

Random Matrix Advances in Large Dimensional Machine Learning

Romain Couillet, Zhenyu Liao

October 29, 2020

Numerous and large dimensional data is now a default setting in modern machine learning (ML). Standard ML algorithms, starting with support vector machines, graphs and kernel methods, were however designed out of small dimensional intuitions and tend to misbehave, if not completely collapse when dealing with real large datasets. Random matrix theory has recently developed a broad spectrum of tools to help understand this new curse of dimensionality, to help repair or completely recreate the misbehaving algorithms, and most importantly to provide new intuitions to deal with real modern data mining.

This monograph primarily aims to deliver these intuitions, by providing a digest of the recent theoretical and applied breakthroughs of random matrix theory into machine learning. Targeting a broad audience, spanning from undergraduate students in statistical learning to AI engineers and researchers alike, the mathematical prerequisites to the book are minimal (basics of probability theory, linear algebra and real and complex analysis are sufficient): as opposed to introductory books in the mathematical literature of random matrix theory and large dimensional statistics, the theoretical focus is restricted to the essential requirements to machine learning applications. These applications range large, including detection, statistical inference and estimation, supervised, semi-supervised and unsupervised classification, mostly using graphs and kernel methods, as well as neural networks: for these, a theoretical understanding of the algorithm performances (often inaccessible when not resorting to a random matrix analysis), large dimensional insights, methods of improvement, along with a fundamental justification of the wide-scope applicability of the methods to real data, are provided.

Most methods, algorithms, and visuals proposed in the monograph are coded in Matlab and made freely available to the readers (<https://github.com/Zhenyu-LIAO/RMT4ML>). The monograph also contains a series of exercises of two types: short exercises with corrections appended to the end of the book to familiarize the reader with the basic theoretical notions of random matrices, as well as long guided exercises to apply these notions to further concrete machine learning applications.

Contents

1	Introduction	7
1.1	Motivation: the pitfalls of large dimensional statistics	7
1.1.1	The big data era: when n is no longer much larger than p	7
1.1.2	Sample covariance matrices in the large n, p regime	8
1.1.3	Kernel matrices of large dimensional data	11
1.1.4	Summarizing	16
1.2	Random matrix theory as an answer	19
1.2.1	Which theory and why?	19
1.2.2	The double asymptotics: turning the curse of dimensionality to a dimensionality blessing	23
1.2.3	Improving machine learning methods	24
1.2.4	Exploiting universality: from large dimensional statistics to practical data	30
1.3	Outline and online toolbox	35
1.3.1	Organization of the manuscript	35
1.3.2	Online codes	38
2	Basics of Random Matrix Theory	39
2.1	Fundamental objects	39
2.1.1	The resolvent	39
2.1.2	Spectral measure and Stieltjes transform	40
2.1.3	Cauchy's integral, linear eigenvalue functionals, and eigenspaces	42
2.1.4	Deterministic and random equivalents	43
2.2	Foundational random matrix results	46
2.2.1	Key lemmas and identities	46
2.2.2	The Marčenko-Pastur and semi-circle laws	52
2.2.3	Large dimensional sample covariance matrices and generalized semi-circles	66
2.3	Advanced spectrum considerations for sample covariances	77
2.3.1	Limiting spectrum	77
2.3.2	"No eigenvalue outside the support"	82
2.4	Preliminaries on statistical inference	84
2.4.1	Linear eigenvalue statistics	85
2.4.2	Eigenvector projections and subspace methods	92

2.5	Spiked models	98
2.5.1	Isolated eigenvalues	98
2.5.2	Isolated eigenvectors	102
2.5.3	Limiting fluctuations	106
2.5.4	Further discussions and other spiked models	109
2.6	Information-plus-noise, deformed Wigner, and other models	111
2.6.1	Why focus on the sample covariance matrix model?	111
2.6.2	Other models	112
2.6.3	Other statistics	122
2.7	Beyond vectors of independent entries: concentration of measure in RMT	125
2.7.1	Limitations of the i.i.d. assumption	125
2.7.2	Concentrated random vectors as the answer	125
2.7.3	Elements of concentration of measure for random matrices	129
2.7.4	A concentration inequality version of Theorem 2.5	135
2.8	Concluding remarks	140
2.9	Exercises	142
2.9.1	Properties of the Stieltjes transform	142
2.9.2	On limiting laws	143
2.9.3	On eigen-inference	144
2.9.4	Spiked models	145
2.9.5	Deterministic equivalent	145
2.9.6	Concentration of measure	146
2.9.7	Beyond matrices	147
3	Statistical Inference in Linear Models	149
3.1	Detection and estimation in information-plus-noise models	150
3.1.1	GLRT asymptotics	150
3.1.2	Linear and Quadratic Discriminant Analysis	153
3.1.3	Subspace methods: the G-MUSIC algorithm	160
3.2	Covariance matrix distance estimation	164
3.2.1	Distances and divergences between Gaussian laws	164
3.2.2	The random matrix framework	166
3.2.3	Closed-form expressions	169
3.2.4	The Wasserstein and Frobenius distances	174
3.2.5	Application to covariance-based spectral clustering	175
3.3	M-estimators of scatter	176
3.3.1	Reminder on robust statistics	176
3.3.2	The M-estimator of scatter	177
3.3.3	The random matrix framework	178
3.3.4	Extensions	186
3.4	Concluding remarks	190
3.5	Practical course material	191

4 Kernel Methods	199
4.1 Basic setting	200
4.1.1 The non-trivial growth rates	200
4.1.2 Statistical data model	202
4.2 Distance and inner-product random kernel matrices	203
4.2.1 Main intuition	203
4.2.2 Main Results	208
4.3 The α - β random kernel model	212
4.3.1 Motivation	212
4.3.2 Main results	214
4.4 Properly scaling kernels	219
4.4.1 Motivation	219
4.4.2 Setting	220
4.4.3 Hermite polynomials	221
4.4.4 Limiting spectrum of the null model \mathbf{K}_N	222
4.4.5 Main results	228
4.5 Implications to kernel methods	232
4.5.1 Application to kernel spectral clustering	232
4.5.2 Application to semi-supervised kernel learning	241
4.5.3 Application to kernel ridge regression	255
4.5.4 Summary of Section 4.5	261
4.6 Concluding remarks	261
4.7 Practical course material	264
5 Large Neural Networks	269
5.1 Random neural networks	269
5.1.1 Regression with random neural networks	270
5.1.2 Delving deeper into limiting kernels	280
5.2 Gradient descent dynamics in learning linear neural nets	287
5.3 Recurrent neural nets: echo-state networks	292
5.3.1 Preliminaries and echo state networks	292
5.3.2 Results on ESN asymptotics	294
5.4 Concluding remarks	299
5.5 Practical course material	302
6 Optimization-based Methods with Non-explicit Solutions	305
6.1 Generalized linear classifier	306
6.1.1 Basic setting	306
6.1.2 Intuitions and main results	307
6.1.3 Practical consequences and further discussions	312
6.2 Large dimensional support vector machines	317
6.3 Conclusion	323
6.4 Practical course material	325

7	Community Detection on Graphs	329
7.1	Community detection in dense graphs	330
7.1.1	The stochastic block model	330
7.1.2	The degree-corrected stochastic block model	339
7.2	From dense to sparse graphs: a different approach	347
7.2.1	The non-backtracking matrix	347
7.2.2	The Bethe Hessian matrix	349
7.2.3	Degree regularization	349
7.2.4	A unifying approach adapted to DC-SBM	350
7.3	Concluding remarks	353
7.4	Practical course material	353
8	Discussions on Universality and Practical Applications	357
8.1	From Gaussian mixtures to concentrated random vectors and GAN images	357
8.1.1	On data models in large dimensions	357
8.1.2	A study of GAN data	359
8.2	Wide-sense universality in large dimensional machine learning	365
8.3	Discussions and conclusions	368
8.3.1	Deterministic equivalent	381

Chapter 1

Introduction

chap:intro

1.1 Motivation: the pitfalls of large dimensional statistics

sec:motivation

1.1.1 The big data era: when n is no longer much larger than p

The big data revolution comes along with the challenging need to parse, mine, compress large amount of large dimensional and possibly heterogeneous data. In many applications, the dimension p of the observations is as large as – if not much larger than – their number n . In array processing and wireless communications, the number of antennas required for fine localization resolution or increased communication throughput may be as large (today in the order of hundreds) as the number of available independent signal observations [Lu et al., 2014, Li and Stoica, 2007]. In genomics, the identification of correlations among hundred of thousands genes based on a limited number of independent (and expensive) samples induces an even larger ratio p/n [Arnold et al., 1994]. In statistical finance, portfolio optimization relies on the opposite need to invest on a large number p of assets to reduce volatility but at the same time to estimate the current (rather than past) asset statistics from a relatively small number n of asset return records [Laloux et al., 2000].

As we shall demonstrate in the next section, the fact that in these problems n is not *much larger* than p annihilates most of the results from standard asymptotic statistics that assume n alone is large [Van der Vaart, 2000]. As a rule of thumb, by *much larger* we mean here that n must be at least 100 times as large as p for standard asymptotic statistics to be of practical convenience (see our argument in Section 1.1.2). Many algorithms in statistics, signal processing, and machine learning are precisely derived from this inappropriate $n \gg p$ assumption. A main objective of this monograph is to cast a light on the resulting biases and problems incurred and to provide a systematic random matrix framework to improve these algorithms.

Possibly more importantly, we will see along this monograph that finite-dimensional intuitions which are at the core of many machine learning algorithms (starting with spectral clustering [Ng et al., 2002, Von Luxburg, 2007]) may strikingly fail when applied in a simultaneously large n, p setting. A compelling example lies in the notion of “distance” between vectors. Most classification methods in machine learning are rooted in the observation that random vectors arising from a mixture distribution (say Gaussian) gather in “groups” of close-by vectors in Euclidean norm. When dealing with large dimensions, concentration phenomena arise that may make Euclidean distances useless, if not counter-productive: vectors of the same Gaussian mixture class may be further away in Euclidean distance than vectors arising from different classes, but classification may still be doable. The monograph intends to prepare the reader for these multiple traps caused by the famous “curse of dimensionality”.

1.1.2 Sample covariance matrices in the large n, p regime

sec:intro-SCM

Let us consider the following illustrating example which shows a first elementary, yet counterintuitive, result: for simultaneously large n, p , sample covariance matrices $\hat{\mathbf{C}} \in \mathbb{R}^{p \times p}$ based on n samples $\mathbf{x}_i \sim \mathcal{N}(\mathbf{0}, \mathbf{C})$ are *entry-wise* consistent estimators of the population covariance $\mathbf{C} \in \mathbb{R}^{p \times p}$ (i.e., $\|\hat{\mathbf{C}} - \mathbf{C}\|_\infty \rightarrow 0$ as $p, n \rightarrow \infty$ for $\|\mathbf{C}\|_\infty \equiv \max_{ij} |\mathbf{C}_{ij}|$) while overall being extremely poor estimators (i.e., $\|\hat{\mathbf{C}} - \mathbf{C}\| \not\rightarrow 0$ with here $\|\cdot\|$ the operator norm). Matrix norms are in particular *not* equivalent from a large n, p standpoint.

Let us detail this claim, in the simplest case where $\mathbf{C} = \mathbf{I}_p$. Consider a data set $\mathbf{X} = [\mathbf{x}_1, \dots, \mathbf{x}_n] \in \mathbb{R}^{p \times n}$ of n independent and identically distributed (i.i.d.) observations from a p -dimensional Gaussian distribution, i.e., $\mathbf{x}_i \sim \mathcal{N}(\mathbf{0}_p, \mathbf{I}_p)$ for $i = 1, \dots, n$. We wish to estimate the population covariance matrix $\mathbf{C} = \mathbf{I}_p$ from the n available samples. The maximum likelihood estimator in this zero-mean Gaussian setting is the sample covariance matrix $\hat{\mathbf{C}}$ defined by

$$\hat{\mathbf{C}} = \frac{1}{n} \sum_{i=1}^n \mathbf{x}_i \mathbf{x}_i^\top = \frac{1}{n} \mathbf{X} \mathbf{X}^\top. \quad \text{eq:scm}(1.1)$$

By the strong law of large numbers, for fixed p , $\hat{\mathbf{C}} \rightarrow \mathbf{I}_p$ almost surely as $n \rightarrow \infty$, so that $\|\hat{\mathbf{C}} - \mathbf{I}_p\| \xrightarrow{a.s.} 0$ holds for any standard matrix norm and in particular for the operator norm.

One must be more careful when dealing with the regime $n, p \rightarrow \infty$ with ratio $p/n \rightarrow c \in (0, \infty)$ (or, from a practical standpoint, n is not much larger than p). First, note that the entry-wise convergence still holds since, invoking by the law of large numbers again

$$\hat{\mathbf{C}}_{ij} = \frac{1}{n} \sum_{l=1}^n \mathbf{X}_{il} \mathbf{X}_{jl} \xrightarrow{a.s.} \begin{cases} 1, & i = j; \\ 0, & i \neq j. \end{cases}$$

1.1. MOTIVATION: THE PITFALLS OF LARGE DIMENSIONAL STATISTICS9

Besides, by a concentration inequality argument, it can even be shown that

$$\max_{1 \leq i, j \leq p} |(\hat{\mathbf{C}} - \mathbf{I}_p)_{ij}| \xrightarrow{a.s.} 0$$

which holds as long as p is no larger than a polynomial function of n , and thus

$$\|\hat{\mathbf{C}} - \mathbf{I}_p\|_\infty \xrightarrow{a.s.} 0$$

with $\|\mathbf{A}\|_\infty$ the largest absolute entry of matrix \mathbf{A} .

Consider now the case $p > n$. Since $\hat{\mathbf{C}}$ is the sum of n rank one matrices (as per the form (1.1)), the rank of $\hat{\mathbf{C}}$ is at most equal to n and thus, being a $p \times p$ matrix with $p < n$, the sample covariance matrix $\hat{\mathbf{C}}$ is a singular matrix having at least $p - n > 0$ null eigenvalues. As a consequence,

$$\|\hat{\mathbf{C}} - \mathbf{I}_p\| \not\rightarrow 0$$

for $\|\cdot\|$ the matrix operator (or spectral) norm. This last result actually extends to the general case where $n, p \rightarrow \infty$ with $p/n \rightarrow c > 0$. As such, matrix norms cannot be considered equivalent in the regime where p is not negligible compared to n . This follows from the fact that the equivalence factors depend on the matrix size p ; here for instance, $\|\mathbf{A}\|_\infty \leq \|\mathbf{A}\| \leq p\|\mathbf{A}\|_\infty$ for $\mathbf{A} \in \mathbb{R}^{p \times p}$.

Unfortunately, in practice, the (non converging) operator norm is of more practical interest than the (converging) infinity norm.

rem:operator-norm

Remark 1.1 (On the importance of operator norm). *For practical purposes, this loss of norm equivalence raises the question of the relevant matrix norm to be considered in any given application. For the purpose of the present monograph, and for most applications in machine learning, the operator (or spectral) norm is the most relevant. Indeed, first, the operator norm is the matrix norm induced by the Euclidean norm of vectors. Thus, the study of regression vectors or label/score vectors in classification is naturally attached to the spectral study of matrices. Besides, we will often be interested in the asymptotic equivalence of families of large dimensional matrices. If $\|\mathbf{A}_p - \mathbf{B}_p\| \rightarrow 0$ for matrix sequences $\{\mathbf{A}_p\}$ and $\{\mathbf{B}_p\}$, indexed by their dimension p , then according to Weyl's inequality (see for example [Horn and Johnson, 2012, Theorem 4.3.1]),*

$$\max_i |\lambda_i(\mathbf{A}_p) - \lambda_i(\mathbf{B}_p)| \rightarrow 0$$

for $\lambda_1(\mathbf{A}) \geq \lambda_2(\mathbf{A}) \geq \dots$ the eigenvalues of \mathbf{A} in a decreasing order. Besides, for $\mathbf{u}_i(\mathbf{A}_p)$ an eigenvector of \mathbf{A}_p associated with an isolated eigenvalue $\lambda_i(\mathbf{A}_p)$ (i.e., such that $\min(|\lambda_{i+1}(\mathbf{A}_p) - \lambda_i(\mathbf{A}_p)|, |\lambda_i(\mathbf{A}_p) - \lambda_{i-1}(\mathbf{A}_p)|) > \varepsilon$ for some $\varepsilon > 0$ uniformly on p),

$$\|\mathbf{u}_i(\mathbf{A}_p) - \mathbf{u}_i(\mathbf{B}_p)\| \rightarrow 0.$$

These results ensure that, as far as spectral properties are concerned, \mathbf{A}_p can be studied equivalently through \mathbf{B}_p . We will often use this argument to investigate intractable random matrices \mathbf{A}_p by means of a tractable ersatz \mathbf{B}_p .

The pitfall that consists in assuming that $\hat{\mathbf{C}}$ is a valid estimator of \mathbf{C} since $\|\hat{\mathbf{C}} - \mathbf{C}\|_\infty \xrightarrow{a.s.} 0$ may thus have deleterious practical consequences when n is not significantly larger than p .

Resuming on our norm convergence discussion, it is now natural to ask whether $\hat{\mathbf{C}}$, which badly estimates \mathbf{C} , has a controlled asymptotic behavior. There precisely lay the first theoretical interests of random matrix theory. While $\hat{\mathbf{C}}$ itself does not converge in any useful way, its eigenvalue distribution does exhibit a traceable limiting behavior [Marcenko and Pastur, 1967, Silverstein and Bai, 1995, Bai and Silverstein, 2010]. The seminal result in this direction, due to Marčenko and Pastur, states that, when $\mathbf{C} = \mathbf{I}_p$, as $n, p \rightarrow \infty$ with $p/n \rightarrow c \in (0, \infty)$, with probability one, the (random) *discrete empirical spectral distribution*

$$\mu_p \equiv \frac{1}{p} \sum_{i=1}^p \delta_{\lambda_i(\hat{\mathbf{C}})}$$

converges in law to a non-random *smooth* limit, today referred to as the “Marčenko-Pastur law” [Marcenko and Pastur, 1967]

$$\mu(dx) = (1 - c^{-1})^+ \delta_0(x) + \frac{1}{2\pi cx} \sqrt{(x - a)^+(b - x)^+} dx \quad \text{eq:MP-law (1.2)}$$

where $a = (1 - \sqrt{c})^2$, $b = (1 + \sqrt{c})^2$ and $(x)^+ \equiv \max(x, 0)$.

Figure 1.1 compares the empirical spectral distribution of $\hat{\mathbf{C}}$ to the limiting Marčenko-Pastur law given in (1.2), for $p = 500$ and $n = 50\,000$.

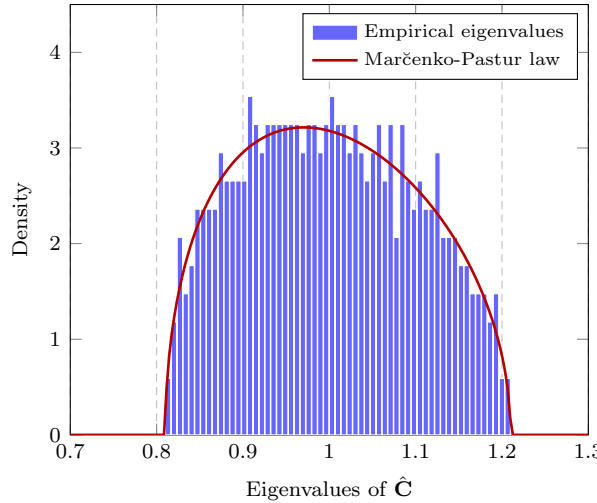


Figure 1.1: Histogram of the empirical spectral distribution of $\hat{\mathbf{C}}$ versus the Marčenko-Pastur law, for $p = 500$ and $n = 50\,000$. [Link to code] fig:MP-law

The elementary Marčenko-Pastur result is already quite instructive and insightful.

Remark 1.2 (When is one under the random matrix regime?). *Equation (1.2) reveals that the eigenvalues of $\hat{\mathbf{C}}$, instead of concentrating at $x = 1$ as a large- n alone analysis would suggest, are spread from $(1 - \sqrt{c})^2$ to $(1 + \sqrt{c})^2$. As such, the eigenvalues span on a range*

$$(1 + \sqrt{c})^2 - (1 - \sqrt{c})^2 = 4\sqrt{c}.$$

This is a slow decaying behavior with respect to c (and thus to increasing n). In particular, for $n = 100p$, where one would expect a sufficiently large number of samples for $\hat{\mathbf{C}}$ to properly estimate $\mathbf{C} = \mathbf{I}_p$, $4\sqrt{c} = 0.4$ which is a large spread around the mean (and true) eigenvalue 1. This is visually confirmed by Figure 1.1 for $p = 500$ and $n = 50\,000$, where the histogram of the eigenvalues is nowhere near concentrated at $x = 1$. As such, random matrix results will be largely more accurate than classical asymptotic statistics even when $n \sim 100p$. As a telling example, estimating the covariance matrix of each digit from the popular MNIST dataset [LeCun et al., 1998], made of no more than 60 000 training samples (and thus about $n = 6\,000$ samples per digit) of size $p = 784$, is likely a hazardous undertaking.

rem:universality

Remark 1.3 (On universality). *Although introduced here in the context of Gaussian distributions for \mathbf{x}_i , the Marčenko-Pastur law applies to much more general cases. Indeed, the result remains valid so long that the \mathbf{x}_i 's have i.i.d. normalized entries of zero mean and unit variance (and even beyond this setting [El Karoui, 2009, Louart and Couillet, 2019]). Similar to the law of large numbers in standard statistics, this universality phenomenon commonly arises in random matrix theory and high dimensional statistics. We will exploit this phenomenon in the monograph to justify the wide applicability of the presented results, even to real datasets.*

1.1.3 Kernel matrices of large dimensional data

sec:intro-kernel

Another less known but equally important example of the curse of dimensionality in machine learning involves the loss of relevance of the notion of Euclidean distance between large dimensional data vectors. To be more precise, we will see in the course of the manuscript that, *under an asymptotically non-trivial classification setting* (that is, ensuring that asymptotic classification is neither too simple nor too hard), large and numerous data vectors $\mathbf{x}_1, \dots, \mathbf{x}_n \in \mathbb{R}^p$ extracted from a few-class mixture model tend to be asymptotically at equal distance from one another, irrespective of their mixture class. Roughly said, in this non-trivial setting and under reasonable statistical assumptions on the \mathbf{x}_i 's, we have

$$\max_{1 \leq i \neq j \leq n} \left\{ \frac{1}{p} \|\mathbf{x}_i - \mathbf{x}_j\|^2 - \tau \right\} \rightarrow 0 \quad \text{eq:distance-constant (1.3)}$$

for some constant $\tau > 0$ as $n, p \rightarrow \infty$, *independently of the classes (same or different) of \mathbf{x}_i and \mathbf{x}_j* (here the distance normalization by p is used for compliance with the notations in the remainder of the manuscript but has no particular importance).

This asymptotic behavior is extremely counterintuitive and conveys the idea that classification by standard methods ought not be doable in this regime. Indeed, in the conventional finite-dimensional intuition that forged many of the leading machine learning algorithms of everyday use (such as spectral clustering [Ng et al., 2002, Von Luxburg, 2007]), two data points belong to the same class if they are “close” in Euclidean distance. Here we claim that, when p is large, *data pairs are neither close nor far* from each other, regardless of their belonging to the same class or not. Despite this troubling loss of individual discriminative power between data pairs, we subsequently show that, thanks to a *collective behavior* of all data belonging to the same (few and thus large) classes, asymptotic data classification or clustering is still achievable. Better, we shall see that, while many conventional methods devised from small dimensional intuitions do fail in the large dimensional regime, some popular approaches (such as the Ng-Jordan-Weiss spectral clustering method [Ng et al., 2002] or the PageRank semi-supervised learning approach [Avrachenkov et al., 2012]) still function. But the core reasons for their functioning are strikingly different from the reasons of their initial designs, and they often operate far from optimally.

1.1.3.1 The non-trivial classification regime

sec:non-trivial-regime

To get a clear picture of the source of Equation (1.3), we first need to clarify what we refer to as the “asymptotically non-trivial” classification setting. Consider the simplest setting of a binary Gaussian mixture classification. We give ourselves a training set $\mathbf{x}_1, \dots, \mathbf{x}_n \in \mathbb{R}^p$ of n samples independently drawn from the two-class (\mathcal{C}_1 and \mathcal{C}_2) Gaussian mixture

$$\begin{aligned}\mathcal{C}_1 : \mathbf{x} &\sim \mathcal{N}(\boldsymbol{\mu}, \mathbf{I}_p) \\ \mathcal{C}_2 : \mathbf{x} &\sim \mathcal{N}(-\boldsymbol{\mu}, \mathbf{I}_p + \mathbf{E})\end{aligned}$$

each drawn with probability 1/2, for some deterministic $\boldsymbol{\mu} \in \mathbb{R}^p$ and $\mathbf{E} \in \mathbb{R}^{p \times p}$ both possibly depending on p . In the ideal case where $\boldsymbol{\mu}$ and \mathbf{E} are perfectly known, one can devise a (decision optimal) Neyman-Pearson test. For an unknown \mathbf{x} , genuinely belonging to \mathcal{C}_1 , the Neyman-Pearson test to decide on the class of \mathbf{x} reads

$$(\mathbf{x} + \boldsymbol{\mu})^\top (\mathbf{I}_p + \mathbf{E})^{-1} (\mathbf{x} + \boldsymbol{\mu}) - (\mathbf{x} - \boldsymbol{\mu})^\top (\mathbf{x} - \boldsymbol{\mu}) \stackrel{\mathcal{C}_1}{\gtrless} \stackrel{\mathcal{C}_2}{\gtrless} -\log \det(\mathbf{I}_p + \mathbf{E}). \quad \text{eq:NP-test (1.4)}$$

Writing $\mathbf{x} = \boldsymbol{\mu} + \mathbf{z}$ so that $\mathbf{z} \sim \mathcal{N}(\mathbf{0}, \mathbf{I}_p)$, the above test is equivalent to

$$\begin{aligned}T(\mathbf{x}) &\equiv 4\boldsymbol{\mu}^\top (\mathbf{I}_p + \mathbf{E})^{-1} \boldsymbol{\mu} + 4\boldsymbol{\mu}^\top (\mathbf{I}_p + \mathbf{E})^{-1} \mathbf{z} + \mathbf{z}^\top ((\mathbf{I}_p + \mathbf{E})^{-1} - \mathbf{I}_p) \mathbf{z} \\ &+ \log \det(\mathbf{I}_p + \mathbf{E}) \stackrel{\mathcal{C}_1}{\gtrless} 0. \quad \text{eq:NP-test-1 (1.5)}\end{aligned}$$

Since \mathbf{Uz} for $\mathbf{U} \in \mathbb{R}^{p \times p}$ an eigenvector basis of $(\mathbf{I}_p + \mathbf{E})^{-1}$ (and thus of $(\mathbf{I}_p + \mathbf{E})^{-1} - \mathbf{I}_p$) follows the same distribution as \mathbf{z} , the random variable $T(\mathbf{x})$ can be written as the sum of p independent random variables. Further assuming

that $\|\boldsymbol{\mu}\| = O(1)$ with respect to p , by Lyapunov's central limit theorem (e.g., [Billingsley, 2012, Theorem 27.3]), we have, as $p \rightarrow \infty$,

$$V_T^{-1/2}(T(\mathbf{x}) - \bar{T}) \xrightarrow{d} \mathcal{N}(0, 1)$$

where

$$\begin{aligned}\bar{T} &\equiv 4\boldsymbol{\mu}^\top(\mathbf{I}_p + \mathbf{E})^{-1}\boldsymbol{\mu} + \text{tr}(\mathbf{I}_p + \mathbf{E})^{-1} - p + \log \det(\mathbf{I}_p + \mathbf{E}), \\ V_T &\equiv 16\boldsymbol{\mu}^\top(\mathbf{I}_p + \mathbf{E})^{-2}\boldsymbol{\mu} + 2\|(\mathbf{I}_p + \mathbf{E})^{-1} - \mathbf{I}_p\|_F^2.\end{aligned}$$

As a consequence, the classification performance of $\mathbf{x} \in \mathcal{C}_1$ is asymptotically non-trivial (i.e., the classification error neither goes to 0 nor 1 as $p \rightarrow \infty$) if and only if \bar{T} is of the same order as $\sqrt{V_T}$. Considering the worst case scenario where $\mathbf{E} = \mathbf{0}$, we must have $\|\boldsymbol{\mu}\| \geq O(1)$ with respect to p (indeed, if instead $\|\boldsymbol{\mu}\| = o(1)$, the classification of \mathbf{x} is asymptotically impossible).

Under the minimal constraint of $\|\boldsymbol{\mu}\| = O(1)$ we move on to considering the case $\mathbf{E} \neq \mathbf{0}$ with $\|\mathbf{E}\| = o(1)$. By a Taylor expansion of both $(\mathbf{I}_p + \mathbf{E})^{-1}$ and $\log \det(\mathbf{I}_p + \mathbf{E})$ around \mathbf{I}_p we obtain

$$\begin{aligned}\bar{T} &= 4\|\boldsymbol{\mu}\|^2 + \frac{1}{2}\|\mathbf{E}\|_F^2 + o(1); \\ V_T &= 16\|\boldsymbol{\mu}\|^2 + 2\|\mathbf{E}\|_F^2 + o(1),\end{aligned}$$

which demands $\|\mathbf{E}\|_F^2$ to be of order $O(1)$ (as $\|\boldsymbol{\mu}\|$) so as to have discriminative power. Since $\|\mathbf{E}\|_F^2 = \text{tr}(\mathbf{E}^2) \leq p\|\mathbf{E}\|^2$, with equality if and only if \mathbf{E} is proportional to identity, i.e., $\mathbf{E} = \epsilon\mathbf{I}_p$, one must have $\|\mathbf{E}\| \geq O(p^{-1/2})$. Also, by the Cauchy–Schwarz inequality, we have $|\text{tr } \mathbf{E}| \leq \sqrt{\text{tr}(\mathbf{E}^2)} \cdot \text{tr } \mathbf{I}_p = O(\sqrt{p})$, with equality if and only if $\mathbf{E} = \epsilon\mathbf{I}_p$, and we must therefore have $|\text{tr } \mathbf{E}| \geq O(\sqrt{p})$. This allows us to conclude on the following non-trivial classification conditions

$$\|\boldsymbol{\mu}\| \geq O(1), \quad \|\mathbf{E}\| \geq O(p^{-1/2}), \quad |\text{tr}(\mathbf{E})| \geq O(\sqrt{p}), \quad \|\mathbf{E}\|_F^2 \stackrel{\text{eq:non-trivial-conditions}}{\geq} O(1). \quad (1.6)$$

These are the minimal conditions for classification in the case of perfectly known means and covariances in the following sense: (i) if none of the inequalities hold (i.e., if means and covariances from both classes are too close), asymptotic classification must fail, (ii) if at least one of the inequalities is not tight (say if $\|\boldsymbol{\mu}\| \geq O(\sqrt{p})$), asymptotic classification becomes trivial.

We shall subsequently see that (1.6) precisely induces the asymptotic loss of distance discrimination raised in (1.3) but that standard spectral clustering methods based on $n \sim p$ data remain valid.

1.1.3.2 Asymptotic loss of pairwise distance discrimination

Under the equality case for the conditions in (1.6), the (normalized) Euclidean distance between two distinct data vectors $\mathbf{x}_i \in \mathcal{C}_a, \mathbf{x}_j \in \mathcal{C}_b$ is thus given by

$$\frac{1}{p}\|\mathbf{x}_i - \mathbf{x}_j\|^2 = \begin{cases} \frac{1}{p}\|\mathbf{z}_i - \mathbf{z}_j\|^2 + Ap^{-1/2}, & \text{eq:distance-constant-concrete} \\ \frac{1}{p}\|\mathbf{z}_i - \mathbf{z}_j\|^2 + Bp^{-1/2}, & \text{for } a = 1, b = 2, \end{cases} \quad (1.7)$$

where

$$\begin{aligned} A &= (\mathbf{z}_i^\top \mathbf{E} \mathbf{z}_i + \mathbf{z}_j^\top \mathbf{E} \mathbf{z}_j - 2\mathbf{z}_i^\top \mathbf{E} \mathbf{z}_j) p^{-1/2} \\ B &= (\mathbf{z}_j^\top (\mathbf{E} + \mathbf{E}^2/4) \mathbf{z}_j - \mathbf{z}_i^\top \mathbf{E} \mathbf{z}_j + 4\|\boldsymbol{\mu}\|^2 + 4\boldsymbol{\mu}^\top (\mathbf{z}_i - \mathbf{z}_j) + o(1)) p^{-1/2} \end{aligned}$$

are both of order $O(1)$ (and thus $Ap^{-1/2}, Bp^{-1/2} = O(p^{-1/2})$) while the leading term $\frac{1}{p}\|\mathbf{z}_i - \mathbf{z}_j\|^2$ of (1.7) is of order $O(1)$ and such that

$$\max_{1 \leq i \neq j \leq n} \left\{ \frac{1}{p}\|\mathbf{z}_i - \mathbf{z}_j\|^2 - 2 \right\} \rightarrow 0$$

almost surely as $n, p \rightarrow \infty$ (this easily follows by exploiting the fact that $\|\mathbf{z}_i - \mathbf{z}_j\|^2$ is a χ -square random variable with p degrees of freedom). As a consequence, as previously claimed,

$$\max_{1 \leq i \neq j \leq n} \left\{ \frac{1}{p}\|\mathbf{x}_i - \mathbf{x}_j\|^2 - \tau \right\} \rightarrow 0$$

for $\tau = 2$ here. Besides, let us suppose first that $\text{tr } \mathbf{E} = 0$ (a situation that arises in practice if the data all have the same covariance or if they, or their entries $[\mathbf{x}_i]_k$, are normalized). Then, on closer inspection of (1.7), beyond this common value τ , the discriminative class information in means $4\|\boldsymbol{\mu}\|^2/p$ and in covariances $\mathbf{z}_j^\top \mathbf{E}^2 \mathbf{z}_j/(4p) \sim \text{tr } \mathbf{E}^2/(4p)$ are both of order $O(p^{-1})$, while, by the central limit theorem, $\frac{1}{p}\|\mathbf{z}_i - \mathbf{z}_j\|^2 = 2 + O(p^{-1/2})$. The class information is thus largely overtaken by the random fluctuations. As a consequence, asymptotically, $\frac{1}{p}\|\mathbf{x}_i - \mathbf{x}_j\|^2$ contains *no* exploitable information (about $\boldsymbol{\mu}$ or \mathbf{E}) to distinguish if \mathbf{x}_i and \mathbf{x}_j vectors belong to the same or different classes.¹

To visually confirm this joint convergence of the data distances, in Figure 1.2 we display the content of the Gaussian (heat) kernel matrix $\mathbf{K} \in \mathbb{R}^{n \times n}$ with $\mathbf{K}_{ij} = \exp\left(-\frac{1}{2p}\|\mathbf{x}_i - \mathbf{x}_j\|^2\right)$ and the associated second top eigenvector \mathbf{v}_2 for a two-class Gaussian mixture $\mathbf{x} \sim \mathcal{N}(\pm \boldsymbol{\mu}, \mathbf{I}_p)$ with $\boldsymbol{\mu} = [2; \mathbf{0}_{p-1}]$. For a constant $n = 500$, we take $p = 5$ in Figure 1.2a and $p = 250$ in Figure 1.2b.

While the “block-structure” in Figure 1.2a does agree with the finite-dimensional intuition: data vectors from the same class are “closer” to one another, corresponding to diagonal blocks with larger values (since $\exp(-x/2)$ decreases with the distance) than in non diagonal blocks, this intuition collapses when large dimensional data vectors are considered. Indeed, in the large data setting of Figure 1.2b, all entries (but obviously on the diagonal) of \mathbf{K} have approximately the same value, which we now know from (1.3) is $\exp(-1)$.

This is no longer surprising to us. However, what remains surprising at this stage of our analysis is that the eigenvector \mathbf{v}_2 of \mathbf{K} is not affected by this

¹The case where $\text{tr } \mathbf{E} = O(p^{1/2})$ leads to slightly different conclusions. There, the term $\frac{1}{p}\mathbf{z}_i^\top \mathbf{E} \mathbf{z}_i + \frac{1}{p}\mathbf{z}_j^\top \mathbf{E} \mathbf{z}_j \sim \frac{2}{p}\text{tr } \mathbf{E}$ in $Ap^{-1/2}$ dominates $\frac{1}{p}\mathbf{z}_j^\top \mathbf{E} \mathbf{z}_j \sim \frac{1}{p}\text{tr } \mathbf{E}$ in $Bp^{-1/2}$ by a factor 2. Both are of order $O(p^{-1/2})$, which is the same as the order of the noise fluctuations. It is thus possible to non-trivially extract the class information in this case, merely by comparing the norms $\|\mathbf{x}_1\|, \dots, \|\mathbf{x}_n\|$.

(asymptotic) loss of class-wise discrimination of individual distances (particularly valid here since $\mathbf{E} = \mathbf{0}$). Thus spectral clustering seems to work equally well for $p = 5$ or $p = 250$, despite the radical and intuitively destructive change in the behavior of \mathbf{K} for $p = 250$.

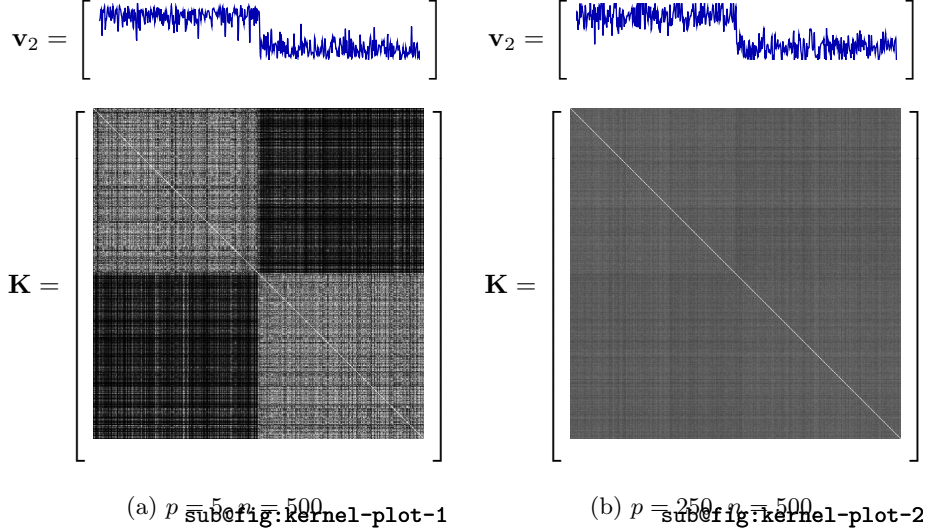


Figure 1.2: Kernel matrices \mathbf{K} and the second top eigenvectors \mathbf{v}_2 for small and large dimensional data $\mathbf{X} = [\mathbf{x}_1, \dots, \mathbf{x}_n] \in \mathbb{R}^{p \times n}$ with $\mathbf{x}_1, \dots, \mathbf{x}_{n/2} \in \mathcal{C}_1$ and $\mathbf{x}_{n/2+1}, \dots, \mathbf{x}_n \in \mathcal{C}_2$.
fig:kernel-plot

1.1.3.3 Explaining kernel methods with random matrix theory

The fundamental reason behind this surprising behavior lies in the *accumulated* effect of the (in total) $n/2$ small “hidden” informative terms $\|\boldsymbol{\mu}\|^2$ and $\text{tr}(\mathbf{E}^2)$, to collectively “steer” the several top eigenvectors of \mathbf{K} . More explicitly, we shall see in the course of this monograph that the RBF kernel matrix \mathbf{K} can be asymptotically expanded as

$$\mathbf{K} = \exp(-1) \left(\mathbf{1}_n \mathbf{1}_n^\top + \frac{1}{p} \mathbf{Z} \mathbf{Z}^\top \right) + g(\boldsymbol{\mu}, \mathbf{E}) \frac{1}{p} \mathbf{j} \mathbf{j}^\top + * + o(1)$$

where $\mathbf{Z} = [\mathbf{z}_1, \dots, \mathbf{z}_n] \in \mathbb{R}^{p \times n}$, $g(\boldsymbol{\mu}, \mathbf{E}) = O(1)$ and $\mathbf{j} = [\mathbf{1}_{n/2}^\top, -\mathbf{1}_{n/2}^\top]^\top$ is the class-information vector (as in the setting of Figure 1.2). Here ‘*’ symbolizes extra terms of marginal importance to the present discussion and $o(1)$ represents terms of asymptotically vanishing operator norm. The important remark to be made here is that

- (i) under this description, $\mathbf{K}_{ij} = \exp(-1) \left(1 + \frac{1}{p} \mathbf{z}_i^\top \mathbf{z}_j \right) \pm \frac{1}{p} g(\boldsymbol{\mu}, \mathbf{E}) + *$ with

$\frac{1}{p}g(\boldsymbol{\mu}, \mathbf{E}) \ll \frac{1}{p}\mathbf{z}_i^\top \mathbf{z}_j = O(p^{-\frac{1}{2}})$; this is consistent with our previous discussion: that the information is *entry-wise* dominated by noise;

- (ii) from a *spectral* viewpoint, $\|\frac{1}{p}\mathbf{Z}^\top \mathbf{Z}\| = O(1)$, as per the Marčenko-Pastur theorem [Marcenko and Pastur, 1967] discussed in the previous section, while $\|g(\boldsymbol{\mu}, \mathbf{E})\frac{1}{p}\mathbf{j}\mathbf{j}^\top\| = O(1)$: thus, *spectrum-wise*, the information stands on even ground with noise.

The mathematical magic at play here lies in $g(\boldsymbol{\mu}, \mathbf{E})\frac{1}{p}\mathbf{j}\mathbf{j}^\top$ having entries of order $O(p^{-1})$ while being a low rank (here unit rank) matrix: all its “energy” concentrates in a single eigenvalue. As for $\frac{1}{p}\mathbf{Z}^\top \mathbf{Z}$, with larger $O(p^{-1/2})$ amplitude entries, it is composed of “essentially independent” zero mean random variables and tends to *spread* its energy over its p eigenvalues. Spectrum-wise, both $g(\boldsymbol{\mu}, \mathbf{E})\frac{1}{p}\mathbf{j}\mathbf{j}^\top$ and $\frac{1}{p}\mathbf{Z}^\top \mathbf{Z}$ meet on even ground “somewhat” under the aforementioned non-trivial classification setting.

We shall see in Section 4 that things are actually not as clear-cut and in particular that not all kernel choices can reach the same (non-trivial) classification rates. In particular, the popular Gaussian (RBF) kernel will be shown to be largely sub-optimal in this respect.

1.1.3.4 Do real data follow small or large dimensional intuitions?

A first glimpse into this riddle, fundamental for the practical design of machine learning algorithm, is provided here in Figure 1.3. Similar to Figure 1.2 for synthetic Gaussian data, Figure 1.3 depicts the content of kernel matrices built from the MNIST [LeCun et al., 1998] and Fashion-MNIST data [Xiao et al., 2017], with $p = 28 \times 28 = 784$ and $n = 500$ in both cases. In Figure 1.4, instead of raw data, we display the *features* extracted from popular deep networks such as VGG-16 [Simonyan and Zisserman, 2014] of the more complex CIFAR-10 images (with $p = 1024$), as well as the so-called “word-embedding” *features* from the popular word2vec method [Mikolov et al., 2013] of the Google-News data (with $p = 300$). In all aforementioned cases, we observe a typical large dimensional behavior (as in Figure 1.2b) not only on raw data but also on efficient features from modern and elaborate machine learning algorithms; strikingly, this behavior is consistently observed both for image and natural language data, despite their being of a fundamentally different nature. Section 1.2.4, at the end of this introductory chapter, provides first clues which justify why this seemingly unexpected observation (recall again that, in the classical motivation behind spectral methods Ng et al. [2002], we rather expect a behavior typical of Figure 1.2a) should in fact not be a surprise.

1.1.4 Summarizing

In this section we discussed two simple, yet counterintuitive examples of common pitfalls in handling large dimensional data.

In the sample covariance matrix example of Section 1.1.2, we made the important remark of the loss of equivalence between matrix norms in the *random*

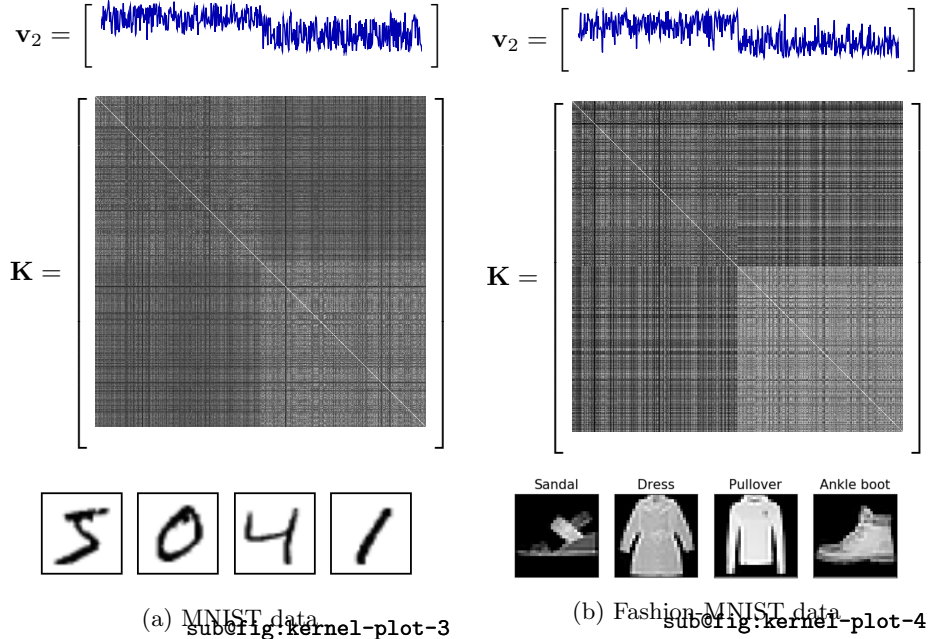


Figure 1.3: Kernel matrices \mathbf{K} and the second top eigenvectors \mathbf{v}_2 for MNIST (classes 8 versus 9) and Fashion-MNIST data (classes 5 versus 7), with $\mathbf{x}_1, \dots, \mathbf{x}_{n/2} \in \mathcal{C}_1$ and $\mathbf{x}_{n/2+1}, \dots, \mathbf{x}_n \in \mathcal{C}_2$. fig:kernel-plot-MNIST

matrix regime where the data (or feature) dimension p and their number n are both large and comparable, which is at the source of many intuition errors. We in particular insist that, for matrices $\mathbf{A}_n, \mathbf{B}_n \in \mathbb{R}^{n \times n}$ of large sizes

$$\forall i, j, (\mathbf{A}_n - \mathbf{B}_n)_{ij} \rightarrow 0 \not\Rightarrow \|\mathbf{A}_n - \mathbf{B}_n\| \rightarrow 0 \quad \text{eq:A-B-n} \quad (1.8)$$

in operator norm.

We also realized, from a basic reading of the Marčenko-Pastur theorem, that the random matrix regime arises more often than one may think: while $n/p \sim 100$ may seem large enough a ratio for classical asymptotic statistics to be accurate, random matrix theory is in general a far more appropriate tool (with as much as 20% gain in precision for the estimation of the eigenvalues of sample covariances).

In Section 1.1.3, we gave a concrete machine learning classification example of the message (1.8) above. We saw that, in the practically most relevant scenario of non-trivial (not too easy, not too hard) large data classification tasks, the distance between any two data vectors “concentrates” around a constant (1.3), regardless of their respective classes. Yet, since again $(\mathbf{A}_n)_{ij} \rightarrow \tau$ does not imply that $\|\mathbf{A}_n - \tau \mathbf{1}_n \mathbf{1}_n^\top\| \rightarrow 0$ in operator norm, we understood that, thanks to a collective effect of the small but similarly “oriented” fluctuations, spectral

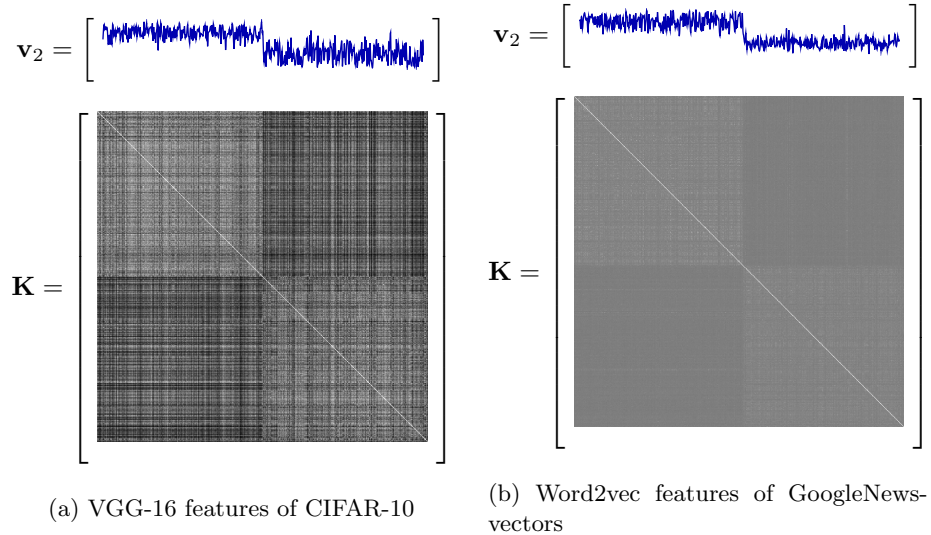


Figure 1.4: Kernel matrices \mathbf{K} and the second top eigenvectors \mathbf{v}_2 for (left) VGG-16 [Simonyan and Zisserman, 2014] features of CIFAR-10 data (airplane versus bird) and (right) word2vec [Mikolov et al., 2013] features of GoogleNews-vectors data (“sports” versus “sales”), with $\mathbf{x}_1, \dots, \mathbf{x}_{n/2} \in \mathcal{C}_1$ and $\mathbf{x}_{n/2+1}, \dots, \mathbf{x}_n \in \mathcal{C}_2$.

`fig:kernel-plot-features`

clustering remains valid for large dimensional problems.

Possibly most importantly, we discovered that the curse of dimensionality induced by the eerie behavior of large dimensional vectors turns into an asset for mathematical analysis. In the sample covariance matrix example, we observed a random-matrix version of the laws of large numbers arises in the convergence to a deterministic limit of the eigenvalue distributions of large sample covariance matrices. As a matter of fact, as we shall see throughout the monograph, the very fact that both p and n are large ensures a generally *fast convergence* of most quantities of practical interest: by exploiting $np = O(n^2)$ rather than n degrees of freedom, central limit theorems may converge at $O(1/n)$ speed (instead of the classical $O(1/\sqrt{n})$).

This fast convergence further induces another important phenomenon, referred to as the *universality* which ensures the robustness of the random matrix asymptotics to a vast range of distributions. Essentially, as we shall see in more details later in this monograph, first and second order statistics are often sufficient to describe most asymptotic behaviors, even of complicated data models and methods. This is a first (yet not the most convincing) justification of the repeatedly observed strong match between random matrix predictions and practical simulations on real datasets.

In a nutshell, the fundamental counterintuitive yet mathematically address-

able changes in behavior of large dimensional data have two major consequences to statistics and machine learning: (i) most algorithms, originally developed under a finite-dimensional intuition, are likely to fail (as we shall discover in this monograph, many of them do) or at least to perform inefficiently, yet (ii) by benefiting from the extra degrees of freedom offered by large data, random matrix theory is apt to analyze, improve, and evoke a whole new paradigm for large dimensional learning.

1.2 Random matrix theory as an answer

1.2.1 Which theory and why?

1.2.1.1 A point of history

Random matrix theory originates from the work of John Wishart [Wishart, 1928] on the study of the eigenvalues of the matrix $\mathbf{X}\mathbf{X}^\top$ (now referred to as a Wishart matrix) for $\mathbf{X} \in \mathbb{R}^{p \times n}$ with $\mathbf{X}_{ij} \sim \mathcal{N}(0, 1)$. Wishart managed to determine a closed-form expression for the joint eigenvalue distribution of $\mathbf{X}\mathbf{X}^\top$ for every pair p, n . Few progress however followed, as matrices with non-Gaussian entries are not amenable to this analysis and, even if they were, the actual study of more elaborate functionals of $\mathbf{X}\mathbf{X}^\top$ is at best cumbersome and often simply intractable.

The works of the physicist Eugene Wigner [Wigner, 1955] gave a new impulse to the theory. Interested in the eigenvalues of symmetric matrices $\mathbf{X} \in \mathbb{R}^{n \times n}$ with independent Bernoulli entries (spins), Wigner opted for an *asymptotic* analysis of the eigenvalue distribution, thereby initiating the important and much richer branch of *large dimensional random matrix theory*. Despite this important inspiration, Wigner exploited standard asymptotic statistics tools (the method of moments) to prove that the *discrete* distribution of the eigenvalues of \mathbf{X} has a *continuous* semi-circle looking density in the limit (the now popular semi-circular law). This approach was particularly convenient as the limiting law is simple and could be visually anticipated.

Only in 1967 with the tour-de-force of Marčenko and Pastur [Marcenko and Pastur, 1967] did random matrix theory take a new dimension. Marčenko and Pastur determined the limiting spectral distribution of the sample covariance matrix model $\mathbf{X}\mathbf{X}^\top$ of Wishart but under relaxed conditions: \mathbf{X}_{ij} are independent entries with zero mean and unit variance, with no further assumption. The independence (or weak dependence) property is key to this method. The proof exploits the powerful Stieltjes transform $\frac{1}{p} \text{tr}(\frac{1}{n} \mathbf{X}\mathbf{X}^\top - z\mathbf{I}_p)^{-1}$ of the empirical spectral distribution of $\frac{1}{n} \mathbf{X}\mathbf{X}^\top$, a tool borrowed from operator theory in Hilbert spaces [Akhiezer and Glazman, 2013], rather than the moments $\frac{1}{p} \text{tr}(\frac{1}{n} \mathbf{X}\mathbf{X}^\top)^k$ (which may not converge since $\mathbb{E}[\mathbf{X}_{ij}^\ell]$ needs not be finite for $\ell > 2$).

The technical approach devised by Marčenko and Pastur was then largely embraced at the turn of the 21st century by Bai and Silverstein who, in a series of significant breakthroughs [Silverstein and Bai, 1995, Bai and Silverstein,

1998], extended [Marcenko and Pastur, 1967] to an exhaustive study of sample covariance matrices.

In parallel, another approach to limiting spectral analysis of random matrices emerged as an application example of the *free probability theory* developed by Voiculescu [Voiculescu et al., 1992]. Free probability was born as a theory to study random variables in non-commutative algebras, such as the algebra of matrices. Rather than relying on independence assumptions as for the Stieltjes transform method, free probability relies on a notion of *asymptotic freeness*. In essence, random matrices are asymptotically free if their eigenvector distribution are sufficiently isotropic with respect to each other; for instance, independent Gaussian matrices (matrices with independent Gaussian entries) are free, independent unitary matrices with isotropic eigenvector distributions are free, a deterministic matrix is free with respect to a Gaussian matrix, etc.

Both free probability and the Stieltjes transform approach have long lived hand-in-hand, and are essentially capable of proving similar results under various assumptions. A classical example, of great importance to this monograph, is that of *spiked models* (i.e., finite-rank deformation of random matrices, such as the nonzero mean sample covariance $(\mathbf{X} + \mu \mathbf{1}_n^\top)(\mathbf{X} + \mu \mathbf{1}_n^\top)^\top$ or the rank-1 perturbed identity covariance $(\mathbf{I}_p + \lambda \mathbf{u} \mathbf{u}^\top)^{\frac{1}{2}} \mathbf{X} \mathbf{X}^\top (\mathbf{I}_p + \lambda \mathbf{u} \mathbf{u}^\top)^\top$ for \mathbf{X} with i.i.d. centered entries) made popular by two key articles [Baik and Silverstein, 2006] and [Benaych-Georges and Nadakuditi, 2012], respectively based on a Stieltjes transform and a free probability approach.

These tools are largely sufficient to cover most of the basic statistical problems in random matrix theory. In particular, the often called *global regime* of random matrices: their limiting eigenvalue spectrum, the behavior of linear statistics of their eigenvalues or eigenvectors, the position of the outlying eigenvalues in spiked models, etc., are all amenable to study by either method. However, this is often not the case of the *local regime*: the limiting distribution of a specific eigenvalue (notably the largest and smallest of practical interest) cannot be study by these methods. There, researchers have rather resorted to a finite dimensional analysis of the joint eigenvalue distribution for the Gaussian case (in the spirit of Wishart), and carefully taken the limits of the distribution, exploiting powerful tools in orthogonal polynomial theory [Johnstone, 2001]. We will not further discuss this approach in the monograph, which is too specific and not of direct use to our applications.

1.2.1.2 Resolvents, Gaussian tools, and concentration of measure theory

More recently, the attraction of the free probability approach decayed, as asymptotic freeness no longer holds for structured random matrix models of importance for application purposes. For this very reason, our focus in this monograph will be on the range of methods surrounding the Stieltjes transform approach.

Precisely, our central object of study throughout the monograph is the so-called *resolvent* of the random matrix $\mathbf{X} \in \mathbb{R}^{n \times n}$ under investigation, that we shall often denote $\mathbf{Q}_{\mathbf{X}}(z)$ or simply $\mathbf{Q}(z)$, and that is defined, for all $z \in \mathbb{C}$ not

in the spectrum of \mathbf{X} , by

$$\mathbf{Q}_{\mathbf{X}}(z) \equiv (\mathbf{X} - z\mathbf{I}_n)^{-1}.$$

The resolvent is a rich mathematical object that gives access to

- the eigenvalue distribution $\mu_{\mathbf{X}} \equiv \frac{1}{n} \sum_{i=1}^n \delta_{\lambda_i(\mathbf{X})}$ of \mathbf{X} through the Stieltjes transform relation (for all $a, b \notin \{\lambda_1(\mathbf{X}), \dots, \lambda_n(\mathbf{X})\}$)

$$\begin{aligned} \int_a^b \mu_{\mathbf{X}}(d\lambda) &= \lim_{\varepsilon \downarrow 0} \int_a^b \frac{1}{\pi} \Im[m_{\mathbf{X}}(x + i\varepsilon)] dx \\ m_{\mathbf{X}}(z) &\equiv \int \frac{\mu_{\mathbf{X}}(d\lambda)}{\lambda - z} = \frac{1}{n} \operatorname{tr} \mathbf{Q}_{\mathbf{X}}(z) = \frac{1}{n} \sum_{i=1}^n \frac{1}{\lambda_i(\mathbf{X}) - z}; \end{aligned}$$

- functionals of these eigenvalues $\frac{1}{n} \sum_{i=1}^n f(\lambda_i(\mathbf{X}))$ through the Cauchy's integral identity

$$\frac{1}{n} \sum_{i=1}^n f(\lambda_i(\mathbf{X})) = -\frac{1}{2\pi i n} \oint_{\Gamma} f(z) \operatorname{tr}(\mathbf{Q}_{\mathbf{X}}(z)) dz$$

for $\Gamma \subset \mathbb{C}$ a positively oriented contour surrounding all the $\lambda_i(\mathbf{X})$'s and $f(z)$ complex analytic in a neighborhood of the inside of Γ ;

- the eigenvectors and subspaces of \mathbf{X} , again through Cauchy's integral relation

$$\mathbf{u}_i(\mathbf{X}) \mathbf{u}_i(\mathbf{X})^T = -\frac{1}{2\pi i} \oint_{\Gamma_{\lambda_i(\mathbf{X})}} \mathbf{Q}_{\mathbf{X}}(z) dz$$

for $(\lambda_i(\mathbf{X}), \mathbf{u}_i(\mathbf{X}))$ an eigenpair of \mathbf{X} and $\Gamma_{\lambda_i(\mathbf{X})}$ a positively oriented contour surrounding only $\lambda_i(\mathbf{X})$.

In addition, the resolvent is a natural object that frequently appears in the solutions to linear regression problems (for machine learning applications, in least-square support vector machines, extreme learning machines, echo-state neural networks, etc.) or to random walk and graph-based semi-supervised learning methods. They will also be shown to appear naturally in not immediately related machine learning problems, such as in large dimensional nonlinear regression (logistic or robust M-regression).

The core of the random matrix approach devised in this monograph consists in determining, for various statistical models of matrices \mathbf{X} a *deterministic equivalent* $\bar{\mathbf{Q}}(z)$ for $\mathbf{Q}(z) = \mathbf{Q}_{\mathbf{X}}(z)$, in the sense that

$$u(\mathbf{Q}(z) - \bar{\mathbf{Q}}(z)) \xrightarrow{a.s.} 0, \quad \text{or} \quad u(\mathbb{E}[\mathbf{Q}(z)] - \bar{\mathbf{Q}}(z)) \rightarrow 0$$

for all 1-Lipschitz linear application $u : \mathbb{R}^n \rightarrow \mathbb{R}$. Of particular interest are the functions $u(\mathbf{Z}) = \frac{1}{n} \operatorname{tr}(\mathbf{A}\mathbf{Z})$ for $\|\mathbf{A}\| \leq 1$, $u(\mathbf{Z}) = \mathbf{a}^T \mathbf{Z} \mathbf{b}$ for $\|\mathbf{a}\|, \|\mathbf{b}\| \leq 1$.

As an example, in the setting of the Marčenko-Pastur law where the random matrix of interest is $\frac{1}{n}\mathbf{XX}^\top$ with \mathbf{X} having i.i.d. zero mean and unit variance entries,

$$\mathbf{Q}(z) = \left(\frac{1}{n}\mathbf{XX}^\top - z\mathbf{I}_p \right)^{-1}$$

admits

$$\bar{\mathbf{Q}}(z) = m_\mu(z)\mathbf{I}_p, \quad m_\mu(z) = \int \frac{\mu(d\lambda)}{\lambda - z}, \quad \mu \text{ defined in (1.2)}$$

as deterministic equivalent. Thus, in particular, $\frac{1}{n} \operatorname{tr} \mathbf{Q}(z) - m_\mu(z) \xrightarrow{a.s.} 0$ and $\mathbf{a}^\top \mathbf{Q}(z) \mathbf{b} - m_\mu(z) \mathbf{a}^\top \mathbf{b} \xrightarrow{a.s.} 0$ for all \mathbf{a}, \mathbf{b} of bounded norm.

In order to determine and investigate these deterministic equivalents, tools from three main mathematical areas are required:

- *linear algebra*, mostly in the exploitation of inverse matrix lemmas, the Schur complement, interlacing and low rank perturbation identities [Horn and Johnson, 2012];
- *complex analysis* (the resolvent $\mathbf{Q}(z)$ is a complex analytic matrix-valued function) and particularly the theory of analytic functions, contour integrals and residue calculus;
- *probability theory*, and particularly notions of convergence, central limit theory, moment methods, etc. [Billingsley, 2012]. More specifically, depending on the underlying random matrix assumptions (independence of entries, Gaussianity, concentration properties), different random matrix-adapted techniques will be discussed: the Gaussian tools developed by Pastur, relying on Stein's lemma and the Nash-Poincaré inequality [Pastur and Shcherbina, 2011], the Bai-Silverstein inductive method [Bai and Silverstein, 2010], the concentration of measure framework developed by Ledoux [Ledoux, 2001] and applied to random matrix endeavors successively by El Karoui, Vershynin, and Louart in [El Karoui, 2009, Vershynin, 2010, Louart and Couillet, 2019], or the double leave-one-out approach devised by El-Karoui in [El Karoui et al., 2013].

In a nutshell, all aforementioned methods are perturbation methods in the sense that they exploit the fact that, by eliminating a row or column (say here both row and column i) of \mathbf{X} to obtain $\mathbf{X}_{-i} \in \mathbb{R}^{(n-1) \times (n-1)}$, the resolvent $\mathbf{Q}_{-i}(z) = (\mathbf{X}_{-i} - z\mathbf{I}_{n-1})^{-1}$ can be related to the original resolvent $\mathbf{Q}(z)$ through both linear algebraic relations and asymptotically comparable statistical behaviors. For instance, in the case of symmetric \mathbf{X} with i.i.d. (properly normalized) entries, it is not difficult to show that $m_{\mathbf{X}}(z) = m_{\mathbf{X}_{-i}}(z) + O(n^{-1})$.

In this regard, Pastur's Gaussian method manages, for models of \mathbf{X} involved Gaussianity, to obtain asymptotic relations of $\mathbb{E}\mathbf{Q}(z)$. Interpolation methods

may then be used to extrapolate the results beyond the Gaussian case. The Bai-Silverstein inductive method is not restricted to matrices of Gaussian entries but is restricted to the specific analysis of either trace forms $\text{tr } \mathbf{AQ}(z)$ or bilinear forms $\mathbf{a}^T \mathbf{Q}(z) \mathbf{b}$ that need be treated individually. The concentration of measure approach is quite versatile: by merely restricting the matrix under study to be constituted of *concentrated random vectors* (so in particular, Lipschitz maps of standard Gaussian random vectors or of vectors with i.i.d. entries), it allows to study $\mathbb{E}\mathbf{Q}(z)$ directly as well.

1.2.2 The double asymptotics: turning the curse of dimensionality to a dimensionality blessing

The major technical difficulty that has long held many machine learning away from tractable analysis and theoretical comprehension relates to the nonlinearity involved in feature extraction (nonlinear kernels, nonlinear activation functions in neural networks), to the implicit nature of some methods (such as for the popular logistic regression), and eventually to the difficulty of a proper (statistical) modeling for arbitrary data (starting with images).

An all-encompassing example of these difficulties could be summarized as the following problem:

Problem. Determine the exact classification performances of logistic regression for n observations of p -dimensional random feature vectors extracted from a set of two-class images (say, images of dogs versus images of cats).

In the conventional wisdom of machine learning research, one cannot conceive to solve this problem: the input data (real images) cannot be easily modelled, the nonlinear features extracted from those data are complex mathematical objects (even in the case where the original data could be modelled as simply as Gaussian vectors), and the logistic regression is an implicit optimization method not easily amenable to mathematical analysis.

We shall demonstrate throughout this monograph that random matrix theory provides a satisfying answer to all these difficulties at once and can actually *solve* the Problem. This is made possible by the powerful joint *universality* and *determinism* effects brought by large dimensional data models and treatments.

Specifically, in the random matrix regime where n, p grow large at a controlled rate, the following key properties arise:

- *fast asymptotic determinism*: the law of large numbers and the central limit theorem tell us that the average of n i.i.d. random variables converges to a deterministic limit at a $O(1/\sqrt{n})$ speed. By gathering independence (or degrees of freedom) both in the sample dimension p and size n , functionals of random matrices (even complex functionals, such as the average of functions of their eigenvalues) also converge to deterministic limits, but at an increased speed of up to $O(1/\sqrt{np})$ which, for $n \sim p$, is $O(1/n)$. In machine learning, performances may be expressed in terms of correct classification rates (i.e., averaged statistics of sometimes involved random

matrix functionals) and can thereby be predicted with high accuracy, even for not too large dimensional datasets;

- *universality*: similarly, again consistently with the law of large numbers and the central limit theorem in the large n alone setting, the above asymptotic deterministic behavior at large n, p is in general independent of the underlying distribution of the random matrix entries. This phenomenon, referred to in the random matrix literature as *universality*, predicts notably that the asymptotic statistics of even complex machine learning procedures only depend on first and second order statistics of the input data;
- *linearization behavior*: the above properties explain that linear statistics are asymptotically predictable. What additionally appears in the large n, p regime is that, due to concentration of even elementary objects (such as distances $\|\mathbf{x}_i - \mathbf{x}_j\|$ previously discussed), the functioning points of many algorithms moves from continuous to discrete and finite. In the kernel random matrix example, only the derivatives of the kernel function f at τ matter. In random neural networks, all the information will be encapsulated in a single deterministic matrix involving the random distribution of the hidden layers and the activation function. In implicit optimization schemes (such as logistic regression), the solution “concentrates” with predictable asymptotics which, despite the initial nonlinear convex optimization problem, only depend on first order statistics;
- *tractable real data modelling*: possibly the most important aspect though relates to the counter-intuitive fact that, as p, n grow large, machine learning algorithms tend to treat real data as if they were mere Gaussian mixture models. This statement, to be discussed thoroughly in the subsequent sections, is both sustained by empirical observations (most theoretical findings tend to fit with performances on real data) and by the theoretical fact that some extremely realistic datasets (in particular artificial images created by generative adversarial networks) are by definition *concentrated random vectors* which are (i) amenable to random matrix analysis, (ii) proved to behave as if mere Gaussian models.

In a word, in large dimensions, data no longer “gather” in groups and do not really “spread” all over their large ambient space neither. But, by accumulation of degrees of freedom, they rather concentrate in a thin lower-dimensional layer. Each scalar observation of the data, even by complicated functions (regressors, classifiers for us), then tends to become deterministic, predictable and simple functions of first order statistics. Random matrix theory exploits these effects and is thus capable to answer seemingly challenging machine learning questions.

1.2.3 Improving machine learning methods

The objective of the monograph is to primarily demonstrate that, under a large dimensional and numerous dataset assumption, many standard machine learn-

ing (low dimensional) intuitions tend to collapse. As a result, many of the algorithms originally designed for small data sizes in turn fail to perform as expected. Some of these algorithms will be shown to remain valid but for unexpected reasons. Some of them will be proved suboptimal, quite largely so sometimes. Finally, some of them will be shown to completely fail to meet their objectives and in need for an adaptation or a change of paradigm.

In a second part, the monograph will further show that the “large dimensional” regime, which one may think synonymous to thousands or millions, in reality appears for much smaller data sizes than the earliest researchers in applied random matrix theory could anticipate. And that a large class of “real data” naturally fall in under the random matrix umbrella.

Our argumentation line and every single treatment of machine learning algorithm analysis and improvement unfolds along the following steps: (i) one first needs to conceive the limitations of low dimensional intuitions and understand the reach of the large dimensional intuitions, (ii) capture the effect of the main mathematical objects at play in machine learning on large data models, (iii) include these objects in a mathematical framework of performance analysis, and (iv) foresee improvement methods based on the newly acquired large dimensional intuitions and mathematical understanding.

1.2.3.1 From low to large dimensional intuitions

Most of the manuscript focuses on large dimensional vector data or graph models. By large dimensional, we will mostly understand vectors $\mathbf{x} \in \mathbb{R}^p$ “built from” numerous ($O(p)$) independent degrees of freedom. That is, as opposed to the compressive sensing paradigm in bigdata, we do not impose the existence of a very low dimensional representation of the data.

From this viewpoint, the simplest mixture data model is the Gaussian mixture model $\mathbf{x} \sim \mathcal{N}(\pm\boldsymbol{\mu}, \mathbf{I}_p)$. As we saw previously, for p small (say, $p = 2$ or $p = 3$), classifying n samples of the mixture is mentally seen from the grouping of two stacks of data, one gathered around $\boldsymbol{\mu} \in \mathbb{R}^p$, the other around $-\boldsymbol{\mu}$. Most of (low dimensional) machine learning algorithms are anchored in this mental image. But the large dimensional image is different. Gaussian vectors $\mathbf{x} \in \mathbb{R}^p$ have a norm of order $\|\mathbf{x}\| \sim \sqrt{p}$ but a spread of order $\|\mathbf{x}\| - \mathbb{E}[\|\mathbf{x}\|] \sim 1$ and non-trivial classification can be performed as long as $\|\boldsymbol{\mu}\|$ is no smaller than 1. The mental image is thus one of two spheres in \mathbb{R}^p with an extremely large radius around which the data of both classes accumulate. Figure 1.5 provides a comparative picture for small versus large dimensions p .

With this image in mind, the Euclidean distance paradigm is shifted. For small p , the information lies in the typical distance from one data point to a “centroid”. For large p , the centroid is far from all points of the class (it lives in an “empty” region of the space) and the class information is summarized in the accumulated small deterministic deviations of all data points from the class; this deviation is not (asymptotically) visible for any entry but can be inferred collectively.

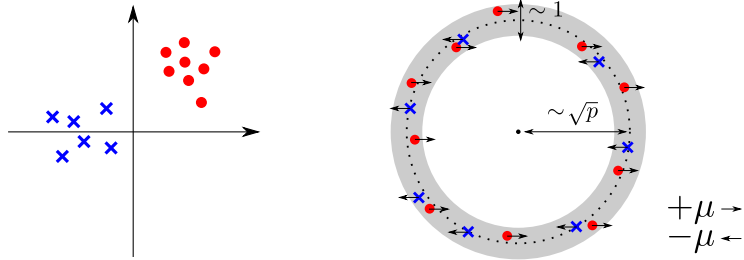


Figure 1.5: Visual representation of classification in (left) small and (right) large dimensions.

fig:p

Consequently, most machine learning algorithms based on evaluations of Euclidean distances $\|\mathbf{x}_i - \mathbf{x}_j\|$, inner products $\mathbf{x}_i^\top \mathbf{x}_j$, nonlinear activations $\sigma(\mathbf{w}^\top \mathbf{x}_i)$ and regressions $f(\boldsymbol{\beta}^\top \mathbf{x}_i)$, etc. of data \mathbf{x}_i or data pairs $\mathbf{x}_i, \mathbf{x}_j$ structurally behave differently in large dimensions.

1.2.3.2 Core random matrices in machine learning algorithms

Be it in a supervised, semi-supervised or unsupervised context, machine learning algorithms essentially consist in extracting structural information from the data by comparing or associating within some available set of data $\mathbf{x}_1, \dots, \mathbf{x}_n \in \mathcal{X}$. At the heart of most algorithms we thus notably find affinity matrices of the type

$$\mathbf{K} \equiv \{\kappa(\mathbf{x}_i, \mathbf{x}_j)\}_{i,j=1}^n \in \mathbb{R}^{n \times n}$$

where $\kappa : \mathcal{X} \times \mathcal{X} \rightarrow \mathbb{R}$ evaluates the closeness or affinity between \mathbf{x}_i and \mathbf{x}_j . For graphs, where the data \mathbf{x}_i are merely the nodes (or vertices) of the graph, $\kappa(\mathbf{x}_i, \mathbf{x}_j) = w_{ij}$ the weight of the edge (i, j) which may be real or binary (i.e., $w_{ij} \in \{0, 1\}$ depending on whether node i attaches to node j).

For $\mathcal{X} = \mathbb{R}^p$ and \mathbf{x}_i statistically distributed, this naturally gives rise to a family of *kernel random matrices*, among which the most popular are for $\kappa(\mathbf{x}, \mathbf{y}) = f(\mathbf{x}^\top \mathbf{y})$ (inner product kernel random matrices), $\kappa(\mathbf{x}, \mathbf{y}) = f(\|\mathbf{x} - \mathbf{y}\|^2)$ (distance-based kernel random matrices) or $\kappa(\mathbf{x}, \mathbf{y}) = \mathbf{x}^\top \mathbf{y} / (\|\mathbf{x}\| \|\mathbf{y}\|)$ (correlation random matrices). In the first case, f is often taken to be either the identity (therefore giving rise to simple sample covariance matrix models) or of a sigmoid-type such as the logistic function $f(t) = (1 + e^{-t})^{-1} - \frac{1}{2}$. In the second case, f is either the identity matrix (and we obtain a Euclidean matrix) or more often $f(t) = \exp(-t/(2\sigma^2))$ for some $\sigma > 0$, which is referred to as a heat kernel, or a Gaussian kernel, or even as a radial basis function kernel.

When the \mathbf{x}_i 's themselves are not directly separable in their ambient space, they are conventionally mapped into a *feature space* in which they become separable. As feature extraction is possibly the single most important but usually hardest task in machine learning, it comes in a variety of forms.

The likely simplest approach is a random extraction by means of *random feature maps* which consist in operating $\sigma(\mathbf{W}\mathbf{x})$ for some (usually randomly and independently drawn) matrix $\mathbf{W} \in \mathbb{R}^{q \times p}$ and some nonlinear function $\sigma : \mathbb{R}^q \rightarrow \mathbb{R}^q$ applying entry-wise, i.e., $\sigma(\mathbf{y}) = [\sigma_0(y_1), \dots, \sigma_0(y_q)]^\top$ for some $\sigma_0 : \mathbb{R} \rightarrow \mathbb{R}$ which, with a slight abuse of notation we simply call σ . Among random feature maps, the most popular is the *random Fourier feature* mapping proposed in [Rahimi and Recht, 2008] and for which $\sigma(t) = \exp(-it)$ (so, formally, $\sigma(\mathbb{R}) \subset \mathbb{C}$ rather than \mathbb{R} in this case).

Neural networks operate likewise. Every size- q layer (i.e., containing q neurons) of a neural network operates $\sigma(\mathbf{W}\mathbf{x})$ for an input \mathbf{x} , a linear mapping \mathbf{W} (the neural weights to be learned) and a nonlinear *activation function* $\sigma : \mathbb{R}^q \rightarrow \mathbb{R}^q$. In this setting, σ is usually taken to be a sigmoid function (the logistic function, the tanh or the Gaussian erf function) or, more recently, the rectifier function $\sigma(t) = \max(0, t)$.

Collecting the data in $\mathbf{X} = [\mathbf{x}_1, \dots, \mathbf{x}_n] \in \mathbb{R}^{p \times n}$ and (again abusively) writing $\sigma(\mathbf{A}) = \{\sigma(\mathbf{A}_{ij})\}_{i,j=1}^n$, the sample covariance matrix of the data then reduces to the following Gram matrix

$$\Phi \equiv \sigma(\mathbf{W}\mathbf{X})^\top \sigma(\mathbf{W}\mathbf{X})$$

which is thus also a central object of interest.

The aforementioned kernels and Gram matrices of feature maps are actually much interrelated. For instance, the random Fourier feature $\sigma(\mathbf{W}\mathbf{x})$, with $\sigma(t) = \exp(-it)$ and \mathbf{W} with i.i.d. standard Gaussian entries, is known to have the fundamental property

$$\mathbb{E}_{\mathbf{W}}[\sigma(\mathbf{W}\mathbf{x})^\top \sigma(\mathbf{W}\mathbf{y})] \equiv \exp\left(-\frac{1}{2}\|\mathbf{x} - \mathbf{y}\|^2\right)$$

so that kernels connect to random feature maps. This property ensures in particular that the kernel function $\kappa(\mathbf{x}, \mathbf{y}) = \exp(-\frac{1}{2}\|\mathbf{x} - \mathbf{y}\|^2)$ is a *nonnegative definite kernel* in the sense that $\mathbf{K} = \{\kappa(\mathbf{x}_i, \mathbf{x}_j)\}_{i,j=1}^n$ is a nonnegative definite matrix, a particularly convenient property in practice. An important subclass of kernel functions, referred to as Mercer kernels, share this nonnegative definite property and have long been privileged in machine learning. We shall see in this monograph that, from a large dimensional perspective, Mercer kernels can be suboptimal and that simple but less intuitive choices of κ can largely outperform these conventional kernels.

A large body of machine learning algorithms (spectral clustering, linear regression, and even logistic regression, support vector machine and neural network learning) one way or another relate to the aforementioned *global properties* (eigenvalues, content of dominant eigenvectors, linear or nonlinear functionals of the resolvent) of the above matrices \mathbf{K} or Φ . A systematic statistical analysis of these global properties for all finite p, n, q is however out of reach, even for the simplest standard Gaussian model of the data \mathbf{x}_i .

In this monograph, we will show that random matrix theory manages to leverage the large dimensional behavior of data to tackle this statistical analysis. We will see in particular that several conventional models for \mathbf{K} can be Taylor-expanded under the form of matrices involving only second order moments. The matrix Φ cannot be Taylor-expanded in this way but will also behave as a kernel random matrix and be decomposed as the sum of elementary random matrices, the statistical properties of which also become tractable in the large dimensional regime.

In short, the intractable matrices \mathbf{K} and Φ will be approximated by tractable ersatz $\tilde{\mathbf{K}}$ and $\tilde{\Phi}$ which behave asymptotically the same in the sense that

$$\|\mathbf{K} - \tilde{\mathbf{K}}\| \xrightarrow{a.s.} 0, \quad \|\Phi - \tilde{\Phi}\| \xrightarrow{a.s.} 0$$

in *operator norm* as $n, p, q \rightarrow \infty$ at a similar rate. These matrices $\tilde{\mathbf{K}}$ and $\tilde{\Phi}$ will allow for further and deeper mathematical analysis.

1.2.3.3 Performance analysis: Spectral properties and functionals

In a classification context, where conventionally $\mathbf{x}_i \in \mathbb{R}^p$ belongs to one of the k classes $\mathcal{C}_1, \dots, \mathcal{C}_k$ with $k \ll n$ (the number of data samples) and thus $k \ll p$ whenever $p \sim n$, the approximation matrices $\tilde{\mathbf{K}}$ and $\tilde{\Phi}$ will often assume a *spiked random matrix* form. That is, for instance,

$$\tilde{\mathbf{K}} = \mathbf{Z} + \mathbf{P}$$

where $\mathbf{Z} \in \mathbb{R}^{n \times n}$ is a random symmetric matrix in general having entries of zero mean and rather uniform variances, while $\mathbf{P} \in \mathbb{R}^{n \times n}$ is a *low rank* (often related to k) matrix comprising the statistical information about the data-class associations and the statistical properties of the classes.

These spiked random matrix models have been extensively studied and it is possible to extract much information about them. In particular, the dominant eigenvectors of $\tilde{\mathbf{K}}$ are known to relate to the dominant eigenvectors of \mathbf{P} (which carry the sought-for information) whenever a *phase transition* threshold is exceeded.

In a regression setting where the \mathbf{x}_i 's may be identically distributed, the regression vector $\beta \in \mathbb{R}^p$ of interest is a certain functional of \mathbf{K} or Φ . For instance, a random feature regression from the observations $\mathbf{X} \in \mathbb{R}^{p \times n}$ to the desired outputs $\mathbf{y} \in \mathbb{R}^n$ entails the regression vector

$$\beta = \sigma(\mathbf{W}\mathbf{X})(\Phi + \alpha\mathbf{I}_n)^{-1}\mathbf{y}$$

which is thus an (indirect) function of the resolvent $\mathbf{Q}_\Phi(-\alpha) = (\Phi + \alpha\mathbf{I}_n)^{-1}$ of Φ for a certain $\alpha > 0$. Random matrix theory possesses tools to analyze the statistical properties of such vectors β as well.

Least-square support vector machine machine and most conventional algorithms of graph-based semi-supervised learning relate to functionals of the same

type. But this also holds true (yet less directly) for nonlinear (e.g., logistic) regression where β is *implicitly defined* as a function of \mathbf{Q}_Φ . Similarly, in their plain form, support vector machines can be seen as nonlinear regression schemes which also fall within this scope.

Since eigenvalues, eigenvectors and regressor statistics are at the core of the algorithm performances, once these central quantities are accessible, the actual (asymptotic) classification error rates, mean square error of regression, etc. become also accessible. It is important to point out here that not only bounds on performances but *actual accurate estimators* of the performances are accessible. Under a random matrix framework, a precise characterization of the anticipated performance (as well as its error margins) for the above algorithms becomes available.

Since these performance indicators depend on the various hyperparameters of the problem, themselves being quantifiable from data statistics, in many scenarios, it becomes possible to fine-tune the algorithms without resorting to cross-validation procedures. We shall notably see how some simple instance of neural networks can be fairly well understood: why the rectifier $\max(t, 0)$ is a convenient choice, how the activation function and the data statistics mix up, etc. We will also understand that kernel methods do not function as one may think it should do and that there exists an elegant interplay between data statistics and the successive derivatives of the kernel function at a precise position.

1.2.3.4 Directions of improvement and new ideas

Due to the complete change in paradigm when comparing data from a small versus large dimensional perspective, the overall behavior and the ensuing performances of the studied algorithms are tainted.

We shall notably see in the course of the manuscript that the conventional heat kernel used in various classification contexts is largely suboptimal. We shall also see that most graph-inspired semi-supervised learning algorithms of the literature fail to properly accomplish their requested task as n, p grow large together. Yet, we will show that the so-called PageRank approach happens not to fail, although the fundamental reasons behind its non-degrading performances are at odds with the initial inspiration for the method. Most importantly, this popular approach will also be shown to perform quite far from expected and in particular not to be capable of benefiting from the large addition of unlabeled data. This observation entails the very unpleasant property that purely unsupervised methods tend to outperform semi-supervised ones when the number of unlabeled data is quite large.

For all these applications, the monograph will list a set of recommendations and improved methods which are tailored to large (as well as not so large) data learning. Optimal but quite counter-intuitive kernel functions will be introduced, new regularization procedures for supervised and semi-supervised learning will be discussed that defeat the curse of dimensionality in semi-supervised learning (that is by fully exploiting the addition of unlabeled data), and some further lights into neural network performances will be cast.

1.2.4 Exploiting universality: from large dimensional statistics to practical data

sec:universality

Before delving into the core of the manuscript, we conclude this section by further elaborating on the universality phenomenon briefly discussed above, which carries a much deeper importance than one may anticipate.

First, let us recall that most random matrix results derived in the literature, even the most recent on machine learning applications (discussed in this monograph), are based on the assumption of data arising either from Gaussian (possibly mixture) distributions or represented by vectors with independent entries. These vector distributions are naturally deemed unrealistic models for realistic data and we will not claim otherwise. It is a fact that real data, such as images, are largely more complex than mere Gaussian vectors.

Yet, what we do claim is that *scalar observations* (regression or classifier outputs, misclassification rates, etc.) obtained from large data or large datasets *tend to behave as if the data were Gaussian* (mixtures) in the first place. This is a fundamental rupture that random matrix theory structurally exploits: rather than assuming data as fixed entities living in a complex manifold, random matrix theory mostly exploits their numerous degrees of freedom which, by universality, induce deterministic behavior in the large dimensional limit.

We justify this claim below with two strong arguments: one empirical and one theoretical.

1.2.4.1 Theory versus practice

Our first argument follows after numerous comparative experiments made between theoretical findings on Gaussian datasets versus real datasets. Indeed, although mostly derived under simple and seemingly unrealistic Gaussian mixture models, many theoretical results mentioned above show an *unexpected close match* when applied to popular real-world large dimensional datasets, such as the MNIST handwritten-digit dataset [LeCun et al., 1998], the related Fashion-MNIST data [Xiao et al., 2017], the German Traffic Sign dataset [Houben et al., 2013], as well as numerous financial and electro-encephalography (EEG) time series data.

To be more precise, the following systematic comparison approach will be pursued in this monograph. An *asymptotically non-trivial* classification or regression problem is studied: that is, we assume that the problem at hand is neither too easy nor too hard to solve and leads, in general, to, say, classification error rates of the order of 5% – 30% and of absolute regression errors also of the order 5% – 30%. In particular, we insist that the random matrix framework under study is in general incapable to thinly grasp error rates below the 1 – 2% region, which is the domain of “outliers” and marginal data.

Having made this non-trivial assumption, we shall generically model our data as a simple mixture model. The simplest random matrix model under this constraint is a Gaussian mixture model which gives access to a large panoply

of powerful technical tools. The theoretical results obtained from our analyses (asymptotic performances notably) are thus function of the statistical means, covariances of the mixture distribution. To compare our theoretical results to real data, we in general conduct the following procedure:

1. exploiting the numerous (often labeled) samples of the real datasets (such as the $\sim 60\,000$ images of the training MNIST database), we empirically compute statistical means and covariances for each class of the database;
2. we then evaluate the asymptotic performance that a genuine Gaussian mixture model having *these means and covariances* would have;
3. we compare these “theoretical” values to actual simulations.

As the monograph will demonstrate in most scenarios, this procedure systematically leads to the conclusion that *performances obtained on mere Gaussian mixtures* approximate surprisingly well the performance observed on the real data.

As already mentioned in Remark 1.3, this surprising accordance between theory and practice is possibly due to the *universality* of random matrix theory results, i.e., only the first several statistical moments of the problem at hand matter in the large random matrix regime (recall for instance that the limiting eigenvalue distribution of $\mathbf{Z}\mathbf{Z}^\top$ for \mathbf{Z} having i.i.d. zero mean and unit variance entries is the *same* Marčenko-Pastur law, irrespective of the other moments of \mathbf{Z}).

Yet, a stronger argument can be made, especially when it comes to machine learning for image processing.

1.2.4.2 Concentrated random vectors and real data modelling

The modelling assumption that data \mathbf{x}_i are linear or affine maps $\mathbf{x}_i = \mathbf{A}\mathbf{z}_i + \mathbf{b}$ of vectors \mathbf{z}_i constituted of i.i.d. entries is simultaneously an asset for random matrix analysis (the exploited degrees of freedom are those of \mathbf{z}_i) but a severe practical limitation as few real datasets are likely of this simplistic form.

In [El Karoui, 2009], El Karoui provided a first means for random matrix theory to go beyond the “vector of independent entries” assumption.² There, relying on concentration of measure theory, extensively developed by Ledoux in [Ledoux, 2001], El Karoui essentially shows (in a rather technical manner) that some of the early random matrix results from Pastur, Bai, and Silverstein, remain valid under the assumption that the \mathbf{x}_i ’s are *concentrated random vectors*. Roughly speaking, a random vector $\mathbf{x} \in \mathbb{R}^p$ is *concentrated* if, for a certain family of functions $f : \mathbb{R}^p \rightarrow \mathbb{R}$, there exists a deterministic scalar $M_f \in \mathbb{R}$ such that

$$\mathbb{P}(|f(\mathbf{x}) - M_f| > t) \leq \alpha(t) \quad \text{eq:concentration (1.9)}$$

²See also [Pajor and Pastur, 2009] published the same year under slightly more constrained assumptions.

for some decreasing function $\alpha : \mathbb{R} \rightarrow \mathbb{R}$; in general, $\alpha(t)$ will be of the form $\alpha(t) = Ce^{-ct^q}$ for some $q > 0$ and $C, c > 0$ constant (which may depend on p though). Intuitively, a concentrated random vector is a (random) point in high dimensional space having “predictable observations” $f(\mathbf{x})$, in the sense that, with (exponentially) high probability, $f(\mathbf{x})$ takes values very close to the deterministic M_f . Thus, in the “observable world”, the observation $f(\mathbf{x})$ (which may typically be any performance metric of a machine learning algorithm on test data \mathbf{x}) appears to be “stable” for any concentrated vector \mathbf{x} .

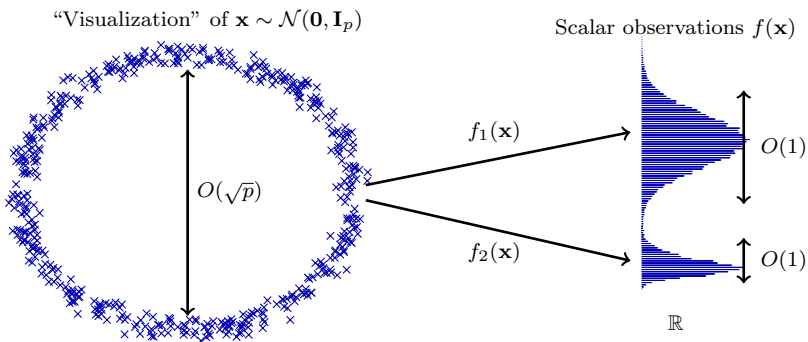


Figure 1.6: Multivariate Gaussian distribution $\mathbf{x} \sim \mathcal{N}(\mathbf{0}, \mathbf{I}_p)$, a fundamental example of concentrated random vectors. (**Left**) A visual “interpretation” of 500 independent drawings of $\mathbf{x} \sim \mathcal{N}(\mathbf{0}, \mathbf{I}_p)$. (**Right**) Concentration of the observables for linear ($f_1(\mathbf{x}) = \mathbf{x}^\top \mathbf{1}_p / \sqrt{p}$) and Lipschitz ($f_2(\mathbf{x}) = \|\mathbf{x}\|_\infty$) maps.

Ledoux and El Karoui mostly focus on concentrated random vectors defined on Lipschitz classes of functions f , i.e., \mathbf{x} is *Lipschitz-concentrated* if (1.9) holds for all f such that $|f(\mathbf{x}) - f(\mathbf{y})| \leq \|\mathbf{x} - \mathbf{y}\|$ for all $\mathbf{x}, \mathbf{y} \in \mathbb{R}^p$. These stringent constraints however make it very hard to find *any* random vectors belonging to this class. As a matter of fact, in this class, the only standard random vectors are the Gaussian random vector $\mathbf{x} \sim \mathcal{N}(\mathbf{0}, \mathbf{I}_p)$ and the uniform vector on the sphere $\mathbf{u} = \frac{\mathbf{x}}{\|\mathbf{x}\|} \sim \mathbb{S}^{p-1}$ for $\mathbf{x} \sim \mathcal{N}(\mathbf{0}, \mathbf{I}_p)$. However, quite importantly, *every* $\mathbb{R}^p \rightarrow \mathbb{R}^q$ Lipschitz-mapping $g(\mathbf{x})$ and $g(\mathbf{u})$ of these two random vectors, by definition, also belongs to the class.

A visual representation of the notion of concentration is presented in Figure 1.6.

Yet, since the widest class of (Lipschitz) concentrated random vectors is apparently restricted to Lipschitz maps of standard Gaussian vectors, at first sight, concentrated random vectors are seemingly no more elaborate models

than linear and affine maps of Gaussian vectors. As a consequence, there is a priori no reason to assume that mixtures of concentrated random vectors model real datasets any better than Gaussian mixtures.

It turns out that this intuition is again tainted by finite dimensional insights. Indeed, there *practically exist extremely data-realistic concentrated random vectors*: the outputs of generative adversarial networks (GANs) [Goodfellow et al., 2014, Brock et al., 2018] as shown in Figure 1.7. GANs generate artificial images $g(\mathbf{x})$ from large dimensional standard Gaussian vectors \mathbf{x} where g is a conventional feedforward neural network trained to mimic real data. As such, g is the combination of Lipschitz nonlinear (the neural activations) and linear (the inter-layer connexions) maps, and is thus a Lipschitz mapping. The output image vectors $g(\mathbf{x})$, see examples in Figure 1.8, are thus also concentrated vectors. Modern GANs are so sophisticated that it has become virtually impossible for human beings to tell whether their outputs are genuine or artificial. This, as a result, strongly suggests that concentrated random vectors are accurate models of real-world data.

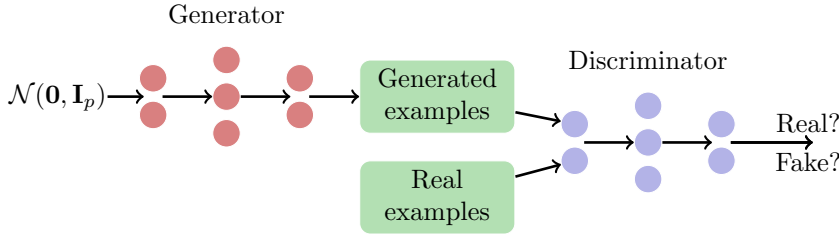


Figure 1.7: Illustration of a generative adversarial network (GAN)
fig:GAN



Figure 1.8: Images samples generated by BigGAN in [Brock et al., 2018]
fig:biggan

A strong emphasis has thus lately been given to these models. The monograph will in particular elaborate on the work of Louart [Louart and Couillet, 2019] which largely generalizes the seminal findings of El Karoui by providing a systematic methodological toolbox of *concentration theory for random matrices*. There, the notion of concentration is generalized by including *linear concentration*, which conveys a consistent framework for the important notion of deterministic equivalents in random matrix theory, and by providing a wide range of properties and lemmas of immediate use for random matrix purposes.

An important finding of [Louart and Couillet, 2019] is that *first order statistics* of functionals of random matrices built from concentrated random vectors, so in particular the asymptotic performances of many machine learning methods, are also universal. Specifically, for most conventional machine learning methods (support vector machines, semi-supervised learning, spectral clustering, random feature maps, linear regression, etc.), the asymptotic performances achieved on Gaussian mixtures $\mathcal{N}(\boldsymbol{\mu}_a, \mathbf{C}_a)$, $a = 1, \dots, k$, coincide with those obtained on concentrated random vectors mixtures $\mathcal{L}_a(\boldsymbol{\mu}_a, \mathbf{C}_a)$, $a = 1, \dots, k$, having the same means $\boldsymbol{\mu}_a$ and covariances \mathbf{C}_a per class.

This strongly suggests that Gaussian mixture models, if not appropriate data “models” per se, are largely sufficient statistical assumptions for the theoretical understanding of real data machine learning.

Remark 1.4 (Concentration of measure, concentration inequalities, and non-asymptotic random matrices). *It is important to raise here that the concentration of measure theory is structurally broader than the scope of the popular concentration inequalities regularly used in statistical learning. Concentration inequalities are merely expressions of (1.9) for specific choices of f and their consequences. Concentration inequalities are in particular not new to random matrix theory. In [Vershynin, 2010, Tao, 2012], Vershynin and Tao exploit the mathematical strength of concentration inequalities (which, thanks to the exponential decay, is stronger and less cumbersome to handle than moment bounds) to prove fundamental results in random matrix theory. Yet, these inequalities are mostly exploited in proofs involving Gaussian random vectors (as an instance of concentrated random vector). Vershynin even defines the notion of a non-asymptotic random matrix theory that exploits concentration inequalities to bound various quantities of theoretical interest (in particular bounds on eigenvalue positions). The monograph instead puts forth the interest of concentration of measure theory for data modeling and not simply as a convenient mathematical tool.*

Concentration of measure theory is also all the more suited to machine learning since it structurally relates to linear, Lipschitz, or convex-Lipschitz functionals of random vectors and matrices. These are precisely the core elements of machine learning algorithms (kernels, activation functions, convex optimization schemes). From this viewpoint, concentration of measure theory is much more adapted to machine learning analysis than simpler data models. Note for instance that concentrated random vectors are stable (i.e., they remain concentrated) when passed through the layers of a neural network; this is not true of Gaussian random vectors or vectors with independent entries which in general no longer have independent entries when passed through non linear layers.

A last convenient aspect of concentration of measure theory is that it flexibly allows one to “decouple” the behavior of the data size p and number n in the large dimensional setting. It is technically much easier to keep track of *independent growth rates* for p and n under a concentration of measure framework than when exploiting more standard random matrix techniques (such as Gaussian tools).

1.3 Outline and online toolbox

1.3.1 Organization of the manuscript

sec:organization

The remainder of the manuscript is essentially divided in two parts.

Chapter 2 introduces the basics of random matrix theory *needed for this manuscript*. In doing so, we shall first revisit the traditional approach found in maths-oriented sources, such as [Bai and Silverstein, 2010] based on a Stieltjes transform and truncation machinery, [Pastur and Shcherbina, 2011] based on a Gaussian-method approach, [Tao, 2012, Vershynin, 2010] based on concentration inequalities and a non-asymptotic random matrix approach, and also say a few words on [Mingo and Speicher, 2017] which follows a free probability framework or on [Anderson et al., 2010] which is more oriented towards a determinantal point process and large deviations direction. Unlike most of these references though (at the possible exception of [Pastur and Shcherbina, 2011]), our methodology is primarily centered on the statistical analysis of the *resolvent* (and only secondarily on the Stieltjes transform) of random matrices, which is the core object of interest to us in most machine learning applications. The particular mathematical toolbox exploited to derive the results is of secondary importance.

In this chapter, we will successively introduce:

- the fundamental notion of the *resolvent* $\mathbf{Q}(z) = (\mathbf{X} - z\mathbf{I}_n)^{-1}$ of a (random) matrix \mathbf{X} and its relations to the eigenvalues of \mathbf{X} , the limiting spectrum of \mathbf{X} , the eigenvectors and eigenspaces associated to some of these eigenvalues, as well as its relations to bilinear and quadratic forms often met in applications (linear or kernel regression, linear and quadratic discriminant analysis, support vector machines, and even the performance of some neural networks);
- the almost equally important notion of *deterministic equivalents* which extend the notion of “limiting behavior” of large dimensional random matrices, when such limits may not exist (which is the case of most structured random matrix models); *deterministic equivalents for the resolvent* of random matrix models are at the core of almost all results derived in this monograph;
- the foundational Marčenko-Pastur and Wigner semi-circle laws which, as we shall see, serve as a reference “null model” to all random matrix models met in the random matrix applied to machine learning literature; even quite sophisticated random matrix transformations (through nonlinear kernels, discontinuous activation functions, etc.) will be seen to boils down, one way or another, to either one (or a mixture of both) of these reference laws;
- a successive presentation of the three main technical tools at our disposal (in this monograph at least) to study random matrix models: the Bai-

Silverstein-Stieltjes transform approach, the Pastur-Scherbina Gaussian tools, and the Louart-Couillet concentration of measure approach;

- the natural extensions of the Marčenko-Pastur- and Wigner-like random matrix models to more structured models: with correlation in either feature or samples, with nonzero mean, divided into sub-classes of correlated nonzero mean models, with a variance profile (in the case of heterogeneous graph matrix models), etc.;
- a refined analysis of the large dimensional spectrum of random matrices using tools arising purely from complex analysis, based on which statistical inference techniques on covariance matrix models are introduced;
- a thorough treatment of the so-called *spiked models* of random matrices which carry a significant importance in the applications to machine learning: spiked models consist in *low rank deviations* from some elementary or structured random matrix models; this “rank sparsity” property simplifies the analyses and appropriately models the presence of classes, communities, principal components, etc., in machine learning data models;
- a short exposition of alternative tools and techniques, not of central focus in this monograph, but which have various advantages in specific random matrix structures;
- a short presentation to the very recent concentration of measure theory for random matrices which extends most of the results presented in this chapter to much more realistic generative models of data for machine learning applications.

This lengthy chapter provides a vast majority of the necessary tools to recover the results and conduct the analyses performed in the subsequent chapters on applications to machine learning. This second part is organized as follows:

- Chapter 3 introduces first applications of the random matrix framework devised in Chapter 2 to detection, estimation and statistical inference; particular emphasis is made on likelihood ratio tests for the detection of presence of information in noise, on linear and quadratic discriminant analysis in a binary hypothesis test, on the estimation of distances between data statistics (particularly here the estimation of distances between unknown covariance matrices and divergences between Gaussian measures of unknown statistics), as well as on the performance of robust estimators of covariance (or scatter) matrices. The estimators of distance between covariance matrices is typical of a classical problem for which classical “large n alone” statistical answers dramatically fail, even when the ratio n/p is quite large, and random matrix methods provide consistent estimators. As for the robust M-estimator analysis, it is typical of a scenario where classical statistics fail to perform any satisfying analysis, while random matrix methods exploit concentration phenomena to fully understand and improve their behavior.

- Chapter 4 follows with a fundamental exposition of kernel random matrices and their applications to kernel methods, neural networks, and beyond in machine learning. This chapter successively exposes the many consequences for these methods of the already several-times discussed *concentration of distances* phenomenon and shows that, as a result, the behavior, performances, and the role of the kernel parameters (kernel function, hyperparameters) become tractable and amenable to improvement. Specific applications to kernel spectral clustering, graph-based semi-supervised learning, and kernel ridge-regression (also referred to as least-squares SVM). All these methods will be shown to be theoretically tractable, easy to optimize and thus improve, with simulations on real data comforting the theoretical findings. The specific example of semi-supervised learning (SSL) is quite telling of the limitations of standard finite-dimensional intuitions as it will be shown that all known classical graph-based SSL methods either dramatically fail or at best do not exhibit the expected SSL behavior (notably failing to account for large numbers of unlabeled data): the random matrix approach proposed in this section is quite simple, it directly points at the above problems and easily solves them.
- Chapter 5 focuses specifically on neural network applications. While modern deep neural networks remain difficult to handle, several studies are reported in this chapter which address simpler models of neural networks (with random and few layers, with a possibly recurrent structure) and for which, again, new insights and exact asymptotic performance behaviors are clarified. An additional discussion of the learning dynamics of gradient descent methods is also exposed in which the step-by-step performances and the importance of early stopping mechanisms are theoretically analyzed.
- Chapter 6 goes a step beyond all previous chapters for which all metrics of interest (algorithm behavior, performances) are all *explicit functions* of the various random matrix models introduced in Chapter 2 (under the form of eigenvalue distribution, eigenvector statistics, bilinear forms on the resolvent, etc.): here we focus on optimization schemes in machine learning having no explicit solution. As such, the performances of these algorithms are *implicitly* related to the random data matrix and look at first sight not related to random matrix theory. The chapter shows instead that most of these problems do exhibit asymptotic (n, p) performances which can be expressed as an explicit function of random matrix models, thereby opening the door to a large random of applications (logistic regression, support vector machines with soft and hard thresholding, empirical risk minimization, etc.).
- Chapter 7 discusses the question of spectral methods for community detection on (mostly dense) graphs and networks. As opposed to all previous application-related chapters for which the elementary random matrix

model under study is the Gram matrix $\mathbf{X}\mathbf{X}^\top$ for data $\mathbf{X} \in \mathbb{R}^{p \times n}$, the question of community detection on graphs naturally relates to symmetric graph models $\mathbf{X} \in \mathbb{R}^{n \times n}$ with independent Bernoulli entries. The chapter discusses at length the so-called stochastic block model (SBM) and degree-corrected SBM which mimic, with a different degree of reality, the behavior of genuine graphs with communities. A short discussion on the (difficult and so far not random matrix-related) modern concern of community detection on the even more realistic case of large dimensional and *sparse* graphs is also reported.

- Chapter 8 closes the application-related chapters by a discussion on the extension of the aforementioned applications to real data. There, using the recent concentration of measure for random matrix framework, simulations of extremely realistic models of data (images mostly) are used to theoretically validate the random matrix results devised in the above chapters. The chapter notably passes across the fundamental but surprising message according to which simple data models are often sufficiently rich to account for the performance of most existing machine learning algorithms.

1.3.2 Online codes

Matlab codes of the algorithms used to obtain most of the visual results (graphs, histograms) provided in the monograph are publicly available at <https://github.com/Zhenyu-LIAO/RMT4ML>. Links to these codes are directly provided in the caption of the corresponding figures.

Chapter 2

Basics of Random Matrix Theory

chap:basis-of-RMT

Random matrix theory, at its inception, primarily dealt with the eigenvalue distribution (also referred to as spectral measure) of large dimensional random matrices. One of the key technical tools to study these measures is the Stieltjes transform, often presented as the central object of the theory [Bai and Silverstein, 2010].

But signal processing and machine learning alike are more fundamentally interested in subspaces and eigenvectors (which often carry the structural data information) than in eigenvalues. Subspace or spectral methods, such as principal component analysis (PCA) [Wold et al., 1987], spectral clustering [Ng et al., 2002] and some semi-supervised learning techniques [Zhu, 2005] are built directly upon the eigenspace spanned by the several top eigenvectors.

Consequently, beyond the Stieltjes transform, a more general mathematical object, the *resolvent* of large random matrices will constitute the cornerstone of the whole monograph. The resolvent of a matrix gives access to its spectral measure, to the location of its isolated eigenvalues, to the statistical behavior of their associated eigenvectors when random, and consequently provides an entry-door to the performance analysis of numerous learning methods.

2.1 Fundamental objects

2.1.1 The resolvent

We first introduce the resolvent of a matrix.

def:resolvent
Definition 1 (Resolvent). *For a symmetric matrix $\mathbf{M} \in \mathbb{R}^{n \times n}$, the resolvent $\mathbf{Q}_{\mathbf{M}}(z)$ of \mathbf{M} is defined, for $z \in \mathbb{C}$ not eigenvalue of \mathbf{M} , as*

$$\mathbf{Q}_{\mathbf{M}}(z) \equiv (\mathbf{M} - z\mathbf{I}_n)^{-1} \quad \text{eq: def-resolvent (2.1)}$$

which is also denoted \mathbf{Q} when there is no ambiguity.

The resolvent operator is in fact a very classical tool, the use of which goes far beyond random matrix theory. It is for instance exploited in the analysis of linear operators in general Hilbert spaces [Akhiezer and Glazman, 2013, Chapter 4] as well as in monotone operator theory of importance to modern convex optimization theory [Bauschke and Combettes, 2011, Chapter 23].

2.1.2 Spectral measure and Stieltjes transform

The first use of the resolvent \mathbf{Q}_M is in its relation to the *empirical spectral measure* μ_M of matrix M , through *Stieltjes transform* m_{μ_M} , which we all define next.

def:esd-and-lsd

Definition 2 (Empirical spectral measure). *For a symmetric matrix $M \in \mathbb{R}^{n \times n}$, the spectral measure or empirical spectral measure or empirical spectral distribution (e.s.d.) μ_M of M is defined as the normalized counting measure of the eigenvalues $\lambda_1(M), \dots, \lambda_n(M)$ of M ,*

$$\mu_M \equiv \frac{1}{n} \sum_{i=1}^n \delta_{\lambda_i(M)}. \quad (2.2)$$

Since $\int_{\mathbb{R}} \mu_M(dx) = 1$, the spectral measure μ_M of a matrix $M \in \mathbb{R}^{n \times n}$ (random or not) is a probability measure. For (probability) measures, we can define their associated Stieltjes transforms as follows.

def:ST

Definition 3 (Stieltjes transform). *For a real probability measure μ with support $\text{supp}(\mu)$, the Stieltjes transform $m_\mu(z)$ is defined, for all $z \in \mathbb{C} \setminus \text{supp}(\mu)$, as*

$$m_\mu(z) \equiv \int \frac{1}{t - z} \mu(dt). \quad (2.3)$$

This definition and the Stieltjes transform framework in reality extends beyond probability measures to σ -finite real measures (i.e., measures μ such that $\mu(\mathbb{R}) < \infty$), which will occasionally be discussed in this monograph.

The Stieltjes transform m_μ has numerous interesting properties: it is complex analytic on its domain of definition $\mathbb{C} \setminus \text{supp}(\mu)$, it is bounded $|m_\mu(z)| \leq 1/\text{dist}(z, \text{supp}(\mu))$, it satisfies $\Im[z] > 0 \Rightarrow \Im[m(z)] > 0$, and it is an increasing function on all connected components of its restriction to $\mathbb{R} \setminus \text{supp}(\mu)$ (since $m'_\mu(x) = \int (t - x)^{-2} dt > 0$) with $\lim_{x \rightarrow \pm\infty} m_\mu(x) = 0$ if $\text{supp}(\mu)$ is bounded.

As a transform, m_μ admits an inverse formula to recover μ , as per the following result.

theo:inverse-ST

Theorem 2.1 (Inverse Stieltjes transform). *For a, b continuity points of the probability measure μ , we have*

$$\mu([a, b]) = \frac{1}{\pi} \lim_{y \downarrow 0} \int_a^b \Im[m_\mu(x + iy)] dx. \quad (2.4)$$

Besides, if μ admits a density f at x (i.e., $\mu(x)$ is differentiable in a neighborhood of x and $\lim_{\epsilon \rightarrow 0} (2\epsilon)^{-1} \mu([x - \epsilon, x + \epsilon]) = f(x)$),

$$f(x) = \frac{1}{\pi} \lim_{y \downarrow 0} \Im[m_\mu(x + iy)]. \quad (2.5)$$

Also, if μ has an isolated mass at x , then

$$\mu(\{x\}) = \lim_{y \downarrow 0} \imath y m_\mu(x + iy). \quad (2.6)$$

Proof. Since $|\frac{y}{(t-x)^2+y^2}| \leq \frac{1}{y}$ for $y > 0$, by Fubini's theorem,

$$\begin{aligned} \frac{1}{\pi} \int_a^b \Im[m_\mu(x + iy)] dx &= \frac{1}{\pi} \int_a^b \left[\int \frac{y}{(t-x)^2+y^2} \mu(dt) \right] dx \\ &= \frac{1}{\pi} \int \left[\int_a^b \frac{y}{(t-x)^2+y^2} dx \right] \mu(dt) \\ &= \frac{1}{\pi} \int \left[\arctan\left(\frac{b-t}{y}\right) - \arctan\left(\frac{a-t}{y}\right) \right] \mu(dt). \end{aligned}$$

As $y \downarrow 0$, the difference in brackets converges either to $\pm\pi$ or 0 depending on the relative position of a, b, t . By the dominated convergence theorem, limits and integrals can be exchanged, and the limit, as $y \downarrow 0$, is $\int 1_{[a,b]} \mu(dt) = \mu([a,b])$. When μ has an isolated mass at x , say $\mu(dt) = a\delta_x(t)$, we similarly have, again by dominated convergence (using in particular $|y(t-x)| \leq \frac{1}{2}(y^2 + (t-x)^2)$),

$$\lim_{y \downarrow 0} \imath y m(x + iy) = \lim_{y \downarrow 0} \int \frac{\imath y(t-x) \mu(dt)}{(t-x)^2+y^2} + \lim_{y \downarrow 0} \int \frac{y^2 \mu(dt)}{(t-x)^2+y^2} = a.$$

□

The important relation between the empirical spectral measure of $\mathbf{M} \in \mathbb{R}^{n \times n}$, the Stieltjes transform $m_{\mu_{\mathbf{M}}}(z)$ and the resolvent $\mathbf{Q}_{\mathbf{M}}$ lies in the fact that

$$m_{\mu_{\mathbf{M}}}(z) = \frac{1}{n} \sum_{i=1}^n \int \frac{\delta_{\lambda_i(\mathbf{M})}(t)}{t-z} = \frac{1}{n} \sum_{i=1}^n \frac{1}{\lambda_i(\mathbf{M}) - z} = \frac{1}{n} \text{tr}(\mathbf{Q}_{\mathbf{M}}). \quad \text{eq:m_trQ} \quad (2.7)$$

Combining inverse Stieltjes transform and the relation above thus provides a link between $\mathbf{Q}_{\mathbf{M}}$ and the eigenvalue distribution of \mathbf{M} . While seemingly contorted, this link is in general the only efficient way to study the spectral measure of *large dimensional random matrices* \mathbf{M} .

In particular, note that Theorem 2.1 raises an interesting fact: the Stieltjes transform $m_\mu(z) = \int (t-z)^{-1} \mu(dt)$ is defined on all $\mathbb{C} \setminus \text{supp}(\mu)$. As z approaches $\text{supp}(\mu)$, the integrand $(t-z)^{-1}$ becomes singular: yet, this is precisely when $x = \Re[z] \in \text{supp}(\mu)$ while $\Im[z] \downarrow 0$ that one can retrieve the density of μ at x from $m_\mu(z)$. This observation is key to the analysis of the spectrum (both eigenvalues and eigenvectors) of (random) matrices: the singular points of the resolvent of a (random) matrix hold the information about its spectrum.

rem:resolvent_as_ST

Remark 2.1 (Resolvent as a matrix-valued Stieltjes transform). As proposed in [Hachem et al., 2007], it can be convenient to extrapolate Definition 3 of Stieltjes transforms to $n \times n$ matrix-valued positive measures $\mathbf{M}(dt)$,¹ in which case Equation (2.7) can be generalized as

$$\mathbf{Q}_{\mathbf{M}}(z) = \int \frac{\mathbf{M}(dt)}{t - z} = \mathbf{U} \operatorname{diag} \left\{ \frac{1}{\lambda_i(\mathbf{M}) - z} \right\}_{i=1}^n \mathbf{U}^T$$

where we used the spectral decomposition $\mathbf{M} = \mathbf{U} \operatorname{diag}\{\lambda_i(\mathbf{M})\}_{i=1}^n \mathbf{U}^T$. In particular, $\mathbf{Q}_{\mathbf{M}}(z)$ enjoys similar properties as Stieltjes transforms of real-valued measures: $\|\mathbf{Q}_{\mathbf{M}}(z)\| \leq \operatorname{dist}(z, \operatorname{supp}(\mu_{\mathbf{M}}))^{-1}$, and $x \mapsto \mathbf{Q}_{\mathbf{M}}(x)$ for $x \in \mathbb{R} \setminus \operatorname{supp}(\mu_{\mathbf{M}})$ is an increasing matrix-valued function with respect to symmetric matrix partial ordering (i.e., $\mathbf{A} \succeq \mathbf{B}$ whenever $\mathbf{z}^T(\mathbf{A} - \mathbf{B})\mathbf{z} \geq 0$ for all \mathbf{z}).

2.1.3 Cauchy's integral, linear eigenvalue functionals, and eigenspaces

subsec:cauchy-integral

Being complex analytic, the resolvent $\mathbf{Q}_{\mathbf{M}}$ can be manipulated using advanced tools from complex analysis. Of particular interest to this monograph is the relation between the resolvent and Cauchy's integral theorem.

theo:cauchy-integral

Theorem 2.2 (Cauchy's integral formula). For $\Gamma \subset \mathbb{C}$ a positively (i.e., counterclockwise) oriented simple closed curve and a complex function $f(z)$ analytic in a region containing Γ and its interior, then

- (i) if $z_0 \in \mathbb{C}$ is enclosed by Γ , $f(z_0) = -\frac{1}{2\pi i} \oint_{\Gamma} \frac{f(z)}{z - z_0} dz$;
- (ii) if not, $\frac{1}{2\pi i} \oint_{\Gamma} \frac{f(z)}{z - z_0} dz = 0$.

This result provides an immediate link between the *linear functionals of the eigenvalues of \mathbf{M}* and the Stieltjes transform through

$$\frac{1}{n} \sum_{i=1}^n f(\lambda_i(\mathbf{M})) = -\frac{1}{2\pi i n} \oint_{\Gamma} f(z) \operatorname{tr}(\mathbf{Q}_{\mathbf{M}}(z)) dz = -\frac{1}{2\pi i} \oint_{\Gamma} f(z) m_{\mu_{\mathbf{M}}}(z) dz$$

for all f complex analytic in a compact neighborhood of $\operatorname{supp}(\mu_{\mathbf{M}})$, by choosing the contour Γ to enclose $\operatorname{supp}(\mu_{\mathbf{M}})$ (i.e., all the $\lambda_i(\mathbf{M})$'s). More generally,

$$\frac{1}{n} \sum_{\lambda_i(\mathbf{M}) \in \Gamma^\circ} f(\lambda_i(\mathbf{M})) = -\frac{1}{2\pi i} \oint_{\Gamma} f(z) m_{\mu_{\mathbf{M}}}(z) dz$$

for Γ° the interior of contour Γ .

¹Defined by the fact that $\mu(dt; \mathbf{z}) = \mathbf{z}^T \mathbf{M}(dt) \mathbf{z} = \sum_{ij} z_i z_j \mathbf{M}_{ij}(dt)$ is a positive real-valued measure for all \mathbf{z} . See [Rozanov, 1967] for an introduction.

Another quantity of interest relates to eigenvectors and eigenspaces. Decomposing the symmetric matrix $\mathbf{M} = \mathbf{U}\Lambda\mathbf{U}^\top$ in its spectral decomposition with $\mathbf{U} = [\mathbf{u}_1, \dots, \mathbf{u}_n] \in \mathbb{R}^{n \times n}$ and $\Lambda = \text{diag}(\lambda_1(\mathbf{M}), \dots, \lambda_n(\mathbf{M}))$, we have

$$\mathbf{Q}_{\mathbf{M}}(z) = \sum_{i=1}^n \frac{\mathbf{u}_i \mathbf{u}_i^\top}{\lambda_i(\mathbf{M}) - z}$$

and thus the access directly to the i -th eigenvector of \mathbf{M} through

$$\mathbf{u}_i \mathbf{u}_i^\top = -\frac{1}{2\pi i} \oint_{\Gamma_{\lambda_i(\mathbf{M})}} \mathbf{Q}_{\mathbf{M}}(z) dz$$

for $\Gamma_{\lambda_i(\mathbf{M})}$ a contour circling around $\lambda_i(\mathbf{M})$ only. More generally,

$$\mathbf{U}f(\Lambda; \Gamma)\mathbf{U}^\top = -\frac{1}{2\pi i} \oint_{\Gamma} f(z) \mathbf{Q}_{\mathbf{M}}(z) dz$$

for f analytic in a neighborhood of Γ and its interior and $f(\Lambda; \Gamma) = \text{diag}(\{f(\lambda_i(\mathbf{M}))\}_{i=1}^n)$.

Of interest in this monograph will be the projection of the individual eigenvectors \mathbf{u}_i of \mathbf{M} onto a deterministic eigenvector \mathbf{v} . In particular, from the above,

$$|\mathbf{v}^\top \mathbf{u}_i|^2 = -\frac{1}{2\pi i} \oint_{\Gamma_{\lambda_i(\mathbf{M})}} \mathbf{v}^\top \mathbf{Q}_{\mathbf{M}}(z) \mathbf{v} dz.$$

It is important to note that the resolvent provides access to *scalar observations* of the eigenstructure of \mathbf{M} through *linear functionals of the resolvent* \mathbf{M} , i.e., the scalar observations $\frac{1}{n} \sum_i f(\lambda_i(\mathbf{M}))$ and $|\mathbf{v}^\top \mathbf{u}_i|$ accessible from $\text{tr } \mathbf{Q}_{\mathbf{M}}$ and $\mathbf{v}^\top \mathbf{Q}_{\mathbf{M}} \mathbf{v}$, respectively.

2.1.4 Deterministic and random equivalents

This monograph is concerned with the situation where \mathbf{M} is a *large dimensional random matrix*, the eigenvalues and eigenvectors of which need be related to the statistical nature of the model design of \mathbf{M} .

In the early days of random matrix theory, the main focus was on the *limiting spectral measure* of \mathbf{M} , that is the characterization of a certain “limit” to the spectral measure $\mu_{\mathbf{M}}$ of \mathbf{M} as the size of \mathbf{M} increases. To this purpose, the natural approach is to study the *random* Stieltjes transform $m_{\mu_{\mathbf{M}}}(z)$ and to show that it admits a limit (in probability or almost surely) $m(z)$. However, this method shows strong limitations today: (i) it supposes that such a limit does exist, therefore restricting the study to very isotropic models for \mathbf{M} and (ii) it only quantifies $\text{tr } \mathbf{Q}_{\mathbf{M}}$ (through the Stieltjes transform), thereby discarding all subspace information about \mathbf{M} carried in $\mathbf{Q}_{\mathbf{M}}$ (as a consequence, a further study of the eigenvectors of \mathbf{M} requires a complete rework).

To avoid these limitations, modern random matrix theory uses the notion of *deterministic equivalents* which are *non-asymptotic* deterministic matrices having (in probability or almost surely) asymptotically the same *scalar observations* as the random ones.²

def : deterministic-equivalent

Definition 4 (Deterministic Equivalent). *We say that $\bar{\mathbf{Q}} \in \mathbb{R}^{n \times n}$ is a deterministic equivalent for the symmetric random matrix $\mathbf{Q} \in \mathbb{R}^{n \times n}$ if, for (sequences of) deterministic matrix $\mathbf{A} \in \mathbb{R}^{n \times n}$ and vectors $\mathbf{a}, \mathbf{b} \in \mathbb{R}^n$ of unit norms (operator and Euclidean, respectively), we have, as $n \rightarrow \infty$,*

$$\frac{1}{n} \operatorname{tr} \mathbf{A}(\mathbf{Q} - \bar{\mathbf{Q}}) \rightarrow 0, \quad \mathbf{a}^\top (\mathbf{Q} - \bar{\mathbf{Q}}) \mathbf{b} \rightarrow 0$$

where the convergence is either in probability or almost surely.

This definition³ has the advantage to bring forth the two key elements giving access to spectral information about a random matrix \mathbf{M} : traces and bilinear forms (of its resolvent $\mathbf{Q}_\mathbf{M}(z)$ for some z). Deterministic equivalents of resolvents $\mathbf{Q}_\mathbf{M}$ then encode most of the information necessary to statistically quantify a random matrix \mathbf{M} .

Remark 2.2 (Generalized definition). *Technically speaking, under a concentration of measure framework, a more natural approach to define deterministic equivalents is under the notion of linear concentration (see Section 2.7 for details) which stipulates that $\bar{\mathbf{Q}}$ is a deterministic equivalent for \mathbf{Q} if, for all deterministic linear functional $u : \mathbb{R}^{n \times n} \rightarrow \mathbb{R}$ with $\sup_{\mathbf{A} \in \mathbb{R}^{n \times n}} |u(\mathbf{A})|/\|\mathbf{A}\| \leq 1$ (i.e., 1-Lipschitz), we have*

$$u(\mathbf{Q} - \bar{\mathbf{Q}}) \rightarrow 0.$$

Using $\frac{1}{n} \operatorname{tr}(\mathbf{A}\mathbf{Q}) \leq \|\mathbf{A}\|\|\mathbf{Q}\| = \|\mathbf{Q}\|$ and $|\mathbf{a}^\top \mathbf{Q}\mathbf{b}| \leq \|\mathbf{a}\|\|\mathbf{b}\|\|\mathbf{Q}\| = \|\mathbf{Q}\|$, we see that Definition 4 is a corollary for this more general (but possibly less explicit) form.

A practical use of deterministic equivalents is to establish that, for a random matrix \mathbf{M} , $\frac{1}{n} \operatorname{tr}(\mathbf{Q}_\mathbf{M}(z) - \bar{\mathbf{Q}}(z)) \rightarrow 0$, say almost surely, for all $z \in \mathcal{C}$ with $\mathcal{C} \subset \mathbb{C}$ some region of \mathbb{C} . Denoting $\bar{m}_n(z) = \frac{1}{n} \operatorname{tr} \bar{\mathbf{Q}}(z)$, this convergence implies that the Stieltjes transform of $\mu_\mathbf{M}$ “converges” in the sense that $m_{\mu_\mathbf{M}}(z) - \bar{m}_n(z) \rightarrow 0$. As we will see, this will indicate that $\mu_\mathbf{M}$ gets increasingly well approximated by a probability measure $\bar{\mu}_n$ having Stieltjes transform $\bar{m}_n(z)$. Identifying $\bar{m}_n(z)$,

²The wide spread of deterministic equivalents in the random matrix literature came along with the necessity of applications, primarily in signal processing and wireless communications, involving too structured matrix models for limiting eigenvalue distributions to be meaningful [Hachem et al., 2007, Couillet et al., 2011]. Yet, they originate to a much earlier period with the works of Girko [2001]. They have even recently been included as a new feature of free probability theory [Speicher and Vargas, 2012], an alternative approach to the resolvent method, which we will shortly discuss in Section 2.6.2.4.

³The very notion of “deterministic equivalent” has not formally been defined in the literature. The present definition is thus restricted to this monograph and is convenient for our present purposes. Note that Section 2.7 will provide an alternative, possibly more satisfying, definition through the notion of *linear concentration* (Definition 8).

which uniquely defines $\bar{\mu}_n$, will often be as far as *the Stieltjes transform method* will lead us. But in some rare cases (such as with the Marčenko–Pastur and the semi-circle laws), $\bar{\mu}_n$ will be identifiable.

In the remainder of the monograph, we will often characterize the large dimensional behavior of random matrix models \mathbf{M} through an approximation by deterministic equivalents $\bar{\mathbf{Q}}(z)$ of their associated resolvents $\mathbf{Q}_{\mathbf{M}}(z)$, as this offers access not only to their asymptotic spectral measure but also to their eigenspaces. We shall therefore often extrapolate some of the core traditional results of the theory, such as the Marčenko–Pastur law [Marcenko and Pastur, 1967], the sample covariance matrix model [Silverstein and Bai, 1995], etc., under this more general form.

Remark 2.3 ($\bar{\mathbf{Q}}$ versus $\mathbb{E}\mathbf{Q}$). *For $\bar{\mathbf{Q}}$ a deterministic equivalent for \mathbf{Q} , the probabilistic convergences $\frac{1}{n} \text{tr } \mathbf{A}(\mathbf{Q} - \bar{\mathbf{Q}}) \rightarrow 0$ and $\mathbf{a}^T(\mathbf{Q} - \bar{\mathbf{Q}})\mathbf{b} \rightarrow 0$ will in general unfold from the fact that*

$$\|\mathbb{E}\mathbf{Q} - \bar{\mathbf{Q}}\| \rightarrow 0$$

and from a control of the variance of $\frac{1}{n} \text{tr } (\mathbf{A}\mathbf{Q})$ and $\mathbf{a}^T\mathbf{Q}\mathbf{b}$; this will often be the strategy followed in our proofs. But note importantly that, if the above relation is met, then $\mathbb{E}\mathbf{Q}$ itself is a deterministic equivalent for \mathbf{Q} by Definition 4. However, $\mathbb{E}\mathbf{Q}$ is often not convenient to work with and a “truly deterministic” matrix $\bar{\mathbf{Q}}$ involving no integration over probability spaces will be systematically preferred.

Deterministic equivalents will be used very regularly in the course of this monograph. To avoid heavy notations, particularly in the main theorems and their proofs, we will use the following shortcut notation for deterministic equivalents.

Notation 1 (Deterministic Equivalents). *For $\mathbf{X}, \mathbf{Y} \in \mathbb{R}^{n \times n}$ two random or deterministic matrices. We write*

$$\mathbf{X} \leftrightarrow \mathbf{Y}$$

if, for all $\mathbf{A} \in \mathbb{R}^{n \times n}$ and $\mathbf{a}, \mathbf{b} \in \mathbb{R}^n$ of unit norms (respectively, operator and Euclidean), we have the simultaneous results

$$\frac{1}{n} \text{tr } \mathbf{A}(\mathbf{X} - \mathbf{Y}) \xrightarrow{a.s.} 0, \quad \mathbf{a}^T(\mathbf{X} - \mathbf{Y})\mathbf{b} \xrightarrow{a.s.} 0, \quad \|\mathbb{E}[\mathbf{X} - \mathbf{Y}]\| \rightarrow 0.$$

In many situations, deterministic equivalents \mathbf{Y} of a matrix \mathbf{X} may not be directly accessible using classical random matrix methods. For these, the access to an intermediary random matrix $\tilde{\mathbf{X}}$ satisfying $\|\tilde{\mathbf{X}} - \mathbf{X}\| \xrightarrow{a.s.} 0$ in operator norm will help “forward” the deterministic equivalents. Indeed, if $\tilde{\mathbf{X}} \leftrightarrow \mathbf{Y}$, then necessarily $\mathbf{X} \leftrightarrow \mathbf{Y}$. When the convergence $\|\tilde{\mathbf{X}} - \mathbf{X}\| \xrightarrow{a.s.} 0$ is too demanding, it may of course be sufficient in some cases to prove that $\mathbf{X} \leftrightarrow \tilde{\mathbf{X}}$ (in which case both left and right matrices are random) to ensure then that $\mathbf{X} \leftrightarrow \mathbf{Y}$. This justifies the need to generalize the notation “ \leftrightarrow ” to arbitrary (random or deterministic) matrices.

2.2 Foundational random matrix results

sec:fundamental-RMT-results

In this section we introduce the main historical results of random matrix theory (appropriately updated under a deterministic equivalent form), which will serve as supporting models to most applications to machine learning.⁴ For readability and accessibility to the readers new to random matrix theory, we mostly stick to intuitive and short sketches of proofs. Yet, for the readers to have a glimpse on the technical details and modern tools of the field, some of the proof sketches will be appended by a complete exhaustive proof.

Both sketches and detailed proofs rely on a set of elementary lemmas and identities need be introduced to understand their spirit and cornerstone arguments. This is done below in Section 2.2.1. The main difference between sketches and detailed proofs then relies on additional technical *probability* theory arguments to prove various convergence results. These arguments strongly depend on the underlying random matrix model hypotheses (Gaussian independent, i.i.d., concentrated random vectors, etc.); for readability, we will focus in our proofs on one specific line of arguments (that we claim to be the “historical” one) and will discuss alternative techniques in side remarks. In particular, the specific *concentration of measure* theoretic approach, which is both more “modern” (yet less mature) and more adapted to machine learning applications, will be given a separate treatment in Section 2.7.

2.2.1 Key lemmas and identities

sec:key_lemmas

2.2.1.1 Resolvent identities

Most results discussed in this section consist in tools meant to help “approximate” random resolvents $\mathbf{Q}(z)$ via deterministic resolvents $\bar{\mathbf{Q}}(z)$ in the sense of the deterministic equivalents definition. The following first identity provides a comparison of matrix inverses (often used in practice to compare the aforementioned resolvents).

lem:resolvent-identity

Lemma 2.1 (Resolvent identity). *For invertible matrices \mathbf{A} and \mathbf{B} , we have*

$$\mathbf{A}^{-1} - \mathbf{B}^{-1} = \mathbf{A}^{-1}(\mathbf{B} - \mathbf{A})\mathbf{B}^{-1}.$$

Proof. This can be easily checked by multiplying both sides on the left by \mathbf{A} and on the right by \mathbf{B} . \square

Another useful lemma that helps directly connect the resolvent of \mathbf{BA} to that of \mathbf{AB} , is given as follows.

⁴Although historically and technically, said “Wigner” models of symmetric random matrices with independent entries came first, are simpler to analyze and spurred more mathematical research efforts [Wigner, 1955, Mehta and Gaudin, 1960, Anderson et al., 2010], for the sake of machine learning applications, our focus is primarily steered towards the slightly more involved sample covariance matrix models [Marcenko and Pastur, 1967, Bai and Silverstein, 2010].

lem:resolvent-trick

Lemma 2.2. *For $\mathbf{A} \in \mathbb{R}^{p \times n}$ and $\mathbf{B} \in \mathbb{R}^{n \times p}$, we have*

$$\mathbf{A}(\mathbf{BA} - z\mathbf{I}_n)^{-1} = (\mathbf{AB} - z\mathbf{I}_p)^{-1}\mathbf{A}$$

for $z \in \mathbb{C}$ distinct from 0 and from the eigenvalues of \mathbf{AB} .

Proof. Left-multiply both ends of the equality by $\mathbf{AB} - z\mathbf{I}_p$ to obtain $\mathbf{A} = \mathbf{A}$. \square

For \mathbf{AB} and \mathbf{BA} symmetric, Lemma 2.2 is a special case of the more general relation $\mathbf{Af}(\mathbf{BA}) = f(\mathbf{AB})\mathbf{A}$, with $f(\mathbf{M}) \equiv \mathbf{U}f(\mathbf{\Lambda})\mathbf{U}^\top$ under the spectral decomposition $\mathbf{M} = \mathbf{U}\mathbf{\Lambda}\mathbf{U}^\top$ and f complex analytic. Since f is analytic, $f(\mathbf{BA}) = \sum_{i=0}^{\infty} c_i(\mathbf{BA})^i$ for some sequence $\{c_i\}_{i=0}^{\infty}$ and thus $\mathbf{Af}(\mathbf{BA}) = \sum_{i=0}^{\infty} c_i(\mathbf{AB})^i\mathbf{A} = f(\mathbf{AB})\mathbf{A}$.

The next lemma, known as *Sylvester's identity* (also known as the Weinstein–Aronszajn identity), similarly relates the resolvents of \mathbf{AB} and \mathbf{BA} through their determinant.

lem:sylvester

Lemma 2.3 (Sylvester's identity). *For $\mathbf{A} \in \mathbb{R}^{p \times n}$, $\mathbf{B} \in \mathbb{R}^{n \times p}$ and $z \in \mathbb{C} \setminus \{0\}$,*

$$\det(\mathbf{AB} - z\mathbf{I}_p) = \det(\mathbf{BA} - z\mathbf{I}_n)(-z)^{p-n}.$$

Proof. It suffices to develop the block-matrix determinant (recall that $\det \begin{bmatrix} \mathbf{A} & \mathbf{B} \\ \mathbf{C} & \mathbf{D} \end{bmatrix} = \det \mathbf{D} \det(\mathbf{A} - \mathbf{B}\mathbf{D}^{-1}\mathbf{C}) = \det \mathbf{A} \det(\mathbf{D} - \mathbf{C}\mathbf{A}^{-1}\mathbf{B})$ when \mathbf{A} and \mathbf{D} are invertible)

$$\det \begin{bmatrix} z\mathbf{I}_p & z\mathbf{A} \\ \mathbf{B} & z\mathbf{I}_n \end{bmatrix} = \det(z\mathbf{I}_p) \det(z\mathbf{I}_n - \mathbf{BA}) = \det(z\mathbf{I}_n) \det(z\mathbf{I}_p - \mathbf{AB}).$$

\square

An immediate consequence of Sylvester's identity is that \mathbf{AB} and \mathbf{BA} have the same nonzero eigenvalues (those nonzero z 's for which both left- and right-hand sides vanish). Thus, say $n \geq p$, $\mathbf{AB} \in \mathbb{R}^{p \times p}$ and $\mathbf{BA} \in \mathbb{R}^{n \times n}$ have the same spectrum, except for the additional $n - p$ zero eigenvalues of \mathbf{AB} . This remark implies the next identity.

Lemma 2.4 (Trace of resolvent and co-resolvent). *Let $\mathbf{A} \in \mathbb{R}^{p \times n}$, $\mathbf{B} \in \mathbb{R}^{n \times p}$, and $z \in \mathbb{C}$ not an eigenvalue of \mathbf{AB} nor zero. Then*

$$\mathrm{tr} \mathbf{Q}_{\mathbf{AB}}(z) = \mathrm{tr} \mathbf{Q}_{\mathbf{BA}}(z) + \frac{n-p}{z}.$$

In particular, if \mathbf{AB} and \mathbf{BA} are symmetric,

$$m_{\mu_{\mathbf{AB}}}(z) = \frac{n}{p} m_{\mu_{\mathbf{BA}}}(z) + \frac{n-p}{pz}.$$

It will be customary, if $\mathbf{Q}_{\mathbf{AB}}$ is the resolvent of the matrix model \mathbf{AB} under study to call $\mathbf{Q}_{\mathbf{BA}}$ the *co-resolvent* of \mathbf{AB} . We will see that the resolvent and co-resolvent of random matrix models (in particular the resolvent and co-resolvent of \mathbf{XX}^\top for \mathbf{X} some structured random matrix model) often intervene together, and quite symmetrically, to define their associated deterministic equivalents.

2.2.1.2 Perturbation identities

Quantifying the asymptotic global (e.g., spectral distribution) or local (e.g., isolated eigenvalues or projection on eigenvector) behavior of random matrices \mathbf{M} will systematically involve a *perturbation approach*. The idea often lies in comparing the behavior of the resolvent $\mathbf{Q} = \mathbf{Q}_{\mathbf{M}}$ to the resolvent \mathbf{Q}_{-i} of \mathbf{M}_{-i} , with \mathbf{M}_{-i} defined as \mathbf{M} with either row and column i , or some i -th contribution (e.g., $\mathbf{M}_{-i} = \sum_{j \neq i} \mathbf{x}_j \mathbf{x}_j^T$ if $\mathbf{M} = \sum_j \mathbf{x}_j \mathbf{x}_j^T$), discarded. A number of so-called *perturbation* identities are then needed.

The first one involves the segmentation of \mathbf{M} under the form of subblocks, in general consisting of one large block and three small submatrices. The corresponding resolvent $\mathbf{Q}_{\mathbf{M}}$ can correspondingly be segmented in subblocks according to the following block inversion lemma.

lem:block-inverse

Lemma 2.5 (Block matrix inversion). *For $\mathbf{A} \in \mathbb{R}^{p \times p}$, $\mathbf{B} \in \mathbb{R}^{p \times n}$, $\mathbf{C} \in \mathbb{R}^{n \times p}$ and $\mathbf{D} \in \mathbb{R}^{n \times n}$ with \mathbf{D} invertible, we have*

$$\begin{pmatrix} \mathbf{A} & \mathbf{B} \\ \mathbf{C} & \mathbf{D} \end{pmatrix}^{-1} = \begin{pmatrix} \mathbf{S}^{-1} & -\mathbf{S}^{-1}\mathbf{BD}^{-1} \\ -\mathbf{D}^{-1}\mathbf{CS}^{-1} & \mathbf{D}^{-1} + \mathbf{D}^{-1}\mathbf{CS}^{-1}\mathbf{BD}^{-1} \end{pmatrix}$$

where $\mathbf{S} \equiv \mathbf{A} - \mathbf{BD}^{-1}\mathbf{C}$ is the Schur complement (for the block \mathbf{D}) of $(\mathbf{A} \ \mathbf{B})$.⁵

As a consequence of Lemma 2.5, we get the following explicit form for all diagonal entries of an invertible matrix \mathbf{A} .

lem:diag-of-inverse

Lemma 2.6 (Diagonal entries of matrix inverse). *For invertible $\mathbf{A} \in \mathbb{R}^{p \times p}$ and $\mathbf{A}_{-i} \in \mathbb{R}^{(p-1) \times (p-1)}$, the matrix obtained by removing the i -th row and column from \mathbf{A} , $i = 1, \dots, p$, we have*

$$(\mathbf{A}^{-1})_{ii} = \frac{1}{\mathbf{A}_{ii} - \boldsymbol{\alpha}_i^T (\mathbf{A}_{-i})^{-1} \boldsymbol{\beta}_i}$$

for $\boldsymbol{\alpha}_i^T, \boldsymbol{\beta}_i \in \mathbb{R}^{p-1}$ the i -th row and column of \mathbf{A} with i -th entries removed, respectively.

The result is a direct consequence of the fact that $\mathbf{A}^{-1} = \frac{\text{adj}(\mathbf{A})}{\det(\mathbf{A})}$, with $\text{adj}(\mathbf{A})$ the adjugate matrix of \mathbf{A} , together with the block determinant formula in Lemma 2.5.

Perturbations by addition or subtraction of low-rank matrices to \mathbf{M} induce modifications in the resolvent \mathbf{Q} that involve Woodbury's identity as follows.

lem:woodbury

Lemma 2.7 (Woodbury). *For $\mathbf{A} \in \mathbb{R}^{p \times p}$, $\mathbf{U}, \mathbf{V} \in \mathbb{R}^{p \times n}$, such that both \mathbf{A} and $\mathbf{A} + \mathbf{UV}^T$ are invertible, we have*

$$(\mathbf{A} + \mathbf{UV}^T)^{-1} = \mathbf{A}^{-1} - \mathbf{A}^{-1}\mathbf{U}(\mathbf{I}_n + \mathbf{V}^T\mathbf{A}^{-1}\mathbf{U})^{-1}\mathbf{V}^T\mathbf{A}^{-1}.$$

⁵The Schur complement $\mathbf{S} = \mathbf{A} - \mathbf{BD}^{-1}\mathbf{C}$ is particularly known for its providing the block determinant formula $\det \begin{pmatrix} \mathbf{A} & \mathbf{B} \\ \mathbf{C} & \mathbf{D} \end{pmatrix} = \det(\mathbf{D}) \det(\mathbf{S})$, already exploited in the proof of Sylvester's identity (Lemma 2.3).

Note importantly that, while $(\mathbf{A} + \mathbf{U}\mathbf{V}^\top)^{-1}$ is of size $p \times p$, $(\mathbf{I}_n + \mathbf{V}\mathbf{A}\mathbf{U})^{-1}$ is of size $n \times n$. This will turn out useful to relate resolvents of large dimensional matrices to resolvents of more elementary fixed small size matrices. In particular, for $n = 1$, i.e., $\mathbf{U}\mathbf{V}^\top = \mathbf{u}\mathbf{v}^\top$ for $\mathbf{U} = \mathbf{u} \in \mathbb{R}^p$ and $\mathbf{V} = \mathbf{v} \in \mathbb{R}^p$, Woodbury's identity specializes to the Sherman–Morrison formula.

lem:sherman-morrison

Lemma 2.8 (Sherman–Morrison). *For $\mathbf{A} \in \mathbb{R}^{p \times p}$ invertible and $\mathbf{u}, \mathbf{v} \in \mathbb{R}^p$, $\mathbf{A} + \mathbf{u}\mathbf{v}^\top$ is invertible if and only if $1 + \mathbf{v}^\top \mathbf{A}^{-1} \mathbf{u} \neq 0$ and*

$$(\mathbf{A} + \mathbf{u}\mathbf{v}^\top)^{-1} = \mathbf{A}^{-1} - \frac{\mathbf{A}^{-1}\mathbf{u}\mathbf{v}^\top\mathbf{A}^{-1}}{1 + \mathbf{v}^\top\mathbf{A}^{-1}\mathbf{u}}.$$

Besides,

$$(\mathbf{A} + \mathbf{u}\mathbf{v}^\top)^{-1}\mathbf{u} = \frac{\mathbf{A}^{-1}\mathbf{u}}{1 + \mathbf{v}^\top\mathbf{A}^{-1}\mathbf{u}}.$$

Letting $\mathbf{A} = \mathbf{M} - z\mathbf{I}_p$, $z \in \mathbb{C}$, and $\mathbf{v} = \tau\mathbf{u}$ for $\tau \in \mathbb{R}$ in the previous lemma leads to the following rank-1 perturbation lemma for the resolvent of \mathbf{M} .

lem:rank-one-update-trace

Lemma 2.9 ([Silverstein and Bai, 1995, Lemma 2.6]). *For $\mathbf{A}, \mathbf{M} \in \mathbb{R}^{p \times p}$ symmetric, $\mathbf{u} \in \mathbb{R}^p$, $\tau \in \mathbb{R}$ and $z \in \mathbb{C} \setminus \mathbb{R}$,*

$$|\operatorname{tr} \mathbf{A}(\mathbf{M} + \tau\mathbf{u}\mathbf{u}^\top - z\mathbf{I}_p)^{-1} - \operatorname{tr} \mathbf{A}(\mathbf{M} - z\mathbf{I}_p)^{-1}| \leq \frac{\|\mathbf{A}\|}{|\Im(z)|}.$$

Also, for $\mathbf{A}, \mathbf{M} \in \mathbb{R}^{p \times p}$ symmetric and nonnegative definite, $\mathbf{u} \in \mathbb{R}^p$, $\tau > 0$ and $z < 0$,

$$|\operatorname{tr} \mathbf{A}(\mathbf{M} + \tau\mathbf{u}\mathbf{u}^\top - z\mathbf{I}_p)^{-1} - \operatorname{tr} \mathbf{A}(\mathbf{M} - z\mathbf{I}_p)^{-1}| \leq \frac{\|\mathbf{A}\|}{|z|}.$$

Exercise 4 at the end of the chapter proposes a partial proof for the case $z < 0$.

It is interesting (and possibly counterintuitive at first) to note that $\|\mathbf{u}\|$ does not intervene in this inequality. In particular, irrespective of the amplitude of the rank-1 perturbation, under the conditions of the lemma

$$m_{\mu_{\mathbf{M} + \tau\mathbf{u}\mathbf{u}^\top}}(z) = m_{\mu_{\mathbf{M}}}(z) + O(p^{-1})$$

and thus, by the link between spectrum and Stieltjes transform, the spectral measure of \mathbf{M} is asymptotically close to that of $\mathbf{M} + \tau\mathbf{u}\mathbf{u}^\top$ for any \mathbf{u} , in the large p limit. This result can be understood through the following two arguments: (i) for large p , the spectrum of \mathbf{M} (say $\|\mathbf{M}\| = O(1)$ without generality restriction) is only non-trivial if the vast majority of the p eigenvalues of \mathbf{M} are of order $O(1)$: thus, as p eigenvalues use a space of size $O(1)$, they tend to aggregate; (ii) by Weyl's interlacing lemma presented next (Lemma 2.10) for symmetric matrices, the eigenvalues of \mathbf{M} and of $\mathbf{M} + \tau\mathbf{u}\mathbf{u}^\top$ are interlaced. Both arguments thus indicate that, in the large p limit, the spectral measures are indeed asymptotically the same.

Unlike non-symmetric matrices, symmetric matrices indeed enjoy the nice property of having stable spectra with respect to rank-1 perturbations. For $\lambda \in \mathbb{R}$ an eigenvalue of $\mathbf{M} + \tau \mathbf{u} \mathbf{u}^\top$ but not of \mathbf{M} with, say $\tau > 0$, we indeed have

$$\begin{aligned} 0 &= \det(\mathbf{M} + \tau \mathbf{u} \mathbf{u}^\top - \lambda \mathbf{I}_p) = \det(\mathbf{Q}_\mathbf{M}(\lambda)) \det(\mathbf{I}_p + \tau \mathbf{Q}_\mathbf{M}(\lambda) \mathbf{u} \mathbf{u}^\top) \\ &= \det(\mathbf{Q}_\mathbf{M}(\lambda)) (1 + \tau \mathbf{u}^\top \mathbf{Q}_\mathbf{M}(\lambda) \mathbf{u}) \end{aligned}$$

where the second equality unfolds from factoring out $\mathbf{M} - \lambda \mathbf{I}_p$ (which is not singular as λ is not an eigenvalue of \mathbf{M}) and the third from Sylvester's identity (Lemma 2.3). As a consequence, λ is one of the solutions to

$$-1 = \tau \mathbf{u}^\top \mathbf{Q}_\mathbf{M}(\lambda) \mathbf{u} = \tau \sum_{i=1}^p \frac{|\mathbf{v}_i^\top \mathbf{u}|^2}{\lambda_i(\mathbf{M}) - \lambda}, \quad \left(\mathbf{M} = \sum_{i=1}^p \lambda_i(\mathbf{M}) \mathbf{v}_i \mathbf{v}_i^\top \right)$$

which, seen as a function of λ , has asymptotes at each $\lambda_i(\mathbf{M})$ and is increasing (from $-\infty$ to ∞) on the segments $(\lambda_i(\mathbf{M}), \lambda_{i+1}(\mathbf{M}))$ (eigenvalues being sorted in increasing order). The eigenvalues of $\mathbf{M} + \tau \mathbf{u} \mathbf{u}^\top$ are therefore *interlaced* with those of \mathbf{M} (see Figure 2.1 for an illustration). This idea generalizes to finite rank perturbation as follows.

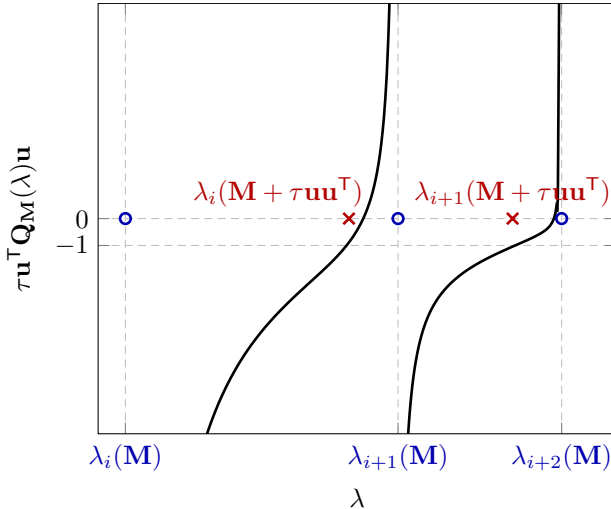


Figure 2.1: Illustration of the eigenvalues of \mathbf{M} and the rank-one perturbation $\mathbf{M} + \tau \mathbf{u} \mathbf{u}^\top$ of \mathbf{M} , as well as the function $\tau \mathbf{u}^\top \mathbf{Q}_\mathbf{M}(\lambda) \mathbf{u}$. [\[Link to code\]](#)

Lemma 2.10 (Weyl, [Horn and Johnson, 2012, Theorem 4.3.1]). Let $\mathbf{A}, \mathbf{B} \in \mathbb{R}^{p \times p}$ be symmetric matrices and let the respective eigenvalues of \mathbf{A} , \mathbf{B} and $\mathbf{A} + \mathbf{B}$ arranged in nondecreasing order, i.e., $\lambda_1 \leq \lambda_2 \leq \dots \lambda_{p-1} \leq \lambda_p$. Then, for all $i \in \{1, \dots, p\}$,

$$\begin{aligned} \lambda_i(\mathbf{A} + \mathbf{B}) &\leq \lambda_{i+j}(\mathbf{A}) + \lambda_{p-j}(\mathbf{B}), \quad j = 0, 1, \dots, p-i, \\ \lambda_{i-j+1}(\mathbf{A}) + \lambda_j(\mathbf{B}) &\leq \lambda_i(\mathbf{A} + \mathbf{B}), \quad j = 1, \dots, i, \end{aligned}$$

lem:weyl

In particular, taking $i = 1$ in the first equation and $i = p$ in the second equation, together with the fact $\lambda_j(\mathbf{B}) = -\lambda_{p+1-j}(-\mathbf{B})$ for $j = 1, \dots, p$, implies

$$\max_{1 \leq j \leq p} |\lambda_j(\mathbf{A}) - \lambda_j(\mathbf{B})| \leq \|\mathbf{A} - \mathbf{B}\|.$$

2.2.1.3 Probability identities

The results of the previous sections are algebraic identities useful to handle the resolvent \mathbf{Q}_M of the deterministic matrix \mathbf{M} . The second ingredient of random matrix analysis lies in asymptotic probability approximations as the dimensions of \mathbf{M} increase. Quite surprisingly, most results essentially revolve around the convergence of a certain quadratic form, which is often nothing more than a mere extension of the *law of large numbers*.

Those quadratic form convergence results come under multiple forms. The historical form, due to Bai and Silverstein, sometimes referred to as the “trace lemma”, is as follows.

Lemma 2.11 (Quadratic-form-close-to-the-trace, [Bai and Silverstein, 2010, Lemma B.26]). *Let $\mathbf{x} \in \mathbb{R}^p$ have i.i.d. entries of zero mean, unit variance and $\mathbb{E}[|x_i|^L] \leq \nu_L$ for some $L \geq 1$. Then for $\mathbf{A} \in \mathbb{R}^{p \times p}$ and $l \geq 1$*

$$\mathbb{E} \left[| \mathbf{x}^\top \mathbf{A} \mathbf{x} - \text{tr } \mathbf{A} |^l \right] \leq K_l \left[(\nu_4 \text{tr}(\mathbf{A} \mathbf{A}^\top))^{l/2} + \nu_{2l} \text{tr}(\mathbf{A} \mathbf{A}^\top)^{l/2} \right]$$

for some constant $K_l > 0$ independent of p . In particular, if $\|\mathbf{A}\| \leq 1$ and the entries of \mathbf{x} have bounded eighth-order moment,

$$\mathbb{E} \left[(\mathbf{x}^\top \mathbf{A} \mathbf{x} - \text{tr } \mathbf{A})^4 \right] \leq Kp^2$$

for some K independent of p , and consequently, as $p \rightarrow \infty$,

$$\frac{1}{p} \mathbf{x}^\top \mathbf{A} \mathbf{x} - \frac{1}{p} \text{tr } \mathbf{A} \xrightarrow{\text{a.s.}} 0.$$

This last result is rather intuitive. For $\mathbf{A} = \mathbf{I}_p$, this is simply an instance of the law of large numbers. For generic \mathbf{A} , first note that, by the independence of the entries of \mathbf{x} , $\mathbb{E}[\mathbf{x}^\top \mathbf{A} \mathbf{x}] = \text{tr } \mathbf{A}$. Exploiting the fact that $\text{var}[\frac{1}{p} \mathbf{x}^\top \mathbf{A} \mathbf{x}] = O(p^{-1})$ then ensures that $\frac{1}{p} \mathbf{x}^\top \mathbf{A} \mathbf{x} - \frac{1}{p} \text{tr } \mathbf{A} \rightarrow 0$, but only in probability; since the variance calculus involves exponentiating the entries x_i of \mathbf{x} up to power 4, they need to be of finite fourth power. The almost sure convergence is achieved by showing the faster moment convergence $\mathbb{E}[(\frac{1}{p} \mathbf{x}^\top \mathbf{A} \mathbf{x} - \frac{1}{p} \text{tr } \mathbf{A})^4] = O(p^{-2})$ which is the second statement of the lemma and requires 8-th order exponentiation of the x_i 's. The request for \mathbf{A} to be of bounded norm with respect to p in this case “stabilizes” the quadratic form $\mathbf{x}^\top \mathbf{A} \mathbf{x}$ by maintaining its concentration properties.

Recalling that $\|\mathbf{Q}_M(z)\| \leq (\text{dist}(z, \text{supp}(\mu_M)))^{-1}$, Lemma 2.11 can be exploited for $\mathbf{A} = \mathbf{Q}_M(z)$ for all z away from the support of μ_M and all \mathbf{x} independent of $\mathbf{Q}_M(z)$. The core of the proofs of the main random matrix results is uniquely based on this last remark.

These identities constitute all the main technical ingredients needed to understand the proofs of both historical and recent random matrix results. The next section introduces the most fundamental of those which will be called after over and over in the remainder of the monograph.

2.2.2 The Marčenko-Pastur and semi-circle laws

We start by illustrating how the aforementioned tools are used to prove the two most popular results in random matrix theory: the Marčenko-Pastur law and the Wigner semi-circle law.

To simplify the exposition of the results, we will use the notation for deterministic equivalents introduced in Notation 1. That is, for $\mathbf{X}, \mathbf{Y} \in \mathbb{R}^{n \times n}$, we will denote $\mathbf{X} \leftrightarrow \mathbf{Y}$ if, for all unit norm $\mathbf{A} \in \mathbb{R}^{n \times n}$ and $\mathbf{a}, \mathbf{b} \in \mathbb{R}^n$, $\frac{1}{n} \text{tr } \mathbf{A}(\mathbf{X} - \mathbf{Y}) \xrightarrow{\text{a.s.}} 0$, $\mathbf{a}^\top (\mathbf{X} - \mathbf{Y}) \mathbf{b} \xrightarrow{\text{a.s.}} 0$ and $\|\mathbb{E}[\mathbf{X} - \mathbf{Y}]\| \rightarrow 0$.

Most of the results involve Stieltjes transforms $m_\mu(z)$ of a probability measure with support $\text{supp}(\mu)$. Since Stieltjes transforms are such that $m_\mu(z) > 0$ for $z < \inf \text{supp}(\mu)$, $m_\mu(z) < 0$ for $z > \sup \text{supp}(\mu)$ and $\Im[z] \Im[m_\mu(z)] > 0$ if $z \in \mathbb{C} \setminus \mathbb{R}$, it will be convenient in the following to consider the set

$$\begin{aligned} \mathcal{Z}(\mathcal{A}) = \{ (z, m) \in \mathcal{A} \times \mathbb{C}, (\Im[z] \Im[m] > 0 \text{ if } \Im[z] \neq 0) \\ \text{or } (zm < 0 \text{ if } \Im[z] = 0) \} \end{aligned}$$

that is, the set of all “licit” Stieltjes transform couples $(z, m(z))$.

2.2.2.1 The Marčenko-Pastur law

We present the Marčenko-Pastur law under the slightly modified form of a deterministic equivalent for the resolvent $\mathbf{Q}(z)$.

theo:MP-law

Theorem 2.3 (From [Marcenko and Pastur \[1967\]](#)). *Consider the resolvent $\mathbf{Q}(z) = (\frac{1}{n} \mathbf{X} \mathbf{X}^\top - z \mathbf{I}_p)^{-1}$, for $\mathbf{X} \in \mathbb{R}^{p \times n}$ having i.i.d. zero mean, unit variance and some smooth tail condition.⁶ Then, as $n, p \rightarrow \infty$ with $p/n \rightarrow c \in (0, \infty)$, we have*

$$\mathbf{Q}(z) \leftrightarrow \bar{\mathbf{Q}}(z), \quad \bar{\mathbf{Q}}(z) = m(z) \mathbf{I}_p \tag{2.8} \quad \text{eq:MP-DE}$$

with $(z, m(z))$ the unique solution in $\mathcal{Z}(\mathbb{C} \setminus [(1 - \sqrt{c})^2, (1 + \sqrt{c})^2])$ of

$$zcm^2(z) - (1 - c - z)m(z) + 1 = 0. \tag{2.9} \quad \text{eq:MP-ST}$$

⁶For this result, and those related, various tail conditions may be used: finite moment of order ℓ for some sufficiently large ℓ (usually $\ell > 4$ is sufficient), subgaussian behavior, concentration of measure condition, etc. Determining the minimalistic conditions for the results to hold has been of long interest to mathematicians, as demonstrated by the huge impact of the complete proof in [\[Tao and Vu, 2008\]](#) of the full-circle law theorem (see also [Bordenave and Chafaï \[2014\]](#)). Yet, for machine learning purposes, these are of minor interest: we shall systematically assume “sufficiently smooth” (and technically convenient) conditions to hold, without hampering the practical applicability of the results.

The function $m(z)$ is the Stieltjes transform of the probability measure μ given explicitly by

$$\mu(dx) = (1 - c^{-1})^+ \delta_0(x) + \frac{1}{2\pi cx} \sqrt{(x - a)^+(b - x)^+} dx \quad \text{eq:MP-law-in-theo}$$
(2.10)

where $a = (1 - \sqrt{c})^2$, $b = (1 + \sqrt{c})^2$ and $(x)^+ = \max(0, x)$, which is known as the Marčenko-Pastur distribution. In particular, with probability one, the empirical spectral measure $\mu_{\frac{1}{n}\mathbf{X}\mathbf{X}^\top}$ converges weakly to μ .

Figure 2.2 depicts the density of the Marčenko-Pastur distribution for different values of c . For a fixed dimension p , the ratio c decreases as the number of samples n grows large, so that the eigenvalues of the sample covariance matrix become more “concentrated” (their spread is given by the length of the support $[(1 - \sqrt{c})^2, (1 + \sqrt{c})^2]$) around the unique population covariance matrix eigenvalue equal to 1.

Note that the “asymmetric bell” shape of the Marčenko-Pastur law gets increasingly skewed towards large values as c increases and that, as $c = 1$, the left-edge has the very peculiar behavior to diverge. This $c = 1$ setting is referred to as the “hard edge” scenario explained by the fact that the limiting density becomes $\frac{1}{2\pi x} \sqrt{x^+((1 - \sqrt{c})^2 - x)^+} \sim \frac{1}{2\pi\sqrt{x}}$ as $x \downarrow 0$ and thus behaves as $1/\sqrt{x}$ near the left edge (the left edge being at $x = 0$) rather than as $\sqrt{x - (1 + \sqrt{c})^2}$ when $c \neq 0$ (the left edge being at $x = (1 + \sqrt{c})^2$). When $c > 1$, a mass at zero is created (of weight $1 - c^{-1}$) while, possibly unexpectedly, the left edge of the main “bulk” of eigenvalues moves towards the right, leaving the open segment $(0, (1 - \sqrt{c})^2)$ empty.

Proof. Before going into the details of the proof, we first give a few intuitive arguments.

Intuitive idea. A first heuristic derivation, essentially due to Bai and Silverstein, consists in iteratively “guessing” the form of $\mathbf{Q}(z) = \mathbf{F}(z)^{-1}$ for some matrix $\mathbf{F}(z)^{-1}$. To this end, from Lemma 2.1, it first appears that

$$\begin{aligned} \mathbf{Q}(z) - \bar{\mathbf{Q}}(z) &= \mathbf{Q}(z) \left(\mathbf{F}(z) + z\mathbf{I}_p - \frac{1}{n} \mathbf{X}\mathbf{X}^\top \right) \bar{\mathbf{Q}}(z) \\ &= \mathbf{Q}(z) \left(\mathbf{F}(z) + z\mathbf{I}_p - \frac{1}{n} \sum_{i=1}^n \mathbf{x}_i \mathbf{x}_i^\top \right) \bar{\mathbf{Q}}(z) \end{aligned}$$

For $\bar{\mathbf{Q}}(z)$ to be a deterministic equivalent for $\mathbf{Q}(z)$, we wish in particular that $\frac{1}{p} \operatorname{tr} \mathbf{A}(\mathbf{Q}(z) - \bar{\mathbf{Q}}(z)) \xrightarrow{a.s.} 0$, for \mathbf{A} deterministic with $\|\mathbf{A}\| = 1$. That is

$$\frac{1}{p} \operatorname{tr} (\mathbf{F}(z) + z\mathbf{I}_p) \bar{\mathbf{Q}}(z) \mathbf{A} \mathbf{Q}(z) - \frac{1}{n} \sum_{i=1}^n \frac{1}{p} \mathbf{x}_i^\top \bar{\mathbf{Q}}(z) \mathbf{A} \mathbf{Q}(z) \mathbf{x}_i \xrightarrow{a.s.} 0. \quad \text{eq:MPproof-1}$$
(2.11)

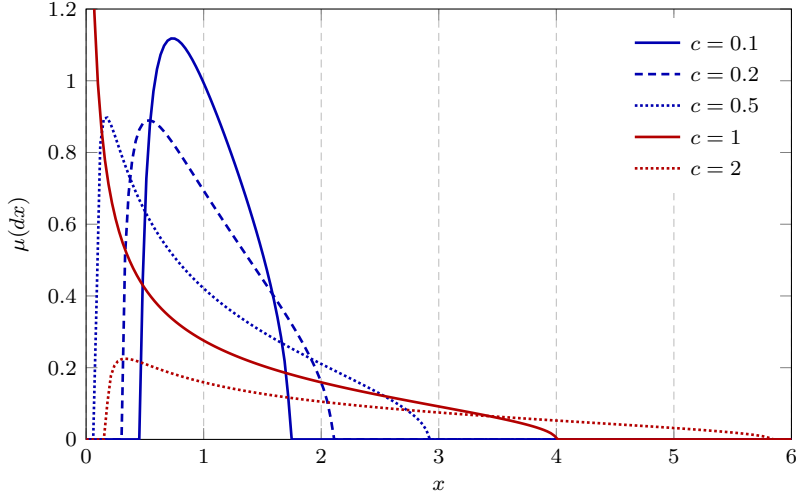


Figure 2.2: Marčenko-Pastur distribution for different c . Note the peculiar “hard-edge” behavior at $c = 1$, quite unlike other values of c .

We recognize in $\frac{1}{p} \mathbf{x}_i^\top \bar{\mathbf{Q}}(z) \mathbf{A} \mathbf{Q}(z) \mathbf{x}_i$ a quadratic form on which we would like to use Lemma 2.11 to turn it into a trace term independent of \mathbf{x}_i . Yet, Lemma 2.11 cannot be used as $\mathbf{Q}(z)$ depends on \mathbf{x}_i . To counter the difficulty, we then use Lemma 2.8 to write

$$\mathbf{Q}(z) \mathbf{x}_i = \frac{\mathbf{Q}_{-i}(z) \mathbf{x}_i}{1 + \frac{1}{n} \mathbf{x}_i^\top \mathbf{Q}_{-i}(z) \mathbf{x}_i}$$

where $\mathbf{Q}_{-i}(z) = (\frac{1}{n} \sum_{j \neq i} \mathbf{x}_j \mathbf{x}_j^\top - z \mathbf{I}_p)^{-1}$ which is now independent of \mathbf{x}_i . Now legitimately applying Lemma 2.11, we find that

$$\frac{1}{p} \mathbf{x}_i^\top \bar{\mathbf{Q}}(z) \mathbf{A} \mathbf{Q}(z) \mathbf{x}_i = \frac{\frac{1}{p} \mathbf{x}_i^\top \bar{\mathbf{Q}}(z) \mathbf{A} \mathbf{Q}_{-i}(z) \mathbf{x}_i}{1 + \frac{1}{n} \mathbf{x}_i^\top \mathbf{Q}_{-i}(z) \mathbf{x}_i} \simeq \frac{\frac{1}{p} \operatorname{tr} \bar{\mathbf{Q}}(z) \mathbf{A} \mathbf{Q}_{-i}(z)}{1 + \frac{1}{n} \operatorname{tr} \mathbf{Q}_{-i}(z)}. \quad \text{[Eq.: MP proof 3]}$$

From Lemma 2.9, normalized traces involving $\mathbf{Q}_{-i}(z)$ or $\mathbf{Q}(z)$ are asymptotically identical and thus this further reads

$$\frac{1}{p} \mathbf{x}_i^\top \bar{\mathbf{Q}}(z) \mathbf{A} \mathbf{Q}(z) \mathbf{x}_i \simeq \frac{\frac{1}{p} \operatorname{tr} \bar{\mathbf{Q}}(z) \mathbf{A} \mathbf{Q}(z)}{1 + \frac{1}{n} \operatorname{tr} \mathbf{Q}(z)}.$$

Getting back to (2.11), we thus end up with the approximation

$$\frac{1}{p} \operatorname{tr} (\mathbf{F}(z) + z \mathbf{I}_p) \bar{\mathbf{Q}}(z) \mathbf{A} \mathbf{Q}(z) \simeq \frac{\frac{1}{p} \operatorname{tr} \bar{\mathbf{Q}}(z) \mathbf{A} \mathbf{Q}(z)}{1 + \frac{1}{n} \operatorname{tr} \mathbf{Q}(z)}.$$

As a consequence, we can now “guess” the form of $\mathbf{F}(z)$. Indeed, if it is to exist, $\mathbf{F}(z)$ must be of the type

$$\mathbf{F}(z) \simeq \left(-z + \frac{1}{1 + \frac{1}{n} \operatorname{tr} \mathbf{Q}(z)} \right) \mathbf{I}_p$$

for the approximation above to hold. To close the loop, taking $\mathbf{A} = \mathbf{I}_p$, $\frac{1}{n} \operatorname{tr} \mathbf{Q}(z)$ appearing in this display must be well approximated by $m(z) \equiv \frac{1}{p} \operatorname{tr} \bar{\mathbf{Q}}(z)$ so that

$$\frac{1}{p} \operatorname{tr} \mathbf{Q}(z) \simeq m(z) = \frac{1}{-z + \frac{1}{1 + \frac{p}{n} \frac{1}{p} \operatorname{tr} \mathbf{Q}(z)}} \simeq \frac{\text{eq:MPproof_fixed_point}}{-z + \frac{1}{1 + \frac{p}{n} m(z)}} \quad (2.13)$$

and we thus have finally

$$\bar{\mathbf{Q}}(z) = \mathbf{F}(z)^{-1} = m(z) \mathbf{I}_p$$

where, in the large n, p limit, $m(z)$ is solution to

$$m(z) = \frac{1}{-z + \frac{1}{1 + cm(z)}}$$

or equivalently

$$zcm^2(z) - (1 - c - z)m(z) + 1 = 0.$$

This equation has two solutions defined by the two roots of the complex square root function

$$m(z) = \frac{1 - c - z}{2cz} + \frac{\sqrt{((1 + \sqrt{c})^2 - z)((1 - \sqrt{c})^2 - z)}}{2cz}$$

only one of which is such that $\Im[z]\Im[m(z)] > 0$ as imposed by the definition of Stieltjes transforms. Now, from the inverse Stieltjes transform theorem, Theorem 2.1, we find that $m(z)$ is the Stieltjes transform of the measure μ with

$$\mu([a, b]) = \frac{1}{\pi} \lim_{\epsilon \downarrow 0} \int_a^b \Im[m(x + i\epsilon)] dx$$

for all continuity points $a, b \in \mathbb{R}$ of μ . The term under the square root in $m(z)$ being negative only in the set $[(1 - \sqrt{c})^2, (1 + \sqrt{c})^2]$, the latter defines the support of the continuous part of the measure μ with density $\frac{\sqrt{((1 + \sqrt{c})^2 - x)(x - (1 - \sqrt{c})^2)}}{2c\pi x}$ at point x in the set. The case $x = 0$ brings a discontinuity in μ with weight equal to

$$\mu(\{0\}) = -\lim_{y \downarrow 0} y \Im[m(iy)] = \frac{c - 1}{2c} \pm \frac{c - 1}{2c}$$

where the sign is established by a second order development of $zm(z)$ in the neighborhood of zero.

Detailed proof. Having heuristically identified $\bar{\mathbf{Q}}(z)$, we shall now use sound mathematical tools to prove that, indeed, $\bar{\mathbf{Q}}(z)$ is a deterministic equivalent for $\mathbf{Q}(z)$ in the sense of the theorem statement. Let us first show that $\mathbb{E}[\mathbf{Q}(z)] = \bar{\mathbf{Q}}(z) + o_{\|\cdot\|}(1)$, where $o_{\|\cdot\|}(1)$ denotes a matrix term of vanishing operator norm as $n, p \rightarrow \infty$.

Convergence in mean. For mathematical convenience, we will take $z < 0$ in what follows. Since $\mathbf{Q}(z)$ and $\bar{\mathbf{Q}}(z)$ from the theorem statement are complex analytic functions for $z \notin \mathbb{R}^+$ (matrix-valued Stieltjes transforms are analytic), obtaining the convergence results on \mathbb{R}^- is equivalent to obtaining the result on all of $\mathbb{C} \setminus \mathbb{R}^+$.

We proceed in two steps by first introducing the intermediate deterministic quantities $\alpha(z) \equiv \frac{1}{n} \text{tr } \mathbb{E}[\mathbf{Q}(z)]$ and $\bar{\mathbf{Q}} \equiv (-z + \frac{1}{1+\alpha(z)})^{-1} \mathbf{I}_p$. From Lemma 2.1, we have (the argument z in $\alpha(z)$, $\mathbf{Q}(z)$ and $\bar{\mathbf{Q}}(z)$ is dropped when confusion is not possible)

$$\begin{aligned} \mathbb{E}[\mathbf{Q} - \bar{\mathbf{Q}}] &= \mathbb{E}\mathbf{Q} \left(\frac{\mathbf{I}_p}{1+\alpha} - \frac{1}{n} \mathbf{X} \mathbf{X}^\top \right) \bar{\mathbf{Q}} = \frac{\mathbb{E}[\mathbf{Q}]}{1+\alpha} \bar{\mathbf{Q}} - \frac{1}{n} \mathbb{E}[\mathbf{Q} \mathbf{X} \mathbf{X}^\top] \bar{\mathbf{Q}} \\ &= \frac{\mathbb{E}[\mathbf{Q}]}{1+\alpha} \bar{\mathbf{Q}} - \sum_{i=1}^n \frac{1}{n} \mathbb{E}[\mathbf{Q} \mathbf{x}_i \mathbf{x}_i^\top] \bar{\mathbf{Q}} = \frac{\mathbb{E}[\mathbf{Q}]}{1+\alpha} \bar{\mathbf{Q}} - \sum_{i=1}^n \mathbb{E} \left[\frac{\mathbf{Q}_{-i} \frac{1}{n} \mathbf{x}_i \mathbf{x}_i^\top}{1 + \frac{1}{n} \mathbf{x}_i^\top \mathbf{Q}_{-i} \mathbf{x}_i} \right] \bar{\mathbf{Q}} \end{aligned}$$

where we applied Lemma 2.8 to obtain the last equality and denoted $\mathbf{Q}_{-i} \equiv (\sum_{j \neq i} \frac{1}{n} \mathbf{x}_j \mathbf{x}_j^\top - z \mathbf{I}_p)^{-1}$ as previously.

Since we expect $\frac{1}{n} \mathbf{x}_i^\top \mathbf{Q}_{-i} \mathbf{x}_i$ to be close to α (as a consequence of Lemma 2.11), we rewrite

$$\frac{\mathbf{Q}_{-i} \frac{1}{n} \mathbf{x}_i \mathbf{x}_i^\top}{1 + \frac{1}{n} \mathbf{x}_i^\top \mathbf{Q}_{-i} \mathbf{x}_i} = \frac{\mathbf{Q}_{-i} \frac{1}{n} \mathbf{x}_i \mathbf{x}_i^\top}{1 + \alpha} - \frac{\mathbf{Q}_{-i} \frac{1}{n} \mathbf{x}_i \mathbf{x}_i^\top (\frac{1}{n} \mathbf{x}_i^\top \mathbf{Q}_{-i} \mathbf{x}_i - \alpha)}{(1 + \alpha)(1 + \frac{1}{n} \mathbf{x}_i^\top \mathbf{Q}_{-i} \mathbf{x}_i)}$$

so that

$$\begin{aligned} \mathbb{E}[\mathbf{Q} - \bar{\mathbf{Q}}] &= \frac{\mathbb{E}[\mathbf{Q}]}{1+\alpha} \bar{\mathbf{Q}} - \sum_{i=1}^n \frac{\mathbb{E} [\mathbf{Q}_{-i} \frac{1}{n} \mathbf{x}_i \mathbf{x}_i^\top] \bar{\mathbf{Q}}}{1+\alpha} + \sum_{i=1}^n \frac{\mathbb{E} [\mathbf{Q}_{-i} \frac{1}{n} \mathbf{x}_i \mathbf{x}_i^\top d_i] \bar{\mathbf{Q}}}{1+\alpha} \\ &= \frac{\mathbb{E}[\mathbf{Q}]}{1+\alpha} \bar{\mathbf{Q}} - \sum_{i=1}^n \frac{\mathbb{E} [\mathbf{Q}_{-i} \frac{1}{n} \mathbf{x}_i \mathbf{x}_i^\top] \bar{\mathbf{Q}}}{1+\alpha} + \frac{\mathbb{E} [\mathbf{Q}_{-i} \frac{1}{n} \mathbf{x}_i \mathbf{x}_i^\top \mathbf{D}] \bar{\mathbf{Q}}}{1+\alpha} \end{aligned}$$

where we introduced $\mathbf{D} = \text{diag}\{d_i\}_{i=1}^n$ for $d_i = \frac{1}{n} \mathbf{x}_i^\top \mathbf{Q}_{-i} \mathbf{x}_i - \alpha$, and used again Lemma 2.8 to write $\frac{\mathbf{Q}_{-i} \frac{1}{n} \mathbf{x}_i \mathbf{x}_i^\top}{1 + \frac{1}{n} \mathbf{x}_i^\top \mathbf{Q}_{-i} \mathbf{x}_i} = \mathbf{Q}_{-i} \frac{1}{n} \mathbf{x}_i \mathbf{x}_i^\top$ in the first equality. Since $\mathbb{E}[\mathbf{Q}_{-i} \mathbf{x}_i \mathbf{x}_i^\top] = \mathbb{E}[\mathbf{Q}_{-i}]$, this further reads

$$\mathbb{E}[\mathbf{Q} - \bar{\mathbf{Q}}] = \frac{1}{n} \sum_{i=1}^n (\mathbb{E}[\mathbf{Q}] - \mathbb{E}[\mathbf{Q}_{-i}]) \frac{\bar{\mathbf{Q}}}{1+\alpha} + \frac{\mathbb{E} [\frac{1}{n} \mathbf{Q} \mathbf{X} \mathbf{D} \mathbf{X}^\top] \bar{\mathbf{Q}}}{1+\alpha}.$$

Again from Lemma 2.1 and 2.8,

$$\begin{aligned} \frac{1}{n} \sum_{i=1}^n \mathbb{E}[\mathbf{Q} - \mathbf{Q}_{-i}] &= -\frac{1}{n} \sum_{i=1}^n \mathbb{E}\left[\mathbf{Q} \frac{1}{n} \mathbf{x}_i \mathbf{x}_i^\top \mathbf{Q}_{-i}\right] \\ &= -\frac{1}{n} \sum_{i=1}^n \mathbb{E}\left[\mathbf{Q} \frac{1}{n} \mathbf{x}_i \mathbf{x}_i^\top \mathbf{Q} \left(1 + \frac{1}{n} \mathbf{x}_i^\top \mathbf{Q}_{-i} \mathbf{x}_i\right)\right] \\ &= -\frac{1}{n} \mathbb{E}\left[\mathbf{Q} \frac{1}{n} \mathbf{X} \mathbf{D}_2 \mathbf{X}^\top \mathbf{Q}\right] \end{aligned}$$

where $\mathbf{D}_2 = \text{diag}\left\{1 + \frac{1}{n} \mathbf{x}_i^\top \mathbf{Q}_{-i} \mathbf{x}_i\right\}_{i=1}^n$ and thus

$$\mathbb{E}[\mathbf{Q} - \bar{\mathbf{Q}}] = -\frac{1}{n} \mathbb{E}\left[\mathbf{Q} \frac{1}{n} \mathbf{X} \mathbf{D}_2 \mathbf{X}^\top \mathbf{Q}\right] \frac{\bar{\mathbf{Q}}}{1+\alpha} + \frac{\mathbb{E}\left[\frac{1}{n} \mathbf{Q} \mathbf{X} \mathbf{D}_2 \mathbf{X}^\top \mathbf{Q}\right] \bar{\mathbf{Q}}}{1+\alpha}. \quad (\text{Eq:MPproof 2})$$

It remains to show that the right-hand side terms vanish in the large p, n limit.

For the first term, note that

$$0 \preceq \mathbf{Q} \frac{1}{n} \mathbf{X} \mathbf{D}_2 \mathbf{X}^\top \mathbf{Q} \preceq \mathbf{Q} \frac{1}{n} \mathbf{X} \mathbf{X}^\top \mathbf{Q} \max_{1 \leq i \leq n} [\mathbf{D}_2]_{ii}$$

in the order of symmetric matrices. Since $\mathbf{Q} \frac{1}{n} \mathbf{X} \mathbf{X}^\top = \mathbf{I}_p + z\mathbf{Q}$ which is of bounded operator norm (by 2), controlling $\|\mathbb{E}[\mathbf{Q} \frac{1}{n} \mathbf{X} \mathbf{D}_2 \mathbf{X}^\top \mathbf{Q}]\|$ boils down to controlling $\mathbb{E}[\max_i [\mathbf{D}_2]_{ii}]$. This can be established in various ways. From the union bound and the i.i.d. nature of the \mathbf{x}_i 's,

$$\mathbb{P}\left(\max_i [\mathbf{D}_2]_{ii} > t\right) \leq n \mathbb{P}([\mathbf{D}_2]_{11} > t).$$

Now, by Markov's inequality $\mathbb{P}(X > a) \leq \mathbb{E}[X^l]/a^l$ for every l (for $X, a > 0$) and the moment inequality in Lemma 2.11 for, say $l = 4$, $\mathbb{P}(\max_i [\mathbf{D}_2]_{ii} > t)$ may be bounded by a function decreasing as t^{-4} , for all $t > 1 + \alpha(z)$, and of order n^{-1} . Since $\mathbb{E}[X] = \int_{X>0} \mathbb{P}(X > t) dt$, we then find that $\mathbb{E}[\max_i [\mathbf{D}_2]_{ii}]$ is bounded. Alternatively, one may have used a concentration inequality argument to show the same. Consequently, due to the leading $1/n$ factor in front of the first right-hand side term of (2.14), this term vanishes as $n, p \rightarrow \infty$.

To handle the second right-hand side term in (2.14), one needs to control the norm of $\frac{1}{n} \mathbf{Q} \mathbf{X} \mathbf{D}_2 \mathbf{X}^\top \bar{\mathbf{Q}}$. This is not a symmetric matrix, but $\mathbb{E}[\mathbf{Q} - \bar{\mathbf{Q}}]$ is. We may thus rewrite (2.14) as the half-sum of itself and its transpose and we are thus left to controlling the operator norm of $\frac{1}{n} \mathbf{Q} \mathbf{X} \mathbf{D}_2 \mathbf{X}^\top \bar{\mathbf{Q}} + \frac{1}{n} \bar{\mathbf{Q}} \mathbf{X} \mathbf{D}_2 \mathbf{X}^\top \mathbf{Q}$. Using the matrix inequalities $\mathbf{A}\mathbf{B}^\top + \mathbf{B}\mathbf{A}^\top \preceq \mathbf{A}\mathbf{A}^\top + \mathbf{B}\mathbf{B}^\top$ (from $(\mathbf{A} - \mathbf{B})(\mathbf{A} - \mathbf{B})^\top \succeq 0$) and $\mathbf{A}\mathbf{B}^\top + \mathbf{B}\mathbf{A}^\top \succeq -\mathbf{A}\mathbf{A}^\top - \mathbf{B}\mathbf{B}^\top$ (from $(\mathbf{A} + \mathbf{B})(\mathbf{A} + \mathbf{B})^\top \succeq 0$), we are left to bounding the norm of

$$\mathbb{E}\left[\frac{1}{n\sqrt{n}} \mathbf{Q} \mathbf{X} \mathbf{X}^\top \mathbf{Q}\right] + \mathbb{E}\left[\frac{1}{\sqrt{n}} \bar{\mathbf{Q}} \mathbf{X} \mathbf{D}_2 \mathbf{X}^\top \bar{\mathbf{Q}}\right]$$

where the distribution of the $1/n^2$ term into $1/(n\sqrt{n})$ and $1/\sqrt{n}$ is essential. The first term above is easily seen to be of order $1/\sqrt{n}$. As for the second, using as above the moment inequality in Lemma 2.11, the concentration result of $\frac{1}{n} \operatorname{tr} \mathbf{Q}_{-i}$ around its expectation (that shall be proved with for instance Lemma 2.12 below), together with Markov's inequality, it appears to be also of order $1/\sqrt{n}$. This can be anticipated by noticing that $d_i = \frac{1}{n} \mathbf{x}_i^\top \mathbf{Q}_{-i} \mathbf{x}_i - \alpha$ fluctuates as $1/\sqrt{n}$ (by a central limit theorem argument) and thus d_i^2 is essentially of order $1/n$.

Gathering the pieces together, we thus conclude that

$$\|\mathbb{E}[\mathbf{Q}] - \bar{\mathbf{Q}}\| \rightarrow 0, \quad \text{with } \bar{\mathbf{Q}} = \left(\frac{1}{1 + \alpha(z)} - z \right)^{-1} \mathbf{I}_p.$$

Since

$$\alpha(z) = \frac{1}{n} \operatorname{tr} \mathbb{E}[\mathbf{Q}(z)] = \frac{1}{n} \operatorname{tr} \bar{\mathbf{Q}}(z) + o(1) = \frac{c}{\frac{1}{1 + \alpha(z)} - z} + o(1)$$

by defining $m(z)$ as the unique Stieltjes transform solution such that $\Im(z)\Im[m(z)] > 0$ of

$$\frac{1}{m(z)} = \frac{1}{1 + cm(z)} - z \Leftrightarrow zcm^2(z) - (1 - c - z)m(z) + 1 = 0$$

(the uniqueness is easily shown by solving the quadratic equation), we finally have $cm(z) - \alpha(z) \rightarrow 0$, which concludes the proof of (2.8).

Almost sure convergence. To now prove the almost sure convergence $\frac{1}{p} \operatorname{tr} \mathbf{A}(\mathbf{Q} - \bar{\mathbf{Q}}) \xrightarrow{a.s.} 0$ and $\mathbf{a}^\top (\mathbf{Q} - \bar{\mathbf{Q}}) \mathbf{b} \xrightarrow{a.s.} 0$, it suffices to show

$$\frac{1}{p} \operatorname{tr} \mathbf{A}(\mathbf{Q} - \mathbb{E}\mathbf{Q}) \xrightarrow{a.s.} 0, \quad \mathbf{a}^\top (\mathbf{Q} - \mathbb{E}\mathbf{Q}) \mathbf{b} \xrightarrow{a.s.} 0.$$

We will only show here the left-most convergence. This follows from either a moment or a concentration argument. The historical approach, due to [Bai and Silverstein \[2010\]](#), exploits the following martingale difference inequality.

lem:Burkholder

Lemma 2.12 (Burkholder inequality, Lemma 2.13 in [Bai and Silverstein \[2010\]](#)). *Let $\{X_i\}_{i=1}^\infty$ be a martingale difference for the increasing σ -field $\{\mathcal{F}_i\}$ and denote \mathbb{E}_k the expectation with respect to \mathcal{F}_k . Then, for $k \geq 2$, and some constant C_k only dependent on k ,*

$$\mathbb{E} \left[\left| \sum_{i=1}^n X_i \right|^k \right] \leq C_k \left(\mathbb{E} \left[\sum_{i=1}^n \mathbb{E}_{k-1}[|X_i|^2] \right]^{k/2} + \sum_{i=1}^n \mathbb{E}[|X_i|^k] \right).$$

Remark that

$$\begin{aligned} \frac{1}{p} \operatorname{tr} \mathbf{A}(\mathbf{Q} - \mathbb{E}\mathbf{Q}) &= \sum_{i=1}^n \mathbb{E}_i \left[\frac{1}{p} \operatorname{tr} \mathbf{A}\mathbf{Q} \right] - \mathbb{E}_{i-1} \left[\frac{1}{p} \operatorname{tr} \mathbf{A}\mathbf{Q} \right] \\ &= \frac{1}{p} \sum_{i=1}^n (\mathbb{E}_i - \mathbb{E}_{i-1}) [\operatorname{tr} \mathbf{A}(\mathbf{Q} - \mathbf{Q}_{-i})] \end{aligned}$$

(since $\mathbb{E}_i[\text{tr } \mathbf{A}\mathbf{Q}_{-i}] = \mathbb{E}_{i-1}[\text{tr } \mathbf{A}\mathbf{Q}_{-i}]$) for \mathcal{F}_i the σ -field generating the columns $\mathbf{x}_{i+1}, \dots, \mathbf{x}_n$ of \mathbf{X} and with the convention $\mathbb{E}_0[f(\mathbf{X})] = f(\mathbf{X})$, which forms a martingale difference sequence, we fall under the scope of Burkholder lemma. Now, from the identity $\mathbf{Q} = \mathbf{Q}_{-i} - \frac{1}{n} \frac{\mathbf{Q}_{-i}\mathbf{x}_i\mathbf{x}_i^\top \mathbf{Q}_{-i}}{1 + \frac{1}{n} \mathbf{x}_i^\top \mathbf{Q}_{-i}\mathbf{x}_i}$ (Lemma 2.8),

$$(\mathbb{E}_i - \mathbb{E}_{i-1}) \left[\frac{1}{p} \text{tr } \mathbf{A}(\mathbf{Q} - \mathbf{Q}_{-i}) \right] = -(\mathbb{E}_i - \mathbb{E}_{i-1}) \frac{\frac{1}{pn} \mathbf{x}_i^\top \mathbf{Q}_{-i} \mathbf{A} \mathbf{Q}_{-i} \mathbf{x}_i}{1 + \frac{1}{n} \mathbf{x}_i^\top \mathbf{Q}_{-i} \mathbf{x}_i}$$

which is order $O(p^{-1})$. As a consequence, from Lemma 2.12,

$$\mathbb{E} \left[\left| \frac{1}{p} \text{tr } \mathbf{A}(\mathbf{Q} - \mathbb{E}\mathbf{Q}) \right|^4 \right] = O(n^{-2}).$$

From Markov's inequality (i.e., $\mathbb{P}(|X| > t) \leq \mathbb{E}[|X|^k]/t^k$) and Borel-Cantelli lemma (i.e., $\mathbb{P}(|X_n| > t) = O(n^{-\ell})$ for some $\ell > 1$ for all $t > 0$ implies $X_n \xrightarrow{a.s.} 0$), we then conclude that

$$\frac{1}{p} \text{tr } \mathbf{A}(\mathbf{Q} - \mathbb{E}\mathbf{Q}) \xrightarrow{a.s.} 0$$

as requested. \square

Remark 2.4 (On the convergence rates). *In the course of the proofs above, we saw examples of a general concentration trend for linear statistics and quadratic forms of random matrices. We shall indeed typically have for most of the models of random matrices $\mathbf{X} \in \mathbb{R}^{n \times n}$ under study in this monograph that*

- linear statistics $\frac{1}{n} \sum_{i=1}^n f(\lambda_i(\mathbf{X}))$ for sufficiently well-behaved f (so for instance $\frac{1}{n} \text{tr } \mathbf{Q}_\mathbf{X}(z) = \frac{1}{n} \sum_i (\lambda_i(\mathbf{X}) - z)^{-1}$) converge at a speed $O(1/n)$ (their variance scales as $O(1/n^2)$). From a central-limit theorem viewpoint, this is as fast as it can get. Indeed, \mathbf{X} is maximally composed of $O(n^2)$ “degrees of freedom” and thus, by the central limit theorem, fluctuations are at most at speed $O(1/\sqrt{n^2}) = O(1/n)$.
- quadratic forms $\mathbf{a}^\top f(\mathbf{X}) \mathbf{b}$ where $f(\mathbf{X}) = \mathbf{U} \text{diag}(f(\lambda_i(\mathbf{X}))) \mathbf{U}^\top$ (in the spectral decomposition of \mathbf{X}) typically converge at a slower $O(1/\sqrt{n})$ speed.

This remark is particularly interesting as it indicates, from a statistics viewpoint that, for $\mathbf{X} \in \mathbb{R}^{p \times n}$, asymptotic approximations may gain accuracy by doubly exploiting the degrees of freedom in both the sample (n) and feature (p) direction.

Remark 2.5 (On the assumptions on \mathbf{X}). *Let us pursue here on the footnote introduced to clarify the “smooth tail condition” phrase of Theorem 2.3. The Marčenko–Pastur law has been widely generalized and several times proved using different techniques. For instance [Adamczak et al., 2011, O’Rourke et al., 2012] assume the \mathbf{X}_{ij} are “weakly” dependent in the sense that their correlation or higher order cross-moments vanish at a certain speed as $n, p \rightarrow \infty$. Alternatively, the works of Bai and Silverstein (see [Baik and Silverstein, 2006]) tend to*

assume that the entries of \mathbf{X} are not necessarily identically distributed; in this case, an additional condition on the tails $\mathbb{P}(|\mathbf{X}_{ij}| > t)$ of the probability measures of the entries (for instance a uniform bound on some moment higher than 2) is needed. In [El Karoui, 2009], El Karoui provides a first result which assumes the columns \mathbf{x}_i of $\mathbf{X} = [\mathbf{x}_1, \dots, \mathbf{x}_n]$ are independent concentrated random vectors, an assumption that we will thoroughly discuss in Section 2.7; (very) roughly speaking, concentrated random vectors $\mathbf{x} \in \mathbb{R}^p$ can be written as $\mathbf{x} = \varphi(\tilde{\mathbf{x}})$ where $\tilde{\mathbf{x}}$ has standard i.i.d. entries with either a Gaussian law or a bounded support, and $\varphi : \mathbb{R}^p \rightarrow \mathbb{R}^p$ is any 1-Lipschitz function: this assumption maintains the p degrees of freedom in \mathbf{x} (arising from $\tilde{\mathbf{x}}$) while allowing for strong correlation between the entries of \mathbf{x} . In this case, the Marčenko–Pastur law is indeed still valid if $\varphi(\mathbf{x})$ has zero mean and identity covariance.

2.2.2.2 The “Gaussian method” alternative

subsubsec:Gaussian-calculus

In [Pastur and Shcherbina, 2011], Pastur and Scherbina propose an alternative proof scheme for Theorem 2.3, based on a two-step approach: (i) a proof for Gaussian \mathbf{X} and (ii) an interpolation method to non-Gaussian \mathbf{X} ; together known as the “Gaussian method”. Although less intuitive when compared to the Bai and Silverstein’s approach presented in the previous section, this method is much more flexible as it can handle more structured random matrix models, in particular when the “guessing” part (of the ultimate deterministic equivalent $\bar{\mathbf{Q}}$ for \mathbf{Q}) of Bai-Silverstein’s method is non trivial.

The Gaussian case itself is handled in two steps (or more precisely is based on two ingredients): (i-a) convergence in means of the resolvent with Stein’s lemma, and (i-b) control of the variance with the Nash–Poicaré inequality to establish convergence (in probability or almost surely).

Convergence in mean by Stein’s lemma.

lem:Stein

Lemma 2.13 (Stein [1981]). *Let $x \sim \mathcal{N}(0, 1)$ and $f : \mathbb{R} \rightarrow \mathbb{R}$ a continuously differentiable function such that $\mathbb{E}[f'(x)] < \infty$. Then,*

$$\mathbb{E}[xf(x)] = \mathbb{E}[f'(x)]. \quad (2.15)$$

In particular, for $\mathbf{x} \sim \mathcal{N}(\mathbf{0}, \mathbf{C})$ with $\mathbf{C} \in \mathbb{R}^{p \times p}$ and $f : \mathbb{R}^p \rightarrow \mathbb{R}$ a continuously differentiable function with derivatives having at most polynomial growth with respect to p ,

$$\mathbb{E}[[\mathbf{x}]_i f(\mathbf{x})] = \sum_{j=1}^p \mathbf{C}_{ij} \mathbb{E} \left[\frac{\partial f(\mathbf{x})}{\partial [\mathbf{x}]_j} \right] \quad (2.16)$$

where $\partial/\partial[\mathbf{x}]_i$ indicates differentiation with respect to the i -th entry of \mathbf{x} .

The lemma, sometimes referred to as the integration-by-parts formula for

Gaussian variables, simply follows from

$$\begin{aligned}\mathbb{E}[xf(x)] &= \int xf(x)e^{-\frac{1}{2}x^2}dx \\ &= [-f(x)e^{-\frac{1}{2}x^2}]_{-\infty}^{\infty} + \int f'(x)e^{-\frac{1}{2}x^2}dx = \mathbb{E}[f'(x)]\end{aligned}$$

by integration by parts $\int u'v = [uv] - \int uv'$ for $u(x) = -e^{-\frac{1}{2}x^2}$ and $v(x) = f(x)$.

To exploit Lemma 2.13, let us thus assume \mathbf{X} Gaussian, i.e., $\mathbf{X}_{ij} \sim \mathcal{N}(0, 1)$. Observe that $\mathbf{Q} = \frac{1}{z} \frac{1}{n} \mathbf{X} \mathbf{X}^\top \mathbf{Q} - \frac{1}{z} \mathbf{I}_p$, so that

$$\mathbb{E}[\mathbf{Q}_{ij}] = \frac{1}{zn} \sum_{k=1}^n \mathbb{E}[\mathbf{X}_{ik} [\mathbf{X}^\top \mathbf{Q}]_{kj}] - \frac{1}{z} \delta_{ij}$$

in which $\mathbb{E}[\mathbf{X}_{ik} [\mathbf{X}^\top \mathbf{Q}]_{kj}] = \mathbb{E}[xf(x)]$ for $x = \mathbf{X}_{ik}$ and $f(x) = [\mathbf{X}^\top \mathbf{Q}]_{kj}$. Therefore, from the lemma and the fact that $\partial \mathbf{Q} = -\frac{1}{n} \mathbf{Q} \partial(\mathbf{X} \mathbf{X}^\top) \mathbf{Q}$,

$$\begin{aligned}\mathbb{E}[\mathbf{X}_{ik} [\mathbf{X}^\top \mathbf{Q}]_{kj}] &= \mathbb{E}\left[\frac{\partial[\mathbf{X}^\top \mathbf{Q}]_{kj}}{\partial \mathbf{X}_{ik}}\right] \\ &= \mathbb{E}[\mathbf{Q}_{ij}] - \mathbb{E}\left[\frac{1}{n} [\mathbf{X}^\top \mathbf{Q} \mathbf{X}]_{kk} \mathbf{Q}_{ij}\right] - \mathbb{E}\left[\frac{1}{n} [\mathbf{X}^\top \mathbf{Q}]_{ki} [\mathbf{X}^\top \mathbf{Q}]_{kj}\right].\end{aligned}$$

so that, summing over k ,

$$\begin{aligned}\frac{1}{z} \frac{1}{n} \sum_{k=1}^n \mathbb{E}[\mathbf{X}_{ik} [\mathbf{X}^\top \mathbf{Q}]_{kj}] &= \frac{1}{z} \mathbb{E}[\mathbf{Q}_{ij}] - \frac{1}{z} \frac{1}{n^2} \mathbb{E}[\mathbf{Q}_{ij} \operatorname{tr}(\mathbf{Q} \mathbf{X} \mathbf{X}^\top)] \\ &\quad - \frac{1}{z} \frac{1}{n^2} \mathbb{E}[\mathbf{Q} \mathbf{X} \mathbf{X}^\top \mathbf{Q}]_{ij}^{\text{eq:derivation_MP_law_Stein}}.\end{aligned}\tag{2.17}$$

It is not too difficult to see that the rightmost term has vanishing operator norm (of order $O(1/n)$) as $n, p \rightarrow \infty$ (see later Remark 2.6, which shows that for complex-valued Gaussian \mathbf{X} , this terms does not even appear in the derivation). Also recall that $\operatorname{tr}(\mathbf{Q} \mathbf{X} \mathbf{X}^\top) = np + zn \operatorname{tr} \mathbf{Q}$. As a result, matrix-wise, we obtain

$$\mathbb{E}[\mathbf{Q}] + \frac{1}{z} \mathbf{I}_p = \mathbb{E}[\mathbf{X}_{\cdot k} [\mathbf{X}^\top \mathbf{Q}]_{k \cdot}] = \frac{1}{z} \mathbb{E}[\mathbf{Q}] - \frac{1}{z} \frac{1}{n} \mathbb{E}[\mathbf{Q}(p + z \operatorname{tr} \mathbf{Q})] + o_{\|\cdot\|}(1).$$

As $\frac{1}{n} \operatorname{tr} \mathbf{Q}$ is expected to converge to some $m(z)$, it can be taken out of the expectation in the limit so that, gathering all terms proportional to $\mathbb{E}[\mathbf{Q}]$ on the left-hand side, we finally have

$$\mathbb{E}[\mathbf{Q}](1 - p/n - z - p/nzm(z)) = \mathbf{I}_p + o_{\|\cdot\|}(1)$$

which, taking the trace to identify $m(z)$, concludes the proof for the Gaussian case.

Almost sure convergence by Nash–Poincaré inequality. To prove the almost sure convergence of traces and bilinear forms of the resolvent in the case of Gaussian \mathbf{X} , one may then use the powerful Nash–Poincaré inequality proposed by Pastur.

lem:Nash-Poincare

Lemma 2.14 (Nash–Poincaré inequality [Pastur, 2005]). *For $\mathbf{x} \sim \mathcal{N}(\mathbf{0}, \mathbf{C})$ with $\mathbf{C} \in \mathbb{R}^{p \times p}$ and $f : \mathbb{R}^p \rightarrow \mathbb{R}$ continuously differentiable with derivatives having at most polynomial growth with respect to p ,*

$$\text{var}[f(\mathbf{x})] \leq 2 \sum_{i,j=1}^d \mathbf{C}_{ij} \mathbb{E} \left[\frac{\partial f(\mathbf{x})}{\partial x_i} \frac{\partial f(\mathbf{x})}{\partial x_j} \right].$$

In the present case, for Gaussian \mathbf{X} with $\mathbf{X}_{ij} \sim \mathcal{N}(0, 1)$,

$$\text{var} \left[\frac{1}{p} \text{tr} \mathbf{A} \mathbf{Q} \right] \leq \frac{2}{p^2} \sum_{i=1}^p \sum_{j=1}^n \mathbb{E} \left[\left| \frac{\partial \text{tr} \mathbf{A} \mathbf{Q}}{\partial \mathbf{X}_{ij}} \right|^2 \right].$$

Again using $\partial \mathbf{Q} = -\frac{1}{n} \mathbf{Q} \partial (\mathbf{X} \mathbf{X}^\top) \mathbf{Q}$, we find

$$\frac{\partial \text{tr} \mathbf{A} \mathbf{Q}}{\partial \mathbf{X}_{ij}} = -\frac{1}{n} [\mathbf{Q} \mathbf{A} \mathbf{Q} \mathbf{X} + \mathbf{Q} \mathbf{A}^\top \mathbf{Q} \mathbf{X}]_{ij}$$

so that, from $(a+b)^2 \leq 2(a^2 + b^2)$ and $\|\mathbf{A}\| = 1$,

$$\begin{aligned} \frac{2}{p^2} \sum_{i=1}^p \sum_{j=1}^n \mathbb{E} \left[\left| \frac{\partial \text{tr} \mathbf{A} \mathbf{Q}}{\partial \mathbf{X}_{ij}} \right|^2 \right] &\leq \frac{4}{p^2 n^2} (\text{tr}(\mathbf{Q} \mathbf{A} \mathbf{Q} \mathbf{X} \mathbf{X}^\top \mathbf{Q} \mathbf{A}^\top \mathbf{Q}) \\ &\quad + \text{tr}(\mathbf{Q} \mathbf{A}^\top \mathbf{Q} \mathbf{X} \mathbf{X}^\top \mathbf{Q} \mathbf{A} \mathbf{Q})) = O(n^{-2}). \end{aligned}$$

By Markov's inequality and the Borel Cantelli lemma, we thus have that $\frac{1}{p} \text{tr} \mathbf{A} (\mathbf{Q} - \mathbb{E} \mathbf{Q}) \xrightarrow{a.s.} 0$.

When it comes to evaluating the fluctuations of $\mathbf{a}^\top (\mathbf{Q} - \mathbb{E} \mathbf{Q}) \mathbf{b}$ with the same approach, it appears that $\text{var}[\mathbf{a}^\top (\mathbf{Q} - \mathbb{E} \mathbf{Q}) \mathbf{b}] = O(n^{-1})$ which is enough to ensure convergence in probability (by Markov's inequality) but not almost surely (as the Borel Cantelli lemma cannot be applied). Thus one needs to resort to evaluating a higher moment bound, such as $\mathbb{E}[|\mathbf{a}^\top (\mathbf{Q} - \mathbb{E} \mathbf{Q}) \mathbf{b}|^4]$. To this end, we may use the fact that

$$\begin{aligned} \mathbb{E}[|\mathbf{a}^\top (\mathbf{Q} - \mathbb{E} \mathbf{Q}) \mathbf{b}|^4] &= \text{var}[|\mathbf{a}^\top (\mathbf{Q} - \mathbb{E} \mathbf{Q}) \mathbf{b}|^2] + \mathbb{E}[|\mathbf{a}^\top (\mathbf{Q} - \mathbb{E} \mathbf{Q}) \mathbf{b}|^2]^2 \\ &= \text{var}[|\mathbf{a}^\top (\mathbf{Q} - \mathbb{E} \mathbf{Q}) \mathbf{b}|^2] + \text{var}[|\mathbf{a}^\top (\mathbf{Q} - \mathbb{E} \mathbf{Q}) \mathbf{b}|]^2. \end{aligned}$$

Since we know that the rightmost term is of order $O(n^{-2})$, it remains to show, again through Nash–Poincaré inequality, that $\text{var}[|\mathbf{a}^\top (\mathbf{Q} - \mathbb{E} \mathbf{Q}) \mathbf{b}|^2] = O(n^{-2})$ which is a cumbersome but easily obtained result as well.

Interpolation trick to non-Gaussian \mathbf{X} . To “interpolate” these results from Gaussian \mathbf{X} to non-Gaussian \mathbf{X} , one may then use a generalized version of Stein’s lemma to non-Gaussian distributions, for which we have the following lemma.

Lemma 2.15 (Interpolation trick, [Lytova et al., 2009, Corollary 3.1]). *For $x \in \mathbb{R}$ a random variable with zero mean and unit variance, $y \sim \mathcal{N}(0, 1)$, and f a $k + 2$ -differentiable function with bounded derivatives,*

$$\mathbb{E}[f(x)] - \mathbb{E}[f(y)] = \sum_{l=2}^k \frac{\kappa_{l+1}}{2l!} \int_0^1 \mathbb{E}[f^{(l+1)}x(t)]t^{(l-1)/2}dt + \epsilon_k$$

where κ_l is the l^{th} cumulant of x , $x(t) = \sqrt{t}x + (1 - \sqrt{t})y$, and $|\epsilon_k| \leq C_k \mathbb{E}[|x|^{k+2}] \sup_t |f^{(k+2)}(t)|$ for some constant C_k only dependent on k .

All Gaussian expectations (means and variance) in the proof above can then be expressed as their non-Gaussian form up to a sum of moment control on the derivatives of f .

rem:Stein_complex_case

Remark 2.6 (Simplification in the complex case). *The Marčenko-Pastur result presented in Theorem 2.3 is also universal with respect to the field (\mathbb{R} or \mathbb{C}) of the entries of \mathbf{X} , where the Gram matrix of interest is now \mathbf{XX}^* for \mathbf{A}^* the Hermitian conjugate (transpose conjugate) of \mathbf{A} . The resolvent is in particular now $\mathbf{Q}(z) = (\frac{1}{n}\mathbf{XX}^* - z\mathbf{I}_p)^{-1}$. More interestingly, Stein’s lemma, Lemma 2.13, is simplified in the complex case into*

$$\mathbb{E}[\mathbf{X}_{ij} f(\mathbf{X}, \mathbf{X}^*)] = \mathbb{E}\left[\frac{d}{d\bar{\mathbf{X}}_{ij}} f(\mathbf{X}, \mathbf{X}^*)\right]$$

for $f(\mathbf{X}, \mathbf{X}^*)$ a (polynomially bounded) smooth function of both \mathbf{X} and \mathbf{X}^* , and $\bar{\mathbf{X}}_{ij}$ the complex conjugate of \mathbf{X}_{ij} , where the complex derivation rules become $(d/d\bar{x})(x) = 0$ and $(d/d\bar{x})\bar{x} = 1$ (see details in [Pastur and Shcherbina, 2011]). From these identities, we in particular find that

$$\frac{d}{d\mathbf{X}_{ij}} \mathbf{XX}^* = \mathbf{E}_{ij} \mathbf{X}^*$$

for \mathbf{E}_{ij} the matrix with entry $[\mathbf{E}_{ij}]_{lm} = \delta_{il}\delta_{jm}$. This relation is more convenient to use than in the real case where

$$\frac{d}{d\mathbf{X}_{ij}} \mathbf{XX}^\top = \mathbf{E}_{ij} \mathbf{X}^\top + \mathbf{X} \mathbf{E}_{ij}^\top$$

and thus two terms instead of one appear; in recollection of the derivation above of the Marčenko-Pastur theorem in the real case with Stein’s lemma, this extra term was anticipated to vanish (see Equation (2.17)).

This remark is particularly useful when universality is anticipated (essentially for all such “first order” deterministic equivalents) and when elaborate random matrix models are to be treated. That is, in these settings, it is convenient (at least as a preliminary exploration) to assume \mathbf{X} has complex rather than real Gaussian entries.

2.2.2.3 Wigner's semi-circle law

While the Marčenko-Pastur law is at the heart of sample covariance matrix models and thus a starting point in kernel methods for machine learning, Wigner's semi-circle law concerns symmetric matrices of independent entries (over and on the diagonal) which is more akin to random graphs and will be used in this monograph almost exclusively to this purpose.⁷

The main result, again presented under the form of a deterministic equivalent for the resolvent, is as follows.

theo:semi-circle

Theorem 2.4 (By Wigner [1955]). *Let $\mathbf{X} \in \mathbb{R}^{n \times n}$ be symmetric and such that the $\mathbf{X}_{ij} \in \mathbb{R}$, $j \geq i$, are independent zero mean and unit variance random variables, with smooth tail conditions. Then, for $\mathbf{Q}(z) = (\frac{\mathbf{X}}{\sqrt{n}} - z\mathbf{I}_n)^{-1}$, as $n \rightarrow \infty$,*

$$\mathbf{Q}(z) \leftrightarrow \bar{\mathbf{Q}}(z), \quad \bar{\mathbf{Q}}(z) = m(z)\mathbf{I}_n \quad (2.18)$$

with $(z, m(z))$ the unique solution in $\mathcal{Z}(\mathbb{C} \setminus [-2, 2])$ of

$$m^2(z) + zm(z) + 1 = 0. \quad (2.19)$$

The function $m(z)$ is the Stieltjes transform of the probability measure

$$\mu(dx) = \frac{1}{2\pi} \sqrt{(4-x^2)^+} dx \quad \text{eq:semi-circle} \quad (2.20)$$

which is known as the Wigner semi-circle law.

Figure 2.3 compares the empirical spectral measure of $\frac{\mathbf{X}}{\sqrt{n}}$ defined in Theorem 2.4 with the Wigner semi-circle law (which, for a proper scaling of the axes, has a half circular shape as the name suggests), for $n = 1\,000$.

Sketch of proof of Theorem 2.4. Although not the historical proof approach due to Wigner,⁸ we propose here to follow exactly the approach detailed in the proof of the Marčenko–Pastur theorem. Only the main heuristic arguments will be presented.

Similar to the proof of the Marčenko-Pastur law with Gaussian methods in Section 2.2.2.2, observe that, for $\mathbf{Q} = (\frac{\mathbf{X}}{\sqrt{n}} - z\mathbf{I}_n)^{-1}$, we have

$$\frac{1}{\sqrt{n}} \mathbb{E}[\mathbf{X}\mathbf{Q}] = \mathbf{I}_n + z\mathbb{E}[\mathbf{Q}] \quad \text{eq:proof-in-semi-circle} \quad (2.21)$$

⁷Up to an important exception when dealing with “properly scaled kernels” in Section 4.4.

⁸Wigner's proof in [Wigner, 1955] relied on a method of moment approach: having inferred that the limiting measure should be a semi-circle, he proved via a combinatorial approach, that the successive “moments” $\frac{1}{n} \text{tr}(n^{-\frac{1}{2}} \mathbf{X})^k$ for $k = 1, 2, \dots$ must converge, as $n \rightarrow \infty$, to the moments of the semi-circle measure $\int t^k \mu(dt)$. However, this method is only useful if indeed the limiting measure can be guessed. In the Marčenko-Pastur case of Theorem 2.3, the limiting measure μ is less obvious to infer.

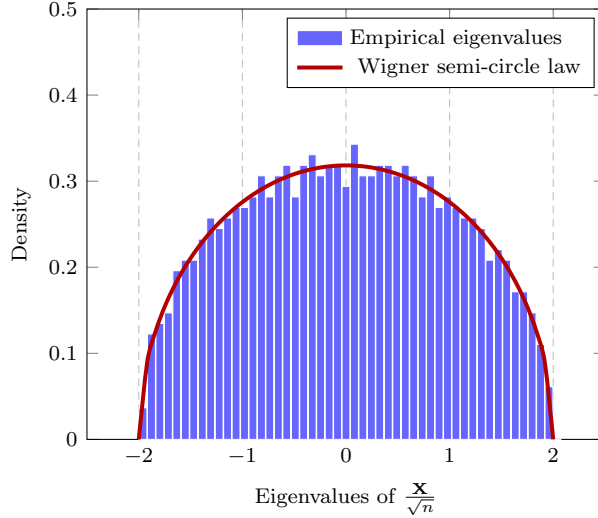


Figure 2.3: Histogram of the empirical spectral measure of $\frac{\mathbf{X}}{\sqrt{n}}$ versus the Wigner semi-circle law, for $n = 1\,000$. [\[Link to code\]](#)

`fig:semi-circle-law`

so that by Lemma 2.13 and the fact that $\partial \mathbf{Q} = -\frac{1}{\sqrt{n}} \mathbf{Q} \partial \mathbf{X} \mathbf{Q}$,

$$\begin{aligned}\mathbb{E}[\mathbf{Q}_{ij}] &= \frac{1}{z} \frac{1}{\sqrt{n}} \sum_{k=1}^n \mathbb{E}[\mathbf{X}_{ik} \mathbf{Q}_{kj}] - \frac{1}{z} \delta_{ij} \\ &= \frac{1}{z} \frac{1}{\sqrt{n}} \sum_{k=1}^n \mathbb{E} \left[\frac{\partial \mathbf{Q}_{kj}}{\partial \mathbf{X}_{ik}} \right] - \frac{1}{z} \delta_{ij} \\ &= -\frac{1}{z} \frac{1}{n} \sum_{k=1}^n \mathbb{E}[\mathbf{Q}_{ki} \mathbf{Q}_{kj} + \mathbf{Q}_{kk} \mathbf{Q}_{ij}] - \frac{1}{z} \delta_{ij} \\ &= -\frac{1}{z} \frac{1}{n} \mathbb{E}[\mathbf{Q}_{ij}^2 + \mathbf{Q}_{ij} \operatorname{tr} \mathbf{Q}] - \frac{1}{z} \delta_{ij}\end{aligned}$$

which can be summarized in matrix form as

$$\mathbb{E}[\mathbf{Q}] \simeq -\frac{1}{z} \frac{1}{n} \mathbb{E}[\mathbf{Q}^2] - \frac{1}{z} \mathbb{E}[\mathbf{Q}] m(z) \underset{(2.22)}{\overset{\text{eq:proof-in-semi-circle-2}}{\mathbf{I}_n}}$$

where we used the fact that the random quantity $\frac{1}{n} \operatorname{tr} \mathbf{Q} \simeq \frac{1}{n} \operatorname{tr} \mathbb{E} \mathbf{Q}$ is expected to converge to some deterministic $m(z)$ and can therefore be taken out of the expectation.

Since the first term on the right-hand side asymptotically vanishes (of operator norm order $O(1/n)$) as $n, p \rightarrow \infty$, we reach

$$\mathbb{E}[\mathbf{Q}] \simeq -\frac{1}{z} \left(1 + \frac{1}{z} \frac{1}{n} \operatorname{tr} \mathbb{E} \mathbf{Q} \right)^{-1} \mathbf{I}_n$$

which, after taking the trace and using $m(z) \simeq \frac{1}{n} \text{tr } \mathbb{E}\mathbf{Q}(z)$, gives the limiting formula

$$m^2(z) + zm(z) + 1 = 0.$$

The solution of the above equation is explicitly given by

$$m(z) = \frac{1}{2}(-z + \sqrt{z^2 - 4})$$

with $\sqrt{\cdot}$ chosen as the branch of the square root for which $m(z)$ is a Stieltjes transform. Taking the imaginary part and the limit when $z \rightarrow x \in \mathbb{R}$ gives the form of the density $\mu(dx)$ in the theorem statement. \square

The result could of course also be obtained using Bai and Silverstein's method used in our first proof of the Marčenko-Pastur theorem.

2.2.3 Large dimensional sample covariance matrices and generalized semi-circles

The Marčenko–Pastur and semi-circle theorems have long been the gold-standard in both theoretical and applied random matrix theory, in the sense that most mathematical studies and practical results concerned the Wishart and Wigner random matrix models.⁹ But the assumption of data \mathbf{X} with i.i.d., let alone standard Gaussian, entries is often limiting. In statistics where one is interested in the correlation \mathbf{XX}^\top , it is expected that the columns $\mathbf{x}_i \in \mathbb{R}^p$ of \mathbf{X} exhibit a correlation structure and be non-necessarily independent (in particular when they are samples from a time series). In graph theory, where the affinity matrix $\mathbf{X} \in \mathbb{R}^{n \times n}$ is the central object of study, one may wish to model graph patterns, degree heterogeneity, community structures, etc., which go against the i.i.d. Bernoulli assumption of so-called Erdős–Rényi graphs.

This section introduces generalizations of these results, to a level that is convenient to machine learning applications. In particular, in order to model the existence of classes within the data, \mathbf{X} will often be subdivided into subblocks that can be identified with each class.

2.2.3.1 Large sample covariance matrix model and its generalizations

Our first result generalizes the Marčenko–Pastur law to sample covariance matrices and is originally due to a long line of works by Bai and Silverstein [Silverstein and Bai, 1995].

theo:baisilverstein95

Theorem 2.5 (Sample covariance matrix, from Silverstein and Bai [1995]). *Let $\mathbf{X} = \mathbf{C}^{\frac{1}{2}}\mathbf{Z} \in \mathbb{R}^{p \times n}$ with symmetric nonnegative definite $\mathbf{C} \in \mathbb{R}^{p \times p}$ of bounded*

⁹Among those studies are generalizations of the data model assumptions to matrices \mathbf{X} with non independent entries [Pajor and Pastur, 2009], studies and characterization of the limiting spectra [Silverstein and Choi, 1995], deeper considerations on the local behavior of eigenvalues [Johnstone, 2001, 2008], etc.

operator norm (i.e., $\limsup_p \|\mathbf{C}\| < \infty$),¹⁰ $\mathbf{Z} \in \mathbb{R}^{p \times n}$ having i.i.d. zero mean and unit variance entries with smooth tail conditions. Then, as $n, p \rightarrow \infty$ with $p/n \rightarrow c \in (0, \infty)$, letting $\mathbf{Q}(z) = (\frac{1}{n} \mathbf{X} \mathbf{X}^\top - z \mathbf{I}_p)^{-1}$ and $\tilde{\mathbf{Q}}(z) = (\frac{1}{n} \mathbf{X}^\top \mathbf{X} - z \mathbf{I}_n)^{-1}$, we have

$$\begin{aligned}\mathbf{Q}(z) &\leftrightarrow \tilde{\mathbf{Q}}(z) = -\frac{1}{z} (\mathbf{I}_p + \tilde{m}_p(z) \mathbf{C})^{-1} \\ \tilde{\mathbf{Q}}(z) &\leftrightarrow \bar{\tilde{\mathbf{Q}}}(z) = \tilde{m}_p(z) \mathbf{I}_n\end{aligned}$$

where $(z, \tilde{m}_p(z))$ is the unique solution in $\mathcal{Z}(\mathbb{C} \setminus \mathbb{R}^+)$ of

$$\tilde{m}_p(z) = \left(-z + \frac{1}{n} \text{tr } \mathbf{C} (\mathbf{I}_p + \tilde{m}_p(z) \mathbf{C})^{-1} \right)^{-1}.$$

In particular, if $\mu_{\mathbf{C}} \rightarrow \nu$ as $p \rightarrow \infty$, then $\mu_{\frac{1}{n} \mathbf{X} \mathbf{X}^\top} \xrightarrow{\text{a.s.}} \mu$, $\mu_{\frac{1}{n} \mathbf{X}^\top \mathbf{X}} \xrightarrow{\text{a.s.}} \tilde{\mu}$ as $p, n \rightarrow \infty$ where $\mu, \tilde{\mu}$ are the unique measures having Stieltjes transforms $m(z)$ and $\tilde{m}(z)$, respectively, with

$$m(z) = \frac{1}{c} \tilde{m}(z) + \frac{1-c}{cz}, \quad \tilde{m}(z) = \left(-z + c \int \frac{t \nu(dt)}{1 + \tilde{m}(z)t} \right)^{-1}.$$

A few remarks are in order to better understand the statement of the theorem.

Remark 2.7 (On the implicit statement). As opposed to Theorem 2.3, the statement of the theorem is here implicit in the sense that μ is only defined through $m_\mu(z)$, itself implicitly defined as the solution of a fixed-point equation. The main reason for the explicit nature of Theorem 2.3 is that Equation (2.13), which provides the connection between $m(z)$ and a function of itself, boils down to a quadratic equation in $m(z)$ which can be solved and from which Theorem 2.1 can be applied. Due to the presence of \mathbf{C} , in the present situation, the equivalent to (2.13) will here maintain an implicit form. This will hold true for almost all generalizations of the Marčenko–Pastur theorem to be introduced in this monograph.

rem:fixed_point

Remark 2.8 (Numerical evaluation of $m(z)$). Due to its implicit nature, determining $m(z)$ for $z \in \mathbb{C} \setminus \mathbb{R}^+$ requires to solve an implicit equation. Using contraction and analyticity arguments, it can be shown that the standard fixed-point algorithm converges, i.e.,

$$m(z) = \lim_{\ell \rightarrow \infty} m^{(\ell)}(z)$$

for $\tilde{m}^{(0)}(z) = 0$ (say) and, for $\ell \geq 0$, $m^{(\ell)}(z) = \frac{1}{c} \tilde{m}^{(\ell)}(z) + \frac{1-c}{cz}$, $\tilde{m}^{(\ell+1)}(z) = (-z + c \int \frac{t \nu(dt)}{1 + \tilde{m}^{(\ell)}(z)t})^{-1}$.

¹⁰In the original article [Silverstein and Bai, 1995], the constraint on the bounded norm of $\|\mathbf{C}\|$ is relaxed and unnecessary. Yet, this complicates the proof and is never of actual use for the purpose of this monograph.

One must be careful here that, since $m(z)$ is not formally defined for $z \in \text{supp}(\mu)$, the above argument does not hold in this set. In practice, trying to solve for $m(z)$ with $z \in \text{supp}(\mu)$ numerically leads to a non-converging $m^{(\ell)}(z)$ sequence. This, in passing, can be used in practice to actually determine the support $\text{supp}(\mu)$ as the set of z 's for which the above algorithm does not converge.

In practice, when evaluating $m(z)$ close to the real axis (say for $z = x + i\epsilon$, $|\epsilon| \ll 1$), the convergence can appear to be quite slow for $x \in \text{supp}(\mu)$. A convenient workaround is to sequentially evaluate $m(z)$ for all z 's of the form $x + i\epsilon$, starting from some $z_0 = x_0 + i\epsilon$ with $x_0 \notin \text{supp}(\mu)$, then moving on to $z_1 = (x_0 + \epsilon') + i\epsilon$, then $z_2 = (x_0 + 2\epsilon') + i\epsilon$, etc., (for some $\epsilon' > 0$ small) and systematically initializing the fixed-point iterations at position z_i with the value $m(z_{i-1})$. This way, the z_i 's for which $\Re[z_i] \in \text{supp}(\mu)$ are initialized closed to the (non real) solution.

rem:drawing_mu

Remark 2.9 (Drawing μ). As shall be seen in Section 2.3, the limiting measure μ in Theorem 2.5 admits a density, which, from the inverse Stieltjes transform formula in Theorem 2.1 and Remark 2.8 above, can be approximated by solving for $m(z)$ with $z \in \mathbb{R} + i\epsilon$ for some $\epsilon > 0$ small (say $\epsilon = 10^{-5}$) and retrieving the density at x as $\frac{1}{\pi} \Im[m(x + i\epsilon)]$.

This procedure however only allows for a numerical approximation (rather than theoretical evaluation) of μ and of its support (in particular, the support consists approximately in all values of x 's such that $|\frac{1}{\pi} \Im[m(x + i\epsilon)]| \sim \epsilon \ll 1$). Section 2.3 will go beyond this naive approach and provide an exact determination of both $\lim_{z \rightarrow x \in \mathbb{R}^*} m(x)$ and the support of μ .

Figure 2.4 depicts the empirical versus limiting measure of $\mu_{\frac{1}{n}\mathbf{XX}^\top}$ for \mathbf{C} having three distinct and evenly numerous eigenvalues. In this particular setting, the limiting spectrum is akin to Marčenko–Pastur shaped connected components. For sufficiently distinct eigenvalues of \mathbf{C} , these components are disjoint (top) while for close eigenvalues they tend to merge (middle), while for $n < p$ a Dirac mass at zero is observed and the eigenvalues spread out even further (bottom).

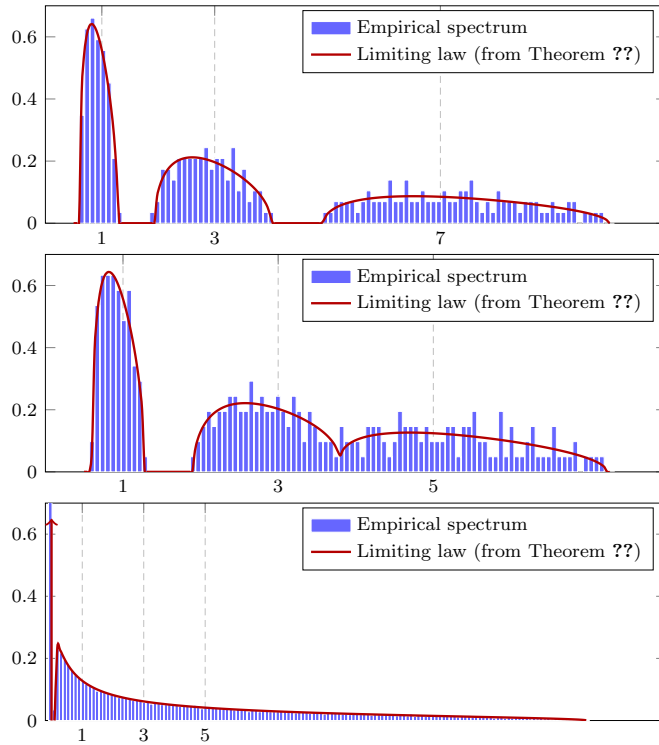


Figure 2.4: Histogram of the eigenvalues of $\frac{1}{n} \mathbf{X} \mathbf{X}^\top$ with $n = 3000$, for $p = 300$ and \mathbf{C} having spectral measure $\mu_{\mathbf{C}} = \frac{1}{3}(\delta_1 + \delta_3 + \delta_7)$ (**top**), $\mu_{\mathbf{C}} = \frac{1}{3}(\delta_1 + \delta_3 + \delta_5)$ (**middle**) and $p = 4500$ with $\mu_{\mathbf{C}} = \frac{1}{3}(\delta_1 + \delta_3 + \delta_5)$ (**bottom**). [\[Link to code\]](#) Fig. baisilverstein95

Remark 2.10 (Deterministic equivalent for $\mu_{\frac{1}{n}\mathbf{XX}^\top}$). *The convergence result $\mu_{\frac{1}{n}\mathbf{XX}^\top} \xrightarrow{\text{a.s.}} \mu$ in Theorem 2.5 imposes that there exists a limit ν to which $\mu_{\mathbf{C}}$ converges as $p \rightarrow \infty$: this may not be practically meaningful. In generalized versions of Theorem 2.5 (see e.g., Theorem 2.7 below), even if the spectral measure of the covariance matrices are to converge, $\mu_{\frac{1}{n}\mathbf{XX}^\top}$ may not have a limit.*

One may instead consider the deterministic equivalent μ_p for $\mu_{\frac{1}{n}\mathbf{XX}^\top}$ which is a sequence of probability measures, such that $\text{dist}(\mu_{\frac{1}{n}\mathbf{XX}^\top}, \mu_p) \xrightarrow{\text{a.s.}} 0$ for some distance between distributions (for instance, such that $\mu_{\frac{1}{n}\mathbf{XX}^\top} - \mu_p \xrightarrow{\text{a.s.}} 0$ vaguely) as $n, p \rightarrow \infty$.

Practically speaking, since the data dimension p is in general a fixed quantity and \mathbf{C} a given covariance matrix (rather than specific values in a growing sequence of p 's and \mathbf{C} 's), one will always consider that the “effective” limiting measure ν actually coincides with (or is “frozen” to) $\mu_{\mathbf{C}} = \frac{1}{p} \sum_{i=1}^p \delta_{\lambda_i(\mathbf{C})}$.

Sketch of proof of Theorem 2.5. The proof of Theorem 2.5 generally follows the same line of arguments as that of Theorem 2.3. The main difference is that

(2.12) here becomes

$$\frac{1}{n} \mathbf{x}_i^\top \bar{\mathbf{Q}} \mathbf{A} \mathbf{Q} \mathbf{x}_i = \frac{\frac{1}{n} \mathbf{x}_i^\top \bar{\mathbf{Q}} \mathbf{A} \mathbf{Q}_{-i} \mathbf{x}_i}{1 + \frac{1}{n} \mathbf{x}_i^\top \mathbf{Q}_{-i} \mathbf{x}_i} \simeq \frac{\frac{1}{n} \operatorname{tr} \bar{\mathbf{Q}} \mathbf{A} \mathbf{Q}_{-i} \mathbf{C}}{1 + \frac{1}{n} \operatorname{tr} \mathbf{Q}_{-i} \mathbf{C}}$$

where we used the fact that, denoting $\mathbf{x}_i = \mathbf{C}^{\frac{1}{2}} \mathbf{z}_i$ for \mathbf{z}_i the i -th column of \mathbf{Z} having i.i.d. zero mean and unit variance entries, by Lemma 2.11,

$$\frac{1}{n} \mathbf{x}_i^\top \mathbf{Q}_{-i} \mathbf{x}_i = \frac{1}{n} \mathbf{z}_i^\top \mathbf{C}^{\frac{1}{2}} \mathbf{Q}_{-i} \mathbf{C}^{\frac{1}{2}} \mathbf{z}_i \simeq \frac{1}{n} \operatorname{tr} \mathbf{Q}_{-i} \mathbf{C}.$$

Again with Lemma 2.9 and the fact that $\frac{1}{n} \operatorname{tr} \mathbf{Q}_{-i} \mathbf{C} \leq \|\mathbf{C}\| \frac{1}{n} \operatorname{tr} \mathbf{Q}_{-i}$, we obtain the approximation

$$\frac{1}{n} \operatorname{tr} (\mathbf{F} + z \mathbf{I}_p) \bar{\mathbf{Q}} \mathbf{A} \mathbf{Q} \simeq \frac{\frac{1}{n} \operatorname{tr} \mathbf{C} \bar{\mathbf{Q}} \mathbf{A} \mathbf{Q}}{1 + \frac{1}{n} \operatorname{tr} \mathbf{Q} \mathbf{C}}$$

with $\mathbf{F}(z) = \bar{\mathbf{Q}}^{-1}(z)$ the sought-for deterministic equivalent, which then must admit the form

$$\mathbf{F}(z) \simeq \frac{\mathbf{C}}{1 + \frac{1}{n} \operatorname{tr} \mathbf{Q} \mathbf{C}} - z \mathbf{I}_p$$

for the previous approximation to hold. Ultimately, taking $\mathbf{A} = \mathbf{C}$ in $\frac{1}{n} \operatorname{tr} \mathbf{A}(\mathbf{Q} - \bar{\mathbf{Q}}) \xrightarrow{a.s.} 0$ we deduce

$$\frac{1}{n} \operatorname{tr} \mathbf{C} \mathbf{Q} \simeq \frac{1}{n} \operatorname{tr} \mathbf{C} \bar{\mathbf{Q}} \simeq \frac{1}{n} \operatorname{tr} \mathbf{C} \left(-z \mathbf{I}_p + \frac{\text{Eq:SCM}^{-1} \text{proof_fixed_point}}{1 + \frac{1}{n} \operatorname{tr} \mathbf{C} \bar{\mathbf{Q}}} \right) \quad (2.23)$$

or equivalently

$$\tilde{m}_p(z) = \left(-z + \frac{1}{n} \operatorname{tr} \mathbf{C} (\mathbf{I}_p + \tilde{m}_p(z) \mathbf{C})^{-1} \right)^{-1}$$

if we denote $\tilde{m}_p(z) = -\frac{1}{z} (1 + \frac{1}{n} \operatorname{tr} \mathbf{C} \bar{\mathbf{Q}}(z))^{-1}$, as requested. Note that we implicitly used here the fact that $\|\mathbf{C}\|$ is bounded.

With the deterministic equivalent for \mathbf{Q} in hand, the deterministic equivalent for $\tilde{\mathbf{Q}}$ follows from the direct observation that $\tilde{\mathbf{Q}} = \frac{1}{z} \frac{1}{n} \mathbf{X}^\top \mathbf{Q} \mathbf{X} - \frac{1}{z} \mathbf{I}_n$ so that

$$\begin{aligned} \mathbb{E}[\tilde{\mathbf{Q}}]_{ij} &= \frac{1}{z} \frac{1}{n} \mathbb{E}[\mathbf{x}_i^\top \mathbf{Q} \mathbf{x}_j] - \frac{1}{z} \delta_{ij} = \frac{1}{z} \mathbb{E} \left[\frac{\frac{1}{n} \mathbf{x}_i^\top \mathbf{Q}_{-i} \mathbf{x}_j}{1 + \frac{1}{n} \mathbf{x}_i^\top \mathbf{Q}_{-i} \mathbf{x}_i} \right] - \frac{1}{z} \delta_{ij} \\ &\simeq -\frac{1}{z} \left(1 + \frac{1}{n} \operatorname{tr} \mathbf{C} \bar{\mathbf{Q}} \right)^{-1} \delta_{ij} = \tilde{m}_p(z) \delta_{ij}. \end{aligned}$$

□

Remark 2.11 (On singular population covariance). *It is interesting to note from Theorem 2.5 that, if the population covariance \mathbf{C} contains some zero eigenvalues, for example if $\mu_{\mathbf{C}} \rightarrow \nu$ as $p \rightarrow \infty$ with*

$$\nu(dx) = (1 - c_\nu)\delta_0(x) + \tilde{\nu}(dx)$$

for $c_\nu \in (0, 1)$ and $\int \tilde{\nu}(dx) = c_\nu$, then (as properly shown in [Silverstein and Choi, 1995]) $\tilde{\mu}(\{0\}) = \max(0, 1 - cc_\nu)$ which further implies

$$\mu(\{0\}) = \begin{cases} 1 - c_\nu & \text{if } cc_\nu \leq 1 \\ 1 - c^{-1} & \text{if } cc_\nu > 1. \end{cases}$$

This differs from the systematic $\mu(\{0\}) = \max(0, 1 - c^{-1})$ in the Marčenko-Pastur scenario, and takes into consideration the intrinsic dimension $c_\nu p$ of the random vector $\mathbf{C}^{\frac{1}{2}}\mathbf{z}_i \in \mathbb{R}^p$.

When the data $\mathbf{X} = [\mathbf{x}_1, \dots, \mathbf{x}_n]$ arise from a time series, or when each data sample is weighted by an independent coefficient (as shall be seen in Section 3.3 on robust statistical methods), the sample covariance matrix model is not sufficiently expressive but can be generalized to the *bi-correlated* model

$$\frac{1}{n} \mathbf{C}^{\frac{1}{2}} \mathbf{Z} \tilde{\mathbf{C}} \mathbf{Z}^\top \mathbf{C}^{\frac{1}{2}}.$$

for $\mathbf{C} \in \mathbb{R}^{p \times p}$ and $\tilde{\mathbf{C}} \in \mathbb{R}^{n \times n}$ two nonnegative definite matrices and \mathbf{Z}_{ij} i.i.d. random variables with zero mean and unit variance. In particular, for \mathbf{Z} Gaussian and $\tilde{\mathbf{C}}^{\frac{1}{2}}$ Toeplitz (i.e., such that $[\tilde{\mathbf{C}}^{\frac{1}{2}}]_{ij} = \alpha_{|i-j|}$ for some sequence $\alpha_0, \dots, \alpha_{n-1}$), the columns of $\mathbf{Z} \tilde{\mathbf{C}}^{\frac{1}{2}}$ model a first order auto-regressive process [Hamilton, 1994].¹¹

For this model, we have the following theorem.

Theorem 2.6 (Bi-correlated model, from Paul and Silverstein [2009]). *Let $\mathbf{Z} \in \mathbb{R}^{p \times n}$ be a random matrix with i.i.d. zero mean, unit variance and smooth tail entries, and $\mathbf{C} \in \mathbb{R}^{p \times p}$, $\tilde{\mathbf{C}} \in \mathbb{R}^{n \times n}$ be symmetric nonnegative definite matrices with bounded operator norm. Then, as $n, p \rightarrow \infty$ with $p/n \rightarrow c \in (0, \infty)$, letting $\mathbf{Q}(z) = (\frac{1}{n} \mathbf{C}^{\frac{1}{2}} \mathbf{Z} \tilde{\mathbf{C}} \mathbf{Z}^\top \mathbf{C}^{\frac{1}{2}} - z \mathbf{I}_p)^{-1}$ and $\tilde{\mathbf{Q}}(z) = (\frac{1}{n} \tilde{\mathbf{C}}^{\frac{1}{2}} \mathbf{Z}^\top \mathbf{C} \mathbf{Z} \tilde{\mathbf{C}}^{\frac{1}{2}} - z \mathbf{I}_n)^{-1}$, we have*

$$\begin{aligned} \mathbf{Q}(z) \leftrightarrow \bar{\mathbf{Q}}(z) &= -\frac{1}{z} \left(\mathbf{I}_p + \tilde{\delta}_p(z) \mathbf{C} \right)^{-1} \\ \tilde{\mathbf{Q}}(z) \leftrightarrow \bar{\tilde{\mathbf{Q}}}(z) &= -\frac{1}{z} \left(\mathbf{I}_n + \delta_p(z) \tilde{\mathbf{C}} \right)^{-1} \end{aligned}$$

¹¹In passing, Toeplitz matrices involved in time series analyses also exhibit interesting large dimensional behavior. In [Gray, 2006], Gray shows that, under some decay condition on the sequence α_n , their spectral behavior is the same as that of equivalent *circulant* matrices, the latter having the nice property to be diagonalizable in the Fourier basis: the asymptotic eigenvalues of the Toeplitz matrix are in particular the coefficients of the discrete Fourier transform of the series $\alpha_0, \alpha_1, \dots$

with $(z, \delta_p(z)), (z, \tilde{\delta}_p(z)) \in \mathcal{Z}(\mathbb{C} \setminus \mathbb{R}^+)$ unique solutions to

$$\delta_p(z) = \frac{1}{n} \operatorname{tr} \mathbf{C} \bar{\mathbf{Q}}(z), \quad \tilde{\delta}_p(z) = \frac{1}{n} \operatorname{tr} \tilde{\mathbf{C}} \bar{\mathbf{Q}}(z).$$

In particular, if $\mu_{\mathbf{C}} \rightarrow \nu$ and $\mu_{\tilde{\mathbf{C}}} \rightarrow \tilde{\nu}$, then $\mu_{\frac{1}{n} \mathbf{C}^{\frac{1}{2}} \mathbf{Z} \tilde{\mathbf{C}} \mathbf{Z}^T \mathbf{C}^{\frac{1}{2}}} \rightarrow \mu$ and $\mu_{\frac{1}{n} \tilde{\mathbf{C}}^{\frac{1}{2}} \mathbf{Z}^T \mathbf{C} \mathbf{Z} \tilde{\mathbf{C}}^{\frac{1}{2}}} \rightarrow \tilde{\mu}$ where $\mu, \tilde{\mu}$ are defined by their Stieltjes transforms $m(z)$ and $\tilde{m}(z)$ given by

$$m(z) = -\frac{1}{z} \int \frac{\nu(dt)}{1 + \tilde{\delta}(z)t}, \quad \tilde{m}(z) = -\frac{1}{z} \int \frac{\tilde{\nu}(dt)}{1 + \delta(z)t}$$

where $(\delta, \tilde{\delta})$ are solutions to

$$\delta(z) = -\frac{c}{z} \int \frac{t\nu(dt)}{1 + \tilde{\delta}(z)t}, \quad \tilde{\delta}(z) = -\frac{1}{z} \int \frac{t\tilde{\nu}(dt)}{1 + \delta(z)t}.$$

Sketch of proof of Theorem 2.6. For simplicity and readability, only the case where both \mathbf{C} and $\tilde{\mathbf{C}}$ are diagonal is presented here. In this case, similar to the decomposition performed in Theorem 2.5, one has the following symmetric re-expression of $\mathbf{Q}(z)$ and $\tilde{\mathbf{Q}}(z)$

$$\begin{aligned} \mathbf{Q}(z) &= \left(\frac{1}{n} \sum_{i=1}^n \mathbf{C}^{\frac{1}{2}} \tilde{\mathbf{y}}_i (\mathbf{C}^{\frac{1}{2}} \tilde{\mathbf{y}}_i)^T - z \mathbf{I}_p \right)^{-1} \\ \tilde{\mathbf{Q}}(z) &= \left(\frac{1}{n} \sum_{i=1}^n \tilde{\mathbf{C}}^{\frac{1}{2}} \mathbf{y}_i (\tilde{\mathbf{C}}^{\frac{1}{2}} \mathbf{y}_i)^T - z \mathbf{I}_n \right)^{-1} \end{aligned}$$

where we denote $\tilde{\mathbf{y}}_i \in \mathbb{R}^p$ the i -th column of $\mathbf{Z} \tilde{\mathbf{C}}^{\frac{1}{2}}$ and $\mathbf{y}_i \in \mathbb{R}^n$ the i -th column of $\mathbf{Z}^T \mathbf{C}^{\frac{1}{2}}$ so that, for \mathbf{C} and $\tilde{\mathbf{C}}$ both diagonal, one has $\tilde{\mathbf{y}}_i = \tilde{\mathbf{C}}_{ii}^{\frac{1}{2}} \mathbf{z}_i$ and $\mathbf{y}_i = \mathbf{C}_{ii}^{\frac{1}{2}} \tilde{\mathbf{z}}_i$ with $\mathbf{z}_i \in \mathbb{R}^p$ the i -th column and $\tilde{\mathbf{z}}_i \in \mathbb{R}^n$ the i -th row of $\mathbf{Z} \in \mathbb{R}^{p \times n}$.

As a consequence, with $\bar{\mathbf{Q}}(z) = \mathbf{F}(z)^{-1}$ and $\bar{\tilde{\mathbf{Q}}}(z) = \tilde{\mathbf{F}}(z)^{-1}$, one obtains again with Lemma 2.8 that

$$\begin{aligned} \mathbf{Q}(z) - \bar{\mathbf{Q}}(z) &= \mathbf{Q}(z) \left(\mathbf{F}(z) + z \mathbf{I}_p - \frac{1}{n} \sum_{i=1}^n \mathbf{C}^{\frac{1}{2}} \tilde{\mathbf{y}}_i (\mathbf{C}^{\frac{1}{2}} \tilde{\mathbf{y}}_i)^T \right) \bar{\mathbf{Q}}(z) \\ &= \mathbf{Q}(\mathbf{F} + z \mathbf{I}_p) \bar{\mathbf{Q}} - \frac{1}{n} \sum_{i=1}^n \frac{\mathbf{Q}_{-i} \mathbf{C}^{\frac{1}{2}} \tilde{\mathbf{C}}_{ii} \mathbf{z}_i \mathbf{z}_i^T \mathbf{C}^{\frac{1}{2}} \bar{\mathbf{Q}}}{1 + \frac{1}{n} \mathbf{C}_{ii} \mathbf{z}_i^T \mathbf{C}^{\frac{1}{2}} \mathbf{Q}_{-i} \mathbf{C}^{\frac{1}{2}} \mathbf{z}_i} \\ \tilde{\mathbf{Q}}(z) - \bar{\tilde{\mathbf{Q}}}(z) &= \tilde{\mathbf{Q}}(z) \left(\tilde{\mathbf{F}}(z) + z \mathbf{I}_n - \frac{1}{n} \sum_{i=1}^p \tilde{\mathbf{C}}^{\frac{1}{2}} \mathbf{y}_i (\tilde{\mathbf{C}}^{\frac{1}{2}} \mathbf{y}_i)^T \right) \bar{\tilde{\mathbf{Q}}}(z) \\ &= \tilde{\mathbf{Q}}(\tilde{\mathbf{F}} + z \mathbf{I}_n) \bar{\tilde{\mathbf{Q}}} - \frac{1}{n} \sum_{i=1}^p \frac{\tilde{\mathbf{Q}}_{-i} \tilde{\mathbf{C}}^{\frac{1}{2}} \mathbf{C}_{ii} \tilde{\mathbf{z}}_i \tilde{\mathbf{z}}_i^T \tilde{\mathbf{C}}^{\frac{1}{2}} \bar{\tilde{\mathbf{Q}}}}{1 + \frac{1}{n} \tilde{\mathbf{C}}_{ii} \tilde{\mathbf{z}}_i^T \tilde{\mathbf{C}}^{\frac{1}{2}} \tilde{\mathbf{Q}}_{-i} \tilde{\mathbf{C}}^{\frac{1}{2}} \tilde{\mathbf{z}}_i} \end{aligned}$$

where we denote $\mathbf{Q}_{-i}(z) \equiv \left(\frac{1}{n} \sum_{j \neq i} \mathbf{C}^{\frac{1}{2}} \tilde{\mathbf{C}}_{jj} \mathbf{z}_j \mathbf{z}_j^T \mathbf{C}^{\frac{1}{2}} - z \mathbf{I}_p \right)^{-1}$ and symmetrically $\tilde{\mathbf{Q}}_{-i}(z) \equiv \left(\frac{1}{n} \sum_{j \neq i} \tilde{\mathbf{C}}^{\frac{1}{2}} \mathbf{C}_{jj} \tilde{\mathbf{z}}_j \tilde{\mathbf{z}}_j^T \tilde{\mathbf{C}}^{\frac{1}{2}} - z \mathbf{I}_n \right)^{-1}$ which are independent of \mathbf{z}_i and $\tilde{\mathbf{z}}_i$, respectively.

With this independence of \mathbf{Q}_{-i} on \mathbf{z}_i and $\tilde{\mathbf{Q}}_{-i}$ on $\tilde{\mathbf{z}}_i$, one deduces again with Lemma 2.11 that

$$\begin{aligned} \frac{1}{n} \tilde{\mathbf{C}}_{ii} \mathbf{z}_i^\top \mathbf{C}^{\frac{1}{2}} \mathbf{Q}_{-i} \mathbf{C}^{\frac{1}{2}} \mathbf{z}_i - \frac{1}{n} \tilde{\mathbf{C}}_{ii} \operatorname{tr}(\mathbf{Q}_{-i} \mathbf{C}) &\xrightarrow{a.s.} 0 \\ \frac{1}{n} \mathbf{C}_{ii} \tilde{\mathbf{z}}_i^\top \tilde{\mathbf{C}}^{\frac{1}{2}} \tilde{\mathbf{Q}}_{-i} \tilde{\mathbf{C}}^{\frac{1}{2}} \tilde{\mathbf{z}}_i - \frac{1}{n} \mathbf{C}_{ii} \operatorname{tr}(\tilde{\mathbf{Q}}_{-i} \tilde{\mathbf{C}}) &\xrightarrow{a.s.} 0 \end{aligned}$$

so that $\mathbf{F}(z)$ and $\tilde{\mathbf{F}}(z)$ must take the following forms

$$\begin{aligned} \mathbf{F}(z) &= \frac{1}{n} \sum_{i=1}^n \frac{\tilde{\mathbf{C}}_{ii}}{1 + \tilde{\mathbf{C}}_{ii} \frac{1}{n} \operatorname{tr}(\mathbf{Q}_{-i} \mathbf{C})} \mathbf{C} - z \mathbf{I}_p \simeq \frac{1}{n} \sum_{i=1}^n \frac{\tilde{\mathbf{C}}_{ii}}{1 + \tilde{\mathbf{C}}_{ii} \frac{1}{n} \operatorname{tr} \mathbf{C} \bar{\mathbf{Q}}} \mathbf{C} - z \mathbf{I}_p \\ \tilde{\mathbf{F}}(z) &= \frac{1}{n} \sum_{i=1}^p \frac{\mathbf{C}_{ii}}{1 + \mathbf{C}_{ii} \frac{1}{n} \operatorname{tr}(\tilde{\mathbf{Q}}_{-i} \tilde{\mathbf{C}})} \tilde{\mathbf{C}} - z \mathbf{I}_n \simeq \frac{1}{n} \sum_{i=1}^p \frac{\mathbf{C}_{ii}}{1 + \mathbf{C}_{ii} \frac{1}{n} \operatorname{tr} \tilde{\mathbf{C}} \bar{\mathbf{Q}}} \tilde{\mathbf{C}} - z \mathbf{I}_n \end{aligned}$$

which, by denoting $\delta_p(z) = \frac{1}{n} \operatorname{tr} \mathbf{C} \bar{\mathbf{Q}}(z)$ and $\tilde{\delta}_p(z) = \frac{1}{n} \operatorname{tr} \tilde{\mathbf{C}} \bar{\mathbf{Q}}(z)$, can be further reduced to

$$\begin{aligned} \bar{\mathbf{Q}}(z) &= \mathbf{F}(z)^{-1} \simeq -\frac{1}{z} \left(\mathbf{I}_p - \frac{1}{z} \frac{1}{n} \sum_{i=1}^n \frac{\tilde{\mathbf{C}}_{ii}}{1 + \tilde{\mathbf{C}}_{ii} \delta_p(z)} \mathbf{C} \right)^{-1} \\ \bar{\tilde{\mathbf{Q}}}(z) &= \tilde{\mathbf{F}}(z)^{-1} \simeq -\frac{1}{z} \left(\mathbf{I}_n - \frac{1}{z} \frac{1}{n} \sum_{i=1}^p \frac{\mathbf{C}_{ii}}{1 + \mathbf{C}_{ii} \tilde{\delta}_p(z)} \tilde{\mathbf{C}} \right)^{-1}. \end{aligned}$$

To eventually close the loop and obtain the relation on $(\delta_p, \tilde{\delta}_p)$, one may plug in the above approximation into the definition of δ_p and $\tilde{\delta}_p$ to obtain the following symmetric equation

$$\begin{aligned} \delta_p(z) &\simeq -\frac{1}{z} \frac{1}{n} \sum_{i=1}^p \frac{\mathbf{C}_{ii}}{1 - \frac{1}{z} \frac{1}{n} \sum_{j=1}^n \frac{\tilde{\mathbf{C}}_{jj}}{1 + \tilde{\mathbf{C}}_{jj} \delta_p(z)}} \\ \tilde{\delta}_p(z) &\simeq -\frac{1}{z} \frac{1}{n} \sum_{i=1}^n \frac{\tilde{\mathbf{C}}_{ii}}{1 - \frac{1}{z} \frac{1}{n} \sum_{j=1}^p \frac{\mathbf{C}_{jj}}{1 + \mathbf{C}_{jj} \tilde{\delta}_p(z)}} \end{aligned}$$

which retrieves the expressions of Theorem 2.6. \square

It is quite interesting to note the almost perfect symmetry in the equations for the resolvent and co-resolvent in the bi-correlated model. From a machine learning perspective, wherein $\mathbf{X} = \mathbf{C}^{\frac{1}{2}} \mathbf{Z} \tilde{\mathbf{C}}^{\frac{1}{2}}$ are the observed data, this symmetry between “space” and “time” correlations, or between the sample covariance matrix \mathbf{XX}^\top and the kernel matrix $\mathbf{X}^\top \mathbf{X}$, will often allow for a natural connection between results in the spatial (e.g., PCA, subspace methods) and in the temporal (classification, regression) domains.

These kernel methods involve matrices of the type $\mathbf{K} = \{\frac{1}{p} \mathbf{x}_i^\top \mathbf{x}_j\}_{i,j=1}^n = \frac{1}{p} \mathbf{X}^\top \mathbf{X}$ (inner product kernels) or $\mathbf{K} = \{\frac{1}{p} \|\mathbf{x}_i - \mathbf{x}_j\|^2\}_{i,j=1}^n$ (distance kernels).¹²

¹²The prefactor $1/p$ is necessary under our notation framework to ensure that the spectrum of \mathbf{K} remains of order $O(1)$ as p, n increase.

Assuming, as is the basic setting in a multi-class machine learning classification context, that the vectors \mathbf{x}_i arise from a mixture model, the following generalization of Theorem 2.5 will thus be of practical relevance.

theo:SCMmixture

Theorem 2.7 (Sample covariance of k -class mixture models, from [Benaych-Georges and Couillet, 2016]). *Let $\mathbf{X} = [\mathbf{X}^{(1)}, \dots, \mathbf{X}^{(k)}] \in \mathbb{R}^{p \times n}$ with $\mathbf{X}^{(a)} = [\mathbf{x}_1^{(a)}, \dots, \mathbf{x}_{n_a}^{(a)}] \in \mathbb{R}^{p \times n_a}$ and $\mathbf{x}_i^{(a)} = \mathbf{C}_a^{\frac{1}{2}} \mathbf{z}_i^{(a)}$ for $\mathbf{z}_i^{(a)}$ a vector with i.i.d. zero mean, unit variance and smooth tail entries. Then, as $n_a, p \rightarrow \infty$ in such a way that k is fixed and $n_a/n \rightarrow c_a \in (0, 1)$, $p/n \rightarrow c \in (0, \infty)$ for $a \in \{1, \dots, k\}$, letting $\mathbf{Q}(z) = (\frac{1}{n} \mathbf{X} \mathbf{X}^T - z \mathbf{I}_p)^{-1}$ and $\bar{\mathbf{Q}}(z) = (\frac{1}{n} \mathbf{X}^T \mathbf{X} - z \mathbf{I}_n)^{-1}$, we have*

$$\begin{aligned}\mathbf{Q}(z) &\leftrightarrow \bar{\mathbf{Q}}(z) = -\frac{1}{z} \left(\mathbf{I}_p + \sum_{a=1}^k c_a \tilde{g}_a(z) \mathbf{C}_a \right)^{-1} \\ \tilde{\mathbf{Q}}(z) &\leftrightarrow \bar{\tilde{\mathbf{Q}}}(z) = \text{diag}\{\tilde{g}_a(z) \mathbf{1}_{n_a}\}_{a=1}^k\end{aligned}$$

with $(z, \tilde{g}_a(z))$, $a \in \{1, \dots, k\}$, the unique solutions in $\mathcal{Z}(\mathbb{C} \setminus \mathbb{R}^+)$ of

$$\tilde{g}_a(z) = -\frac{1}{z} (1 + g_a(z))^{-1}, \quad g_a(z) = -\frac{1}{z} \frac{1}{n} \text{tr} \mathbf{C}_a \left(\mathbf{I}_p + \sum_{b=1}^k c_b \tilde{g}_b(z) \mathbf{C}_b \right)^{-1}.$$

Sketch of proof of Theorem 2.7. Similar to the proof of Theorem 2.5, we obtain, with the initial guess $\bar{\mathbf{Q}}(z) = \mathbf{F}^{-1}(z)$ that

$$\mathbf{Q} - \bar{\mathbf{Q}} = \mathbf{Q} \left(\mathbf{F} + z \mathbf{I}_p - \frac{1}{n} \sum_{a=1}^k \sum_{i=1}^{n_a} \mathbf{x}_i^{(a)} (\mathbf{x}_i^{(a)})^T \right) \bar{\mathbf{Q}}$$

which, different from the proof of Theorem 2.5, contains the (first) sum over a due to the different class covariance \mathbf{C}_a . To establish $\frac{1}{n} \text{tr} \mathbf{A}(\mathbf{Q} - \bar{\mathbf{Q}}) \xrightarrow{a.s.} 0$, one must have

$$\frac{1}{n} \text{tr}(\mathbf{F} + z \mathbf{I}_p) \bar{\mathbf{Q}} \mathbf{A} \mathbf{Q} - \frac{1}{n} \sum_{a=1}^k \sum_{i=1}^{n_a} \frac{1}{n} (\mathbf{x}_i^{(a)})^T \bar{\mathbf{Q}} \mathbf{A} \mathbf{Q} \mathbf{x}_i^{(a)} \xrightarrow{a.s.} 0.$$

Applying Lemma 2.8 to remove the dependence in \mathbf{Q} of $\mathbf{x}_i^{(a)}$, together with Lemma 2.9, we deduce

$$\frac{1}{n} \sum_{a=1}^k \sum_{i=1}^{n_a} \frac{1}{n} (\mathbf{x}_i^{(a)})^T \bar{\mathbf{Q}} \mathbf{A} \mathbf{Q} \mathbf{x}_i^{(a)} \simeq \sum_{a=1}^k \frac{n_a}{n} \frac{\frac{1}{n} \text{tr} \mathbf{C}_a \bar{\mathbf{Q}} \mathbf{A} \bar{\mathbf{Q}}}{1 + \frac{1}{n} \text{tr} \bar{\mathbf{Q}} \mathbf{C}_a}$$

so that \mathbf{F} must be written as the following sum over a

$$\mathbf{F} \simeq \sum_{a=1}^k c_a \frac{\mathbf{C}_a}{1 + \frac{1}{n} \text{tr} \bar{\mathbf{Q}} \mathbf{C}_a} - z \mathbf{I}_p.$$

To close the loop, we take $\mathbf{A} = \mathbf{C}_b$ for $b \in \{1, \dots, k\}$ to establish

$$\begin{aligned}\frac{1}{n} \operatorname{tr} \mathbf{C}_b \mathbf{Q} &\simeq \frac{1}{n} \operatorname{tr} \mathbf{C}_b \bar{\mathbf{Q}} \equiv g_b(z) \simeq \frac{1}{n} \operatorname{tr} \mathbf{C}_b \left(-z \mathbf{I}_p + \sum_{a=1}^k c_a \frac{\mathbf{C}_a}{1 + \frac{1}{n} \operatorname{tr} \bar{\mathbf{Q}} \mathbf{C}_a} \right)^{-1} \\ &\equiv -\frac{1}{z} \frac{1}{n} \operatorname{tr} \mathbf{C}_b \left(\mathbf{I}_p + \sum_{a=1}^k c_a \tilde{g}_a(z) \mathbf{C}_a \right)\end{aligned}$$

where we denote $\tilde{g}_a(z) \equiv -\frac{1}{z} \left(1 + \frac{1}{n} \operatorname{tr} \bar{\mathbf{Q}} \mathbf{C}_a \right)^{-1} = -\frac{1}{z} (1 + g_a(z))^{-1}$, as desired.

To derive the deterministic equivalent for $\tilde{\mathbf{Q}}$ from that for \mathbf{Q} , we use again the fact that $\tilde{\mathbf{Q}} = \frac{1}{z} \frac{1}{n} \mathbf{X}^\top \mathbf{Q} \mathbf{X} - \frac{1}{z} \mathbf{I}_n$ and therefore, indexing the set $\{1, \dots, n\}$ as $\{(1)1, \dots, (1)n_1, \dots, (k)1, \dots, (k)n_k\}$,

$$\begin{aligned}\mathbb{E}[\mathbf{Q}]_{(a)i,(b)j} &= \frac{1}{z} \frac{1}{n} \mathbb{E} \left[(\mathbf{x}_i^{(a)})^\top \mathbf{Q} \mathbf{x}_j^{(b)} \right] - \frac{1}{z} \delta_{(a)i,(b)j} \\ &\simeq -\frac{1}{z} \left(1 + \frac{1}{n} \operatorname{tr} \bar{\mathbf{Q}} \mathbf{C}_a \right)^{-1} \delta_{(a)i,(b)j} = \tilde{g}_a(z) \delta_{(a)i,(b)j}\end{aligned}$$

concludes the proof of Theorem 2.7. \square

With some further control, Theorem 2.7 may in fact be extended to $k = n$, i.e., each data vector \mathbf{x}_i has its own, possibly distinct, covariance matrix, as shown in [Wagner et al., 2012]. When the covariance matrices are diagonal, this is then equivalent to letting \mathbf{X} have a *variance profile*, i.e., the \mathbf{X}_{ij} 's are then all independent with zero mean and variance $\sigma_{ij}^2 \equiv [\mathbf{C}_i]_{jj}$ (with $\mathbf{C}_i = \mathbb{E}[\mathbf{x}_i \mathbf{x}_i^\top]$), a setting studied in depth in [Hachem et al., 2007] but originally found in [Girko, 2001].

The application of a variance profile to random matrices with independent entries finds an even more relevant application to Wigner matrices, as detailed next.

2.2.3.2 Generalized semi-circle law with a variance profile

Similar to the large sample covariance matrix model, generalizations also exist for the Wigner semi-circle law in Theorem 2.4. In the following theorem, a variance profile for the entries of the symmetric random matrix is taken into account.

theo:deformed-semi-circle

Theorem 2.8 (From Pastur and Shcherbina [2011]). *Let $\mathbf{X} \in \mathbb{R}^{n \times n}$ be symmetric and such that \mathbf{X}_{ij} , $j \geq i$, is of zero mean, bounded variance $\operatorname{var}[\mathbf{X}_{ij}] = \sigma_{ij}^2$, and smooth tail condition. Then, for $\mathbf{Q}(z) = (\frac{\mathbf{X}}{\sqrt{n}} - z \mathbf{I}_n)^{-1}$, we have*

$$\mathbf{Q}(z) \leftrightarrow \bar{\mathbf{Q}}(z), \quad \bar{\mathbf{Q}}(z) = (-z \mathbf{I}_n + \operatorname{diag}\{\tilde{g}_i(z)\}_{i=1}^n)^{-1} \quad \text{eq:deformed-semi-circle-Q} \quad (2.24)$$

with $(z, g_i(z)) \in \mathcal{Z}(\mathbb{C} \setminus \mathbb{R}^+)$, $i \in \{1, \dots, n\}$, uniquely determined by

$$g_i(z) = \frac{1}{n} \operatorname{tr} \left(\operatorname{diag}(\sigma_{ij}^2)_{j=1}^n \bar{\mathbf{Q}}(z) \right).$$

Sketch of proof of Theorem 2.8. The proof of Theorem 2.8 differs from that of Theorem 2.4 in the application of Lemma 2.13. Taking into consideration the variance $\mathbb{E}[\mathbf{X}_{ik}^2] = \sigma_{ik}^2$, Equation (2.21) gives

$$\begin{aligned}\mathbb{E}[\mathbf{Q}_{ij}] &= \frac{1}{z} \frac{1}{\sqrt{n}} \sum_{k=1}^n \mathbb{E}[\mathbf{X}_{ik}^2] \mathbb{E}\left[\frac{\partial \mathbf{Q}_{kj}}{\partial \mathbf{X}_{ik}}\right] - \frac{1}{z} \delta_{ij} \\ &= -\frac{1}{z} \frac{1}{n} \sum_{k=1}^n \sigma_{ik}^2 \mathbb{E}[\mathbf{Q}_{ki} \mathbf{Q}_{kj} + \mathbf{Q}_{kk} \mathbf{Q}_{ij}] - \frac{1}{z} \delta_{ij} \\ &= -\frac{1}{z} \frac{1}{n} \mathbb{E}[\mathbf{Q} \Sigma_i \mathbf{Q}]_{ij} - \frac{1}{z} \frac{1}{n} \mathbb{E}[\text{tr}(\Sigma_i \mathbf{Q}) \mathbf{Q}_{ij}] - \frac{1}{z} \delta_{ij}\end{aligned}$$

with $\Sigma_i \equiv \text{diag}(\sigma_{ik}^2)_{k=1}^n$ so that $\|\Sigma_i\| = O(1)$ uniformly over all i .

Note that the semi-circle law in Theorem 2.4 is indeed a special case with $\sigma_{ij}^2 = \delta_{ij}$ and $\Sigma_i = \mathbf{I}_n$. As a consequence, similar to the term $\frac{1}{n} \mathbb{E}[\mathbf{Q}^2]$ in (2.22), the first term on the right-hand side vanishes as $n, p \rightarrow \infty$. Following the same reasoning, the random variable $\frac{1}{n} \text{tr} \Sigma_i \mathbf{Q}(z)$ essentially plays the role of $\frac{1}{n} \text{tr} \mathbf{Q}(z)$ in (2.22) and is expected to converge to some deterministic $g_i(z) \equiv \frac{1}{n} \text{tr} \Sigma_i \mathbf{Q}(z)$ which can be taken out of the expectation. This gives, in matrix form

$$\mathbb{E}[\mathbf{Q}(z)] \simeq -\frac{1}{z} \text{diag}\{g_i(z)\}_{i=1}^n \mathbb{E}[\mathbf{Q}(z)] - \frac{1}{z} \mathbf{I}_n.$$

Solving this equation for $\mathbb{E}[\mathbf{Q}(z)] \simeq \bar{\mathbf{Q}}(z)$ we conclude the proof of Theorem 2.8. \square

Theorem 2.8 plays a significant role in the study of random graphs, with applications to community detection in large graphs or networks. We shall come back to this model in more details later in Section 7.1.

Summarizing, this lengthy first technical section provided the necessary technical ingredients, along with several key results to obtain the (large n, p) spectrum of “data samples” from the population statistics. In Section 2.4, we will seek to go backwards, trying to infer the population statistics from the observed *empirical* spectrum of the samples. To this end though, subtle supplementary results on the limiting spectra must be introduced. This is the objective of the next section.

The subsequent section, possibly the most technical of the monograph, may be skipped at first read, the main ideas of Section 2.4 being understandable if some results are admitted. Yet, for a clear and rigorous treatment of the limitations of statistical inference, the reader will need to grasp the notions of Section 2.3 below.

2.3 Advanced spectrum considerations for sample covariances

`sec:advanced_spectrum`

As opposed to the Marčenko–Pastur result, Theorem 2.3, the generalized sample covariance matrix model of Theorem 2.5 (and beyond) only provides a characterization of the limiting spectral measure μ of $\mu_n^{\frac{1}{n}} \mathbf{X} \mathbf{X}^\top$ (or a deterministic equivalent μ_p for it) through its Stieltjes transform $m(z)$ for $z \in \mathbb{C} \setminus \mathbb{R}^+$ (respectively, through a sequence $m_p(z)$ of Stieltjes transforms) which itself assumes an implicit form. Since the Stieltjes transform inversion formula (Theorem 2.1) involves the limit of $m(z)$ for $z \rightarrow x \in \mathbb{R}$, the sole information about $m(z)$ for all $z \in \mathbb{C} \setminus \mathbb{R}^+$ does not immediately quantifies the measure μ .

From a theoretical standpoint, one may wonder whether μ admits a density as in the Marčenko–Pastur case and, if so, whether one can determine this density and its exact support. As recalled in Remarks 2.8 and 2.9, the density of μ (provided it exists) can be “numerically depicted” by solving for $m(z)$ with z close to, but formally *away* from, the real axis. We aim here at a more theoretical and precise characterization of μ .

From a practical standpoint, a fundamental byproduct of this characterization is the introduction of the function $z \mapsto -\frac{1}{m(z)}$ which plays a key role in statistical inference. Indeed, we shall see in Section 2.4 and the many applications of Chapter 3 that statistical information related to the population covariance \mathbf{C} (such as functionals of its eigenvalues, projections on its eigenvectors) can be accessed from the measurement matrix \mathbf{X} by means of a complex integral method involving the change of variable $z \mapsto -\frac{1}{m(z)}$.

2.3.1 Limiting spectrum

`sec:limiting_spectrum`

In [Silverstein and Choi, 1995] (generalized later in [Couillet and Hachem, 2014] with a more systematic approach), the authors prove that, for any measure ν , the limiting measures μ and $\tilde{\mu}$ introduced in Theorem 2.5 indeed have a density with a well-defined support.¹³

¹³It may come as very surprising but very few works in the random matrix literature have actually studied the actual spectrum of the limiting measure μ of advanced random matrix models. The few exceptions are the works [Silverstein and Choi, 1995, Couillet and Hachem, 2014] which study the defining equation of the Stieltjes transform m_μ of μ associated to the sample covariance matrix models $\mathbf{C}^{\frac{1}{2}} \mathbf{X} \mathbf{X}^\top \mathbf{C}^{\frac{1}{2}}$ and $\mathbf{C}^{\frac{1}{2}} \mathbf{X} \tilde{\mathbf{C}} \mathbf{X}^\top \mathbf{C}^{\frac{1}{2}}$, respectively, as well as the very extensive work [Ajanki et al., 2019] on the defining equation of m_μ attached to generalized Wigner models (for instance the deformed semi-circle law for Wigner models with a variance profile, Theorem 2.8). The small number of these studies testifies of the greater importance of the Stieltjes transform relation defining m_μ over the measure μ itself which, both in theory and in practice, is quite often of lesser interest.

2.3.1.1 Density and support of μ (and $\tilde{\mu}$)

Precisely, recall that $\mu = \frac{1}{c}\tilde{\mu} + (1 - \frac{1}{c})\delta_0$ (with δ_x the Dirac mass at x) with $\tilde{\mu}$ defined by its Stieltjes transform $\tilde{m}(z)$ solution to

$$\tilde{m}(z) = \left(-z + c \int \frac{t\nu(dt)}{1+t\tilde{m}(z)} \right)^{-1}.$$

This functional expression has the interesting key property of being invertible, in the sense that it is formally equivalent to

$$z = -\frac{1}{\tilde{m}(z)} + c \int \frac{t\nu(dt)}{1+t\tilde{m}(z)}.$$

As a consequence, the function $\tilde{m}(\cdot) : \mathbb{C} \setminus \text{supp}(\tilde{\mu}) \rightarrow \mathbb{C}$, $z \mapsto \tilde{m}(z)$ admits the functional inverse

$$\begin{aligned} z(\cdot) &: \tilde{m}(\mathbb{C} \setminus \text{supp}(\tilde{\mu})) \rightarrow \mathbb{C} \\ \tilde{m} &\mapsto -\frac{1}{\tilde{m}} + c \int \frac{t\nu(dt)}{1+t\tilde{m}}. \end{aligned}$$

The important point to notice here is that $z(\cdot)$, seen as the functional inverse of $\tilde{m}(\cdot)$, is only defined on the domain $\tilde{m}(\mathbb{C} \setminus \text{supp}(\tilde{\mu}))$. Yet, formally, this function could be *extended* to all values $\tilde{m} \in \mathbb{C}$ such that $0 \notin 1 + \tilde{m} \cdot \text{supp}(\nu)$ (i.e., all values that do not cancel the denominator $1 + t\tilde{m}$ for some $t \in \text{supp}(\nu)$).

The idea of Silverstein and Choi, originally expressed in the seminal work of Marčenko and Pastur [Marcenko and Pastur, 1967], is twofold:

- **Outside the support.** (i) the Stieltjes transform $m_\mu(x) = \int (t-x)^{-1}\mu(dt)$ of a measure μ is an increasing function on its restriction to $x \in \mathbb{R} \setminus \text{supp}(\mu)$ (it has positive derivative there), hence (ii) so must be its functional inverse $x(\cdot)$ on its restriction to $m_\mu(\mathbb{R} \setminus \text{supp}(\mu))$, (iii) consequently, if $x(\cdot)$ admits an extension to some domain \mathcal{S} with $m_\mu(\mathbb{R} \setminus \text{supp}(\mu)) \subset \mathcal{S} \subset \mathbb{R}$, $x(\cdot)$ *should* only be increasing on $m_\mu(\mathbb{R} \setminus \text{supp}(\mu))$;¹⁴ (iv) therefore, the complementary $\mathbb{R} \setminus \text{supp}(\mu)$ to the support of μ can be determined as the image by $x(\cdot)$ of all increasing sections of $x(\cdot)$. See Figure 2.5, commented below, for a simplified visual understanding.

In our setting, this thus defines the support of the limiting measure μ of $\mu_{\frac{1}{n}\mathbf{X}\mathbf{X}^\top}$.

- **In the support.** Inside this support, one then needs to determine the density of μ . To this end, one may first prove the existence of $\tilde{m}^\circ(x) = \lim_{\epsilon \rightarrow 0} \tilde{m}(x + i\epsilon)$. Upon existence, since $\Im[\tilde{m}^\circ(x)] > 0$ for $x \in \text{supp}(\mu)$,

¹⁴Formally, it is clear that all decreasing sections of (the extended version of) $x(\cdot)$ cannot correspond to the functional inverse of a Stieltjes transform. It is less evident though that all increasing sections do correspond to the inverse of a Stieltjes transform; this was settled in [Silverstein and Choi, 1995].

dominated convergence can be applied on the defining equation for $\tilde{m}(z)$ to find that $\tilde{m}^\circ(x)$ is a solution *with positive imaginary part* of

$$\tilde{m}^\circ(x) = \left(-x + c \int \frac{t\nu(dt)}{1 + \tilde{m}^\circ(x)t} \right)^{-1}$$

which is then shown to be unique.

These arguments are formally stated in the following theorem.

Theorem 2.9 (From Silverstein and Choi [1995]). *Under the setting of Theorem 2.5 with $\mu_C \rightarrow \nu$, define*

$$\begin{aligned} x(\cdot) : \mathbb{R} \setminus \{\tilde{m} \mid (-1/\tilde{m}) \in \text{supp}(\nu)\} &\rightarrow \mathbb{R} \\ \tilde{m} &\mapsto -\frac{1}{\tilde{m}} + c \int \frac{t\nu(dt)}{1 + \tilde{m}t}. \end{aligned}$$

Then, $\tilde{\mu}$ has a density \tilde{f} on $\mathbb{R} \setminus \{0\}$ and

- for $y \in \text{supp}(\tilde{\mu})$, $\tilde{f}(y) = \frac{1}{\pi} \Im[\tilde{m}^\circ(y)]$ with $\tilde{m}^\circ(y)$ the unique solution with positive imaginary part of $x(\tilde{m}^\circ(y)) = y$;
- the support $\text{supp}(\tilde{\mu}) \setminus \{0\}$, and thus $\text{supp}(\mu) \setminus \{0\}$, is defined by

$$\begin{aligned} \text{supp}(\mu) \setminus \{0\} \\ = \mathbb{R} \setminus \{x(\tilde{m}) \mid (-1/\tilde{m}) \in \mathbb{R} \setminus \{\text{supp}(\nu) \cup \{0\}\} \text{ and } x'(\tilde{m}) > 0\}. \end{aligned}$$

Figure 2.5 depicts the function $x(\tilde{m})$ for $\tilde{m} < 0$ under a similar setting as Figure 2.4 with ν composed of three Dirac masses. The top display shows four increasing regions of $x(\cdot)$, thus corresponding (on the y -axis) to four connected components of $\mathbb{R} \setminus \text{supp}(\mu)$. The complementary, depicted in blue on the y -axis, corresponds to the (three) connected components of $\text{supp}(\mu)$. The middle display only shows three growing regions for $x(\cdot)$, thus restricting the support of μ to two connected components. Analogously, in the bottom display there is only one growing region for $x(\cdot)$ (close to the y -axis from above), which now corresponds to a single connected component for $\text{supp}(\mu) \setminus \{0\}$. This is in accordance with the observations made in Figure 2.4, when altering either ν or c .

A careful analysis of the function $x(\cdot)$ actually reveals additional interesting properties:

1. the restriction of $x(\cdot)$ to its growing sections is a growing function. This follows from the fact that, there, $x(\cdot)$ is the functional inverse of $\tilde{m}(\cdot)$ restricted to $\mathbb{R} \setminus \text{supp}(\mu)$ which is a growing function.
2. in the case of Figure 2.5, since ν is discrete, $x(\cdot)$ presents asymptotes at each $-1/t$, $t \in \text{supp}(\nu)$. Thus, from the previous item, $\text{supp}(\mu)$ is here determined by the union $\bigcup_k [\tilde{m}_k^-, \tilde{m}_k^+]$ for $\tilde{m}_1^- < \tilde{m}_1^+ < \tilde{m}_2^- < \dots$ the successive values of \tilde{m} such that $x'(\tilde{m}) = 0$. This remark may however not hold for ν with continuous support. Detailed conditions for this characterization to hold are discussed in [Coutillet and Hachem, 2014].

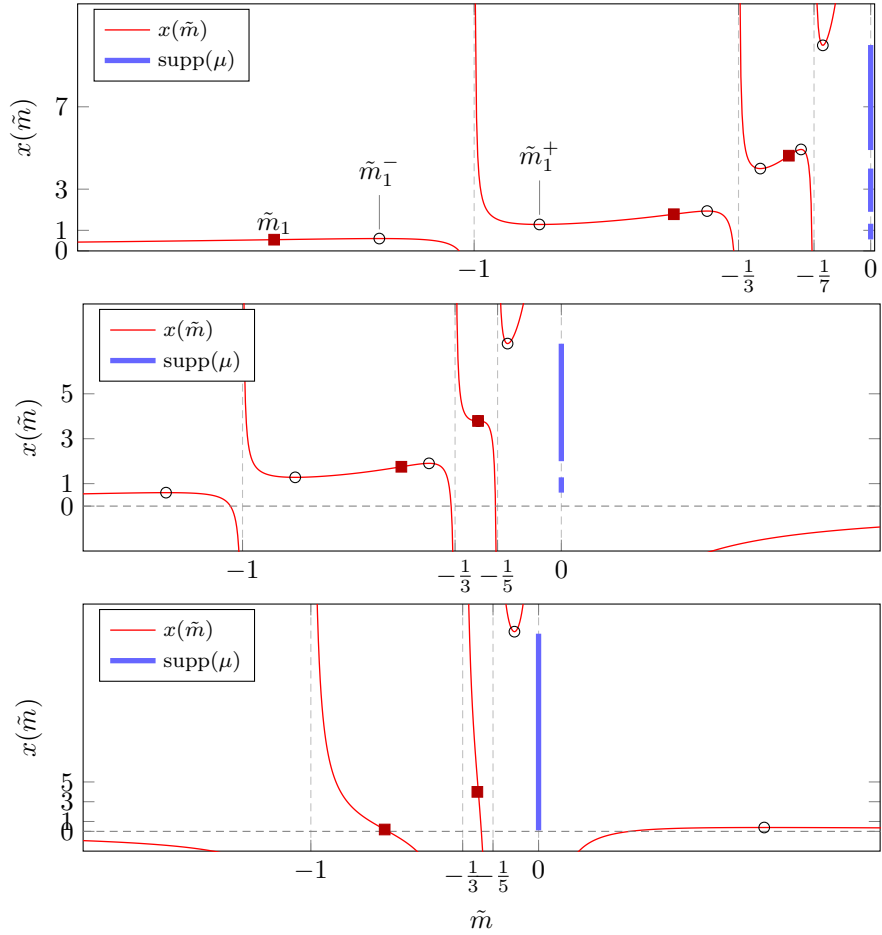


Figure 2.5: $x(\tilde{m})$ for $-1/\tilde{m} \in \mathbb{R} \setminus \text{supp}(\nu)$, with $\nu = \frac{1}{3}(\delta_1 + \delta_3 + \delta_7)$ (**top**) and $\nu = \frac{1}{3}(\delta_1 + \delta_3 + \delta_5)$ (**middle**), $c = 1/10$ in both cases, and $\nu = \frac{1}{3}(\delta_1 + \delta_3 + \delta_5)$ with $c = 2$ (**bottom**). Local extrema are marked by circles, inflection points by squares. The support of μ can be read on the vertical axes. [Link to code]

item:contour_position

3. the derivative of $x(\cdot)$ is given by

$$x'(\tilde{m}) = \frac{1}{\tilde{m}^2} - c \int \frac{t^2 \nu(dt)}{(1+t\tilde{m})^2}$$

and thus $\tilde{m}^2 x'(\tilde{m})$ converges to $1 - c$ as $|\tilde{m}| \rightarrow \infty$, while $x(\tilde{m}) \rightarrow 0$. Thus $x(\cdot)$ is either decreasing or increasing at $\pm\infty$ depending on whether $c < 1$ or $c > 1$. In particular, the pre-image by $x(\cdot)$ of 0^+ is $-\infty$ if $c < 1$ (top and middle displays of Figure 2.5) and some positive value if $c > 1$ (bottom display of Figure 2.5): this remark is fundamental for the next section.

2.3.1.2 Variable change: relating $\text{supp}(\nu)$ and $\text{supp}(\mu)$.

An important side consequence of the study above of $z(\cdot)$ (and its restriction $x(\cdot)$ to the real axis) is that the function

$$\begin{aligned}\gamma : \mathbb{C} \setminus \{\text{supp}(\mu) \cup \{0\}\} &\rightarrow \mathbb{C} \\ z = z(\tilde{m}) &\mapsto -\frac{1}{\tilde{m}} \quad \text{eq:injective-map-z}\end{aligned}$$
(2.25)

provides an *injective* mapping between points outside the support of μ and points outside the support of ν with the property that

$$\gamma(\mathbb{C} \setminus \mathbb{R}) \subset \mathbb{C} \setminus \mathbb{R} \quad \text{and} \quad \gamma(\mathbb{R} \setminus \text{supp}(\mu)) \subset \mathbb{R} \setminus \text{supp}(\nu)$$

but where the *inclusion is strict* in general.

To understand this statement, first consider $z \in \mathbb{C} \setminus \mathbb{R}^+$. Then, by Theorem 2.5, there exists a unique pair $(z, \tilde{m}(z)) \in \mathcal{Z}$ and we may thus write $z = z(\tilde{m})$ for the value $\tilde{m} \in \mathbb{C} \setminus \mathbb{R}^-$ given by $\tilde{m} = \tilde{m}(z)$. For $z = x \in \mathbb{R}^+ \setminus \text{supp}(\mu)$, we have just seen in our discussion of Theorem 2.9 and in Figure 2.5 that there also exists $\tilde{m} \in \mathbb{R}^-$ (it must be real because $\Im[\tilde{m}(x)] = 0$ outside the support) such that $x = x(\tilde{m})$. As a consequence, for $z \in \mathbb{C} \setminus \mathbb{R}$, $\tilde{m} = \tilde{m}(z) \in \mathbb{C} \setminus \mathbb{R}$ and thus $-1/\tilde{m} \in \mathbb{C} \setminus \mathbb{R}$. Similarly, for $x \in \mathbb{R} \setminus \text{supp}(\mu)$, from Figure 2.5, $-1/\tilde{m} \in \mathbb{R} \setminus \text{supp}(\nu)$.

The map is however only injective (in general not surjective) as not all values of $\mathbb{C} \setminus \text{supp}(\nu)$ can be reached. For instance, in Figure 2.5, the sets $(-1/\tilde{m}_1^-, 1)$ and $(1, -1/\tilde{m}_1^+)$ cannot be reached by γ . This remark will constitute a fundamental limitation to statistical inference methods.

More visually, Figure 2.6 depicts in blue the complementary to the image $\gamma(\mathbb{C} \setminus \text{supp}(\mu))$. This blue region is inaccessible in the sense that no point in $\mathbb{C} \setminus \text{supp}(\mu)$ can have an image by $\gamma(\cdot)$ in it. In red are depicted typical images by $\gamma(\cdot)$ of rectangular contours surrounding $\text{supp}(\mu)$. Intuitively, we observe that, as c increases (compare left to right displays), the exclusion region increases in size and one thus cannot get “too close” to the support of ν (which is here the discrete union of three point masses).

In particular, for $c > 1$, the exclusion region includes $\{0\}$. This is a consequence of Item 3 in the remarks of the previous paragraph: while the right real crossing of a contour $\Gamma_\mu \subset \{z \in \mathbb{C}, \Re[z] > 0\}$ surrounding the support of μ will have an image by $\gamma(\cdot)$ somewhere on the right side of $\text{supp}(\nu)$, (i) for $c < 1$, the left real crossing will have 0^+ for image, and (ii) for $c > 1$, the left real crossing will have a negative value for image.

This, we shall see next in Section 2.4, is an important problem when it comes to estimating certain functionals $\int f d\nu$ of ν based on the sample measure $\mu_{\frac{1}{n}} \mathbf{X} \mathbf{X}^\top$.

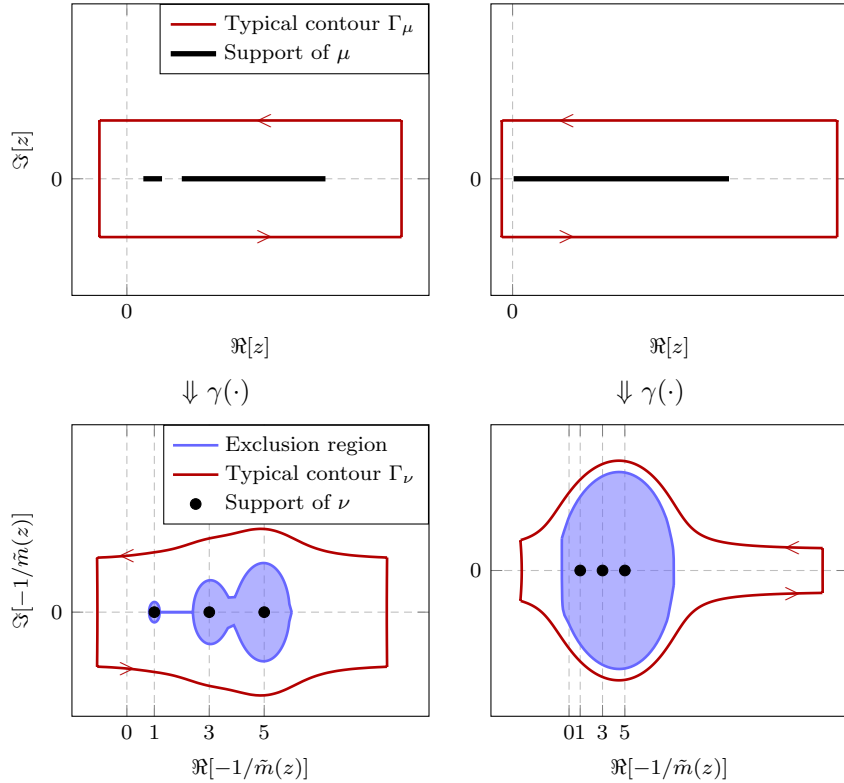


Figure 2.6: Domain of validity of variable changes, for $\nu = \frac{1}{3}(\delta_1 + \delta_3 + \delta_5)$, with $c = \frac{1}{10}$ (**left**) and $c = 2$ (**right**). The filled region in the bottom display is the (inaccessible) complementary to the image of $-1/\tilde{m}(\cdot)$. The **red** contour Γ_ν is the image by $-1/\tilde{m}(\cdot)$ of a rectangular contour Γ_μ surrounding $\text{supp}(\mu)$. [Link to code]

`fig:contour_valid`

2.3.2 “No eigenvalue outside the support”

Before exploiting the aforementioned change of variable for statistical inference, an important extension of Theorem 2.5 is needed.

It must be stressed that the limiting results of Theorem 2.5 are *weak convergences* for the *normalized* counting measure $\frac{1}{p} \sum_{i=1}^p \delta_{\lambda_i(\frac{1}{n}\mathbf{XX}^\top)}$ (i.e., the spectral measure) of the eigenvalues of $\frac{1}{n}\mathbf{XX}^\top$. This, by definition, means that, for every continuous bounded f ,

$$\frac{1}{p} \sum_{i=1}^p f\left(\lambda_i\left(\frac{1}{n}\mathbf{XX}^\top\right)\right) - \int f(t)\mu(dt) \xrightarrow{\text{a.s.}} 0.$$

Letting for instance f be a smoothed version of the indicator $1_{[a,b]}$ for $a, b \notin \text{supp}(\mu)$, this thus only says that the *averaged* number of eigenvalues of $\frac{1}{n}\mathbf{XX}^\top$

within $[a, b]$ converges to $\mu([a, b])$.

In the example of Figure 2.4 (top or middle), if p_1 is the number of eigenvalues falling in the neighborhood of the leftmost connected component of μ , we thus only know that $p_1/p = 1/3 + o(1)$ (almost surely), that is $p_1 = p/3 + o(p)$. This thus does *not* guarantee that $p_1 - p/3 \xrightarrow{a.s.} 0$ exactly as $n, p \rightarrow \infty$.

Worse, Theorem 2.5 only guarantees that, for $[a, b]$ a connected component of $\mathbb{R} \setminus \text{supp}(\mu)$, the number of eigenvalues of $\frac{1}{n}\mathbf{XX}^\top$ inside $[a, b]$ is asymptotically of order $o(p)$. As such, $[a, b]$ may never be empty, even for arbitrarily large n, p (it can contain a fixed finite number of eigenvalues or even a growing number of eigenvalues, so long that this number is much less than $O(p)$).

The following result, again originally due to Bai and Silverstein, settles this non-trivial issue.

Theorem 2.10 (“No eigenvalue outside the support” and exact separation: from [Bai and Silverstein \[1998, 1999\]](#), [Bai et al. \[1988\]](#)). *Under the setting of Theorem 2.5,¹⁵ let $\|\mathbf{C}\|$ be bounded with $\mu_{\mathbf{C}} \rightarrow \nu$ and $\max_{1 \leq i \leq p} \text{dist}(\lambda_i(\mathbf{C}), \text{supp}(\nu)) \rightarrow 0$ as $p \rightarrow \infty$. Consider also $-\infty \leq a < b \leq \infty$ such that $a, b \in \mathbb{R}^+ \setminus \text{supp}(\mu)$. Then the following results hold*

- if $\mathbb{E}[|\mathbf{Z}_{ij}|^4] < \infty$, then

$$\left| \left\{ \lambda_i \left(\frac{1}{n} \mathbf{XX}^\top \right) \in [a, b] \right\} \right| - |\{\lambda_i(\mathbf{C}) \in [\gamma(a), \gamma(b)]\}| \xrightarrow{a.s.} 0$$

with $\gamma(\cdot)$ defined by (2.25). In particular, if $[a, b]$ is a connected component of $\mathbb{R}^+ \setminus \text{supp}(\mu)$, then

$$\left| \left\{ \lambda_i \left(\frac{1}{n} \mathbf{XX}^\top \right) \in [a, b] \right\} \right| \xrightarrow{a.s.} 0.$$

- if $\mathbb{E}[\mathbf{Z}_{ij}^4] = \infty$,

$$\max_{1 \leq i \leq p} \lambda_i \left(\frac{1}{n} \mathbf{XX}^\top \right) \xrightarrow{a.s.} \infty.$$

In plain words, the theorem precisely states that:

- under the condition that $\mathbb{E}[\mathbf{Z}_{ij}^4] < \infty$ and that no eigenvalue of \mathbf{C} isolates from its associated limiting spectrum ν , (i) there asymptotically exists no eigenvalue outside the support of μ and (ii) the eigenvalues assembled in “bulks” are found in asymptotically expected numbers. For instance, in the setting of Figure 2.4, it can be verified that not a single eigenvalue is found away from the support of μ and, in addition, that the exact number of eigenvalues around each connected component of μ is in exact proportion (for the top exactly $p/3$ values for each component and for the middle, $2p/3$ in the largest component).

¹⁵Here formally, the theorem statement must be understood with the “smooth tail condition” discarded, i.e., the only condition on \mathbf{Z} is that it is composed of i.i.d. entries with zero mean and unit variance.

- if $\mathbb{E}[\mathbf{Z}_{ij}^4] = \infty$ (for instance for a Student t-distribution with low degree of freedom), this ‘exact separation’ collapses: while in correct asymptotic proportion, up to $o(p)$ eigenvalues may be found away from the support of μ , with in particular the largest eigenvalue going to infinity.

For future reference, we insist on the condition

$$\max_{1 \leq i \leq p} \text{dist}(\lambda_i(\mathbf{C}), \text{supp}(\nu)) \rightarrow 0$$

which is also fundamental for the theorem to hold. Not surprisingly, if a single eigenvalue of \mathbf{C} were to diverge as $p \rightarrow \infty$, it is expected that an eigenvalue of $\frac{1}{n}\mathbf{XX}^\top$ would also diverge. For instance, say $\lambda_1(\mathbf{C}) = p$ and $\lambda_2(\mathbf{C}) = \dots = \lambda_p(\mathbf{C}) = 1$; then $\mu_{\mathbf{C}} \rightarrow \delta_1$ so that Theorems 2.5 and 2.3 ensure that $\mu_{\frac{1}{n}\mathbf{XX}^\top}$ converges weakly to the Marčenko–Pastur law, while the largest eigenvalue of $\frac{1}{n}\mathbf{XX}^\top$ is strongly expected to diverge to infinity (which it indeed does in this case). Section 2.5 on *spiked models* is strongly inspired by this remark.

2.4 Preliminaries on statistical inference

sec:preliminaries_inference_stats

Section 2.3 provides the necessary ingredients for basic statistical inference considerations of large dimensional sample covariance matrix models.

In this section, we will successively consider the estimation (i) of linear eigenvalue statistics of the type $\frac{1}{p} \sum_{i=1}^p f(\lambda_i(\mathbf{C}))$ and (ii) of eigenvector projections $\mathbf{a}^\top \mathbf{u}_i$ (\mathbf{u}_i an eigenvector of \mathbf{C}) for deterministic vectors \mathbf{a} , from the sample observation $\mathbf{X} = [\mathbf{x}_1, \dots, \mathbf{x}_n]$, $\mathbf{x}_i = \mathbf{C}^{\frac{1}{2}} \mathbf{z}_i$ and \mathbf{z}_i with standard i.i.d. entries, as defined in Theorem 2.5.

Before entering the topic, it must be mentioned that *large dimensional statistical inference*, from a random matrix approach, has stood for long as a complex problem. In particular, retrieving information about a population covariance \mathbf{C} from the samples $\mathbf{C}^{\frac{1}{2}} \mathbf{X}$ may be seen as inverting Theorem 2.5, a problem tentatively tackled in [El Karoui et al., 2008] and later in [Bun et al., 2017] using convex optimization (thus non exact) schemes, but with limited success. Some specific objects, such as traces of powers of \mathbf{C} , traces of its resolvent, quadratic forms, etc., may be estimated by detoured means and formed the extensive database of the more-than-fifty *G-estimators* due to Girko [Girko, 2001] (the phrase ‘G-estimator’ should be understood to stand for ‘generalized estimators’, according to Girko). In this section, we instead concentrate on a contour integral approach to *systematically* estimate a broad class of functionals of \mathbf{C} : the idea, found scattered in the literature, was revived by Mestre in a [Mestre, 2008]. The ideas developed in this section are not easily found in the literature but are strongly inspired by (a simplified treatment of) [Mestre, 2008].

2.4.1 Linear eigenvalue statistics

2.4.1.1 Relating population and sample Stieltjes transforms

A first observation is that the defining equation for $\tilde{m}(z)$ in Theorem 2.5, that is

$$\tilde{m}(z) = \left(-z + c \int \frac{t\nu(dt)}{1+t\tilde{m}(z)} \right)^{-1}$$

can be equivalently rewritten under the form

$$m_\nu \left(-\frac{1}{\tilde{m}(z)} \right) = -zm(z)\tilde{m}(z) \quad \text{eq:mnu_mmuv} \quad (2.26)$$

where we recall that $m(z) = \frac{1}{c}\tilde{m}(z) + \frac{1-c}{c}\frac{1}{z}$. This simply follows from noticing that

$$\begin{aligned} \int \frac{t\nu(dt)}{1+t\tilde{m}(z)} &= \frac{1}{\tilde{m}(z)} \int \frac{t\tilde{m}(z)\nu(dt)}{1+t\tilde{m}(z)} \\ &= \frac{1}{\tilde{m}(z)} \left(1 - \int \frac{\nu(dt)}{1+t\tilde{m}(z)} \right) \\ &= \frac{1}{\tilde{m}(z)} \left(1 - \frac{1}{\tilde{m}(z)} \int \frac{\nu(dt)}{t - (-1/\tilde{m}(z))} \right) \end{aligned}$$

where, from Definition 3, we recognize $\int \frac{\nu(dt)}{t - (-1/\tilde{m}(z))}$ to be the Stieltjes transform m_ν of ν evaluated at $-1/\tilde{m}(z)$.

Theorem 2.5 thus establishes a relation between the population statistics \mathbf{C} and the sample covariance matrix $\frac{1}{n}\mathbf{XX}^\top$, through the Stieltjes transforms of their *limiting* measures.

2.4.1.2 Eigen-inference

Now, observe that, for $f : \mathbb{C} \rightarrow \mathbb{C}$ a function analytic in a neighborhood of the eigenvalues of \mathbf{C} , by Cauchy's integral theorem, the linear statistics $\frac{1}{p} \sum_{i=1}^p f(\lambda_i(\mathbf{C}))$ of the eigenvalues of \mathbf{C} can be expressed as¹⁶

$$\begin{aligned} \frac{1}{p} \sum_{i=1}^p f(\lambda_i(\mathbf{C})) &\simeq \int f(t)\nu(dt) \\ &= \int \left[\frac{1}{2\pi i} \oint_{\Gamma_\nu} \frac{f(z)}{z-t} dz \right] \nu(dt) \\ &= -\frac{1}{2\pi i} \oint_{\Gamma_\nu} f(z) \left[\int \frac{\nu(dt)}{t-z} \right] dz \\ &= -\frac{1}{2\pi i} \oint_{\Gamma_\nu} f(z)m_\nu(z)dz \quad \text{eq:f(nu)-->f(mmuv)} \quad (2.27) \end{aligned}$$

¹⁶Here again the “ \simeq ” sign can be turned into an equality if one assumes $\nu = \frac{1}{p} \sum_{i=1}^p \delta_{\lambda_i(\mathbf{C})}$.

where $\Gamma_\nu \subset \mathbb{C}$ is a (positively oriented) contour encircling the support of ν but no singularity of f . Thus, one can express (smooth) linear statistics of the eigenvalues of \mathbf{C} by means of a complex integral involving the Stieltjes transform $m_\nu(z)$.

As a consequence of (2.26), it is now possible to relate the non-observable $m_\nu(z)$ to $\tilde{m}(z)$, which is the large n, p limit of the observable Stieltjes transform $m_{\frac{1}{n}\mathbf{X}^\top \mathbf{X}}(z)$. To be able to plug (2.26) in (2.27), one needs to perform the change of variable $z \mapsto -1/\tilde{m}(z)$. This is however only possible if there indeed exists a $\Gamma_\nu \subset \mathbb{C}$ (the contour in (2.27)) such that $\Gamma_\nu = -1/\tilde{m}(\Gamma_\mu)$. The discussions in Section 2.3.1 have clarified the conditions under which such a Γ_ν exists.

Let us assume for the moment that Γ_ν is indeed well defined as $\Gamma_\nu = -1/\tilde{m}(\Gamma_\mu)$ for a valid Γ_μ . Then, Equation (2.27) along with (2.26) imply

$$\begin{aligned} \int f(t)\nu(dt) &= -\frac{1}{2\pi i} \oint_{\Gamma_\mu} f\left(-\frac{1}{\tilde{m}(\omega)}\right) m_\nu\left(-\frac{1}{\tilde{m}(\omega)}\right) \frac{\tilde{m}'(\omega)}{\tilde{m}(\omega)^2} d\omega \\ &= \frac{1}{2\pi i} \oint_{\Gamma_\mu} f\left(-\frac{1}{\tilde{m}(\omega)}\right) \omega \frac{m(\omega)\tilde{m}'(\omega)}{\tilde{m}(\omega)} d\omega \end{aligned}$$

where we wrote $z = -1/\tilde{m}(\omega)$. Recalling that $m(\omega) = \frac{1}{c}\tilde{m}(\omega) + (1-c)/(cz)$, this further reads

$$\begin{aligned} \int f(t)\nu(dt) &= \frac{1}{2c\pi i} \oint_{\Gamma_\mu} f\left(-\frac{1}{\tilde{m}(\omega)}\right) \frac{(\omega\tilde{m}(\omega) + (1-c))\tilde{m}'(\omega)}{\tilde{m}(\omega)} d\omega \\ &= \frac{1}{2c\pi i} \oint_{\Gamma_\mu} f\left(-\frac{1}{\tilde{m}(\omega)}\right) \omega\tilde{m}'(\omega) d\omega - \frac{1-c}{c} f(0) 1_{\{0 \in \Gamma_\nu^\circ\}} \end{aligned}$$

where Γ_ν° is the interior of the surface described by Γ_ν , and where for the last equality we used

$$\oint_{\Gamma_\mu} f\left(-\frac{1}{\tilde{m}(\omega)}\right) \frac{\tilde{m}'(\omega)}{\tilde{m}(\omega)} d\omega = - \oint_{\Gamma_\nu} z^{-1} f(z) dz = -f(0) 1_{\{0 \in \Gamma_\nu^\circ\}}$$

by residue calculus, assuming again that f is analytic on a sufficiently large region (in particular here in zero).

To complete the statistical inference framework, one finally needs to relate the above expression to the observation \mathbf{X} . The idea is to use the fact that $m_{\frac{1}{n}\mathbf{X}^\top \mathbf{X}}(z) \xrightarrow{a.s.} \tilde{m}(z)$. To ensure that $\tilde{m}(z)$ can be replaced by $m_{\frac{1}{n}\mathbf{X}^\top \mathbf{X}}(z)$ in the above expression, one however needs to ensure that dominated convergence on the compact set Γ_ν holds. For this, two ingredients are needed: (i) first guarantee that the convergence $m_{\frac{1}{n}\mathbf{X}^\top \mathbf{X}}(z) \xrightarrow{a.s.} \tilde{m}(z)$ is uniform on Γ_ν , which easily follows from the analytic nature of Stieltjes transform, and most importantly (ii) prove that $f(-1/m_{\frac{1}{n}\mathbf{X}^\top \mathbf{X}}(\omega))\omega m'_{\frac{1}{n}\mathbf{X}^\top \mathbf{X}}(\omega)$ is uniformly bounded on Γ_μ . This second item follows from Theorem 2.10 which guarantees that all eigenvalues remain in the vicinity of $\text{supp}(\mu)$ under the additional conditions (i) $\mathbb{E}[|\mathbf{X}_{ij}|^4] < \infty$ and (ii) $\max_i \text{dist}(\lambda_i(\mathbf{C}), \text{supp}(\nu)) \rightarrow 0$.

As a consequence, we have the following fundamental statistical inference result, the original ideas of which are due to Mestre.

Theorem 2.11 (Inspired from Mestre [2008]). *Under the setting of Theorem 2.5 with $\mathbb{E}[|\mathbf{X}_{ij}|^4] < \infty$ and $\max_{1 \leq i \leq p} \text{dist}(\lambda_i(\mathbf{C}), \text{supp}(\nu)) \rightarrow 0$, let $f : \mathbb{C} \rightarrow \mathbb{C}$ be a complex function analytic on the complement of $\gamma(\mathbb{C} \setminus \text{supp}(\mu))$ in \mathbb{C} with γ defined in (2.25). Then,*

$$\frac{1}{p} \sum_{i=1}^p f(\lambda_i(\mathbf{C})) - \frac{1}{2c\pi i} \oint_{\Gamma_\mu} f\left(\frac{-1}{m_{\frac{1}{n}\mathbf{X}^\top \mathbf{X}}(\omega)}\right) \omega m'_{\frac{1}{n}\mathbf{X}^\top \mathbf{X}}(\omega) d\omega \xrightarrow{a.s.} 0$$

for some complex positively oriented contour $\Gamma_\mu \subset \mathbb{C}$ surrounding $\text{supp}(\mu) \setminus \{0\}$. In particular, if $c < 1$, the result holds for any f analytic on $\{z \in \mathbb{C}, \Re[z] > 0\}$ with Γ_μ chosen as any such contour within $\{z \in \mathbb{C}, \Re[z] > 0\}$.

From a numerical standpoint, for $c < 1$, Theorem 2.11 is rather simple: it indicates that any complex contour Γ_μ in $\{z \in \mathbb{C}, \Re[z] > 0\}$ guarantees the result. For $c > 1$, the choice of Γ_μ is less trivial. For safety, it is advised to take Γ_μ a contour closely fitting the support of $\mu_{\frac{1}{n}\mathbf{X}^\top \mathbf{X}}$, excluding zero (such as a small rectangle).

Remark 2.12 (On the $c > 1$ case). *The case $c > 1$ of Theorem 2.11 hides a fundamental limitation: for f not analytic at zero (for instance $f(z) = \log(z)$, $f(z) = z^{-1}$, or even $f(z) = \sqrt{z}$), Theorem 2.11 cannot be applied. This precisely means that, for these functions,*

$$\frac{1}{p} \sum_{i=1}^p f(\lambda_i(\mathbf{C}))$$

cannot be consistently estimated using this contour integral approach. This somehow means that, when $p > n$ and thus the sample covariance matrix $\frac{1}{n}\mathbf{X}\mathbf{X}^\top$ is of rank $n < p$, one lacks information to estimate some functionals of the p eigenvalues of \mathbf{C} .

2.4.1.3 Application example: estimating population eigenvalues of large multiplicity

The top and middle displays in Figure 2.4 present two scenarios where the population measure $\nu_{\mathbf{C}}$ is a discrete sum of three distinct eigenvalues. A natural concern in the large n, p dimension is whether it is possible to estimate these eigenvalues consistently from the sample data \mathbf{X} of size n .

In the top display of Figure 2.4, it a priori appears that averaging the sample eigenvalues of each connected component of μ_p may provide such a consistent estimator. This is however not the case: this estimator is indeed biased. In the middle display, the problem looks even harder as the two eigenvalues (3 and 5) of \mathbf{C} associated to the same connected component of μ are a priori hard to

jointly estimate: we will see, perhaps even more surprisingly, that a procedure can indeed consistently estimate them both.

Consider then the following generalized setting of Figure 2.4, where

$$\nu_{\mathbf{C}} = \frac{1}{p} \sum_{i=1}^k p_i \delta_{\ell_i} \rightarrow \sum_{i=1}^k c_i \delta_{\ell_i}$$

for $\ell_1 > \dots > \ell_k > 0$, k fixed with respect to n, p , and $p_i/p \rightarrow c_i > 0$ as $p \rightarrow \infty$ (i.e., each eigenvalue has a large multiplicity).

Fully separable case. We additionally assume for the moment that the sample size $n > p$ of $\mathbf{X} = [\mathbf{x}_1, \dots, \mathbf{x}_n]$ (where $\mathbf{x}_i = \mathbf{C}^{\frac{1}{2}} \mathbf{z}_i$, \mathbf{z}_i having standard i.i.d. entries) is sufficiently large for the number of connected components in μ to be exactly k , i.e., each eigenvalue of \mathbf{C} is “mapped” to a single connected component of $\text{supp}(\mu)$.

Then, to estimate a given ℓ_a , Theorem 2.11 may be applied to the mere function $f(z) = z$, however for Γ_μ changed into $\Gamma_\mu^{(a)}$ a contour circling around the a -th connected component of $\text{supp}(\mu)$ only (sorted descendingly from ∞ to 0). Adapting Theorem 2.11 according to Theorem 2.10 and our previous line of reasoning, we then have

$$\ell_a - \hat{\ell}_a \xrightarrow{a.s.} 0, \quad \hat{\ell}_a = -\frac{n}{p_a} \frac{1}{2\pi i} \oint_{\Gamma_\mu^{(a)}} \omega \frac{m'_{\frac{1}{n}\mathbf{X}^\top \mathbf{X}}(\omega)}{m_{\frac{1}{n}\mathbf{X}^\top \mathbf{X}}(\omega)} d\omega \xrightarrow{a.s.} 0.$$

The estimator $\hat{\ell}_a$ can be numerically evaluated. However, recalling that $m_{\frac{1}{n}\mathbf{X}^\top \mathbf{X}}(\omega)$ (and its derivative) are rational functions, this integral is prone to estimation by a simple residue calculus.

Indeed, first observe that the integrand in the expression of $\hat{\ell}_a$ has two types of poles: (i) the $\lambda_i = \lambda_i(\frac{1}{n}\mathbf{X}^\top \mathbf{X})$ falling inside the surface described by $\Gamma_\mu^{(a)}$, since in the neighborhood of λ_i ,

$$\begin{aligned} -\frac{n}{p_a} \omega \frac{m'_{\frac{1}{n}\mathbf{X}^\top \mathbf{X}}(\omega)}{m_{\frac{1}{n}\mathbf{X}^\top \mathbf{X}}(\omega)} &= -\frac{n}{p_a} \omega \frac{\frac{1}{n} \sum_{i=1}^n \frac{1}{(\lambda_i - \omega)^2}}{\frac{1}{n} \sum_{i=1}^n \frac{1}{\lambda_i - \omega}} \\ &\sim_{\omega \sim \lambda_i} -\frac{n}{p_a} \frac{\omega}{\lambda_i - \omega} \end{aligned}$$

and (ii) the zeros of $m_{\frac{1}{n}\mathbf{X}^\top \mathbf{X}}$ falling within $\Gamma_\mu^{(a)}$.

For readability in what follows, we sort the eigenvalues of $\frac{1}{n}\mathbf{X}^\top \mathbf{X}$ as $\lambda_1 > \dots > \lambda_n$. Dealing with the first poles is easy: the λ_i falling within $\Gamma_\mu^{(1)}$ are precisely the p_1 largest, within $\Gamma_\mu^{(2)}$ the next p_2 largest, etc., as per Theorem 2.10. The residue associated to λ_i is then

$$\lim_{\omega \rightarrow \lambda_i} (\omega - \lambda_i) \frac{n}{p_a} \frac{-\omega}{\lambda_i - \omega} = \frac{n}{p_a} \lambda_i.$$

The second set of poles is less immediate to retrieve. An important remark is that the zeros, call them η_j (sorted also as $\eta_1 > \eta_2 > \dots$), of $m_{\frac{1}{n}\mathbf{X}^\top \mathbf{X}}(\omega)$ are necessarily real (since the Stieltjes transform has nonzero imaginary part for $\Re[\omega] \neq 0$) and satisfy

$$\frac{1}{n} \sum_{i=1}^n \frac{1}{\lambda_i - \eta_j} = 0.$$

Since the function

$$x \mapsto \frac{1}{n} \sum_{i=1}^n \frac{1}{\lambda_i - x}$$

is increasing and has ∞ and $-\infty$ asymptotes in $x = \lambda_i - 0$ and $x = \lambda_i + 0$, respectively, each η_j falls exactly in one of the intervals $[\lambda_i, \lambda_{i+1}]$ and thus each λ_i pole is accompanied by its η_i pole (if sorted similarly, see Figure 2.7 for an illustration). The residue calculus then gives, by Taylor expanding the denominator,

$$\lim_{\omega \rightarrow \eta_j} (\omega - \eta_j) \frac{n}{p_a} \frac{-\omega m'_{\frac{1}{n}\mathbf{X}^\top \mathbf{X}}(\omega)}{0 + m'_{\frac{1}{n}\mathbf{X}^\top \mathbf{X}}(\eta_j)(\omega - \eta_j)} = -\frac{n}{p_a} \eta_j.$$

As a result, we finally have the estimator

$$\hat{\ell}_a = \frac{n}{p_a} \sum_{i=p_1+\dots+p_{a-1}+1}^{p_1+\dots+p_a} \lambda_i - \eta_i.$$

Surprisingly at first, it appears that the estimator is the sum of $p_a = O(p)$ terms, which may seem to conduct to an estimate of order $O(p)$. However, recall that $\lambda_1, \dots, \lambda_p$ are “compacted” in a support of size $O(1)$ and that $\lambda_i < \eta_i < \lambda_{i+1}$ so that $\lambda_i - \eta_i = O(1/p)$, which settles the problem.

This formulation is nonetheless still not fully closed in the sense that the η_i are so far only provided in terms of the zeros of $m_{\frac{1}{n}\mathbf{X}^\top \mathbf{X}}$. The following remark provides an explicit form.

`rem:explicit-express-zeros`

Remark 2.13 (Explicit expression for the zeros of $m_{\mathbf{X}}(z)$). *For $\mathbf{X} \in \mathbb{R}^{n \times n}$ symmetric with eigenvalues $\lambda_1 > \dots > \lambda_n$, the zeros $\eta_1 > \eta_2 > \dots$ of $m_{\mathbf{X}}(z)$*

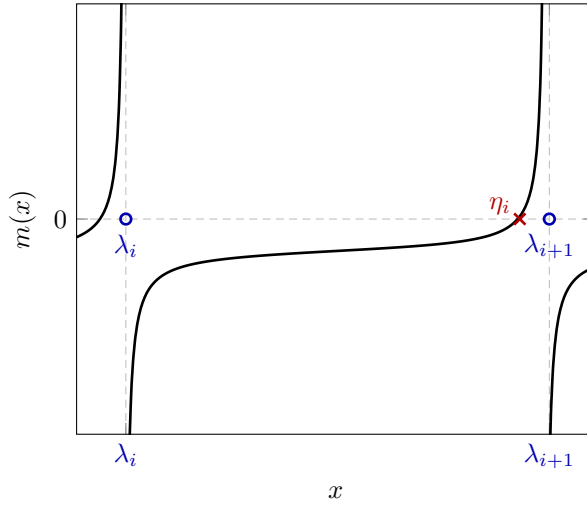


Figure 2.7: Illustration of the zeros (η_i) and poles (λ_i) of the (restriction to the real axis of the) Stieltjes transform $m_{\frac{1}{n}\mathbf{X}^\top \mathbf{X}}(x)$. [Link to code] [fig:zeros_of_m](#)

satisfy the following equivalence relations

$$\begin{aligned}
 \frac{1}{n} \sum_{i=1}^n \frac{1}{\lambda_i - \eta_j} = 0 &\Leftrightarrow \frac{1}{n} \sum_{i=1}^n \frac{-\eta_j}{\lambda_i - \eta_j} = 0 \\
 &\Leftrightarrow \frac{1}{n} \sum_{i=1}^n \frac{\lambda_i}{\lambda_i - \eta_j} - 1 = 0 \\
 &\Leftrightarrow \frac{1}{n} \sqrt{\boldsymbol{\lambda}}^\top (\boldsymbol{\Lambda} - \eta_j \mathbf{I}_n)^{-1} \sqrt{\boldsymbol{\lambda}} - 1 = 0 \\
 &\Leftrightarrow \det \left(\frac{1}{n} \sqrt{\boldsymbol{\lambda}} \sqrt{\boldsymbol{\lambda}}^\top (\boldsymbol{\Lambda} - \eta_j \mathbf{I}_n)^{-1} - \mathbf{I}_n \right) = 0 \\
 &\Leftrightarrow \det \left(\frac{1}{n} \sqrt{\boldsymbol{\lambda}} \sqrt{\boldsymbol{\lambda}}^\top - \boldsymbol{\Lambda} + \eta_j \mathbf{I}_n \right) = 0
 \end{aligned}$$

where we denoted $\sqrt{\boldsymbol{\lambda}} \in \mathbb{R}^p$ the (column) vector of the $\sqrt{\lambda_i}$'s and $\boldsymbol{\Lambda} \in \mathbb{R}^{p \times p}$ the diagonal matrix $\text{diag}(\lambda_1, \dots, \lambda_p)$, sorted in the same way, and used Lemma 2.3 as well as the fact that $\det(\boldsymbol{\Lambda} - \eta_j \mathbf{I}_n) \neq 0$ according to our discussion above.

Consequently, the zeros of $m_{\mathbf{X}}$ are exactly the eigenvalues of

$$\boldsymbol{\Lambda} - \frac{1}{n} \sqrt{\boldsymbol{\lambda}} \sqrt{\boldsymbol{\lambda}}^\top.$$

Figure 2.8 depicts the estimation error in the setting of two population eigenvalues ℓ_1 and ℓ_2 (with $\ell_1 = 1$ and $p/n = 1/4$), as a function of the difference $\Delta\lambda = \ell_2 - \ell_1$. The error grows rapidly once $\Delta\lambda < 1$: this is a typical “avalanche

effect” which appears below the phase transition threshold when the two connected components of the support of the empirical measure μ are no longer separable.

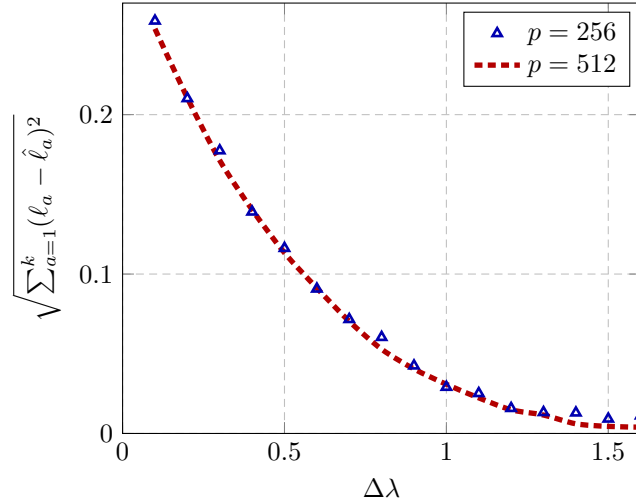


Figure 2.8: Eigenvalue estimation error as a function of $\Delta\lambda$, for $\ell_1 = 1$, $\ell_2 = 1 + \Delta\lambda$ and $p/n = 1/4$. Results averaged over 10 runs. [\[Link to code\]](#)

`fig.popu-eigenvalue-estim`

Non-separable case. The estimator introduced above is only valid if the contour $\Gamma_\mu^{(a)}$ is licit, in the sense that its image by the variable change $z \mapsto -1/\tilde{m}(z)$ leads to a valid contour surrounding ℓ_a only. However, we have seen (in Figure 2.6 notably) that there may not exist any such licit $\Gamma_\mu^{(a)}$. In our present setting, Figures 2.5 (both middle and bottom) and Figure 2.6 (both left and right) reveal that, if say ℓ_1 and ℓ_2 are associated to a single connected component of $\text{supp}(\mu)$, then all contours $\Gamma_\mu^{(1)}$ surrounding the p_1 largest λ_i are illicit.

In order to estimate both ℓ_1 and ℓ_2 individually, one must then resort to using at least *two* estimates of functionals of ℓ_1 and ℓ_2 . One approach is to estimate simultaneously both $\frac{p_1}{p}\ell_1 + \frac{p_2}{p}\ell_2$ and $\frac{p_1}{p}\ell_1^2 + \frac{p_2}{p}\ell_2^2$, which are accessible from our present adaptation of Theorem 2.11 for $f(z) = z$ and $f(z) = z^2$, with a contour $\Gamma_\mu^{(1,2)}$ surrounding the connected component of μ encompassing the $p_1 + p_2$ largest λ_i .

Assuming p_1 and p_2 are known, this thus boils down to solving a second order polynomial in $\hat{\ell}_1$ and $\hat{\ell}_2$. This procedure however has several limitations: (i) the polynomial equations may lead to nonreal solutions, and (ii) assuming p_1 and p_2 known is quite demanding as they cannot be easily estimated from the λ_i themselves (an additional third equation is then needed here), (iii) generally speaking, a known issue in statistics is that estimates of high order moments are

increasingly prone to large variances as the order increases: as such, the need for additional equations to estimate the individual ℓ_a and their multiplicity must pass through generalized (non polynomial) moments, which are possibly cumbersome to estimate.

2.4.2 Eigenvector projections and subspace methods

sec:subspace-method

In the previous section on the inference methods for the linear statistics (of eigenvalues) of the population covariance \mathbf{C} , we exploited the relation

$$m_\nu(-1/\tilde{m}(z)) = -zm(z)\tilde{m}(z)$$

between the Stieltjes transform m_ν of the population measure ν and the Stieltjes transform m (and \tilde{m}) of the sample measure μ (and $\tilde{\mu} = c\mu + (1-c)\delta_0$), which are immediate consequences of Theorem 2.5.

The deterministic equivalent statements $\mathbf{Q}(z) \leftrightarrow \bar{\mathbf{Q}}(z)$ (as well as $\tilde{\mathbf{Q}}(z) \leftrightarrow \bar{\tilde{\mathbf{Q}}}(z)$) in Theorem 2.5 go beyond Stieltjes transform relations by connecting the whole resolvent $\mathbf{Q}(z) = (\frac{1}{n}\mathbf{XX}^\top - z\mathbf{I}_p)^{-1}$ of the sample covariance (almost directly) to the resolvent $(\mathbf{C} - z\mathbf{I}_p)^{-1}$ of the population covariance.

These relations allow for two main estimates: (i) when \mathbf{C} is known, they provide asymptotic characterizations of some functionals of \mathbf{X} involving its singular vectors (i.e., the eigenvectors $\mathbf{u}_i(\mathbf{X}^\top \mathbf{X})$ of $\mathbf{X}^\top \mathbf{X}$ or $\mathbf{u}_i(\mathbf{XX}^\top)$ of \mathbf{XX}^\top), in particular projections $\mathbf{u}_i(\mathbf{XX}^\top)^\top \mathbf{u}(\mathbf{C})$ onto the corresponding eigenvectors $\mathbf{u}(\mathbf{C})$ of \mathbf{C} ; (ii) when \mathbf{C} is unknown, they provide estimates for some functionals of the eigenvectors of \mathbf{C} , notably projections $\mathbf{a}^\top \mathbf{u}(\mathbf{C})$ onto deterministic vectors \mathbf{a} . The latter case is particularly suited to the so-called subspace methods, based on the fact that $\mathbf{u}(\mathbf{C})$ is known to be aligned (or be equal) to some vector \mathbf{a}_θ parametrized by θ and one aims to solve for θ maximizing this alignment.

2.4.2.1 Estimates of functionals of \mathbf{X}

In some applications, the observed data \mathbf{X} will be processed in a nonlinear fashion that may nonetheless preserve its eigenvector structure. The spectral behavior of the resulting matrix may here be typically evaluated by means of its projection onto specific vector structures. This is for instance the case of some simple gradient descent mechanisms for supervised learning discussed in Section 5.2, where the learning performance can be measured from the alignment between the gradient descent iterates and the classification vectors (such as the vector $[-\mathbf{1}_{n_1}, \mathbf{1}_{n_2}]$ in a binary classification setting).

For $\mathbf{M} \in \mathbb{R}^{p \times p}$ a symmetric matrix with spectral decomposition $\mathbf{M} = \mathbf{U}\Lambda\mathbf{U}^\top$ and $\Lambda = \text{diag}(\lambda_1, \dots, \lambda_p)$, and $f : \mathbb{R} \rightarrow \mathbb{R}$, we shall here denote

$$f(\mathbf{M}) = \mathbf{U} \text{diag}(f(\lambda_i))_{i=1}^p \mathbf{U}^\top.$$

Assume f is extensible to a complex function $f : \mathbb{C} \rightarrow \mathbb{C}$, analytic on a neighborhood of $\lambda_1, \dots, \lambda_p$. Then, we have that

$$f(\mathbf{M}) = -\frac{1}{2\pi i} \oint_{\Gamma} f(z) \mathbf{Q}_{\mathbf{M}}(z) dz$$

for $\Gamma \subset \mathbb{C}$ a contour closely encompassing $\lambda_1, \dots, \lambda_p$ but no singularity of f . This result arises from a simple residue calculus. Indeed, writing

$$\mathbf{Q}_{\mathbf{M}} = \mathbf{U}(\Lambda - z\mathbf{I}_p)^{-1}\mathbf{U}^T = \sum_{i=1}^p \frac{\mathbf{u}_i \mathbf{u}_i^T}{\lambda_i - z}$$

with $\mathbf{U} = [\mathbf{u}_1, \dots, \mathbf{u}_p]$, each λ_j is a pole of the integrand and the associated residue is

$$\lim_{z \rightarrow \lambda_j} (z - \lambda_j) f(z) \sum_{i=1}^p \frac{\mathbf{u}_i \mathbf{u}_i^T}{\lambda_i - z} = -f(\lambda_j) \mathbf{u}_j \mathbf{u}_j^T.$$

Summing this result over j gives the result.

Now, assuming $\mathbf{Q}_{\mathbf{M}}(z)$ has a deterministic equivalent $\bar{\mathbf{Q}}(z)$, we have in particular, for $\mathbf{A} \in \mathbb{R}^{p \times p}$ and $\mathbf{a}, \mathbf{b} \in \mathbb{R}^p$, deterministic and of bounded norms,

$$\begin{aligned} \frac{1}{p} \operatorname{tr} \mathbf{A} f(\mathbf{M}) &= -\frac{1}{2\pi i} \oint_{\Gamma} f(z) \frac{1}{p} \operatorname{tr} \mathbf{A} \mathbf{Q}_{\mathbf{M}}(z) dz \\ &= -\frac{1}{2\pi i} \oint_{\Gamma} f(z) \frac{1}{p} \operatorname{tr} \mathbf{A} \bar{\mathbf{Q}}(z) dz + o(1) \\ \mathbf{a}^T f(\mathbf{M}) \mathbf{b} &= -\frac{1}{2\pi i} \oint_{\Gamma} f(z) \mathbf{a}^T \mathbf{Q}_{\mathbf{M}}(z) \mathbf{b} dz \\ &= -\frac{1}{2\pi i} \oint_{\Gamma} f(z) \mathbf{a}^T \bar{\mathbf{Q}}(z) \mathbf{b} dz + o(1) \end{aligned}$$

thereby giving access to the asymptotics of these eigenvector functionals.

Under the notations of Theorem 2.5, for $\mathbf{M} = \frac{1}{n} \mathbf{X} \mathbf{X}^T$ the sample covariance matrix under study, we have in particular

$$\begin{aligned} \frac{1}{p} \operatorname{tr} \mathbf{A} f\left(\frac{1}{n} \mathbf{X} \mathbf{X}^T\right) &= \frac{1}{2\pi i} \oint_{\Gamma_\mu} \frac{f(z)}{z} \frac{1}{p} \operatorname{tr} \mathbf{A} (\mathbf{I}_p + \tilde{m}(z) \mathbf{C})^{-1} dz + o(1) \quad \text{eq:alignment_to_A} \\ \mathbf{a}^T f\left(\frac{1}{n} \mathbf{X} \mathbf{X}^T\right) \mathbf{b} &= \frac{1}{2\pi i} \oint_{\Gamma_\mu} \frac{f(z)}{z} \mathbf{a}^T (\mathbf{I}_p + \tilde{m}(z) \mathbf{C})^{-1} \mathbf{b} dz + o(1) \end{aligned}$$

for Γ_μ a contour circling around $\operatorname{supp}(\mu)$.

Example: Eigenspace correlation. Returning to Figure 2.4, we have seen that, when ν is a discrete measure $\nu = \sum_{a=1}^k \frac{p_a}{p} \delta_{\ell_a}$ and c is small enough, μ has a density that spreads in k connected components $\operatorname{supp}(\mu) = \mathcal{S}_1 \cup \dots \cup \mathcal{S}_k$,

with \mathcal{S}_a mapped to the atom ℓ_a of ν ; these connected components spread more when c increases. A natural subsequent question would be to know whether the eigenvectors $\hat{\mathbf{u}}_i$ associated to the p_a eigenvalues of $\frac{1}{n}\mathbf{XX}^\top$ of a given connected component \mathcal{S}_a share the same eigenspace as that spanned by the eigenvectors \mathbf{u}_i of \mathbf{C} corresponding to population eigenvalue ℓ_a (with multiplicity p_a) of ν .

This question is readily answered by evaluating

$$\frac{1}{p_a} \operatorname{tr} \mathbf{\Pi}_a \hat{\mathbf{\Pi}}_a, \quad \mathbf{\Pi}_a = \sum_{\lambda_i(\mathbf{C})=\ell_a} \mathbf{u}_i \mathbf{u}_i^\top, \quad \hat{\mathbf{\Pi}}_a = \sum_{i \sim \mathcal{S}_a} \hat{\mathbf{u}}_i \hat{\mathbf{u}}_i^\top$$

and where the relation $i \sim \mathcal{S}_a$ stands for $\operatorname{dist}(\lambda_i, \mathcal{S}_a) \rightarrow 0$ (i.e., those eigenvalues of $\frac{1}{n}\mathbf{XX}^\top$ converging to the limiting connected component \mathcal{S}_a).

This quantity can be evaluated by letting $\mathbf{A} = \mathbf{\Pi}_a$, $f(z) = 1$ and changing Γ_μ into $\Gamma_{\mathcal{S}_a}$ a contour surrounding only the component \mathcal{S}_a of $\operatorname{supp}(\mu)$ in (2.28). We precisely get

$$\begin{aligned} \frac{1}{p_a} \operatorname{tr} \mathbf{\Pi}_a \hat{\mathbf{\Pi}}_a &= \frac{1}{2\pi i} \oint_{\Gamma_{\mathcal{S}_a}} \frac{1}{z} \frac{1}{p_a} \operatorname{tr} \mathbf{\Pi}_a (\mathbf{I}_p + \tilde{m}(z)\mathbf{C})^{-1} dz + o(1) \\ &= \frac{1}{2\pi i} \oint_{\Gamma_{\mathcal{S}_a}} \frac{1}{z} \frac{\text{leq:eigenspace-corr-contour-integral}}{1 + \tilde{m}(z)\ell_a} dz + o(1) \end{aligned} \quad (2.29)$$

which, for a given population eigenvalue ℓ_a , can be evaluated numerically with the following two-step procedure:

1. with Theorem 2.9, determine the support of μ , which is assumed to have exactly k disjoint components, i.e., $\operatorname{supp}(\mu) = \bigcup_{i=1}^k \mathcal{S}_i$ with say $\mathcal{S}_i = [s_i^-, s_i^+]$ and $s_i^+ < s_{i+1}^-$;
2. choose *any* licit contour $\Gamma_{\mathcal{S}_a}$ that carefully circles around *only* the component \mathcal{S}_a , for instance the rectangular $\Gamma_{\mathcal{S}_a}$ as depicted in Figure 2.6 (which was adopted e.g., in [Bai and Silverstein, 2008]).

But we may go beyond numerical evaluation and obtain an explicit expression of the integral. To this end, for the chosen rectangular contour $\Gamma_{\mathcal{S}_a}$ (Figure 2.9), this consists in evaluating the sum of four line integrals (two “horizontal” and two “vertical”). We provide here the full derivation as it is instrumental of many such calculus arising in similar inference problems and, to the best of our knowledge, this specific calculus was not derived elsewhere in the random matrix literature. Let us first focus on the sum of two horizontal integrals

$$\int_{s_a^+ + \varepsilon_x}^{s_a^- - \varepsilon_x} g(x + \imath\varepsilon_y) dx + \int_{s_a^- - \varepsilon_x}^{s_a^+ + \varepsilon_x} g(x - \imath\varepsilon_y) dx$$

for $g(z) \equiv \frac{1}{z} \frac{1}{1 + \tilde{m}(z)\ell_a}$ our object of interest here. Note from the definition of Stieltjes transform (Definition 3) that

$$\Re[m(x + \imath y)] = \Re[m(x - \imath y)], \quad \Im[m(x + \imath y)] = -\Im[m(x - \imath y)]$$

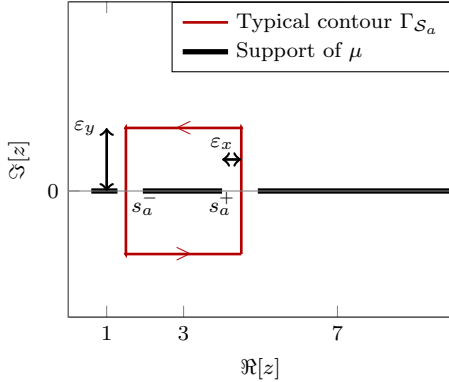


Figure 2.9: Typical contour Γ_{S_a} , for $\nu = \frac{1}{3}(\delta_1 + \delta_2 + \delta_5)$ with $c = 1/10$.

for any Stieltjes transform $m(z)$ and, consequently,

$$\Re[g(x + iy)] = \Re[g(x - iy)], \quad \Im[g(x + iy)] = -\Im[g(x - iy)].$$

A direct consequence of this observation is that

$$\int_{s_a^+ + \varepsilon_x}^{s_a^- - \varepsilon_x} g(x + i\varepsilon_y) dx + \int_{s_a^- - \varepsilon_x}^{s_a^+ + \varepsilon_x} g(x - i\varepsilon_y) dx = -2i \int_{s_a^- - \varepsilon_x}^{s_a^+ + \varepsilon_x} \Im[g(x + i\varepsilon_y)] dx$$

and it thus remains only the imaginary part of $g(z) = \frac{1}{z} \frac{1}{1 + \tilde{m}(z)\ell_a}$, explicitly given by

$$\Im[g(x + i\varepsilon_y)] = -\frac{\varepsilon_y + \ell_a (x \Im[\tilde{m}(x + i\varepsilon_y)] + \varepsilon_y \Re[\tilde{m}(x + i\varepsilon_y)])}{(x^2 + \varepsilon_y^2)(1 + 2\ell_a \Re[\tilde{m}(x + i\varepsilon_y)] + \ell_a^2 |\tilde{m}(x + i\varepsilon_y)|^2)}.$$

To handle the two vertical integrals (from $-\varepsilon_y$ to ε_y), we would like to take the limit $\varepsilon_y \rightarrow 0$ so that these two vertical integrals can be neglected. We already know from Theorem 2.9 that the limit

$$\tilde{m}^\circ(x) = \lim_{\varepsilon_y \rightarrow 0} \tilde{m}(x + i\varepsilon_y)$$

exists for $x \in \text{supp}(\mu)$ and similarly for $\tilde{g}^\circ(x) = \lim_{\varepsilon_y \rightarrow 0} g(x + i\varepsilon_y)$. This finally leads to

$$\frac{1}{p_a} \text{tr } \boldsymbol{\Pi}_a \hat{\boldsymbol{\Pi}}_a = \frac{1}{\pi} \int_{s_a^-}^{s_a^+} \frac{\ell_a \Im[\tilde{m}^\circ(x)]}{1 + 2\ell_a \Re[\tilde{m}^\circ(x)] + \ell_a^2 |\tilde{m}^\circ(x)|^2} \frac{dx}{x} \quad \text{eq: eigenspace-corr (2.30)}$$

where we recall that, for x inside the support, $\tilde{m}^\circ(x)$ is the unique solution with positive imaginary part of

$$\tilde{m}^\circ(x) = \left(-x + c \int \frac{t\nu(dt)}{1 + \tilde{m}^\circ(x)t} \right)^{-1}.$$

We will show in Section 2.5 on the “spiked models” that, when the multiplicity p_a of atom ℓ_a is small – technically, if one assumes that $p_a = O(1)$ with respect to p –, the alignment $\text{tr } \boldsymbol{\Pi}_a \hat{\boldsymbol{\Pi}}_a$ just derived assumes a much simpler and fully explicit form (see Theorem 2.13). Yet, the present estimate, which we set under the opposite scenario where $p_a = O(p)$, turns out (as numerical observations suggest) to be more precise even when p_a is small.

To make this claim more precise, consider the setting where the population covariance $\mathbf{C} \in \mathbb{R}^{p \times p}$ has its $p - m$ eigenvalues equal to 1 and the remaining m eigenvalues equal to $\ell > 1$, so that the population spectral measure ν is a discrete measure having two components: $\nu = \frac{p-m}{p} \delta_1 + \frac{m}{p} \delta_\ell$. In the case where $m, n, p \rightarrow \infty$ with $\lim m/p, p/n \in (0, \infty)$, the correlation of eigenspaces that correspond to the leading eigenvalues of \mathbf{C} (equal to ℓ with multiplicity m) and of $\frac{1}{n} \mathbf{X} \mathbf{X}^\top$, can be fully characterized by (2.30). Figure 2.10 compares the empirical eigenspace correlation with different limiting behavior predicted by the “separate bulk” model in (2.30) versus the spiked model in Theorem 2.13. For small values of m , both limiting predictions are close, although (2.30) already shows a surprisingly marked advantage over the spiked model, even though $m \ll p$ (which goes against our assumptions). But as m increases, the spiked model-based Theorem 2.13 tends to overestimate the correlation where the prediction (2.30) is a close match to the empirical observation.

This observation, which appears to be quite systematic in random matrix theory, is interesting for applicative considerations: in practice, \mathbf{C} is fixed (instead of growing large) and so are m , p and n . And yet, the random matrix predictions based on simultaneously large m, p, n are always extremely accurate, and most importantly, systematically more accurate than when one assumes one of the dimensions (be it m , p , or n) is fixed.

As a side remark, if we only have access to the empirical covariance $\frac{1}{n} \mathbf{X}^\top \mathbf{X}$ and its Stieltjes transform (i.e., if \mathbf{C} is unknown), then the contour integration in (2.29) asymptotically and practically reduces to residue calculus as

$$\begin{aligned} \frac{1}{p_a} \text{tr } \boldsymbol{\Pi}_a \hat{\boldsymbol{\Pi}}_a &= \frac{1}{2\pi i} \oint_{\Gamma_{S_a}} \frac{1}{z} \frac{1}{1 + m \frac{1}{n} \mathbf{X}^\top \mathbf{X}(z) \ell_a} dz + o(1) \\ &= \sum_{i \sim S_a} \frac{-m \frac{1}{n} \mathbf{X}^\top \mathbf{X}(\zeta_i)}{\zeta_i m' \frac{1}{n} \mathbf{X}^\top \mathbf{X}(\zeta_i)} + o(1) \end{aligned}$$

with ζ_i the roots of $m \frac{1}{n} \mathbf{X}^\top \mathbf{X}(\zeta_i) = -1/\ell_a$, which, by an argument similar to Remark 2.13, are the (sorted) eigenvalues of $\boldsymbol{\Lambda} + \frac{\ell_a}{n} \mathbf{1}_n \mathbf{1}_n^\top$, for $\boldsymbol{\Lambda}$ the diagonal matrix containing the eigenvalue of $\frac{1}{n} \mathbf{X}^\top \mathbf{X}$. The residue calculus technique performed in the last equation is described in the previous section.

2.4.2.2 Eigenvector inference and subspace methods

The second interest of the deterministic equivalent $\mathbf{Q}(z) \leftrightarrow \bar{\mathbf{Q}}(z)$ of Theorem 2.5, already underlined in the previous example, now concerns the statistical inference of the eigenvectors and eigenspace of \mathbf{C} . Of course, unless a strong a priori

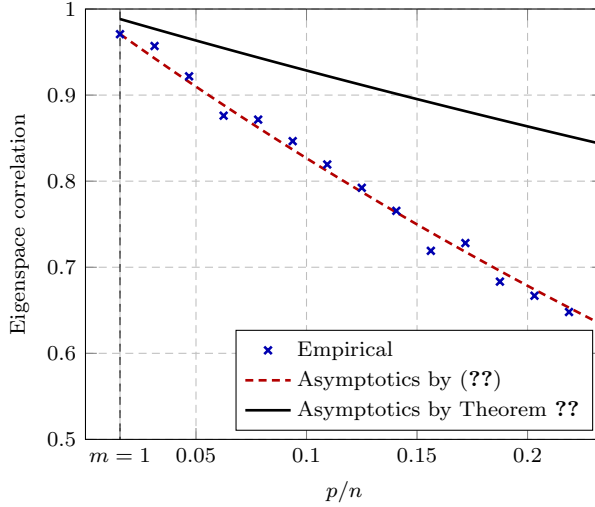


Figure 2.10: Empirical versus limiting eigenspace correlation as a function of $\frac{p}{n} = \frac{p}{m} \frac{m}{n}$ for $\nu = (1 - \frac{m}{p})\delta_1 + \frac{m}{p}\delta_2$, $\frac{m}{p} = \frac{1}{16}$ and $n = 1024$. [Link to code]
fig:eigenspace-corr

structure is imposed, the eigenvectors themselves cannot be consistently estimated from \mathbf{X} . But their projections onto deterministic vectors are accessible. Precisely, for $\mathbf{a}, \mathbf{b} \in \mathbb{R}^p$ of bounded Euclidean norm, denoting Π_i a projector on the eigenspace associated to the eigenvalue $\lambda_i(\mathbf{C})$,

$$\mathbf{a}^\top \Pi_i \mathbf{b} = -\frac{1}{2\pi i} \oint_{\Gamma_\nu^i} \mathbf{a}^\top (\mathbf{C} - z\mathbf{I}_p)^{-1} \mathbf{b} dz$$

for Γ_ν^i a contour circling around $\lambda_i(\mathbf{C})$ only. From Theorem 2.5 and our subsequent discussions of Section 2.3, it is strongly desirable to use again the variable change $z = -1/\tilde{m}(\omega)$ in order to estimate $\mathbf{a}^\top \Pi_i \mathbf{b}$ from an integral over $\mathbf{a}^\top \mathbf{Q}(z) \mathbf{b}$. However, this is again only possible if there exists a pair of contours (Γ_ν^i, Γ) such that $-1/\tilde{m}(\Gamma) = \Gamma_\nu^i$. This is in general not possible unless $\lambda_i(\mathbf{C})$ “induces” its own associated connected component in $\text{supp}(\mu)$. This is precisely the case again of the example of Figure 2.4. Assuming the validity of the variable change, we thus have

$$\begin{aligned} \mathbf{a}^\top \Pi_i \mathbf{b} &= -\frac{1}{2\pi i} \oint_{\Gamma} \mathbf{a}^\top \left(\mathbf{C} + \frac{1}{\tilde{m}(\omega)} \mathbf{I}_p \right)^{-1} \mathbf{b} \frac{\tilde{m}'(\omega)}{\tilde{m}(\omega)^2} d\omega \\ &= \frac{1}{2\pi i} \oint_{\Gamma} \mathbf{a}^\top \mathbf{Q}(\omega) \mathbf{b} \frac{\omega \tilde{m}'(\omega)}{\tilde{m}(\omega)} d\omega + o(1). \end{aligned}$$

This formula reveals handy when testing whether an expected “structure” vector $\mathbf{a} \in \mathbb{R}^p$ is present in the dominant subspace associated to the largest eigenvalue (possibly with multiplicity) $\lambda_1(\mathbf{C})$ of the data covariance structure

C. The value $\mathbf{a}^\top \mathbf{\Pi} \mathbf{a} / \|\mathbf{a}\|^2 \in [0, 1]$ precisely evaluates a score for the structure \mathbf{a} to be in the span of the dominant eigenvectors of \mathbf{C} .

This analysis finds several applications in detection and estimation, notably in the field of array processing. A concrete example, the G-MUSIC algorithm, is discussed in Section 3.1.3 but more results are available in the dedicated array processing literature [Mestre and Lagunas, 2008, Kammoun et al., 2018].

2.5 Spiked models

sec:spiked-model

The statistical methods discussed in the previous sections for the sample covariance matrix model offer a flexible estimation and inference framework, which can be extended to a large spectrum of random matrix models. However, they have a certain number of practical limitations: (i) they rely on the implicit nature of Theorem 2.5 and thus their behavior is not easily understood, (ii) the complex integration framework, while theoretically satisfying, may be difficult to handle in practice (conditions of existence of valid contours need be ensured, the complex integrals do not necessarily lend themselves to simple analytical evaluation, etc.).

In this section, we will consider a very special, yet practically far reaching, case of sample covariance matrix models for which the limiting spectral measure coincides with the Marčenko–Pastur law, while the population covariance matrix has a non-trivial informative structure. Since the Marčenko–Pastur law assumes an explicit well-understood expression (recall Theorem 2.3), the various estimates of interest will be explicit, thus intuitions on their behavior are easily derived. Besides, the various change of variable difficulties for contour integral methods met in the previous sections are greatly simplified in this setting.

These special models fundamentally rely on letting the covariance matrix \mathbf{C} be a *low rank* perturbation of the identity matrix \mathbf{I}_p , i.e., $\mathbf{C} = \mathbf{I}_p + \mathbf{P}$ for $\mathbf{P} \in \mathbb{R}^{p \times p}$ with $\text{rank}(\mathbf{P}) = k$ fixed with respect to n, p .

Such statistical models corresponding to a *low rank update* of a classical random matrix model with well-known behavior are generically called *spiked models*.

2.5.1 Isolated eigenvalues

sec:spiked-model_eigenvalues

Let us then consider again the model $\mathbf{X} = [\mathbf{x}_1, \dots, \mathbf{x}_n] \in \mathbb{R}^{p \times n}$ with $\mathbf{x}_i = \mathbf{C}^{\frac{1}{2}} \mathbf{z}_i$, $\mathbf{z}_i \in \mathbb{R}^p$ with standard i.i.d. entries and where

$$\mathbf{C} = \mathbf{I}_p + \mathbf{P}, \quad \mathbf{P} = \sum_{i=1}^k \ell_i \mathbf{u}_i \mathbf{u}_i^\top$$

with k and $\ell_1 \geq \dots \geq \ell_k > 0$ fixed with respect to n, p .

According to Theorem 2.5, $\mu_{\frac{1}{n}\mathbf{XX}^\top}$ has a limiting measure μ defined through the limiting measure ν of $\mu_{\mathbf{C}}$. But clearly $\nu = \delta_1$ here since

$$\mu_{\mathbf{C}} = \frac{p-k}{p}\delta_1 + \frac{1}{p}\sum_{i=1}^k \delta_{1+\ell_i} \rightarrow \delta_1.$$

As a consequence, while \mathbf{C} is not the identity matrix, μ is the Marčenko–Pastur law introduced in Theorem 2.3. Yet, the assumptions of the “no eigenvalue outside the support theorem”, Theorem 2.10, do not hold here since $\text{dist}(1 + \ell_1, \text{supp}(\nu)) \not\rightarrow 0$. Therefore, one cannot claim that *all* the eigenvalues of $\frac{1}{n}\mathbf{XX}^\top$ will converge to the support $\text{supp}(\mu)$.

We will precisely show here that, depending on the values of ℓ_i and the ratio $c = \lim p/n$, the i -th largest eigenvalue of $\frac{1}{n}\mathbf{XX}^\top$ may indeed *isolate* from $\text{supp}(\mu)$. As such, since most of the eigenvalues of $\frac{1}{n}\mathbf{XX}^\top$ aggregate but possibly for a few ones (up to k of them), the latter isolated eigenvalues are seen as isolated “spikes” in the histogram of eigenvalues. See Figure 2.11, commented next, for a visual representation of these “spikes”.

The specific result, here due to Baik (not Bai) and Silverstein, is given in the following theorem.¹⁷

theo:spikes

Theorem 2.12 (Spiked models, from Baik and Silverstein [2006]). *Under the setting of Theorem 2.5 with $\mathbb{E}[\mathbf{Z}_{ij}^4] < \infty$, let $\mathbf{C} = \mathbf{I}_p + \mathbf{P}$ with $\mathbf{P} = \sum_{i=1}^k \ell_i \mathbf{u}_i \mathbf{u}_i^\top$ its spectral decomposition, where k and $\ell_1 \geq \dots \geq \ell_k > 0$ are fixed with respect to n, p . Then, denoting $\lambda_1 \geq \dots \geq \lambda_p$ the eigenvalues of $\frac{1}{n}\mathbf{XX}^\top$, as $n, p \rightarrow \infty$ with $p/n \rightarrow c \in (0, \infty)$,*

$$\lambda_i \xrightarrow{\text{a.s.}} \begin{cases} \rho_i = 1 + \ell_i + c \frac{1+\ell_i}{\ell_i} > (1 + \sqrt{c})^2 & , \ell_i > \sqrt{c} \\ (1 + \sqrt{c})^2 & , \ell_i \leq \sqrt{c}. \end{cases}$$

The theorem thus identifies an abrupt change in the behavior of the i -th dominant eigenvalue λ_i of $\frac{1}{n}\mathbf{XX}^\top$: if $\ell_i \leq \sqrt{c}$, λ_i converges to the right-edge $(1 + \sqrt{c})^2$ of the support of the Marčenko–Pastur law μ and thus does *not* isolate. However, as soon as $\ell_i > \sqrt{c}$, λ_i converges to a limit *beyond* the right-edge of μ and thus *does isolate*.

With a physics inspiration, this phenomenon is often referred to as the *phase transition* of the spiked models.

From a statistical viewpoint, the fact that the i -th eigenvalue λ_i of the sample covariance matrix “macroscopically” exceeds or not the other eigenvalues according to whether $\ell_i > \sqrt{c}$ or $\ell_i \leq \sqrt{c}$ can be interpreted as a test of whether

¹⁷These same results were later retrieved using a free probability approach (so formally under slightly different assumptions on \mathbf{Z}) in the work [Benaych-Georges and Nadakuditi, 2011] and were generalized to a larger class of random matrix models. This last article, a richer set of dedicated and better digested techniques (such as those exposed presently), as well as the growing evidence of fundamental applications of the results [Bianchi et al., 2011, Donoho et al., 2013, Candes et al., 2015, Couillet, 2015, Couillet and Hachem, 2013], triggered a renewed wave of interest for spiked models [Loubaton et al., 2011, Capitaine, 2014].

the “signal strength” ℓ_i of the structured data exceeds the minimal *detectability* threshold \sqrt{c} : this can be achieved if the signal strength ℓ_i is strong enough, or alternatively if the number of observed independent data n is large enough (so that $c = \lim p/n$ is small), as common sense would suggest. Indeed, if $\ell_1 < \sqrt{c}$, the eigenvalues of $\frac{1}{n}\mathbf{XX}^\top$ are all asymptotically compacted in the support $[(1 - \sqrt{c})^2, (1 + \sqrt{c})^2]$ and thus it is theoretically (asymptotically) impossible to tell whether $\mathbf{C} = \mathbf{I}_p$ or \mathbf{C} is more structured from the mere observation of the spectral measure of $\frac{1}{n}\mathbf{XX}^\top$. This phase transition effect, for all successive spikes, is well illustrated in Figure 2.11.

Proof of Theorem 2.12. When it comes to assessing the eigenvalues of a given matrix \mathbf{M} , the first thing that comes to mind is to solve the determinant equation $\det(\mathbf{M} - \lambda\mathbf{I}) = 0$. This approach is not convenient for \mathbf{M} of increasing dimensions and we have seen that the Stieltjes transform method is an appropriate substitute in that case. Here, since the low rank matrix \mathbf{P} only induces a low rank perturbation of $\frac{1}{n}\mathbf{ZZ}^\top$, the use of Sylvester’s identity (Lemma 2.3) will turn the large dimensional determinant equation into a small (fixed) dimensional one, and the determinant equation method is now valid. This is the approach we pursue here.

Specifically, let us seek for the presence of an eigenvalue λ of $\frac{1}{n}\mathbf{XX}^\top$ that is asymptotically greater than $(1 + \sqrt{c})^2$. Our approach is to “isolate” the low rank contribution due to \mathbf{P} from the “whitened” sample covariance matrix model $\frac{1}{n}\mathbf{ZZ}^\top$ with identity covariance. To this end, we use the following sequence of equivalences

$$\begin{aligned} 0 &= \det\left(\frac{1}{n}\mathbf{XX}^\top - \lambda\mathbf{I}_p\right) \\ &= \det\left(\frac{1}{n}(\mathbf{I}_p + \mathbf{P})^{\frac{1}{2}}\mathbf{ZZ}^\top(\mathbf{I}_p + \mathbf{P})^{\frac{1}{2}} - \lambda\mathbf{I}_p\right) \\ &= \det(\mathbf{I}_p + \mathbf{P}) \det\left(\frac{1}{n}\mathbf{ZZ}^\top - \lambda(\mathbf{I}_p + \mathbf{P})^{-1}\right) \end{aligned}$$

where we denoted $\mathbf{X} = \mathbf{C}^{\frac{1}{2}}\mathbf{Z}$. Obviously, $\det(\mathbf{I}_p + \mathbf{P}) \neq 0$ so that the first determinant can be discarded. For the second determinant, first recall from the resolvent identity (Lemma 2.1) that

$$(\mathbf{I}_p + \mathbf{P})^{-1} = \mathbf{I}_p - (\mathbf{I}_p + \mathbf{P})^{-1}\mathbf{P}$$

so that we can isolate the (now well-understood) resolvent of the “whitened” model. That is, letting $\mathbf{Q}(\lambda) = (\frac{1}{n}\mathbf{ZZ}^\top - \lambda\mathbf{I}_p)^{-1}$, we write

$$\begin{aligned} 0 &= \det\left(\frac{1}{n}\mathbf{ZZ}^\top - \lambda\mathbf{I}_p + \lambda(\mathbf{I}_p + \mathbf{P})^{-1}\mathbf{P}\right) \\ &= \det\mathbf{Q}^{-1}(\lambda) \det(\mathbf{I}_p + \lambda\mathbf{Q}(\lambda)(\mathbf{I}_p + \mathbf{P})^{-1}\mathbf{P}). \end{aligned}$$

Inverting the matrix $\frac{1}{n}\mathbf{ZZ}^\top - \lambda\mathbf{I}_p$ is (almost surely) licit for all large n, p as we demanded $\lambda > (1 + \sqrt{c})^2$. Now, denoting $\mathbf{P} = \mathbf{U}\mathbf{L}\mathbf{U}^\top$ with $\mathbf{L} = \text{diag}(\ell_1, \dots, \ell_k)$

and $\mathbf{U} = [\mathbf{u}_1, \dots, \mathbf{u}_k] \in \mathbb{R}^{p \times k}$, we further have

$$(\mathbf{I}_p + \mathbf{P})^{-1} \mathbf{P} = (\mathbf{I}_p + \mathbf{U} \mathbf{L} \mathbf{U}^\top)^{-1} \mathbf{U} \mathbf{L} \mathbf{U}^\top = \mathbf{U} (\mathbf{I}_k + \mathbf{L})^{-1} \mathbf{L} \mathbf{U}^\top.$$

Plugging into the above determinant equation, this is

$$\begin{aligned} 0 &= \det \mathbf{Q}^{-1}(\lambda) \det (\mathbf{I}_p + \lambda \mathbf{Q}(\lambda) \mathbf{U} (\mathbf{I}_k + \mathbf{L})^{-1} \mathbf{L} \mathbf{U}^\top) \\ &= \det \mathbf{Q}^{-1}(\lambda) \det (\mathbf{I}_k + \lambda \mathbf{U}^\top \mathbf{Q}(\lambda) \mathbf{U} (\mathbf{I}_k + \mathbf{L})^{-1} \mathbf{L}) \end{aligned}$$

where in the last equality we applied Sylvester's identity. Since $\det \mathbf{Q}^{-1}(\lambda) = \det(\frac{1}{n} \mathbf{Z} \mathbf{Z}^\top - \lambda \mathbf{I}_p)$ for $\lambda > (1 + \sqrt{c})^2$, we finally have for all large n, p ,

$$0 = \det (\mathbf{I}_k + \lambda \mathbf{U}^\top \mathbf{Q}(\lambda) \mathbf{U} (\mathbf{I}_k + \mathbf{L})^{-1} \mathbf{L}).$$

From Theorem 2.3, we now know that

$$\mathbf{U}^\top \mathbf{Q}(\lambda) \mathbf{U} = m(\lambda) \mathbf{I}_k + o_{\|\cdot\|}(1)$$

almost surely, for $m(z)$ the Stieltjes transform of the Marčenko–Pastur law μ (the term \mathbf{I}_k arises from the fact that $\mathbf{U}^\top \mathbf{U} = \mathbf{I}_k$). Consequently, by continuity of the determinant (this is a polynomial of its entries), we have

$$0 = \det (\mathbf{I}_k + \lambda m(\lambda) (\mathbf{I}_k + \mathbf{L})^{-1} \mathbf{L}) + o(1)$$

and thus, if such a λ exists, it must satisfy

$$\lambda m(\lambda) = -\frac{1 + \ell_i}{\ell_i} + o(1).$$

for some $i \in \{1, \dots, k\}$. We thus need to understand when this equation has a solution. To this end, observe that the function $\mathbb{R} \setminus \text{supp}(\mu) \rightarrow \mathbb{R}$, $x \mapsto xm(x) = \int \frac{x}{t-x} \mu(dt)$ is increasing on its domain of definition and that $xm(x) \rightarrow -1$ as $x \rightarrow \infty$. Solving for $m(z)$ in Theorem 2.3, i.e.,

$$\begin{aligned} zcm^2(z) - (1 - c - z)m(z) + 1 &= 0 \\ \Leftrightarrow zm(z) &= \frac{\text{eq: proof spike expression of } m}{1 - z - czm(z)} \quad (2.31) \end{aligned}$$

(from which we may isolate $zm(z)$ and express it as a function of z alone) we further reach

$$\lim_{x \downarrow (1+\sqrt{c})^2} xm(x) = -\frac{1 + \sqrt{c}}{\sqrt{c}}.$$

Thus, $xm(x)$ increases from $-\frac{1+\sqrt{c}}{\sqrt{c}}$ to -1 on the set $((1 + \sqrt{c})^2, \infty)$. The equation $\lambda m(\lambda) = -\frac{1 + \ell_i}{\ell_i}$ thus only has a solution if and only if

$$-\frac{1 + \ell_i}{\ell_i} > -\frac{1 + \sqrt{c}}{\sqrt{c}}$$

that is, whenever $\ell_i > \sqrt{c}$. Assuming this holds, we may then use again (2.31) (replacing $zm(z)$ by $-(1 + \ell_i)/\ell_i$) to obtain

$$\lambda \rightarrow 1 + \ell_i + c \frac{1 + \ell_i}{\ell_i}$$

which concludes the proof of Theorem 2.12. \square

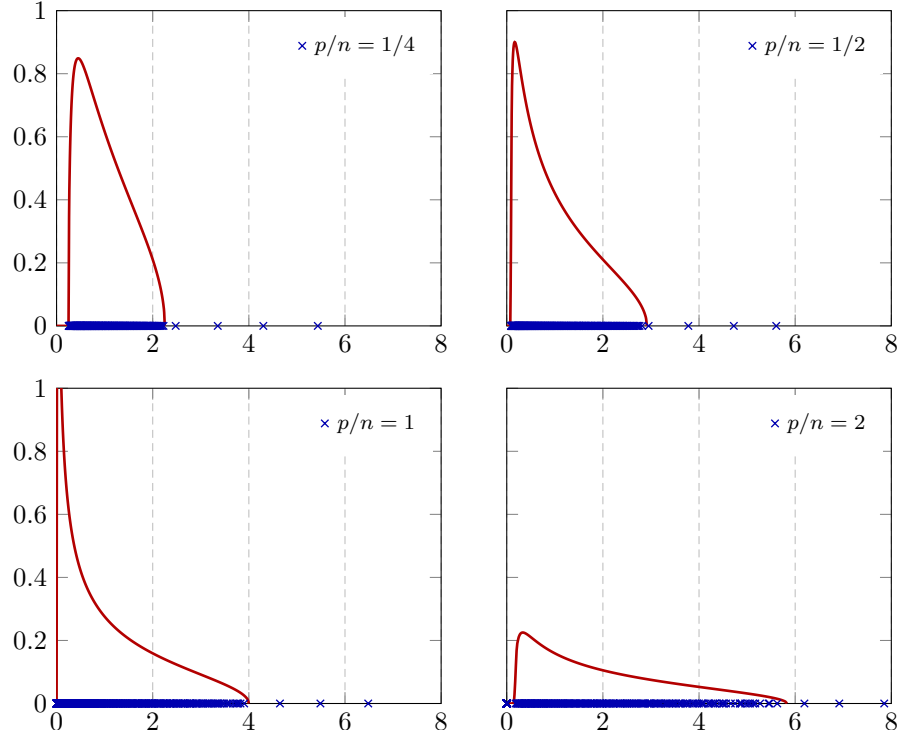


Figure 2.11: Eigenvalues of $\frac{1}{n} \mathbf{X} \mathbf{X}^\top$ (blue crosses) and the Marčenko–Pastur law (red line) for $\mathbf{X} = \mathbf{C}^{\frac{1}{2}} \mathbf{Z}$, $\mathbf{C} = \mathbf{I}_p + \mathbf{P}$ with $\mu_{\mathbf{P}} = \frac{p-4}{p} \delta_0 + \frac{1}{p} (\delta_1 + \delta_2 + \delta_3 + \delta_4)$, for $p = 512$ and different values of n . [Link to code] fig:spikes

Figure 2.11 depicts the eigenvalues of $\frac{1}{n} \mathbf{X} \mathbf{X}^\top$ versus the Marčenko–Pastur law, in the scenario where $\mathbf{C} = \mathbf{I}_p + \mathbf{P}$ with \mathbf{P} of rank four, for various ratios p/n . As predicted by Theorem 2.12, the number of visible “spikes” outside the limiting support of $\frac{1}{n} \mathbf{X} \mathbf{X}^\top$ varies with p/n : as the ratio decreases, less spikes are visible.

2.5.2 Isolated eigenvectors

sec:spiked-model_eigenvectors

From a practical standpoint, we have seen that the presence of isolated eigenvalues in the spectrum of the sample covariance $\frac{1}{n} \mathbf{X} \mathbf{X}^\top$ reveals the presence of

some “structure” in the population covariance \mathbf{C} in the sense that $\mathbf{C} \neq \mathbf{I}_p$. We have however also seen that the converse is not true: assuming a spiked model for \mathbf{C} , the absence of isolated eigenvalue does not imply $\mathbf{C} = \mathbf{I}_p$.

More interestingly, whether this “structure” is detected or not, one may wonder whether it can be estimated at all. More specifically, for $\mathbf{C} = \mathbf{I}_p + \mathbf{P}$ with $\mathbf{P} = \sum_{i=1}^k \ell_i \mathbf{u}_i \mathbf{u}_i^\top$, are the eigenvectors $\hat{\mathbf{u}}_1, \dots, \hat{\mathbf{u}}_k$ of $\frac{1}{n} \mathbf{X} \mathbf{X}^\top$ associated to the k largest eigenvalues $\lambda_1 \geq \dots \geq \lambda_k$ good estimators of $\mathbf{u}_1, \dots, \mathbf{u}_k$?

Not surprisingly, the answer is here again twofold: (i) if $\ell_i \leq \sqrt{c}$ then $\hat{\mathbf{u}}_i$ tends to be totally uncorrelated from and thus asymptotically orthogonal to \mathbf{u}_i , while (ii) if $\ell_i > \sqrt{c}$, $\hat{\mathbf{u}}_i$ is to some extent aligned to \mathbf{u}_i . The following theorem, due to Paul, quantifies this “to some extent”.¹⁸

theo:spikes_vep

Theorem 2.13 (Eigenvector alignment, from Paul [2007]). *Under the setting of Theorem 2.12, let $\hat{\mathbf{u}}_1, \dots, \hat{\mathbf{u}}_k$ be the eigenvectors associated with the largest k eigenvalues $\lambda_1 > \dots > \lambda_k$ of $\frac{1}{n} \mathbf{X} \mathbf{X}^\top$. Further assume that $\ell_1 > \dots > \ell_k > 0$ are all distinct. Then, for $\mathbf{a}, \mathbf{b} \in \mathbb{R}^k$ unit norm deterministic vectors*

$$\mathbf{a}^\top \hat{\mathbf{u}}_i \hat{\mathbf{u}}_i \mathbf{b} - \mathbf{a}^\top \mathbf{u}_i \mathbf{u}_i^\top \mathbf{b} \frac{1 - c\ell_i^{-2}}{1 + c\ell_i^{-1}} 1_{\ell_i > \sqrt{c}} \xrightarrow{\text{a.s.}} 0.$$

In particular, with $\mathbf{a} = \mathbf{b} = \mathbf{u}_i$ we obtain

$$|\mathbf{u}_i^\top \hat{\mathbf{u}}_i|^2 \xrightarrow{\text{a.s.}} \zeta_i \equiv \frac{1 - c\ell_i^{-2}}{1 + c\ell_i^{-1}} 1_{\ell_i > \sqrt{c}}.$$

Proof of Theorem 2.13. We may first write that, for all large n, p almost surely,

$$\mathbf{a}^\top \hat{\mathbf{u}}_i \hat{\mathbf{u}}_i \mathbf{b} = -\frac{1}{2\pi i} \oint_{\Gamma_{\rho_i}} \mathbf{a}^\top \left(\frac{1}{n} \mathbf{X} \mathbf{X}^\top - z \mathbf{I}_p \right)^{-1} \mathbf{b} dz$$

for Γ_{ρ_i} a small contour enclosing the almost sure limit $\rho_i = 1 + \ell_i + c\frac{1+\ell_a}{\ell_i}$ of the eigenvalue λ_i of $\frac{1}{n} \mathbf{X} \mathbf{X}^\top$ given in Theorem 2.12 only. Isolating $\frac{1}{n} \mathbf{Z} \mathbf{Z}^\top$ from $\frac{1}{n} \mathbf{X} \mathbf{X}^\top$ as in the proof of Theorem 2.12, we have from Woodbury’s identity

¹⁸Here again, a large body of literature and modernized tools were set in place to study asymptotic eigenvector behaviors. Some of them are only valid (or only convenient) for rank-one spike models [Paul, 2007, Benaych-Georges and Nadakuditi, 2011, 2012], but the techniques now widely used (such as the contour-integral method presented in this monograph) generally apply to an arbitrary number of spikes [Couillet and Hachem, 2013, Baik et al., 2005].

(Lemma 2.7) that

$$\begin{aligned}
& \mathbf{a}^\top \left(\frac{1}{n} \mathbf{X} \mathbf{X}^\top - z \mathbf{I}_p \right)^{-1} \mathbf{b} \\
&= \mathbf{a}^\top \left(\frac{1}{n} (\mathbf{I}_p + \mathbf{P})^{\frac{1}{2}} \mathbf{Z} \mathbf{Z}^\top (\mathbf{I}_p + \mathbf{P})^{\frac{1}{2}} - z \mathbf{I}_p \right)^{-1} \mathbf{b} \\
&= \mathbf{a}^\top (\mathbf{I}_p + \mathbf{P})^{-\frac{1}{2}} \left(\frac{1}{n} \mathbf{Z} \mathbf{Z}^\top - z \mathbf{I}_p - z \mathbf{P} \right)^{-1} (\mathbf{I}_p + \mathbf{P})^{-\frac{1}{2}} \mathbf{b} \\
&= \mathbf{a}^\top (\mathbf{I}_p + \mathbf{P})^{-\frac{1}{2}} \mathbf{Q}(z) (\mathbf{I}_p + \mathbf{P})^{-\frac{1}{2}} \mathbf{b} \\
&\quad + z \mathbf{a}^\top (\mathbf{I}_p + \mathbf{P})^{-\frac{1}{2}} \mathbf{Q}(z) \mathbf{U} \mathbf{L} (\mathbf{I}_k - z \mathbf{U}^\top \mathbf{Q}(z) \mathbf{U} \mathbf{L})^{-1} \mathbf{U}^\top \mathbf{Q}(z) (\mathbf{I}_p + \mathbf{P})^{-\frac{1}{2}} \mathbf{b} \\
&= \mathbf{a}^\top (\mathbf{I}_p + \mathbf{P})^{-\frac{1}{2}} \mathbf{Q}(z) (\mathbf{I}_p + \mathbf{P})^{-\frac{1}{2}} \mathbf{b} \\
&\quad + z m^2(z) \mathbf{a}^\top \mathbf{U} (\mathbf{I}_k + \mathbf{L})^{-\frac{1}{2}} \mathbf{L} (\mathbf{I}_k - z m(z) \mathbf{L})^{-1} (\mathbf{I}_k + \mathbf{L})^{-\frac{1}{2}} \mathbf{U}^\top \mathbf{b} + o(1)
\end{aligned}$$

where $\mathbf{Q}(z) = (\frac{1}{n} \mathbf{Z} \mathbf{Z}^\top - z \mathbf{I}_p)^{-1}$ and for the last equality we used $(\mathbf{I}_p + \mathbf{P})^{-\frac{1}{2}} = \mathbf{U} (\mathbf{I}_k + \mathbf{L})^{-\frac{1}{2}} \mathbf{U}^\top$ and $\mathbf{U}^\top \mathbf{Q}(z) \mathbf{U} = m(z) \mathbf{I}_k + o_{\|\cdot\|}(1)$, as per Theorem 2.3. The complex integration of $\mathbf{Q}(z)$ on the contour Γ_{ρ_i} only brings a positive residue for the second right-hand side term owing to the inverse $(\mathbf{I}_k - z m(z) \mathbf{L})^{-1}$ which is singular for $z = \rho_i$. We thus finally have

$$\begin{aligned}
\mathbf{a}^\top \hat{\mathbf{u}}_i \hat{\mathbf{u}}_i^\top \mathbf{b} &= -\frac{1}{2\pi i} \oint_{\Gamma_{\rho_i}} z m^2(z) \mathbf{a}^\top \mathbf{U} (\mathbf{I}_k + \mathbf{L})^{-\frac{1}{2}} \mathbf{L} (\mathbf{I}_k - z m(z) \mathbf{L})^{-1} \\
&\quad \times (\mathbf{I}_k + \mathbf{L})^{-\frac{1}{2}} \mathbf{U}^\top \mathbf{b} dz + o(1).
\end{aligned}$$

By a residue calculus, we obtain that

$$\lim_{z \rightarrow \rho_i} (z - \rho_i) (\mathbf{I}_k - z m(z) \mathbf{L})^{-1} = -(\rho_i m'(\rho_i) + m(\rho_i))^{-1} \ell_i^{-1} \mathbf{e}_i \mathbf{e}_i^\top$$

with $\mathbf{e}_i \in \mathbb{R}^k$ the canonical basis vector defined as $[\mathbf{e}_i]_j = \delta_{ij}$. Using the form

$$m(z) = \frac{1}{-z + \frac{1}{1+cm(z)}}$$

of the Stieltjes transform of the Marčenko-Pastur law gives

$$m'(z) = \frac{m(z)^2}{1 - \frac{cm(z)^2}{(1+cm(z))^2}}$$

from which we obtain in particular that $m(\rho_i) = -1/(\ell_i + c)$ and $m'(\rho_i) = \ell_i^2(\ell_i + c)^{-2}(\ell_i^2 - c)^{-1}$. It unfolds that the residue associated to $(\mathbf{I}_k - z m(z) \mathbf{L})^{-1}$ reads

$$(-\rho_i m'(\rho_i) - m(\rho_i))^{-1} \ell_i^{-1} \mathbf{e}_i \mathbf{e}_i^\top = -(\ell_i^2 - c) \ell_i^{-1} \mathbf{e}_i \mathbf{e}_i^\top$$

and we finally get

$$\mathbf{a}^\top \hat{\mathbf{u}}_i \hat{\mathbf{u}}_i \mathbf{b} = \mathbf{a}^\top \mathbf{u}_i \mathbf{u}_i^\top \mathbf{b} \frac{\rho_i m^2(\rho_i) \ell_i}{1 + \ell_i} (\ell_i^2 - c) \ell_i^{-1} = \mathbf{a}^\top \mathbf{u}_i \mathbf{u}_i^\top \mathbf{b} \frac{1 - c \ell_i^{-2}}{1 + c \ell_i^{-1}}$$

which concludes the proof of Theorem 2.13. \square

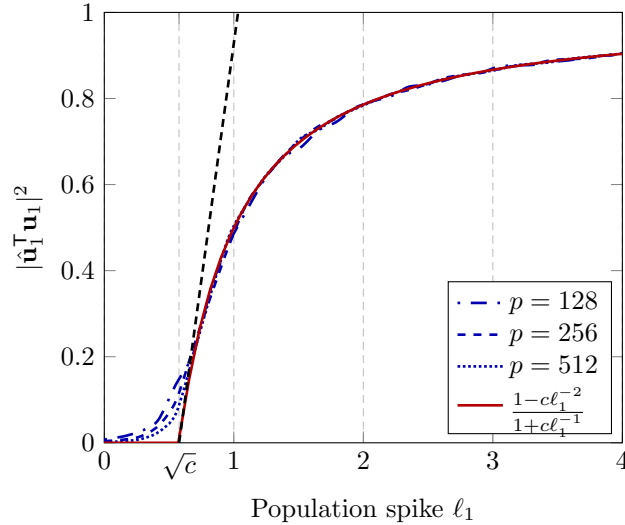


Figure 2.12: Empirical versus limiting $|\hat{\mathbf{u}}_1^\top \mathbf{u}_1|^2$ for $\mathbf{X} = \mathbf{C}^{\frac{1}{2}} \mathbf{Z}$, $\mathbf{C} = \mathbf{I}_p + \ell_1 \mathbf{u}_1 \mathbf{u}_1^\top$, $p/n = 1/3$, for varying ℓ_1 . Results obtained by averaging over 100 runs. In black dashed line the local behavior around \sqrt{c} . [Link to code] [fig:spike_eigenvector](#)

Figure 2.12 compares, in a single-spike scenario, the theoretical limit of $|\hat{\mathbf{u}}_1^\top \mathbf{u}_1|^2$ (in red) versus its empirical value for different ℓ_1 and different p, n with constant ratio p/n . It is important to note that the theoretical *asymptotic* phase transition phenomenon at $\ell_1 = \sqrt{c}$ corresponds to a sharp non-differentiable change in the function $\ell_1 \mapsto |\hat{\mathbf{u}}_1^\top \mathbf{u}_1|^2$; a local analysis in the limit of $\ell_1 = \sqrt{c} + \varepsilon$ reveals that $|\hat{\mathbf{u}}_1^\top \mathbf{u}_1|^2$ is locally equal to $|\hat{\mathbf{u}}_1^\top \mathbf{u}_1|^2 \simeq \frac{2\varepsilon}{\sqrt{c}(1+\sqrt{c})}$ and thus,

$$|\hat{\mathbf{u}}_1^\top \mathbf{u}_1|_{=\ell_1=\sqrt{c}+\varepsilon} \sqrt{\frac{2}{\sqrt{c}(1+\sqrt{c})}} \sqrt{\varepsilon} + O(\varepsilon)$$

thus having an infinite derivative in the limit $\ell_1 \downarrow \sqrt{c}$. On real data of finite size, this sharp transition is only observed for extremely large values of n, p . This in particular means that, in practice, residual information is present below the phase transition.

2.5.3 Limiting fluctuations

Theorem 2.12 on the *limiting* presence and position of isolated eigenvalues in the spectrum of $\frac{1}{n}\mathbf{XX}^T$ establishes that it suffices to evaluate whether the largest eigenvalue λ_1 of $\frac{1}{n}\mathbf{XX}^T$ “isolates from the other eigenvalues $\lambda_2 > \dots > \lambda_p$ ” to determine the presence of a structure in the population covariance \mathbf{C} .

However, in practice, from the empirical observation of $\lambda_1, \dots, \lambda_p$, how can one decide whether λ_1 is isolated? On a random realization of \mathbf{X} , λ_1 may haphazardly be found “rather far” from λ_2 by a mere probabilistic finite-dimensional effect. The natural question is then to determine whether this “haphazard” event can be evaluated.

A whole line of works, based on significantly different tools from the Stieltjes transform approach adopted in this monograph,¹⁹ settles this question by evaluating, for $\mathbf{C} = \mathbf{I}_p$ or $\mathbf{C} = \mathbf{I}_p + \mathbf{P}$ with the eigenvalues of \mathbf{P} below the phase transition, the asymptotic probability for λ_1 to escape its limiting value $(1 + \sqrt{c})^2$.

The main result of importance is the following.

Theorem 2.14 (Fluctuation of the largest eigenvalue, from Baik et al. [2005]).
theo:TW
Under the setting of Theorem 2.12, assume $0 \leq \ell_k < \dots < \ell_1 < \sqrt{c}$. Then,

$$n^{\frac{2}{3}} \frac{\lambda_1 - (1 + \sqrt{c})^2}{(1 + \sqrt{c})^{\frac{4}{3}} c^{-\frac{1}{6}}} \rightarrow \text{TW}_1$$

in law, where TW_1 is the (real) Tracy-Widom distribution, historically defined in [Tracy and Widom, 1996].²⁰

Specifically, the theorem is here placed under the setting where the “population spikes” are *below* the phase transition and thus asymptotically *not isolated* (as per Theorem 2.12). In this setting, the largest eigenvalue λ_1 thus converges to the right edge $(1 + \sqrt{c})^2$ of the Marčenko-Pastur law and more precisely behaves, according to the theorem, as $\lambda_1 = (1 + \sqrt{c})^2 + n^{-\frac{2}{3}} T$ where T is a (scaled) Tracy-Widom random variable.

This result is of practical interest as it allows one to estimate, for sufficiently large n, p , the probability for λ_1 to be found away from its theoretical limit $(1 + \sqrt{c})^2$ below the phase transition.

Precisely, the result shows that the limiting fluctuations of λ_1 are not Gaussian but follow the Tracy-Widom distribution and that, possibly surprisingly,

¹⁹Unlike the Stieltjes transform method, these tools start from the explicit (finite dimensional) formula of the joint eigenvalue distribution of matrix models \mathbf{X} or \mathbf{XX}^T , which is known in the Gaussian case (and only in this case) and given by (2.34). Exploiting the theory of orthogonal polynomials and determinantal processes, (2.34) can be marginalized so to retrieve the exact (finite dimensional) law of one or several specific eigenvalues (inside the bulk or on the edge). Taking the large dimensional limit relates the law of the eigenvalues to the determinant of a specific kernel [Soshnikov, 2000] (Airy kernel for the edge eigenvalues [Johnstone, 2001, Soshnikov, 1999], sine kernel in the bulk [Ben Arous and Péché, 2005, Erdős et al., 2010]). Details on these techniques can be found in [Anderson et al., 2010].

²⁰The Tracy-Widom distribution does not have an explicit form. Several works have provided approximated forms as well as tables of TW_1 [Chiani, 2014, Ma et al., 2012].

the rate of this fluctuation is of order $O(n^{-\frac{2}{3}})$ (instead of $O(n^{-\frac{1}{2}})$ or $O(n^{-1})$ as one would usually expect). This rate is strongly related to the following result, initially observed by Silverstein and Choi in [Silverstein and Choi, 1995]: close to the right-edge of its support, the Marčenko–Pastur law behaves proportionally to $\sqrt{(1 + \sqrt{c})^2 - x}$. As such, the typical number of eigenvalues in a space of size ϵ in the neighborhood of the edge is

$$\int_{(1+\sqrt{c})^2-\epsilon}^{(1+\sqrt{c})^2} \sqrt{(1+\sqrt{c})^2 - x} dx \propto \epsilon^{\frac{3}{2}}.$$

This explains the typical $O(n^{-\frac{2}{3}})$ fluctuation of the eigenvalues in this neighborhood.

The original result from [Baik et al., 2005] also provides the limiting fluctuations of $\lambda_1, \dots, \lambda_k$ beyond the phase transition (i.e., when $\ell_i > \sqrt{c}$). Interestingly, after the transition, the fluctuation of λ_1 is now a classical central limit with speed $O(n^{-\frac{1}{2}})$. The surprising “transition” from $O(n^{-\frac{2}{3}})$ to $O(n^{-\frac{1}{2}})$ of the fluctuations of λ_1 (which has little meaning or interpretability for finite n, p) is often called the *BBP phase transition* after the names of the authors of [Baik et al., 2005]. The authors in [Couillet and Hachem, 2013] go beyond by even providing the joint fluctuations of the eigenvalues and eigenvector projections as follows.

Theorem 2.15 (Joint fluctuations beyond the phase transition (from [Couillet and Hachem, 2013])). *Under the setting and notations of Theorem 2.12 and Theorem 2.13, assume $\ell_1 > \dots > \ell_k > \sqrt{c}$ and define $L = \sqrt{p}[\lambda_1 - \rho_1, \dots, \lambda_k - \rho_k]^T$ and $V = \sqrt{p}[|\mathbf{u}_1^T \hat{\mathbf{u}}_1|^2 - \zeta_1, \dots, |\mathbf{u}_k^T \hat{\mathbf{u}}_k|^2 - \zeta_k]^T$. Then, as $p, n \rightarrow \infty$ with $p/n \rightarrow c \in (0, \infty)$,*

$$\begin{pmatrix} L \\ V \end{pmatrix} \rightarrow \mathcal{N} \left(\mathbf{0}_{2k}, \text{BlockDiag} \left(\begin{bmatrix} \frac{c^2(1+\ell_i)^2 \left(1+c\frac{(1+\ell_i)^2}{(c+\ell_i)^2}\right)}{(c+\ell_i)^2(\ell_i^2-c)} & \frac{(1+\ell_i)^3 c^2}{(\ell_i+c)^2 \ell_i} \\ \frac{(1+\ell_i)^3 c^2}{(\ell_i+c)^2 \ell_i} & \frac{c(1+\ell_i)^2 (\ell_i^2-c)}{\ell_i^2} \end{bmatrix}_{i=1}^k \right) \right)$$

where BlockDiag is the “block-diagonal” operator.

The theorem notably states that, in the large n, p limit, while each eigenvalue-eigenvector projector pair fluctuates together, the k pairs fluctuate independently.

Remark 2.14 (Tracy-Widom law: beyond the real field and universality). *The Tracy-Widom law was first introduced in the context of Wigner random matrices (Theorem 2.4). More precisely, Tracy and Widom [1996] showed that the fluctuation of the largest eigenvalue of a real Gaussian Wigner random matrix ($\frac{1}{\sqrt{n}} \mathbf{X}$ with $\mathbf{X} \in \mathbb{R}^{n \times n}$ of i.i.d. zero mean and unit variance Gaussian entries) asymptotically follows a Tracy-Widom distribution*

$$n^{\frac{2}{3}}(\lambda_1 - 2) \rightarrow \text{TW}_1.$$

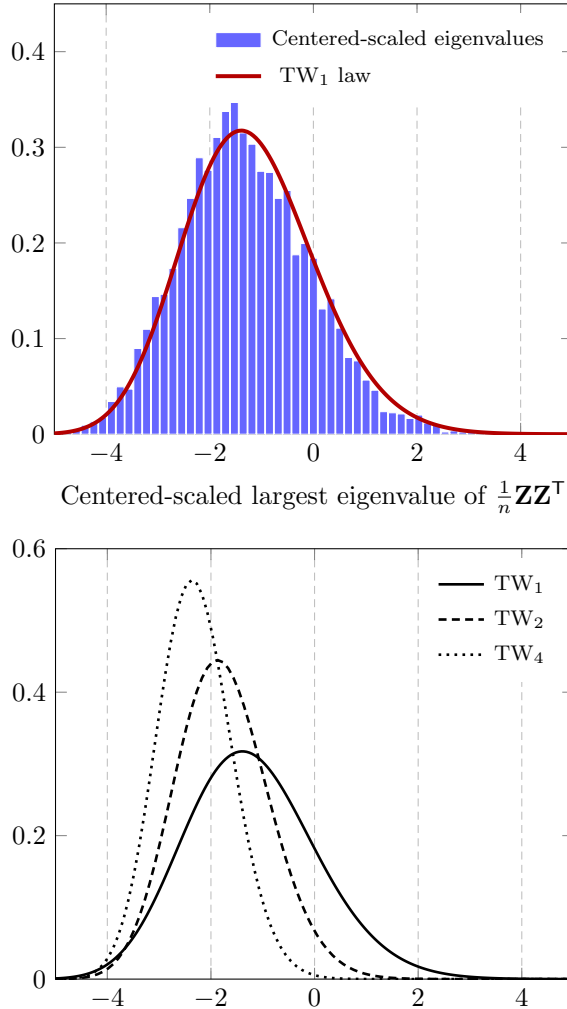


Figure 2.13: **(Top)** Empirical histogram of $n^{\frac{2}{3}} \frac{\lambda_1 - (1 + \sqrt{c})^2}{(1 + \sqrt{c})^{\frac{4}{3}} c^{-\frac{1}{6}}}$ for $p = 256$, $n = 512$ versus the real Tracy-Widom law TW₁. Histogram obtained over 5 000 independent runs. **(Bottom)** Tracy-Widom distribution TW _{β} for $\beta = 1$ (real \mathbf{X}_{ij}), 2 (complex \mathbf{X}_{ij}), and 4 (symplectic \mathbf{X}_{ij}). [Link to code] fig:TW

The Tracy-Widom law also extends beyond the largest eigenvalue: it holds true for the finitely many largest as well as smallest eigenvalues of the Wigner and the Wishart matrix (in the latter case only if $p/n \not\rightarrow 1$). It also goes beyond real-valued symmetric Gaussian matrices (often referred to as the Gaussian orthogonal ensemble (GOE)) and the real-valued Wishart random matrices, to complex (Gaussian Unitary Ensemble (GUE)) and quaternionic (Gaussian Symplectic

Ensemble (GSE)) Gaussian matrices. See Figure 2.13 below for an illustration.

The Tracy-Widom law has also been proved, to some extent, to be universal with respect to the Gaussian distribution. In [Soshnikov, 1999] and [Erdős, 2011], the authors prove that, for fast decaying distributions, it is sufficient to match the first two moments of the entries of \mathbf{X} to obtain asymptotic Tracy-Widom fluctuations.

2.5.4 Further discussions and other spiked models

As briefly discussed above, the “spiked model” terminology goes beyond sample covariance matrix models with $\mathbf{C} = \mathbf{I}_p + \mathbf{P}$, for \mathbf{P} a low rank matrix. In the literature, spiked models loosely refer to as “low rank perturbative” models in the following sense: there exists an underlying random matrix model \mathbf{X} , the spectral measure of which converges to a well-defined measure with compact support *and* having eigenvalues converging to the support (i.e., no single eigenvalue isolates) which is then modified in some way by a low rank perturbation matrix \mathbf{P} ; the resulting matrix has the same limiting spectral measure as that of \mathbf{X} but with possibly some spurious (isolated) eigenvalues.

Baik and Silverstein [2006] were the first to study spiked models, but their approach relied on applying the results on sample covariance matrix models (i.e., Theorem 2.5) to the specific case where $\mathbf{C} = \mathbf{I}_p + \mathbf{P}$. This approach requires to have a full understanding of a “more complex” statistical model before particularizing it to a low rank perturbation. Pursuing on the footnote introducing Theorem 2.12, more modern tools launched a second wave of advances in spiked models, mostly triggered by the ideas found in Benaych-Georges and Nadakuditi [2012] (with a free probability approach), which is based on relating the perturbation matrix model to the underlying simple (non perturbed) matrix; this is mathematically simpler and opened the path to a broader scope of generalizations to more advanced random matrix models.

Among the popular spiked models, we have the following cases:

- the *information-plus-noise* model of the type

$$\frac{1}{n}(\mathbf{X} + \mathbf{P})(\mathbf{X} + \mathbf{P})^\top$$

with $\mathbf{X} \in \mathbb{R}^{p \times n}$ having i.i.d. standard entries (zero mean, unit variance and finite fourth moment) and $\mathbf{P} \in \mathbb{R}^{p \times n}$ deterministic (or at least independent of \mathbf{X}) of fixed rank k .

- the *additive* model of the type

$$\mathbf{M} + \mathbf{P}$$

where $\mathbf{M} \in \mathbb{R}^{p \times p}$ is either of the type $\mathbf{M} = \frac{1}{n}\mathbf{XX}^\top$, $\mathbf{X} \in \mathbb{R}^{p \times n}$ with standard i.i.d. entries, or of $\mathbf{M} = \frac{1}{\sqrt{n}}\mathbf{X}$ with \mathbf{X} symmetric with standard i.i.d. entries above and on the diagonal and $\mathbf{P} \in \mathbb{R}^{n \times n}$ deterministic of low rank.

Each of these models has its own phase transition threshold (i.e., the value that eigenvalues of \mathbf{P} must exceed for a spike to be observed), dominant eigenvalue limits, and eigenvector projections. These can all be determined with the aforementioned proof approaches (see examples in the exercise list, Section 2.9).

However, we will see in several applications in Chapter 4 that, in practice, we will be confronted with more general forms of low rank perturbation models that do not fit this conventional “random matrix \mathbf{X} and deterministic perturbation \mathbf{P} ” assumption.

In particular, \mathbf{P} will often be a (possibly elaborate) function of \mathbf{X} . Also, \mathbf{X} itself, which will often stand for the “noisy” part of the data model (while \mathbf{P} will in general comprise both the relevant information and possibly some extra noise), may induce its own isolated eigenvalues. For instance, we shall see that, depending on the ratios p/n and $\text{tr } \mathbf{C}^4 / (\text{tr } \mathbf{C}^2)^2$, the random matrix $\{[\mathbf{X}\mathbf{X}^\top]_{ij}^2 1_{i \neq j}\}_{i,j=1}^p$ where $\mathbf{X} = \mathbf{C}^{\frac{1}{2}} \mathbf{Z}$ and \mathbf{Z} with i.i.d. standard entries, may have two isolated eigenvalues although all the eigenvalues of \mathbf{C} remain in their limiting support. Also, in the context of robust estimation of covariance matrices, it will not be natural for the statistical model to impose that all its population eigenvalues to converge to their limiting support (in particular to mimic the action of a few outliers).

Yet, despite these technical differences, the proof approaches of Theorem 2.12 and Theorem 2.13 remain essentially valid. We thus propose here to generalize the notion of “spiked models” to models of the type $\mathbf{X} + \mathbf{P}$ where \mathbf{X} is some reference, well understood, random matrix model (possibly inducing its own spikes) and \mathbf{P} is a low rank matrix, possibly depending on \mathbf{X} .

With this definition, the aforementioned *sample covariance*, *information-plus-noise* and *additive* models are in fact all equivalent to an additive model. Precisely, we may write

$$\begin{aligned} \frac{1}{n}(\mathbf{X} + \mathbf{P})(\mathbf{X} + \mathbf{P})^\top &= \mathbf{M} + \mathbf{P}' \\ \mathbf{M} &= \frac{1}{n}\mathbf{X}\mathbf{X}^\top, \quad \mathbf{P}' = \frac{1}{n}(\mathbf{X}\mathbf{P}^\top + \mathbf{P}\mathbf{X}^\top + \mathbf{P}\mathbf{P}^\top) \end{aligned}$$

and

$$\begin{aligned} \frac{1}{n}(\mathbf{I}_p + \mathbf{P})^{\frac{1}{2}}\mathbf{X}\mathbf{X}^\top(\mathbf{I}_p + \mathbf{P})^{\frac{1}{2}} &= \mathbf{M} + \mathbf{P}' \\ \mathbf{M} &= \frac{1}{n}\mathbf{X}\mathbf{X}^\top, \quad \mathbf{P}' = \frac{1}{n}(\mathbf{X}\mathbf{P}''^\top + \mathbf{P}''\mathbf{X} + \mathbf{P}''\mathbf{P}''^\top) \end{aligned}$$

where we denote $\mathbf{P}'' = \mathbf{U}((\mathbf{I}_k + \mathbf{L})^{\frac{1}{2}} - \mathbf{I}_k)\mathbf{U}^\top$ with $\mathbf{P} = \mathbf{U}\mathbf{L}\mathbf{U}^\top$. In the remainder of the monograph, we shall systematically exploit this generic modelling approach to treat all spiked models.

2.6 Information-plus-noise, deformed Wigner, and other models

sec:other_models

2.6.1 Why focus on the sample covariance matrix model?

The previous sections have mostly been concerned with the sample covariance matrix (as well as more marginally with Wigner matrices), as an instrumental statistical model for the introduction of the main technical tools of interest to the monograph: the Stieltjes transform method, the spiked model approach, statistical inference based on contour integrals, etc.

Several other classical random matrix models, of interest in statistics, will be listed in this section. The technical methods required to study these models are however not very different and thus not worth detailing. Only pointers to relevant references will be provided here for the interested reader.

It is in particular important to stress that many statistical models arising in machine learning applications are so specific that they may not (strictly) fall in any of the conventional models discussed above. Yet, up to some additional tricks, the analytical tools required to study these models are in general not much different from those presented in this chapter. Among examples met in the next chapters of this monograph, we may list:

- Graph Laplacian matrices

$$\mathbf{D} - \mathbf{A}, \quad \mathbf{D}^{-\frac{1}{2}} \mathbf{A} \mathbf{D}^{-\frac{1}{2}}, \quad \mathbf{D}^{-1} \mathbf{A}$$

for $\mathbf{A} \in \mathbb{R}^{n \times n}$ a symmetric matrix with independent entries (up to symmetry) and $\mathbf{D} = \text{diag}(\mathbf{A}\mathbf{1}_n)$. The dependence between \mathbf{A} and \mathbf{D} makes these random matrices slightly different from *deformed Wigner matrices* (see below) of the type $\mathbf{A} + \mathbf{D}$ where \mathbf{A} has independent entries and \mathbf{D} is *deterministic*.

- Kernel random matrices of the inner-product or distance type

$$\mathbf{K} = \{f(\mathbf{x}_i^\top \mathbf{x}_j)\}_{i,j=1}^n, \quad \mathbf{K} = \{f(\|\mathbf{x}_i - \mathbf{x}_j\|^2)\}_{i,j=1}^n.$$

There, the non-trivial dependence between the entries of \mathbf{K} differs significantly from sample covariance models (except for the linear kernel function $f(t) = t$ in the inner-product case).

- Robust estimators of scatter $\hat{\mathbf{C}}$ defined by the solutions to

$$\hat{\mathbf{C}} = \frac{1}{n} \sum_{i=1}^n u\left(\frac{1}{p} \mathbf{x}_i^\top \hat{\mathbf{C}}^{-1} \mathbf{x}_i\right) \mathbf{x}_i \mathbf{x}_i^\top$$

for some non-increasing function $u(t)$. There, due to the implicit nature of $\hat{\mathbf{C}}$, sample covariance matrix results cannot be strictly applied.

- F-matrix models $\hat{\mathbf{C}}_1^{-1}\hat{\mathbf{C}}_2$ and product models $\hat{\mathbf{C}}_1\hat{\mathbf{C}}_2$ for $\hat{\mathbf{C}}_a = \frac{1}{n}\mathbf{X}_a\mathbf{X}_a^\top$, $a \in \{1, 2\}$, with $\mathbf{X}_1, \mathbf{X}_2$ independent (notably Gaussian) random matrices, used in covariance matrix distance evaluation (e.g., Fisher distance, KL divergence, Wasserstein distance, etc.). By successive conditioning, these models are more directly related to the sample covariance matrix models, although not strictly equivalent.

Nonetheless, most models and applications listed above appear to be strongly related, one way or another, to sample covariance matrices. Of the examples above, kernel matrices, robust estimators, F-matrices and sample covariance products all relate to sample covariance matrices. The graph Laplacian (as well, to some extent, as the kernel random matrix models) is rather connected to Wigner matrices. This justifies the particularly focused vision of this chapter.²¹

2.6.2 Other models

2.6.2.1 Advanced sample covariance matrices

From a historical standpoint, the model studied by [Silverstein and Bai \[1995\]](#) is slightly more general than that presented in [Theorem 2.5](#). This model indeed assumes

$$\mathbf{A} + \frac{1}{n}\mathbf{X}^\top \mathbf{C} \mathbf{X}$$

for $\mathbf{X} \in \mathbb{R}^{p \times n}$ with independent entries and \mathbf{A}, \mathbf{C} deterministic matrices (in fact, \mathbf{C} was imposed to be diagonal in [\[Silverstein and Bai, 1995\]](#) but this condition was later relaxed).

The bi-correlated model of the type $\frac{1}{n}\mathbf{C}^{\frac{1}{2}}\mathbf{X}\tilde{\mathbf{C}}\mathbf{X}^\top\mathbf{C}^{\frac{1}{2}}$ introduced in [Theorem 2.6](#) was later studied in [\[Paul and Silverstein, 2009\]](#), where not only the limiting spectrum but also the exact separation of the eigenvalues is studied. The extension of the spectral analysis of [\[Silverstein and Choi, 1995\]](#) for this model was then provided in [\[Couillet and Hachem, 2014\]](#); a convenient explicit Stieltjes transform inverse $z(\tilde{m})$ no longer exists for this model (due to the presence of a coupled system of equations), but inverse mapping theorems guarantee its existence and enable similar results.

For wireless communication purposes, this model was further extended in [\[Couillet et al., 2011\]](#) to

$$\sum_{i=1}^k \frac{1}{n_i} \mathbf{R}_i^{\frac{1}{2}} \mathbf{X}_i \mathbf{T}_i \mathbf{X}_i^\top \mathbf{R}_i^{\frac{1}{2}}$$

²¹In effect and to the best of our knowledge, most, if not all, random matrix results directly related to machine learning applications boil down, in simple data model settings at least, to combinations (usually sums, sometimes products) of asymptotically independent matrices of the Wishart (Marčenko-Pastur related) and Wigner (semi-circle related) types.

where $\mathbf{T}_i \in \mathbb{R}^{n_i \times n_i}$ and $\mathbf{R}_i \in \mathbb{C}^{p \times p}$ are symmetric nonnegative definite matrices standing respectively for the transmit (T) and receive (R) correlation matrices at each end of a communication channel between k devices equipped with n_1, \dots, n_k antennas and a single receiver equipped with p antennas. Establishing the limiting spectral measure of this model allows one to establish for instance the maximally achievable communication rates between k simultaneously transmitting mobile phones and a local base station. Further extensions of this model were then proposed to model more involved wireless communication models, but they mostly all consist in summing independent versions of Gram matrices $\mathbf{Z}_i \mathbf{Z}_i^\top$ where \mathbf{Z}_i is a Gaussian (or beyond Gaussian) matrix with possibly nonzero mean, side correlations, a variance profile, etc.; see e.g., [Wen et al., 2012, Hachem et al., 2007, Wagner et al., 2012, Papazafeiropoulos and Ratnarajah, 2015] out of a much larger list of articles on the topic.

Of interest to statistics is also the *information-plus-noise* model of the type

$$\frac{1}{n}(\mathbf{X} + \mathbf{A})(\mathbf{X} + \mathbf{A})^\top$$

which is the sample “correlation” matrix between non-centered independent data $\mathbf{X} + \mathbf{A}$. This model also finds some interest in wireless communications where $[\mathbf{X} + \mathbf{A}]_{ij}$ models the statistical link between transmit antenna j and receive antenna i which may not be at the same mean-distance (controlled by \mathbf{A}_{ij}) than another antenna pair. This model was first studied by Dozier and Silverstein [2007] who established the (unique) canonical equation ruling the limiting spectral distribution of the model, as a function of the limiting Stieltjes transform of $\mu_{\mathbf{A}}$. Surprisingly enough, this model induces specific technical difficulties that left open for long the question of the exact location of the eigenvalues. Only much later in [Loubaton et al., 2011] for the Gaussian case and then in [Capitaine, 2014] for the generic i.i.d. setting was the result fully established: that is, as for the sample covariance matrix result (Theorem 2.10), under compacity assumption on the eigenvalues of \mathbf{A} , none of the eigenvalues of $\frac{1}{n}(\mathbf{X} + \mathbf{A})(\mathbf{X} + \mathbf{A})^\top$ asymptotically escapes their limiting support with high probability.

Yet, for practical applications, if the vectors of means $\mathbf{A}_{\cdot 1}, \dots, \mathbf{A}_{\cdot n}$ in the model $\mathbf{X} + \mathbf{A}$ are equal (to say vector $\boldsymbol{\mu}$), then $\mathbf{A} = \boldsymbol{\mu} \mathbf{1}_n^\top$ reduces to a rank-one matrix, and $\frac{1}{n}(\mathbf{X} + \mathbf{A})(\mathbf{X} + \mathbf{A})^\top$ is a mere spiked model, which does not necessitate the technical intricacies of the aforementioned articles. If instead the entries \mathbf{A}_{ij} are distinct with no specific structure, then it is in general not natural to assume that the \mathbf{X}_{ij} have equal variance (as the variance should scale with the mean). To handle this setting, Hachem et al. [2007], Dumont et al. [2007] study the generic *non-centered variance profile* model

$$\frac{1}{n}(\mathbf{B} \odot \mathbf{X} + \mathbf{A})(\mathbf{B} \odot \mathbf{X} + \mathbf{A})^\top$$

where \mathbf{B} is a symmetric matrix and \odot is the entry-wise Hadamard product. There is no natural limiting spectral measure for this model (even when requiring the spectra of \mathbf{A}, \mathbf{B} to converge) but deterministic equivalents can be

established. Those rely on a set of pn fixed-point equations. To our knowledge, no result on the conditions for the exact spectrum separation has been established in this setting. In the “separable case” where $\mathbf{B} = \mathbf{b}_1\mathbf{b}_2^\top$ for some vectors $\mathbf{b}_1, \mathbf{b}_2$ (in which case $\mathbf{B} \odot \mathbf{X} = \text{diag}(\mathbf{b}_1)\mathbf{X}\text{diag}(\mathbf{b}_2)$), the solution reduces to two fixed-point equations and the exact asymptotic location of the eigenvalues is almost a direct application of the “no-eigenvalue outside the support” theorem for the bi-correlated and the information-plus-noise models (i.e., the extension of Theorem 2.10 to these models).

2.6.2.2 Advanced Wigner matrices

The generalizations of Wigner random matrix model ($\frac{1}{\sqrt{n}}\mathbf{X}$ with \mathbf{X} having i.i.d. zero mean and unit variance entries) have been studied quite in parallel to the generalization surrounding the sample covariance matrix model $\frac{1}{n}\mathbf{XX}^\top$, as the technical tools and proofs are quite alike (if not simpler).

The first extended model of historical interest was that of the deformed (i.e., nonzero mean) Wigner model of the type

$$\frac{1}{\sqrt{n}}(\mathbf{X} + \mathbf{A})$$

for \mathbf{A} symmetric and deterministic [Khorunzhy and Pastur, 1994]. Yet again, if $\mathbf{A} \neq 0$, of utmost interest in practice is the case where the independent entries of \mathbf{X} have differing variances, which brings forth the model

$$\frac{1}{\sqrt{n}}(\mathbf{B} \odot \mathbf{X} + \mathbf{A}).$$

The set of the n^2 canonical implicit (Stieltjes transform related) equations induced for this model, or for its separable version ($\mathbf{B} = \mathbf{b}_1\mathbf{b}_2^\top$), have been thoroughly investigated in [Ajanki et al., 2019].

In practice, these models are directly applicable to the adjacency matrices of random graphs ($[\mathbf{X} + \mathbf{A}]_{ij}$ is the connectivity between node i and node j) with independent link probabilities. The elementary case of such random graph models is the so-called Erdős–Rényi graph for which $\mathbf{X} + \mathbf{A}$ has i.i.d. Bernoulli $\{0, 1\}$ entries with parameter p . In this case $\mathbf{A} = p\mathbf{1}_n\mathbf{1}_n^\top$ is a rank-one matrix and \mathbf{X} has i.i.d. $\{-p, 1 - p\}$ entries such that $\mathbb{P}(\mathbf{X}_{ij} = 1 - p) = p$ and $\mathbb{P}(\mathbf{X}_{ij} = -p) = 1 - p$. This here boils down to a spiked model. Assuming the graph has *heterogeneous degrees*, in the sense that every particular node has its own probability q_i to connect to any other arbitrary node in the graph, we end up with the model $\text{diag}(\mathbf{q})\mathbf{X}\text{diag}(\mathbf{q}) + \mathbf{A}$ with $\mathbf{q} = [q_1, \dots, q_n]$, $\mathbf{X}_{ij} \in \{-q_i q_j, 1 - q_i q_j\}$ and $\mathbf{A}_{ij} = q_i q_j$. Here again $\mathbf{A} = \mathbf{q}\mathbf{q}^\top$ is a rank-one matrix.

2.6.2.3 (Real) Haar random matrices

subsubsec:haar

Many algorithms and techniques in machine learning and data (or signal) processing involve random projections, in general on lower dimensional subspaces.

This naturally calls for the study of matrix models involving random isometric matrices $\mathbf{U} \in \mathbb{R}^{p \times n}$, $n \leq p$, such that $\mathbf{U}^\top \mathbf{U} = \mathbf{I}_n$. These can be alternatively seen as the concatenated n columns of an underlying orthogonal matrix $\tilde{\mathbf{U}} \in \mathbb{R}^{p \times p}$.

Assuming $\tilde{\mathbf{U}}$ to be drawn uniformly in the space of unitary $p \times p$ matrices (this is called the *Haar measure*), \mathbf{U} is an *orthogonally invariant* random matrix, i.e., $\mathbf{V}\mathbf{U}\mathbf{W}$ has the same law as \mathbf{U} for any pair of deterministic orthogonal matrices $\mathbf{V} \in \mathbb{R}^{p \times p}$, $\mathbf{W} \in \mathbb{R}^{n \times n}$. However, unlike Gaussian random matrices $\mathbf{X} \in \mathbb{R}^{p \times n}$, which are also orthogonally invariant, the entries of \mathbf{U} are *not* independent as they must satisfy $\mathbf{U}^\top \mathbf{U} = \mathbf{I}_n$. This makes the study of the family of *Haar random matrices* more involved than the classical Gaussian case.

Yet, strong analogies exist between the Gaussian and the Haar random matrices. To start with, note that \mathbf{U} can be constructed from Gaussian random matrices by letting $\mathbf{U} = \mathbf{Z}(\mathbf{Z}^\top \mathbf{Z})^{-\frac{1}{2}}$ where $\mathbf{Z} \in \mathbb{R}^{p \times n}$, $n \leq p$, is a random matrix with i.i.d. standard Gaussian entries. Using this property, the fundamental trace lemma, Lemma 2.11, can be extended to a Haar-matrix equivalent [Debbah et al., 2003, Couillet et al., 2012].

lem:trace-lemma-Haar

Lemma 2.16 (Trace lemma for isometric matrices, [Couillet et al., 2012, Lemma 5]).
Let $\mathbf{U} \in \mathbb{R}^{p \times n}$ be $n < p$ columns of a $p \times p$ Haar random matrix and let $\mathbf{u} \in \mathbb{R}^p$ be a column of \mathbf{U} . Then, for $\mathbf{X} \in \mathbb{R}^{p \times p}$ a matrix function of the columns of \mathbf{U} , except \mathbf{u} , and of bounded operator norm,

$$\mathbb{E} \left[\left| \mathbf{u}^\top \mathbf{X} \mathbf{u} - \frac{1}{p-n} \operatorname{tr} \mathbf{\Pi} \mathbf{X} \right|^4 \right] \leq \frac{C}{p^2}$$

where $\mathbf{\Pi} = \mathbf{I}_p - \mathbf{U} \mathbf{U}^\top + \mathbf{u} \mathbf{u}^\top$ and C a constant depending only on the operator norm $\|\mathbf{X}\|$ and the ratio n/p .

Of course, since $\mathbf{U} \mathbf{U}^\top$ is a projection matrix, all its eigenvalues are 1 and 0 and there is thus no interest in the spectrum of $\mathbf{U} \mathbf{U}^\top$ itself. The above trace lemma however becomes handy when dealing with more structured models, such as $\mathbf{C}^{\frac{1}{2}} \mathbf{U} \mathbf{U}^\top \mathbf{C}^{\frac{1}{2}}$; the latter may be seen as a generalization of the sample covariance matrix model of Theorem 2.5. Specifically, we have the following result which provides a deterministic equivalent (and consequently the limiting eigenvalue distribution **** Why the lsd? the convergence is only for $z < 0$, no? When I tried to do simulations this seems not working ****) for this model.

theo:bai-silverstein_Haar

Theorem 2.16 (Haar sample covariance [Couillet et al., 2012, Theorem 1]).
Let $\mathbf{X} = \mathbf{C}^{\frac{1}{2}} \mathbf{U} \in \mathbb{R}^{p \times n}$, where $\mathbf{U} \in \mathbb{R}^{p \times n}$ are the $n < p$ columns of a $p \times p$ Haar random matrix and $\mathbf{C} \in \mathbb{R}^{p \times p}$ be symmetric nonnegative definite with bounded operator norm. Then, for $z < 0$, as $p/n \rightarrow c \in (1, \infty)$, letting $\mathbf{Q}(z) = (\frac{p}{n} \mathbf{X} \mathbf{X}^\top - z \mathbf{I}_p)^{-1}$, we have the deterministic equivalent

$$\mathbf{Q}(z) \leftrightarrow \bar{\mathbf{Q}}(z) = -\frac{1}{z} (\mathbf{I}_p + \tilde{m}_p(z) \mathbf{C})^{-1}$$

where $\tilde{m}_p(z)$ is the unique positive solution to

$$\tilde{m}_p(z) = \left(-z + (1 + zc^{-1}\tilde{m}_p(z)) \frac{1}{n} \operatorname{tr} \mathbf{C}(\mathbf{I}_p + \tilde{m}_p(z)\mathbf{C})^{-1} \right)^{-1}.$$

In the statement of the theorem, we used a correction $\frac{p}{n}$ in front of $\mathbf{X}\mathbf{X}^\top$ to ensure the correspondence between $\mathbb{E}[\mathbf{U}\mathbf{U}^\top] = \frac{n}{p}\mathbf{I}_p$ and the setting of Theorem 2.5 where $\mathbb{E}[\frac{1}{n}\mathbf{Z}\mathbf{Z}^\top] = \mathbf{I}_p$. Indeed, it is quite interesting to observe the tight relation between Theorem 2.5 and Theorem 2.16 which, despite the major difference imposed by the strongly dependent structure of \mathbf{U} versus the independent structure of \mathbf{Z} , leads almost to the same deterministic equivalent. The only difference lies in the extra term $zc^{-1}\tilde{m}_p(z)$ in the defining equation for $\tilde{m}_p(z)$.

Similar to the case of random matrices with i.i.d. entries versus Gaussian entries, it is nonetheless more convenient to work with Gaussian-specific identities rather than the “independence”-related trace lemma. Specifically, an equivalent for Stein’s lemma, Lemma 2.13, also exists for Haar matrices.

lem:Stein-Haar

Lemma 2.17 (Stein’s lemma for Haar matrices (from [Pastur and Shcherbina, 2011, Chapter 8])). Let $\tilde{\mathbf{U}} \in \mathbb{R}^{p \times p}$ be a Haar matrix and $f : \mathbb{R}^{p \times p} \rightarrow \mathbb{R}$ a function admitting an analytic extension in the neighborhood of the set of unitary matrices in $\mathbb{R}^{p \times p}$. Then we have, for all $j, j' \in \{1, \dots, p\}$,

$$\mathbb{E} \left[\sum_{i=1}^p f'_{ij}(\tilde{\mathbf{U}}) \tilde{\mathbf{U}}_{ij'} - f'_{ij'}(\tilde{\mathbf{U}}) \tilde{\mathbf{U}}_{ij} \right] = 0$$

where f'_{ij} is the classical derivative over $\tilde{\mathbf{U}}_{ij}$ (not accounting for the dependence of the other entries in $\tilde{\mathbf{U}}$). In the complex case ($\tilde{\mathbf{U}} \in \mathbb{C}^{p \times p}$ and $f(\tilde{\mathbf{U}}) \in \mathbb{C}$), this reduces to

$$\mathbb{E} \left[\sum_{i=1}^p f'_{ij}(\tilde{\mathbf{U}}) \tilde{\mathbf{U}}_{ij'} \right] = 0.$$

Similarly a Nash-Poincaré inequality for Haar matrix models is defined.

lem:NP-Haar

Lemma 2.18 (Nash-Poincaré for Haar matrices). Under the setting of Lemma 2.17, we have

$$\operatorname{Var}(f(\tilde{\mathbf{U}})) \leq \frac{1}{p} \sum_{i,j=1}^p \mathbb{E} \left[|f'_{ij}(\tilde{\mathbf{U}})|^2 \right].$$

Although seemingly less exploitable, Stein’s lemma for Haar matrices is in fact quite convenient and easily leads to results such as the aforementioned Theorem 2.16 (for instance, by considering matrix functions of the form $f(\tilde{\mathbf{U}}\mathbf{D})$ for $\mathbf{D} \in \mathbb{R}^{p \times p}$ diagonal with $\mathbf{D}_{ii} = \delta_{i \leq n}$ — so that $f(\tilde{\mathbf{U}}\mathbf{D})$ only selects $n < p$

columns of $\tilde{\mathbf{U}} \in \mathbb{R}^{p \times p}$). See Exercise 12 for a concrete example of the application of Lemma 2.17 and 2.18.

To the best of our knowledge, very few works have so far fully exploited the strength of these identities to study large dimensional random matrix models for machine learning applications. They may reveal fundamental for the analysis of specific random projection-based methods with isometric constraints.

2.6.2.4 The free probability approach

sec:freeprob

Free probability theory is a drastically different approach to study random matrices. It is particularly efficient in some scenarios, such as when the sum or product of random matrices are involved. The theory was developed in parallel to the Stieltjes transform method developed in this monograph and originates from the works of Voiculescu et al. [1992], who originally aimed to describe a theory of probabilities on non-commutative algebras. A detailed introduction of the theory is beyond the scope of this monograph and we refer the interested readers to [Hiai and Petz, 2000, Biane, 1998] and [Couillet and Debbah, 2011, Chapter 4 and Chapter 5]. Although free probability theory is rooted in a combinatorial approach (see e.g., [Nica and Speicher, 2006]), it also contains some elegant analytic results, which can be related to the Stieltjes transform: in the sequel, we emphasize those useful results.

For μ and ν two compactly supported probability measures on $[0, \infty)$, Hiai and Petz [2000] proved that there always exist two free random variables a and b in some non-commutative probability space having distributions μ and ν , respectively. The distribution of $a + b$ and ab depend solely on μ, ν and can be associated with probability measures called *free additive convolution* and *free multiplicative convolution* of the distributions μ and ν , denoted $\mu \boxplus \nu$ and $\mu \boxtimes \nu$, respectively. These measures are both compactly supported on $[0, \infty)$ [Voiculescu et al., 1992].

These free additive and multiplicative convolutions satisfy convenient analytic expressions, through the so-called R - and S -transforms introduced below.

def:RT-and-ST

Definition 5 (R - and S -transform). *Let μ be a real probability measure with support $\text{supp}(\mu)$ and Stieltjes transform $m_\mu(z)$, for $z \in \mathbb{C}^+$. The R -transform of μ , denoted R_μ , is defined as the solution to*

$$m_\mu(R_\mu(z) + z^{-1}) = -z$$

or equivalently

$$m_\mu(z) = \frac{1}{R_\mu(-m_\mu(z)) - z}.$$

Let $\psi_\mu(z)$ be the formal power series defined as

$$\psi_\mu(z) = \sum_{k=1}^{\infty} z^k \int t^k \mu(dt) = \int \frac{zt}{1-zt} \mu(dt)$$

and let χ_μ be the (unique) inverse under composition of such series that is analytic in a neighborhood of zero so that $\chi_\mu(\psi_\mu(z)) = z$ for $|z|$ small enough, then the S -transform of μ , denoted S_μ , is given by

$$S_\mu(z) = \chi_\mu(z) \frac{1+z}{z}.$$

In particular, $S_\mu(z)$ satisfies

$$m_\mu \left(\frac{z+1}{zS_\mu(z)} \right) = -zS_\mu(z).$$

**** uniqueness is clear? in which way? ****

The main property of R - and S -transforms is summarized below, and requires the notion of *freeness* between non-commutative random variables. Freeness is not an easy notion, and is defined through a series of moment conditions, which we will not go into here (see again [Hiai and Petz, 2000, Biane, 1998] for details). One needs just remember at this point that freeness extends the notion of independence to non-commutative random variables.

lem:RT-ST-of-sum-and-product

Lemma 2.19 (R - and S -transforms of sums and products). *For a and b two free random variables with compactly supported distributions μ and ν , respectively, the law $\mu \boxplus \nu$ of $a + b$ satisfies*

$$R_{\mu \boxplus \nu}(z) = R_\mu(z) + R_\nu(z).$$

Similarly, the law $\mu \boxtimes \nu$ of ab satisfies

$$S_{\mu \boxtimes \nu}(z) = S_\mu(z)S_\nu(z).$$

Of interest to the present monograph is that “asymptotically large random matrices” are typical examples of non-commutative random variables for which freeness can be ensured. To avoid dealing with infinite-size linear operators, it is more appropriate to define a notion of *asymptotic freeness* for finite-dimensional random matrices, which translates the freeness of their respective limiting operators.

As such, the main result of interest to us is the following: for $\mathbf{A} \in \mathbb{R}^{n \times n}$ and $\mathbf{B} \in \mathbb{R}^{n \times n}$ two asymptotically free random matrices with respective *limiting spectral measures* $\mu_{\mathbf{A}}$ and $\mu_{\mathbf{B}}$ (with a slight abuse of notation), the limiting spectral measure $\mu_{\mathbf{A}+\mathbf{B}}$ of $\mathbf{A} + \mathbf{B}$ exists and satisfies

$$\mu_{\mathbf{A}+\mathbf{B}} = \mu_{\mathbf{A}} \boxplus \mu_{\mathbf{B}}, \quad R_{\mathbf{A}+\mathbf{B}}(z) = R_{\mathbf{A}}(z) + R_{\mathbf{B}}(z)$$

for $R_{\mathbf{A}}(z)$, $R_{\mathbf{B}}(z)$ and $R_{\mathbf{A}+\mathbf{B}}(z)$ the R -transforms of $\mu_{\mathbf{A}}$, $\mu_{\mathbf{B}}$ and $\mu_{\mathbf{A}+\mathbf{B}}$, respectively. Similarly, $\mu_{\mathbf{AB}}$, the limiting spectral measure of the matrix product \mathbf{AB} , exists and satisfies

$$\mu_{\mathbf{AB}} = \mu_{\mathbf{A}} \boxtimes \mu_{\mathbf{B}}, \quad S_{\mathbf{AB}}(z) = S_{\mathbf{A}}(z)S_{\mathbf{B}}(z)$$

for $S_{\mathbf{A}}(z)$, $S_{\mathbf{B}}(z)$ and $S_{\mathbf{A}+\mathbf{B}}(z)$ the S -transforms of $\mu_{\mathbf{A}}$, $\mu_{\mathbf{B}}$ and $\mu_{\mathbf{A}+\mathbf{B}}$. The above equalities should be understood to hold in the almost sure sense.

Clearly, the asymptotically freeness assumption plays a key role in relating the limiting spectrum of $\mathbf{A}+\mathbf{B}$ or \mathbf{AB} to that of \mathbf{A} and \mathbf{B} , which unfortunately in practice only applies to a limited range of random matrices. Essentially, \mathbf{A} and \mathbf{B} are asymptotically free if they are both independent and if the distribution of their respective eigenvectors are sufficiently “isotropic” with respect to one another: so essentially, when one of the two matrices is invariant by left and right product by arbitrary unitary matrices. Typically, the two typical cases of matrix pairs known to be asymptotically free are: (i) a Gaussian standard random matrix and any other independent random matrix (for instance a deterministic matrix or another Gaussian standard random matrix, independent of the first), (ii) a Haar random matrix and any other independent random matrix. One may for instance easily determine the limiting spectral measure of models of the type $\mathbf{X} + \mathbf{A}$ for \mathbf{X} a Wigner matrix or a Wishart matrix and \mathbf{A} deterministic, or even $\mathbf{X}\mathbf{A}\mathbf{X}^T$ with \mathbf{X} Gaussian or Haar distributed. Free probability theory is however more difficult to use when summing or multiplying two random matrices with structured eigenvectors, such as as simple models as $\mathbf{X} \odot \mathbf{B} + \mathbf{A}$ for \mathbf{X} a Wigner matrix and \mathbf{B} a deterministic variance profile; this very fact has strongly limited the reach and importance of free probability theory in the past decade.

A fundamental result to efficiently use the additive and product rules of Lemma 2.19 are the basic forms of the R - and S -transforms of elementary random matrix models. Specifically, the R - and S -transforms of the Marčenko-Pastur and semi-circle distributions are known in closed-form as follows.

1em:RT-ST-of-MP-SC

Lemma 2.20 (R and S -transforms of Marčenko-Pastur and semi-circle law).

The R -transform $R_{MP,c}(z)$ and S -transform $S_{MP,c}(z)$ of the Marčenko-Pastur law $\mu_{MP,c}$ of parameter c , i.e., the limiting spectral measure of $\frac{1}{n}\mathbf{Z}\mathbf{Z}^T$, $\mathbf{Z} \in \mathbb{R}^{p \times n}$ with i.i.d. zero mean, unit variance entries, as $p/n \rightarrow c \in (0, \infty)$, given explicitly by (2.10), read

$$R_{MP,c}(z) = \frac{1}{1 - cz}, \quad S_{MP,c}(z) = \frac{1}{1 + cz}. \quad (2.32)$$

As for the R -transform $R_{SC}(z)$ of the semi-circle law μ_{SC} , given by (2.20), it is simply

$$R_{SC}(z) = z. \quad (2.33)$$

With Lemma 2.20, one is able to derive, with a free probability approach, the limiting spectral measure of the information-plus-noise-type random matrix model $\mathbf{M} = \mathbf{A} + \frac{1}{n}\mathbf{XX}^T$ for $\mathbf{X} \in \mathbb{R}^{p \times n}$ having i.i.d. standard Gaussian entries and $\mathbf{A} \in \mathbb{R}^{p \times p}$ a deterministic matrix. Specifically, calling (with a slight abuse of notation) $\mu_{\mathbf{A}}$ and $\mu_{\mathbf{M}}$ the limiting spectral measure of \mathbf{A} and \mathbf{M} as $n, p \rightarrow \infty$ with $p/n \rightarrow c$, we have

$$\mu_{\mathbf{M}} = \mu_{\mathbf{A}} \boxplus \mu_{MP,c}, \quad R_{\mathbf{M}}(z) = R_{\mathbf{A}}(z) + R_{MP,c}(z)$$

so that, by Definition 5 and Lemma 2.20,

$$m_{\mathbf{M}}(z) = \frac{1}{R_{\mathbf{M}}(-m_{\mathbf{M}}(z)) - z} = \frac{1}{R_{\mathbf{A}}(-m_{\mathbf{M}}(z)) + \frac{1}{1+cm_{\mathbf{M}}(z)} - z}$$

or equivalently

$$R_{\mathbf{A}}(-m_{\mathbf{M}}(z)) + \frac{1}{-m_{\mathbf{M}}(z)} = z - \frac{1}{1+cm_{\mathbf{M}}(z)}$$

which, by taking the Stieltjes transform $m_{\mathbf{A}}(\cdot)$ of \mathbf{A} on both sides, together with Definition 5, gives

$$m_{\mathbf{M}}(z) = m_{\mathbf{A}}\left(z - \frac{1}{1+cm_{\mathbf{M}}(z)}\right).$$

The same result would have been more painstaking to derive using a purely Stieltjes transform approach. However, very few matrix models being asymptotically free, the free probability framework quickly fails to operate in more structured random matrix models.

Recent works try to cope for these limitations as well as open the range of applicability of free probability theory to handle sums and products of matrices under weaker forms of asymptotic freeness conditions (to characterize for instance the limiting spectrum of the sum of random matrices with row and columns permutation invariance [Au et al., 2018], or to extend the notion of deterministic equivalents to a free probability setting [Speicher and Vargas, 2012]). Despite these efforts, the major trend and most flexible tools in random matrix theory remain the approaches linked to the Stieltjes transform which is the focus of the monograph.

2.6.2.5 Full circle law, β -ensembles, sparse random matrices, etc. sec:full_circle_beta_sparse

Mathematicians have long been intrigued by the “simplest” random matrix model in appearance that is $\frac{1}{\sqrt{n}}\mathbf{X} \in \mathbb{R}^{n \times n}$ (non-symmetric) with i.i.d. zero mean and unit variance entries. Being non-symmetric (at least with probability one), the eigenvalues of $\frac{1}{\sqrt{n}}\mathbf{X}$ are complex. They have been long known to spread uniformly on the unit complex disc $\{z \in \mathbb{C}, |z| < 1\}$. Surprisingly, despite its simple statement, this result, known as the *full circle law* or the *circular law*, has only been proved in full generality by Tao and Vu [2008]. To explain the difficulties: (i) the Stieltjes transform method cannot be applied directly as the spectrum is complex (and thus taking a limit $z \rightarrow z_0$ for z_0 in the support does not allow to “enter” the complex-supported support as in the real-supported one); there the solution was provided earlier by Girko who introduced the alternative V-transform; (ii) the V-transform involves the limit of an integral form on the logarithm of the singular values of \mathbf{X} which, being square, tends to have a lot of singular values tending to zero; this technical difficulty, previously solved by invoking the existence of high order moments for

\mathbf{X}_{ij} was solved by Tao and Vu by means of the *ϵ -net technique*, popular today in compressive sensing.

From the perspective of the present monograph, the eigenvalues of non-symmetric models are of marginal interest. These could be used for the analysis of directed random graphs although, to our knowledge, not much works exist in this direction.

Another purely mathematical interest relates to the fact that Gaussian random matrices are much better known than random matrices with i.i.d. entries and, consequently, come along with a host of other technical tools. In particular, not only the limiting spectral measure, but actually the exact *finite-dimensional joint distribution* $\mathbb{P}(\lambda_1, \dots, \lambda_n)$ of (real, complex, or quaternionic) Gaussian symmetric random matrix \mathbf{X} and $\frac{1}{n}\mathbf{XX}^\top$ having independent entries are known. The expression for all these cases are quite related.

In particular, the joint eigenvalue distribution for the Gaussian Wigner matrix $\mathbf{X} \in \mathbb{R}^{n \times n}$ is explicitly given by

$$\mathbb{P}(\lambda_1, \dots, \lambda_n) \propto \prod_{i=1}^n e^{-\frac{1}{4}\beta n \lambda_i} \prod_{1 \leq i < j \leq n} |\lambda_i - \lambda_j|^\beta \quad \text{eq:joint_eig} \quad (2.34)$$

for real Gaussian \mathbf{X} when $\beta = 1$ (the random ensemble is called here the Gaussian orthogonal ensemble, GOE), complex Gaussian \mathbf{X} when $\beta = 2$ (referred to as the Gaussian unitary ensemble, GUE), and quaternionic Gaussian \mathbf{X} when $\beta = 4$ (the Gaussian symplectic ensemble, GSE). Much work has been devoted to the study of the asymptotics of the joint law of this now called β -ensemble of random matrices. In particular, the Tracy-Widom limit for the largest eigenvalue introduced in Theorem 2.14 is obtained by marginalizing the joint measure to obtain the probability $\mathbb{P}(\lambda_1 > x)$. See [Anderson et al., 2010] for an introduction to these quite different methods.

Most of the aforementioned random matrix models however share as a common denominator their relying on $O(n^2)$ “degrees of freedom”, in the sense that they are designed out of $O(n^2)$ independent random variables. For the sample covariance matrix model $\frac{1}{n}\mathbf{XX}^\top$, we have $\mathbf{X} = \mathbf{C}^{\frac{1}{2}}\mathbf{Z} \in \mathbb{R}^{p \times n}$ with \mathbf{Z} made of np independent entries. For the Wigner model, $\mathbf{X} \in \mathbb{R}^{n \times n}$ has $n(n+1)/2$ independent entries on and above the diagonal. This large number of degrees of freedom is the *major asset of random matrix theory*, as presented in this monograph: (i) it triggers concentration properties that do not appear if p is fixed and only $n \rightarrow \infty$ (such as quadratic form concentration $\frac{1}{p}\|\mathbf{z}_i\|^2 \xrightarrow{a.s.} 1$), (ii) fast convergence rates with typical central limit speeds of order up to $O(1/n)$ and, possibly most importantly, (iii) *universality* with respect to the underlying distribution of the independent entries (i.e., asymptotic statistics loosely depend on the actual law of the entries) which simplifies the analysis and provides robustness of the studied objects to deviations from the statistical model.

Yet, a host of practical random matrix models demand less degrees of freedom. Realistic networks for instance (social nets, brain connectivity, molecular

networks, etc.) are naturally modelled by *sparse* random (say symmetric) adjacency matrices $\mathbf{A} \in \mathbb{R}^{n \times n}$ with typical number of nonzero elements scaling as $O(n)$ rather than $O(n^2)$. Every row/column \mathbf{a}_i of \mathbf{A} typically has $O(1)$ nonzero elements, and thus $\|\mathbf{a}_i\|$ does not concentrate. Kernel random matrices $\mathbf{K} = \{f(\|\mathbf{x}_i - \mathbf{x}_j\|^2)\}_{i,j=1}^n$ of finite-dimensional vectors $\mathbf{x}_1, \dots, \mathbf{x}_n \in \mathbb{R}^p$ with p small (such as used in the context of classification or clustering of 2D or 3D points) are also more challenging to study than their large- p counterpart, as every entry of \mathbf{K} remains a random variable. The consequences are numerous: (i) the analysis of these objects is more difficult, if doable at all, and only slow large- n statistics can be studied (ii) universality and robustness to model assumptions are lost: large- n asymptotics remain a function of the law of the data vectors \mathbf{x}_i . The hard-to-obtain results are thus additionally less applicable in practice.

Nevertheless, a branch of random matrix theory is interested in these important models. Stieltjes transform methods are here mostly ineffective so that, for lack of better alternatives, one has to rely essentially on moment approaches and combinatorics. A particularly interesting approach when it comes to sparse random graphs of size n is that, as $n \rightarrow \infty$, the graph has a “tree-like” structure; indeed, with a probability $O(1/n)$ for each node to reach out any another node, the probability of presence of cycles in the graph is vanishingly small. This has motivated the independent development of a graph-based random matrix framework, strongly pushed by Bordenave and Lelarge in e.g., [Bordenave and Lelarge, 2010a,b]. The results are however generally “weak” from a practical standpoint. For instance, while it has long been known that the spectral measure of a *dense* Erdős–Rényi random graph \mathbf{A} with Bernoulli i.i.d. entries (i.e., with $O(n^2)$ degrees of freedom) converges to the semi-circle law, it is still unknown to which measure a *sparse* random graph \mathbf{A} converges: the limiting law is known to exist, to be decomposed as the sum of a (known) discrete measure and a (unknown) continuous measure, and to have an unbounded support (as opposed to the semi-circular distribution) [Salez, 2011].

The specific kernel random matrix $\mathbf{K} = \{\|\mathbf{x}_i - \mathbf{x}_j\|^2\}_{i,j=1}^n$ with \mathbf{x}_i of fixed dimension, known as a Euclidean random matrix, has also been studied in [Bordenave, 2008], but again with results of limited practical reach.

Aside from side comments, the monograph will not dig into these fundamentally different problems, tools, and results. We exclusively concentrate on dense random matrix models.

2.6.3 Other statistics

sec:other_statistics

Most of the statistics of practical interest in the application chapters of the monograph are directly related to deterministic equivalents of the resolvent of random matrices and to their linear statistics. For instance, we shall see that the performance of classification methods (correct classification rates) of n data vectors $\mathbf{x}_1, \dots, \mathbf{x}_n$ in a k -class ($\mathcal{C}_1, \dots, \mathcal{C}_k$) problem can in general be estimated

from the k -dimensional matrix of quadratic forms

$$\frac{1}{n} \mathbf{J}^\top \mathbf{Q}(z) \mathbf{J}$$

(or some closely related statistics) where $\mathbf{Q}(z)$ is the resolvent of the underlying affinity matrix of the data (kernel, graph Laplacian, etc.) and $\mathbf{J} = [\mathbf{j}_1, \dots, \mathbf{j}_k] \in \mathbb{R}^{n \times k}$ with $[\mathbf{j}_a]_i = \delta_{\mathbf{x}_i \in C_a}$ the canonical vector of the classes.

Yet, some specific results (such as the classification rate of some random neural networks, the exact proof of the asymptotic Gaussian behavior of the dominant eigenvector entries in graph adjacency and kernel matrices, etc.) demand more than just *first order* limiting statistics. A further common statistics of interest lies in the *second order fluctuations*, i.e., in central limit theorems, of the objects under study.

These statistics have long been studied in the random matrix litterature, starting with the works of [Bai and Silverstein \[2008\]](#) who, under the sample covariance setting of Theorem 2.5, establish a central limit of the type

$$n \int f(t) (\mu_{\frac{1}{n}} \mathbf{X} \mathbf{X}^\top - \mu)(dt) \rightarrow \mathcal{N}(M(f), \sigma^2(f))$$

for all analytic functions f . This result (and all similar results in related models) has the following noteworthy properties:

- the convergence speed is of order $O(n^{-1})$. This however only stands for linear statistics of the eigenvalues; fluctuations of bilinear forms $\mathbf{a}^\top (\mathbf{Q}(z) - \bar{\mathbf{Q}}(z)) \mathbf{b}$ fluctuate at a slower $O(n^{-\frac{1}{2}})$ speed;
- the mean (or bias term) $M(f)$ and variance $\sigma^2(f)$ depend on $\mathbb{E}[|\mathbf{Z}_{ij}|^4]$. Both can be decomposed as a sum $A + \kappa B$ with κ the kurtosis of \mathbf{Z}_{ij} . The mean in particular vanishes in the complex Gaussian case and the variance is twice large in the real Gaussian than in the complex Gaussian case.

Many results on central limit theorems for a vast spectrum of linear statistics of random models have been established, for instance in [\[Hachem et al., 2008\]](#) for sample covariance matrices $\frac{1}{n} \mathbf{X} \mathbf{X}^\top$ with \mathbf{X} having a variance profile, or in [\[Zheng et al., 2017\]](#) for F-matrix models of the type $(\frac{1}{n_1} \mathbf{X}_1 \mathbf{X}_1^\top)^{-1} \frac{1}{n_2} \mathbf{X}_2 \mathbf{X}_2^\top$. A generalization to less smooth functions f (three-times differentiable) is proposed in [\[Najim et al., 2016\]](#). Central limit theorems for bilinear forms are found for instance in [\[Kammoun et al., 2009\]](#). Fluctuations of the spikes and eigenvector projections in a spiked random matrix model can also be found in [\[Baik et al., 2005, Bai and Yao, 2008, Couillet and Hachem, 2013\]](#). These fluctuations are at the slowest $O(n^{-\frac{1}{2}})$ rate.

A central limit result for the linear statistical inference method of Theorem 2.11 has also been established in [\[Yao et al., 2013\]](#). There again it is shown that the convergence speed is of order $O(n^{-1})$ with a bias and a variance of the form $A + \kappa B$ with κ the kurtosis of the underlying distribution (and, again,

the bias is only zero in the complex Gaussian case). An estimation method is also proposed for the means and variances, which is of practical interest to empirically assess the confidence interval of the estimator.

Due to a strong motivation from the field of wireless communications, some specific linear statistics have been particularly widely studied in the random matrix literature. This is notably the case of the logarithm. Statistics of the type

$$\int \log(1 + st) \mu_{\frac{1}{n} \mathbf{X} \mathbf{X}^T}(dt)$$

are particularly important in wireless communications as they give access to the achievable communication rate over a linear wireless communication channel \mathbf{X} . This $\log(1 + st)$ terms arises from the entropy of Gaussian random variables and is also found in many other applications, such as with the estimation of the Kullbach-Liebler divergence between two multivariate Gaussian vectors discussed in Chapter 3. A particularly convenient feature of $\log(1 + st)$ is that its derivative is immediately related to the Stieltjes transform. It is thus not required to use a complex contour integral method to assess these quantities (a real integration is sufficient). See [Tulino et al., 2004, Couillet and Debbah, 2011] for a detailed account of all these findings.

In technical terms, there are essentially two major methods to obtain central limit theorems of random matrix quantities. Recalling that linear functionals $u(\mathbf{Q})$ of the resolvent $\mathbf{Q} = (\mathbf{X} - z\mathbf{I}_n)^{-1}$ of the random matrix \mathbf{X} under study (e.g., bilinear forms $\mathbf{a}^T \mathbf{Q} \mathbf{b}$ or traces $\text{tr } \mathbf{A} \mathbf{Q}$) is usually the central object of interest, it cannot in general be expressed as a sum of independent random variables. Instead, Silverstein and Bai propose to use a martingale difference approach by noting that, if \mathbf{X} has independent columns

$$u(\mathbf{Q}) - \mathbb{E}u(\mathbf{Q}) = \sum_{i=1}^n \mathbb{E}_{i-1}[u(\mathbf{Q})] - \mathbb{E}_i[u(\mathbf{Q})]$$

where \mathbb{E}_i is the expectation conditioned on the columns $\mathbf{x}_1, \dots, \mathbf{x}_i$ of \mathbf{X} , with the convention $\mathbb{E}_0 u(\mathbf{Q}) = u(\mathbf{Q})$. This is a sum of martingale differences, for which [Billingsley, 2012, Theorem 35.12] provides a central limit theorem (see also [Bai and Silverstein, 2010, Chapter 9]).

Alternatively, Pastur proposes to use Gaussian techniques, advocated in [Pastur and Shcherbina, 2011], and the characteristic function approach to show that

$$\mathbb{E} \left[e^{-it u(\mathbf{Q})} \right] \rightarrow e^{-it\mu - \frac{1}{2}t^2\sigma^2}$$

which is the Gaussian characteristic function. To this end, the approach consists in exploiting the Gaussian integration-by-parts formula (Stein's lemma) on the differentiated (along t) left-hand expectation, i.e.,

$$\mathbb{E} \left[-iu(\mathbf{Q})e^{-it u(\mathbf{Q})} \right].$$

Exploiting the fact that u is linear and that $\mathbf{Q} = -\frac{1}{z}\mathbf{I}_n - \frac{1}{z}\mathbf{QX}$, this expectation can be reduced as a function of the type $\mathbb{E}[\mathbf{X}f(\mathbf{X})]$ on which the Gaussian integration-by-parts method can be applied. The objective is then to show that this differentiated characteristic function converges to the derivative of the limiting Gaussian characteristic function, i.e., $(-\imath\mu - t\sigma^2)e^{-\imath t\mu - \frac{1}{2}t^2\sigma^2}$. This is in particular performed by controlling the small terms using the Poincaré-Nash inequality.

2.7 Beyond vectors of independent entries: concentration of measure in RMT

sec:concentration

2.7.1 Limitations of the i.i.d. assumption

In the previous sections, we have shown that the Stieltjes transform and resolvent approaches are quite versatile tools which, in a way, form a surrounding “complex analysis and linear algebra core” for random matrix theory analysis that, however, must be *independently supplemented* by appropriate probabilistic tools.

When it comes to these probabilistic methods, we have seen that a major driver for most of the results lies in exploiting the *independence both in sample and features* of the entries of the underlying random matrix \mathbf{X} . It is thus no wonder that a natural and long-standing assumption in the early works in random matrix theory was to request for \mathbf{X} to have all independent entries. Most generalizations of these results generally assume mere deviations from this setting (by allowing weak correlation between the entries for instance).

However, while for random graphs it is largely conceivable to request independent “noise” associated to each link and for random vector observations it is natural to ask for these observations to be independent, requesting that every single observation is made of independent entries is very constraining. Note in particular that what we referred to as the *sample covariance matrix model* in Theorem 2.5 is in fact a very restricted model where every observation \mathbf{x}_i needs be of the form $\mathbf{x}_i = \mathbf{C}^{\frac{1}{2}}\mathbf{z}_i$ for some \mathbf{z}_i with independent entries. This model is mostly convenient only for the Gaussian case where $\mathbf{z}_i \sim \mathcal{N}(\mathbf{0}, \mathbf{I}_p)$ and as a result $\mathbf{x}_i \sim \mathcal{N}(\mathbf{0}, \mathbf{C})$. Most multivariate random vectors \mathbf{x}_i with zero mean and covariance \mathbf{C} (elliptical distributions, correlated vectors of Bernoulli entries, etc.) cannot be factorized under this form.

Most importantly, the “real data” \mathbf{x}_i (images, sounds, videos) met in machine learning applications tend to live in very contorted manifolds that cannot be linearly “whitened” into a vector of independent entries by merely operating $\mathbf{C}^{-\frac{1}{2}}\mathbf{x}_i$.

2.7.2 Concentrated random vectors as the answer

In [El Karoui, 2009] and [Pajor and Pastur, 2009], El Karoui and Pajor–Pastur were the first to realize that, from a probability standpoint, the proof of the

sample covariance matrix result in Theorem 2.5 from [Silverstein and Bai, 1995], only relies on (i) the independence between the (column) vectors \mathbf{x}_i composing $\mathbf{X} = \mathbf{C}^{\frac{1}{2}}\mathbf{Z}$, and (ii) the convergence

$$\frac{1}{n}\mathbf{x}_i^\top \mathbf{Q}_{-i}(z)\mathbf{x}_i - \frac{1}{n} \operatorname{tr} \mathbf{Q}_{-i}\mathbf{C} \xrightarrow{\text{eq:quadform_convergence}} 0 \quad (2.35)$$

in some probabilistic sense, where $\mathbf{Q}_{-i}(z) = (\frac{1}{n}\mathbf{XX}^\top - \frac{1}{n}\mathbf{x}_i\mathbf{x}_i^\top - z\mathbf{I}_p)^{-1}$. For the latter, it is sufficient but not necessary for $\mathbf{z}_i = \mathbf{C}^{-\frac{1}{2}}\mathbf{x}_i$ to have standard i.i.d. entries. In particular, El Karoui showed that this convergence also holds if \mathbf{x}_i is a *concentrated random vector*.

In a nutshell, the concentration of measure theory, as extensively developed by Ledoux [2001], considers random vectors $\mathbf{x} \in \mathbb{R}^p$ having the property that every 1-Lipschitz functional $\phi : \mathbb{R}^p \rightarrow \mathbb{R}$ of \mathbf{x} is “predictable” in the sense that there exists a deterministic value $M_\phi \in \mathbb{R}$ such that random variable $\phi(\mathbf{x})$ remains in the neighborhood of M_ϕ and the diameter of this neighborhood vanishes as $p \rightarrow \infty$. More formally, assuming $M_\phi = O(1)$ with respect to p (otherwise, it needs to be appropriately scaled), there exists a function $\alpha(t, p)$ decreasing to zero in both t and p such that

$$\mathbb{P}(|\phi(\mathbf{x}) - M_\phi| > t) \leq \alpha(t, p). \quad \text{eq:concentration_nutshell} \quad (2.36)$$

Of particular interest is the function $\alpha(t, p) = e^{-t^\beta p^\gamma}$ for some $\beta, \gamma > 0$ which, since the exponential grows faster than any polynomial, provides a more powerful and much more flexible inequality than the moment bounds introduced in the proof of the Marčenko–Pastur law. The mapping $\mathbf{x}_i \rightarrow \frac{1}{n}\mathbf{x}_i^\top \mathbf{Q}_{-i}(z)\mathbf{x}_i$ in (2.35) is however not Lipschitz, and thus more profound technical considerations are requested to show that Theorem 2.5 extends to the case where the vectors \mathbf{x}_i are independent concentrated random vectors. This is performed in an intricate manner in [El Karoui, 2009]. A more systematic approach has been recently developed in [Louart and Couillet, 2019], the basics of which are discussed in the next section.

Paradoxically, very few “classical” multivariate distributions are known to produce concentrated random vectors, and yet, this is enough to bring an outstanding practical competitive advantage against vectors with independent entries, when it comes to modelling real data for machine learning.

Of these popular distributions, only the Gaussian random vector $\mathbf{x} \sim \mathcal{N}(\mathbf{0}, \mathbf{I}_p)$, the uniformly distributed vector \mathbf{x} on the unit sphere of \mathbb{R}^p , and the vector \mathbf{x} with i.i.d. entries with bounded support (i.e., $|x_i| < K$ for some $K > 0$) are known to be concentrated random vectors. Worse, for the latter, the definition (2.36) only holds for all 1-Lipschitz and convex maps, which is practically inconvenient.

Let us thus stick for the moment to the example of $\mathbf{x} \sim \mathcal{N}(\mathbf{0}, \mathbf{I}_p)$. The major advantage of being a concentrated random vector is that this concentration property is stable under any 1-Lipschitz map $f : \mathbb{R}^p \rightarrow \mathbb{R}^q$. So, if \mathbf{x} is concentrated, so is $\mathbf{x}' = f(\mathbf{x})$, which can be a vector with intricate nonlinear dependence between its entries.

Now, the key reasons why the class of random vectors $\{f(\mathbf{x})\}$ spanned by 1-Lipschitz maps f is so fundamental to machine learning are that:

- (i) there exist machine learning techniques that *learn* to produce artificial but highly realistic data, exclusively based on Lipschitz maps. The most popular of these methods are the generative adversarial networks (GANs) initially proposed by Goodfellow et al. [2014]. Those are feedforward neural networks which, after training, generate highly realistic data $f(\mathbf{x})$ (so realistic that even human beings cannot distinguish synthetic data from real ones) from a standard Gaussian vector input $\mathbf{x} \sim \mathcal{N}(\mathbf{0}, \mathbf{I}_p)$. Since a feedforward neural network is a sequence of linear operators (inter-layer connections and convolution operators) and Lipschitz nonlinear activation functions (sigmoidal, rectified linear, etc.), f is indeed Lipschitz (as a combination of Lipschitz operators remains Lipschitz).
- (ii) feature extraction procedures in machine learning are also mostly Lipschitz maps. Again, the most popular of these today are convolution neural networks, which are again feedforward neural nets and thus, by definition, Lipschitz maps of the input data.

As a consequence of (i) and (ii), since real data can trust-worthily be approximated by outputs \mathbf{x}' of some Lipschitz function $\mathbf{x}' = f(\mathbf{x})$ of random Gaussian vectors \mathbf{x} , the class of concentrated random vectors encompasses a broad “set of realistic data”. Furthermore, in practice, the actual data features exploited in most machine learning algorithms can be seen as yet another Lipschitz mapping $g(\mathbf{x}')$ of the data \mathbf{x}' . Since \mathbf{x}' is well modelled under the form $\mathbf{x}' = f(\mathbf{x})$ for standard Gaussian \mathbf{x} , $\mathbf{x}' = (g \circ f)(\mathbf{x})$ is again a Lipschitz map of a standard Gaussian vector.

It then becomes natural to model a wide range of realistic data as concentrated random vectors.

Remark 2.15 (Concentration inequalities versus concentration of measure theory). *The concentration of measure theory developed by Ledoux provides as corollaries a list of popular concentration inequalities such as Gaussian concentration inequalities, Bernstein's and Talagrand's inequalities for random variables with bounded entries,²² McDiarmid's inequalities for functionals of bounded deviations of independent random variables, etc. These few results, quite popular in statistics, can however only marginally be used as a full-fledged concentration of measure-oriented random matrix framework. As already pointed out, quadratic forms are not naturally handled by these concentration inequalities. More importantly, while quadratic form concentration is essentially sufficient to prove the convergence of Stieltjes transforms, proving the resolvent convergence $\mathbb{E}[\mathbf{Q}] - \bar{\mathbf{Q}} \rightarrow 0$ under a concentration inequality setting actually demands to further expand the works of Ledoux, as will be shown next.*

²²To be more exact, Talagrand's work was developed in parallel to Ledoux's theory and are rather complementary than a consequence of one another.

It must also be pointed out that in [Tao, 2012, Vershynin, 2010], Tao and Vershynin provide an introduction to what Vershynin refers to as non-asymptotic random matrix theory based on popular concentration inequalities. The approach followed by the authors however significantly differs from the present “asymptotic” random matrix considerations. There, the variables n, p are left “free” to grow at any relative speed to infinity and their use of concentration inequalities aims at retrieving bounds on largest or smallest eigenvalues or singular values of random matrices, without resorting to Stieltjes transform approach. For Tao, this control step is at the crux of the proof of the circular law (based on the ϵ -net theory developed by the author) for non-symmetric matrix \mathbf{X} with i.i.d. entries. For Vershynin, these spectrum support controls are exploited in applications to compressive sensing, where random matrix theory also plays a key role, for instance in providing “typical” matrices fulfilling the popular restricted isometry property [Candes, 2008].

The approach proposed in this monograph also provides a set of inequalities where n, p have an untied growth to infinity, but the application of these convergence results are mostly of interest in a joint growth rate for n, p . Besides, additional tools to Ledoux’s original framework, such as the notion of linear concentration will be needed.

Remark 2.16 (Limitations of the concentration of measure framework). *It is important to raise here (somewhat ironically) that the concentration of measure framework, which finds important corollaries to the field of compressive sensing [Baraniuk, 2007], is, as presented here, at odds with the compressive sensing framework. Indeed, compressive sensing is a major field of research in large dimensional statistics and machine learning which assumes that large dimensional data are intrinsically of low dimension. That is, in the simplest linear setting, data vector $\mathbf{x} \in \mathbb{R}^p$ can be written as $\mathbf{x} = \mathbf{Ay}$ for some matrix $\mathbf{A} \in \mathbb{R}^{p \times q}$ (generally unknown) and $\mathbf{y} \in \mathbb{R}^q$ for q very small. From there, the idea of compressive sensing is that meaningful statistical inference on \mathbf{y} can be performed based on few independent realizations $n \ll p$ (which is convenient if p is extremely large). There, concentration inequalities are mostly used to deal with the (random) observation matrix \mathbf{A} , rather than with the data.*

In the present random matrix framework, concentration of measure is used to model the data, not the data operating matrices. These data however must not be of intrinsic low dimension $q \ll n$. Or, at least, if it were, we would impose in our framework that $n \sim q$ and $n, q \rightarrow \infty$. If $q = O(1) \ll n$, then we would in general fall back under the sparse setting discussed at the end of Section 2.6.2.5 where the proposed framework is ineffective.

As shall be seen in the concrete applications presented in this monograph, large dimensional images are very appropriately modelled by concentrated random vectors of intrinsically large dimensions. However, feature vectors such as bag-of-words for text classification (which are very large but extremely sparse vectors) cannot be handled by random matrix theory so far.

This however does not mean that compressive sensing is complementary to random matrix theory. Compressive sensing indeed tackles the “difficult” prob-

lem analyzing sparse recovery algorithms by somehow “loose” inequalities and bounds: that is, it cannot accurately predict the exact performance of a given algorithm (however it can ensure its convergence and its efficiency as $n \rightarrow \infty$ at a certain rate with respect to p , while q is in general fixed). Random matrix theory instead requests that the intrinsic dimension $q \rightarrow \infty$ but manages in exchange (by exploiting the q degrees of freedom in the feature space) to provide accurate performance estimates of machine learning algorithms for all finite (but at least moderately large) n, q .

2.7.3 Elements of concentration of measure for random matrices

We recall here basic elements of the concentration of measure theory of immediate interest to random matrix applications. More advanced considerations can be found in [Ledoux, 2001] from a mathematical standpoint, and in [Louart and Couillet, 2019] specifically with a more random matrix-oriented flavor.

2.7.3.1 Concentration of random variables

We start with the concept of concentration of a (univariate) random *variable*. Concentration of measure can be defined in two parallel ways.

Definition 6 (Concentration of a random variable). *Let $\alpha : \mathbb{R}^+ \rightarrow [0, 1]$ be a non-increasing function with $\alpha(\infty) = 0$. A random variable x is α -concentrated and we write $x \propto \alpha$ if, for an independent copy x' of x , and all $t > 0$,*

$$\mathbb{P}(|x - x'| > t) \leq \alpha(t).$$

The definition suggests that any two independent realizations of x cannot live far from one another. Alternatively, we may define x as concentrated if there exists a deterministic *pivot* a close to which x remains.

Definition 7 (Concentration around a pivot). *Let $\alpha : \mathbb{R}^+ \rightarrow [0, 1]$ be a non-increasing function and $a \in \mathbb{R}$. Then x is α -concentrated around the pivot a , denoted $x \in a \pm \alpha$, if for all $t > 0$,*

$$\mathbb{P}(|x - a| > t) \leq \alpha(t).$$

These two definitions are not formally equivalent. However, we have the implication

$$x \propto \alpha \Rightarrow x \in M_x \pm 2\alpha \Rightarrow x \propto 4\alpha(\cdot/2)$$

where $M_x \in \mathbb{R}$ is a *median* of x , i.e., is such that $\mathbb{P}(x \geq M_x) \geq \frac{1}{2}$ and $\mathbb{P}(x \leq M_x) \geq \frac{1}{2}$. The loss of a factor 1/2 arises here from the bound $\mathbb{P}(|x - x'| > t) \leq \mathbb{P}(|x - a| > t/2) + \mathbb{P}(|x' - a| > t/2)$. Up to constants, it is then possible to use either definition interchangeably (the proofs of subsequent results are usually more accessible to one or the other definition).

A particularly appealing result is that 1-Lipschitz maps $f : \mathbb{R} \rightarrow \mathbb{R}$ of a concentrated random variable x maintain the concentration, i.e.,

$$x \propto \alpha \Rightarrow f(x) \propto \alpha. \quad \text{eq:concentration_lipschitz} \quad (2.37)$$

This is a particularly fundamental result which suggests that all smooth map of sub-linear growth of x satisfies the same concentration property. This result naturally arises from the fact that $|f(x) - f(x')| \leq |x - x'|$ and thus $\mathbb{P}(|f(x) - f(x')| > t) \leq \mathbb{P}(|x - x'| > t)$.

Evidently, sums of concentrated random variables are concentrated:

$$\begin{aligned} x_1 \propto \alpha, x_2 \propto \beta &\Rightarrow x_1 + x_2 \propto \alpha(\cdot/2) + \beta(\cdot/2) \\ x_1 \in a \pm \alpha, x_2 \in b \pm \beta &\Rightarrow x_1 + x_2 \in a + b \pm [\alpha(\cdot/2) + \beta(\cdot/2)] \end{aligned}$$

where in the first line the factor $1/2$ unfolds from the bound $\mathbb{P}(|x_1 + x_2 - x'_1 - x'_2| > t) \leq \mathbb{P}(|x_1 - x'_1| > t/2) + \mathbb{P}(|x_2 - x'_2| > t/2)$, and similarly for the second line.

However, products, particularly of dependent random variables, are less obvious to tackle, as one needs to avoid conditioning. The problem can be worked around using the following two relations

$$\begin{aligned} x_1 x_2 - ab &= (x_1 - a)(x_2 - b) + a(x_2 - b) + b(x_1 - a) \\ |x_1 - a||x_2 - b| > t &\Rightarrow (|x_1 - a| > \sqrt{t}) \text{ or } (|x_2 - b| > \sqrt{t}) \end{aligned}$$

so to obtain

$$\begin{aligned} x_1 \in a \pm \alpha, x_2 \in b \pm \beta &\Rightarrow x_1 x_2 \in ab \pm \\ \begin{cases} \alpha(\sqrt{\cdot/3}) + \alpha(\cdot/3|b|) + \beta(\sqrt{\cdot/3}) + \beta(\cdot/3|a|), & a, b \neq 0 \\ \alpha(\sqrt{\cdot/2}) + \alpha(\cdot/2|b|) + \beta(\sqrt{\cdot/3}), & a = 0, b \neq 0 \\ \alpha(\sqrt{\cdot}) + \beta(\sqrt{\cdot}), & a = b = 0. \end{cases} \end{aligned}$$

For large t , the probability $\mathbb{P}(|x_1 x_2 - t|)$ is here dominated by the terms $\alpha(\sqrt{\cdot})$ and $\beta(\sqrt{\cdot})$ which is not surprising. In the particular case where $x_1 = x_2 = x$, or more generally for powers x^k of concentrated random variables x , we have

$$x \in a \pm \alpha \Rightarrow x^k \in a^k \pm \left[\alpha(\cdot/2^k |a|^{k-\frac{1}{2}}) + \alpha((\cdot/2)^{\frac{1}{k}}) \right] \quad \text{eq:concentration_power_of_x} \quad (2.38)$$

with $\alpha(\cdot/0) = \alpha(\infty)$ by convention, which is based on noticing that

$$|x^k - a^k| \leq (2|a|)^k \left(\frac{x - a}{a} + \frac{|x - a|^k}{|a|^k} \right).$$

This result will be particularly useful for random matrix applications to quadratic forms.

Remark 2.17 (Exponential concentration). *Of utmost interest is the case where $\alpha(t) = Ce^{-(t/\sigma)^q}$ for some $C, \sigma, q > 0$. In particular, it is known that standard random Gaussian variables x satisfy*

$$x \sim \mathcal{N}(0, 1) \Rightarrow x \in 0 \pm 2e^{-(\cdot)^2/2}.$$

Exponential concentrations are fast and induce a lot of convenient properties. In particular, using the formula $\mathbb{E}[|x|^k] = \int_0^\infty \mathbb{P}(|x|^k > t) dt$, it appears that all (absolute) moments of exponentially concentrated random variables exist. In particular,

$$x \propto C e^{-(\cdot/\sigma)^q} \Rightarrow x \in \mathbb{E}[x] \pm e^{\frac{Cq}{q}} e^{-(\cdot/2\sigma)^q} \quad (2.39)$$

so that an exponentially concentrated random variable concentrates around its mean. But most importantly, we have the implications

$$\begin{aligned} x \in a \pm C e^{-(\cdot/\sigma)^q} &\Rightarrow \forall r \geq q, \mathbb{E}[|x - a|^r] \leq C\Gamma(r/q + 1)\sigma^r \\ &\Rightarrow x \in a \pm C e^{-(\cdot/\sigma)^q}/e \end{aligned}$$

with Γ the gamma-distribution. Thus, exponential concentration is “equivalent” to controlled growth by σ^r of all moments $r \geq q$. This is particularly appealing when moments occasionally turn out more convenient to deal with than bounds on tail probabilities.

2.7.3.2 Concentration of random vectors

The concept of concentration of random variables, stating that x does not deviate much from a given pivot a , cannot be straightforwardly extended to that of random vectors. Indeed random vectors (in particular large dimensional ones) rather tend to “avoid” their statistical means or medians: e.g., Gaussian random vectors $\mathbf{x} \sim \mathcal{N}(\mathbf{0}, \mathbf{I}_p)$ are of zero mean but they “concentrate” on a $O(1)$ -thick layer around the sphere of \mathbb{R}^p of diameter \sqrt{p} .

Instead, for a normed vector space $(E, \|\cdot\|)$, we will consider that a random vector $\mathbf{x} \in E$ is concentrated *for some class of functions* $\mathcal{F} : \mathbb{R}^p \rightarrow \mathbb{R}$ if, for all $f \in \mathcal{F}$, $f(\mathbf{x})$ is a concentrated random variable. Depending on the “broadness” of the class, being a concentrated random vector can be more demanding. [Ledoux \[2001\]](#) originally defined two such classes \mathcal{F} : the class of 1-Lipschitz maps (appropriate for Gaussian or random unitary vectors) and the class of convex (or weakly convex) 1-Lipschitz maps (adapted to vectors of independent bounded entries). There, the Lipschitz definition (i.e., the fact that $|f(\mathbf{x}) - f(\mathbf{y})| \leq \|\mathbf{x} - \mathbf{y}\|$) is with respect to the norm $\|\cdot\|$ in E , and thus the concentration rates may depend on $\|\cdot\|$. In order to better encompass random matrices in the concentration inequality framework, a looser additional class \mathcal{F} will be introduced here: that of unit-norm linear functionals.

Linear concentration Linear concentration is an important concept in random matrix theory as it provides a quite general and flexible definition for the notion of *deterministic equivalents*.

def:linear_concentration

Definition 8 (Linear concentration). A random vector $\mathbf{x} \in E$ is linearly α -concentrated around the deterministic equivalent $\bar{\mathbf{x}}$, with respect to the norm $\|\cdot\|$ in E , if, for all unit norm linear functional $u : E \rightarrow \mathbb{R}$ (i.e., $|u(\mathbf{x})| \leq \|\mathbf{x}\|$),

$$u(\mathbf{x}) \in u(\bar{\mathbf{x}}) \pm \alpha.$$

The expectation being a linear operator (from E to E), an advantage of linear concentration is that, upon existence, $\mathbb{E}[\mathbf{x}]$ is a deterministic equivalent for the concentrated random vector \mathbf{x} . In particular, if \mathbf{Q} is a random (resolvent) matrix in the “vector space” $(\mathbb{R}^{p \times p}, \|\cdot\|)$, with $\|\cdot\|$ the operator norm, and that \mathbf{Q} is linearly concentrated with respect to $\|\cdot\|$, then $\mathbb{E}\mathbf{Q}$ is a deterministic equivalent for \mathbf{Q} and we have in particular, for all $\mathbf{A} \in \mathbb{R}^{p \times p}$ and $\mathbf{a}, \mathbf{b} \in \mathbb{R}^p$ of bounded norms,

$$\frac{1}{p} \operatorname{tr} \mathbf{A}(\mathbf{Q} - \mathbb{E}\mathbf{Q}) \rightarrow 0, \quad \mathbf{a}^\top (\mathbf{Q} - \mathbb{E}\mathbf{Q}) \mathbf{b} \rightarrow 0, \quad \|\mathbf{Q} - \mathbb{E}\mathbf{Q}\| \rightarrow 0$$

where the convergence is in probability and, if $\alpha(t) = Ce^{-t^q}$ for some $q > 0$, the convergence is also almost sure. These convergences hold since the three operators are linear and of bounded norm with respect to the norm $\|\cdot\|$.

Lipschitz concentration Lipschitz concentration is the most popular type of concentrations (due to its compatibility with (2.37)). This notion is even in general merely called “concentration” (rather than Lipschitz concentration); it is defined as follows.

Definition 9 (Lipschitz concentration). *A random vector $\mathbf{x} \in E$ is Lipschitz α -concentrated with respect to the norm $\|\cdot\|$ if, for all 1-Lipschitz function $f : E \rightarrow \mathbb{R}$, we have either of the conditions*

$$\begin{aligned} f(\mathbf{x}) &\propto \alpha, \text{ denoted } \mathbf{x} \propto \alpha \\ f(\mathbf{x}) &\in M_f \pm \alpha, \text{ denoted } \mathbf{x} \overset{M}{\propto} \alpha \\ f(\mathbf{x}) &\in \mathbb{E}[f(\mathbf{x})] \pm \alpha, \text{ denoted } \mathbf{x} \overset{\mathbb{E}}{\propto} \alpha \end{aligned}$$

hold, where M_f is a median of $f(\mathbf{x})$.

As for the concentration of random variables, the three notions are not fully equivalent. For generic α -concentration,

$$\mathbf{x} \propto \alpha \Rightarrow \mathbf{x} \overset{\mathbb{E}}{\propto} \alpha \Rightarrow \mathbf{x} \propto 4\alpha(\cdot/2)$$

and, in the case of exponential concentrations, the expectation is well defined and we further have

$$\mathbf{x} \overset{\mathbb{E}}{\propto} Ce^{-(\cdot/\sigma)^q} \Rightarrow \mathbf{x} \overset{M}{\propto} e^{C^q/q} e^{-(\cdot/2\sigma)^q} \Rightarrow \mathbf{x} \overset{M}{\propto} e^{C^q/q} e^{-(\cdot/4\sigma)^q}.$$

The most fundamental result at the very heart of the concentration of measure theory is that Gaussian random vectors $\mathbf{x} \sim \mathcal{N}(\mathbf{0}, \mathbf{I}_p)$ are Lipschitz concentrated in $(\mathbb{R}^p, \|\cdot\|)$ for $\|\cdot\|$ the Euclidean norm, that is

$$\mathbf{x} \sim \mathcal{N}(\mathbf{0}, \mathbf{I}_p) \Rightarrow \mathbf{x} \overset{M}{\propto} 2e^{-(\cdot/2)^2} \text{ and } \mathbf{x} \overset{\mathbb{E}}{\propto} 2e^{-(\cdot/2)^2}.$$

A fundamental fact about the above concentration is that it does *not* depend on the size p of the space (neither in the tail nor in the head parameters). As such,

arbitrarily large standard Gaussian vectors (and thus concatenation of n such vectors, as well as matrices $\mathbf{X} = [\mathbf{x}_1, \dots, \mathbf{x}_n]$ built from independent standard Gaussian vectors \mathbf{x}_i endowed with the Frobenius norm) also concentrate with no dependence on p, n .

This is in fact far from natural as, even for independent vectors $\mathbf{x}_1, \dots, \mathbf{x}_n$, all of which being concentrated, the joint concentration of $(\mathbf{x}_1, \dots, \mathbf{x}_n)$ with respect to the Euclidean norm in the product space generally comes along with a loss of concentration rate proportional to n . Besides, if the vectors \mathbf{x}_1 and \mathbf{x}_2 are both concentrated but not independent, the vector $(\mathbf{x}_1, \mathbf{x}_2)$ may not even be concentrated.

Remark 2.18 (On the location of Gaussian vectors). *To clearly understand the relation between standard Gaussian $\mathbf{x} \sim \mathcal{N}(\mathbf{0}, \mathbf{I}_p)$ and its dimension, note that, $\|\mathbf{x}\|$ having a chi-distribution with median $\sqrt{p} + O(1/\sqrt{p})$, its exponential concentration precisely implies*

$$\mathbb{P}(|\|\mathbf{x}\| - \sqrt{p}| > t) \leq 2e^{-(t+O(1/p))^2/4}.$$

Thus, \mathbf{x} is a random variable that essentially lives close to a sphere of radius $O(\sqrt{p})$ and of thickness $O(1)$ or, equivalently, \mathbf{x}/\sqrt{p} is a random vector distributed close to the unit sphere in \mathbb{R}^p with actual distance to the sphere vanishing as $O(1/\sqrt{p})$. The vector \mathbf{x} is in particular nowhere near its expected value $\mathbf{0}$.

This remark is fundamental as it disrupts with the finite dimensional case where \mathbf{x} lives close to its mean. In 1D to 3D, one indeed visualizes (independent) Gaussian random vectors as densely “concentrated” around their mean. The intuitive extension of this visualization to larger dimensions would be erroneous.

As for concentrated random variables, Lipschitz concentrated random vectors are stable through Lipschitz mapping in the sense that, for all 1-Lipschitz $\phi : E \rightarrow E'$ with respect to norms $\|\cdot\|_E$ and $\|\cdot\|_{E'}$,

$$\mathbf{x} \stackrel{M}{\propto} \alpha \Rightarrow \phi(\mathbf{x}) \stackrel{M}{\propto} \alpha. \quad \text{eq:lipschitz_stability} \quad (2.40)$$

Convex (Lipschitz) concentration. To define convex concentration, we need to recall the notion of quasi-convex functions: $f : E \rightarrow \mathbb{R}$ is quasi-convex if, for all $t \in \mathbb{R}$, the sets $\{\mathbf{x} \in E \mid f(\mathbf{x}) \leq t\}$ are convex sets, i.e., for all $t \in [0, 1]$ and $\mathbf{x}, \mathbf{y} \in E$, $f(t\mathbf{x} + (1-t)\mathbf{y}) \leq \max\{f(\mathbf{x}), f(\mathbf{y})\}$. In particular, convex functions are quasi-convex (thus the notion generalizes convexity) and, for $E = \mathbb{R}$, all monotonous functions (even concave ones) are quasi-convex.

Then we have the following definition of convex concentration.

Definition 10 (Convex concentration). *A vector $\mathbf{x} \in E$ is (Lipschitz) convexly concentrated for the norm $\|\cdot\|$ if, for any 1-Lipschitz and quasi-convex function*

$f : \mathbb{E} \rightarrow \mathbb{R}$, we have either of the conditions

$$\begin{aligned} f(\mathbf{x}) &\propto \alpha, \text{ denoted } \mathbf{x} \propto_c \alpha \\ f(\mathbf{x}) &\in M_f \pm \alpha, \text{ denoted } \mathbf{x} \stackrel{M}{\propto}_c \alpha \\ f(\mathbf{x}) &\in \mathbb{E}[f(\mathbf{x})] \pm \alpha, \text{ denoted } \mathbf{x} \stackrel{\mathbb{E}}{\propto}_c \alpha \end{aligned}$$

where M_f is a median of $f(\mathbf{x})$.

Obviously, all Lipschitz convex functions being Lipschitz, Lipschitz concentration implies convex concentration (which itself implies the even less demanding linear concentration); for instance, in the case of exponential concentration,

$$\mathbf{x} \stackrel{\mathbb{E}}{\propto} C e^{-(\cdot/\sigma)^q} \Rightarrow \mathbf{x} \stackrel{\mathbb{E}}{\propto}_c C e^{-(\cdot/\sigma)^q} \Rightarrow \mathbf{x} \in \mathbb{E}[\mathbf{x}] \pm e^{-(\cdot/\sigma)^q}.$$

The interest for convex concentration is related to the following result due to Talagrand [Talagrand, 1995, Theorem 4.1.1]: let $\mathbf{x} \in [0, 1]^p$ be a vector of independent entries, then

$$\mathbf{x} \stackrel{M}{\propto}_c 4e^{-\cdot^2/4}.$$

However, convex concentration has a major limitation that quasi-convex functions are *not* stable by composition. This prevents the simple adaptation of numerous results obtained for Lipschitz concentration. Yet, for f quasi-convex and g affine, $f \circ g$ is still quasi-convex.

Nonetheless, the results necessary to our present random matrix analysis of sample covariance matrix models can fortunately be extended.

Convex concentration transversally to a group action. A last convenient notion of concentration, dedicated to random matrix theory, consists in transferring concentration from \mathbf{X} to the vector of its singular values. This will help transfer concentration from the data to linear statistics of the eigenvalues of the sample covariance matrix. To this end though, convex concentration is too demanding and we need to further restrict the space of functions as follows.

Definition 11 (Convex concentration transversally to group action). *Let $\mathbf{x} \in E$ and G a group acting on E . Then, \mathbf{x} is convexly α -concentrated transversally to the action of G if, for all quasi-convex 1-Lipschitz and G -invariant function f (i.e., $f(g \cdot \mathbf{x}) = f(\mathbf{x})$ for $g \in G$) $f(\mathbf{x}) \propto \alpha$. This is denoted $\mathbf{x} \propto_G^T \alpha$.*

In particular, denote $\sigma(\mathbf{X}) = (\sigma_1(\mathbf{X}), \dots, \sigma_{\min\{p,n\}}(\mathbf{X}))$ the vector of the singular values of $\mathbf{X} \in \mathbb{R}^{p \times n}$ (i.e., $\sigma_i(\mathbf{X}) = \sqrt{\lambda_i(\mathbf{X}\mathbf{X}^\top)}$ for $i \leq \min\{p, n\}$), and define the group $\mathcal{O}_{p,n} = \{(\mathbf{U}, \mathbf{V}) \in \mathbb{R}^{p \times p} \times \mathbb{R}^{n \times n} \text{ orthonormal}\}$ acting on $\mathbb{R}^{p \times n}$ by $(\mathbf{U}, \mathbf{V}) \cdot \mathbf{M} = \mathbf{U}\mathbf{M}\mathbf{V}^\top$ and the group \mathcal{S}_p of permutations of size p acting on \mathbb{R}^p by $\tau \cdot \mathbf{y} = (\mathbf{y}_{\tau(1)}, \dots, \mathbf{y}_{\tau(p)})$. Then, we have the following result, inspired by [Davis, 1957],

$$\mathbf{X} \propto_{\mathcal{O}_{p,n}}^T \alpha \Leftrightarrow \sigma(\mathbf{X}) \propto_{\mathcal{S}_{\min\{p,n\}}}^T \alpha. \quad \text{eq:concentration-group (2.41)}$$

2.7.4 A concentration inequality version of Theorem 2.5

Equipped with these elementary results, we can now provide an extension of Theorem 2.5 to the case of concentrated data vectors.

Before getting to the main result, we introduce some preliminary lemmas, which generalize classical random matrix results to the concentration of measure framework.

2.7.4.1 Trace lemma

A first result of importance concerns the extension of the “quadratic-form-close-to-the-trace” lemma, Lemma 2.11, from a moment-based version to a concentration of measure setting. We have precisely

Lemma 2.21 (Trace lemma for concentrated vectors). *Let $\mathbf{A} \in \mathbb{R}^{p \times p}$ and $\mathbf{x} \in \mathbb{R}^p$ such that $\mathbf{x} \stackrel{\mathbb{E}}{\propto_c} C e^{-(\cdot/\sigma)^q}$. Then,*

$$\mathbf{x}^\top \mathbf{A} \mathbf{x} \in \text{tr}(\mathbb{E}[\mathbf{x} \mathbf{x}^\top] \mathbf{A}) \pm 2C \left(e^{-(\cdot/4\sigma\|\mathbf{A}\| \mathbb{E}[\|\mathbf{x}\|])^q} + e^{-(\cdot/2\|\mathbf{A}\|\sigma^2)^{\frac{q}{2}}} \right).$$

This lemma follows almost automatically from two elementary ingredients of the concentration of measure theory: (i) assuming first that \mathbf{A} is nonnegative definite, $\mathbf{x}^\top \mathbf{A} \mathbf{x} = \|\mathbf{A}^{\frac{1}{2}} \mathbf{x}\|^2$ with $\|\mathbf{A}^{\frac{1}{2}} \mathbf{x}\|$ a concentrated random variable (it is a Lipschitz and convex function of \mathbf{x}) which, (ii) from the concentration of powers of concentrated random variables (2.38) for $k = 2$, gives the result. For generic \mathbf{A} , it suffices to write \mathbf{A} as the sum of its symmetric nonnegative and symmetric negative parts (which explains the leading factor 2).

This lemma particularly stresses the technical convenience of the concentration of measure framework. The key random matrix results, such as Lemma 2.11 for vectors of i.i.d. entries, often rely on dedicated tools and possibly heavy (combinatorial) proof techniques. Here, the concentration of measure alternative to Lemma 2.11 follows from a mere two-line argument (once the elementary tools of the theory are in place). Besides the exponential rate of convergence is very versatile and particularly ensures the uniform convergence of $\{\mathbf{x}_i^\top \mathbf{A} \mathbf{x}_i, i = 1, \dots, n\}$, for n any polynomial in p ; using the moment method would demand to systematically compute high order moments of $\mathbf{x}_i^\top \mathbf{A} \mathbf{x}_i$ to obtain uniform convergence over large n (using Markov’s inequality).

2.7.4.2 Concentration of the Stieltjes transform

Next, we generalize the convergence of Stieltjes transforms in a generic concentration of measure form.

lem:concentration_ST

Lemma 2.22 (Trace of Resolvent). *For $\mathbf{X} \in \mathbb{R}^{p \times n}$ equipped with the Frobenius norm, and $\mathbf{Q}(z) = (\frac{1}{n} \mathbf{X} \mathbf{X}^\top - z \mathbf{I}_p)^{-1}$ for $z < 0$,*

$$\mathbf{X} \propto_c \alpha \text{ in } (\mathbb{R}^{p \times n}, \|\cdot\|_F) \Rightarrow \text{tr } \mathbf{Q}(z) \propto 2\alpha \left(\frac{\sqrt{n|z|^3}}{8 \min\{p, n\}} \right).$$

To prove this lemma, first recall that $\mathbf{X} \propto_c \alpha \Rightarrow \sigma(\mathbf{X}) \propto_{\mathcal{S}_d}^T \alpha$ with $d = \min\{p, n\}$. Also, $\text{tr } \mathbf{Q}(z) = \sum_{i=1}^d f(\sigma_i(\mathbf{X}))$ for $f : \mathbb{R}_+ \rightarrow \mathbb{R}$, $s \mapsto 1/(s^2 - z)$. This function f is $(2|z|^{-\frac{2}{3}})$ -Lipschitz (checked by bounding its derivative) and the mapping $(s_1, \dots, s_d) \mapsto \sum_{i=1}^d s_i$ is evidently \mathcal{S}_d -invariant. However, f is not quasi-convex but can be written as the sum $f = g - h$ of two quasi-convex $4|z|^{-\frac{2}{3}}$ -Lipschitz functions $(h(s) = (s/|z| - 1/\sqrt{|z|})^2 1_{\{s \in [0, \sqrt{|z|}]\}}$ and $g = f + h$). Consequently, since $\mathbf{X} \propto_c \alpha \Rightarrow \mathbf{X} \propto_{\mathcal{O}_{p,n}}^T \alpha$, we have from (2.41) both the concentration of $\sum_i g(\sigma_i(\mathbf{X}))$ and of $\sum_i h(\sigma_i(\mathbf{X}))$, and it then remains to apply the result on the concentration of the sum of two concentrated random variables to obtain the result.

Again here, the proof is elegantly immediate although the mapping $\mathbf{X} \mapsto \text{tr } \mathbf{Q}(z)$ is highly non-trivial from a statistical standpoint. Note in particular that the technical difficulty raised by the non-convexity of f would not have been a problem if we had rather assumed Lipschitz concentration $\mathbf{X} \propto \alpha$ for \mathbf{X} (which we recall is more demanding for \mathbf{X} and would exclude the case of \mathbf{X} with bounded i.i.d. entries).

2.7.4.3 Concentration of the resolvent \mathbf{Q} and deterministic equivalents

The approach followed in the previous lemma uses the convenient expression of $f : \mathbb{R}^{p \times n} \rightarrow \mathbb{R}$ as $f = g - h$ for two convex and Lipschitz functions g and h . It does not seem that the mapping $f(\mathbf{X}) = \mathbf{Q}_{\frac{1}{n}\mathbf{XX}^\top}(z)$ from $\mathbb{R}^{n \times p}$ to $\mathbb{R}^{p \times p}$ can be treated similarly, as no such Lipschitz function division can be exploited. One must therefore resort to the additional strength of exponential concentration to divide the space $\mathbb{R}^{p \times n}$ into a compact space for the operator norm $\{\mathbf{X} \mid \|\mathbf{X}\| \leq K\sqrt{n}\}$ where f will be shown to be automatically Lipschitz (as its image is bounded) and the complement space $\{\mathbf{X} \mid \|\mathbf{X}\| > K\sqrt{n}\}$ which is of vanishing probability for all large $K > 0$.

Regrouping these two results, we have the following concentration for the resolvent.

Lemma 2.23 (Concentration of $\mathbf{Q}_{\frac{1}{n}\mathbf{XX}^\top}$). *For $\mathbf{X} \in \mathbb{R}^{p \times n}$ and $z < 0$, let $\mathbf{Q}(z) = (\frac{1}{n}\mathbf{XX}^\top - z\mathbf{I}_p)^{-1}$. Then we have the following two results*

$$\begin{aligned} \mathbf{X} \propto \alpha \Rightarrow \mathbf{Q}(z) &\propto \alpha \left(\sqrt{n|z|^3} \cdot /2 \right) \\ \mathbf{X} \stackrel{\mathbb{E}}{\propto}_c C e^{-(\cdot)^q} \Rightarrow \mathbf{Q}(z) &\in \mathbb{E}\mathbf{Q}(z) \pm 2C e^{-\left(\sqrt{|z|^3 n} \cdot /4\sigma\right)^q}. \end{aligned}$$

where the left-hand side concentrations are understood in $(\mathbb{R}^{p \times n}, \|\cdot\|_F)$ and the right-hand side in $(\mathbb{R}^{p \times p}, \|\cdot\|_F)$.

This result is in fact quite powerful and automatically induces (and vastly generalizes) the notion of deterministic equivalent of Definition 4, i.e., it implies that $\frac{1}{n} \text{tr } \mathbf{A}(\mathbf{Q} - \mathbb{E}\mathbf{Q}) \xrightarrow{a.s.} 0$ and $\mathbf{a}^\top(\mathbf{Q} - \mathbb{E}\mathbf{Q})\mathbf{b} \xrightarrow{a.s.} 0$ for all $\mathbf{A}, \mathbf{a}, \mathbf{b}$ of unit

norm. Indeed, first recall that the first statement (of Lipschitz concentration) implies that

$$\mathbf{X} \xrightarrow{\mathbb{E}} \alpha \Rightarrow \mathbf{Q}(z) \in \mathbb{E}\mathbf{Q}(z) \pm \alpha \left(\sqrt{n|z|^3} \cdot / 2 \right)$$

(since Lipschitz concentration around the mean implies linear concentration around the mean). Next, note that the linear concentrations of \mathbf{Q} (under either Lipschitz or convex-Lipschitz-exponential concentration for \mathbf{X}) hold here with respect to the Frobenius norm of $\mathbf{X} \in \mathbb{R}^{p \times n}$. That is, for $\mathbf{A} \in \mathbb{R}^{p \times p}$ of bounded Frobenius (rather than only spectral) norm,²³

$$\text{tr } \mathbf{A}(\mathbf{Q} - \mathbb{E}\mathbf{Q}) = O(n^{-\frac{1}{2}}).$$

In particular, letting $p/n \rightarrow c > 0$, from $\|\mathbf{A}\|_F \leq \sqrt{\text{rank}(\mathbf{A})}\|\mathbf{A}\|$ (with $\|\cdot\|$ the operator norm) and $\|\mathbf{A}\| \leq \|\mathbf{A}\|_F$, we have (i) if $\mathbf{A} = \mathbf{ab}^\top$ is of unit rank, $\text{tr } \mathbf{ab}^\top(\mathbf{Q} - \mathbb{E}\mathbf{Q}) = \mathbf{a}^\top(\mathbf{Q} - \mathbb{E}\mathbf{Q})\mathbf{b} = O(n^{-1/2})$, while (ii) if \mathbf{A} is of arbitrary rank (say $\text{rank}(\mathbf{A}) = p$), $p^{-\frac{1}{2}} \text{tr } \mathbf{A}(\mathbf{Q} - \mathbb{E}\mathbf{Q}) = O(n^{-1/2})$ so that $\frac{1}{p} \text{tr } \mathbf{A}(\mathbf{Q} - \mathbb{E}\mathbf{Q}) = O(n^{-1})$.

Of course, since $\|\cdot\| \leq \|\cdot\|_F$ in $\mathbb{R}^{p \times p}$, Lemma 2.23 applies to \mathbf{Q} in $(\mathbb{R}^{p \times p}, \|\cdot\|)$ as well.

The proof of the first part of the lemma is again extremely simple, once the basic concentration of measure arguments are in place. Here we simply use the fact that the mapping $f : \mathbb{R}^{p \times n} \rightarrow \mathbb{R}^{p \times p}$, $\mathbf{X} \mapsto \mathbf{Q}(z)$ is $(2/\sqrt{|z|^3 n})$ -Lipschitz. Indeed, by the resolvent identity, Lemma 2.1,

$$f(\mathbf{X} + \mathbf{H}) - f(\mathbf{X}) = \frac{1}{n} f(\mathbf{X} + \mathbf{H})((\mathbf{X} + \mathbf{H})\mathbf{H}^\top + \mathbf{H}\mathbf{X}^\top)f(\mathbf{X})$$

so that, from $\|f(\mathbf{X})\mathbf{X}\| \leq \sqrt{n/|z|}$, $\|f(\mathbf{X})\| \leq 1/|z|$ and $\|\mathbf{AB}\|_F \leq \|\mathbf{A}\|\|\mathbf{B}\|_F$ (where $\|\cdot\|$ is the operator norm), we have $\|f(\mathbf{X} + \mathbf{H}) - f(\mathbf{X})\|_F \leq 2\|\mathbf{H}\|_F/\sqrt{|z|^3 n}$ and thus the result.

The proof of the second part is less immediate. Since the result is a linear concentration of the resolvent, one needs to control the concentration of the random variable $\text{tr } \mathbf{AQ}$ obtained for arbitrary $\mathbf{A} \in \mathbb{R}^{p \times p}$ with $\|\mathbf{A}\|_F \leq 1$. This is obtained by considering the mapping $f : \mathbf{X} \mapsto \text{tr } \mathbf{AQ}$, with the major difference from Lemma 2.22 that $f(\mathbf{Q})$ is now not a mere combination of the singular values of \mathbf{Q} . The function f is not convex (as already discussed in Lemma 2.22) but can be divided as $f = h - g$ with $g : \mathbf{X} \mapsto \frac{1}{n|z|^2} \text{tr } \mathbf{XX}^\top$ and $h = f + g$ both convex, with h Lipschitz and g Lipschitz on the bounded region $\{\mathbf{X} \mid \|\mathbf{X}\| \leq K\sqrt{n}\}$. Using a truncation method by considering $(\mathbf{X}^K)_{ij} = \mathbf{X}_{ij} 1_{\mathbf{X}_{ij} < K\sqrt{n}}$ for growing K , one obtains that the sequence of concentrated random variables $\text{tr } \mathbf{AQ}^K = \text{tr } \mathbf{AQ}_{\perp \mathbf{X}^K(\mathbf{X}^K)^\top}$ converges in law to $\text{tr } \mathbf{AQ}$, which can then be shown to imply that $\text{tr } \tilde{\mathbf{AQ}}$ is also a concentrated random variable.

²³One must be careful not to confuse the steps of the proof which, as shown next, use a smart division of $\mathbb{R}^{p \times n}$ into bounded and unbounded operator norm $\|\mathbf{X}\|$, and the fact that the ultimate concentration results hold with respect to the Frobenius norm.

2.7.4.4 Main result

Let us rephrase the setting of Theorem 2.5 by letting $\mathbf{x}_1, \dots, \mathbf{x}_n \in \mathbb{R}^p$ be n i.i.d. random vectors with law \mathcal{L} such that

$$\mathbf{X} = [\mathbf{x}_1, \dots, \mathbf{x}_n] \propto C e^{-(\cdot)^q/c}$$

for some $C, c, q > 0$ with respect to the Frobenius norm (which implies in particular, by the action of the 1-Lipschitz mapping $f : (\mathbf{x}_1, \dots, \mathbf{x}_n) \mapsto \mathbf{x}_i$, that each \mathbf{x}_i is concentrated). This request of joint rather than individual vector concentration may be considered demanding, but is at least satisfied by (i) $\mathbf{x}_i = \phi(\mathbf{y}_i)$ with 1-Lipschitz maps $\phi : \mathbb{R}^{p'} \rightarrow \mathbb{R}^p$ for (i-a) $\mathbf{y}_i \sim \mathcal{N}(0, \mathbf{I}_{p'})$ or (i-b) \mathbf{y}_i uniformly distributed on the $\sqrt{p'}$ -radius sphere of $\mathbb{R}^{p'}$, or (ii) for \mathbf{x}_i composed of (an affine mapping of) i.i.d. entries with support in $[-1, 1]$.

With the above results, and some specific technical arguments, we have the following *concentration of measure version* of Theorem 2.5.

theo:baisilverstein95_concentrated

Theorem 2.17 (Sample covariance of concentrated random vectors). *Let $\mathbf{X} = [\mathbf{x}_1, \dots, \mathbf{x}_n] \propto C e^{-(\cdot)^q/c}$ with $\mathbf{x}_i \in \mathbb{R}^p$, and $z < 0$. Further assume that $\frac{1}{\sqrt{p}} \mathbb{E} \|\mathbf{x}_i\|$ (or, if $q \geq 2$, simply $\frac{1}{\sqrt{p}} \|\mathbb{E}[\mathbf{x}_i]\|$), $\frac{1}{p} \operatorname{tr} \Phi$ with $\Phi = \mathbb{E}[\frac{1}{n} \mathbf{X} \mathbf{X}^\top]$, as well as p/n are all bounded. Then, for all large n ,*

$$\mathbf{Q}(z) \in \bar{\mathbf{Q}}(z) \pm C' e^{-(\sqrt{n})^q/c'} \text{ in } (\mathbb{R}^{p \times n}, \|\cdot\|)$$

for some $C', c' > 0$, where

$$\bar{\mathbf{Q}}(z) = \left(\frac{\Phi}{1 + \delta(z)} - z \mathbf{I}_p \right)^{-1}$$

and $\delta(z)$ is the unique positive solution to $\delta(z) = \frac{1}{n} \operatorname{tr} \Phi \bar{\mathbf{Q}}(z)$.

Remark 2.19 (On real $z < 0$). *It must be noted here that the concentration framework devised in this section is only valid for real-valued matrices and thus Theorem 2.17 holds here for $z < 0$ only. Using additional arguments (of complex analytic extension of $\mathbf{Q}(z)$ and $\bar{\mathbf{Q}}(z)$), Theorem 2.17 naturally extends to all $z \in \mathbb{C} \setminus \mathbb{R}^+$.*

Denoting $\delta(z) = -1 - \frac{1}{z \tilde{m}_p(z)}$ and $\Phi = \mathbf{C}$, it comes immediately that the deterministic equivalent $\bar{\mathbf{Q}}$ in Theorem 2.17 above has the same ‘‘formal statement’’ as in Theorem 2.5; we shall see that using $\delta(z)$ rather than $\tilde{m}_p(z)$ is more convenient under the concentration of measure framework. Yet, there are a few key difference to raise between both theorems. First, $\Phi = \mathbb{E}[\frac{1}{n} \mathbf{X} \mathbf{X}^\top]$ is not a covariance matrix as the present concentration of measure on \mathbf{X} do not impose that $\mathbb{E}[\mathbf{X}] = \mathbf{0}$. Also, the deterministic equivalent $\bar{\mathbf{Q}}(z)$ comes along with a convergence speed and an exponential tail, which are both more practical than a mere almost sure convergence of specific statistics.

Theorem 2.17 unfolds from the same idea introduced in the proof of the Marčenko–Pastur law (Theorem 2.3), by successively introducing two deterministic equivalents. We provide here the basic arguments of the proof. We already know from Lemma 2.23 that $\mathbf{Q}(z) \in \mathbb{E}\mathbf{Q}(z) \pm Ce^{-c(\sqrt{n} \cdot)^q}$ for some $C, c > 0$ and it only remains to show that $\|\mathbb{E}\mathbf{Q}(z) - \bar{\mathbf{Q}}(z)\|$ is small.

To this end, we introduce the first deterministic equivalent

$$\bar{\mathbf{Q}}(z) = \left(\frac{\Phi}{1 + \delta'(z)} - z\mathbf{I}_p \right)^{-1}$$

where $\delta'(z) = \frac{1}{n}\mathbb{E}[\mathbf{x}^\top \mathbf{Q}_-(z)\mathbf{x}] = \frac{1}{n}\text{tr } \Phi \mathbb{E}\mathbf{Q}_-$ for $\mathbf{Q}_- \in \mathbb{R}^{p \times p}$ the resolvent of $\frac{1}{n}\mathbf{X}\mathbf{X}^\top - \frac{1}{n}\mathbf{x}\mathbf{x}^\top$ and \mathbf{x} any column of \mathbf{X} . Applying the same ideas as in the proof of Theorem 2.3 shows that (we discard the z 's for readability),

$$\begin{aligned} \mathbb{E}\mathbf{Q} - \bar{\mathbf{Q}} &= \mathbb{E} \left[\mathbf{Q} \left(\frac{\Phi}{1 + \delta'} - \frac{1}{n}\mathbf{X}\mathbf{X}^\top \right) \right] \bar{\mathbf{Q}} \\ &= \frac{1}{n} \sum_{i=1}^n \mathbb{E} \left[\mathbf{Q} \left(\frac{\Phi}{1 + \delta'} - \mathbf{x}_i \mathbf{x}_i^\top \right) \right] \bar{\mathbf{Q}} = \mathbb{E} \left[\mathbf{Q} \left(\frac{\Phi}{1 + \delta'} - \mathbf{x}\mathbf{x}^\top \right) \right] \bar{\mathbf{Q}} \end{aligned}$$

which, along with $\mathbf{Q} = \mathbf{Q}_- - \frac{1}{n} \frac{\mathbf{Q}_-\mathbf{x}\mathbf{x}^\top\mathbf{Q}_-}{1 + \frac{1}{n}\mathbf{x}^\top\mathbf{Q}_-\mathbf{x}}$ and $\mathbf{Q}\mathbf{x} = \frac{\mathbf{Q}_-\mathbf{x}}{1 + \frac{1}{n}\mathbf{x}^\top\mathbf{Q}_-\mathbf{x}}$, gives

$$\begin{aligned} \mathbb{E}\mathbf{Q} - \bar{\mathbf{Q}} &= \mathbb{E}[\mathbf{E}_1] - \mathbb{E}[\mathbf{E}_2] \\ \mathbf{E}_1 &= \mathbf{Q}_- \left(\frac{\Phi}{1 + \delta'} - \frac{\mathbf{x}\mathbf{x}^\top}{1 + \frac{1}{n}\mathbf{x}^\top\mathbf{Q}_-\mathbf{x}} \right) \bar{\mathbf{Q}} \\ \mathbf{E}_2 &= \frac{1}{n(1 + \delta')} \mathbf{Q}_-\mathbf{x}\mathbf{x}^\top\mathbf{Q}\Phi\bar{\mathbf{Q}}. \end{aligned}$$

To bound $\|\mathbb{E}\mathbf{Q} - \bar{\mathbf{Q}}\|$ it suffices to bound $|\mathbf{a}^\top (\mathbb{E}\mathbf{Q} - \bar{\mathbf{Q}})\mathbf{a}|$ for any unit norm \mathbf{a} . From Hölder's inequality

$$\begin{aligned} |\mathbf{a}^\top \mathbb{E}[\mathbf{E}_1]\mathbf{a}| &= \left| \mathbb{E} \left[\mathbf{a}^\top \mathbf{Q}_-\mathbf{x}\mathbf{x}^\top \bar{\mathbf{Q}}\mathbf{a} \frac{\frac{1}{n}\mathbf{x}^\top \mathbf{Q}_-\mathbf{x} - \delta'}{(1 + \delta')(1 + \frac{1}{n}\mathbf{x}^\top \mathbf{Q}_-\mathbf{x})} \right] \right| \\ &\leq \mathbb{E} \left[|\mathbf{a}^\top \mathbf{Q}_-\mathbf{x}| |\mathbf{x}^\top \bar{\mathbf{Q}}\mathbf{a}| \left| \frac{1}{n}\mathbf{x}^\top \mathbf{Q}_-\mathbf{x} - \delta' \right| \right] \\ &\leq \mathbb{E}[|\mathbf{a}^\top \mathbf{Q}_-\mathbf{x}|] \mathbb{E}[|\mathbf{x}^\top \bar{\mathbf{Q}}\mathbf{a}|] \mathbb{E} \left[\left| \frac{1}{n}\mathbf{x}^\top \mathbf{Q}_-\mathbf{x} - \delta' \right| \right] \\ &= O(n^{-\frac{1}{2}}) \end{aligned}$$

where we used here: (i) $\mathbf{a}^\top \bar{\mathbf{Q}}\mathbf{x} \propto Ce^{-(\cdot)^q}$ and $\mathbf{a}^\top \mathbf{Q}_-\mathbf{x} \propto Ce^{-c(\cdot)^q}$ (from which $\mathbb{E}[|\mathbf{a}^\top \bar{\mathbf{Q}}\mathbf{x}|^k] = O(1)$ and $\mathbb{E}[|\mathbf{a}^\top \mathbf{Q}_-\mathbf{x}|^k] = O(1)$) and (ii) $\frac{1}{n}\mathbf{x}^\top \mathbf{Q}_-\mathbf{x} \in \delta' \pm Ce^{-c(n \cdot)^{q/2}} + Ce^{-c(\sqrt{n} \cdot)^q}$ (from which $\mathbb{E}[|\frac{1}{n}\mathbf{x}^\top \mathbf{Q}_-\mathbf{x} - \delta'|^k] = O(n^{-\frac{k}{2}})$). The concentration results (i) and (ii) themselves unfold from the previous generic results on concentration of vectors and bilinear forms. Similarly,

$$|\mathbf{a}^\top \mathbb{E}[\mathbf{E}_2]\mathbf{a}| \leq \frac{1}{n} \mathbb{E}[|\mathbf{a}^\top \mathbf{Q}_-\mathbf{x}|] \mathbb{E}[|\mathbf{x}^\top \mathbf{Q}_-\Phi\bar{\mathbf{Q}}\mathbf{a}|] = O(n^{-1}).$$

Letting \mathbf{a} be the dominant singular vector of $\mathbb{E}\mathbf{Q} - \bar{\mathbf{Q}}$, we thus find that $\|\mathbb{E}\mathbf{Q} - \bar{\mathbf{Q}}\| = O(n^{-\frac{1}{2}})$. Integrated into $\mathbf{Q}(z) \in \mathbb{E}\mathbf{Q}(z) \pm Ce^{-c(\sqrt{n})^q}$, this gives $\mathbf{Q}(z) \in \bar{\mathbf{Q}} \pm Ce^{-c(\sqrt{n})^q}$.

It thus remains to show similarly that $\|\bar{\mathbf{Q}} - \tilde{\mathbf{Q}}\|$ is small. We have

$$\|\bar{\mathbf{Q}} - \tilde{\mathbf{Q}}\| = \frac{|\delta' - \delta|}{(1 + \delta)(1 + \delta')} \|\bar{\mathbf{Q}}\Phi\tilde{\mathbf{Q}}\| \leq \frac{|\delta - \delta'|}{|z|}$$

and it thus suffices to control $\delta - \delta'$, which, by the implicit form of δ , satisfies

$$\begin{aligned} |\delta - \delta'| &= \frac{1}{n} |\operatorname{tr} \Phi(\bar{\mathbf{Q}} - \bar{\mathbf{Q}} + \bar{\mathbf{Q}} - \mathbb{E}\mathbf{Q} + \mathbb{E}[\mathbf{Q} - \mathbf{Q}_-])| \\ &\leq \frac{1}{n} |\operatorname{tr} \Phi(\bar{\mathbf{Q}} - \bar{\mathbf{Q}})| + \frac{1}{n} \operatorname{tr} \Phi \|\bar{\mathbf{Q}} - \mathbb{E}\mathbf{Q}\| + \frac{1}{n} \operatorname{tr} \Phi \|\mathbb{E}[\mathbf{Q} - \mathbf{Q}_-]\| \\ &\leq \sqrt{\frac{1}{n(1 + \delta)^2} \operatorname{tr} \Phi^2 \bar{\mathbf{Q}}^2} \sqrt{\frac{1}{n(1 + \delta')^2} \operatorname{tr} \Phi^2 \bar{\mathbf{Q}}^2} |\delta - \delta'| + O(n^{-\frac{1}{2}}) \end{aligned}$$

where we used $\operatorname{tr} \mathbf{AB} \leq \|\mathbf{B}\| \operatorname{tr} \mathbf{A}$ for symmetric and nonnegative definite $\mathbf{A} \in \mathbb{R}^{p \times p}$, and $\|\mathbb{E}[\mathbf{Q} - \mathbf{Q}_-]\| = O(n^{-1/2})$, which unfolds from

$$\|\mathbb{E}[\mathbf{Q} - \mathbf{Q}_-]\| = \frac{1}{n} \left\| \mathbb{E} \frac{\mathbf{Q}_- \mathbf{x} \mathbf{x}^\top \mathbf{Q}_-}{1 + \frac{1}{n} \mathbf{x}^\top \mathbf{Q}_- \mathbf{x}} \right\| = \frac{1}{n} \left\| \frac{\mathbb{E}[\mathbf{Q}_- \Phi \mathbf{Q}_-]}{1 + \delta'} \right\| + O(n^{-\frac{1}{2}}).$$

The prefactor of $|\delta - \delta'|$ is strictly less than 1 for all large n , and thus $|\delta - \delta'| = O(n^{-\frac{1}{2}})$, which concludes the proof.

2.8 Concluding remarks

This section explored basic to advanced spectral properties of a family of random matrix models, with a strong emphasis on the sample covariance matrix model, in the regime of large and commensurable data number n and dimension p . Despite the simplicity of its definition, we saw that the limiting eigenvalue distribution of the sample covariance matrix is far from trivial, that quite advanced techniques from complex analysis are needed to perform statistical inference, and that, unlike in the classical $n \rightarrow \infty$ and p fixed regime, phase transition phenomena arise, below which some inference problems are asymptotically insoluble.

Fortunately, even if the statistical models used in concrete machine learning applications are often more involved, we will see that the main techniques and tools used to understand and improve machine learning algorithms and methods are essentially the same as those presented so far. In particular, we will see in the following sections that

- in (not necessarily linear) regression problems, the resolvent (of the sample covariance, of kernel matrices, of the Gram matrix of random feature maps, etc.) will systematically appear as the central object of interest (which is reminiscent of the fact that regression is an inverse problem);

- in classification problems, the spectrum of kernel random matrices and Laplacian random matrices (for spectral clustering or spectral community detection), or alternatively functionals of these kernel and Laplacian random matrices (for supervised or semi-supervised graph-based learning) will play an important role; the performance achieved by these methods, given in terms of misclassification rates, probability of false alarms, etc., will in particular demand the evaluation of the limiting means and variances of these functionals;
- in the specific case of spectral or subspace methods, such as PCA, manifold-based clustering, spectral clustering, and community detection, the aforementioned phase transition phenomena will arise and show that there exist strict limitations for these methods, in particular, a minimal samples/dimension ratio exists below which no detection or classification is possible;
- even for optimization-based machine learning problems, such as generalized linear models [Nelder and Wedderburn, 1972], that rarely offer a solution explicitly defined from (the resolvent of) a particular random matrix, their large dimensional (limiting) performance will be shown ultimately to depend in an almost explicit way on some slightly more involved random matrices; there, the twist will be to realize that some random quantities (not always easy to identify) converge and can asymptotically be replaced by deterministic equivalents obtained from a perturbation analysis (e.g., some sort of a local “linearization”), which naturally induces matrices and resolvent forms.

Before delving into these applications, it is important to recall that we shall purposely place ourselves under the “realistic” situation where the number of samples n cannot be chosen arbitrarily large (samples do not always come for free in practice) and particularly not overwhelmingly larger than the typical dimension p of the data. More importantly, we also impose that the problem being addressed is not “asymptotically trivial”, i.e., for p, n realistically large, the misclassification probability or the cost to be minimized will not vanish. This way, the asymptotic analysis ($n, p \rightarrow \infty$) will be a realistic representative of the finite (but not too small) dimensional and (moderately) difficult machine learning problem. This is quite different from many parallel theoretical machine learning works which often aim at concluding (usually through the evaluation of error bounds, rather than exact results) that the algorithm under analysis provides an asymptotic perfect performance (vanishing misclassification rate or cost) in a certain growth regime of n with respect to p . Our vision instead is that, for a realist and meaningful analysis, n and p must be considered as both fixed (only not to too small values).

As such, to best appreciate the many results to come in the next chapters, these must be seen under this “finite dimensional and realistic” lens.

2.9 Exercises

sec:exercises

In this section, we provide short exercises to familiarize the reader with various useful notions and properties in random matrices calculus discussed in this Section, with detailed solutions deferred to the end of the monograph.

2.9.1 Properties of the Stieltjes transform

ex:ST_moments

Exercise 1 (Stieltjes transform and moments). *Show that the Stieltjes transform $m_\mu(z)$, of a probability measure μ with bounded support (and thus finite moments), is a moment generating function in the sense that, for all $z \in \mathbb{C}$ such that $|z| > \max\{|\inf(\text{supp}(\mu))|, |\sup(\text{supp}(\mu))|\}$,*

$$m_\mu(z) = -\frac{1}{z} \sum_{n=0}^{\infty} M_n z^{-n}$$

where $M_n = \int t^n \mu(dt)$.

From this formulation, propose a method to evaluate the successive moments of μ .

Exercise 2 (Non-immediate Stieltjes transforms). *Let $\mathbf{X} \in \mathbb{R}^{n \times n}$ be a Hermitian matrix and $\mathbf{Q}(z) = (\mathbf{X} - z\mathbf{I}_n)^{-1}$ its resolvent. Show that, for any $\mathbf{u} \in \mathbb{R}^n$ unitary ($\|\mathbf{u}\| = 1$) and any \mathbf{A} with $\text{tr } \mathbf{A} = 1$, the quantities $\mathbf{u}^\top \mathbf{Q}(z) \mathbf{u}$ and $\text{tr } \mathbf{A} \mathbf{Q}(z)$ are the Stieltjes transform of probability measures.*

What are these measures and what are their supports?

Exercise 3 (Stieltjes transform and singular values). *Let μ be a probability measure on \mathbb{R}^+ and ν, ν' be the measures defined by*

$$\begin{aligned} \int f(t) \nu(dt) &= \int f(\sqrt{t}) \mu(dt) \\ \int f(t) \nu'(dt) &= \frac{1}{2} \left(\int f(t) \nu(dt) + \int f(-t) \nu(dt) \right) \end{aligned}$$

for all bounded continuous f .

What are ν, ν' when $\mu = \frac{1}{n} \sum_{i=1}^n \delta_{x_i}$ for $x_1, \dots, x_n \geq 0$?

Show that the Stieltjes transform $m_{\nu'}$ of ν' satisfies

$$m_{\nu'}(z) = zm_\mu(z^2).$$

Letting $\mathbf{X} \in \mathbb{R}^{n \times n}$ and μ the empirical spectral distribution of \mathbf{XX}^\top , relate the Stieltjes transform of the matrix

$$\Gamma = \begin{bmatrix} 0 & \mathbf{X} \\ \mathbf{X}^\top & 0 \end{bmatrix}$$

to that of the measure μ , and conclude on the nature of this Stieltjes transform.

ex:proof_rank1perturbation

Exercise 4 (Partial proof of Lemma 2.9). *For \mathbf{A}, \mathbf{M} symmetric nonnegative definite matrices, $\tau > 0$ and $z < 0$, using inversion lemmas and norm inequalities, prove that*

$$\left| \operatorname{tr} \mathbf{A} (\mathbf{M} + \tau \mathbf{u} \mathbf{u}^\top - z \mathbf{I}_p)^{-1} - \operatorname{tr} \mathbf{A} (\mathbf{M} - z \mathbf{I}_p)^{-1} \right| \leq \frac{\|\mathbf{A}\|}{|z|}.$$

2.9.2 On limiting laws

ex:edges

Exercise 5 (The $\sqrt{|x-b|}$ behavior of the edges). *Show that both the semi-circle and the Marčenko-Pastur laws (for $c \neq 1$) have a local $\sqrt{|x-b|}$ behavior at each of the edges b of their support.*

Conclude on the typical number of eigenvalues of the Wishart matrix $\frac{1}{n} \mathbf{X} \mathbf{X}^\top \in \mathbb{R}^{p \times p}$ with $\mathbf{X}_{ij} \sim \mathcal{N}(0, 1)$ independent, and the Wigner $\mathbf{X} \in \mathbb{R}^{n \times n}$ with $\mathbf{X}_{ij} = \mathbf{X}_{ji} \sim \mathcal{N}(0, 1)$ independent up to symmetry, found near the edges of their respective supports.

Relate this finding to the fluctuations of the Tracy-Widom distribution of the largest and smallest eigenvalues.

What happens for the left-edge of the support of the Marčenko-Pastur law and to the associated smallest eigenvalues of Wishart matrices when $\lim p/n = c = 1$? How many eigenvalues are then found close to the left edge in this so-called “hard-edge” setting? Conclude on the typical fluctuations of these eigenvalues and confirm numerically.

ex:edges2

Exercise 6 (The $\sqrt{|x-b|}$ behavior in elaborate models). *We here seek to extend the results of Exercise 5 to the sample covariance matrix model $\frac{1}{n} \mathbf{X} \mathbf{X}^\top$ where $\mathbf{X} = \mathbf{C}^{\frac{1}{2}} \mathbf{Z}$ with \mathbf{Z} having independent standard Gaussian entries and \mathbf{C} having a bounded limiting spectral measure ν with fast decaying tails. We denote $\tilde{m}(z)$ the Stieltjes transform of the limiting spectral measure $\tilde{\mu}$ of $\frac{1}{n} \mathbf{X}^\top \mathbf{X}$.*

Using Figure 2.5 as a reference and recalling the formulation for the inverse Stieltjes transform

$$x(\tilde{m}) = -\frac{1}{\tilde{m}} + c \int \frac{t \nu(dt)}{1 + t \tilde{m}}$$

visually justify that $x''(\tilde{m})$ can be (complex) analytically extended in the neighborhood of each point \tilde{m} where $x'(\tilde{m}) = 0$ into a function $z(\tilde{m})$ which must locally coincide with the inverse Stieltjes transform of $\tilde{m}(z)$.

Deduce that $\tilde{m}(z)$ must be of the form $\sqrt{z-b}$ near an edge and conclude.

Exercise 7 (Further results on $x(\tilde{m})$). *We aim in this exercise to justify some of the visual observations made on Figure 2.5.*

Show that, for $\tilde{m}_1 \neq \tilde{m}_2$ such that $x'(\tilde{m}_1), x'(\tilde{m}_2) > 0$, we cannot have $x(\tilde{m}_1) = x(\tilde{m}_2)$: that is, the increasing segments of $x(\tilde{m})$ never “overlap”.

Besides, show that, if $\tilde{m}_1 < \tilde{m}_2$ are both of the same sign, and $x'(\tilde{m}_1), x'(\tilde{m}_2) > 0$, then $x(\tilde{m}_1) < x(\tilde{m}_2)$: that is, the increasing segments of $x(\tilde{m})$ never “swap”.

To this end, we may prove the intermediary result

$$(\tilde{m}_1 - \tilde{m}_2) \left(1 - \int \frac{c\tilde{m}_1\tilde{m}_2 t^2 \nu(dt)}{(1+t\tilde{m}_1)(1+t\tilde{m}_2)} \right) = \tilde{m}_1\tilde{m}_2(x(\tilde{m}_1) - x(\tilde{m}_2))$$

and use Cauchy-Schwarz inequality to control the left-hand side parenthesis.

Finally show that, if ν has bounded support, then $x(\tilde{m}) \rightarrow 0$ as $\tilde{m} \rightarrow \pm\infty$.

As a final remark, note that the only important observation about Figure 2.5 which we have not shown here is the fact that the points \tilde{m} where $x'(\tilde{m}) = 0$ must exist. In fact, this is not always the case and heavily depends on the nature of the tails of the underlying measure ν . Justify in particular that, for some ν , there may be no asymptote on the edges of the domain of definition of $x(\cdot)$ (as opposed to what is seen in Figure 2.5).

2.9.3 On eigen-inference

Exercise 8 (Alternative estimates of $\frac{1}{p} \text{tr}(\frac{1}{n} \mathbf{X} \mathbf{X}^\top)^2$). Let $\mathbf{X} = \mathbf{C}^{\frac{1}{2}} \mathbf{Z}$ for $\mathbf{Z} \in \mathbb{R}^{p \times n}$ with independent standard Gaussian entries, and \mathbf{C} deterministic symmetric nonnegative definite, of bounded spectral norm, and limiting eigenvalue distribution ν .

By a direct calculus, determine the limit, as $n, p \rightarrow \infty$ and $p/n \rightarrow c > 0$ of the second order moment

$$M_2 = \frac{1}{p} \text{tr} \left(\frac{1}{n} \mathbf{X} \mathbf{X}^\top \right)^2$$

as a function of the moments of ν .

Retrieve the same result using the results of Exercise 1 along with the expression of the Stieltjes transform $m(z)$ of the limiting spectrum μ of $\frac{1}{n} \mathbf{X} \mathbf{X}^\top$. Hint: It may be useful here to first show that $m(z)$ is solution to

$$m(z) = \int \frac{\nu(dt)}{-z(1 + ctm(z)) + (1 - c)t}$$

with ν the limiting spectral measure of \mathbf{C} .

Exercise 9 (Location of the zeros of $\tilde{m}(z)$). Figure 2.7 and Remark 2.13 both show that the zeros η_1, \dots, η_n of $m_{\mathbf{X}}(z)$, the Stieltjes transform of a symmetric matrix $\mathbf{X} \in \mathbb{R}^{n \times n}$, are interlaced with the eigenvalues $\lambda_1, \dots, \lambda_n$ of \mathbf{X} .

In the sample covariance matrix case $\frac{1}{n} \mathbf{Z}^\top \mathbf{C} \mathbf{Z}$ with $\mathbf{Z} \in \mathbb{R}^{p \times n}$ having independent standard Gaussian entries and \mathbf{C} with limited spectral measure ν of bounded and connected support, this means that (up to zero eigenvalues) the roots η_i of $m_{\frac{1}{n} \mathbf{Z}^\top \mathbf{C} \mathbf{Z}}(z)$ are all found in the limiting support $\tilde{\mu}$ of the empirical spectral distribution, at the possible exception of the leftmost η_1 .

Using a variable change involving $\tilde{m}(z)$ on the formula

$$0 = \frac{1}{2\pi i} \oint_{\Gamma} \frac{1}{w} dw$$

for all Γ not enclosing zero, then the approximation $\tilde{m}(z) = m_{\frac{1}{n}\mathbf{Z}^\top \mathbf{C} \mathbf{Z}}(z) + o(1)$ and finally a residue calculus, show that no root of $m_{\frac{1}{n}\mathbf{Z}^\top \mathbf{C} \mathbf{Z}}(z)$ can be found at macroscopic distance from the limiting support of μ . Conclude.

2.9.4 Spiked models

ex:additive_spike_MP

Exercise 10 (Additive spiked model). Similar to Theorem 2.12, show the phase transition threshold for the additive model $\mathbf{Y} \equiv \frac{1}{n}\mathbf{X}\mathbf{X}^\top + \mathbf{P}$ for \mathbf{X} having i.i.d. entries of zero mean, unit variance and low rank $\mathbf{P} = \sum_{i=1}^k \ell_i \mathbf{u}_i \mathbf{u}_i^\top$, with $\ell_1 > \dots > \ell_k > 0$, is determined by the condition

$$\ell_i > \sqrt{c}(1 + \sqrt{c})$$

with $c = \lim p/n$ as $p, n \rightarrow \infty$. Under this condition, show that the (almost sure) limiting value of the corresponding isolated eigenvalue $\hat{\gamma}_i$ of \mathbf{Y} is given by

$$\hat{\gamma}_i \xrightarrow{a.s.} \gamma_i = 1 + \ell_i + \frac{c}{\ell_i - c}.$$

Further show that, letting $\hat{\mathbf{u}}_i$ be the eigenvector of \mathbf{Y} associated with $\hat{\gamma}_i$, we have the convergence

$$|\hat{\mathbf{u}}_i^\top \mathbf{u}_i|^2 \xrightarrow{a.s.} 1 - \frac{c}{(\ell_i - c)^2}.$$

ex:additive_spike_Wigner

Exercise 11 (Additive spiked model: the Wigner case). Let \mathbf{X} be symmetric with X_{ij} , $i \geq j$, i.i.d. zero mean and unit variance. As in Exercise 10, show that the “spiked” phase transition threshold for the model $\mathbf{Y} \equiv \frac{1}{\sqrt{n}}\mathbf{X} + \mathbf{P}$, where $\mathbf{P} = \sum_{i=1}^k \ell_i \mathbf{u}_i \mathbf{u}_i^\top$, with $\ell_1 > \dots > \ell_k > 0$, is determined by the condition

$$\ell_i > 1$$

and that, under this condition, the isolated eigenvalue $\hat{\gamma}_i$ of \mathbf{Y} associated with ℓ_i is given by

$$\hat{\gamma}_i \xrightarrow{a.s.} \gamma_i = \ell_i + \frac{1}{\ell_i}.$$

Show finally that, for $\hat{\mathbf{u}}_i$ the eigenvector of \mathbf{Y} associated with $\hat{\gamma}_i$, we have

$$|\hat{\mathbf{u}}_i^\top \mathbf{u}_i|^2 \xrightarrow{a.s.} 1 - \frac{1}{\ell_i^2}.$$

2.9.5 Deterministic equivalent

exo:proof-of-SCM_Haar

Exercise 12 (Proof of Theorem 2.16). Inspired by the proofs of Theorem 2.5, prove Theorem 2.16 using

1. the trace method adapted to Haar random matrices, Lemma 2.16; and

2. the Stein's lemma adapted to Haar random matrices, Lemma 2.17.

exo:higher-order-DE

Exercise 13 (Higher-order deterministic equivalent). *Theorem 2.3 provides an deterministic equivalent for the resolvent $\mathbf{Q} = (\frac{1}{n}\mathbf{XX}^\top - z\mathbf{I}_p)^{-1}$ for $\mathbf{X} \in \mathbb{R}^{p \times n}$ having i.i.d. zero mean and unit variance entries, which, according to Notation 1, provides access to the asymptotic behavior of $\mathbf{a}^\top \mathbf{Q} \mathbf{b}$. In many machine learning applications, however, the object of natural interest (e.g., mean squared error in regression analysis and variance analysis in a classification context) often involves the asymptotic behavior of $\mathbf{a}^\top \mathbf{Q} \mathbf{A} \mathbf{Q} \mathbf{b}$ which requires a deterministic equivalent for random matrices of the type $\mathbf{Q} \mathbf{A} \mathbf{Q}$, for arbitrary \mathbf{A} independent of \mathbf{Q} . In particular, for $\mathbf{Q} \leftrightarrow \bar{\mathbf{Q}}$ (such that $\|\mathbb{E}[\mathbf{Q}] - \bar{\mathbf{Q}}\| \rightarrow 0$), $\bar{\mathbf{Q}} \mathbf{A} \bar{\mathbf{Q}}$ is in general not a deterministic equivalent for $\mathbf{Q} \mathbf{A} \mathbf{Q}$, due to the fact that*

$$\mathbb{E}[\mathbf{Q} \mathbf{A} \mathbf{Q}] \not\simeq \mathbb{E}[\mathbf{Q}] \mathbf{A} \mathbb{E}[\mathbf{Q}].$$

Instead, prove that, in the setting of Theorem 2.3, one has

$$\mathbf{Q}(z) \mathbf{A} \mathbf{Q}(z) \leftrightarrow m(z)^2 \mathbf{A} + \frac{1}{n} \operatorname{tr} \mathbf{A} \cdot \frac{m'(z)m(z)^2}{(1+cm(z))^2} \mathbf{I}_p. \quad (2.42)$$

For sanity check, using the fact that $\partial \mathbf{Q}(z)/\partial z = \mathbf{Q}^2(z)$ and taking $\mathbf{A} = \mathbf{I}_p$ in the equation above, confirm that

$$\mathbf{Q}^2(z) \leftrightarrow m'(z)\mathbf{I}_p$$

for $m'(z) = \frac{m(z)^2}{1 - \frac{cm(z)^2}{(1+cm(z))^2}}$ obtained by differentiating the Marčenko–Pastur equation (2.9).

2.9.6 Concentration of measure

** Exercise from Cosme, to clean **

exo:concentration_convexe_produit_odot_Rp

Exercise 14 (Concentration of matrix quadratic forms). *Recalling the definitions and notations of Section 2.7, let $\mathbf{X} \in \mathbb{R}^{p \times n}$ be a random matrix satisfying*

$$\mathbf{X} \propto C e^{c^2}, \text{ and } \|\mathbb{E}[\mathbf{X}]\| \leq K$$

for some $K, C, c > 0$. Given $\mathbf{A} \in \mathbb{R}^{p \times p}$ deterministic, we wish to prove the linear concentration of $\mathbf{X}^\top \mathbf{A} \mathbf{X}$ in $(\mathbb{R}^{n \times n}, \|\cdot\|_F)$. To this end, we thus consider a deterministic matrix $\mathbf{B} \in \mathbb{R}^{n \times n}$ such that $\|\mathbf{B}\|_F \leq 1$ and study the behavior of $\operatorname{tr}(\mathbf{B} \mathbf{X}^\top \mathbf{A} \mathbf{X})$. First decompose

$$\mathbf{A} = \mathbf{P}_A \boldsymbol{\Lambda} \mathbf{Q}_A \text{ and } \mathbf{B} = \mathbf{P}_B \boldsymbol{\Gamma} \mathbf{Q}_B,$$

with $\mathbf{P}_A, \mathbf{Q}_A \in \mathbb{R}^{p \times p}$ and $P_B, Q_B \in \mathbb{R}^{n \times n}$ orthogonal matrices and $\boldsymbol{\Lambda} \in \mathbb{R}^{p \times p}$, $\boldsymbol{\Gamma} \in \mathbb{R}_+^{n \times n}$ diagonal matrices, and define $\tilde{\mathbf{X}} = \mathbf{P}_A \mathbf{X} \mathbf{Q}_B \in \mathbb{R}^{p \times n}$. In the next items, the constants $K', C', c' > 0$ are understood only depending on K, C, c and might change from one line to the other.

First show that there exist $K', C', c' > 0$ such that, for any $t > K' \log(np)$,

$$\mathbb{P}(\|\check{\mathbf{X}} - \mathbb{E}[\check{\mathbf{X}}]\|_\infty \geq t) \leq C'e^{-c't^2/\log(np)},$$

and deduce from Fubini's theorem and the bound on $\|\mathbb{E}[\check{\mathbf{X}}]\|$ that there exists a constant $K' > 0$ depending only on K, C, c such that:

$$\mathbb{E}[\|\check{\mathbf{X}}\|_\infty] \leq K' \sqrt{\log(pn)}.$$

This established, introduce the subset $\mathcal{A}_\theta = \{\mathbf{M} \in \mathbb{R}^{p \times n}, \|\mathbf{P}_A \mathbf{M} \mathbf{Q}_B\|_\infty \leq \theta\} \subset \mathbb{R}^{p \times n}$ and show that for all $\theta \geq K' \sqrt{\log(pn)}$, $\mathbb{P}(\mathbf{X} \in \mathcal{A}_\theta^c) \leq Ce^{-c\theta^2/4}$ and that the mapping $\mathbf{M} \mapsto \text{tr}(\mathbf{B}\mathbf{M}^\top \mathbf{A}\mathbf{M})$ is $\theta\|\mathbf{A}\|_F$ -Lipschitz on \mathcal{A}_θ .

Introducing m , a median of $\text{tr}(\mathbf{B}\mathbf{X}^\top \mathbf{A}\mathbf{X})$, denote now

$$\mathcal{C} = \{\mathbf{M} \in \mathbb{R}^{p \times n} \mid \text{tr}(\mathbf{B}\mathbf{M}^\top \mathbf{A}\mathbf{M}) \leq m\},$$

and for $\mathcal{B} \subset \mathbb{R}^{p \times n}$, $\mathcal{B} \neq \emptyset$, define the map $d(\cdot, \mathcal{B}) : z \mapsto \inf\{\|z - b\|, b \in \mathcal{B}\}$ and show that

$$\begin{aligned} & \mathbb{P}(|\text{tr}(\mathbf{B}\mathbf{X}^\top \mathbf{A}\mathbf{X}) - m| \geq t, \mathbf{X} \in \mathcal{A}_\theta) \\ & \leq \mathbb{P}\left(d(\mathbf{X}, \mathcal{C}) \geq \frac{t}{\theta\|\mathbf{A}\|_F}\right) + \mathbb{P}\left(d(\mathbf{X}, \mathcal{C}^c) \geq \frac{t}{\theta\|\mathbf{A}\|_F}\right). \end{aligned}$$

Cleverly choosing the parameter $\theta \geq K' \sqrt{\log(pn)}$, conclude by showing that

$$\mathbf{X}^\top \mathbf{A} \mathbf{X} \in \mathbb{E}[\mathbf{X}^\top \mathbf{A} \mathbf{X}] \pm C'e^{-c'.2/(\log(np)\|\mathbf{A}\|_F)} + C'e^{-c'./\|\mathbf{A}\|_F}.$$

2.9.7 Beyond matrices

**** J'attends l'avancement d'Henrique là dessus. Cet exo peut devenir un TP plus intéressant. ****

Exercise 15 (Towards Spiked Models in Random Tensors). Let $\mathcal{Y} \in \mathbb{R}^{n \times n \times n}$ be a three-way symmetric tensor, i.e., such that \mathcal{Y}_{ijk} is constant to exchanges of its indexes, defined by

$$\mathcal{Y} = \lambda \mathbf{x} \otimes \mathbf{x} \otimes \mathbf{x} + \frac{1}{\sqrt{n}} \mathcal{W}$$

where $\mathcal{W} \in \mathbb{R}^{n \times n \times n}$ has independent $\mathcal{N}(0, 1)$ entries up to symmetry, $\mathbf{x} \in \mathbb{R}^n$ is of unit norm, and $[\mathbf{a} \otimes \mathbf{b} \otimes \mathbf{c}]_{ijk} = a_i b_j c_k$.

A possible definition of the “eigenvalue-eigenvector” pair (ℓ, \mathbf{u}) with $\|\mathbf{u}\| = 1$ of the symmetric tensor \mathcal{Y} is given by the solutions to

$$\mathcal{Y} \cdot \mathbf{u} \cdot \mathbf{u} = \ell \mathbf{u}$$

where $\mathcal{A} \cdot \mathbf{a} \cdot \mathbf{b} = \sum_{ijk} \mathcal{A}_{ijk} a_i b_j \in \mathbb{R}^n$ is the contraction of tensor \mathcal{A} on the vectors \mathbf{a}, \mathbf{b} . The objective is to characterize the largest eigenvalue ℓ_{\max} as well as the associated alignment $|\mathbf{u}_{\max}^\top \mathbf{x}|$ between the dominant eigenvector and the spike \mathbf{x} .

Show first that the matrix $\mathbf{Y}_x = \mathcal{Y} \cdot \mathbf{x} = \sum_{i=1}^n \mathcal{Y}_{i,\cdot,\cdot} x_i$ is given by

$$\mathbf{Y}_x = \lambda \mathbf{x} \mathbf{x}^\top + \frac{1}{\sqrt{n}} \sum_{i=1}^n x_i \mathbf{W}_{i,\cdot,\cdot}$$

where $\mathbf{W}_{i,\cdot,\cdot} \in \mathbb{R}^{n \times n}$ is the i -th “layer” matrix of the tensor \mathcal{W} with $[\mathbf{W}_{i,\cdot,\cdot}]_{ab} = \mathcal{W}_{iab}$.

Using Pastur’s Stein approach, show that the limiting empirical spectral measure of \mathbf{Y}_x is the semi-circle distribution supported on $[-2, 2]$ (we may discard the rank-one matrix $\lambda \mathbf{x} \mathbf{x}^\top$ to retrieve this result). Then, using a spiked analysis, show that

- for all $\lambda > 0$, there must exist an isolated eigenvalue $\hat{\gamma}$ of \mathbf{Y}_x (thus no phase transition) asymptotically equal to (with high probability)

$$\hat{\gamma} \rightarrow \gamma = \sqrt{\lambda^2 + 4};$$

- the eigenvector $\hat{\mathbf{u}}$ associated with $\hat{\gamma}$ satisfies (with high probability)

$$|\hat{\mathbf{u}}^\top \mathbf{x}|^2 \rightarrow \frac{\lambda}{\sqrt{\lambda^2 + 4}}.$$

Conclude on a (asymptotic) bound for the quantity $\ell_{\max} |\mathbf{u}_{\max}^\top \mathbf{x}|$.

Chapter 3

Statistical Inference in Linear Models

chap:stats_inf

Sections 2.2 through 2.5 provided the basic material to perform fundamental signal and data processing tasks such as detection (hypothesis testing) and estimation (statistical inference) for sample covariance matrix models.

These sections can be summarized as follows: if no a priori information is known about the population covariance matrix $\mathbf{C} \in \mathbb{R}^{p \times p}$ (i.e., it is not known to be sparse, Toeplitz, etc.), the observation of i.i.d. (say zero mean) samples $\mathbf{X} = [\mathbf{x}_1, \dots, \mathbf{x}_n] \in \mathbb{R}^{p \times n}$ with covariance $\text{cov}(\mathbf{x}_i) = \mathbf{C}$ is not sufficient to estimate \mathbf{C} itself if p and n are of the same order of magnitude (essentially because the np degrees of freedom in \mathbf{X} are not enough to evaluate the $O(p^2)$ distinct elements of \mathbf{C}). As such, the standard methods for detection and estimation involving \mathbf{C} which conventionally substitute $\hat{\mathbf{C}} = \frac{1}{n}\mathbf{XX}^\top$ for \mathbf{C} are bound to fail when p is not too small compared to n .

Yet, \mathbf{C} itself may not be the object of central interest. One is often rather interested in a scalar functional of \mathbf{C} : the binary answer to a signal detection procedure, the probability of an hypothesis test, the class-label in a classification method, or more generally the estimation of a certain more-or-less involved functional of \mathbf{C} (its dominant eigenvalue, the distribution of its dominant eigenvector, etc.).

Section 2.3 showed that, while $\hat{\mathbf{C}} \not\rightarrow \mathbf{C}$ in the random matrix regime, there exist complex analytic relations between the resolvents $\mathbf{Q}_{\hat{\mathbf{C}}}(z)$ of $\hat{\mathbf{C}}$ and $\mathbf{Q}_{\mathbf{C}}(z)$ of \mathbf{C} . This relation allows one to connect a large class of functionals of \mathbf{C} (linear functionals of its eigenvalues, subspace projections of some of its eigenvectors) to those of $\hat{\mathbf{C}}$, allowing for random-matrix improved estimates of these functionals. However, these estimates can be quite involved and limited in practice by complex integration boundaries. In many cases of practical interest where information and noise can be decoupled in a *low rank* information and a *high rank* noise, spiked models previously discussed in Section 2.5 give access to much simplified versions of these inference methods.

In this chapter, examples of concrete problems involving covariance matrix-based estimators (and beyond) are discussed:

1. **Hypothesis testing in signal-plus-noise model:** assuming $\mathbf{x}_i = \mathbf{z}_i$ is pure noise or $\mathbf{x}_i = \boldsymbol{\mu} + \mathbf{z}_i$ contains an unknown signal and noise, we discuss in Section 3.1.1 the generalized likelihood ratio test (GLRT) aiming to detect the presence of a signal, using asymptotic results on the eigenvalues of the sample covariance model.
2. **Linear and quadratic discriminant analysis:** the objective of LDA and QDA discussed in Section 3.1.2 is to classify a test datum \mathbf{x} into one of the two Gaussian hypotheses $\mathcal{N}(\boldsymbol{\mu}_0, \mathbf{C}_0)$ or $\mathcal{N}(\boldsymbol{\mu}_1, \mathbf{C}_1)$, based on some (linear) discrimination rule $T(\mathbf{x})$ obtained from the available training set. Random matrix results will be used here to analyze the (surprisingly far from obvious) performance of LDA/QDA.
3. **Estimation with subspace methods:** given noisy signals parameterized by some specific “direction of arrival” angles $\theta_1, \dots, \theta_k$, the so-called subspace methods, in particular the MUSIC algorithm, can be used to recover this “angular” information from the signal covariance. In Section 3.1.3, we discuss the random matrix improved G-MUSIC algorithm, and discuss its significant performance gain in the large dimensional signal scenario;
4. **Distance estimation:** as a concrete example of statistical inference procedures commonly used in machine learning, we will estimate the distance between two centered (population) data distributions (or covariance matrices) based on few samples from each distribution in Section 3.2. Here random matrix theory provides original estimators which are consistent in the regime of simultaneously large sample size and data dimension.
5. **Robust covariance estimation:** in presence of outliers, sample covariance matrices are known to be non-robust estimators of population covariance matrices, already in the $n \gg p$ case: robust estimators of scatter is an efficient alternative in these situations; these objects are however hard to theoretically grasp in the classical $n \gg p$ setting, we present here a random matrix understanding for these estimates in Section 3.3.

3.1 Detection and estimation in information-plus-noise models

3.1.1 GLRT asymptotics

sec:GLRT

The most immediate and telling use of random matrix theory, and particularly of spiked models, in practical statistics deals with the decision of the presence of some “information” buried in white noise.

Denoting $\mathbf{X} = [\mathbf{x}_1, \dots, \mathbf{x}_n] \in \mathbb{R}^{p \times n}$ a matrix with i.i.d. columns \mathbf{x}_i , the decision problem is formulated as the binary hypothesis test:

$$\mathbf{X} = \begin{cases} \sigma \mathbf{Z}, & \mathcal{H}_0 \\ \mathbf{a} \mathbf{s}^\top + \sigma \mathbf{Z}, & \mathcal{H}_1 \end{cases}$$

where $\mathbf{Z} = [\mathbf{z}_1, \dots, \mathbf{z}_n]$ with $\mathbf{z}_i \sim \mathcal{N}(\mathbf{0}, \mathbf{I}_p)$, $\mathbf{a} \in \mathbb{R}^p$ deterministic with unit norm $\|\mathbf{a}\| = 1$, $\mathbf{s} = [s_1, \dots, s_n]^\top \in \mathbb{R}^n$ with s_i i.i.d. random scalars, and $\sigma > 0$. Let also also denote $c = p/n$ (and demand as usual that $0 < \liminf c \leq \limsup c < \infty$).

This model describes the reception of either pure noise data $\sigma \mathbf{z}_i$ with zero mean and covariance $\sigma^2 \mathbf{I}_p$ or a deterministic information \mathbf{a} possibly modulated by a scalar (random) signal s_i (which could simply be ± 1) added to the noise. Obviously, if the parameters \mathbf{a} , σ as well as the statistics of s_i are known, a mere Neyman-Pearson test allows one to discriminate between \mathcal{H}_0 and \mathcal{H}_1 with optimal detection probability, for all finite n, p ; precisely, one will decide on the genuine hypothesis according to the ratio of posterior probabilities

$$\frac{\mathbb{P}(\mathbf{X} | \mathcal{H}_1)}{\mathbb{P}(\mathbf{X} | \mathcal{H}_0)} \stackrel{\mathcal{H}_1}{\gtrless} \alpha$$

for some $\alpha > 0$ controlling the desired Type I and Type II error rates.

However, in practice, unless the existence of a set of previous pure-noise acquisitions is assumed, it is quite unlikely that σ is already known. Similarly, the ultimate objective being to estimate the data structure \mathbf{a} under \mathcal{H}_1 , \mathbf{a} is often assumed completely unknown (it may likely be known though to belong to a subset of \mathbb{R}^p in which case more elaborate procedures than proposed here can be carried on). Nonetheless, assuming the data of zero mean in either scenario, we may impose that $\mathbb{E}[s_i] = 0$ and $\mathbb{E}[s_i^2] = 1$. If such is the case, instead of the maximum likelihood test, one may resort to a *generalized likelihood ratio test* (GLRT) defined as

$$\frac{\sup_{\sigma, \mathbf{a}} \mathbb{P}(\mathbf{X} | \mathcal{H}_1)}{\sup_{\sigma, \mathbf{a}} \mathbb{P}(\mathbf{X} | \mathcal{H}_0)} \stackrel{\mathcal{H}_1}{\gtrless} \alpha.$$

Under both a Gaussian noise and signal s_i assumption, the GLRT has an explicit expression which is precisely a monotonous increasing function of $\|\mathbf{X}\mathbf{X}^\top\|/\text{tr}(\mathbf{X}\mathbf{X}^\top)$. That is, the test is equivalent to

$$T_p \equiv \frac{\left\| \frac{1}{n} \mathbf{X} \mathbf{X}^\top \right\|}{\frac{1}{p} \text{tr} \left(\frac{1}{n} \mathbf{X} \mathbf{X}^\top \right)} \stackrel{\mathcal{H}_1}{\gtrless} f(\alpha)$$

for some known monotonously increasing function f , where we introduced the scales $1/p$ and $1/n$ to maintain both numerator and denominator of order $O(1)$ as $n, p \rightarrow \infty$.

Obviously, since the ratio has limit $(1 + \sqrt{c})^2$ (over 1) under the \mathcal{H}_0 asymptotics, $f(\alpha)$ must be of the form $f(\alpha) = (1 + \sqrt{c})^2 + g(\alpha)$ for some $g(\alpha) > 0$. Now, since $\frac{1}{p} \text{tr} \left(\frac{1}{n} \mathbf{X} \mathbf{X}^\top \right)$ fluctuates at the “fast” speed $O(n^{-1})$, while $\left\| \frac{1}{n} \mathbf{X} \mathbf{X}^\top \right\|$

fluctuates at the slower speed $O(n^{-2/3})$ (as per Theorem 2.14), the global fluctuation is thus dominated by the numerator at a rate of order $O(n^{-2/3})$, i.e., under \mathcal{H}_0 we have

$$T_p \xrightarrow{\mathcal{H}_0} (1 + \sqrt{c})^2 + O(n^{-2/3}).$$

Since the denominator is essentially converging while the numerator still fluctuates, despite the dependence between them, it indeed turns out that

$$T_p \xrightarrow{\mathcal{H}_0} (1 + \sqrt{c})^2 + (1 + \sqrt{c})^{\frac{4}{3}} c^{-\frac{1}{6}} n^{-\frac{2}{3}} \text{TW}_1 + o(n^{-2/3}).$$

As a consequence, in order to set a maximum false alarm rate (or false positive, or Type I error) of $r > 0$, one must choose a threshold $f(\alpha)$ for T_p such that

$$\mathbb{P}(T_p \leq f(\alpha)) = r$$

that is, such that

$$\mu_{\text{TW}_1}((-\infty, A_p]) = r, \quad A_p = (f(\alpha) - (1 + \sqrt{c})^2)(1 + \sqrt{c})^{-\frac{4}{3}} c^{\frac{1}{6}} n^{\frac{2}{3}} \stackrel{\text{eq:GLRT-Ap}}{=} (3.1)$$

with $\mu_{\text{TW}_1}(dt)$ the Tracy-Widom measure.

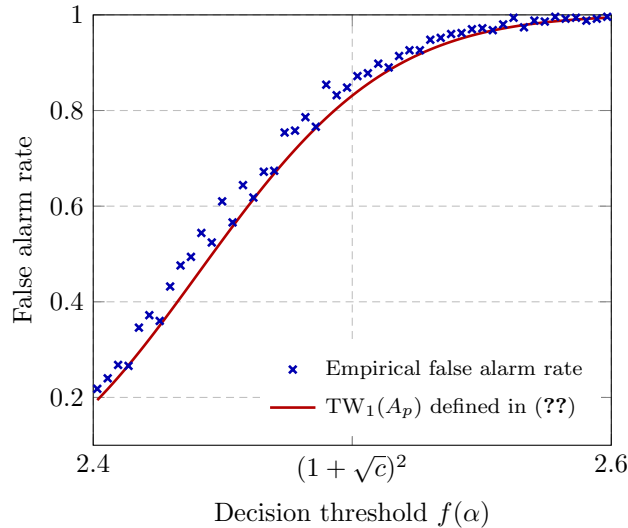


Figure 3.1: Comparison between empirical false alarm rates and $\text{TW}_1(A_p)$ for A_p defined in (3.1), as a function of the threshold $f(\alpha) \in [(1 + \sqrt{c})^2 - 5n^{-2/3}, (1 + \sqrt{c})^2 + 5n^{-2/3}]$, for $p = 256$, $n = 1024$ and $\sigma = 1$. Results obtained from 100 runs. [Link to code].

`fig:GLRT`

Figure 3.1 depicts this the empirical false alarm rate obtained from different choices of thresholds $f(\alpha) = (1 + \sqrt{c})^2 + O(n^{-2/3})$ to the asymptotic estimate

$\text{TW}_1(A_p)$. For a given maximum false alarm rate r , one can thus numerically determine the threshold $f(\alpha)$ that ensures that $\text{TW}_1(A_p(f(\alpha))) = r$.

Assume now that, under the \mathcal{H}_1 hypothesis, $s \sim \mathcal{N}(\mathbf{0}, \mathbf{I}_n)$. We may then write

$$\mathbf{X} = \mathbf{a}\mathbf{s}^\top + \sigma\mathbf{Z} = [\mathbf{a} \quad \sigma\mathbf{I}_p] \tilde{\mathbf{Z}}, \quad \tilde{\mathbf{Z}} = \begin{bmatrix} \mathbf{s}^\top \\ \mathbf{Z} \end{bmatrix}$$

with $\tilde{\mathbf{Z}} \in \mathbb{R}^{(p+1) \times n}$ having i.i.d. $\mathcal{N}(0, 1)$ entries. Hence $\sigma^{-1}\mathbf{X}$ has independent columns with zero mean and covariance

$$\mathbf{C} \equiv \mathbb{E} \left[\sigma^{-2} \frac{1}{n} \mathbf{X} \mathbf{X}^\top \right] = \mathbf{I}_p + \sigma^{-2} \mathbf{a} \mathbf{a}^\top.$$

This is a spiked model with population eigenvalues $\sigma^{-2} + 1$ with unit multiplicity and 1 with multiplicity $p-1$. We thus know from Theorem 2.12 that T_p converges to a quantity strictly greater than $(1 + \sqrt{c})^2$ if and only if the “signal-to-noise ratio” σ^{-2} satisfies $\sigma^{-2} > \sqrt{c}$.

Assuming $\sigma = \sigma_p$ depends on p, n , we thus have that, for the signal detection to be asymptotically non-trivial, σ_p^{-2} must be of the form $\sqrt{c} + O(n^{-2/3})$, in which case $T_p = (1 + \sqrt{c})^2 + O(n^{-2/3})$. These considerations are given a detailed account in [Bianchi et al., 2011].

3.1.2 Linear and Quadratic Discriminant Analysis

sec:LDA-QDA

The application of the random matrix framework to linear (LDA) and quadratic (QDA) discriminant analyses is a very telling example of the counter-intuitive behavior of large dimensional statistics.

Specifically, LDA and QDA aim at selecting one out of two Gaussian model hypotheses $\mathcal{N}(\boldsymbol{\mu}_0, \mathbf{C}_0)$ (hypothesis \mathcal{H}_0) versus $\mathcal{N}(\boldsymbol{\mu}_1, \mathbf{C}_1)$ (hypothesis \mathcal{H}_1) for an observed vector $\mathbf{x} \in \mathbb{R}^p$.

The means and covariances under \mathcal{H}_0 and \mathcal{H}_1 are however unknown, and are instead directly estimated from two sets of training data $\mathbf{x}_1^{(\ell)}, \dots, \mathbf{x}_{n_\ell}^{(\ell)} \sim \mathcal{N}(\boldsymbol{\mu}_\ell, \mathbf{C}_\ell)$ with $\ell \in \{0, 1\}$, as per the standard empirical estimators

$$\begin{aligned} \hat{\boldsymbol{\mu}}_\ell &\equiv \frac{1}{n_\ell} \sum_{i=1}^{n_\ell} \mathbf{x}_i^{(\ell)} \\ \hat{\mathbf{C}}_\ell &\equiv \frac{1}{n_\ell - 1} \sum_{i=1}^{n_\ell} (\mathbf{x}_i^{(\ell)} - \hat{\boldsymbol{\mu}}_\ell)(\mathbf{x}_i^{(\ell)} - \hat{\boldsymbol{\mu}}_\ell)^\top. \end{aligned}$$

The test decision the unknown \mathbf{x} is then carried out using a standard Neyman–Pearson likelihood-ratio procedure under the assumption that $\boldsymbol{\mu}_\ell$ and \mathbf{C}_ℓ are correctly estimated by $\hat{\boldsymbol{\mu}}_\ell$ and $\hat{\mathbf{C}}_\ell$. In the context of LDA, it is assumed that $\mathbf{C}_0 = \mathbf{C}_1$ (which may be an invalid assumption), in which case the discrimination is based on the test:

$$T_{\text{LDA}}(\mathbf{x}) \equiv (\mathbf{x} - \hat{\boldsymbol{\mu}})^\top \hat{\mathbf{C}}^{-1} (\hat{\boldsymbol{\mu}}_0 - \hat{\boldsymbol{\mu}}_1) \stackrel{\mathcal{H}_0}{\geqslant} 0$$

where $\hat{\boldsymbol{\mu}} = \frac{1}{2}(\hat{\boldsymbol{\mu}}_0 + \hat{\boldsymbol{\mu}}_1)$, $\hat{\mathbf{C}} = \frac{n_0-1}{n-2}\hat{\mathbf{C}}_0 + \frac{n_1-1}{n-2}\hat{\mathbf{C}}_1$, and we implicitly assumed that \mathcal{H}_0 and \mathcal{H}_1 are equally probable. As for QDA, it instead fully accounts for the possible difference between \mathbf{C}_0 and \mathbf{C}_1 , and the corresponding test is

$$\begin{aligned} T_{\text{QDA}}(\mathbf{x}) &\equiv -\frac{1}{2}(\mathbf{x} - \hat{\boldsymbol{\mu}}_0)^\top \hat{\mathbf{C}}_0^{-1}(\mathbf{x} - \hat{\boldsymbol{\mu}}_0) + \frac{1}{2}(\mathbf{x} - \hat{\boldsymbol{\mu}}_1)^\top \hat{\mathbf{C}}_1^{-1}(\mathbf{x} - \hat{\boldsymbol{\mu}}_1) \\ &+ \frac{1}{2} \log \frac{|\hat{\mathbf{C}}_0|}{|\hat{\mathbf{C}}_1|} \stackrel{\mathcal{H}_0}{\gtrless} 0. \end{aligned}$$

Of course, due to the involved inverses, these estimators are only defined (only surely) for $n_0, n_1 \geq p$. If this condition is not met, the estimates of $\hat{\mathbf{C}}_\ell$ are generally regularized as $\hat{\mathbf{C}}_\ell^{(\gamma)} \equiv \hat{\mathbf{C}}_\ell + \gamma \mathbf{I}_p$ for some $\gamma > 0$. As a matter of fact, even when $n_0, n_1 \geq p$, the conditioning of the empirical inverses significantly degrades the performances and imposes this regularization in practice.

The objective of this section is to analyze the impact of a large dimensional assumption on n_0, n_1, p on the performances of (regularized) LDA and QDA.

In a nutshell, and quite surprisingly, we will observe that LDA almost systematically outperforms QDA, even when $\mathbf{C}_0 \neq \mathbf{C}_1$: specifically, the minimal regime for $\|\boldsymbol{\mu}_0 - \boldsymbol{\mu}_1\|$, when seen as a function of p , under which hypotheses \mathcal{H}_0 and \mathcal{H}_1 can be discriminated is $O(1)$ for LDA but only $O(\sqrt{p})$ for QDA. That is, quite paradoxically, in possibly wrongly assuming that $\mathbf{C}_0 = \mathbf{C}_1$, LDA is capable to discriminate \mathcal{H}_0 from \mathcal{H}_1 when $\|\boldsymbol{\mu}_0 - \boldsymbol{\mu}_1\| = O(1)$, where QDA must fail.

This remark is all the more counter-intuitive that we will see later in Section 4.5.3 that a mere least-squares regression method, which does not even need to know that the data are Gaussian distributed, will in the present setting outperform QDA. This fundamental statement must be understood as follows: the performance gain induced by a perfect modelling of the data statistics (Neyman-Pearson test over two Gaussian hypotheses) is insufficient to outweigh the huge loss incurred by the inappropriate estimation of \mathbf{C}_ℓ by $\hat{\mathbf{C}}_\ell$, entailing that more ill-matched procedures may perform better.

In the following two sections, we first provide a full account of the large dimensional behavior and performance of regularized LDA. We will then only justify the main reasons behind the comparatively poor performances of QDA, or at least its inability to perform at the same optimal $\|\boldsymbol{\mu}_0 - \boldsymbol{\mu}_1\| = O(1)$ rate. A detailed analysis of regularized QDA is provided in [Elkhalil et al., 2020a].

3.1.2.1 Linear discriminant analysis

The performance of LDA is provided by the statistics $\mathbb{P}(T_{\text{LDA}}(\mathbf{x}) > 0 \mid \mathbf{x} \sim \mathcal{H}_\ell)$ for $\ell \in \{0, 1\}$.

In the large n_0, n_1, p regime where $n_\ell/n \rightarrow c_\ell \in (0, 1)$ and $p/n \rightarrow c \in (0, \infty)$, in order for this quantity to remain non-trivial (i.e., neither converging to 0, 1 or 1/2), some growth rate constraints need be set on the distance $\|\boldsymbol{\mu}_0 - \boldsymbol{\mu}_1\|$. Assuming $\|\mathbf{C}_\ell\| = O(1)$ (which is a natural assumption), it appears in the calculus that this non-trivial regime corresponds to $\|\boldsymbol{\mu}_0 - \boldsymbol{\mu}_1\| = O(1)$. Recalling

Equation 1.6 in Section 1.1.3, this regime happens to be the minimal possible growth rate for detection in the oracle case where μ_0 and μ_1 were perfectly known; as such, in terms of optimally allowed growth rates for $\|\mu_0 - \mu_1\|$, LDA does not loose in performance.

Under this assumption, one then needs to evaluate the statistics of $T_{\text{LDA}}(\mathbf{x})$. This study is performed in [Elkhalil et al., 2020a] with a (slightly different form of) regularization γ , where

$$T_{\text{LDA}}^{(\gamma)}(\mathbf{x}) = (\mathbf{x} - \hat{\mu})^\top [\hat{\mathbf{C}}^{(\gamma)}]^{-1} (\hat{\mu}_0 - \hat{\mu}_1)$$

is shown to satisfy a central limit theorem in the large n_0, n_1, p limit. To obtain the limiting behavior of $T_{\text{LDA}}^{(\gamma)}$, let us assume that $\mathbf{x} = \mu_\ell + \mathbf{C}_\ell^{\frac{1}{2}} \mathbf{z} \sim \mathcal{H}_\ell$ and observe that we may write the complete training data set as $\mathbf{X} = [\mathbf{C}_0^{\frac{1}{2}} \mathbf{Z}_0 + \mu_0 \mathbf{1}_{n_0}^\top, \mathbf{C}_1^{\frac{1}{2}} \mathbf{Z}_1 + \mu_1 \mathbf{1}_{n_1}^\top]$ and its hypothesis-wise empirically centered version as $\mathbf{X}^\circ = [\mathbf{C}_0^{\frac{1}{2}} \mathbf{Z}_0, \mathbf{C}_1^{\frac{1}{2}} \mathbf{Z}_1] - [\frac{1}{n_0} \mathbf{C}_0^{\frac{1}{2}} \mathbf{Z}_0 \mathbf{1}_{n_0} \mathbf{1}_{n_0}^\top, \frac{1}{n_1} \mathbf{C}_1^{\frac{1}{2}} \mathbf{Z}_1 \mathbf{1}_{n_1} \mathbf{1}_{n_1}^\top]$, with $\mathbf{Z}_0, \mathbf{Z}_1$ having i.i.d. $\mathcal{N}(0, 1)$ entries, so that

$$T_{\text{LDA}}^{(\gamma)}(\mathbf{x}) = \left(\mathbf{C}_\ell^{\frac{1}{2}} \mathbf{z} + \frac{1}{2} \mathbf{U} \begin{bmatrix} (-1)^\ell \\ (-1)^{\ell+1} \\ -1 \\ -1 \end{bmatrix} \right)^\top \mathbf{Q} \mathbf{U} \begin{bmatrix} 1 \\ -1 \\ 1 \\ -1 \end{bmatrix}$$

where

$$\begin{aligned} \mathbf{Q}^{-1} &= \frac{1}{n-2} \mathbf{C}_0^{\frac{1}{2}} \mathbf{Z}_0 \mathbf{Z}_0^\top \mathbf{C}_0^{\frac{1}{2}} + \frac{1}{n-2} \mathbf{C}_1^{\frac{1}{2}} \mathbf{Z}_1 \mathbf{Z}_1^\top \mathbf{C}_1^{\frac{1}{2}} \\ &\quad - \mathbf{U} \begin{bmatrix} 0 & 0 \\ 0 & 1 \end{bmatrix} \otimes \begin{bmatrix} \frac{n_0}{n-2} & 0 \\ 0 & \frac{n_1}{n-2} \end{bmatrix} \mathbf{U}^\top + \gamma \mathbf{I}_p \\ \mathbf{U} &= \begin{bmatrix} \mu_0 & \mu_1 & \frac{1}{n_0} \mathbf{C}_0^{\frac{1}{2}} \mathbf{Z}_0 \mathbf{1}_{n_0} & \frac{1}{n_1} \mathbf{C}_1^{\frac{1}{2}} \mathbf{Z}_1 \mathbf{1}_{n_1} \end{bmatrix} \end{aligned}$$

where ‘ \otimes ’ is the Kronecker product.

The matrix \mathbf{Q}^{-1} takes the form of a “spiked” random matrix model, and we may therefore use Woodbury’s identity to isolate the low rank from the large rank parts in \mathbf{Q} as

$$\begin{aligned} \mathbf{Q} &= \mathbf{Q}^\circ + \mathbf{Q}^\circ \mathbf{U} \begin{bmatrix} 0 & 0 \\ 0 & 1 \end{bmatrix} \otimes \begin{bmatrix} \frac{n_0}{n-2} & 0 \\ 0 & \frac{n_1}{n-2} \end{bmatrix} \\ &\quad \times \left(\mathbf{I}_4 - \mathbf{U}^\top \mathbf{Q}^\circ \mathbf{U} \begin{bmatrix} 0 & 0 \\ 0 & 1 \end{bmatrix} \otimes \begin{bmatrix} \frac{n_0}{n-2} & 0 \\ 0 & \frac{n_1}{n-2} \end{bmatrix} \right)^{-1} \mathbf{U}^\top \mathbf{Q}^\circ \end{aligned}$$

in which $\mathbf{Q}^\circ = \mathbf{Q}^\circ(-\gamma) = (\frac{1}{n-2} \mathbf{C}_0^{\frac{1}{2}} \mathbf{Z}_0 \mathbf{Z}_0^\top \mathbf{C}_0^{\frac{1}{2}} + \frac{1}{n-2} \mathbf{C}_1^{\frac{1}{2}} \mathbf{Z}_1 \mathbf{Z}_1^\top \mathbf{C}_1^{\frac{1}{2}} + \gamma \mathbf{I}_p)^{-1}$. We may then invoke Theorem 2.7 for which we have in particular that

$$\begin{aligned} \mathbf{Q}^\circ(z) \leftrightarrow \bar{\mathbf{Q}}^\circ(z) &\equiv -\frac{1}{z} \left(\mathbf{I}_p + \sum_{\ell=0}^1 c_\ell \tilde{g}_\ell(z) \mathbf{C}_\ell \right)^{-1} \\ \tilde{\mathbf{Q}}^\circ(z) \leftrightarrow \bar{\tilde{\mathbf{Q}}}^\circ(z) &\equiv \text{diag}(\{\tilde{g}_\ell(z) \mathbf{1}_{n_\ell}\}_{\ell=0}^1) \end{aligned}$$

where $(g_\ell(z), \tilde{g}_\ell(z))_{\ell=0}^1$ are solutions to

$$g_\ell(z) = \frac{1}{n} \operatorname{tr} \mathbf{C}_\ell \bar{\mathbf{Q}}^\circ(z), \quad \tilde{g}_\ell(z) = -\frac{1}{z} \frac{1}{1 + g_\ell(z)}.$$

Developing $T_{\text{LDA}}^{(\gamma)}$, multiple instances of the form $\mathbf{U}^\top \mathbf{Q}^\circ \mathbf{U}$ appear, which can be expressed in the large n_0, n_1, p limit as

$$\mathbf{U}^\top \mathbf{Q}^\circ \mathbf{U} = \begin{bmatrix} \mu_0^\top \mathbf{Q}^\circ \mu_0 & \mu_0^\top \mathbf{Q}^\circ \mu_1 & 0 & 0 \\ \mu_1^\top \mathbf{Q}^\circ \mu_0 & \mu_1^\top \mathbf{Q}^\circ \mu_1 & 0 & 0 \\ 0 & 0 & \frac{1-\gamma\tilde{g}_0(-\gamma)}{c_0} & 0 \\ 0 & 0 & 0 & \frac{1-\gamma\tilde{g}_1(-\gamma)}{c_1} \end{bmatrix} + o(1).$$

Plugging this result into the expression of $T_{\text{LDA}}^{(\gamma)}(\mathbf{x})$, we find that in the large n_0, n_1, p limit,

$$\begin{aligned} T_{\text{LDA}}^{(\gamma)}(\mathbf{x}) &= \frac{(-1)^\ell}{2} (\mu_0 - \mu_1)^\top \bar{\mathbf{Q}}^\circ (\mu_0 - \mu_1) - \frac{1}{2} g_0(-\gamma) + \frac{1}{2} g_1(-\gamma) \\ &\quad + \mathbf{z}^\top \mathbf{C}_\ell^{\frac{1}{2}} \mathbf{Q}^\circ \mathbf{U} \begin{bmatrix} 1 \\ -1 \\ \frac{1}{\gamma\tilde{g}_0(-\gamma)} \\ -\frac{1}{\gamma\tilde{g}_1(-\gamma)} \end{bmatrix} + o(1) \end{aligned}$$

where we used in particular the fact that $\frac{1-\gamma\tilde{g}_0(-\gamma)}{\gamma\tilde{g}_0(-\gamma)} = g_0(-\gamma)$.

rem:LDA-threshold

Remark 3.1 (Optimal decision threshold). Since $\mathbf{z} \sim \mathcal{N}(\mathbf{0}, \mathbf{I}_p)$, it is clear that $\mathbb{E}[T_{\text{LDA}}^{(\gamma)}(\mathbf{x})]$ is dominated by the quantity $\pm(\mu_0 - \mu_1)^\top \bar{\mathbf{Q}}^\circ (\mu_0 - \mu_1)$ which is positive when $\ell = 0$ and negative when $\ell = 1$, as expected. Yet, the term $\frac{1}{2}(g_1(-\gamma) - g_0(-\gamma))$ intervenes as a bias. If $\mathbf{C}_0 = \mathbf{C}_1$, then $g_0 = g_1$ and this bias disappears; however, for $\mathbf{C}_0, \mathbf{C}_1$ distinct, this bias remains and must be accounted for in the decision threshold which, therefore, should not be zero.

In passing, note that the first three terms in the expansion of $T_{\text{LDA}}^{(\gamma)}(\mathbf{x})$ are of order $O(1)$ with respect to p , where the fourth term is Gaussian conditionally to \mathbf{X} , with variance also of order $O(1)$ (see below for detail). This thus justifies the need for $\|\mu_0 - \mu_1\|$ to be of order $O(1)$ (if instead $\|\mu_0 - \mu_1\| = O(p^t)$ for $t > 0$, the first term dominates and $T_{\text{LDA}}^{(\gamma)}(\mathbf{x})$ becomes deterministic: the decision is trivial; while if $t < 0$ the first term vanishes when compared to the other three and the decision is asymptotically equivalent to random guess).

To estimate now the variance of $T_{\text{LDA}}^{(\gamma)}(\mathbf{x})$, one now needs to evaluate the second order moment of the term involving z , that is

$$\operatorname{Var}(T_{\text{LDA}}^{(\gamma)}(\mathbf{x})) = \begin{bmatrix} 1 \\ -1 \\ \frac{1}{\gamma\tilde{g}_0(-\gamma)} \\ \frac{1}{\gamma\tilde{g}_1(-\gamma)} \end{bmatrix}^\top \mathbf{U}^\top \mathbf{Q}^\circ \mathbf{C}_\ell \mathbf{Q}^\circ \mathbf{U} \begin{bmatrix} 1 \\ -1 \\ \frac{1}{\gamma\tilde{g}_0(-\gamma)} \\ \frac{1}{\gamma\tilde{g}_1(-\gamma)} \end{bmatrix} + o(1).$$

To proceed, the deterministic equivalent for \mathbf{Q}° is not sufficient and we must resort to a deterministic equivalent for $\mathbf{Q}^\circ \mathbf{C}_\ell \mathbf{Q}^\circ$ (similar to Exercise 13).

This result was derived in [Benaych-Georges and Couillet, 2016] and states

$$\mathbf{Q}^\circ \mathbf{C}_\ell \mathbf{Q}^\circ \leftrightarrow \overline{\mathbf{Q}^\circ \mathbf{C}_\ell \mathbf{Q}^\circ} \equiv \bar{\mathbf{Q}}^\circ \mathbf{C}_\ell \bar{\mathbf{Q}}^\circ + \bar{\mathbf{Q}}^\circ (R_{0\ell} \mathbf{C}_0 + R_{1\ell} \mathbf{C}_1) \bar{\mathbf{Q}}^\circ$$

with $R_{ij} = \frac{c_i}{c_j} [(\mathbf{I}_2 - \mathbf{S})^{-1} \mathbf{S}]_{i+1,j+1}$, $[\mathbf{S}]_{i+1,j+1} = c_j \gamma^2 \tilde{g}_i(-\gamma)^2 \frac{1}{n} \operatorname{tr} \mathbf{C}_i \bar{\mathbf{Q}}^\circ \mathbf{C}_j \bar{\mathbf{Q}}^\circ$.

This result gives a direct access to a deterministic approximation for the upper 2×2 matrix of $\mathbf{U}^\top \mathbf{Q}^\circ \mathbf{C}_\ell \mathbf{Q}^\circ \mathbf{U}$. The off-diagonal 2×2 blocks vanish. As for the bottom-right 2×2 matrix, it involves the inner products

$$\frac{1}{n_\ell^2} \mathbf{1}_{n_\ell}^\top \mathbf{Z}_\ell^\top \mathbf{C}_\ell^{\frac{1}{2}} \mathbf{Q}^\circ \mathbf{C}_\ell \mathbf{Q}^\circ \mathbf{C}_{\ell'}^{\frac{1}{2}} \mathbf{Z}_{\ell'} \mathbf{1}_{n_{\ell'}}.$$

By asymmetry, this is non-vanishing only for $\ell = \ell'$ but \mathbf{Z}_ℓ and \mathbf{Q}° are not independent. To deal with this case, we may write,

$$\mathbf{C}_\ell^{\frac{1}{2}} \mathbf{Z}_\ell \mathbf{Z}_\ell^\top \mathbf{C}_\ell^{\frac{1}{2}} = \mathbf{C}_\ell^{\frac{1}{2}} \mathbf{Z}_\ell (\mathbf{I}_{n_\ell} - \frac{1}{n_\ell} \mathbf{1}_{n_\ell} \mathbf{1}_{n_\ell}^\top) \mathbf{Z}_\ell \mathbf{C}_\ell^{\frac{1}{2}} + \frac{1}{n_\ell^2} \mathbf{C}_\ell^{\frac{1}{2}} \mathbf{Z}_\ell \mathbf{1}_{n_\ell} \mathbf{1}_{n_\ell}^\top \mathbf{Z}_\ell^\top \mathbf{C}_\ell^{\frac{1}{2}}$$

in which the columns of $\mathbf{Z}_\ell (\mathbf{I}_{n_\ell} - \frac{1}{n_\ell} \mathbf{1}_{n_\ell} \mathbf{1}_{n_\ell}^\top)$ and $\mathbf{Z}_\ell \frac{1}{n_\ell} \mathbf{1}_{n_\ell}$ are orthogonal and thus independent Gaussian vectors. As such, with a rank-1 perturbation argument,

$$\mathbf{1}_{n_\ell}^\top \mathbf{Z}_\ell^\top \mathbf{C}_\ell^{\frac{1}{2}} \mathbf{Q}^\circ = \frac{\mathbf{1}_{n_\ell}^\top \mathbf{Z}_\ell^\top \mathbf{C}_\ell^{\frac{1}{2}} \mathbf{Q}_{-\ell}^\circ}{1 + \frac{1}{n_\ell(n-2)} \mathbf{1}_{n_\ell}^\top \mathbf{Z}_\ell^\top \mathbf{C}_\ell^{\frac{1}{2}} \mathbf{Q}_{-\ell}^\circ \mathbf{C}_\ell^{\frac{1}{2}} \mathbf{Z}_\ell \mathbf{1}_{n_\ell}}$$

with $\mathbf{Q}_{-\ell}^\circ$ the matrix \mathbf{Q}° with contribution from $\frac{1}{n_\ell^2} \mathbf{C}_\ell^{\frac{1}{2}} \mathbf{Z}_\ell \mathbf{1}_{n_\ell} \mathbf{1}_{n_\ell}^\top \mathbf{Z}_\ell^\top \mathbf{C}_\ell^{\frac{1}{2}}$ discarded. By the induced independence, we may then apply a trace lemma, Lemma 2.11, to obtain

$$\begin{aligned} \frac{1}{n_\ell^2} \mathbf{1}_{n_\ell}^\top \mathbf{Z}_\ell^\top \mathbf{C}_\ell^{\frac{1}{2}} \mathbf{Q}^\circ \mathbf{C}_\ell \mathbf{Q}^\circ \mathbf{C}_{\ell'}^{\frac{1}{2}} \mathbf{Z}_{\ell'} \mathbf{1}_{n_{\ell'}} &= \delta_{\ell\ell'} \frac{\frac{1}{n_\ell} \operatorname{tr} (\mathbf{C}_\ell \mathbf{Q}^\circ)^2}{(1 + \frac{1}{n} \operatorname{tr} \mathbf{C}_\ell \mathbf{Q}^\circ)^2} + o(1) \\ &= \delta_{\ell\ell'} \gamma^2 \tilde{g}_\ell(-\gamma)^2 \frac{1}{n_\ell} \operatorname{tr} \mathbf{C}_\ell \overline{\mathbf{Q}^\circ \mathbf{C}_\ell \mathbf{Q}^\circ} + o(1). \end{aligned}$$

Plugging these results in the expression of the variance, we thus conclude that, for $\mathbf{x} \sim \mathcal{H}_\ell$,

$$\begin{aligned} \operatorname{Var}(T_{\text{LDA}}^{(\gamma)}(\mathbf{x})) &= (\boldsymbol{\mu}_0 - \boldsymbol{\mu}_1)^\top \overline{\mathbf{Q}^\circ \mathbf{C}_\ell \mathbf{Q}^\circ} (\boldsymbol{\mu}_0 - \boldsymbol{\mu}_1) \\ &\quad + \frac{1}{n_0} \operatorname{tr} \mathbf{C}_0 \overline{\mathbf{Q}^\circ \mathbf{C}_\ell \mathbf{Q}^\circ} + \frac{1}{n_1} \operatorname{tr} \mathbf{C}_1 \overline{\mathbf{Q}^\circ \mathbf{C}_\ell \mathbf{Q}^\circ}. \end{aligned}$$

We finally conclude that, for a decision threshold $\xi \in \mathbb{R}$,

$$\begin{aligned} \mathbb{P}\left(T_{\text{LDA}}^{(\gamma)}(\mathbf{x}) > \xi \mid \mathbf{x} \sim \mathcal{H}_\ell\right) \\ = Q\left(\frac{\xi - \frac{1}{2} [(-1)^\ell (\boldsymbol{\mu}_0 - \boldsymbol{\mu}_1)^\top \bar{\mathbf{Q}}^\circ (\boldsymbol{\mu}_0 - \boldsymbol{\mu}_1) - g_0(-\gamma) + g_1(-\gamma)]}{\sqrt{(\boldsymbol{\mu}_0 - \boldsymbol{\mu}_1)^\top \overline{\mathbf{Q}^\circ \mathbf{C}_\ell \mathbf{Q}^\circ} (\boldsymbol{\mu}_0 - \boldsymbol{\mu}_1) + \operatorname{tr} \left(\frac{\mathbf{C}_0}{n_0} + \frac{\mathbf{C}_1}{n_1}\right) \overline{\mathbf{Q}^\circ \mathbf{C}_\ell \mathbf{Q}^\circ}}} + o(1)\right) \end{aligned}$$

where $Q(t) = \frac{1}{\sqrt{2\pi}} \int_t^\infty e^{-u^2/2} du$ is the Gaussian Q -function. This expression emphasizes again the optimality of the decision threshold $\xi = \frac{1}{2}g_1(-\gamma) - \frac{1}{2}g_0(-\gamma)$ pointed out in Remark 3.1.

Figure 3.2 depicts the histograms of the output of $T_{\text{LDA}}^{(\gamma)}(\mathbf{x})$ in the practical case of MNIST data, here for $\gamma = 1$ and $n_0 = n_1 = 1024$ samples per class. The optimal decision threshold appears to be quite close to $\xi = 0$ in this balanced training sample setting, thereby suggesting that the quantities $g_0(-\gamma) = \frac{1}{n} \text{tr } \mathbf{C}_0 \bar{\mathbf{Q}}^o(-\gamma)$ and $g_1(-\gamma) = \frac{1}{n} \text{tr } \mathbf{C}_1 \bar{\mathbf{Q}}^o(-\gamma)$ are very similar. This does not necessarily implies that \mathbf{C}_0 and \mathbf{C}_1 are similar, but rather that their “structures” are similar so that $g_0(-\gamma) \approx g_1(-\gamma)$.

In practice, these quantities $g_\ell(-\gamma)$ are simple to estimate. Indeed, it suffices to notice, from the trace lemma (Lemma 2.11) that, for every sample $\mathbf{x}_i \sim \mathcal{H}_\ell$ from the training set,

$$\frac{1}{p} (\mathbf{x}_i - \hat{\boldsymbol{\mu}}_\ell)^\top [\hat{\mathbf{C}}_{-i}^{(\gamma)}]^{-1} (\mathbf{x}_i - \hat{\boldsymbol{\mu}}_\ell) = g_\ell(-\gamma) + O(p^{-\frac{1}{2}})$$

where $\hat{\mathbf{C}}_{-i}^{(\gamma)} = \hat{\mathbf{C}} - \frac{1}{n-2} \mathbf{x}_i \mathbf{x}_i^\top + \gamma \mathbf{I}_p$. Or equivalently, using the rank-one perturbation lemma,

$$\frac{\frac{1}{p} (\mathbf{x}_i - \hat{\boldsymbol{\mu}}_\ell)^\top [\hat{\mathbf{C}}^{(\gamma)}]^{-1} (\mathbf{x}_i - \hat{\boldsymbol{\mu}}_\ell)}{1 - \frac{1}{n-2} (\mathbf{x}_i - \hat{\boldsymbol{\mu}}_\ell)^\top [\hat{\mathbf{C}}^{(\gamma)}]^{-1} (\mathbf{x}_i - \hat{\boldsymbol{\mu}}_\ell)} = g_\ell(-\gamma) + O(p^{-\frac{1}{2}})$$

which, averaging over $i = 1, \dots, n_\ell$, gives the even more accurate estimate

$$\frac{1}{n_\ell} \sum_{i=1}^{n_\ell} \frac{\frac{1}{p} (\mathbf{x}_i^{(\ell)} - \hat{\boldsymbol{\mu}}_\ell)^\top [\hat{\mathbf{C}}^{(\gamma)}]^{-1} (\mathbf{x}_i^{(\ell)} - \hat{\boldsymbol{\mu}}_\ell)}{1 - \frac{1}{n-2} (\mathbf{x}_i^{(\ell)} - \hat{\boldsymbol{\mu}}_\ell)^\top [\hat{\mathbf{C}}^{(\gamma)}]^{-1} (\mathbf{x}_i^{(\ell)} - \hat{\boldsymbol{\mu}}_\ell)} = g_\ell(-\gamma) + O(p^{-1}).$$

3.1.2.2 Quadratic discriminant analysis

To best understand the large dimensional behavior of (regularized) QDA and to fine-tune the non-trivial assumptions on $\boldsymbol{\mu}_0, \boldsymbol{\mu}_1$ and $\mathbf{C}_0, \mathbf{C}_1$, an important preliminary step of order of magnitude estimation is needed.

Under the regularized setting, let us define

$$\begin{aligned} T_{\text{QDA}}^{(\gamma)}(\mathbf{x}) &\equiv \frac{1}{2\sqrt{p}} \log \frac{|\hat{\mathbf{C}}_0^{(\gamma)}|}{|\hat{\mathbf{C}}_1^{(\gamma)}|} - \frac{1}{2\sqrt{p}} (\mathbf{x} - \hat{\boldsymbol{\mu}}_0)^\top [\hat{\mathbf{C}}_0^{(\gamma)}]^{-1} (\mathbf{x} - \hat{\boldsymbol{\mu}}_0) \\ &\quad + \frac{1}{2\sqrt{p}} (\mathbf{x} - \hat{\boldsymbol{\mu}}_1)^\top [\hat{\mathbf{C}}_1^{(\gamma)}]^{-1} (\mathbf{x} - \hat{\boldsymbol{\mu}}_1) \end{aligned}$$

where $\hat{\mathbf{C}}_\ell^{(\gamma)} = \hat{\mathbf{C}}_\ell + \gamma \mathbf{I}_p$, and the division by $1/\sqrt{p}$ is chosen here so that $T_{\text{QDA}}^{(\gamma)}(\mathbf{x})$ be of order $O(1)$ in the non-trivial regime, as we shall see.

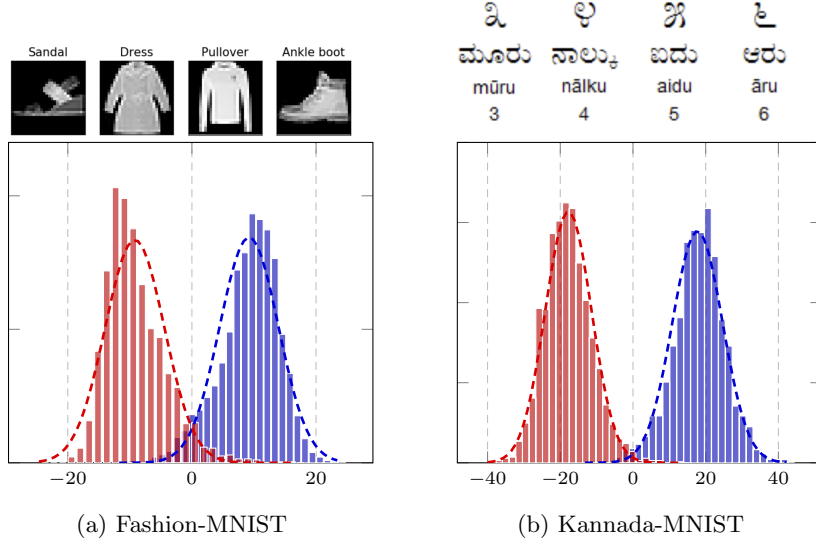


Figure 3.2: Empirical histogram of $T_{\text{LDA}}^{(\gamma)}(\mathbf{x})$ versus the Gaussian limiting prediction (dashed), \mathcal{H}_0 in **blue** and \mathcal{H}_1 in **red**, $n_0 = n_1 = 1024$, $p = 784$, $\gamma = 0.1$, for Fashion-MNIST (**left**) and Kannada-MNIST (**right**) data, class 3 versus 4. Empirical results averaged over 30 runs on test sets of size 128. [\[Link to code\]](#)

First observe that $T_{\text{QDA}}^{(\gamma)}(\mathbf{x})$ is the sum of two quadratic forms ($\frac{1}{2\sqrt{p}}(\mathbf{x} - \hat{\mu}_\ell)^T[\hat{\mathbf{C}}_\ell^{(\gamma)}]^{-1}(\mathbf{x} - \hat{\mu}_\ell)$) and of two linear statistics ($\frac{1}{\sqrt{p}} \log |\hat{\mathbf{C}}_\ell^{(\gamma)}|$) of the eigenvalues of large dimensional random matrices. Under the present $1/\sqrt{p}$ normalization, it is not difficult to see that the leading order of the quadratic forms is $O(\sqrt{p})$ while their fluctuations of order $O(1)$; as for the linear statistics, their means are of order $O(\sqrt{p})$ and their fluctuations of order $O(1/\sqrt{p})$ (recall from the discussion in Section 2.6.3 that linear statistics have a fast convergence rate with central limit theorems of speed $O(1/\sqrt{pn}) = O(1/p)$).

As such, if \mathbf{C}_0 and \mathbf{C}_1 are too ‘distinct’ in the large n, p regime, that is $\|\mathbf{C}_0 - \mathbf{C}_1\| \geq O(1)$, the sum of these means remains of order $O(\sqrt{p})$ and the fluctuations at most of order $O(1)$: the (random) $T_{\text{QDA}}^{(\gamma)}(\mathbf{x})$ is asymptotically deterministic and the problem becomes trivially easy. One thus needs a stronger assumption on the difference $\|\mathbf{C}_0 - \mathbf{C}_1\|$ for the decision not to be trivial. Not surprisingly, since the objective is to lower the dominant order by a factor $1/\sqrt{p}$, we must thus demand here that

$$\|\mathbf{C}_0 - \mathbf{C}_1\| = O(1/\sqrt{p}).$$

Yet, due to the independence of \mathbf{Z}_0 and \mathbf{Z}_1 , and the fact that p/n remains away from zero, this condition still implies that

$$\|\hat{\mathbf{C}}_0 - \hat{\mathbf{C}}_1\| = O(1)$$

which holds even when $\mathbf{C}_0 = \mathbf{C}_1$. To see why $\|\hat{\mathbf{C}}_0 - \hat{\mathbf{C}}_1\|$ must be $O(1)$, it suffices to note that, for say $\mathbf{C}_0 = \mathbf{C}_1 = \mathbf{I}_p$, $\hat{\mathbf{C}}_0 - \hat{\mathbf{C}}_1 = [\mathbf{Z}_0, \mathbf{Z}_1]\text{diag}(\frac{1}{n_0}\mathbf{1}_{n_0}^\top, \frac{1}{n_1}\mathbf{1}_{n_1}^\top)[\mathbf{Z}_0, \mathbf{Z}_1]^\top$, the eigenvalues of which are known from Theorem 2.5 to be of order $O(1)$.

As a consequence of this critical remark, observe that in the case $\mathbf{C}_0 = \mathbf{C}_1 = \mathbf{I}_p$, for say $\mathbf{x} = \boldsymbol{\mu}_0 + \mathbf{z}$ with $\mathbf{z} \sim \mathcal{N}(\mathbf{0}, \mathbf{I}_p)$,

$$\begin{aligned} & (\mathbf{x} - \hat{\boldsymbol{\mu}}_1)^\top [\hat{\mathbf{C}}_1^{(\gamma)}]^{-1} (\mathbf{x} - \hat{\boldsymbol{\mu}}_1) - (\mathbf{x} - \hat{\boldsymbol{\mu}}_0)^\top [\hat{\mathbf{C}}_0^{(\gamma)}]^{-1} (\mathbf{x} - \hat{\boldsymbol{\mu}}_0) \\ &= \left(\mathbf{z} + \boldsymbol{\mu}_0 - \boldsymbol{\mu}_1 - \frac{1}{n_0} \mathbf{Z}_0 \mathbf{1}_{n_0} \right)^\top [\hat{\mathbf{C}}_1^{(\gamma)}]^{-1} \left(\mathbf{z} + \boldsymbol{\mu}_0 - \boldsymbol{\mu}_1 - \frac{1}{n_1} \mathbf{Z}_1 \mathbf{1}_{n_1} \right) \\ &\quad - \left(\mathbf{z} - \frac{1}{n_0} \mathbf{Z}_0 \mathbf{1}_{n_0} \right)^\top [\hat{\mathbf{C}}_0^{(\gamma)}]^{-1} \left(\mathbf{z} - \frac{1}{n_1} \mathbf{Z}_1 \mathbf{1}_{n_1} \right). \end{aligned}$$

Note that $\|\frac{1}{n_\ell} \mathbf{Z}_\ell \mathbf{1}_{n_\ell}\| = O(1)$ and is thus negligible when compared to $\|\mathbf{z}\| = O(\sqrt{p})$. Further developing, we find that, if $\|\boldsymbol{\mu}_0 - \boldsymbol{\mu}_1\| = O(1)$, the dominant term is

$$\mathbf{z}^\top [\hat{\mathbf{C}}_1^{(\gamma)}]^{-1} (\hat{\mathbf{C}}_0 - \hat{\mathbf{C}}_1) [\hat{\mathbf{C}}_0^{(\gamma)}]^{-1} \mathbf{z} \quad \text{eq:QDA_dominant_term (3.2)}$$

which is of order $O(p)$, while the informative means-discriminating term

$$(\boldsymbol{\mu}_0 - \boldsymbol{\mu}_1)^\top [\hat{\mathbf{C}}_1^{(\gamma)}]^{-1} (\boldsymbol{\mu}_0 - \boldsymbol{\mu}_1) \quad \text{eq:QDA_informative_term (3.3)}$$

is of order $O(1)$ and thus negligible. When in particular $\mathbf{C}_0 = \mathbf{C}_1$ and $n_0 = n_1$, while $\|\boldsymbol{\mu}_0 - \boldsymbol{\mu}_1\| = O(1)$, the dominant term of Equation (3.2) is a random noise term of arbitrary sign, and thus leads the asymptotic detection performance to be no better than random guess.

To avoid this trivial scenario it is thus required to let

$$\|\boldsymbol{\mu}_0 - \boldsymbol{\mu}_1\| = O(\sqrt{p})$$

thereby turning the informative term of Equation (3.3) to be comparative to the term of Equation (3.2). Note however that, if \mathbf{C}_0 and \mathbf{C}_1 had been perfectly known, letting $\hat{\mathbf{C}}_\ell = \mathbf{C}_\ell$, the dominant term in Equation (3.2) would vanish and detection would be achievable at the optimal $\|\boldsymbol{\mu}_0 - \boldsymbol{\mu}_1\| = O(1)$ rate.

Being largely suboptimal (when compared to simpler methods developed in the course of the monograph such as the LS-SVM approach to be discussed in Section 4.5.3), we do not further expose the technical development of the regularized QDA performance. An exhaustive account is performed in [Elkhalil et al., 2020a]. It is also worth mentioning that, by applying different regularization $\gamma_0 \neq \gamma_1$ to the sample covariance matrix $\hat{\mathbf{C}}_0^{\gamma_0}$ and $\hat{\mathbf{C}}_1^{\gamma_1}$, significant performance improvement can be achieved, particularly in the case of unbalanced classification [Bejaoui et al., 2020].

3.1.3 Subspace methods: the G-MUSIC algorithm

sec:GMUSIC

In several applied contexts, such as in array processing, or brain signal processing, the statistical covariance of a sequence of multivariate observations in \mathbb{R}^p

testifies of specific “directions of arrival” of a sought-for signal (arising from radar bounces in array processing, or brain regions in brain signal processing). In these scenarios, the covariance matrix is quite structured and, if few (say $k \ll p$) distinct signals, or directions of arrival, are to be retrieved (compared to the dimension p of the data collecting array), this population covariance matrix is both structured and of a “spiked model type”.

The so-called subspace methods are used to retrieve this structural information in the covariance, and to infer the directions of arrival, from the dominant eigenvectors of the sample covariance matrix. These methods are known to perform well only when the typical angular distance between the angles $\theta_1, \dots, \theta_k$ to be estimated is sufficiently large, but fail to be discriminative otherwise.

We shall see in this section that these algorithms, and particularly the most popular of them – the MUSIC algorithm [Schmidt, 1986] – are based on the assumption that the population covariance can be consistently estimated by the sample covariance matrix. Paradoxically, this approximation, which we now know is quite rough and hazardous, will not alter the consistency of classical MUSIC in the individual estimation of the angles $\theta_1, \dots, \theta_k$. However, we will see that, random matrix analysis allows for a much more accurate estimation of close angles.

3.1.3.1 The MUSIC algorithm

We consider the multivariate data (or signal) model of the form

$$\mathbf{x}_i = \sum_{\ell=1}^k \mathbf{a}(\theta_\ell) s_{\ell,i} + \sigma \mathbf{w}_i$$

for $i \in \{1, \dots, n\}$, where $\mathbf{a}(\theta_\ell) \in \mathbb{R}^p$ is a deterministic “steering vector” parameterized by the scalar angle $\theta_\ell \in (-\pi, \pi]$, $s_{\ell,i} \in \mathbb{R}$ is a deterministic or random signal carried in the direction θ_ℓ at time instant i , $\sigma > 0$ and $\mathbf{w}_i \in \mathbb{R}^p$ is an independent random thermal noise at time i .

Various hypotheses can be formulated on prior knowledge on the signal $s_{\ell,i}$ and its dependence across time instants and across array elements. We consider here the simple setting where $\mathbf{s}_i = [s_{1,i}, \dots, s_{k,i}]^\top \sim \mathcal{N}(\mathbf{0}, \mathbf{P})$ for diagonal $\mathbf{P} \in \mathbb{R}^{k \times k}$ with $\mathbf{P}_{\ell\ell} > 0$ that collects the energy of the sources, with independent $\mathbf{s}_1, \dots, \mathbf{s}_n$. We also assume that $\mathbf{w}_i \sim \mathcal{N}(\mathbf{0}, \mathbf{I}_p)$ and are independent. In particular, source ℓ has an associated signal-to-noise ratio (SNR) $\mathbf{P}_{\ell\ell}/\sigma^2$.

As a consequence, we obtain, for each i that

$$\mathbb{E}[\mathbf{x}_i \mathbf{x}_i^\top] = \sum_{\ell=1}^k \mathbf{P}_{\ell\ell} \mathbf{a}(\theta_\ell) \mathbf{a}(\theta_\ell)^\top + \sigma^2 \mathbf{I}_p = \mathbf{A}_\theta \mathbf{P} \mathbf{A}_\theta^\top + \sigma^2 \mathbf{I}_p$$

where $\mathbf{A}_\theta = [\mathbf{a}(\theta_1), \dots, \mathbf{a}(\theta_k)] \in \mathbb{R}^{p \times k}$.

Let $\mathbb{E}[\mathbf{x}_i \mathbf{x}_i^\top] = \mathbf{U} \Lambda \mathbf{U}^\top$ be the spectral decomposition of $\mathbb{E}[\mathbf{x}_i \mathbf{x}_i^\top]$ with $\mathbf{U} = [\mathbf{u}_1, \dots, \mathbf{u}_p] \in \mathbb{R}^{p \times p}$, and $\Lambda = \text{diag}(\lambda_1, \dots, \lambda_p)$ where $\lambda_1 \geq \dots \geq \lambda_p$. The

MUSIC algorithm is fundamentally based on the fact that the sought-for steering vectors $\mathbf{a}(\theta_1), \dots, \mathbf{a}(\theta_k)$ live in the k -dimensional subspace spanned by the k dominant eigenvectors $\mathbf{U}_S = [\mathbf{u}_1, \dots, \mathbf{u}_k]$ of $\mathbb{E}[\mathbf{x}_i \mathbf{x}_i^\top]$. The $\mathbf{a}(\theta_\ell)$'s are therefore all orthogonal to the complementary subspace $\mathbf{I}_p - \mathbf{U}_S \mathbf{U}_S^\top$ and

$$\mathbf{a}(\theta_\ell)^\top (\mathbf{I}_p - \mathbf{U}_S \mathbf{U}_S^\top) \mathbf{a}(\theta_\ell) = 0$$

for $\ell \in \{1, \dots, k\}$. This equality is then turned into a detection criterion for $\theta_1, \dots, \theta_\ell$ since, for steering vectors that are linearly independent, we have

$$\eta(\theta) \equiv \mathbf{a}(\theta)^\top \mathbf{U}_S \mathbf{U}_S^\top \mathbf{a}(\theta) = \|\mathbf{a}(\theta)\|^2 \Leftrightarrow \theta \in \{\theta_1, \dots, \theta_\ell\}.$$

Would $\mathbb{E}[\mathbf{x}_i \mathbf{x}_i^\top]$ be perfectly known, the identification criterion for the θ_ℓ 's then consists in scanning $\eta(\theta)$ over $(-\pi, \pi]$ and extract the k zeros of the function. Being a quadratic form, all other values of $\eta(\theta)$ are positive. In practice, however, the population covariance $\mathbb{E}[\mathbf{x}_i \mathbf{x}_i^\top]$ is substituted by the sample estimation $\frac{1}{n} \mathbf{X} \mathbf{X}^\top$, where $\mathbf{X} = [\mathbf{x}_1, \dots, \mathbf{x}_n] \in \mathbb{R}^{p \times n}$ and the criterion consists in retrieving the local minima of

$$\mathbf{a}(\theta)^\top (\mathbf{I}_p - \hat{\mathbf{U}}_S \hat{\mathbf{U}}_S^\top) \mathbf{a}(\theta)$$

or alternatively the local maxima of the spike “MUSIC” estimator

$$\hat{\eta}_{\text{MUSIC}}(\theta) \equiv \mathbf{a}(\theta)^\top \hat{\mathbf{U}}_S \hat{\mathbf{U}}_S^\top \mathbf{a}(\theta)$$

for $\hat{\mathbf{U}}_S \in \mathbb{R}^{p \times k}$ the collection of eigenvectors associated with the k largest eigenvalues of the sample covariance $\frac{1}{n} \mathbf{X} \mathbf{X}^\top$.

In the presence of few samples, i.e., if n is not much larger than p , $\hat{\eta}(\theta)$ is *not* a consistent estimator for $\eta(\theta)$. Surprisingly enough though, it has been shown that, despite this inconsistency in estimating $\eta(\theta)$, under the classical detectability conditions inherent to spiked models (see details below), the corresponding estimates $\hat{\theta}_1, \dots, \hat{\theta}_k$ of the angles are consistent estimates. This means that, while $\hat{\eta}(\theta) - \eta(\theta) \not\rightarrow 0$ as $n, p \rightarrow \infty$, we still have that $\arg \max_{\theta \in \partial \theta_\ell} \hat{\eta}(\theta) - \arg \max_{\theta \in \partial \theta_\ell} \eta(\theta) \rightarrow 0$ (where $\partial \theta_\ell$ is a sufficiently small neighborhood of the genuine angle θ_ℓ).

This remark possibly explains the widespread usage of the MUSIC algorithm, despite its inherently using an erroneous estimate of $\eta(\theta)$. This ill-estimate however has the major defect of exhibiting only one local minimum where two close minima are in presence (see an illustration in the right display of Figure 3.3), thereby disrupting the resolution capability of the MUSIC algorithm. The next section revisits the large n, p estimation of $\eta(\theta)$ with the spiked covariance matrix results established in Section 2.5.

The following results are immediate consequences of Section 2.5 but were primarily developed, under a broader scope of assumptions in a long series of works on the topic (see in particular [Mestre, 2008, Loubaton et al., 2011]).

3.1.3.2 Spiked G-MUSIC

Assuming that the ratio p/n between the number of sensors p (antenna array elements, electrodes, etc.) and the number of independent snapshots n of \mathbf{x}_i 's is not small, estimating \mathbf{U}_S by $\hat{\mathbf{U}}_S$ is quite inappropriate, as $\|\mathbf{U}_S - \hat{\mathbf{U}}_S\| \not\rightarrow 0$ as $p, n \rightarrow \infty$ with a non-trivial ratio.

However, the objective of interest is $\eta(\theta) = \mathbf{a}(\theta)^T \mathbf{U}_S \mathbf{U}_S^T \mathbf{a}(\theta)$, which is a quadratic form involving the deterministic vector $\mathbf{a}(\theta)$ and the rank- k matrix $\mathbf{U}_S \mathbf{U}_S^T \equiv \sum_{i=1}^k \mathbf{u}_{S,i} \mathbf{u}_{S,i}^T$, and can thus be estimated consistently using the results of Section 2.5 on spiked random matrices.

More precisely, note that $\frac{1}{\sigma^2 n} \mathbf{X} \mathbf{X}^T$ is a Wishart random matrix with $\mathbf{x}_i/\sigma \sim \mathcal{N}(\mathbf{0}, \sigma^{-2} \mathbf{A}_\theta \mathbf{P} \mathbf{A}_\theta^T + \mathbf{I}_p)$ and $\text{rank}(\sigma^{-2} \mathbf{A}_\theta \mathbf{P} \mathbf{A}_\theta^T) = k$, which thus falls under the setting of Theorems 2.12 and 2.13. Writing

$$\sigma^{-2} \mathbf{A}_\theta \mathbf{P} \mathbf{A}_\theta^T = \mathbf{U}_S \mathbf{L}_S \mathbf{U}_S^T = \sum_{i=1}^k \ell_i \cdot \mathbf{u}_{S,i} \mathbf{u}_{S,i}^T$$

for some diagonal matrix $\mathbf{L}_S = \text{diag}(\ell_1, \dots, \ell_k) \in \mathbb{R}^{k \times k}$, and thus, assuming that $\ell_i > \sqrt{c}$ for each i (high SNR scenario), by Theorem 2.13, for all deterministic unit-norm vector $\mathbf{a} \in \mathbb{R}^p$, as $p, n \rightarrow \infty$ with $p/n \rightarrow c \in (0, \infty)$,

$$\mathbf{a}^T \mathbf{U}_S \mathbf{U}_S^T \mathbf{a} = \sum_{i=1}^k |\mathbf{a}^T \mathbf{u}_{S,i}|^2 = \sum_{i=1}^k |\mathbf{a}^T \hat{\mathbf{u}}_{S,i}|^2 \frac{1 + c\ell_i^{-1}}{1 - c\ell_i^{-2}} + o(1).$$

In the specific case of array processing, it is most convenient to assume that $\|\mathbf{a}(\theta)\| = 1$ and $\mathbf{a}(\theta)^T \mathbf{a}(\theta') \rightarrow 0$ for all fixed $\theta \neq \theta'$ as $p \rightarrow \infty$. This is particularly valid for the canonical example of a “uniform linear array” (that is, an array of sensor evenly spaced on a line). Therefore, in these scenarios, one can identify

$$\ell_i = \frac{\mathbf{P}_{ii}}{\sigma^2} + o(1)$$

the SMR for the i -th signal source. As a result, we have a first estimator:

$$\sum_{i=1}^k |\mathbf{a}(\theta)^T \hat{\mathbf{u}}_{S,i}|^2 \frac{1 + \frac{p}{n} (\frac{\mathbf{P}_{ii}}{\sigma^2})^{-1}}{1 - \frac{p}{n} (\frac{\mathbf{P}_{ii}}{\sigma^2})^{-2}} = \eta(\theta) + o(1).$$

However, \mathbf{P}_{ii}/σ^2 is in general not known and also needs to be estimated. To this end, one may use Theorem 2.12 by noticing that, still under the condition that $\ell_i = \mathbf{P}_{ii}/\sigma^2 + o(1) > \sqrt{c}$, the i -th largest eigenvalue λ_i of $\frac{1}{\sigma^2 n} \mathbf{X} \mathbf{X}^T$ satisfies

$$\lambda_i \xrightarrow{a.s.} 1 + \ell_i + c \frac{1 + \ell_i}{\ell_i} = 1 + c + \frac{\mathbf{P}_{ii}}{\sigma^2} + c \frac{\sigma^2}{\mathbf{P}_{ii}} + o(1)$$

so that, by inverting the expression,

$$\hat{\ell}_i \equiv \frac{\lambda_i - (1 + p/n)}{2} + \frac{1}{2} \sqrt{\left(\lambda_i - \left(1 + \frac{p}{n} \right) \right)^2 - \frac{4p}{n}} = \frac{\mathbf{P}_{ii} \text{eq:hat_pi_sigma2}}{\sigma^2} + o(1) \quad (3.4)$$

entailing the final spike “G-MUSIC” estimate

$$\hat{\eta}_{\text{GMUSIC}}(\theta) \equiv \sum_{i=1}^k |\mathbf{a}(\theta)^T \hat{\mathbf{u}}_{S,i}|^2 \frac{1 + \frac{p}{n} \hat{\ell}_i^{-1}}{1 - \frac{p}{n} \hat{\ell}_i^{-2}} = \eta(\theta) + o(1)$$

with $\hat{\ell}_i$ given in (3.4). This approach demands to know σ^2 since λ_i is the i -th largest (and isolated) eigenvalue of $\frac{1}{\sigma^2 n} \mathbf{X} \mathbf{X}^T$. Yet, it is also known that the limiting spectrum of $\frac{1}{\sigma^2 n} \mathbf{X} \mathbf{X}^T$ is the Marčenko-Pastur distribution with right edge equal to (and thus, here, with $(k+1)$ -th largest eigenvalue converging to) $(1 + \sqrt{c})^2 = (1 + \sqrt{p/n})^2 + o(1)$. As such, σ^2 can be estimated from the fact that $\lambda_{k+1}(\frac{1}{n} \mathbf{X} \mathbf{X}^T) = \sigma^2(1 + \sqrt{p/n})^2 + o(1)$. This estimator is however possibly less accurate as λ_{k+1} fluctuates at a rate $O(n^{-2/3})$ by the Tracy-Widom theorem, Theorem 2.14. A better estimate consists in noticing that $\frac{1}{\sigma^2} \frac{1}{p} \text{tr}(\frac{1}{n} \mathbf{X} \mathbf{X}^T) = 1 + O(n^{-1})$, or even more accurately $\frac{1}{\sigma^2} \frac{1}{p-k} \text{tr}(\frac{1}{n} \mathbf{X} \mathbf{X}^T) - \frac{1}{p-k} \sum_{i=1}^k \lambda_i = 1 + O(n^{-1})$.

The resulting G-MUSIC estimator is nothing more than a “weighted” version of the standard MUSIC algorithm where, instead of projecting $\mathbf{a}(\theta)$ against each of the k dominant eigenvectors of $\frac{1}{n} \mathbf{X} \mathbf{X}^T$, $\mathbf{a}(\theta)$ is now projected against an appropriate weighted sum of these eigenvectors. This weighted sum of projections on eigenvectors is no longer a subspace projection though, and one must be careful that $1 - \hat{\eta}_{\text{GMUSIC}}(\theta)$ might, with low but not zero probability, be negative. This is a common artifact of the random matrix approximation of quadratic forms which may not result in nonnegative estimates.

Figure 3.3 depicts, for $\|\mathbf{a}(\theta)\| = 1$, the performances of the estimator of $1 - \hat{\eta}(\theta)$ (more conventionally used than $\hat{\eta}(\theta)$) for both the classical MUSIC and the improved G-MUSIC algorithm. The ground truth $\eta(\theta)$ has zeros precisely at the location of the genuine angles (here -10° , 35° and 37°). It is observed that deep local minima are precisely exhibited by both MUSIC and G-MUSIC around these positions (on a log scale). However, (i) the minima reached by G-MUSIC are deeper and, more importantly, (ii) the precision of estimation is largely improved with G-MUSIC, leading particularly to an improved resolution capability of close angles estimation, as observed in the vicinity of the two angles 35° and 37° in the right display of Figure 3.3.

The improved spike G-MUSIC algorithm is a typical example of the possibility to (quite elementarily) improve over a classical and largely used algorithm (MUSIC), long known to suffer from large p/n ratios.

3.2 Covariance matrix distance estimation

sec:cov_distance_estim

3.2.1 Distances and divergences between Gaussian laws

Most statistical detection, estimation, and classification methods rely exclusively on the first order statistics of the data model. The various notions of “distances” between classes of data are then strongly related to these first moments.

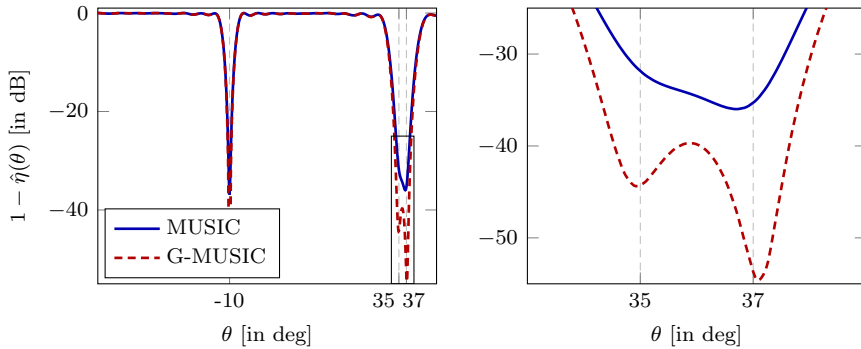


Figure 3.3: **Left:** MUSIC versus G-MUSIC for $k = 3$ sources, $p = 30$, $n = 150$ samples, $\sigma^2 = 0.1$ (-10 dB). Angles of arrival of 10° , 35° , and 37° . **Right:** zoom on the region of interest of close angles. [\[Link to code\]](#). fig:GMUSIC

Since means and covariances are often sufficiently discriminating, especially in large dimensions (see Section 4), distances and divergences revolving around Gaussian distributions are of common interest. Among these, the Kullback–Liebler divergence d_{KL} or the Rényi divergence $d_{\alpha R}$ between two Gaussian $\mathcal{N}(\mu_1, \mathbf{C}_1)$ and $\mathcal{N}(\mu_2, \mathbf{C}_2)$, as well as the Bhattacharyya distance d_B and the Fisher distance d_F (the length of the geodesic in the “natural” Riemannian space of positive definite matrices) between two covariance matrices \mathbf{C}_1 and \mathbf{C}_2 are the most popular.

Assuming the data have zero mean (or equal mean) and positive definite covariance, these distances and divergences, that we shall generically denote $d(\mathbf{C}_1, \mathbf{C}_2; f)$, share the property that

$$d(\mathbf{C}_1, \mathbf{C}_2; f) = \int f(t) \nu_p(dt)$$

for $\nu_p = \frac{1}{p} \sum_{i=1}^p \delta_{\lambda_i(\mathbf{C}_1^{-1} \mathbf{C}_2)}$ and some specific function f . Table 3.1 lists the mappings between distances¹ and functions f and shows in particular that, in order to evaluate all of these distances, it suffices to assess $\int f(t) \nu_p(dt)$ for $f(t)$ one of the functions $t \mapsto t$, $t \mapsto \log(1+st)$ ($s \in (0, \infty)$), with $\log(t) = \lim_{s \rightarrow \infty} \log(1+st) - \log(s)$ and $t \mapsto \log^2(t)$.

rem:Wasserstein

Remark 3.2 (The Wasserstein distance). *Of increasing interest in machine learning lately is the Wasserstein distance which, for the laws $\mathcal{N}(\mathbf{0}, \mathbf{C}_1)$ and*

¹We slightly abuse the definitions here as the Fisher and Bhattacharyya distances and in fact the square roots of $\int f(t) \nu_p(dt)$ and not the integrals themselves.

Divergences	$f(z)$
d_F	$\log^2(z)$
d_B	$-\frac{1}{4} \log(z) + \frac{1}{2} \log(1+z) - \frac{1}{2} \log(2)$
d_{KL}	$\frac{1}{2}z - \frac{1}{2} \log(z) - \frac{1}{2}$
$d_{\alpha, R}$	$\frac{-1}{2(\alpha-1)} \log(\alpha + (1-\alpha)z) + \frac{1}{2} \log(z)$

Table 3.1: Distances and divergences, and their corresponding $f(z)$. tab:f

$\mathcal{N}(\mathbf{0}, \mathbf{C}_2)$, reduces (up to normalization by $1/p$) to

$$\begin{aligned} d_W(\mathbf{C}_1, \mathbf{C}_2) &= \frac{1}{p} \text{tr}(\mathbf{C}_1) + \frac{1}{p} \text{tr}(\mathbf{C}_2) - \frac{2}{p} \text{tr} \left[(\mathbf{C}_1^{\frac{1}{2}} \mathbf{C}_2 \mathbf{C}_1^{\frac{1}{2}})^{\frac{1}{2}} \right] \\ &= \frac{1}{p} \text{tr}(\mathbf{C}_1) + \frac{1}{p} \text{tr}(\mathbf{C}_2) - 2 \int \sqrt{t} \nu'_p(dt), \quad \nu'_p = \frac{1}{p} \sum_{i=1}^p \delta_{\lambda_i(\mathbf{C}_1 \mathbf{C}_2)}. \end{aligned}$$

The Wasserstein distance therefore does not enter the present scheme as it involves the eigenvalues of the product $\mathbf{C}_1 \mathbf{C}_2$ rather than $\mathbf{C}_1^{-1} \mathbf{C}_2$. Yet, the derivations in this section easily extend to this setup. Section 3.2.4 below reports the corresponding results.

3.2.2 The random matrix framework

In practice, to evaluate the distance between data classes $\mathcal{C}_1, \dots, \mathcal{C}_k$, one has access to numbers n_a of vectors $\mathbf{X}^{(a)} = [\mathbf{x}_1^{(a)}, \dots, \mathbf{x}_{n_a}^{(a)}] \in \mathbb{R}^{p \times n_a}$ from class \mathcal{C}_a from which the pairwise distances $d(\mathbf{C}_a, \mathbf{C}_b; f)$ must be estimated. Assuming $n_a > p$ and the $\mathbf{x}_i^{(a)}$ independent zero mean with covariance \mathbf{C}_a , $d(\mathbf{C}_a, \mathbf{C}_b; f)$ is conventionally estimated through the empirical estimate $d(\hat{\mathbf{C}}_a, \hat{\mathbf{C}}_b; f)$ where $\hat{\mathbf{C}}_a = \frac{1}{n_a} \mathbf{X}^{(a)} (\mathbf{X}^{(a)})^\top$.

However, for n_a not much larger than p , $\hat{\mathbf{C}}_a$ is known to be a poor estimator for \mathbf{C}_a and $d(\hat{\mathbf{C}}_a, \hat{\mathbf{C}}_b; f)$ is likely a poor estimator for $d(\mathbf{C}_a, \mathbf{C}_b; f)$. To convince oneself, for say $f(t) = \log(t)$ and $\mathbf{C}_1 = \mathbf{C}_2$, $\mathbf{C}_1^{-1} \mathbf{C}_2 = \mathbf{I}_p$ so that $d(\mathbf{C}_1, \mathbf{C}_2; f) = 0$, while $\hat{\mathbf{C}}_1^{-1} \hat{\mathbf{C}}_2$ is distributed as a F-matrix with eigenvalues asymptotically supported on a compact interval around 1 and with left edge converging to zero as $n_1/p > 1$ or $n_2/p > 1$ is close to 1 [Silverstein, 1985], so that $d(\hat{\mathbf{C}}_1^{-1} \hat{\mathbf{C}}_2; f)$ may be arbitrarily large as either $n_1/p, n_2/p \downarrow 1$.

The idea of the random matrix framework is to evaluate $d(\mathbf{C}_a, \mathbf{C}_b; f)$ consistently from $\mathbf{X}_a, \mathbf{X}_b$ in the spirit of Section 2.4. Since only pairwise distances are of interest, on the following we focus on evaluating the metric $d(\mathbf{C}_1, \mathbf{C}_2; f)$ for some arbitrary analytic function f .

To this end, similar to (2.27), we write

$$d(\mathbf{C}_1, \mathbf{C}_2; f) = \int f(t) \nu_p(dt) = -\frac{1}{2\pi i} \oint_{\Gamma_\nu} f(z) m_{\nu_p}(z) dz$$

for Γ_ν a contour surrounding the support of ν_p , i.e., the eigenvalues of $\mathbf{C}_1^{-1}\mathbf{C}_2$, but no singularity of f . Using the finite-dimensional trick that consists in letting $\nu = \nu_p$ be a fictitious asymptotic limit for ν_p as $p \rightarrow \infty$, this becomes

$$d(\mathbf{C}_1, \mathbf{C}_2; f) = -\frac{1}{2\pi i} \oint_{\Gamma_\nu} f(z)m_\nu(z)dz.$$

Similarly, we will in the following denote $c_1 = n_1/p = \lim n_1/p$, $c_2 = n_2/p = \lim n_2/p$ the fictitious limiting data sample/size ratios.

To connect the unknown ν to the observed $\mu_p = \frac{1}{p} \sum_{i=1}^p \delta_{\lambda_i(\hat{\mathbf{C}}_1^{-1}\hat{\mathbf{C}}_2)}$, we first need to establish a link between m_ν and m_μ , with μ the (almost sure) weak limit of μ_p as $n, p \rightarrow \infty$. For this, it suffices proceed as follows:

- by Sylvester's identity (Lemma 2.3), $\hat{\mathbf{C}}_1^{-1}\hat{\mathbf{C}}_2$ has the same eigenvalues as the symmetric matrix $\hat{\mathbf{C}}_2^{\frac{1}{2}}\hat{\mathbf{C}}_1^{-1}\hat{\mathbf{C}}_2^{\frac{1}{2}}$; which are the inverse eigenvalues of $\hat{\mathbf{C}}_2^{-\frac{1}{2}}\hat{\mathbf{C}}_1\hat{\mathbf{C}}_2^{-\frac{1}{2}}$;
- conditioned on \mathbf{X}_2 , $\hat{\mathbf{C}}_2^{-\frac{1}{2}}\hat{\mathbf{C}}_1\hat{\mathbf{C}}_2^{-\frac{1}{2}}$ is a sample covariance matrix with population covariance $\mathbb{E}_{\mathbf{X}_1}[\hat{\mathbf{C}}_2^{-\frac{1}{2}}\hat{\mathbf{C}}_1\hat{\mathbf{C}}_2^{-\frac{1}{2}}] = \hat{\mathbf{C}}_2^{-\frac{1}{2}}\mathbf{C}_1\hat{\mathbf{C}}_2^{-\frac{1}{2}}$, for which Theorem 2.5 provides a deterministic equivalent, as a function of the “deterministic” limiting spectral measure of $\hat{\mathbf{C}}_2^{-\frac{1}{2}}\mathbf{C}_1\hat{\mathbf{C}}_2^{-\frac{1}{2}}$;
- similarly, the matrix $\hat{\mathbf{C}}_2^{-\frac{1}{2}}\mathbf{C}_1\hat{\mathbf{C}}_2^{-\frac{1}{2}}$ has the same eigenvalues as $\mathbf{C}_1^{\frac{1}{2}}\hat{\mathbf{C}}_2^{-1}\mathbf{C}_1^{\frac{1}{2}}$, which are the inverse eigenvalues of $\mathbf{C}_1^{-\frac{1}{2}}\hat{\mathbf{C}}_2\mathbf{C}_1^{-\frac{1}{2}}$, the latter being a sample covariance matrix with population covariance $\mathbf{C}_1^{-\frac{1}{2}}\mathbf{C}_2\mathbf{C}_1^{-\frac{1}{2}}$ for which Theorem 2.5 also establishes the limiting spectrum.

Thus, iterating Theorem 2.5 twice results in the following fixed-point system

$$\begin{aligned} m_\nu(-1/m_\zeta(z)) &= -zm_\zeta(z)m_\zeta(z) \\ zm_\mu(z) &= \varphi(z)m_\zeta(\varphi(z)) \end{aligned} \quad \text{eq:cov_distance_f(zeta)-->f(mu)} \quad (3.5)$$

where $\varphi(z) = z(1 + c_1 zm_\mu(z))$ and $m_\zeta(z) = c_2 m_\zeta(z) - (1 - c_2)/z$ for ζ the intermediary limiting spectral measure of $\frac{1}{n_2} \mathbf{C}^{\frac{1}{2}} \mathbf{Z} \mathbf{Z}^\top \mathbf{C}^{\frac{1}{2}}$ with $\mathbf{Z} \in \mathbb{R}^{p \times n_2}$ with i.i.d. standard Gaussian entries and $\mathbf{C} = \mathbf{C}_1^{-\frac{1}{2}}\mathbf{C}_2\mathbf{C}_1^{-\frac{1}{2}}$. Precisely, to obtain (3.5), we first write

$$m_{\zeta^{-1}}(-1/m_{\tilde{\mu}^{-1}}(z)) = -zm_{\mu^{-1}}(z)m_{\tilde{\mu}^{-1}}(z)$$

which relates the Stieltjes transform of the limiting spectral measure of $\hat{\mathbf{C}}_2^{-1}\hat{\mathbf{C}}_1$ (denoted μ^{-1} , the empirical measure) to that of $\hat{\mathbf{C}}_2^{-1}\mathbf{C}_1$ (i.e., ζ^{-1} , considered to be the population measure when conditioned on \mathbf{X}_2), with the convention that, for a probability measure θ , θ^{-1} is defined through $\theta^{-1}([a, b]) = \theta([b^{-1}, a^{-1}])$ for

$0 < a < b$ and $m_{\tilde{\mu}^{-1}}(z) = c_1 m_{\mu^{-1}}(z) - (1 - c_1)/z$. Using the Stieltjes transform relation

$$m_{\zeta^{-1}}(z) = -\frac{1}{z} - \frac{1}{z^2} m_\zeta\left(\frac{1}{z}\right)$$

which is a direct consequence of $m_{\zeta^{-1}}(z) = \int \frac{\zeta(dt)}{t^{-1}-z} = -\frac{1}{z} - \frac{1}{z^2} \int \frac{\zeta(dt)}{t-z^{-1}}$, we reach (3.5), as desired.

For further need, note that the derivative along z of (3.5) gives

$$m'_\zeta(\varphi(z)) = \frac{1}{\varphi(z)} \left(-\frac{\psi'(z)}{c_2 \varphi'(z)} - m_\zeta(\varphi(z)) \right)$$

where we introduced here the function $\psi(z) = 1 - c_2 - c_2 z m_\mu(z)$.

Two successive changes of variable ($\omega \mapsto z = -1/m_\zeta(\omega)$ and $u \mapsto \omega = \varphi(u)$) are then needed to relate m_ν first to m_ζ and then m_ζ to m_μ . Assuming the existence of a contour Γ_μ with valid pre-image Γ_ν by these changes of variable, we find

$$\begin{aligned} d(\mathbf{C}_1, \mathbf{C}_2; f) &= -\frac{1}{2\pi i} \oint_{\Gamma_\nu} f(z) m_\nu(z) dz \\ &= \frac{1}{2\pi i} \oint_{\Gamma_\mu} f\left(\frac{\varphi(u)}{\psi(u)}\right) \frac{\psi(u)}{c_2} \left[\frac{\varphi'(u)}{\varphi(u)} - \frac{\psi'(u)}{\psi(u)} \right] du \\ &\quad - \frac{1-c_2}{c_2} \frac{1}{2\pi i} \oint_{\Gamma_\mu} f\left(\frac{\varphi(u)}{\psi(u)}\right) \left[\frac{\varphi'(u)}{\varphi(u)} - \frac{\psi'(u)}{\psi(u)} \right] du \end{aligned}$$

where we recall that $\varphi(u) = u(1 + c_1 u m_\mu(u))$ and $\psi(u) = 1 - c_2 - c_2 u m_\mu(u)$. Performing the variable changes backwards, the term in the last line writes

$$\begin{aligned} &- \frac{1-c_2}{c_2} \frac{1}{2\pi i} \oint_{\Gamma_\mu} f\left(\frac{\varphi(u)}{\psi(u)}\right) \left[\frac{\varphi'(u)}{\varphi(u)} - \frac{\psi'(u)}{\psi(u)} \right] du \\ &= -\frac{1-c_2}{c_2} \frac{1}{2\pi i} \oint_{\Gamma_\mu} f\left(\frac{\varphi(u)}{\psi(u)}\right) \left(\frac{\varphi(u)}{\psi(u)} \right)^{-1} \left(\frac{\varphi(u)}{\psi(u)} \right)' du \\ &= -\frac{1-c_2}{c_2} \frac{1}{2\pi i} \oint_{\Gamma_\nu} \frac{f(z)}{z} dz. \end{aligned}$$

The contour change analyses performed in Section 2.3.1 are fundamental at this point. Since we here operate twice sample-covariance matrix variable changes, it can be shown that, if $c_1, c_2 < 1$ (i.e., $n_1, n_2 > p$), then any contour $\Gamma_\mu \subset \{z \in \mathbb{C}, \Re[z] > 0\}$ enclosing the support of μ has $\Gamma_\nu \subset \{z \in \mathbb{C}, \Re[z] > 0\}$ as pre-image by the variable changes. Note importantly that, being subsets of the complementary of $\{z \in \mathbb{C}, \Re[z] > 0\}$, both Γ_μ and Γ_ν must exclude $z = 0$.

Thus, if f is analytic on $\{z \in \mathbb{C}, \Re[z] > 0\}$, we have

$$-\frac{1-c_2}{c_2} \frac{1}{2\pi i} \oint_{\Gamma_\nu} \frac{f(z)}{z} dz = 0.$$

It then suffices to replace the limiting measure μ by its empirical version $\mu_p = \frac{1}{p} \sum_{i=1}^p \delta_{\lambda_i(\hat{\mathbf{C}}_1^{-1} \hat{\mathbf{C}}_2)}$ to obtain the final estimate.

theo:cov_dist

Theorem 3.1 (Covariance distance estimate, from [Couillet et al., 2019]). *Let $f : \mathbb{R}^+ \rightarrow \mathbb{R}$ be a real function with a complex analytic extension on $\{z \in \mathbb{C}, \Re[z] > 0\}$ and $c_1, c_2 < 1$. Then, with the above notations²*

$$d(\mathbf{C}_1, \mathbf{C}_2; f) - \hat{d}(\mathbf{X}_1, \mathbf{X}_2; f) \xrightarrow{a.s.} 0$$

where

$$\hat{d}(\mathbf{X}_1, \mathbf{X}_2; f) = \frac{1}{2\pi i} \oint_{\Gamma_\mu} f\left(\frac{\varphi_p(u)}{\psi_p(u)}\right) \frac{\psi_p(u)}{c_2} \left[\frac{\varphi'_p(u)}{\varphi_p(u)} - \frac{\psi'_p(u)}{\psi_p(u)} \right] du$$

where $\varphi_p(z) = z(1 + c_1 z m_{\mu_p}(z))$ and $\psi_p(z) = 1 - c_2 - c_2 z m_{\mu_p}(z)$.

3.2.3 Closed-form expressions

Theorem 3.1 is quite generic, as valid for any f analytic on $\{z \in \mathbb{C}, \Re[z] > 0\}$. Yet, it practically demands a numerical complex integration procedure and thus conveys little insights on the actual estimate being computed.

Since most distances of practical interest (recall Table 3.1) involve linear combinations of the functions $f(t) = t$, $f(t) = \log(t)$, $f(t) = \log(1 + st)$ and $f(t) = \log^2(t)$, it suffices to compute these integrals for their complex analytic extensions.

Since $m_{\mu_p}(z) = \frac{1}{p} \sum_{i=1}^p (\lambda_i (\hat{\mathbf{C}}_1^{-1} \hat{\mathbf{C}}_2) - z)^{-1}$ is a rational function, for f also a rational function, the integrand in Theorem 3.1 is itself a rational function for which residue calculus can be performed. Among the functions above, this is the case only for $f(t) = t$. The other functions (involving logarithms) are “multi-valued” complex functions for which the integral must be computed using more advanced complex analytic calculus.

In all cases, a first requirement is to precisely understand the function $\varphi_p(z)/\psi_p(z)$ on $\{z \in \mathbb{C}, \Re[z] > 0\}$ where f is evaluated. This function can be shown to only have null imaginary part on the real axis and one thus needs to investigate $\varphi_p(z)/\psi_p(z)$ for z real. Also, similar to the proof of Remark 2.13, it can be shown that $\varphi_p(z)$ vanishes exactly at $0 < \eta_1 < \dots < \eta_p$ the eigenvalues of $\mathbf{\Lambda} + \frac{\sqrt{\mathbf{\lambda}}\sqrt{\mathbf{\lambda}}^\top}{n_1-p}$ while $\psi_p(z)$ vanishes exactly at $0 < \zeta_1 < \dots < \zeta_p$ the eigenvalues of $\mathbf{\Lambda} - \frac{\sqrt{\mathbf{\lambda}}\sqrt{\mathbf{\lambda}}^\top}{n_2}$, for diagonal $\mathbf{\Lambda} \in \mathbb{R}^{p \times p}$ and $\mathbf{\lambda} = (\lambda_1, \dots, \lambda_p)^\top \in \mathbb{R}^p$ the increasingly sorted eigenvalues of $\hat{\mathbf{C}}_1^{-1} \hat{\mathbf{C}}_2$. Figure 3.4 depicts the function $x \mapsto xm_{\mu_p}(x)$ at the core of the definition of both $\varphi_p(x)$ and $\psi_p(x)$. The ordering of the triplets $\zeta_i < \lambda_i < \eta_i$ is easily established and it appears that $\varphi_p(z)/\psi_p(z)$ is everywhere positive on \mathbb{R}_+ but on the p intervals $[\zeta_i, \eta_i]$. These segments are important as they correspond to *branch cuts* for the multivalued functions $z \mapsto \log^a(\varphi_p(z)/\psi_p(z))$ ($a \in \{1, 2\}$), i.e., they are discontinuity intervals for the function.

²To avoid too heavy notations, we maintain c_1, c_2 in the empirical estimates (and in the subsequent discussions) but one should in reality replace them systematically with n_1/n and n_2/n .

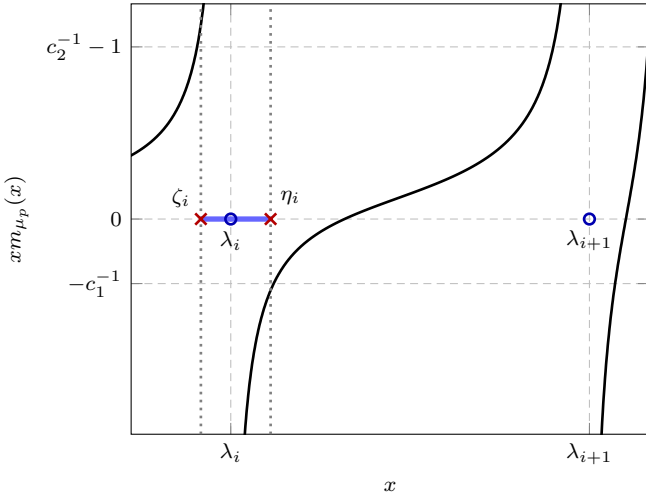


Figure 3.4: Typical behavior of the function $x \mapsto xm_{\mu_p}(x)$. The Blue bar stresses the range of negative values for $\varphi_p(x)/\psi_p(x)$. [Link to code]. `fig:xmx`

For $f(t) = t$, a mere residue calculus accounting for the singularities at ζ_i , λ_i and η_i allows one to establish the following simple corollary.

Corollary 3.1 (Case $f(t) = t$). *Under the setting of Theorem 3.1, for $f(t) = t$,*

$$\hat{d}(\mathbf{X}_1, \mathbf{X}_2; f) = (1 - c_1) \int t \mu_p(dt).$$

That is, the sought-for metric $(\int t \nu_p(dt))$ is consistently estimated by a scaled version (with a $1 - c_1$ prefactor) of the standard estimator $\int t \mu_p(dt)$. We notably recover the standard large- n estimator when $c_1, c_2 \rightarrow 0$. It may be surprising at first to see c_2 not appearing in this expression; this is explained by the fact that $\frac{1}{p} \text{tr } \mathbf{A} \hat{\mathbf{C}}_2$ is a consistent estimator of $\frac{1}{p} \text{tr } \mathbf{A} \mathbf{C}_2$ for all \mathbf{A} of bounded norm, as long as $\liminf n_2/p > 0$ (but the same is not true for $\frac{1}{p} \text{tr } \mathbf{A} \hat{\mathbf{C}}_1^{-1}$ which is not a consistent estimate of $\frac{1}{p} \text{tr } \mathbf{A} \mathbf{C}_1^{-1}$).

To handle the case $f(t) = \log(t)$, one needs to “deform” the contour Γ_μ to avoid the aforementioned branch cuts. A possibility is to proceed as depicted in Figure 3.5 by appending Γ_μ into a circuit surrounding the whole segment $[\zeta_1, \eta_p]$ slightly from above and from below in the complex plane, with small half-circles of vanishing radius around all possible singularities (ζ_i 's, λ_i 's and η_i 's). The whole circuit, call it Γ , has zero integral (as it encompasses no singularity) and is the sum of the sought-for integral over Γ_μ , of linear (asymptotically real) integrals, and of half-circle integrals around the poles (evaluated by a variable change $z = \varepsilon e^{i\theta}$ and then taking $\varepsilon \rightarrow 0$).

The result for the case $f(t) = \log(t)$ again assumes a simple form and is as follows.

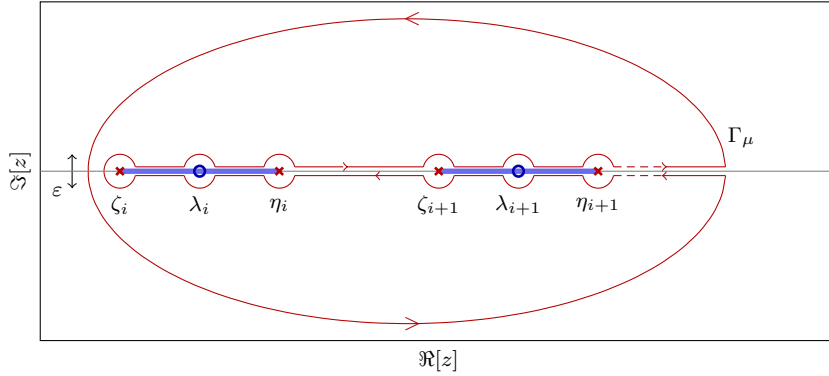


Figure 3.5: Deformed contour Γ to evaluate Theorem 3.1 for $f(z) = \log^a(z)$, $a \in \{1, 2\}$. Branch cuts are displayed in blue bars.

[fig:contour_](#)

Corollary 3.2 (Case $f(t) = \log(t)$). *Under the setting of Theorem 3.1, for $f(t) = \log(t)$,*

$$\hat{d}(\mathbf{X}_1, \mathbf{X}_2; f) = \int \log(t) \mu_p(dt) - \frac{1 - c_1}{c_1} \log(1 - c_1) + \frac{1 - c_2}{c_2} \log(1 - c_2).$$

Interestingly, while the case $f(t) = t$ was a mere scaling of the large- n estimator, here the estimate is a biased version of the large- n estimator by a constant. Besides, for $c_1 = c_2$, the constant vanishes and thus, quite surprisingly, the standard large- n estimator is consistent.

The case $f(t) = \log^2(t)$ is technically more involved to evaluate than $f(t) = \log(t)$. Precisely, the core of both results lies in the evaluation of the real integrals right above and under the branch cuts (as illustrated in Figure 3.5). The sum of every pair of integrals is of the form $\int_{\zeta_i+i0}^{\eta_i+i0} - \int_{\zeta_i-i0}^{\eta_i-i0} \log^a([\varphi_p/\psi_p](z))g(z)dz$ for some rational function $g(z)$ and $a \in \{1, 2\}$. Using the fact that $\log(\omega) = \log|\omega| + i\arg(\omega)$, for $a = 1$, $\log([\varphi_p/\psi_p](x+i0)) - \log([\varphi_p/\psi_p](x-i0)) = 2i\pi$ and the resulting real integral is thus still a rational function. For $a = 2$ though, $\log^2([\varphi_p/\psi_p](x+i0)) - \log^2([\varphi_p/\psi_p](x-i0)) = 2i\pi \log|[\varphi_p/\psi_p](x)|$ and thus the resulting integral involves products of logarithm and rational functions.

After careful calculus, we reach the following corollary.

Corollary 3.3 (Case $f(t) = \log^2(t)$). *Under the setting of Theorem 3.1, for*

$$f(t) = \log^2(t),$$

$$\begin{aligned} \hat{d}(\mathbf{X}_1, \mathbf{X}_2; f) &= \frac{c_1 + c_2 - c_1 c_2}{c_1 c_2} \left[\sum_{i=1}^p \log^2((1 - c_1)\eta_i) - \log^2((1 - c_1)\lambda_i) \right. \\ &\quad \left. + 2 \sum_{i,j=1}^p \left(\text{Li}_2\left(1 - \frac{\zeta_i}{\lambda_j}\right) - \text{Li}_2\left(1 - \frac{\eta_i}{\lambda_j}\right) + \text{Li}_2\left(1 - \frac{\eta_i}{\eta_j}\right) - \text{Li}_2\left(1 - \frac{\zeta_i}{\eta_j}\right) \right) \right] \\ &\quad - \frac{1 - c_2}{c_2} \left[\log^2(1 - c_2) - \log^2(1 - c_1) + \sum_{i=1}^p (\log^2(\eta_i) - \log^2(\zeta_i)) \right] \\ &\quad - \frac{1}{p} \left[2 \sum_{i,j=1}^p \left(\text{Li}_2\left(1 - \frac{\zeta_i}{\lambda_j}\right) - \text{Li}_2\left(1 - \frac{\eta_i}{\lambda_j}\right) \right) - \sum_{i=1}^p \log^2((1 - c_1)\lambda_i) \right] \end{aligned}$$

where $\text{Li}_2(x) = - \int_0^x \frac{\log(1-u)}{u} du$ is the dilogarithm function.

The case $f(t) = \log(1 + st)$, $s \in (0, \infty)$ is treated similarly as the case $f(t) = \log(t)$, with the main difference being a modification in the branch cuts that now occur when $\varphi_p(x)/\psi_p(x) < -1/s$ (rather than < 0). A new set of singularities $\kappa_0 < 0 < \kappa_1 < \dots < \kappa_p$, the zeros of $\varphi_p(x)/\psi_p(x) + 1/s$, are introduced. A simplification nonetheless allows one to express the resulting expression of the integral only as a function of κ_0 , as follows.

Corollary 3.4 (Case $f(t) = \log(1 + st)$). *Under the setting of Theorem 3.1, let $s > 0$ and $f(t) = \log(1 + st)$. Then,*

$$\begin{aligned} \hat{d}(\mathbf{X}_1, \mathbf{X}_2; f) &= \frac{c_1 + c_2 - c_1 c_2}{c_1 c_2} \log \left(\frac{c_1 + c_2 - c_1 c_2}{(1 - c_1)(c_2 - sc_1 \kappa_0)} \right) \\ &\quad + \frac{1}{c_2} \log(-s\kappa_0(1 - c_1)) + \int \log(1 - t/\kappa_0) \mu_p(dt) \end{aligned}$$

where $\kappa_0 < 0$ is the unique negative solution to $\varphi_p(\kappa_0)/\psi_p(\kappa_0) = -1/s$.

Details on the derivation of these results are available in [Couillet et al., 2019].

Table 3.2 illustrates, for the Fisher distance, the comparative performance gain of the large n, p -consistent estimator $\hat{d}_F(\mathbf{X}_1, \mathbf{X}_2) = \hat{d}(\mathbf{X}_1, \mathbf{X}_2; \log^2)$ proposed in Theorem 3.1 with respect to the traditional sample covariance plug-in estimator $d_F(\hat{\mathbf{C}}_1, \hat{\mathbf{C}}_2)$. It clearly appears that, as p/n_1 and p/n_2 become large (bottom part of the table), the standard large- n estimator dramatically fails, while the large- n, p consistent estimator remains quite accurate. More surprisingly is the fact that, even for small p , the large- n, p estimator still overtakes the large- n estimator. An evaluation of the respective estimate variances also reveals that both approaches have similar fluctuations around their mean estimate.

p	$d_F(\mathbf{C}_1, \mathbf{C}_2)$	$\hat{d}_F(\mathbf{X}_1, \mathbf{X}_2)$	$d_F(\hat{\mathbf{C}}_1, \hat{\mathbf{C}}_2)$
2	0.0533	0.0524	0.0568
4	0.0796	0.0840	0.0913
8	0.0927	0.0917	0.1048
16	0.0992	0.1007	0.1253
32	0.1025	0.1029	0.1509
64	0.1042	0.1049	0.2009
128	0.1050	0.1044	0.3023
256	0.1054	0.1057	0.5341
512	0.1056	0.1086	1.1556

Table 3.2: Estimation of the Fisher distance $d_F(\mathbf{C}_1, \mathbf{C}_2)$. Simulation example for $\mathbf{x}_i^{(a)} \sim \mathcal{N}(\mathbf{0}, \mathbf{C}_a)$ with $[\mathbf{C}_1]_{ij} = .2|i-j|$, $[\mathbf{C}_2]_{ij} = .4|i-j|$, $n_1 = 1024$, $n_2 = 2048$, as a function of p , results averaged over 30 runs. [Link to code]
tab:perf_cov_dist

rem:distance-estim-n12>p

Remark 3.3 (On the cases $c_1, c_2 > 1$). While the large- n standard estimator requires $n \gg p$ and thus $n > p$, most random matrix analyses only demand that n, p be simultaneously large. Yet, Theorem 3.1 explicitly demands that $c_1 = \lim p/n_1 < 1$ and $c_2 = \lim p/n_2 < 1$. A careful control of the two successive changes of variable indeed reveals that, for say $c_2 > 1$, the pre-image Γ_ν of a contour Γ_μ around $\text{supp}(\mu)$ necessarily encloses zero. For $f(z)$ analytic in a neighborhood of $z = 0$, this has no consequence. But for $f(z) = \log^a(z)$, this annihilates the derivation; to the best of our knowledge, no simple workaround exists in this case. The case $f(z) = \log(1 + sz)$ may still be valid, however only for sufficiently small values of s (that depend on c_1, c_2).

Remark 3.4 (Fluctuations). Being a linear statistics (although a rather involved one) of the eigenvalues of $\hat{\mathbf{C}}_1^{-1}\hat{\mathbf{C}}_2$ with n_1, n_2, p of similar order, the estimate $\hat{d}(\mathbf{X}_1, \mathbf{X}_2; f)$ can be shown to satisfy a central limit theorem with optimal speed $O(1/p)$, i.e.,

$$\hat{d}(\mathbf{X}_1, \mathbf{X}_2; f) = d(\mathbf{C}_1, \mathbf{C}_2; f) + \frac{1}{p}\mathcal{N}(M, \sigma^2) + o(p^{-1})$$

for some $M, \sigma^2 = O(1)$. Besides, in the complex Gaussian case (i.e., $\mathbf{x}_i^{(a)} \sim \mathcal{CN}(\mathbf{0}, \mathbf{C}_a)$, $M = 0$).

Remark 3.5 (On nonnegativity). It is important to stress that, although $\hat{d}(\mathbf{X}_1, \mathbf{X}_2; f) - d(\mathbf{C}_1, \mathbf{C}_2; f) \xrightarrow{a.s.} 0$, the nonnegativity of the distance $d(\mathbf{C}_1, \mathbf{C}_2; f)$ does not imply that of $\hat{d}(\mathbf{X}_1, \mathbf{X}_2; f)$. In particular, for f such that $d(\cdot, \cdot; f)$ is an actual distance, if $\mathbf{C}_1 = \mathbf{C}_2 = \mathbf{C}$, $d(\mathbf{C}, \mathbf{C}; f) = 0$ while $\hat{d}(\mathbf{X}_1, \mathbf{X}_2; f) = 0 + \frac{1}{p}\mathcal{N}(M, \sigma^2) + o(p^{-1})$ which is thus often negative (with nonzero probability).

3.2.4 The Wasserstein and Frobenius distances

sec:c1c2

As recalled in Remark 3.2, the Wasserstein distance between two centered Gaussian measures $\mathcal{N}(\mathbf{0}, \mathbf{C}_1)$ and $\mathcal{N}(\mathbf{0}, \mathbf{C}_2)$ is defined as

$$d_W(\mathbf{C}_1, \mathbf{C}_2) = \frac{1}{p} \text{tr}(\mathbf{C}_1) + \frac{1}{p} \text{tr}(\mathbf{C}_2) - 2 \int \sqrt{t} \nu_p^+(dt), \quad \nu_p^+ = \frac{1}{p} \sum_{i=1}^p \delta_{\lambda_i(\mathbf{C}_1 \mathbf{C}_2)}$$

where the $+$ sign in the exponent is here to recall that we take the product $\mathbf{C}_1^{+1} \mathbf{C}_2^{+1}$ rather than $\mathbf{C}_1^{-1} \mathbf{C}_2^{+1}$ as in the previous section.

In a similar manner, the Frobenius distance between \mathbf{C}_1 and \mathbf{C}_2 can be written as

$$d_{\text{Fro}}(\mathbf{C}_1, \mathbf{C}_2) = \frac{1}{p} \text{tr} \mathbf{C}_1^2 + \frac{1}{p} \text{tr} \mathbf{C}_2^2 - 2 \int t \nu_p^+(dt), \quad \nu_p^+ = \frac{1}{p} \sum_{i=1}^p \delta_{\lambda_i(\mathbf{C}_1 \mathbf{C}_2)}.$$

Yet, $\frac{1}{p} \text{tr} \hat{\mathbf{C}}_1 \hat{\mathbf{C}}_2$ is known to be a consistent estimate for $\frac{1}{p} \text{tr} \mathbf{C}_1 \mathbf{C}_2 = \int t \nu_p^+(dt)$, so that the present framework is of marginal interest for the covariance Frobenius distance.

For the square-root function in the case of Wasserstein distance and generic functions f though, the same framework as above may be used to estimate integral forms of the type

$$\int f(t) \nu_p^+(dt), \quad \nu_p^+ = \frac{1}{p} \sum_{i=1}^p \delta_{\lambda_i(\mathbf{C}_1 \mathbf{C}_2)}.$$

This is performed in [Tiomoko and Couillet, 2019] with the following result.

theo:cov_dist_product

Theorem 3.2 (Covariance distance estimate for product matrices, from [Tiomoko and Couillet, 2019]). *Let $f : \mathbb{R}^+ \rightarrow \mathbb{R}$ be a real function with a complex analytic extension on $\{z \in \mathbb{C}, \Re[z] > 0\}$ and $c_1, c_2 < 1$. Then, with the same notations as in Theorem 3.1,*

$$d_+(\mathbf{C}_1, \mathbf{C}_2; f) - \hat{d}_+(\mathbf{X}_1, \mathbf{X}_2; f) \xrightarrow{a.s.} 0$$

where

$$d_+(\mathbf{C}_1, \mathbf{C}_2; f) = \int f(t) \nu_p^+(dt), \quad \nu_p^+ = \frac{1}{p} \sum_{i=1}^p \delta_{\lambda_i(\mathbf{C}_1 \mathbf{C}_2)}$$

and

$$\hat{d}_+(\mathbf{X}_1, \mathbf{X}_2; f) = \frac{1}{2\pi i} \oint_{\Gamma_{\mu_p^+}} f\left(\frac{\varphi_p^+(u)}{\psi_p^+(u)}\right) \frac{\psi_p^+(u)}{c_2} \left[\frac{\varphi_p^{+'}(u)}{\varphi_p^+(u)} - \frac{\psi_p^{+'}(u)}{\psi_p^+(u)} \right] du$$

where $\varphi_p^+(z) = z/(1 - c_1 - c_1 z m_{\mu_p^+}(z))$, $\psi_p^+(z) = 1 - c_2 - c_2 z m_{\mu_p^+}(z)$ and μ_p^+ is the empirical spectral measure of $\hat{\mathbf{C}}_1 \hat{\mathbf{C}}_2$.

It is interesting to note that, “formally”, Theorem 3.2 only differs from Theorem 3.1 from the expression of $\psi_p(z)$, but of course μ_p is also now changed into μ_p^+ . Applied to the Wasserstein metric, a suitable complex integration calculus for the function $f(t) = \sqrt{t}$ leads to the following corollary.

coro:Wasserstein_dist

Corollary 3.5 (Wasserstein distance estimate). *Under the setting of Theorem 3.2, let $\lambda = (\lambda_1, \dots, \lambda_p)^\top$ and $\Lambda = \text{diag}(\lambda)$, for $\lambda_1 \leq \dots \leq \lambda_p$ the eigenvalues of $\hat{\mathbf{C}}_1 \hat{\mathbf{C}}_2$. Then,*

$$\hat{d}_+(\mathbf{C}_1, \mathbf{C}_2; \sqrt{\cdot}) - \hat{d}_+(\mathbf{X}_1, \mathbf{X}_2; \sqrt{\cdot}) \xrightarrow{a.s.} 0$$

where, for $n_1 \neq n_2$,

$$\hat{d}_+(\mathbf{X}_1, \mathbf{X}_2; \sqrt{\cdot}) = \frac{2}{\sqrt{c_1 c_2}} \sum_{j=1}^p \sqrt{\lambda_j} + \frac{2}{\pi c_2} \sum_{j=1}^p \int_{\xi_j}^{\eta_j} \sqrt{-\frac{\varphi_p^+(x)}{\psi_p^+(x)}} \psi_p^{+'}(x) dx$$

while, for $n_1 = n_2$,

$$\hat{d}_+(\mathbf{X}_1, \mathbf{X}_2; \sqrt{\cdot}) = \frac{2}{c_2} \sum_{j=1}^p (\sqrt{\lambda_j} - \sqrt{\xi_j})$$

with $\{\xi_j\}_{j=1}^p$ and $\{\eta_j\}_{j=1}^p$ the increasing eigenvalues of $\Lambda - \frac{\sqrt{\lambda} \sqrt{\lambda}^\top}{n_1}$ and $\Lambda - \frac{\sqrt{\lambda} \sqrt{\lambda}^\top}{n_2}$, respectively.

The formula is particularly attractive in the case where $n_1 = n_2$, although its formal interpretation is not obvious. In Section 3.5, the detailed derivation and empirical evaluation of Corollary 3.5 above are provided in the form of a practical lecture material.

3.2.5 Application to covariance-based spectral clustering

In machine learning, the distance $d(\cdot, \cdot)$ between statistical covariance matrices \mathbf{C}_i is a popular *feature* to compare and classify data sets of, say, m data $\mathbf{X}_1, \dots, \mathbf{X}_m$, where each datum \mathbf{X}_i is composed of n_i vectors $\mathbf{X}_i = [\mathbf{x}_1^{(i)}, \dots, \mathbf{x}_{n_i}^{(i)}]$ with $\mathbb{E}[\mathbf{x}_j^{(i)}] = 0$ and $\mathbb{E}[\mathbf{x}_j^{(i)} \mathbf{x}_j^{(i)\top}] = \mathbf{C}_i$ (for instance, \mathbf{X}_i is n_i consecutive samples from a multivariate time series). These data can then be discriminated from their covariances. Here, we will not be concerned with the size of m (which may be small or growing with n_i, p) but will impose that n_1, \dots, n_m, p all large and comparable (and in particular $n_1, \dots, n_m > p$ according to Remark 3.3).

With these m observations $\mathbf{X}_1, \dots, \mathbf{X}_m$, classification based on a standard Gaussian kernel method would typically consist in assessing the kernel matrix

$$\mathbf{K} = \left\{ \exp \left(-\frac{1}{2} d(\mathbf{C}_i, \mathbf{C}_j) \right) \right\}_{i,j=1}^m$$

and then proceed to either a support vector classifier in a supervised setting or spectral clustering when unsupervised. As we now know that estimating $d(\mathbf{C}_i, \mathbf{C}_j)$ by $d(\hat{\mathbf{C}}_i, \hat{\mathbf{C}}_j)$ may lead to dramatically erroneous results, \mathbf{K}_{ij} may be more appropriately estimated by

$$\hat{\mathbf{K}}_{ij} = \left\{ \exp \left(-\frac{1}{2} \hat{d}(\mathbf{X}_i, \mathbf{X}_j) \right) \right\}_{i,j=1}^m.$$

Figure 3.6 illustrates this idea in the context of spectral clustering of two classes, where $\mathbf{C}_1 = \dots = \mathbf{C}_{m/2} = \mathbf{C}^{(1)}$ (class 1) and $\mathbf{C}_{m/2+1} = \dots = \mathbf{C}_m = \mathbf{C}^{(2)}$ (class 2). There are depicted the dominant two eigenvectors of $\hat{\mathbf{K}}$, compared with those obtained by the classical estimates $d(\hat{\mathbf{C}}_i, \hat{\mathbf{C}}_j)$. The difference between these two methods is particularly remarkable as the number of samples n_i for each data differs: in this case, the estimation bias induced by $d(\hat{\mathbf{C}}_i, \hat{\mathbf{C}}_j)$ strongly depends on n_i, n_j and thus differently affects each single estimate. This is seen in the left display by the important spread of the pairs of eigenvector entries when the n_i 's are all different, and in the right display by the singular behavior of the only pair with different n_i value. Spectral clustering performs significantly better with the random matrix-improved kernel.

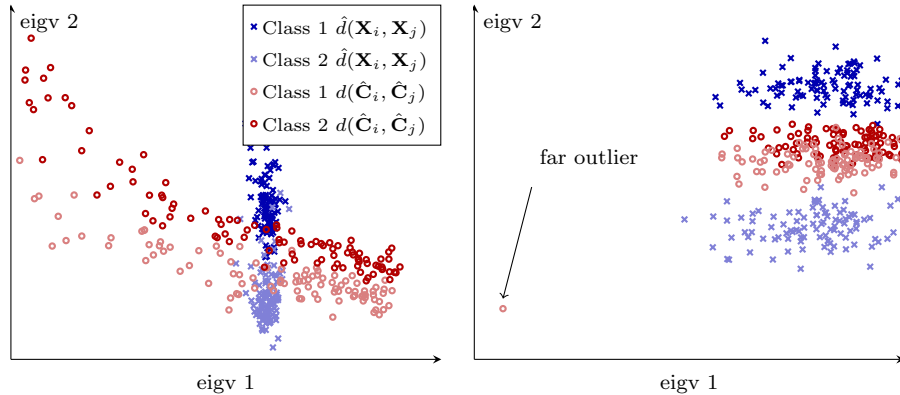


Figure 3.6: First and second eigenvectors of $\hat{\mathbf{K}}$ with $\hat{\mathbf{K}}_{ij} = \exp(-\frac{1}{2}\hat{d}(\mathbf{X}_i, \mathbf{X}_j))$ (blue crosses) versus $\hat{\mathbf{K}}_{ij} = \exp(-\frac{1}{2}d(\hat{\mathbf{C}}_i, \hat{\mathbf{C}}_j))$ (red circles); with random number of snapshots n_i (left) and $n_1 = \dots = n_{m-1} = 512$ and $n_m = 256$ (right).
[\[Link to code\]](#)

`fig:cov_estimate_spectral_clustering`

3.3 M-estimators of scatter

`sec:M-estimator`

3.3.1 Reminder on robust statistics

Most probabilistic data models revolve around a Gaussian assumption: in signal processing additive noise models are mostly Gaussian, while in machine

learning the Gaussian mixture model is quite popular. As already mentioned in Section 2.7, Gaussian models may adequately be replaced by a larger class of concentrated random vector models in large dimensions with little impact on the behavior of many machine learning algorithms. Yet, Gaussian as well as concentrated random vectors precisely share the property that “behave in a smooth and controllable way”. Data polluted by outliers, missing entries, duplicates, etc., can typically not be accounted for by Gaussian or even concentrated vector models.

To consider these outlying data in the models, Huber and his successors developed in the sixties the field of *robust statistics* [Huber, 2011, Maronna et al., 2018]. The basic observation of Huber lies in the lack of “robustness” of sample estimators (sample mean, sample variance and covariance matrix) to the presence of a single arbitrarily deviant outlying sample. Typically, for i.i.d. scalar samples $x_1, \dots, x_n \in \mathbb{R}$ with mean $M = \mathbb{E}[x_i]$, $\frac{1}{n} \sum_{i=1}^n x_i \xrightarrow{a.s.} M$ by the law of large numbers. Yet, the addition of x_0 with arbitrarily large amplitude to the sample average can drive $\frac{1}{n+1} \sum_{i=0}^n x_i$ arbitrarily far from M .

Huber proposed a min-max statistical mean and covariance estimation procedure in [Huber, 2011] that reduces the negative impact of outliers. The underlying assumption of Huber’s work is that the data x_i arise from a mixture of laws $(1 - \epsilon)\mu + \epsilon\mu'$ with μ a known “well-behaved” measure, μ' an unknown arbitrary measure and $\epsilon > 0$ small. The work of Maronna in [Maronna, 1976] generalizes that of Huber by letting x_i belong to a class of (multivariate) generalized Gaussian distributions, and notably of elliptical measures. A vector $\mathbf{x}_i \in \mathbb{R}^p$ is elliptically distributed if it can be written under the form

$$\mathbf{x}_i = \boldsymbol{\mu} + \sqrt{\tau_i} \mathbf{C}^{\frac{1}{2}} \mathbf{z}_i \quad \text{eq: def-elliptical (3.6)}$$

where \mathbf{z}_i is drawn uniformly at random on the sphere centered at zero and of radius \sqrt{p} , $\tau_i > 0$ is also drawn at random independently of \mathbf{z}_i and nonnegative definite $\mathbf{C} \in \mathbb{R}^{p \times p}$ is the so-called *scatter matrix*. The law of the parameters τ_i (and notably its moments) controls the degree of “impulsivity” of the data. When $\boldsymbol{\mu} = \mathbf{0}$ and $\mathbb{E}[\tau_i]$ is finite, then \mathbf{C} is proportional to the population covariance of \mathbf{x}_i ; if $\mathbb{E}[\tau_i] = \infty$, the covariance is not defined. Multivariate Gaussian (for which $\tau_i \xrightarrow{a.s.} 1$ as $p \rightarrow \infty$) and Student-t distributions belong to the class of elliptical distributions. Maronna derived the maximum likelihood estimators for $\boldsymbol{\mu}$ and \mathbf{C} for generic measures \mathcal{T} of the τ_i ’s. These generalize the sample covariance matrix, include Huber’s estimator as a special case, and are particularly resilient to “outlying” samples from the dataset.

3.3.2 The M-estimator of scatter

Of particular interest to the sample covariance matrix thoroughly explored in this monograph is its relation to the M-estimators of scatter matrices. Under both Huber and Maronna’s framework, for $\mathbf{x}_1, \dots, \mathbf{x}_n \in \mathbb{R}^p$ data samples with $n > p$, Maronna’s estimator of scatter $\hat{\mathbf{C}} \in \mathbb{R}^{p \times p}$ is defined as a solution to the

fixed-point equation

$$\hat{\mathbf{C}} = \frac{1}{n} \sum_{i=1}^n u \left(\frac{1}{p} \mathbf{x}_i^\top \hat{\mathbf{C}}^{-1} \mathbf{x}_i \right) \mathbf{x}_i \mathbf{x}_i^\top \quad \text{eq:robust_estimator} \quad (3.7)$$

for $u : \mathbb{R}^+ \rightarrow \mathbb{R}^+$ a non-increasing function such that $\varphi(x) = xu(x)$ is increasing and bounded. Typical examples of such functions are $u(x) = (1+\alpha)/(x+\alpha)$ for some $\alpha > 0$ (this is the prototype of functions met in the maximum likelihood estimator of scatter for Student-t distributions) and $u(x) = \min\{\alpha/x, \beta\}$ for some $\alpha, \beta > 0$ (this is the prototype of Huber's robust estimators).

Under these assumptions for u , if $n > p$ and the \mathbf{x}_i 's are linearly independent, the solution $\hat{\mathbf{C}}$ to (3.7) can be shown to exist and be unique. Besides, the iterative fixed-point algorithm consisting in letting $\hat{\mathbf{C}}_0 = \mathbf{I}_p$ and, for $t \geq 0$,

$$\hat{\mathbf{C}}_{t+1} = \frac{1}{n} \sum_{i=1}^n u \left(\frac{1}{p} \mathbf{x}_i^\top \hat{\mathbf{C}}_t^{-1} \mathbf{x}_i \right) \mathbf{x}_i \mathbf{x}_i^\top$$

converges to $\hat{\mathbf{C}}$ as $t \rightarrow \infty$.

Due to their implicit definition, the behavior of these estimators is particularly difficult to apprehend. Still, it is interesting to observe the mode of action of $\hat{\mathbf{C}}$: u being decreasing, $\hat{\mathbf{C}}$ essentially reduces the impact of those \mathbf{x}_i 's such that $\mathbf{x}_i^\top \hat{\mathbf{C}}^{-1} \mathbf{x}_i$ is large; that is, (i) those \mathbf{x}_i 's having too large amplitude (i.e., large values of τ_i in the case of elliptical distributions) or (ii) those \mathbf{x}_i 's having a weak correlation to the dominant eigenvectors of $\hat{\mathbf{C}}$.

Under a finite n, p regime though, no much more can be said about $\hat{\mathbf{C}}$. However, under a large sample setting where $n \rightarrow \infty$ alone, it was shown that, if the \mathbf{x}_i 's are i.i.d. and elliptically distributed, $\hat{\mathbf{C}}$ converges almost surely to a matrix equal, up to a multiplicative constant, to \mathbf{C} .

A particular difficulty in handling the large- n alone scenario is that the quadratic form $\frac{1}{p} \mathbf{x}_i^\top \hat{\mathbf{C}}^{-1} \mathbf{x}_i$ does not concentrate and thus remains a rather involved random variable. This problem is completely alleviated in the large n, p regime. However, since $\hat{\mathbf{C}}$ depends on \mathbf{x}_i in a non-trivial manner, the large n, p limit of $\frac{1}{p} \mathbf{x}_i^\top \hat{\mathbf{C}}^{-1} \mathbf{x}_i$ is not as simple as for the sample covariance matrix.

3.3.3 The random matrix framework

sec:robust_intuitive

It is not easy to directly obtain a deterministic equivalent, or any asymptotic spectral behavior, for the robust estimator of scatter $\hat{\mathbf{C}}$ from (3.7), due to its implicit definition.

The objective of this section is to show that, when $n, p \rightarrow \infty$, $\hat{\mathbf{C}}$ asymptotically behaves similarly to another random matrix $\hat{\mathbf{S}}$ in the sense that $\|\hat{\mathbf{C}} - \hat{\mathbf{S}}\| \xrightarrow{a.s.} 0$. The matrix $\hat{\mathbf{S}}$ is not observable but tractable via a random matrix analysis. Since the convergence $\|\hat{\mathbf{C}} - \hat{\mathbf{S}}\| \xrightarrow{a.s.} 0$ transfers many spectral properties from $\hat{\mathbf{S}}$ to $\hat{\mathbf{C}}$, the behavior of $\hat{\mathbf{C}}$ can thus be easily understood: deterministic equivalents for $\hat{\mathbf{C}}$ will then be transferred from deterministic equivalents for $\hat{\mathbf{S}}$.

We consider here the setting $\mathbf{x}_1, \dots, \mathbf{x}_n \in \mathbb{R}^p$ arise from a zero-mean elliptical distribution, i.e., $\mathbf{x}_i = \sqrt{\tau_i} \mathbf{C}^{\frac{1}{2}} \mathbf{z}_i$ as above with $\boldsymbol{\mu} = \mathbf{0}$ and $n > p$. Besides, the τ_i 's are positive i.i.d. random variables with measure \mathcal{T} having finite first order moment.

A first key observation is that one may already assume $\mathbf{C} = \mathbf{I}_p$ in the study of $\hat{\mathbf{C}}$. Indeed, by definition

$$\mathbf{C}^{-\frac{1}{2}} \hat{\mathbf{C}} \mathbf{C}^{-\frac{1}{2}} = \frac{1}{n} \sum_{i=1}^n u \left(\frac{1}{p} \mathbf{x}_i^\top \mathbf{C}^{-\frac{1}{2}} (\mathbf{C}^{-\frac{1}{2}} \hat{\mathbf{C}} \mathbf{C}^{-\frac{1}{2}})^{-1} \mathbf{C}^{-\frac{1}{2}} \mathbf{x}_i \right) \mathbf{C}^{-\frac{1}{2}} \mathbf{x}_i \mathbf{x}_i^\top \mathbf{C}^{-\frac{1}{2}}$$

and thus, it is equivalent for $\hat{\mathbf{C}}$ to be the solution to the original problem for the data \mathbf{x}_i and for $\mathbf{C}^{-\frac{1}{2}} \hat{\mathbf{C}} \mathbf{C}^{-\frac{1}{2}}$ to be the solution to the same problem but with $\mathbf{C}^{-\frac{1}{2}} \mathbf{x}_i$. We may then simply assume from now on that

$$\mathbf{x}_i = \sqrt{\tau_i} \mathbf{z}_i.$$

We mostly provide here the intuitive derivation of the main result, with a few words on the actual rigorous proof approach at the end. The idea starts with the following intuition: letting

$$\hat{\mathbf{C}}_{-i} = \hat{\mathbf{C}} - \frac{1}{n} u \left(\frac{1}{p} \mathbf{x}_i^\top \hat{\mathbf{C}}^{-1} \mathbf{x}_i \right) \mathbf{x}_i \mathbf{x}_i^\top = \frac{1}{n} \sum_{j \neq i} u \left(\frac{1}{p} \mathbf{x}_j^\top \hat{\mathbf{C}}^{-1} \mathbf{x}_j \right) \mathbf{x}_j \mathbf{x}_j^\top$$

it is clear that \mathbf{x}_i depends on $\hat{\mathbf{C}}_{-i}$ (because \mathbf{x}_i is part of $\hat{\mathbf{C}}$ appearing in each quadratic form $\frac{1}{p} \mathbf{x}_j^\top \hat{\mathbf{C}}^{-1} \mathbf{x}_j$); yet, this dependence is seemingly “asymptotically weak” as \mathbf{x}_i only accounts for one out of n constitutive elements in $\hat{\mathbf{C}}$ and thus the quadratic forms $\frac{1}{p} \mathbf{x}_j^\top \hat{\mathbf{C}}^{-1} \mathbf{x}_j$, $j \neq i$, barely depend on \mathbf{x}_i .

If this intuition is correct, then we expect the trace-lemma, Lemma 2.11, to hold for $\frac{1}{p} \mathbf{x}_i^\top \hat{\mathbf{C}}_{-i}^{-1} \mathbf{x}_i$, that is we expect

$$\frac{1}{p} \mathbf{x}_i^\top \hat{\mathbf{C}}_{-i}^{-1} \mathbf{x}_i = \tau_i \frac{1}{p} \mathbf{z}_i^\top \hat{\mathbf{C}}_{-i}^{-1} \mathbf{z}_i \simeq \tau_i \frac{1}{p} \text{tr } \hat{\mathbf{C}}_{-i}^{-1} \simeq \tau_i \frac{1}{p} \text{tr } \hat{\mathbf{C}}^{-1} \equiv \tau_i \gamma_p$$

where in the last line we applied the rank-one perturbation Lemma 2.9 and denote $\gamma_p \equiv \frac{1}{p} \text{tr } \hat{\mathbf{C}}^{-1}$.

In order to exploit the concentration $\frac{1}{p} \mathbf{x}_i^\top \hat{\mathbf{C}}_{-i}^{-1} \mathbf{x}_i \simeq \tau_i \gamma_p$, we now need to express $\hat{\mathbf{C}}$ as a function of such quadratic forms. To this end, by Lemma 2.8, first observe that

$$\frac{1}{p} \mathbf{x}_i^\top \hat{\mathbf{C}}^{-1} \mathbf{x}_i = \frac{\frac{1}{p} \mathbf{x}_i^\top \hat{\mathbf{C}}_{-i}^{-1} \mathbf{x}_i}{1 + \frac{1}{n} u(\frac{1}{p} \mathbf{x}_i^\top \hat{\mathbf{C}}^{-1} \mathbf{x}_i) \mathbf{x}_i^\top \hat{\mathbf{C}}_{-i}^{-1} \mathbf{x}_i}$$

which we may equivalently rewrite as

$$\frac{1}{p} \mathbf{x}_i^\top \hat{\mathbf{C}}_{-i}^{-1} \mathbf{x}_i = \frac{\frac{1}{p} \mathbf{x}_i^\top \hat{\mathbf{C}}^{-1} \mathbf{x}_i}{1 - \frac{p}{n} \varphi(\frac{1}{p} \mathbf{x}_i^\top \hat{\mathbf{C}}^{-1} \mathbf{x}_i)} \quad (3.8)$$

assuming $1 - \frac{p}{n}\varphi(\frac{1}{p}\mathbf{x}_i^\top \hat{\mathbf{C}}^{-1} \mathbf{x}_i) \neq 0$, where we recall that $\varphi(x) = xu(x)$.

Consequently, if the mapping

$$\begin{aligned} g : \mathbb{R}^+ &\rightarrow \mathbb{R}^+ \\ x &\mapsto \frac{x}{1 - c\varphi(x)} \end{aligned}$$

with $c = p/n$, is bijective, one can express $\frac{1}{p}\mathbf{x}_i^\top \hat{\mathbf{C}}^{-1} \mathbf{x}_i$ as

$$\frac{1}{p}\mathbf{x}_i^\top \hat{\mathbf{C}}^{-1} \mathbf{x}_i = g^{-1}\left(\frac{1}{p}\mathbf{x}_i^\top \hat{\mathbf{C}}_{-i}^{-1} \mathbf{x}_i\right).$$

This is indeed the case ($g'(x) > 0$ and $g(0) = 0$, $g(\infty) = \infty$) so long that $\|\varphi\|_\infty < c^{-1}$.

Thus, under this assumption, we may rewrite $\hat{\mathbf{C}}$ under the form

$$\hat{\mathbf{C}} = \frac{1}{n} \sum_{i=1}^n v\left(\frac{1}{p}\mathbf{x}_i^\top \hat{\mathbf{C}}_{-i}^{-1} \mathbf{x}_i\right) \mathbf{x}_i \mathbf{x}_i^\top$$

where we introduced the notation $v = u \circ g^{-1}$, a non-increasing function alike u . As $\frac{1}{p}\mathbf{x}_i^\top \hat{\mathbf{C}}_{-i}^{-1} \mathbf{x}_i \simeq \tau_i \gamma_p$, this is further

$$\begin{aligned} \hat{\mathbf{C}} &= \frac{1}{n} \sum_{i=1}^n v(\tau_i \gamma_p) \mathbf{x}_i \mathbf{x}_i^\top + o_{\|\cdot\|}(1) \\ &= \frac{1}{n} \sum_{i=1}^n \tau_i v(\tau_i \gamma_p) \mathbf{z}_i \mathbf{z}_i^\top + o_{\|\cdot\|}(1) \\ &= \frac{1}{\gamma_p} \frac{1}{n} \sum_{i=1}^n \psi(\tau_i \gamma_p) \mathbf{z}_i \mathbf{z}_i^\top + o_{\|\cdot\|}(1) \end{aligned}$$

where we defined $\psi(x) = xv(x)$ which, similar to φ , is increasing and bounded. It finally remains to evaluate γ_p . By definition

$$\gamma_p = \frac{1}{p} \text{tr } \hat{\mathbf{C}}^{-1} \simeq \frac{1}{p} \text{tr} \left(\frac{1}{\gamma_p} \frac{1}{n} \sum_{i=1}^n \psi(\tau_i \gamma_p) \mathbf{z}_i \mathbf{z}_i^\top \right)^{-1}$$

or equivalently

$$1 \simeq \frac{1}{p} \text{tr} \left(\frac{1}{n} \sum_{i=1}^n \psi(\tau_i \gamma_p) \mathbf{z}_i \mathbf{z}_i^\top \right)^{-1}. \quad \text{eq:robust.1=}(3.9)\parallel$$

As you expect $\gamma_p \rightarrow \gamma$ deterministic as $n, p \rightarrow \infty$, the trace above is merely the Stieltjes transform evaluated at zero of the matrix $\frac{1}{n}\mathbf{Z}\mathbf{D}\mathbf{Z}^\top$ where $\mathbf{Z} = [\mathbf{z}_1, \dots, \mathbf{z}_n]$ and \mathbf{D} is diagonal with $\mathbf{D}_{ii} = \psi(\tau_i \gamma)$. Since ψ is bounded, $c = p/n < 1$ and \mathbf{z}_i is a concentrated random vector (that can be seen as a normalized

random Gaussian vector with norm tending to one), the Stieltjes transform for this model is well defined at zero and, from Theorem 2.5 or Theorem 2.17, has limit

$$\begin{aligned} m_{\frac{1}{n}\mathbf{ZDZ}^T}(0) &\xrightarrow{a.s.} m(0) \\ \frac{1}{m(0)} &= \int \frac{\psi(t\gamma)\mathcal{T}(dt)}{1 + c\psi(t\gamma)m(0)} \end{aligned}$$

where we recall that \mathcal{T} is the law of the τ_i 's. Moreover, since $m(0) = 1$ by (3.9), we conclude that γ is solution to:

$$1 = \int \frac{\psi(t\gamma)\mathcal{T}(dt)}{1 + c\psi(t\gamma)}.$$

This derivation allows us to conclude on the following asymptotic behavior for $\hat{\mathbf{C}}$.

theo:robust_est

Theorem 3.3 (Asymptotic equivalent for $\hat{\mathbf{C}}$, from [Couillet et al., 2015]). *Let $\mathbf{x}_1, \dots, \mathbf{x}_n \in \mathbb{R}^p$, $c = p/n < 1$, with $\mathbf{x}_i = \sqrt{\tau_i} \mathbf{C}^{\frac{1}{2}} \mathbf{z}_i$, τ_i i.i.d. with law \mathcal{T} of bounded moment of order $1+\varepsilon$ (for some $\varepsilon > 0$), $\mathbf{C} \in \mathbb{R}^{p \times p}$ positive definite and $\mathbf{z}_i \in \mathbb{R}^p$ i.i.d. uniformly drawn at random on the sphere of mean zero and radius \sqrt{p} . Further $u : \mathbb{R}^+ \rightarrow \mathbb{R}^+$ be a non-increasing function such that $\varphi(x) = xu(x)$ is increasing and bounded by c^{-1} . Then*

$$\|\hat{\mathbf{C}} - \hat{\mathbf{S}}\| \xrightarrow{a.s.} 0$$

where

$$\hat{\mathbf{C}} = \frac{1}{n} \sum_{i=1}^n u\left(\frac{1}{p} \mathbf{x}_i^T \hat{\mathbf{C}}^{-1} \mathbf{x}_i\right) \mathbf{x}_i \mathbf{x}_i^T, \quad \hat{\mathbf{S}} = \frac{1}{n} \sum_{i=1}^n v(\tau_i \gamma) \mathbf{x}_i \mathbf{x}_i^T$$

with $v = u \circ g^{-1}$, $g(x) = x/(1 - c\phi(x))$ and, for $\psi(x) = xv(x)$, γ the unique positive solution to

$$1 = \int \frac{\psi(t\gamma)}{1 + c\psi(t\gamma)} \mathcal{T}(dt).$$

The fundamental result behind Theorem 3.3 is that, under an elliptical data model (the result would of course vary under other statistical assumptions), $\hat{\mathbf{C}}$ has the same asymptotic spectral behavior as the random matrix $\hat{\mathbf{S}}$. Now, unlike $\hat{\mathbf{C}}$, $\hat{\mathbf{S}}$ follows a quite elementary statistical model:

$$\hat{\mathbf{S}} = \frac{1}{n} \mathbf{C}^{\frac{1}{2}} \mathbf{ZDZ}^T \mathbf{C}^{\frac{1}{2}}, \quad \mathbf{Z} = [\mathbf{z}_1, \dots, \mathbf{z}_n], \quad \mathbf{D} = \text{diag}\{\tau_i v(\tau_i \gamma)\}_{i=1}^n.$$

Since the τ_i 's are independent of the \mathbf{z}_i 's, $\hat{\mathbf{S}}$ is merely a sample covariance matrix model with weights \mathbf{D}_{ii} on the samples. This model is thus completely

characterized by Theorem 2.6 which in particular provides the limiting spectral distribution for $\hat{\mathbf{S}}$ which is identical to that of $\hat{\mathbf{C}}$. These are depicted in Figure 3.8 and can be compared to the limiting spectral measure of the sample covariance matrix $\frac{1}{n}\mathbf{XX}^\top$ in Figure 3.7, here for τ_i i.i.d. following a Gamma distribution. Of utmost interest from these figures is to remark that, while the limiting support of $\mu_{\frac{1}{n}\mathbf{XX}^\top}$ is (provably) unbounded, since the Gamma distribution itself has unbounded support, the limiting support of $\mu_{\hat{\mathbf{C}}}$ (and of $\mu_{\hat{\mathbf{S}}}$) are bounded.

Besides, it can be easily checked that $\|\hat{\mathbf{C}}\|$ is also almost surely bounded by writing $\hat{\mathbf{S}} = \frac{1}{n}\mathbf{C}^{\frac{1}{2}}\mathbf{WDW}^\top\mathbf{C}^{\frac{1}{2}}$, where $\|\mathbf{C}\|$ is bounded and $\mathbf{D} = \text{diag}\{\tau_i v(\tau_i \gamma)\}_{i=1}^n$ the entries of which are bounded as $\tau_i v(\tau_i \gamma) = \psi(\tau_i \gamma)/\gamma < \|\psi\|_\infty/\gamma$ which is finite.

The spectrum boundedness has one key consequence to spiked-model versions of the model.

Remark 3.6 (Robust Spiked Model). *The model $\mathbf{x}_i = \sqrt{\tau_i} \mathbf{C}^{\frac{1}{2}} \mathbf{z}_i$ with $\mathbf{C} = \mathbf{I}_p$ is appropriate to model impulsive noise in signal processing applications, particularly so in array processing where radar signals are likely impulsive. In this array processing context, the natural extension to an information-plus-noise model reads*

$$\mathbf{x}_i = \mathbf{a} s_i + \sqrt{\tau_i} \mathbf{z}_i$$

for a certain information vector $\mathbf{a} \in \mathbb{R}^p$ (to be detected and estimated) and possibly some scalar random signal $s_i \in \mathbb{R}$. Writing $\mathbf{X} = [\mathbf{x}_1, \dots, \mathbf{x}_n] \in \mathbb{R}^{p \times n}$,

$$\mathbf{X} = \mathbf{a} \mathbf{s}^\top + \mathbf{Z} \mathbf{T}^{\frac{1}{2}}, \quad \mathbf{T} = \text{diag}\{\tau_i\}_{i=1}^n, \quad \mathbf{s} = [s_1, \dots, s_n]^\top$$

which follows a spiked model.

However, due to the presence of the unbounded norm \mathbf{T} matrix, the sample covariance $\frac{1}{n}\mathbf{XX}^\top$ has unbounded limiting support and thus no visible spike for all large n, p . As a main deleterious consequence, the signal \mathbf{a} can be neither detected nor estimated with spectral methods from the sample covariance.

Letting instead $\hat{\mathbf{C}} = \frac{1}{n} \sum_{i=1}^n u(\frac{1}{p} \mathbf{x}_i^\top \hat{\mathbf{C}}^{-1} \mathbf{x}_i) \mathbf{x}_i \mathbf{x}_i^\top$ be the robust estimator of scatter, it is easily shown that $\|\hat{\mathbf{C}} - \hat{\mathbf{S}}\| \xrightarrow{a.s.} 0$ with $\hat{\mathbf{S}} = \frac{1}{n} \mathbf{Z} \mathbf{D} \mathbf{Z}^\top$ for $\mathbf{D} = \text{diag}\{\tau_i v(\tau_i \gamma)\}_{i=1}^n$ for the same γ defined in the noise-alone model. Since \mathbf{D} is bounded, this model for $\hat{\mathbf{S}}$ now is a proper spiked-model, allowing for the detection and estimation of \mathbf{a} . See details in [Couillet, 2015]. A particular feature of this spiked model is that, since the τ_i 's tend to spread due to their impulsive nature, even for large n , the support of \mathbf{D} may be quite scattered (all the more so when $u(x)$ is close to 1). This is a problem in practice as \mathbf{D} may induce its own “spikes” that is apt to be confused with the genuine informative spikes. Here, a very peculiar phenomenon arises: since $\|\mathbf{D}\| \leq \|\psi\|_\infty/\gamma$, the noise-only model satisfies $\limsup \|\frac{1}{n} \mathbf{Z} \mathbf{D} \mathbf{Z}^\top\| \leq \|\psi\|_\infty(1 + \sqrt{c})^2/\gamma \equiv S^+$ almost surely. Therefore, the noise-induced spikes can (asymptotically) not be found beyond S^+ , while the genuine spikes may. We thus have the typical picture of

Figure 3.9 where (i) between the right-edge S_μ^+ of the support of the limiting spectrum μ of $\hat{\mathbf{C}}$ and S^+ , one can find both genuine and noise-driven spikes, while (ii) beyond S^+ only genuine informative spikes can be found.

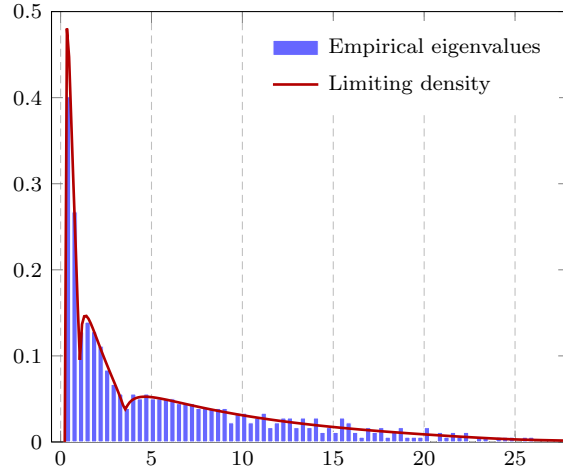


Figure 3.7: Histogram of the eigenvalues of $\frac{1}{n} \mathbf{X} \mathbf{X}^\top$ for $n = 2500$, $p = 500$, $\mathbf{C} = \text{diag}\{\mathbf{I}_{p/4}, 3\mathbf{I}_{p/4}, 10\mathbf{I}_{p/2}\}$, τ_i with $\Gamma(.5, 2)$ -distribution. [\[Link to code\]](#) [fig:robust_est_hist_sample_cov](#)

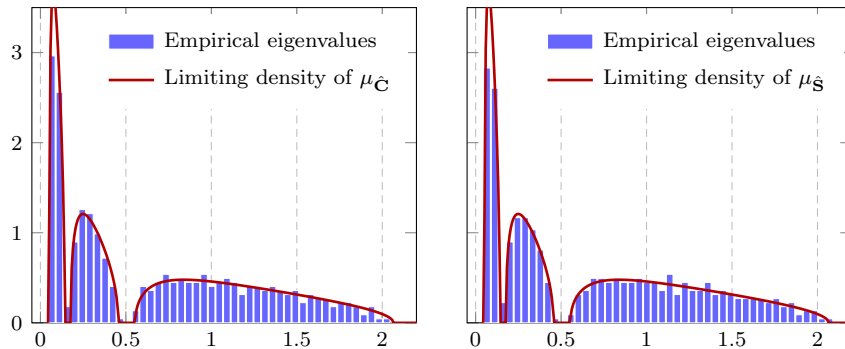


Figure 3.8: Histogram of the eigenvalues of $\hat{\mathbf{C}}$ (left) and $\hat{\mathbf{S}}$ (right) in the same setting of Figure 3.7, for $u(x) = (1 + \alpha)/(\alpha + x)$ with $\alpha = 0.2$. [\[Link to code\]](#) [fig:robust_est_hist_hatS](#)

3.3.3.1 A few words on the rigorous proof

The derivation leading up to Theorem 3.3 strongly relies on the claim that the trace lemma concentration

$$\frac{1}{p} \mathbf{z}_i^\top \hat{\mathbf{C}}_{-i}^{-1} \mathbf{z}_i \simeq \frac{1}{p} \text{tr } \hat{\mathbf{C}}_{-i}^{-1} \simeq \gamma$$

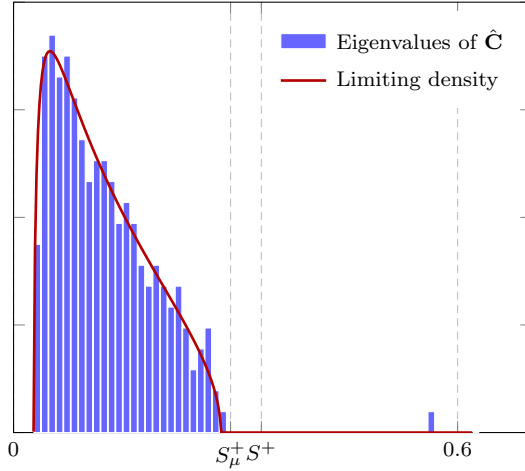


Figure 3.9: Histogram of the eigenvalues of $\hat{\mathbf{C}}$ in a single-spike model, for $u(x) = (1 + \alpha)/(\alpha + x)$ with $\alpha = 0.2$, $p = 256$, $n = 1024$, Student-t \mathcal{T}_ν 's. [\[Link to code\]](#) [fig_robust_est_spike](#)

effectively holds true, uniformly so on $1 \leq i \leq n$, despite the dependence between \mathbf{z}_i and $\hat{\mathbf{C}}_{-i}$. The strategy proposed in [Couillet et al., 2015] to prove this result is to “sandwich” the quantities $\frac{1}{p}\mathbf{z}_i^\top \hat{\mathbf{C}}_{-i}^{-1} \mathbf{z}_i$ for $1 \leq i \leq n$ between two quantities with no dependence problem and which are easily shown to converge to γ .

However, as $\frac{1}{p}\mathbf{z}_i^\top \hat{\mathbf{C}}_{-i}^{-1} \mathbf{z}_i$ appears as arguments of the function v , this sandwiching idea must be extended to a more convenient quantity. Precisely, recalling that we may assume $\mathbf{C} = \mathbf{I}_p$ in the proof, we let

$$e_i = \frac{v\left(\frac{1}{p}\mathbf{x}_i^\top \hat{\mathbf{C}}_{-i}^{-1} \mathbf{x}_i\right)}{v(\tau_i \gamma)}$$

and relabel the e_i 's indices in such a way that $e_1 \leq \dots \leq e_n$. The main idea is then to observe that, letting $d_i = \frac{1}{p}\mathbf{z}_i^\top \hat{\mathbf{C}}_{-i}^{-1} \mathbf{z}_i$, we have $v(\tau_i d_i) = e_i v(\tau_i \gamma)$, and thus

$$\begin{aligned} e_i &= \frac{v\left(\tau_i \frac{1}{p}\mathbf{z}_i^\top \left(\frac{1}{n} \sum_{j \neq i} \tau_j v(\tau_j d_j) \mathbf{z}_j \mathbf{z}_j^\top\right)^{-1} \mathbf{z}_i\right)}{v(\tau_i \gamma)} \\ &= \frac{v\left(\tau_i \frac{1}{p}\mathbf{z}_i^\top \left(\frac{1}{n} \sum_{j \neq i} \tau_j v(\tau_j \gamma) e_j \mathbf{z}_j \mathbf{z}_j^\top\right)^{-1} \mathbf{z}_i\right)}{v(\tau_i \gamma)}. \end{aligned}$$

Using $e_1 \leq e_i \leq e_n$ and the nondecreasing nature of v , we have both

$$\begin{aligned} e_i &\leq \frac{v\left(\frac{1}{e_n}\tau_i\frac{1}{p}\mathbf{z}_i^\top\left(\frac{1}{n}\sum_{j\neq i}\tau_jv(\tau_j\gamma)\mathbf{z}_j\mathbf{z}_j^\top\right)^{-1}\mathbf{z}_i\right)}{v(\tau_i\gamma)}, \\ e_i &\geq \frac{v\left(\frac{1}{e_1}\tau_i\frac{1}{p}\mathbf{z}_i^\top\left(\frac{1}{n}\sum_{j\neq i}\tau_jv(\tau_j\gamma)\mathbf{z}_j\mathbf{z}_j^\top\right)^{-1}\mathbf{z}_i\right)}{v(\tau_i\gamma)}. \end{aligned}$$

Focusing on the first inequality, being valid for each i , it is particularly valid for $i = n$, and thus

$$e_n \leq \frac{v\left(\frac{1}{e_n}\tau_n\frac{1}{p}\mathbf{z}_n^\top\left(\frac{1}{n}\sum_{j\neq n}\tau_jv(\tau_j\gamma)\mathbf{z}_j\mathbf{z}_j^\top\right)^{-1}\mathbf{z}_n\right)}{v(\tau_n\gamma)}.$$

The quadratic form in the numerator above has been cleared of its dependence problems and it is thus only a matter of standard random matrix theory to show that

$$\frac{1}{p}\mathbf{z}_n^\top\left(\frac{1}{n}\sum_{j\neq n}\tau_jv(\tau_j\gamma)\mathbf{z}_j\mathbf{z}_j^\top\right)^{-1}\mathbf{z}_n \xrightarrow{a.s.} \gamma$$

(based on the same Stieltjes transform argument as previously). As a side but important comment, note that, due to the relabeling of e_1, \dots, e_n , \mathbf{z}_n is effectively no longer independent of $\mathbf{z}_1, \dots, \mathbf{z}_{n-1}$ and thus the convergence above in fact follows from a *uniform* convergence to γ of the quadratic forms for all $i = 1, \dots, n$. We thus conclude that, for $\epsilon > 0$ arbitrarily small, for all large n, p ,

$$e_n \leq \frac{v\left(\frac{1}{e_n}\tau_n(\gamma - \epsilon)\right)}{v(\tau_n\gamma)}$$

almost surely which we can equivalently write, by dividing left and right sides by $\tau_n\gamma$,

$$\psi(\tau_n\gamma) \leq v\left(\frac{1}{e_n}\tau_n(\gamma - \epsilon)\right) \frac{1}{e_n}\tau_n\gamma.$$

Let us now assume that $\limsup_n e_n > 1$ (which we want to disprove) and let us restrict ourselves to a subsequence over which e_n is away from one. For simplicity, we consider also that the τ_i 's are all bounded and that ψ is strictly increasing (with the general case treated in [Coulillet et al., 2015]). We may thus extract a further subsequence over which $\tau_n \rightarrow \tau_\infty$, $e_n \rightarrow e_\infty \in (1, \infty]$, $\epsilon \rightarrow 0$, and then in the limit

$$\psi(\tau_\infty\gamma) \leq \psi(e_\infty^{-1}\tau_\infty\gamma).$$

But since ψ is strictly increasing, this implies that $e_\infty \leq 1$ which contradicts the assumption that $\limsup_n e_n > 1$. Thus, $\limsup_n e_n \leq 1$ (almost surely).

With the same arguments, we show that $\liminf_n e_1 \geq 1$ almost surely, so that finally we have that $e_i \xrightarrow{a.s.} 1$ for all $i = 1, \dots, n$ which completes the proof.

3.3.4 Extensions

Tyler's rotational invariant estimator. The class of robust estimators of scatter of the type of $\hat{\mathbf{C}}$ in (3.7) developed by Huber and Maronna imposes that the robustness function u be such that $u(0)$ be defined and that $x \mapsto xu(x)$ be increasing and bounded.

In [Tyler, 1983], Tyler proposed another version of $\hat{\mathbf{C}}$, which can be thought of as a limiting version of (3.7) for $u(x) = 1/x$, i.e.,

$$\hat{\mathbf{C}} = \frac{1}{n} \sum_{i=1}^n \frac{\mathbf{x}_i \mathbf{x}_i^\top}{\frac{1}{p} \mathbf{x}_i^\top \hat{\mathbf{C}}^{-1} \mathbf{x}_i}. \quad \text{eq:robust_est_Tyler (3.10)}$$

Its disrupting from the conditions of Maronna on the function u however changes the behavior of $\hat{\mathbf{C}}$. First, note that $\hat{\mathbf{C}}$ is *no longer unique* as a solution to (3.10): indeed, if $\hat{\mathbf{C}}$ is solution, it is easy to see that so is $\alpha\hat{\mathbf{C}}$ for all $\alpha > 0$. As a matter of fact, it can be shown that this however summarizes all solutions. That is, for $n > p$ and \mathbf{x}_i linearly independent, there exists $\hat{\mathbf{C}}_0$ solution to (3.10) and the set of solutions $\hat{\mathbf{C}}$ is exactly $\{\alpha\hat{\mathbf{C}}_0, \alpha > 0\}$.

The main advantage of this robust formulation lies in its invariance with respect to the amplitude of the outliers. Under this formulation, all the \mathbf{x}_i 's are “normalized” since (3.10) features the ratio $\mathbf{x}_i \mathbf{x}_i^\top / \mathbf{x}_i^\top \hat{\mathbf{C}}^{-1} \mathbf{x}_i$. This advantage however turns into a drawback if one is to somehow maintain and compare the norms of the data.

The asymptotic analysis of Tyler's estimator in the large n, p regime does not unfold from the proof of Theorem 3.3 which strongly exploits the fact that $x \mapsto xu(x)$ is increasing (while here $xu(x) = 1$). In [Zhang et al., 2014], the authors exploit a different approach to prove that, for elliptical data with scatter matrix $\mathbf{C} = \mathbf{I}_p$, Tyler's estimator asymptotically behaves as a sample covariance matrix composed of i.i.d. random vectors with zero mean and identity covariance. Consequently, the limiting spectral measure of $\hat{\mathbf{C}}$ is simply the Marčenko–Pastur law.

In a sense, Tyler's estimator is “as most robust” as one can get since its null-hypothesis spectrum (when $\mathbf{C} = \mathbf{I}_p$) leads to the “most compact” spectral distribution. For all other u function, the limiting spectrum is more spread. This at first seems more advantageous in a spiked model extension of the model, as isolated eigenvalues are likely more visible under this setting. Yet, the harsh normalization of all data points simultaneously “breaks” the low rank eigenspaces *maximally* for Tyler's estimator. A compromise for a suitable u function is demander in this case.

The $p > n$ scenario. The robust estimator of scatter $\hat{\mathbf{C}}$ as defined in (3.7) has the major inconvenience of not being well defined for $p > n$ as $\hat{\mathbf{C}}$ is expressed through its inverse while being the sum of the n rank-one matrices $\frac{1}{n}u(\frac{1}{p}\mathbf{x}_i^\top \hat{\mathbf{C}}^{-1}\mathbf{x}_i)\mathbf{x}_i\mathbf{x}_i^\top$ and is thus of maximum rank $n < p$.

To cover the scenario $p > n$, one usually resorts to a *linear-shrinkage* version of the original $\hat{\mathbf{C}}$ by instead defining $\hat{\mathbf{C}}$ as the solution to

$$\hat{\mathbf{C}} = (1 - \gamma)\frac{1}{n} \sum_{i=1}^n u\left(\frac{1}{p}\mathbf{x}_i^\top \hat{\mathbf{C}}^{-1}\mathbf{x}_i\right) \mathbf{x}_i\mathbf{x}_i^\top + \gamma\mathbf{I}_p$$

for some $\gamma \in (0, 1]$. Thanks to the $\gamma\mathbf{I}_p$ addition, the right-hand side term is positive definite (i.e., $\hat{\mathbf{C}} \succeq \gamma\mathbf{I}_p$ in the sense of symmetric matrices) and it can be shown that, under similar conditions on u as in the previous paragraphs, $\hat{\mathbf{C}}$ is well defined as the unique solution to the equation.

Under this setting, the asymptotic analysis of $\hat{\mathbf{C}}$ essentially boils down to the control of the minimal eigenvalue of $\hat{\mathbf{C}}$ (which could be close to zero and thus lead to an explosion of $\mathbf{x}_i^\top \hat{\mathbf{C}}^{-1}\mathbf{x}_i$). The authors in [Couillet and McKay, 2014, Auguin et al., 2018] extend the results in Theorem 3.3 to this setting.

Robustness to arbitrary outliers. It is important to stress that the asymptotic equivalence $\|\hat{\mathbf{C}} - \hat{\mathbf{S}}\| \xrightarrow{a.s.} 0$ in Theorem 3.3 is only valid for the specific elliptic model of the data \mathbf{x}_i , a scenario which is mostly motivated by Maronna's original works [Maronna, 1976] on the maximum likelihood estimator for elliptical datasets and by the adequate modelling of impulsive noise environments beyond the Gaussian noise model in practice.

In the original works of Huber on robust statistics though, the initial objective of $\hat{\mathbf{C}}$ was to combat the presence of outlying data in the sample. To this end, from a large dimensional random matrix viewpoint, it is more convenient to assume that the data observations $\mathbf{X}_{\mathbf{A}} \in \mathbb{R}^{p \times n}$ are composed in part of *clean data* and in part of *outliers*. We may write

$$\mathbf{X}_{\mathbf{A}} = [\mathbf{X}, \mathbf{A}] = [\mathbf{x}_1, \dots, \mathbf{x}_{(1-\epsilon_n)n}, \mathbf{a}_1, \dots, \mathbf{a}_{\epsilon_n n}]$$

for a proportion ϵ_n (a multiple of $1/n$) of deterministic unknown outliers $\mathbf{A} = [\mathbf{a}_1, \dots, \mathbf{a}_{\epsilon_n n}]$ and $(1 - \epsilon_n)$ of genuine data $\mathbf{X} = [\mathbf{x}_1, \dots, \mathbf{x}_{(1-\epsilon_n)n}]$.

In [Morales-Jimenez et al., 2015], letting \mathbf{x}_i be independent $\mathcal{N}(\mathbf{0}, \mathbf{C})$ and the \mathbf{a}_i 's be such that $\frac{1}{n}\mathbf{C}^{-\frac{1}{2}}\mathbf{A}\mathbf{A}^\top\mathbf{C}^{-\frac{1}{2}}$ has bounded norm, Theorem 3.3 is turned into the following result.

theo:robust_est_outliers

Theorem 3.4 (Robust estimator with outliers, from [Morales-Jimenez et al., 2015]). *Let $\mathbf{X}_{\mathbf{A}} = [\mathbf{X}, \mathbf{A}]$ be as above. Then, under the assumptions and notations of Theorem 3.3 and with $\epsilon_n \rightarrow \epsilon \in (0, 1 - c)$,*

$$\|\hat{\mathbf{C}} - \hat{\mathbf{S}}_{\mathbf{A}}\| \xrightarrow{a.s.} 0, \quad \hat{\mathbf{S}}_{\mathbf{A}} = v(\gamma_n)\frac{1}{n}\mathbf{X}\mathbf{X}^\top + \frac{1}{n}\sum_{i=1}^{\epsilon n} v(\alpha_{i,n})\mathbf{a}_i\mathbf{a}_i^\top$$

where $(\gamma_n, \alpha_{1,n}, \dots, \alpha_{\epsilon n, n})$ are the unique solution to

$$\begin{aligned}\gamma_n &= \frac{1}{p} \operatorname{tr} \mathbf{C} \left(\frac{(1-\epsilon)v(\gamma_n)}{1+cv(\gamma_n)\gamma_n} \mathbf{C} + \frac{1}{n} \sum_{i=1}^{\epsilon n} v(\alpha_{i,n}) \mathbf{a}_i \mathbf{a}_i^\top \right)^{-1} \\ \alpha_{i,n} &= \mathbf{a}_i^\top \left(\frac{(1-\epsilon)v(\gamma_n)}{1+cv(\gamma_n)\gamma_n} \mathbf{C} + \frac{1}{n} \sum_{j \neq i} v(\alpha_{j,n}) \mathbf{a}_j \mathbf{a}_j^\top \right)^{-1} \mathbf{a}_i.\end{aligned}$$

It is already interesting to see that the robust estimator $\hat{\mathbf{S}}_{\mathbf{A}}$ (and thus) properly weighs all genuine data by a constant $v(\gamma_n)$ and then weighs all outliers with a parameter $v(\alpha_{i,n})$ proportional to its “outlying” character.

Of particular interest is the case of a vanishing proportion of outliers with $\epsilon_n \rightarrow 0$ (for instance $\epsilon_n = k/n$, corresponding to exactly k outliers). Then, it is easily seen that $\gamma_n \rightarrow \gamma$ given in the statement of Theorem 3.3 for $\tau_i = 1$, and thus

$$\gamma_n \rightarrow \gamma = \frac{\varphi^{-1}(1)}{1-c}.$$

In this case, we have

$$\hat{\mathbf{S}}_{\mathbf{A}} = \frac{1}{\varphi^{-1}(1)} \frac{1}{n} \mathbf{X} \mathbf{X}^\top + \frac{1}{n} \sum_{i=1}^n v(\alpha_{i,n}) \mathbf{a}_i \mathbf{a}_i^\top.$$

If, in addition, $\epsilon_n n = k$ and $\mathbf{a}_1 = \dots = \mathbf{a}_k \equiv \mathbf{a}$, then $\alpha_{1,n} = \dots = \alpha_{\epsilon n, n} \equiv \alpha_n$ is given by the unique positive solution of

$$\alpha_n = \frac{\gamma \frac{1}{p} \mathbf{a}^\top \mathbf{C}^{-1} \mathbf{a}}{1 + c\gamma(k-1)v(\alpha_n) \frac{1}{p} \mathbf{a}^\top \mathbf{C}^{-1} \mathbf{a}}.$$

Several conclusions can be drawn here: first note that the outlying data are weighed by a factor proportional to $\mathbf{a}^\top \mathbf{C}^{-1} \mathbf{a}$. Thus, the robust estimator behaves *as if aware* of $\mathbf{a}^\top \mathbf{C}^{-1} \mathbf{a}$ although \mathbf{C} itself is not accessible; it thus performs much as expected by only discarding from the sample those data vectors \mathbf{a} not aligned with \mathbf{C} . But also note that, if $\mathbf{C} = \mathbf{I}_p$, then $\mathbf{a}^\top \mathbf{C}^{-1} \mathbf{a} = \|\mathbf{a}\|^2$, in which case the robust estimator only evaluates the amplitude of the outlier, rather than its characteristic covariance structure, to decide on the allocated weight. Consequently, robust estimators are mostly resilient to outliers if the genuine data is quite structured (and outliers are misaligned to this structure, so say not structured at all), but the converse is not true.

However a much more troubling and unexpected effect is that, if k (so finitely many) outliers are *identical*, then α_n scales as $1/k$ and thus quickly vanishes. Ultimately, only few outliers suffice to obtain $\alpha_n < \gamma$ and thus $v(\alpha_n) > v(\gamma)$: the outliers are given *more weight* than the genuine data, going in a stark opposite direction as originally intended. It is interesting that random matrix theory so easily reveals such behaviors which conventional $n \gg 1$ statistics is generally unable to see (or only through approximations).

Second order statistics. The convergence $\|\hat{\mathbf{C}} - \hat{\mathbf{S}}\| \rightarrow 0$ (in Theorems 3.3 and 3.4) is convenient to transfer the *first order* spectral properties of $\hat{\mathbf{S}}$ to $\hat{\mathbf{C}}$. That is, this convergence implies (i) $\max_{1 \leq i \leq p} |\lambda_i(\hat{\mathbf{C}}) - \lambda_i(\hat{\mathbf{S}})| \rightarrow 0$ and (ii) $\|\mathbf{u}_i(\hat{\mathbf{C}}) - \hat{\mathbf{u}}_i(\hat{\mathbf{S}})\| \rightarrow 0$ for all *isolated* eigenpair $(\lambda_i(\hat{\mathbf{C}}), \mathbf{u}_i(\hat{\mathbf{C}}))$ (i.e., such that $|\lambda_i(\hat{\mathbf{C}}) - \lambda_{i \pm 1}(\hat{\mathbf{C}})|$ does not vanish).

As such, $\hat{\mathbf{C}}$ and $\hat{\mathbf{S}}$ have the same limiting spectral distribution, their eigenvalues are point-wise asymptotically equal and they share the same *isolated* eigenvectors in the limit. From a practical standpoint, this in particular means that the asymptotic threshold for signal detection (based on isolated eigenvalues) can be transferred from the statistics of $\hat{\mathbf{S}}$ to $\hat{\mathbf{C}}$ and that the informative content in the eigenvectors of $\hat{\mathbf{C}}$ can be understood from those of $\hat{\mathbf{S}}$.

However, this is as far as the $\|\hat{\mathbf{C}} - \hat{\mathbf{S}}\| \rightarrow 0$ convergence goes. The question of the asymptotic local fluctuations of the individual eigenvalues and of the eigenvector projection statistics cannot be transferred straightforwardly. In particular, it is believed that $\|\hat{\mathbf{C}} - \hat{\mathbf{S}}\| = O(1/\sqrt{n})$. Since the dominant eigenvalues $\lambda_i(\hat{\mathbf{S}})$ and eigenvector projections $\mathbf{u}_i(\hat{\mathbf{S}})^T \mathbf{a}$ for deterministic \mathbf{a} satisfy central limit theorems at this $O(1/\sqrt{n})$ rate precisely, we can at least tell that $\lambda_i(\hat{\mathbf{C}})$ and $\mathbf{u}_i(\hat{\mathbf{C}})^T \mathbf{a}$ also fluctuate at a $O(1/\sqrt{n})$ rate but it is impossible to infer whether a central limit theorem holds and even to estimate the limiting mean and variance of the fluctuation. The problem is even exacerbated when it comes to faster statistics, such as linear functionals $\frac{1}{n} \sum_i f(\lambda_i(\hat{\mathbf{C}}))$: while $\frac{1}{n} \sum_i f(\lambda_i(\hat{\mathbf{C}}))$ is known to satisfy a central limit theorem at rate $O(1/n)$, the convergence $\|\hat{\mathbf{C}} - \hat{\mathbf{S}}\| = O(1/\sqrt{n})$ only allows one to say that $\frac{1}{n} \sum_i f(\lambda_i(\hat{\mathbf{C}}))$ fluctuates at speed $O(1/\sqrt{n})$.

In [Couillet et al., 2016a], it is shown that more can be said for precise statistics. Assuming the case where $u(x) = 1/x$, $\mathbf{C} = \mathbf{I}_p$, and $\hat{\mathbf{C}}$ is regularized by $\gamma \mathbf{I}_p$ for any $\gamma > 0$, it is proved that, for all deterministic vectors $\mathbf{a}, \mathbf{b} \in \mathbb{R}^p$ and for all $k \in \mathbb{Z}$,

$$\mathbf{a}^T \hat{\mathbf{C}}^k \mathbf{b} - \mathbf{a}^T \hat{\mathbf{S}}^k \mathbf{b} \stackrel{\text{eq:transfer_fluctuations_hatC_hatS}}{=} O(n^{1+\epsilon}) \quad (3.11)$$

for all $\epsilon > 0$. This result can be straightforwardly used to show that $\mathbf{u}_i(\hat{\mathbf{C}})^T \mathbf{a}$ satisfies the same asymptotic fluctuations as $\mathbf{u}_i(\hat{\mathbf{S}})^T \mathbf{a}$.

As a concrete application example, the robust estimator $\hat{\mathbf{C}}$ may be used for the following hypothesis testing problem

$$\mathbf{x} = \begin{cases} \sqrt{\tau} \mathbf{z} & , \mathcal{H}_0 \\ s \mathbf{a} + \sqrt{\tau} \mathbf{z} & , \mathcal{H}_1 \end{cases}, \quad \text{given } \mathbf{x}_i = \sqrt{\tau_i} \mathbf{z}_i, \quad 1 \leq i \leq n$$

where \mathbf{z}, \mathbf{z}_i are, say, independent and uniformly distributed on the sphere, $\mathbf{a} \in \mathbb{R}^p$ is some known vector and $s \in \mathbb{R}$ is unknown. Here, one assumes to have access to a single observation \mathbf{x} but also to some prior “pure noise” data $\mathbf{x}_1, \dots, \mathbf{x}_n$, and it is to be tested whether the vector \mathbf{a} is present in \mathbf{x} .

This setting corresponds to that of an impulsive background noise environment within which an informative data \mathbf{a} is expected to be eventually detected (\mathbf{a} could be a signal signature such as a steering vector in array processing).

Since \mathbf{a} is known, the generalized likelihood ratio test (GLRT) in this setting (recall Section 3.1.1 for a definition of the GLRT) reads

$$T_p \equiv \frac{|\mathbf{x}^\top \hat{\mathbf{C}}^{-1} \mathbf{a}|^2}{(\mathbf{x}^\top \hat{\mathbf{C}}^{-1} \mathbf{x})(\mathbf{a}^\top \hat{\mathbf{C}}^{-1} \mathbf{a})} \stackrel{\mathcal{H}_1}{\gtrless}_{\mathcal{H}_0} \alpha.$$

In the absence of \mathbf{a} within \mathbf{x} , $\mathbf{x}^\top \hat{\mathbf{C}}^{-1} \mathbf{a} = O(1/\sqrt{n})$ while in the presence of \mathbf{a} , $\mathbf{x}^\top \hat{\mathbf{C}}^{-1} \mathbf{a}$ is of the order of α . The test is therefore asymptotically non-trivial only if α is of order $O(1/\sqrt{n})$. Under these conditions, the performance of the test (its asymptotic errors of type I and II) are given by the asymptotic behavior of T_p under both \mathcal{H}_0 and \mathcal{H}_1 hypotheses.

This behavior is accessible by showing a central limit theorem for T_p , which itself follows (by the delta-method) from a central limit theorem on the vector $(\mathbf{x}^\top \hat{\mathbf{C}}^{-1} \mathbf{a}, \mathbf{x}^\top \hat{\mathbf{C}}^{-1} \mathbf{x}, \mathbf{a}^\top \hat{\mathbf{C}}^{-1} \mathbf{a})$. From (3.11), this is asymptotically equivalent to establishing a central limit theorem for $(\mathbf{x}^\top \hat{\mathbf{S}}^{-1} \mathbf{a}, \mathbf{x}^\top \hat{\mathbf{S}}^{-1} \mathbf{x}, \mathbf{a}^\top \hat{\mathbf{S}}^{-1} \mathbf{a})$ which, given the elementary modelling of $\hat{\mathbf{S}}$, is within reach of random matrix theory.

A thorough investigation of this GLRT asymptotics is performed in [Coullet et al., 2016a, Kammoun et al., 2018].

3.4 Concluding remarks

All the methods presented in this chapter, from discriminant analysis down to robust covariance estimation, all consist, one way or another, in improving the mismatched estimation of a covariance matrix \mathbf{C} by its sample covariance $\hat{\mathbf{C}}$.

However, as opposed to the conventional idea that one must before everything improve this mismatched estimate $\hat{\mathbf{C}}$ into a “better” plug-in estimate of \mathbf{C} , the random matrix approach developed in this chapter rather consists in the first place to identify the ultimate scalar (or small dimensional) parameter to be optimized, and only then, adapt the estimate of \mathbf{C} appropriately. Specifically, we saw that:

- in the discriminant analysis scenario, we estimated \mathbf{C} through a “linear shrinkage” version $\hat{\mathbf{C}} + \gamma \mathbf{I}_p$ of $\hat{\mathbf{C}}$, and then aim at optimizing γ in such a way to optimize the ultimate detection probability of the underlying hypothesis test;
- in the spike G-MUSIC improvement of the MUSIC algorithm, one aims primarily at estimating quadratic forms of the type $\mathbf{a}^\top \mathbf{u} \mathbf{u}^\top \mathbf{a}$ where \mathbf{u} is an eigenvector (associated to the largest eigenvalues) of \mathbf{C} . There, the covariance \mathbf{C} is never estimated, and only the quadratic form $\mathbf{a}^\top \mathbf{u} \mathbf{u}^\top \mathbf{a}$ is estimated as a function of $\mathbf{a}^\top \hat{\mathbf{u}} \hat{\mathbf{u}}^\top \mathbf{a}$ with $\hat{\mathbf{u}}$ the corresponding eigenvector in $\hat{\mathbf{C}}$;
- in the distance estimation framework between two covariance matrices, again, the ultimate target is the distance $d(\mathbf{C}_1, \mathbf{C}_2)$; instead of correcting the quite erroneous but natural estimate $d(\hat{\mathbf{C}}_1, \hat{\mathbf{C}}_2)$, the strategy is again

to characterize $d(\mathbf{C}_1, \mathbf{C}_2)$ as a function of the resolvents of \mathbf{C}_1 and \mathbf{C}_2 , before connecting them to $\hat{\mathbf{C}}_1$ and $\hat{\mathbf{C}}_2$; in the end, the estimators depend in a non-trivial manner on the eigenvalues of $\hat{\mathbf{C}}_1 \hat{\mathbf{C}}_2$ (or $\hat{\mathbf{C}}_1^{-1} \hat{\mathbf{C}}_2$);

- finally, for the robust covariance estimator method, the asymptotics of the robust estimator are not so trivially related to the underlying covariance matrices being estimated.

While estimating the $p(p-1)/2$ samples of \mathbf{C} from the np samples X_{ij} of the data matrix $\mathbf{X} \in \mathbb{R}^{p \times n}$ cannot be performed consistently in the regime where $n \sim p$ (at least when no strong a priori structure is supposed on \mathbf{C}), this does not necessarily mean that there is no means to improve over the sample covariance matrix.

Specifically, a recent direction is being followed which consists in generalizing the notion of “linear shrinkage”, i.e., estimating \mathbf{C} through the matrix $\hat{\mathbf{C}} + \gamma \mathbf{I}_p$ for some $\gamma > 0$, to “nonlinear shrinkage”. The idea behind nonlinear shrinkage is to design an estimator of the type $\hat{\mathbf{U}} f(\hat{\Lambda}) \hat{\mathbf{U}}^\top$, where $\hat{\mathbf{U}} \hat{\Lambda} \hat{\mathbf{U}}^\top = \hat{\mathbf{C}}$ is the spectral decomposition of $\hat{\mathbf{C}}$ and $f(\cdot)$ is a function applied entry-wise. The function f is then selected in such a way that a distance criterion, such as $\mathbb{E}[\|\mathbf{C} - \hat{\mathbf{U}} f(\hat{\Lambda}) \hat{\mathbf{U}}^\top\|_F^2]$ is minimized or alternatively such that $f(\hat{\lambda}_i)$ estimates the corresponding i -th eigenvalue of \mathbf{C} . In a series of works [Ledoit and Péché, 2011, Ledoit et al., 2012, Bun et al., 2017], the authors proposed several such functions f .

Overall, it is interesting to note the many findings since the seminal article of Marčenko and Pastur in 1967 surrounding the sample covariance matrix model. Clearly ubiquitous in machine learning, second order statistics have for long never been the subject of so deep investigations (as the sample covariance was supposed a good estimator for the covariance) until this fundamental random matrix finding. It is now fully admitted by many research communities (statistics, statistical physics, electrical engineering), and now increasingly by the machine learning community that all methods and algorithms derived from a mere replacement of the population covariance matrix by the sample covariance are at best hazardous, and often counter-productive.

This is another instance of the curse of dimensionality in large and numerous data processing problems, which is being more and more efficiently tackled. The next chapter goes a step further, beyond the linear and quadratic setting, into kernel-based algorithms (and thus nonlinear functions of the data).

3.5 Practical course material

Practical Lecture Material 1 (The Wasserstein distance estimation). *This exercise aims to formally derive the proof of Theorem 3.2 in the specific case of the Wasserstein distance. That is, we aim at estimating, for independent*

centered Gaussian samples covariance matrices \mathbf{C}_1 and \mathbf{C}_2 , the quantity

$$d_W(\mathbf{C}_1, \mathbf{C}_2) = \frac{1}{p} \left(\text{tr}(\mathbf{C}_1) + \text{tr}(\mathbf{C}_2) - 2 \text{tr} \left[(\mathbf{C}_1^{\frac{1}{2}} \mathbf{C}_2 \mathbf{C}_1^{\frac{1}{2}})^{\frac{1}{2}} \right] \right).$$

Prove that only the rightmost term is the challenging one to estimate, i.e., from n_i independent samples $\mathbf{X}_i = [\mathbf{x}_{i1}, \dots, \mathbf{x}_{in_i}] \in \mathbb{R}^{p \times n_i}$ and with $p \sim n_i$, $\frac{1}{p} \text{tr} \hat{\mathbf{C}}_i$ is a consistent estimate for $\frac{1}{p} \text{tr} \mathbf{C}_i$ with $\hat{\mathbf{C}}_i = \frac{1}{n_i} \mathbf{X}_i \mathbf{X}_i^\top$ the sample covariance estimate of \mathbf{C}_i .

In the following we thus aim to estimate $d = \frac{1}{p} \text{tr}[(\mathbf{C}_1^{\frac{1}{2}} \mathbf{C}_2 \mathbf{C}_1^{\frac{1}{2}})^{\frac{1}{2}}]$. First prove that $d = \int \sqrt{t} \nu_p(dt)$ with $\nu_p = \frac{1}{p} \sum_{i=1}^p \delta_{\lambda_i(\mathbf{C}_1 \mathbf{C}_2)}$ and deduce, by Cauchy's integration formula, that $d = \frac{-1}{2\pi i} \oint_{\Gamma_\nu} \sqrt{z} m_{\nu_p}(z) dz$, with $m_{\nu_p}(z)$ the Stieltjes transform of ν_p and Γ_ν an appropriate complex contour.

With Bai-Silverstein's theorem (Theorem 2.5), show that the Stieltjes transform m_{μ_p} of the spectral measure μ_p of $\hat{\mathbf{C}}_1 \hat{\mathbf{C}}_2$ relates to m_{ν_p} through the set of equations

$$zm_{\mu_p}(z) = \varphi_p(z)m_{\zeta_p}(\varphi_p(z)) + o(1) \quad \text{eq:bai1} \quad (3.12)$$

$$m_{\nu_p}\left(\frac{z}{\Psi_p(z)}\right) = m_{\zeta_p}(z)\Psi_p(z) + o(1). \quad \text{eq:bai2} \quad (3.13)$$

where ζ_p is the spectral measure of $\mathbf{C}_2^{\frac{1}{2}} \hat{\mathbf{C}}_1 \mathbf{C}_2^{\frac{1}{2}}$, $\Psi_p(z) \equiv 1 - \frac{p}{n_2} - \frac{p}{n_2} zm_{\zeta_p}(z)$ and $\varphi_p(z) = z/(1 - \frac{p}{n_1} - \frac{p}{n_1} zm_{\mu_p}(z))$.

By means of two successive changes of variables, prove that d can be consistently estimated, as $n, p \rightarrow \infty$ by

$$\hat{d} \equiv \frac{n_2}{2\pi i p} \oint_{\Gamma} \sqrt{\frac{\varphi_p(z)}{\psi_p(z)}} \left[\frac{\varphi'_p(z)}{\varphi_p(z)} - \frac{\psi'_p(z)}{\psi_p(z)} \right] \psi_p(z) dz$$

where $\psi_p(z) \equiv 1 - \frac{p}{n_2} - \frac{p}{n_2} zm_{\mu_p}(z)$, and Γ is some complex contour to be carefully positioned.

The functions $\varphi_p(z)$ and $\psi_p(z)$ are rational functions (as rational functions of m_{μ_p} , itself a relational function). Show that they can be expressed under the rational forms

$$\varphi_p(z) = z \frac{\prod_{i=1}^p z - \lambda_i}{\prod_{i=1}^p z - \eta_i}, \quad \psi_p(z) = \frac{\prod_{i=1}^p z - \xi_i}{\prod_{i=1}^p z - \lambda_i}$$

where $\lambda_1 \leq \dots \leq \lambda_p$ are the increasingly sorted eigenvalues of $\hat{\mathbf{C}}_1 \hat{\mathbf{C}}_2$, and $\{\xi_i\}_{i=1}^p$, $\{\eta_i\}_{i=1}^p$ the increasingly sorted eigenvalues of $\mathbf{\Lambda} - \frac{1}{n_1} \sqrt{\boldsymbol{\lambda}} \sqrt{\boldsymbol{\lambda}}^\top$ and $\mathbf{\Lambda} - \frac{1}{n_2} \sqrt{\boldsymbol{\lambda}} \sqrt{\boldsymbol{\lambda}}^\top$, respectively, where $\boldsymbol{\lambda} = (\lambda_1, \dots, \lambda_p)^\top$, $\mathbf{\Lambda} = \text{diag}(\boldsymbol{\lambda})$ and $\sqrt{\cdot}$ is understood entry wise.

Find the singularities, the poles and the branch cuts of the complex integrand and represent them on the complex plane. You may refer to Figure 3.5, but must be careful on the relative ordering of the $(\xi_i, \eta_i, \lambda_i)$ triplets. Based on this

representation, and as again depicted in Figure 3.5, deform the contour Γ into a more convenient contour (which we still refer to as Γ). Prove then that the integrals over ε -radius circles around ξ_i are null in the small ε limit (using for instance the convenient change of variables $z = \xi_i + \varepsilon e^{i\theta}$). Next prove that the integrals over the real axis (again in the $\varepsilon \rightarrow 0$ limit) between $\xi_j + \varepsilon$ and $\eta_j + \varepsilon$ sum up to

$$A_1 = \frac{2n_2}{\pi p} \sum_{j=1}^p \int_{\xi_j}^{\eta_j} \sqrt{-\frac{\varphi_p(x)}{\psi_p(x)}} \psi'_p(x) dx - \frac{2n_2}{\pi p} \sum_{j=1}^p \frac{1}{\sqrt{\varepsilon \frac{d}{dx} \left(\frac{1}{\varphi_p(x)\psi_p(x)} \right) (\eta_j)}}.$$

Continue the calculus by proving, using the change of variable $z = \eta_i + \varepsilon e^{i\theta}$, that integrals over the ε -radius circles around η_j do not vanish but convey a second contribution summing up in the $\varepsilon \rightarrow 0$ limit to

$$A_2 = \frac{2n_2}{\pi p} \sum_{j=1}^p \frac{1}{\sqrt{\varepsilon \frac{d}{dx} \left(\frac{1}{\varphi_p(x)\psi_p(x)} \right) (\eta_j)}}.$$

Finally prove that the residues associated to the poles sum up to

$$A_3 = \frac{2n_2}{p} \sqrt{\frac{n_1}{n_2}} \sum_{j=1}^p \sqrt{\lambda_j}.$$

Conclude from these three contributions that d can be estimated by the real-line integral form

$$\hat{d}(\mathbf{X}_1, \mathbf{X}_2) \equiv 2\sqrt{n_1 n_2} \frac{1}{p} \sum_{j=1}^p \sqrt{\lambda_j} + \frac{2n_2}{\pi p} \sum_{j=1}^p \int_{\xi_j}^{\eta_j} \sqrt{-\frac{\varphi_p(x)}{\psi_p(x)}} \psi'_p(x) dx.$$

Show in particular that, when $n_1 = n_2 = n/2$, this estimate further simplifies as

$$\hat{d}(\mathbf{X}_1, \mathbf{X}_2) = \frac{n}{p} \sum_{j=1}^p \left(\sqrt{\lambda_j} - \sqrt{\xi_j} \right)$$

using the fact that $\xi_j \rightarrow \eta_j$ in the limit where $n_1/n - n_2/n \rightarrow 0$, and that, by deforming the “real line” part of the contour,

$$\frac{1}{\pi} \lim_{t \rightarrow \xi_j} \int_{\xi_j}^t \sqrt{-\frac{\varphi_p(x)}{\psi_p(x)}} \psi'_p(x) dx = \frac{1}{2\pi i} \lim_{\varepsilon \rightarrow 0} \oint_{\Gamma_{\xi_j}^\varepsilon} \sqrt{-\varphi_p(z)\psi_p(z)} \frac{\psi'_p(z)}{\psi_p(z)} dz$$

where $\Gamma_{\xi_j}^\varepsilon$ is an ε -radius circular contour around ξ_j .

Deduce the final expression for large n, p -consistent estimate of the Wasserstein distance for Gaussian samples, and confirm by reproducing the following example in Table 3.3.

p	$d(\mathbf{C}_1, \mathbf{C}_2)$	$\hat{d}(\mathbf{X}_1, \mathbf{X}_2)$	$d(\hat{\mathbf{C}}_1, \hat{\mathbf{C}}_2)$
2	0.0110	0.0109	0.0115
4	0.0175	0.0189	0.0203
8	0.0208	0.0213	0.0240
16	0.0225	0.0232	0.0286
32	0.0233	0.0237	0.0343
64	0.0237	0.0243	0.0454
128	0.0239	0.0240	0.0663
256	0.0240	0.0243	0.1092
512	0.0241	0.0245	0.1954

Table 3.3: Estimation of the Wasserstein distance for $\mathbf{x}_i^{(a)} \sim \mathcal{N}(\mathbf{0}, \mathbf{C}_a)$ with $[\mathbf{C}_1]_{ij} = .2^{i-j}$, $[\mathbf{C}_2]_{ij} = .4^{i-j}$, $n_1 = 1024$, $n_2 = 2048$, as a function of p , results averaged over 30 runs. [Link to code].

tab:exo_perf_cov_dist

TP:robust_portfolio

Practical Lecture Material 2 (Robust portfolio optimization via Tyler estimator). In computational finance, one of the problems of the popular Markowitz's mean-variance optimization framework consists in determining a portfolio vector $\mathbf{w} \in \mathbb{R}^p$, to allocate to p assets, in such a way to maximize the expected return and/or minimize the risk of the investment. From a statistical perspective, \mathbf{w} is thus set to minimize a certain cost function based on past observations $\mathbf{x}_1, \dots, \mathbf{x}_n \in \mathbb{R}^p$ of the market evolution (the returns) of the p assets. Those are often assumed independent for simplicity, but cannot be considered Gaussian due to the possibly erratic nature of the market.

We consider here for simplicity the problem of minimizing the risk, without constraining the expected return. That is, from a statistical standpoint, assuming independent (centered) elliptically distributed $\mathbf{x}_i = \sqrt{\tau_i} \mathbf{C}^{\frac{1}{2}} \mathbf{z}_i$ returns where $\mathbf{z}_i \in \mathbb{R}^p$ is uniform on the sphere of radius \sqrt{p} and $\tau_i > 0$ are random i.i.d. impulses independent of \mathbf{z}_i , as in (3.6). We wish to determine

$$\mathbf{w}^* = \arg \min_{\mathbf{w} \in \mathbb{R}^p, \mathbf{w}^\top \mathbf{1}_p = 1} \mathbb{E}[|\mathbf{w}^\top \mathbf{x}|^2] \quad \text{eq:portfolio-optim (3.14)}$$

where the constraint $\mathbf{w}^\top \mathbf{1}_p = 1$ ensures that the total wealth remains constant.

Assuming that $\mathbb{E}[\tau] = 1$ (which we can set for convenience), show via the Lagrangian multipliers method, that the solution to (3.14) is explicitly given by

$$\mathbf{w}^* = \frac{\mathbf{C}^{-1} \mathbf{1}_p}{\mathbf{1}_p^\top \mathbf{C}^{-1} \mathbf{1}_p}$$

with the minimal (expected) risk $\mathbb{E}[|(\mathbf{w}^*)^\top \mathbf{x}|^2] = \frac{1}{\mathbf{1}_p^\top \mathbf{C}^{-1} \mathbf{1}_p}$.

The covariance \mathbf{C} being unknown, and the historical returns \mathbf{x}_i being impulsive in nature, we wish to estimate \mathbf{w}^* via a robust estimator of scatter approach as in Section 3.3. That is, we estimate \mathbf{C} in the formulas above by the robust

(shrinkage) Tyler estimator $\hat{\mathbf{C}}(\gamma)$ defined, for $\gamma \in (\max\{0, 1 - n/p\}, 1]$, as the unique solution to

$$\hat{\mathbf{C}}(\gamma) = (1 - \gamma) \frac{1}{n} \mathbf{X} \mathbf{D}^{-1} \mathbf{X}^\top + \gamma \mathbf{I}_p, \quad \mathbf{D} = \text{diag} \left\{ \frac{1}{p} \mathbf{x}_i^\top \hat{\mathbf{C}}(\gamma)^{-1} \mathbf{x}_i \right\}_{i=1}^n.$$

The regularization term $\gamma \mathbf{I}_p$ allows for $p > n$ and offers an additional degree of freedom, and the choice of a Tyler estimator (i.e., $u(t) = 1/t$ in our previous notations) is here for computational convenience.

First show that, replacing the unknown \mathbf{C} by $\hat{\mathbf{C}}(\gamma)$, letting $\hat{\mathbf{w}} = \frac{\hat{\mathbf{C}}(\gamma)^{-1} \mathbf{1}_p}{\mathbf{1}_p^\top \hat{\mathbf{C}}(\gamma)^{-1} \mathbf{1}_p}$, the resulting portfolio risk is given by

$$\mathbb{E}_{\mathbf{x}}[|\hat{\mathbf{w}}^\top \mathbf{x}|^2] = \frac{\mathbf{1}_p^\top \hat{\mathbf{C}}(\gamma)^{-1} \mathbf{C} \hat{\mathbf{C}}(\gamma)^{-1} \mathbf{1}_p}{(\mathbf{1}_p^\top \hat{\mathbf{C}}(\gamma)^{-1} \mathbf{1}_p)^2} \quad (3.15)$$

and confirm that we retrieve the correct result as $\hat{\mathbf{C}}(\gamma)$ coincides with \mathbf{C} . Our objective here is to estimate this quantity to retrieve the performance of this robust portfolio design as a function of γ .

Similar to the intuitive approach developed in Section 3.3.3 for generic $u(t)$ functions (but without regularization), show that the following random equivalent asymptotics hold:

$$\begin{aligned} \|\hat{\mathbf{C}}(\gamma) - \hat{\mathbf{S}}(\gamma)\| &\xrightarrow{\text{a.s.}} 0 \\ \hat{\mathbf{S}}(\gamma) &\equiv \frac{1}{\delta(\gamma)} \frac{1 - \gamma}{1 - (1 - \gamma)c} \frac{1}{n} \mathbf{C}^{\frac{1}{2}} \mathbf{Z} \mathbf{Z}^\top \mathbf{C}^{\frac{1}{2}} + \gamma \mathbf{I}_p \end{aligned}$$

where $c = \lim p/n$, $\mathbf{Z} = [\mathbf{z}_1, \dots, \mathbf{z}_n]$ and $\delta(\gamma)$ is the unique solution to

$$1 = \frac{1}{p} \text{tr } \mathbf{C} ((1 - \gamma) \mathbf{C} + \delta(\gamma) \gamma \mathbf{I}_p)^{-1}$$

and that we have the following deterministic equivalent for the inverse of $\hat{\mathbf{C}}(\gamma)$:

$$\hat{\mathbf{C}}(\gamma)^{-1} \leftrightarrow \left(\frac{1 - \gamma}{\delta(\gamma)} \mathbf{C} + \gamma \mathbf{I}_p \right)^{-1}.$$

To this end, one may first evaluate $\hat{\mathbf{C}}(\gamma)^{-1} - \hat{\mathbf{C}}_{-i}(\gamma)^{-1}$, where $\hat{\mathbf{C}}_{-i}$ is defined as $\hat{\mathbf{C}}$ but with the summation over $1 \leq j \neq i \leq n$, i.e.,

$$\hat{\mathbf{C}}_{-i}(\gamma) = (1 - \gamma) \frac{1}{n} \sum_{j \neq i} \frac{\mathbf{x}_j \mathbf{x}_j^\top}{\frac{1}{p} \mathbf{x}_j^\top \hat{\mathbf{C}}(\gamma) \mathbf{x}_j} + \gamma \mathbf{I}_p$$

then show that

$$\frac{1}{p} \mathbf{z}_i^\top \mathbf{C}^{\frac{1}{2}} \hat{\mathbf{C}}(\gamma)^{-1} \mathbf{C}^{\frac{1}{2}} \mathbf{z}_i = \left(1 - (1 - \gamma) \frac{p}{n} \right) \frac{1}{p} \mathbf{z}_i^\top \mathbf{C}^{\frac{1}{2}} \hat{\mathbf{C}}_{-i}(\gamma)^{-1} \mathbf{C}^{\frac{1}{2}} \mathbf{z}_i \quad (3.16)$$

and then use the intuition that

$$\frac{1}{p} \mathbf{z}_i^\top \mathbf{C}^{\frac{1}{2}} \hat{\mathbf{C}}_{-i}(\gamma)^{-1} \mathbf{C}^{\frac{1}{2}} \mathbf{z}_i \simeq \frac{1}{p} \operatorname{tr} \mathbf{C} \hat{\mathbf{C}}(\gamma)^{-1}$$

the right-end side term corresponding in the limit to $\delta(\gamma)$. Complete the proof by using appropriately Theorem 2.5.

With this result and (3.15) at hand, show that

$$\mathbb{E}[|(\hat{\mathbf{w}})^\top \mathbf{x}|^2] = \sigma^2(\gamma) + o(p^{\text{eq.1-exo-portfolio-conclusion}}) \quad (3.17)$$

where

$$\begin{aligned} \sigma^2(\gamma) &\equiv \frac{\delta(\gamma)^2}{\delta(\gamma)^2 - c\beta(\gamma)(1-\gamma)^2} \frac{\mathbf{1}_p^\top \left(\frac{1-\gamma}{\delta(\gamma)} \mathbf{C} + \gamma \mathbf{I}_p \right)^{-1} \mathbf{C} \left(\frac{1-\gamma}{\delta(\gamma)} \mathbf{C} + \gamma \mathbf{I}_p \right)^{-1} \mathbf{1}_p}{\left(\mathbf{1}_p^\top \left(\frac{1-\gamma}{\delta(\gamma)} \mathbf{C} + \gamma \mathbf{I}_p \right)^{-1} \mathbf{1}_p \right)^2} \\ \beta(\gamma) &\equiv \frac{1}{p} \operatorname{tr} \mathbf{C}^2 \left(\frac{1-\gamma}{\delta(\gamma)} \mathbf{C} + \gamma \mathbf{I}_p \right)^{-2}. \end{aligned}$$

To this end, one may first demonstrate (for the more technical numerator) that

$$\hat{\mathbf{C}}(\gamma)^{-1} \mathbf{C} \hat{\mathbf{C}}(\gamma)^{-1} = -\frac{d}{d\omega} \left\{ (\hat{\mathbf{C}}(\gamma) + \omega \mathbf{C})^{-1} \right\}_{\omega=0}$$

and construct (for instance based on the proof of Theorem 2.5) a deterministic equivalent for $(\hat{\mathbf{C}}(\gamma) + \omega \mathbf{C})^{-1}$, or equivalently for $(\hat{\mathbf{S}}(\gamma) + \omega \mathbf{C})^{-1}$, which we may then differentiate and evaluate at $\omega = 0$ to retrieve the result.

Hint: In detail, obtaining this deterministic equivalent may be performed with the following steps: (i) show, using the Bai-Silverstein approach of the proof of Theorem 2.5, that

$$(\hat{\mathbf{S}} + \omega \mathbf{C})^{-1} \leftrightarrow (\alpha_\omega \mathbf{C} + \gamma \mathbf{I}_p + \omega \mathbf{C})^{-1}$$

where

$$\alpha_\omega = \frac{1 - \gamma}{\delta(\gamma)(1 - (1 - \gamma)c) + (1 - \gamma)c\Delta_\omega},$$

and Δ_ω is solution to

$$\Delta_\omega = \frac{1}{p} \operatorname{tr} \mathbf{C} (\alpha_\omega \mathbf{C} + \gamma \mathbf{I}_p + \omega \mathbf{C})^{-1}.$$

and in particular confirm that $\Delta_0 = \delta(\gamma)$ and $\alpha_0 = (1 - \gamma)/\delta(\gamma)$. Then proceed (ii) by showing that

$$\begin{aligned} -\frac{d}{d\omega} (\hat{\mathbf{S}} + \omega \mathbf{C})^{-1} &\leftrightarrow -\frac{d}{d\omega} (\alpha_\omega \mathbf{C} + \gamma \mathbf{I}_p + \omega \mathbf{C})^{-1} \\ &= \left(1 - c\alpha_\omega^2 \frac{d}{d\omega} \Delta_\omega \right) (\alpha_\omega \mathbf{C} + \gamma \mathbf{I}_p + \omega \mathbf{C})^{-1} \\ &\quad \times \mathbf{C} (\alpha_\omega \mathbf{C} + \gamma \mathbf{I}_p + \omega \mathbf{C})^{-1} \end{aligned}$$

and prove that

$$\frac{d}{d\omega} \Delta_\omega = -\frac{\frac{1}{p} \text{tr } \mathbf{C}^2 (\alpha_\omega \mathbf{C} + \gamma \mathbf{I}_p + \omega \mathbf{C})^{-2}}{1 - c\alpha_\omega^2 \frac{1}{p} \text{tr } \mathbf{C}^2 (\alpha_\omega \mathbf{C} + \gamma \mathbf{I}_p + \omega \mathbf{C})^{-2}}.$$

Put all things together (iii) and set ω to zero to conclude.

For the expression of $\sigma^2(\gamma)$ to be of practical interest, one needs a consistent estimate for $\sigma^2(\gamma)$ for all $\gamma > 0$, upon which an estimate of the optimal γ (i.e., the one achieving the minimum estimated risk) can be obtained. We will proceed here in two steps. From (3.16), first establish that

$$\begin{aligned} \hat{\delta}(\gamma) - \frac{\delta(\gamma)}{\frac{1}{p} \text{tr } \mathbf{C}} &\xrightarrow{\text{a.s.}} 0 \\ \hat{\delta}(\gamma) &\equiv \frac{1}{1 - (1 - \gamma) \frac{p}{n}} \frac{1}{n} \text{tr } \mathbf{X}^\top \hat{\mathbf{C}}(\gamma)^{-1} \mathbf{X} \text{ diag}\{\|\mathbf{x}_i\|^{-2}\}_{i=1}^n \\ &= \frac{1}{1 - (1 - \gamma) \frac{p}{n}} \frac{1}{n} \sum_{i=1}^n \frac{\mathbf{x}_i^\top \hat{\mathbf{C}}(\gamma)^{-1} \mathbf{x}_i}{\|\mathbf{x}_i\|^2} = \frac{1}{1 - (1 - \gamma) \frac{p}{n}} \frac{1}{n} \sum_{i=1}^n \frac{\mathbf{x}_i^\top \hat{\mathbf{C}}(\gamma)^{-1} \mathbf{x}_i}{\|\mathbf{x}_i\|^2}. \end{aligned}$$

Then, establish that

$$\begin{aligned} \hat{\sigma}^2(\gamma) - \frac{\sigma^2(\gamma)}{\frac{1}{p} \text{tr } \mathbf{C}} &\xrightarrow{\text{a.s.}} 0 && \text{eq:exo-portfolio-conclusion-estim} \quad (3.18) \\ \hat{\sigma}^2(\gamma) &\equiv \frac{\hat{\delta}(\gamma)}{1 - \gamma - (1 - \gamma)^2 \frac{p}{n}} \frac{\mathbf{1}_p^\top \hat{\mathbf{C}}(\gamma)^{-1} (\hat{\mathbf{C}}(\gamma) - \gamma \mathbf{I}_p) \hat{\mathbf{C}}(\gamma)^{-1} \mathbf{1}_p}{\left(\mathbf{1}_p^\top \hat{\mathbf{C}}(\gamma)^{-1} \mathbf{1}_p \right)^2} \end{aligned}$$

by developing $\hat{\mathbf{C}}(\gamma)^{-1} \mathbf{C}^{\frac{1}{2}} \mathbf{z}_i \mathbf{z}_i^\top \mathbf{C}^{\frac{1}{2}} \hat{\mathbf{C}}(\gamma)^{-1}$ (or equivalently $\hat{\mathbf{S}}(\gamma)^{-1} \mathbf{C}^{\frac{1}{2}} \mathbf{z}_i \mathbf{z}_i^\top \mathbf{C}^{\frac{1}{2}} \hat{\mathbf{S}}(\gamma)^{-1}$) as a function of the matrix form $\hat{\mathbf{S}}_{-i}(\gamma)^{-1} \mathbf{C}^{\frac{1}{2}} \mathbf{z}_i \mathbf{z}_i^\top \mathbf{C}^{\frac{1}{2}} \hat{\mathbf{S}}_{-i}(\gamma)^{-1}$ and taking the expectation over \mathbf{z}_i , together with the asymptotic approximation $\mathbf{1}_n^\top \hat{\mathbf{S}}_{-i}(\gamma)^{-1} \mathbf{C} \hat{\mathbf{S}}_{-i}(\gamma)^{-1} \mathbf{1}_n \simeq \mathbf{1}_n^\top \hat{\mathbf{C}}(\gamma)^{-1} \mathbf{C} \hat{\mathbf{C}}(\gamma)^{-1} \mathbf{1}_n$.

Confirm the results in (3.17) and (3.18) by reproducing Figure 3.10 in the setting where \mathbf{z}_i are i.i.d. student-t distribution, $\sqrt{\tau_i} = \sqrt{\chi_d^2/d}$ for χ_d^2 a Chi-square random variable with $d = 3$ degree of freedom (so that $\mathbb{E}[\tau_i] = 1$) and $\mathbf{C} = 5 \cdot \mathbf{u} \mathbf{u}^\top + \mathbf{I}_p$ for uniformly distributed $[\mathbf{u}]_i \sim \text{Unif}(0.5, 1.5)/\sqrt{p}$.

These results may also be simulated on real financial time series from leading international markets (e.g., based on daily historical returns from the NYSE, HSI, CAC-40, etc., over a time window of typically a few years). An exhaustive analysis is provided in [Yang et al., 2015].

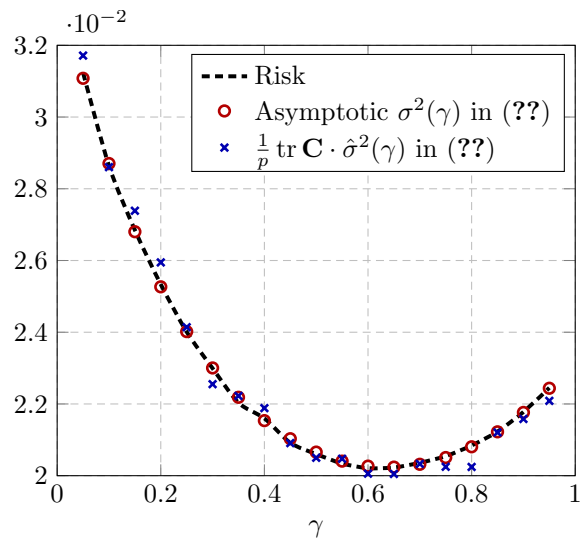


Figure 3.10: Portfolio risk, the asymptotic approximation $\sigma^2(\gamma)$, and the estimate $\frac{1}{p} \text{tr } \mathbf{C} \cdot \hat{\sigma}^2(\gamma)$ versus regularization penalty γ , for Student-t \mathbf{z}_i , Chi-square τ_i , $p = 256$ and $n = 512$. Results averaged over 50 runs. [Link to code]
[fig:exo-portfolio](#)

Chapter 4

Kernel Methods

chap:kernel-methods

In a broad sense, kernel methods are at the core of many, if not most, machine learning algorithms. Given a set of data $\mathbf{x}_1, \dots, \mathbf{x}_n \in \mathbb{R}^p$, most learning mechanisms rely on extracting the structural data information from direct pairwise comparisons $\kappa(\mathbf{x}_i, \mathbf{x}_j)$ for some *affinity metric* $\kappa(\cdot, \cdot)$. Gathered in an $n \times n$ matrix

$$\mathbf{K} = \{\kappa(\mathbf{x}_i, \mathbf{x}_j)\}_{i,j=1}^n$$

the “cumulative” effect of these comparisons for numerous ($n \gg 1$) data is at the heart of various supervised, semi-supervised, or unsupervised methods such as support vector machines, graph Laplacian-based learning, spectral clustering, and has deep connections to neural networks.

These applications will be thoroughly discussed in Section 4.5. For the moment though, our main interest lies in the mathematical characterization of the kernel matrix \mathbf{K} for various choices of affinity functions κ and for various statistical models of the data \mathbf{x}_i .

Clearly, from a purely machine learning perspective, the choice of the affinity function $\kappa(\cdot, \cdot)$ is central to a good performance of the learning method under study. Since real data in general have highly complex structures, a typical viewpoint is to assume that any pair of data \mathbf{x}_i and \mathbf{x}_j are not directly comparable in their ambient space but that there exists a convenient *feature extraction* function $\phi : \mathbb{R}^p \rightarrow \mathbb{R}^q$ ($q \in \mathbb{N} \cup \{+\infty\}$) such that $\phi(\mathbf{x}_i)$ and $\phi(\mathbf{x}_j)$ are more amenable to comparison. Otherwise stated, in the image of $\phi(\cdot)$, the data are more “linear” (or more “linearly separable” if one seeks to group the data in affinity classes). The simplest affinity function between \mathbf{x}_i and \mathbf{x}_j would then read $\phi(\mathbf{x}_i)^\top \phi(\mathbf{x}_j)$.

Since q is often much larger than p , the mere cost of evaluating $\phi(\mathbf{x}_i)^\top \phi(\mathbf{x}_j)$ can be deleterious to practical implementation. The so-called kernel trick is anchored in the remark that, for a wide class of such functions ϕ , $\phi(\mathbf{x}_i)^\top \phi(\mathbf{x}_j) = f(\|\mathbf{x}_i - \mathbf{x}_j\|^2)$ or $= f(\mathbf{x}_i^\top \mathbf{x}_j)$ for some function $f : \mathbb{R} \rightarrow \mathbb{R}$ and it suffices to simply evaluate $\|\mathbf{x}_i - \mathbf{x}_j\|^2$ or $\mathbf{x}_i^\top \mathbf{x}_j$ in the ambient space and then apply some f in an entry-wise manner, leading to more practically convenient methods.

Although the class of such functions f is inherently restricted by the need for a mapping ϕ to exist such that, say, $\phi(\mathbf{x})^\top \phi(\mathbf{y}) = f(\|\mathbf{x} - \mathbf{y}\|^2)$ (these are sometimes called Mercer kernel functions),¹ with time, practitioners have started to use arbitrary functions f and worked with generic kernel matrices of the form

$$\mathbf{K} = \{f(\|\mathbf{x}_i - \mathbf{x}_j\|^2)\}_{i,j=1}^n, \quad \text{or} \quad \mathbf{K} = \{f(\mathbf{x}_i^\top \mathbf{x}_j)\}_{i,j=1}^n$$

for diverse functions f . There are in particular empirical evidences showing that well-chosen “indefinite” (i.e., non-Mercer type) kernels can sometimes outperform conventional positive definite kernels that satisfy the Mercer’s condition [Haasdonk, 2005, Luss and d’Aspremont, 2008].

Remark 4.1 (Typical family of functions f and finite-dimensional setting). *It is important to raise here a direct consequence of the “finite-dimensional intuitions” inherent to kernel methods in machine learning. For an affinity of the type $\kappa(\mathbf{x}_i, \mathbf{x}_j) = f(\|\mathbf{x}_i - \mathbf{x}_j\|^2)$, it is natural to assume that f be a non-increasing function, as close-by data $\mathbf{x}_i, \mathbf{x}_j$ should have a stronger affinity than distant $\mathbf{x}_i, \mathbf{x}_j$. The popular choice $f(t) = \exp(-t/2)$ (known as the Gaussian or heat kernel, related to an infinite-dimensional map ϕ) is particularly appealing as it brings arbitrarily close data to a unit affinity ($\kappa(\mathbf{x}_i, \mathbf{x}_j) \rightarrow 1$ as $\|\mathbf{x}_i - \mathbf{x}_j\| \rightarrow 0$) and far data to a null affinity ($\kappa(\mathbf{x}_i, \mathbf{x}_j) \rightarrow 0$ as $\|\mathbf{x}_i - \mathbf{x}_j\| \rightarrow \infty$).*

We will subsequently show in this section that this natural reasoning often collapses when dealing with realistic large dimensional data, leading to erroneous intuitions and disrupting many conventional ideas behind kernel-based machine learning.

4.1 Basic setting

As pointed out in Remark 4.1 and shall become evident from the coming analysis, the finite dimensional intuition according to which f should be a “valid” Mercer function becomes rather meaningless when dealing with large dimensional data.

To fully capture this aspect, a first important consideration is to deal with “non-trivial” relative growth rates between p, n and the statistical data parameters. By non-trivial, we mean that the underlying classification or regression problem for which the kernel method is designed should neither be impossible nor too easy to solve as $p, n \rightarrow \infty$. In this section we will mostly focus on the use of kernel methods for classification, and thus the non-trivial settings are given in terms of the growth rate of the “distance” between data classes.

4.1.1 The non-trivial growth rates

In classical large- n only asymptotic statistics, laws of large numbers demand a scaling by $1/n$ of the summed observations. When centered, central limit

¹In particular, since the matrix $\{\phi(\mathbf{x}_i)^\top \phi(\mathbf{x}_j)\}_{i,j=1}^n$ is nonnegative definite, f must be such that $\{f(\|\mathbf{x}_i - \mathbf{x}_j\|^2)\}_{i,j=1}^n$ is also nonnegative definite irrespective of n and $\mathbf{x}_1, \dots, \mathbf{x}_n$.

theorems then occur after multiplication of the average by \sqrt{n} . A similar requirement is needed when we now assume that the dimension p of the data is also large. In particular, we will demand that the norm of each observation remains bounded. Assuming $\mathbf{x} \in \mathbb{R}^p$ is a vector of (bounded) entries, i.e., each of order $O(1)$ with respect to p , the correct normalization is typically \mathbf{x}/\sqrt{p} .

In the context of kernel methods, one wishes that the argument of $f(\cdot)$ in the inner-product kernel $f(\mathbf{x}_i^\top \mathbf{x}_j)$ or the distance kernel $f(\|\mathbf{x}_i - \mathbf{x}_j\|^2)$ be of order $O(1)$, when f is assumed fixed with respect to p .

The “correct” scaling appears not to be fully immediate. Letting \mathbf{x}_i have entries of order $O(1)$, one naturally has that $\|\mathbf{x}_i - \mathbf{x}_j\|^2 = O(p)$ and thus it seems natural to scale $\|\mathbf{x}_i - \mathbf{x}_j\|^2$ by $1/p$. Similarly, if the norm of the mean $\|\mathbb{E}[\mathbf{x}_i]\|$ of \mathbf{x}_i has the same order of magnitude as $\|\mathbf{x}_i\|$ itself (as it should in general), then for $\mathbf{x}_i, \mathbf{x}_j$ independent, $\mathbb{E}[\mathbf{x}_i^\top \mathbf{x}_j] = O(p)$. So again, one should scale the inner-product also by $1/p$. Hence the kernels

$$\mathbf{K} = \left\{ f\left(\frac{1}{p}\|\mathbf{x}_i - \mathbf{x}_j\|^2\right) \right\}_{i,j=1}^n, \quad \text{and} \quad \left\{ f\left(\frac{1}{p}\mathbf{x}_i^\top \mathbf{x}_j\right) \right\}_{i,j=1}^n.$$

Section 4.2 (and most applications thereafter) will be placed under these kernel forms. The most commonly used Gaussian (or heat, or radial-basis-function) kernel, defined as $\mathbf{K} = \{\exp(-\|\mathbf{x}_i - \mathbf{x}_j\|^2/2\sigma^2)\}_{i,j=1}^n$, falls into this family as one usually demands that $\sigma^2 \sim \mathbb{E}[\|\mathbf{x}_i - \mathbf{x}_j\|^2]$ (to avoid evaluating the exponential close to zero or infinity).

However, as already demonstrated in Section 1.1.3.1, if n scales like p , then, for the resulting classification problem to be asymptotically non-trivial, the difference $\|\mathbb{E}[\mathbf{x}_i] - \mathbb{E}[\mathbf{x}_j]\|^2$ need to scale as $O(1)$ rather than $O(p)$ (otherwise data would be too easy to cluster), resulting in $\|\mathbf{x}_i - \mathbf{x}_j\|^2/p$ possibly converging to a constant value irrespective of the data classes (of \mathbf{x}_i and \mathbf{x}_j), with a typical “spread” of order $O(1/\sqrt{p})$. Similarly, up to re-centering,² $\mathbf{x}_i^\top \mathbf{x}_j/p$ scales like $O(1/\sqrt{p})$ rather than $O(1)$. As such, it seems more appropriate to normalize the kernels as

$$[\mathbf{K}]_{ij} = f\left(\frac{\|\mathbf{x}_i - \mathbf{x}_j\|^2}{\sqrt{p}} - \frac{1}{n^2} \sum_{i',j'} \frac{\|\mathbf{x}_{i'} - \mathbf{x}_{j'}\|^2}{\sqrt{p}}\right), \quad \text{or} \quad [\mathbf{K}]_{ij} = f\left(\frac{1}{\sqrt{p}} \mathbf{x}_i^\top \mathbf{x}_j\right)$$

in order here to avoid evaluating f essentially at a single value (equal to zero for the inner-product kernel and the average data distance for the distance kernel).

This “properly scaling” setting is in fact much richer than the $1/p$ normalization when n, p are of the same order of magnitude. Sections 4.3 and 4.4 elaborate on this scenario.

²More precisely, $[\mathbf{P}\mathbf{X}^\top \mathbf{X}\mathbf{P}]_{ij}$ with $\mathbf{P} = \mathbf{I}_n - \frac{1}{n}\mathbf{1}_n\mathbf{1}_n^\top$ the data centering projector.

4.1.2 Statistical data model

In the remainder of this section, we assume the observation of n independent data vectors from in total k classes gathered as $\mathbf{X} = [\mathbf{x}_1, \dots, \mathbf{x}_n] \in \mathbb{R}^{p \times n}$ where

$$\begin{aligned}\mathbf{x}_1, \dots, \mathbf{x}_{n_1} &\sim \mathcal{N}(\boldsymbol{\mu}_1, \mathbf{C}_1) \\ &\vdots \quad \vdots \\ \mathbf{x}_{n-n_k+1}, \dots, \mathbf{x}_n &\sim \mathcal{N}(\boldsymbol{\mu}_k, \mathbf{C}_k)\end{aligned}$$

which is a k -class *Gaussian mixture model* (GMM) with a fixed cardinality n_1, \dots, n_k in each class. The fact that the data are labeled according to classes simplifies the notation but has no practical consequence in the analysis.

We will denote

$$\mathbf{x}_i \sim \mathcal{N}(\boldsymbol{\mu}_a, \mathbf{C}_a) \Leftrightarrow \mathbf{x}_i \in \mathcal{C}_a$$

for $a \in \{1, \dots, k\}$ and use the matrix

$$\mathbf{J} = [\mathbf{j}_1, \dots, \mathbf{j}_k] \in \mathbb{R}^{n \times k}, \quad \mathbf{j}_a = [\underbrace{0, \dots, 0}_{n_1 + \dots + n_{a-1}}, \underbrace{1, \dots, 1}_{n_a}, \underbrace{0, \dots, 0}_{n_{a+1} + \dots + n_k}]^\top$$

to summarize the class label information (which is known in a supervised learning setting and is to be recovered in unsupervised learning).

We shall systematically make the following simplifying growth rate assumption for p, n, n_1, \dots, n_k .

Assumption 1 (Growth rate of data size and number). *As $n \rightarrow \infty$, we have $p/n \rightarrow c \in (0, \infty)$ and $n_a/n \rightarrow c_a \in (0, 1)$.*

This assumption in particular implies that each class is “large” in the sense that their cardinality increases with n .³

Accordingly with the discussions in Chapter 2, from a random matrix “universal” perspective, the Gaussian mixture assumption will often (yet not always) turn out equivalent to demanding that

$$\mathbf{x}_i = \boldsymbol{\mu}_a + \mathbf{C}_a^{\frac{1}{2}} \mathbf{z}_i$$

for $\mathbf{x}_i \in \mathcal{C}_a$, with $\mathbf{z}_i \in \mathbb{R}^p$ a random vector with i.i.d. entries of zero mean, finite variance and bounded (say fourth) order moment.

This hypothesis is thus seemingly quite restrictive as it imposes that the data, up to centering and linear scaling, are composed of i.i.d. entries. Equivalently, this suggests that only data that are the resultant of affine transformations of

³If we were to relax the assumption by letting, say \mathcal{C}_a to be of much smaller cardinality than $O(n)$, it would then be necessary to counterbalance this lack of redundancy by increasing the rate of the “distances” between the statistics of \mathcal{C}_a (mean and covariance in particular) and the other classes.

vectors with i.i.d. entries can be studied. This is obviously quite restrictive in practice as “real data” are deemed much more complex.

Exploring the notion of concentrated random vectors introduced in Section 2.7, Chapter 8 will open up this discussion by showing that a much larger class of (statistical) data models embrace the same asymptotic statistics.

4.2 Distance and inner-product random kernel matrices

sec:basic-scaling-kernels

The most widely used kernel model in machine learning applications is the heat kernel $\mathbf{K} = \{\exp(-\|\mathbf{x}_i - \mathbf{x}_j\|^2/2\sigma^2)\}_{i,j=1}^n$, for some $\sigma > 0$. It is thus natural to start our large dimensional analysis of kernel random matrices by focusing on this model.

As mentioned in the previous sections, for the Gaussian mixture model above, as the dimension p increases, σ^2 needs to scale as $O(p)$, so say $\sigma^2 = \tilde{\sigma}^2 p$, to avoid evaluating the exponential at increasingly large values. As such, the prototypical kernel of present interest is

$$\mathbf{K} = \left\{ f \left(\frac{1}{p} \|\mathbf{x}_i - \mathbf{x}_j\|^2 \right) \right\}_{i,j=1}^n$$

for f a sufficiently smooth function (e.g., $f(t) = \exp(-t/2\tilde{\sigma}^2)$ for the heat kernel).

4.2.1 Main intuition

Euclidean random matrix with equal covariances. In order to get a first picture of the large dimensional behavior of \mathbf{K} , let us develop the distance $\|\mathbf{x}_i - \mathbf{x}_j\|^2/p$ for $\mathbf{x}_i \in \mathcal{C}_a$ and $\mathbf{x}_j \in \mathcal{C}_b$, with $i \neq j$.

For simplicity, let us assume for the moment $\mathbf{C}_1 = \dots = \mathbf{C}_k = \mathbf{I}_p$ and recall the notation $\mathbf{x}_i = \boldsymbol{\mu}_a + \mathbf{z}_i$. We have, for $i \neq j$,

$$\begin{aligned} \frac{1}{p} \|\mathbf{x}_i - \mathbf{x}_j\|^2 &= \frac{1}{p} \|\boldsymbol{\mu}_a - \boldsymbol{\mu}_b\|^2 + \frac{2}{p} (\boldsymbol{\mu}_a - \boldsymbol{\mu}_b)^\top (\mathbf{z}_i - \mathbf{z}_j) \\ &\quad + \frac{1}{p} \|\mathbf{z}_i\|^2 + \frac{1}{p} \|\mathbf{z}_j\|^2 - \frac{2}{p} \mathbf{z}_i^\top \mathbf{z}_j. \end{aligned}$$

For $\|\mathbf{x}_i\|$ of order $O(\sqrt{p})$, if $\|\boldsymbol{\mu}_a\| = O(\sqrt{p})$ for all $a \in \{1, \dots, k\}$ (which would be natural), then $\|\boldsymbol{\mu}_a - \boldsymbol{\mu}_b\|^2/p$ is a priori of order $O(1)$ while, by the central limit theorem, $\|\mathbf{z}_i\|^2/p = 1 + O(p^{-\frac{1}{2}})$. Also, again by the central limit theorem, $\mathbf{z}_i^\top \mathbf{z}_j/p = O(p^{-\frac{1}{2}})$ and $2(\boldsymbol{\mu}_a - \boldsymbol{\mu}_b)^\top (\mathbf{z}_i - \mathbf{z}_j)/p = O(p^{-\frac{1}{2}})$.

As a consequence, as $p \rightarrow \infty$, $\|\mathbf{x}_i - \mathbf{x}_j\|^2/p$ is dominated by $\|\boldsymbol{\mu}_a - \boldsymbol{\mu}_b\|^2/p + 2$ and easily discriminates classes from the pairwise observations of $\mathbf{x}_i, \mathbf{x}_j$, making the classification problem asymptotically trivial (without having to resort to any kernel method). It is thus of interest to understand how kernels come into play in the more practical scenario where the class distances are less significant.

To this end, we now demand that $\|\boldsymbol{\mu}_a - \boldsymbol{\mu}_b\| = O(1)$, which is the minimal distance rate that can be discriminated from a mere Bayesian inference analysis as discussed in Section 1.1.3.1. Since the kernel operates only on the distances $\|\mathbf{x}_i - \mathbf{x}_j\|$, we may even request (up to centering all data by, say, the constant vector $\frac{1}{n} \sum_{i=1}^n n_a \boldsymbol{\mu}_a$) that $\|\boldsymbol{\mu}_a\| = O(1)$ for each a .

In this case though, $\|\boldsymbol{\mu}_a - \boldsymbol{\mu}_b\|^2/p = O(p^{-1})$ which is dominated by the noise terms $2\mathbf{z}_i^\top \mathbf{z}_j/p$ and $\|\mathbf{z}_i\|^2/p + \|\mathbf{z}_j\|^2/p - 2$, both of order $O(p^{-1/2})$. It thus seems at first that $\|\boldsymbol{\mu}_a - \boldsymbol{\mu}_b\| = O(1)$ is too demanding a constraint.

However, “matrix-wise”, the situation appears to be quite different. Indeed, we have

$$\begin{aligned} \left\{ \frac{1}{p} \|\mathbf{x}_i - \mathbf{x}_j\|^2 \right\}_{i,j=1}^n &= 2 \cdot \mathbf{1}_n \mathbf{1}_n^\top + \frac{1}{p} \mathbf{J} \left\{ \|\boldsymbol{\mu}_a - \boldsymbol{\mu}_b\|^2 \right\}_{i,j=1}^k \stackrel{\text{eq:euclidean-matrix}}{=} \\ &\quad + \boldsymbol{\psi} \mathbf{1}_n^\top + \mathbf{1}_n \boldsymbol{\psi}^\top - \frac{2}{p} \mathbf{Z}^\top \mathbf{Z} \\ &\quad + \frac{2}{p} (\mathbf{d} \mathbf{1}_n^\top + \mathbf{1}_n \mathbf{d}^\top) - \frac{2}{p} (\mathbf{J} \mathbf{M}^\top \mathbf{Z} + \mathbf{Z}^\top \mathbf{M} \mathbf{J}) - \text{diag}(\cdot) \end{aligned} \quad (4.1)$$

where $\mathbf{M} = [\boldsymbol{\mu}_1, \dots, \boldsymbol{\mu}_k] \in \mathbb{R}^{p \times k}$, $\boldsymbol{\psi} \in \mathbb{R}^n$ is the vector with independent (asymptotically Gaussian) entries $\psi_i = 1 - \|\mathbf{z}_i\|^2/p = O(p^{-1/2})$, $\mathbf{d} = \text{diag}(\mathbf{J} \mathbf{M}^\top \mathbf{Z}) \in \mathbb{R}^n$ having independent entries of zero mean and variance $\|\boldsymbol{\mu}_a\|^2 = O(1)$ if the i -th entry has mean $\mathbb{E}[\mathbf{x}_i] = \boldsymbol{\mu}_a$, and the operator $\mathbf{X} - \text{diag}(\cdot)$ returns matrix \mathbf{X} with diagonal entries replaced by zeros.

From a spectral viewpoint, observe that this matrix is largely dominated by the matrix $2 \cdot \mathbf{1}_n \mathbf{1}_n^\top$ which has norm $2n$. Next in norm comes the rank-2 matrix $\boldsymbol{\psi} \mathbf{1}_n^\top + \mathbf{1}_n \boldsymbol{\psi}^\top$. The sum of these being of rank 2 (since $\mathbf{1}_n$ is common), these matrices marginally affect the spectrum of the whole matrix. What is particularly interesting now is to observe that the resulting matrix is an (in fact not quite standard) “properly normalized” spiked model, as studied in Section 2.5. Indeed, $2\mathbf{Z}^\top \mathbf{Z}/p$ is a Wishart matrix having limiting spectral measure the Marčenko-Pastur distribution with support of order $O(1)$ and all eigenvalues remaining asymptotically close to the support (Theorem 2.10); then $\mathbf{J} \left\{ \|\boldsymbol{\mu}_a - \boldsymbol{\mu}_b\|^2 \right\}_{i,j=1}^k \mathbf{J}^\top/p + 2(\mathbf{d} \mathbf{1}_n^\top + \mathbf{1}_n \mathbf{d}^\top)/p - 2(\mathbf{J} \mathbf{M}^\top \mathbf{Z} + \mathbf{Z}^\top \mathbf{M} \mathbf{J})/p$ is a rank at most $2k + 2$ matrix with the fundamental property also to be of norm $O(1)$ (which is easily verified from our assumptions).

This may seem surprising at first. Indeed, while $\|\boldsymbol{\mu}_a - \boldsymbol{\mu}_b\|^2/p = O(p^{-1})$ is largely dominated by $2\mathbf{z}_i^\top \mathbf{z}_j/p = O(p^{-1/2})$ (and thus the class information is asymptotically *not* accessible from *any* entry $\|\mathbf{x}_i - \mathbf{x}_j\|^2/p$ alone), matrix-wise, the operator norm of $\mathbf{J} \left\{ \|\boldsymbol{\mu}_a - \boldsymbol{\mu}_b\|^2 \right\}_{i,j=1}^k \mathbf{J}^\top/p$ is of the same order as that of $2\mathbf{Z}^\top \mathbf{Z}/p$. This can be understood by the “redundant” effect of the multiple copies (of order $O(n)$) of \mathbf{x}_i sharing the same mean $\boldsymbol{\mu}_a$, for each a , which together “coherently align” into a matrix with all “energy” concentrated into few nonzero eigenvalues (up to $k \ll n$); this is to be opposed to $2\mathbf{Z}^\top \mathbf{Z}/p$ the entries of which are all centered (except on the diagonal) with essentially independent fluctuations, that result in a more or less even spread of the matrix

energy in its n eigenvalues. Altogether, this redundancy effect compensates the individual weak information carried by each \mathbf{x}_i as opposed to the noise.

From the results of Section 2.5 on spiked models, it is thus expected that, as $p, n \rightarrow \infty$ with $p/n \rightarrow c \in (0, \infty)$, if the dominant eigenvalues of the matrix $\{\|\boldsymbol{\mu}_a - \boldsymbol{\mu}_b\|^2\}_{a,b=1}^k$ exceed a certain threshold (that depends on c), the Euclidean distance matrix of (4.1) asymptotically has isolated eigenvalues.

More importantly, the eigenvectors associated with these eigenvalues are, as a consequence, to some extent aligned to the eigenvectors of the rank- k matrix $\mathbf{J} \{\|\boldsymbol{\mu}_a - \boldsymbol{\mu}_b\|^2\}_{i,j=1}^k \mathbf{J}^\top / p$. The latter precisely lie in the span of the columns $\mathbf{j}_1, \dots, \mathbf{j}_k$ of \mathbf{J} . Thus, the (possible isolated) eigenvectors shall correlate to the linear combinations of the indicator vectors \mathbf{j}_a , which is exactly what is observed in practice: the class information can be recovered (in a fully unsupervised manner) from the dominant eigenvectors of \mathbf{K} . This suggests that, while the class of any \mathbf{x}_i cannot be retrieved from a mere pairwise comparison of the distances $\|\mathbf{x}_i - \mathbf{x}_j\|$, matrix-wise, the eigenvectors of \mathbf{K} provide this information. This remark is at the heart of the large dimensional analysis of the spectral clustering algorithms discussed in Section 4.5.1.

Including covariance structures. The kernel matrix \mathbf{K} in (4.1) has so far only been described under the setting where (i) $f(t) = t$ and (ii) $\mathbf{C}_a = \mathbf{I}_p$. A first observation is that, for $\mathbf{C}_1, \dots, \mathbf{C}_k$ distinct (from \mathbf{I}_p), we naturally have $\text{tr}(\mathbf{C}_a - \mathbf{C}_b)/p = O(1)$ (with $\text{tr} \mathbf{C}/p \leq \|\mathbf{C}\| = O(1)$) and thus, defining $\mathbf{C}^\circ = \sum_{a=1}^k \frac{n_a}{n} \mathbf{C}_a$ and $\mathbf{C}_a^\circ = \mathbf{C}_a - \mathbf{C}^\circ$ the centered covariance, we necessarily find $\text{tr} \mathbf{C}_a^\circ/p = O(1)$ for $a = 1, \dots, k$.

Accounting for covariance matrices, for $\mathbf{x}_i = \boldsymbol{\mu}_a + \mathbf{C}_a^{1/2} \mathbf{z}_i$, in the development of $\|\mathbf{x}_i - \mathbf{x}_j\|^2/p$, we thus now have $\mathbf{z}_i^\top \mathbf{C}_a \mathbf{z}_i/p + \mathbf{z}_j^\top \mathbf{C}_b \mathbf{z}_j/p = \text{tr} \mathbf{C}_a/p + \text{tr} \mathbf{C}_b/p + O(p^{-\frac{1}{2}}) = 2 \text{tr} \mathbf{C}^\circ/p + \text{tr} \mathbf{C}_a^\circ/p + \text{tr} \mathbf{C}_b^\circ/p + O(p^{-1/2})$. As a consequence, here again, $\text{tr} \mathbf{C}_a^\circ/p + \text{tr} \mathbf{C}_b^\circ/p = O(1)$ predominates the noise terms $2\mathbf{z}_i^\top \mathbf{C}_a^{1/2} \mathbf{C}_b^{1/2} \mathbf{z}_j/p = O(p^{-1/2})$ and $\mathbf{z}_i^\top \mathbf{C}_a \mathbf{z}_i/p - \text{tr} \mathbf{C}_a/p = O(p^{-1/2})$, and classification becomes trivial. For this not to arise, we further demand that $\text{tr} \mathbf{C}_a^\circ/p = O(p^{-1/2})$, i.e., that “trace-wise” the covariances $\mathbf{C}_1, \dots, \mathbf{C}_k$ are at most distinct by $O(\sqrt{p})$ rather than $O(p)$. This appears to be the correct (and again, from the analysis of Section 1.1.3, this Bayesian minimal) regime of non-trivial classification when n, p scale proportionally.

Remark that this constraint is quite interesting as, in an effort not to trivialize classification, it in turn has the effect to “entry-wise trivialize the Euclidean

distance matrix". Indeed, under this assumption, for $i \neq j$,

$$\begin{aligned} \frac{1}{p} \|\mathbf{x}_i - \mathbf{x}_j\|^2 &= \frac{2}{p} \operatorname{tr} \mathbf{C}^\circ + \frac{1}{p} \|\boldsymbol{\mu}_a - \boldsymbol{\mu}_b\|^2 + \frac{1}{p} \operatorname{tr}(\mathbf{C}_a^\circ + \mathbf{C}_b^\circ) - \frac{2}{p} \mathbf{z}_i^\top \mathbf{C}_a^{\frac{1}{2}} \mathbf{C}_b^{\frac{1}{2}} \mathbf{z}_j \\ &\quad + \left(\frac{1}{p} \mathbf{z}_i^\top \mathbf{C}_a \mathbf{z}_i - \frac{1}{p} \operatorname{tr} \mathbf{C}_a \right) + \left(\frac{1}{p} \mathbf{z}_i^\top \mathbf{C}_b \mathbf{z}_i - \frac{1}{p} \operatorname{tr} \mathbf{C}_b \right) \\ &\quad + \frac{2}{p} (\boldsymbol{\mu}_a - \boldsymbol{\mu}_b)^\top (\mathbf{C}_a^{\frac{1}{2}} \mathbf{z}_i - \mathbf{C}_b^{\frac{1}{2}} \mathbf{z}_j) \\ &= \frac{2}{p} \operatorname{tr} \mathbf{C}^\circ + O(p^{-\frac{1}{2}}). \end{aligned}$$

As such, all of the entries are dominated by the constant $2 \operatorname{tr} \mathbf{C}^\circ / p$.

On the other hand, note that similar to (4.1), matrix-wise, it appears that

$$\begin{aligned} \left\{ \frac{1}{p} \|\mathbf{x}_i - \mathbf{x}_j\|^2 \right\}_{i,j=1}^n &= \frac{2}{p} \operatorname{tr} \mathbf{C}^\circ \cdot \mathbf{1}_n \mathbf{1}_n^\top + \frac{1}{p} \mathbf{J} \{ \|\boldsymbol{\mu}_a - \boldsymbol{\mu}_b\|^2 \}_{i,j=1}^k \mathbf{J}^\top \\ &\quad + (\boldsymbol{\psi} + \mathbf{J}\mathbf{t}) \mathbf{1}_n^\top + \mathbf{1}_n (\boldsymbol{\psi} + \mathbf{J}\mathbf{t})^\top - \frac{2}{p} \mathbf{W}^\top \mathbf{W} \\ &\quad + \frac{2}{p} (\mathbf{d}\mathbf{1}_n^\top + \mathbf{1}_n \mathbf{d}^\top) - \frac{2}{p} (\mathbf{J}\mathbf{M}^\top \mathbf{W} + \mathbf{W}^\top \mathbf{M}\mathbf{J}) \\ &\quad - \operatorname{diag}(\cdot) \end{aligned} \tag{4.2}$$

where we denoted $\mathbf{W} = [\mathbf{C}_1^{\frac{1}{2}} \mathbf{Z}_1, \dots, \mathbf{C}_k^{\frac{1}{2}} \mathbf{Z}_k] \in \mathbb{R}^{p \times n}$, $\mathbf{t} = \{\operatorname{tr} \mathbf{C}_a^\circ / p\}_{a=1}^k \in \mathbb{R}^k$, $\boldsymbol{\psi}_i = \mathbf{z}_i^\top \mathbf{C}_a \mathbf{z}_i / p - \operatorname{tr} \mathbf{C}_a / p = O(p^{-1/2})$ for $\mathbf{x}_i \in \mathcal{C}_a$, and similar to previously used $\mathbf{d} = \operatorname{diag}(\mathbf{J}\mathbf{M}^\top \mathbf{W})$. Again, the matrix is dominated by the $O(n)$ -norm matrix $2 \operatorname{tr} \mathbf{C}^\circ / p \cdot \mathbf{1}_n \mathbf{1}_n^\top$, but the second dominant term, the $O(\sqrt{n})$ -norm rank-2 matrix $(\boldsymbol{\psi} + \mathbf{J}\mathbf{t}) \mathbf{1}_n^\top + \mathbf{1}_n (\boldsymbol{\psi} + \mathbf{J}\mathbf{t})^\top$ is now informative as $\mathbf{J}\mathbf{t}$ is block-wise composed of elements from each class. This matrix being norm-dominant (once the irrelevant rank-1 matrix $2 \operatorname{tr} \mathbf{C}^\circ / p \cdot \mathbf{1}_n \mathbf{1}_n^\top$ discarded), the vector $\boldsymbol{\psi} + \mathbf{J}\mathbf{t}$ is directly accessible (for all large p, n). Thus, a mere principle component analysis gives access to its entries (for $\mathbf{x}_i \in \mathcal{C}_a$):

$$t_a + [\boldsymbol{\psi}]_i \stackrel{\mathcal{L}}{=} \frac{1}{p} \operatorname{tr} \mathbf{C}_a^\circ + \sqrt{\frac{3}{p^2} \operatorname{tr} \mathbf{C}_a^2} \cdot \mathcal{N}(0, 1) \tag{4.3}$$

in law, where the factor 3 arises from the fourth order moment of the standard Gaussian, which follows from the central limit theorem on $\|\mathbf{z}_i\|^2$. Since both $\operatorname{tr} \mathbf{C}_a^\circ / p$ and $\sqrt{3 \operatorname{tr} \mathbf{C}_a^2 / p^2}$ are of order $O(p^{-1/2})$, non-trivial clustering can be performed based on the covariance traces directly using the second dominant eigenvector of the Euclidean matrix.

Setting $(\boldsymbol{\psi} + \mathbf{J}\mathbf{t}) \mathbf{1}_n^\top + \mathbf{1}_n (\boldsymbol{\psi} + \mathbf{J}\mathbf{t})^\top$ aside, we are then left with the smaller order terms

$$\begin{aligned} &- \frac{2}{p} \mathbf{W} \mathbf{W}^\top + \frac{1}{p} \mathbf{J} \{ \|\boldsymbol{\mu}_a - \boldsymbol{\mu}_b\|^2 \}_{i,j=1}^k \mathbf{J}^\top + \frac{2}{p} (\mathbf{d}\mathbf{1}_n^\top + \mathbf{1}_n \mathbf{d}^\top) \\ &- \frac{2}{p} (\mathbf{J}\mathbf{M}^\top \mathbf{W} + \mathbf{W}^\top \mathbf{M}\mathbf{J}) \end{aligned}$$

from which discrimination based on the means μ_1, \dots, μ_k can be performed.

This is as far as the Euclidean distance random matrix can go. In particular, consider the case where $\mu_1 = \dots = \mu_k$ and $\text{tr } \mathbf{C}_1 = \dots = \text{tr } \mathbf{C}_k$ while the $\mathbf{C}_1, \dots, \mathbf{C}_k$ are different. Then, asymptotically, no spectral information can be retrieved from the Euclidean distance matrix which can be used to discriminate the data classes (the covariance matrices appear in \mathbf{W} but the singular vectors of \mathbf{W} do not provide straightforward access to this information).

This is where the limitations of the linear kernel $f(t) = t$ first appear. To go further and be capable to classify data with different covariance structures, f must be taken nonlinear.

Non-linear kernel model. To analyze the general nonlinear kernel, we start from (4.2) of the Euclidean matrix $\{\|\mathbf{x}_i - \mathbf{x}_j\|^2/p\}_{i,j=1}^n$. We recall that, entrywise, the matrix is dominated by $\tau_p \equiv 2 \text{tr } \mathbf{C}^\circ/p$. As such, if f is smooth around τ_p , a Taylor-expansion can be performed to obtain (for $i \neq j$)

$$\begin{aligned} f\left(\frac{1}{p}\|\mathbf{x}_i - \mathbf{x}_j\|^2\right) &= f(\tau_p) + f'(\tau_p)\left(\frac{1}{p}\|\mathbf{x}_i - \mathbf{x}_j\|^2 - \tau_p\right) \\ &\quad + \frac{f''(\tau_p)}{2}\left(\frac{1}{p}\|\mathbf{x}_i - \mathbf{x}_j\|^2 - \tau_p\right)^2 \\ &\quad + O\left(\left(\frac{1}{p}\|\mathbf{x}_i - \mathbf{x}_j\|^2 - \tau_p\right)^3\right). \end{aligned}$$

Let us assume for the moment that $f'(\tau_p) \neq 0$, that is f does not have a minimum at (or in a vanishing vicinity of) τ_p . Since τ_p is of order $O(1)$ and f is smooth around τ_p , all derivatives $f^{(\ell)}(\tau_p)$ are of order $O(1)$. As for $(\|\mathbf{x}_i - \mathbf{x}_j\|^2/p - \tau_p)^\ell$, from our previous calculus, it is of order $O(p^{-\ell/2})$.

As a consequence, $(\|\mathbf{x}_i - \mathbf{x}_j\|^2/p - \tau_p)^3 = O(p^{-3/2})$ so that, in the best case the matrix $\{(\|\mathbf{x}_i - \mathbf{x}_j\|^2/p - \tau_p)^3\}_{i,j=1}^n$ has operator norm of order $O(p^{-1/2})$. Given the presence of the full-rank “noise” term $-2f'(\tau_p)\mathbf{W}\mathbf{W}^\top/p$ in the Taylor expansion, this third-order term vanishes in operator norm. This is not the case for the second-order term that may be of operator norm of order $O(1)$ (which, as we shall see, it indeed does). This is valid provided that $f'(\tau_p) \neq 0$: the case where $f'(\tau_p) \simeq 0$ has a fundamentally different behavior and will be treated subsequently in Section 4.3.

As such, for $f'(\tau_p) \neq 0$, a second order Taylor expansion of the kernel matrix \mathbf{K} is sufficient to fully characterize the spectral behavior of \mathbf{K} in the large n,p regime.

rem:centering_kernel

Remark 4.2 (On data/feature centering). *Replacing all \mathbf{x}_i by $\mathbf{x}_i - \mathbf{u}$ for some fixed vector \mathbf{u} should not impede classification. As such, one may freely work with $\mathbf{x}_i^\circ = \mathbf{x}_i - \frac{1}{n} \sum_{j=1}^n \mathbf{x}_j$. This is particularly relevant when dealing with inner-product kernels of the type $f(\mathbf{x}_i^\top \mathbf{x}_j)$ since then f is applied in other positions, but is irrelevant for distance kernels since $f(\|\mathbf{x}_i - \mathbf{x}_j\|^2) = f(\|\mathbf{x}_i^\circ - \mathbf{x}_j^\circ\|^2)$.*

Now, recall that for Mercer kernels, $f(\|\mathbf{x}_i - \mathbf{x}_j\|^2) = \phi(\mathbf{x}_i)^\top \phi(\mathbf{x}_j)$ for some function $\phi : \mathbb{R}^p \rightarrow \mathbb{R}^q$ (say). Then it may seem natural to also center data in the feature space \mathbb{R}^q . That is, instead of working with \mathbf{K} one may equivalently work with \mathbf{PKP} where $\mathbf{P} = \mathbf{I}_n - \frac{1}{n}\mathbf{1}_n\mathbf{1}_n^\top$ is the centering operator.

This has a major technical advantage: since $\mathbf{P}\mathbf{1}_n = \mathbf{0}$, from the calculus above, many terms that are irrelevant to classification vanish and the study of \mathbf{PKP} is made simpler. It is however not so clear what the impact of this centering operation to non-Mercer kernels really is.

4.2.2 Main Results

4.2.2.1 Kernel random equivalent.

A careful derivation of all terms in the second-order Taylor expansion of \mathbf{K} above is rigorously performed in [Couillet and Benaych-Georges, 2016]. The result is summarized as follows.

theo:K

Theorem 4.1 (Couillet and Benaych-Georges [2016]). *Let f be three-times continuously differentiable in the vicinity of $\tau_p = \frac{2}{p} \operatorname{tr} \mathbf{C}^\circ$ and such that $0 < \liminf_p |f'(\tau_p)| \leq \limsup_p |f'(\tau_p)| < \infty$. Further assume the growth rates*

$$\begin{aligned} \mathbf{M} &= [\boldsymbol{\mu}_1^\circ, \dots, \boldsymbol{\mu}_k^\circ] = O_{\|\cdot\|}(1), \quad \boldsymbol{\mu}_\ell^\circ = \boldsymbol{\mu}_\ell - \sum_{a=1}^k \frac{n_a}{n} \boldsymbol{\mu}_a \\ \mathbf{t} &= [t_1, \dots, t_k]^\top = O_{\|\cdot\|}(1), \quad t_a = \frac{1}{\sqrt{p}} \operatorname{tr}(\mathbf{C}_a - \mathbf{C}^\circ) \\ \mathbf{S} &= \{S_{ab}\}_{a,b=1}^k = O_{\|\cdot\|}(1), \quad S_{ab} = \frac{1}{p} \operatorname{tr} \mathbf{C}_a \mathbf{C}_b. \end{aligned}$$

Then, with previous notations, as $p, n \rightarrow \infty$ with $p/n \rightarrow c \in (0, \infty)$ and $n_a/n \rightarrow c_a \in (0, 1)$,

$$\|\mathbf{K} - \tilde{\mathbf{K}}\| \xrightarrow{a.s.} 0$$

where $\mathbf{K} = \left\{ f\left(\frac{1}{p}\|\mathbf{x}_i - \mathbf{x}_j\|^2\right) \right\}_{i,j=1}^n$ and

$$\tilde{\mathbf{K}} = -2f'(\tau_p) \left(\frac{1}{p} \mathbf{W}^\top \mathbf{W} + \mathbf{V} \mathbf{A} \mathbf{V}^\top \right) + (f(0) - f(\tau_p) + \tau_p f'(\tau_p)) \mathbf{I}_n$$

with $\mathbf{W} = [\mathbf{W}_1, \dots, \mathbf{W}_k]$, $\mathbf{W}_a \in \mathbb{R}^{p \times n_a}$,

$$\begin{aligned} \mathbf{V} &= \left[\frac{\mathbf{J}}{\sqrt{p}}, \frac{\mathbf{W}^\top \mathbf{M}}{\sqrt{p}}, \tilde{\mathbf{v}}, \boldsymbol{\psi}, \sqrt{p}\boldsymbol{\psi}^2, \tilde{\boldsymbol{\psi}} \right], \quad \tilde{\mathbf{v}} = \left\{ \frac{1}{\sqrt{p}} \mathbf{W}_a^\top \boldsymbol{\mu}_a \right\}_{a=1}^k, \\ \tilde{\boldsymbol{\psi}} &= \operatorname{diag}(t_a \mathbf{1}_{n_a}) \boldsymbol{\psi}, \quad \boldsymbol{\psi} = \frac{1}{p} \{ \|\mathbf{w}_i\|^2 - \mathbb{E}[\|\mathbf{w}_i\|^2] \}_{i=1}^n \end{aligned}$$

with $\psi^2 \equiv [\psi_1^2, \dots, \psi_n^2]$ and

$$\mathbf{A} = \mathbf{A}_n + \mathbf{A}_{\sqrt{n}} + \mathbf{A}_1$$

with $\mathbf{A}_{n^\alpha} \in \mathbb{R}^{(2k+4) \times (2k+4)}$ the symmetric matrices of operator norm of order $O(n^\alpha)$ described as

$$\begin{aligned} \mathbf{A}_n &= -\frac{f(\tau_p)}{2f'(\tau_p)} p \begin{bmatrix} \mathbf{1}_k \mathbf{1}_k^\top & \mathbf{0} \\ * & \mathbf{0} \end{bmatrix} \\ \mathbf{A}_{\sqrt{n}} &= -\frac{1}{2}\sqrt{p} \begin{bmatrix} \{t_a + t_b\}_{a,b=1}^k & \mathbf{0} & \mathbf{0} & \mathbf{1}_k & \mathbf{0} & \mathbf{0} \\ * & \mathbf{0} & \mathbf{0} & \mathbf{0} & \mathbf{0} & \mathbf{0} \\ * & * & 0 & 0 & 0 & 0 \\ * & * & * & 0 & 0 & 0 \\ * & * & * & 0 & 0 & 0 \\ * & * & * & * & 0 & 0 \\ * & * & * & * & * & 0 \end{bmatrix} \\ \mathbf{A}_1 &= \begin{bmatrix} \mathbf{A}_{1,11} & \mathbf{I}_k & -\mathbf{1}_k & -\frac{f''(\tau_p)}{2f'(\tau_p)} \mathbf{t} & -\frac{f''(\tau_p)}{4f'(\tau_p)} \mathbf{1}_k & -\frac{f''(\tau_p)}{2f'(\tau_p)} \mathbf{1}_k \\ * & \mathbf{0} & \mathbf{0} & \mathbf{0} & \mathbf{0} & \mathbf{0} \\ * & * & 0 & 0 & 0 & 0 \\ * & * & * & -\frac{f''(\tau_p)}{2f'(\tau_p)} & 0 & 0 \\ * & * & * & * & 0 & 0 \\ * & * & * & * & * & 0 \end{bmatrix} \\ \mathbf{A}_{1,11} &= \left\{ -\frac{1}{2} \|\boldsymbol{\mu}_a - \boldsymbol{\mu}_b\|^2 - \frac{f''(\tau_p)}{4f'(\tau_p)} (t_a + t_b)^2 - \frac{f''(\tau_p)}{f'(\tau_p)} S_{ab} \right\}_{a,b=1}^k. \end{aligned}$$

The first two leading-order terms in $\tilde{\mathbf{K}}$ are $\mathbf{V}\mathbf{A}_n\mathbf{V}^\top = O_{\|\cdot\|}(n)$ and $\mathbf{V}\mathbf{A}_{\sqrt{n}}\mathbf{V}^\top = O_{\|\cdot\|}(\sqrt{n})$. Note that they are (i) low rank matrices and in particular (ii) orthogonal to the projection matrix \mathbf{P} . As a consequence of Remark 4.2, the following corollary provides an asymptotic equivalent for the centered distance random kernel matrix \mathbf{PKP} that takes a much simpler form.

coro:K

Corollary 4.1 (Centered distance random kernel matrix). *With the same notations and assumptions as in Theorem 4.1, as $p, n \rightarrow \infty$ with $p/n \rightarrow c \in (0, \infty)$ and $n_a/n \rightarrow c_a \in (0, 1)$,*

$$\|\mathbf{PKP} - \mathbf{P}\tilde{\mathbf{K}}\mathbf{P}\| \xrightarrow{a.s.} 0$$

where

$$\tilde{\mathbf{K}} = -2f'(\tau_p) \left(\frac{1}{p} \mathbf{W}^\top \mathbf{W} + \mathbf{V} \mathbf{A} \mathbf{V}^\top \right) + (f(0) - f(\tau_p) + \tau_p f'(\tau_p)) \mathbf{I}_n$$

with $\mathbf{W} = [\mathbf{W}_1, \dots, \mathbf{W}_k]$, $\mathbf{W}_a \in \mathbb{R}^{p \times n_a}$,

$$\mathbf{V} = \left[\frac{\mathbf{J}}{\sqrt{p}}, \frac{\mathbf{W}^\top \mathbf{M}}{\sqrt{p}}, \tilde{\mathbf{v}}, \boldsymbol{\psi} \right], \quad \tilde{\mathbf{v}} = \left\{ \frac{1}{\sqrt{p}} \mathbf{W}_a^\top \boldsymbol{\mu}_a \right\}_{a=1}^k, \quad \boldsymbol{\psi} = \frac{1}{p} \{ \|\mathbf{w}_i\|^2 - \mathbb{E}[\|\mathbf{w}_i\|^2] \}_{i=1}^n$$

and

$$\mathbf{A} = \mathbf{A}_1 = \begin{bmatrix} \mathbf{A}_{1,11} & \mathbf{I}_k & -\mathbf{1}_k & -\frac{f''(\tau_p)}{2f'(\tau_p)}\mathbf{t} \\ * & \mathbf{0} & \mathbf{0} & \mathbf{0} \\ * & * & 0 & 0 \\ * & * & * & -\frac{f''(\tau_p)}{2f'(\tau_p)} \end{bmatrix}$$

$$\mathbf{A}_{1,11} = \left\{ -\frac{1}{2}\|\boldsymbol{\mu}_a - \boldsymbol{\mu}_b\|^2 - \frac{f''(\tau_p)}{2f'(\tau_p)}t_a t_b - \frac{f''(\tau_p)}{f'(\tau_p)}S_{ab} \right\}_{a,b=1}^k.$$

Remark 4.3 (Loss of first informative eigenvector due to centering). Note that, compared to Theorem 4.1 without centering, in the asymptotic approximation of PKP in Corollary 4.1 the information on the covariance traces \mathbf{t} (in $\mathbf{A}_{\sqrt{n}}$ in Theorem 4.1), which takes the form $\boldsymbol{\psi} + \mathbf{J}\mathbf{t}$ as in (4.3), is now lost. This is, however, not really an issue: this information is readily accessible through a simple evaluation of the norms $\|\mathbf{x}_i^\circ\|^2$ with the same accuracy.

To fully understand this result, let us make a list of successive observations:

- discarding the term proportional to \mathbf{I}_n (which follows from the treatment of the diagonal elements of \mathbf{K}), after centering, $\tilde{\mathbf{K}}$ is the sum of the full-rank $O(1)$ -norm $\frac{1}{p}\mathbf{W}^\top \mathbf{W}$ matrix and of the low rank (up to $2k+2$) matrix $\mathbf{V}\mathbf{A}\mathbf{V}^\top$. This matrix is of the family of spiked random matrix models and can be studied as per Section 2.5: its asymptotic spectrum, eigenvalue positions, phase transitions, angles between its eigenvectors and those of $\mathbf{V}\mathbf{A}\mathbf{V}^\top$, etc., can all be studied.
- the matrix \mathbf{V} is built such in a way that its vector components are $O(1)$ -norm and asymptotically “essentially” orthogonal (in the sense that $\mathbf{V}_{\cdot a}^\top \mathbf{V}_{\cdot b} \xrightarrow{a.s.} 0$ for $a \neq b$ as $p, n \rightarrow \infty$). Besides, \mathbf{V} mainly contains two types of submatrices: the class (informative) matrix \mathbf{J} and the “noise” (uninformative) remaining random vectors of zero mean. The latter are claimed uninformative in a spectral sense, as their class-wise means are all zero (only the variances of their entries depend on the classes, but a spectral method cannot directly detect this information).
- being a spiked model, the relevance of the dominant eigenvectors of $\tilde{\mathbf{K}}$ for classification depends on the ratio between the largest “informative” eigenvalues of $\mathbf{V}\mathbf{A}\mathbf{V}^\top$ and the typical spread of the eigenvalues of the noise matrix $\frac{1}{p}\mathbf{W}^\top \mathbf{W}$. The useful vector here is \mathbf{J} which contains the class information. As such, by examining the block entry $(1, 1)$ of the matrices \mathbf{A}_{n^α} above, and in particular the block entry $\mathbf{A}_{1,11}$ in the centered case, it appears that asymptotically, the eigenspectrum of the distance random kernel matrix \mathbf{K} *only* depends on:
 - the first three derivatives $f(\tau_p)$, $f'(\tau_p)$ and $f''(\tau_p)$ of the function f ;
 - the vector \mathbf{t} and the matrices \mathbf{M} and \mathbf{S} .

As a consequence of these observations, it appears that when performed on large dimensional data, spectral classification methods based on the kernel matrix \mathbf{K} do not exploit any other information than those contained in \mathbf{M} , \mathbf{t} and \mathbf{S} . Besides, since $\tilde{\mathbf{K}}$ only depends on $f(\tau_p)$, $f'(\tau_p)$ and $f''(\tau_p)$, *most* (if not all) classification methods based on \mathbf{K} asymptotically perform equivalently for f taken as a polynomial of order two having the same first derivatives at τ_p .

Now, further note that the coefficients $f(\tau_p)$, $f'(\tau_p)$ and $f''(\tau_p)$ are prefactors of \mathbf{M} , \mathbf{t} , \mathbf{S} , as well as of the (noisy) random matrix $\mathbf{W}^\top \mathbf{W}$. This leads to several fundamental remarks:

- letting $f''(\tau_p) = 0$, the term \mathbf{S} vanishes from $\tilde{\mathbf{K}}$. As such, spectral methods based on \mathbf{K} cannot distinguish different classes from their covariance “shapes” (but they can still discriminate clusters having different covariance traces, if no centering is applied). This in particular explains why spectral clustering with the linear kernel $f(t) = t$ does not allow to distinguish Gaussian mixtures of equal means and covariance traces;
- more fundamentally, the analysis reveals a non-trivial fact: letting $f'(\tau_p) \rightarrow 0$, the noisy term $-2f'(\tau_p)\mathbf{W}^\top \mathbf{W}/p$ vanishes, while the informative term $-2f'(\tau_p)\mathbf{V}\mathbf{A}\mathbf{V}^\top$ remains. Indeed, since $\mathbf{A}_{1,11}$ contains terms having $f'(\tau_p)$ in the denominator, in this $f'(\tau_p) \rightarrow 0$ limit with $\mathbf{t} = o_{\|\cdot\|}(1)$ (e.g., for normalized data vectors such that $\|\mathbf{x}_i\| = \sqrt{p}$ for all i , of particular interest in a subspace clustering context [Couillet and Kamoun, 2016]), $\tilde{\mathbf{K}}$ becomes essentially deterministic with the covariance shape information \mathbf{S} remaining (\mathbf{M} being discarded), indicating that (asymptotic) perfect classification can be achieved in this case. See also for an application to the LS-SVM classifier in Figure 4.22 later in Section 4.5.3.

The latter remark is quite surprising: it indicates that, for f a kernel function having a local extremum (minimum or maximum) at τ_p , up to data normalization, for $\mathbf{S} = O_{\|\cdot\|}(1)$ as requested in our previous “non-trivial classification” analysis, the classification does become trivially easy. This is not met for any commonly used monotonously decreasing function in the machine learning literature, such as the Gaussian kernel function $f(t) = \exp(-t/2)$. This somewhat changes the perspective of kernel methods that originally request f to define a positive definite kernel, i.e., that f be such that there exists a function $\phi : \mathbb{R}^p \rightarrow \mathbb{R}^q$ (for some $q \in \mathbb{N} \cup \{\infty\}$) for which $f(\|\mathbf{x} - \mathbf{y}\|^2) = \phi(\mathbf{x})^\top \phi(\mathbf{y})$. For f satisfying $f'(\tau_p) = 0$, it is unlikely that f defines a positive definite kernel.

Going further, the possibility to turn the non-trivial classification problem into a trivial one means that, instead of requiring $\mathbf{M}, \mathbf{t}, \mathbf{S}$ to be of order $O(1)$, it might be possible to perform classification for more stringent discriminative rates. Since \mathbf{M} and \mathbf{t} are already rate-optimal in the Neyman-Pearson test analysis, only the growth rate of \mathbf{S} can be improved. More precisely, denote $\mathbf{C}_a^\circ \equiv \mathbf{C}_a - \mathbf{C}^\circ$ and assume $\|\mathbf{C}_a^\circ\| = O_{\|\cdot\|}(p^{-1/2})$ (such that $t_a = \text{tr } \mathbf{C}_a^\circ / \sqrt{p} = O(1)$ that achieves the Bayes optimal rate), we have

$$S_{ab} \equiv \frac{1}{p} \text{tr } \mathbf{C}_a \mathbf{C}_b = \frac{1}{p} \text{tr} (\mathbf{C}^\circ)^2 + \frac{1}{p} \text{tr } \mathbf{C}^\circ (\mathbf{C}_a^\circ + \mathbf{C}_b^\circ) + \frac{1}{p} \text{tr } \mathbf{C}_a^\circ \mathbf{C}_b^\circ \quad (4.4)$$

where we recall $\mathbf{C}^\circ \equiv \sum_{a=1}^k \frac{n_a}{n} \mathbf{C}_a = O_{\|\cdot\|}(1)$ so that $\frac{1}{p} \text{tr}(\mathbf{C}^\circ)^2 = O(1)$ and $\frac{1}{p} \text{tr} \mathbf{C}^\circ (\mathbf{C}_a^\circ + \mathbf{C}_b^\circ) \leq \|\mathbf{C}^\circ\| (t_a + t_b) / \sqrt{p} = O(p^{-1/2})$.

Based on this expansion, we shall show in the subsequent sections that, for a careful choice of f , it is indeed possible, in the $n \sim p$ regime, to perform non-trivial classification down to $\mathbf{S} = \frac{1}{p} \text{tr}(\mathbf{C}^\circ)^2 \mathbf{1}_k \mathbf{1}_k^\top + O_{\|\cdot\|}(p^{-1/2})$ (which is still not Neyman-Pearson optimal, as recall from (1.6), but likely the optimal rate of unsupervised classification methods).

rem:estim_tau

Remark 4.4 (Estimation of τ_p). *The above results suggest that, depending on the discriminating information practitioners wish to emphasize, it suffices to tune the kernel function f by properly selecting its successive derivatives at τ_p . This thus demands an estimate of τ_p in the large n, p setting.*

It can be shown that

$$\frac{1}{n(n-1)} \sum_{i,j=1}^n \frac{1}{p} \|\mathbf{x}_i - \mathbf{x}_j\|^2 - \tau_p = O(p^{-1})$$

in probability. Thus τ_p is fast and easy to estimate. For future use, we raise here the importance of the small fluctuations (of order $1/p$) of the estimate which, in the above derivation in the successive orders $1, 1/\sqrt{p}, 1/p$, etc., is a small (second) order fluctuation.

rem:inner-product

Remark 4.5 (The inner-product kernel case). *The case where $\mathbf{K} = \{f((\mathbf{x}_i^\circ)^\top \mathbf{x}_j^\circ / p)\}_{i,j=1}^n$ (with \mathbf{x}_i centered as per Remark 4.2) gives an inner-product kernel that is simpler to deal with. Note that $\|\mathbf{x}_i - \mathbf{x}_j\|^2 / p = \|\mathbf{x}_i^\circ\|^2 / p + \|\mathbf{x}_j^\circ\|^2 / p - 2(\mathbf{x}_i^\circ)^\top \mathbf{x}_j^\circ / p$, the Taylor expansion of the inner-product case is now performed around the limit (equal to 0) of $(\mathbf{x}_i^\circ)^\top \mathbf{x}_j^\circ / p$, with much less terms involved than for the distance kernel model. For instance, the covariance trace information $\mathbf{t} = \{\text{tr } \mathbf{C}_a^\circ / \sqrt{p}\}_{a=1}^k$ disappears in the (asymptotic) expansion of inner-product kernel matrices and, as a consequence, the inner-product kernels are not able to separate two “nested balls” $\mathcal{N}(\mathbf{0}, (1 \pm \epsilon/\sqrt{p}) \mathbf{I}_p)$ while the distance kernel can.⁴ Figure 4.1 illustrates this remark by displaying the eigenvalues and top eigenvectors of distance and inner-product kernel matrices, respectively. While an informative spike and the associated eigenvector are observed for the distance kernel, this is not the case for the inner-product kernel.*

4.3 The α - β random kernel model

sec:alpha-beta-kernel

4.3.1 Motivation

We have seen above that, with the particular choice $f'(\tau_p) = 0$, the classification becomes (asymptotically) trivial if the eigenvalues of \mathbf{S} are of order $O(1)$. In a two-class setting, this is equivalent to $\frac{1}{p} \text{tr}(\mathbf{C}_1 - \mathbf{C}_2)^2 = O(1)$ (which is also

⁴Note here that, the covariance “shape” $\mathbf{S} = \mathbf{1}_2 \mathbf{1}_2^\top + O_{\|\cdot\|}(p^{-1/2})$ is not discriminative.

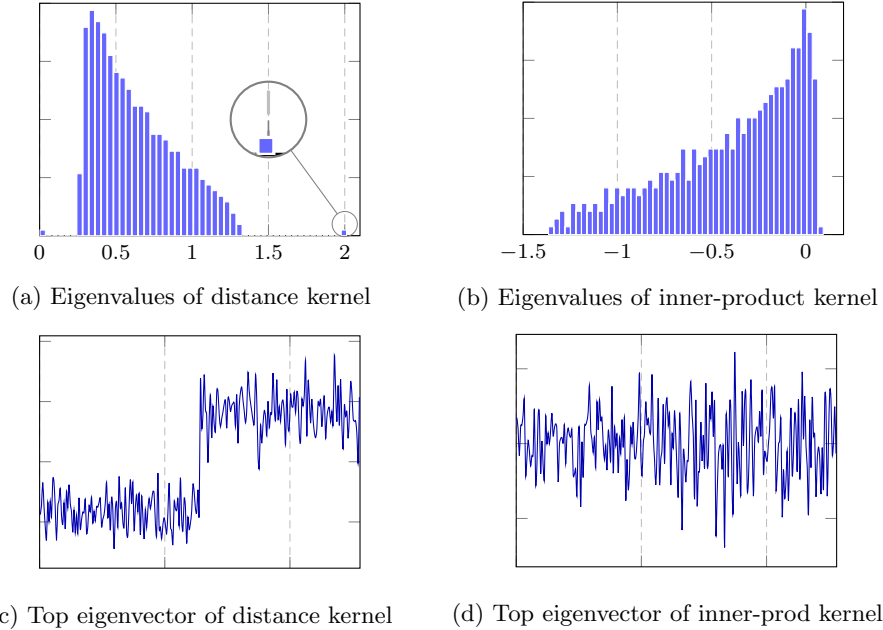


Figure 4.1: Eigenvalues and top eigenvector of recentered distance $f(\|\mathbf{x}_i^\circ - \mathbf{x}_j^\circ\|^2/p)$ and inner product $f((\mathbf{x}_i^\circ)^\top \mathbf{x}_j^\circ/p)$ kernel matrices \mathbf{PKP} , with $f(t) = \exp(-t/2)$, $p = 1024$, $n = 512$, $\boldsymbol{\mu} = \mathbf{0}$ and $\mathbf{C}_a = (1 + 5 \cdot (-1)^a/\sqrt{p})\mathbf{I}_p$ for $a \in \{1, 2\}$, $\mathbf{x}_1, \dots, \mathbf{x}_{n/2} \in \mathcal{C}_1$ and $\mathbf{x}_{n/2+1}, \dots, \mathbf{x}_n \in \mathcal{C}_2$. [Link to fig:nested-balls code]

the normalized Frobenius distance $\frac{1}{p}\|\mathbf{C}_1 - \mathbf{C}_2\|_F^2$ between covariances \mathbf{C}_1 and \mathbf{C}_2). It is thus theoretically possible to discriminate closer covariance matrices. As we shall see next, in the $n \sim p$ context, one can lower the constraint on \mathbf{S} to $\mathbf{S} = \frac{1}{p}\text{tr}(\mathbf{C}^\circ)^2\mathbf{1}_k\mathbf{1}_k^\top + O_{\|\cdot\|}(p^{-1/2})$, that is, to be able to discriminate data classes under the weaker condition

$$\text{tr}(\mathbf{C}_a - \mathbf{C}_b)^2 = O(\sqrt{p}).$$

However, in the random kernel models discussed in Section 4.2 (with f independent of n, p), choosing $f'(\tau_p) = 0$ simultaneously discards the information in \mathbf{M} about the class means.

A careful analysis of our previous derivations reveals the fact that the information about $\mathbf{M} = O_{\|\cdot\|}(1)$ and $\mathbf{S} = \frac{1}{p}\text{tr}(\mathbf{C}^\circ)^2\mathbf{1}_k\mathbf{1}_k^\top + O_{\|\cdot\|}(p^{-1/2})$ can be set on “even grounds” by letting f depend on p in such a way that

$$f(\tau_p) = O(1), \quad f'(\tau_p) = O(p^{-\frac{1}{2}}), \quad f''(\tau_p) = O(1).$$

That is, instead of requesting $f'(\tau_p) = 0$, we merely demand $f'(\tau_p) = \alpha/\sqrt{p}$ and $f''(\tau_p) = 2\beta$ (where the factor 2 is here for future convenience) for some

$\alpha, \beta \in (0, \infty)$. Examples of such kernel functions include

$$f(t) = \beta \left(t - \tau_p + \frac{\alpha}{2\beta\sqrt{p}} \right)^2, \quad f(t) = \exp \left(- \left(t - \tau_p + \frac{\alpha}{2\beta\sqrt{p}} \right)^2 \right).$$

The first function may be seen as a generalized second-order polynomial kernel, and the second as a generalized (properly normalized) Gaussian heat-kernel.

Note importantly that, from Remark 4.4, τ_p can be estimated within $O(p^{-1})$. Therefore, writing $f'(\tau_p) \simeq f'(\hat{\tau}_p) + (\tau_p - \hat{\tau}_p)f''(\hat{\tau}_p)$ with $f'(\tau_p) = O(p^{-1/2})$ and $f''(\hat{\tau}_p) = O(1)$, the relative estimation error $(f'(\tau_p) - f'(\hat{\tau}_p))/f'(\tau_p)$ vanishes as $O(p^{-1/2})$. This means one can still accurately select f to fulfill the above conditions on derivatives, with the estimate $\hat{\tau}_p$ proposed in Remark 4.4.

For simplicity of analysis (see Remarks 4.2 and 4.5), we here consider the inner-product random kernel matrix with feature centering

$$\mathbf{PKP} = \mathbf{P} \left\{ f \left(\frac{1}{p} (\mathbf{x}_i^\circ)^\top \mathbf{x}_j^\circ \right) \right\}_{i,j=1}^n \mathbf{P} \quad \text{eq:PKP_alpha_beta (4.5)}$$

where we recall that $\mathbf{x}_i^\circ = \mathbf{x}_i - \frac{1}{n} \sum_{j=1}^n \mathbf{x}_j$ and $\mathbf{P} = \mathbf{I}_n - \frac{1}{n} \mathbf{1}_n \mathbf{1}_n^\top$. This double-centering has the advantage of both ensuring that the inner products concentrate at 0 and also eliminating many terms in the Taylor expansion around 0 thanks to the projection matrix \mathbf{P} (as in Corollary 4.1). We now demand that f depend on p and satisfy the conditions

$$f(0) = O(1), \quad f'(0) = \frac{\alpha}{\sqrt{p}}, \quad f''(0) = 2\beta$$

with $\alpha, \beta \in \mathbb{R}$ fixed with respect to p . Here, typical kernel functions are

$$f(t) = \beta \left(t + \frac{\alpha}{2\beta\sqrt{p}} \right)^2, \quad f(t) = \exp \left(- \left(t + \frac{\alpha}{2\beta\sqrt{p}} \right)^2 \right).$$

In terms of data statistics, we consider here the same setting for means $\mathbf{M} = O_{\|\cdot\|}(1)$ as in the previous section. For covariances, recalling the expansion of $S_{ab} = \frac{1}{p} \text{tr } \mathbf{C}_a \mathbf{C}_b$ in (4.4), we introduce the *centered and rescaled* (by \sqrt{p}) covariance “shape” information

$$\mathbf{S}^\circ = \left\{ \frac{1}{\sqrt{p}} \text{tr } \mathbf{C}_a^\circ \mathbf{C}_b^\circ \right\}_{a,b=1}^k$$

for which we demand $\mathbf{S}^\circ = O_{\|\cdot\|}(1)$, rather than $O(\sqrt{p})$ as in the previous setting.

4.3.2 Main results

For the inner-product random kernel matrix \mathbf{K} above, we have the following asymptotics.

theo:alpha_beta_kernel

Theorem 4.2 (α - β kernel [Tiomoko Ali et al., 2018]). Let $\mathbf{K} \in \mathbb{R}^{n \times n}$ be defined as in (4.5) with $\mathbf{x}_i \sim \mathcal{N}(\boldsymbol{\mu}_a, \mathbf{C}_a)$ for $\mathbf{x}_i \in \mathcal{C}_a$ satisfying the following growth rate conditions

$$\mathbf{M} = O_{\|\cdot\|}(1), \quad \mathbf{S}^\circ = \frac{1}{\sqrt{p}} \{ \text{tr } \mathbf{C}_a^\circ \mathbf{C}_b^\circ \}_{a,b=1}^k = O_{\|\cdot\|}(1)$$

Then, as $n, p \rightarrow \infty$ with $p/n \rightarrow c \in (0, \infty)$,

$$\left\| \sqrt{p} (\mathbf{P} \tilde{\mathbf{K}} \mathbf{P} + (f(0) + (\text{tr } \mathbf{C}^\circ / p) \cdot f'(0)) \mathbf{P}) - \mathbf{P} \tilde{\mathbf{K}} \mathbf{P} \right\| \xrightarrow{a.s.} 0$$

where

$$\begin{aligned} \tilde{\mathbf{K}} &= \alpha \cdot \frac{1}{p} \mathbf{W}^\top \mathbf{W} + \beta \cdot \Phi + \mathbf{V} \mathbf{A} \mathbf{V}^\top \\ \mathbf{A} &= \begin{bmatrix} \alpha \cdot \mathbf{M}^\top \mathbf{M} + \beta \cdot \mathbf{S}^\circ & \alpha \mathbf{I}_k \\ \alpha \mathbf{I}_k & \mathbf{0} \end{bmatrix} \\ \mathbf{V} &= \begin{bmatrix} \frac{\mathbf{J}}{\sqrt{p}}, & \frac{\mathbf{W}^\top \mathbf{M}}{\sqrt{p}} \end{bmatrix} \\ \frac{\Phi}{\sqrt{p}} &= \left\{ \left(\frac{1}{p} \mathbf{w}_i^\top \mathbf{w}_j \right)^2 \right\}_{i,j=1}^n - \left\{ \frac{1}{p^2} \text{tr}(\mathbf{C}_a \mathbf{C}_b) \mathbf{1}_{n_a} \mathbf{1}_{n_b}^\top \right\}_{a,b=1}^k - \text{diag}(\cdot) \end{aligned}$$

where we recall that $\mathbf{Z} - \text{diag}(\cdot)$ sets the diagonal entries of the matrix \mathbf{Z} to zero.

It is worth mentioning that, similar to Remark 4.5 for “classical” inner-product kernel with f independent of p , the covariance trace information \mathbf{t} also disappear in the α - β inner-product kernel model and the covariance “shape” information \mathbf{S} in Theorem 4.1 appears here in the form of \mathbf{S}° .

It is fundamental to see here that, by reducing the amplitude of $f'(\tau_p)$ by a factor \sqrt{p} , the formerly leading noise term $\mathbf{W}^\top \mathbf{W}/p$ in Theorem 4.1 is now on even grounds to the second-order noise term Φ . Thus, \mathbf{K} can be here seen to asymptotically behave like a very special spiked model, for which the full rank (or noise) matrix is the sum $\alpha \mathbf{W}^\top \mathbf{W}/p + \beta \Phi$ constituted of the *dependent* \mathbf{W} and Φ .

Individually, $\mathbf{W}^\top \mathbf{W}/p$ has a limiting spectrum akin to the Bai-Silverstein law (Theorem 2.5), with \mathbf{C}° as population covariance (or to the Marčenko-Pastur law for $\mathbf{C}^\circ = \mathbf{I}_p$). Indeed, taking $\mathbf{S}^\circ = O_{\|\cdot\|}(1)$ ensures that the covariance matrices $\mathbf{C}_1, \dots, \mathbf{C}_k$ cannot be too different from \mathbf{C}° (e.g., all eigenvalues of $\mathbf{C}_a^\circ = \mathbf{C}_a - \mathbf{C}^\circ$ are of the order $O(p^{-1/4})$) and it can then be shown that the limiting spectrum of $\mathbf{W}^\top \mathbf{W}/p$ is the same as if all columns of \mathbf{W} have the same covariance matrix \mathbf{C}° . This largely simplifies the theoretical analysis.

As for Φ , note that it has identically distributed entries (but on the diagonal) of zero mean that are however not independent. Yet, it can be shown [Kammoun and Couillet, 2017] that the limiting spectrum of Φ is indeed a semi-circle distribution, similar to the Wigner case (Theorem 2.4) where the entries are independent; there is nonetheless a major difference in the spectrum of Φ to

that of a matrix with i.i.d. entries: Φ may present *up to two* isolated eigenvalues outside the semi-circle bulk. This unfolds from the fact that the deterministic equivalent for the resolvent $(\Phi - z\mathbf{I}_n)^{-1}$ is of the form

$$(\Phi - z\mathbf{I}_n)^{-1} \leftrightarrow m(z)\mathbf{I}_n + \frac{\Omega^2 m^3(z)}{c^2 - \Omega^2 m^2(z)} \cdot \frac{\mathbf{1}_n \mathbf{1}_n^\top}{n} \quad (4.6)$$

where

$$\omega = \frac{\sqrt{2}}{p} \text{tr}(\mathbf{C}^\circ)^2, \quad \Omega = \sqrt{\frac{2}{p} \text{tr}(\mathbf{C}^\circ)^4}$$

and $m(z)$ is the Stieltjes transform of the (rescaled) semi-circle law with support $[-2\omega/\sqrt{c}, 2\omega/\sqrt{c}]$ which is the solution to

$$m(z) = -\frac{1}{z + c^{-1}\omega^2 m(z)}$$

and admits the (limiting) spectral measure having density

$$\mu(dx) = \frac{c}{2\omega^2 \pi} \sqrt{(4\omega^2/c - x^2)^+} dx.$$

In particular, if $\Omega \leq \sqrt{c}\omega$, the contribution $\mathbf{1}_n \mathbf{1}_n^\top/n$ in the deterministic equivalent does not induce a (symmetric) pair of isolated spikes in the eigenspectrum of Φ . Otherwise, spikes can be found at the position $\pm(c^{-1}\Omega + \omega^2/\Omega)$ (see for an illustration in Figure 4.2). Yet, this is of little relevance here since $\mathbf{P}\Phi\mathbf{P}$ naturally discards the contribution from $\mathbf{1}_n \mathbf{1}_n^\top$ and thus no spurious spike appears in $\mathbf{P}\Phi\mathbf{P}$.

Now, the main issue in determining the limiting spectral measure of $\alpha\mathbf{W}^\top\mathbf{W}/p + \beta\Phi$ (and its centered version) is to deal with the dependence between \mathbf{W} and Φ . Intuitively, note that the main “driving randomness” in $\mathbf{W}^\top\mathbf{W}/p$ are the *first-order fluctuations* of the inner products $\mathbf{w}_i^\top \mathbf{w}_j/p$ ($i \neq j$) around 0, while for Φ this driving randomness are the *second-order fluctuations* of the type $(\mathbf{w}_i^\top \mathbf{w}_j/p)^2 - \mathbb{E}[(\mathbf{w}_i^\top \mathbf{w}_j/p)^2]$. These two fluctuations (of different order) essentially “behave” independently in the large n, p limit. Rigorously, it can be proved that the limiting spectral measure of $\alpha\mathbf{W}^\top\mathbf{W}/p + \beta\Phi$ is a so-called *free additive convolution* (recall from Definition 5) of the limiting measures of each component, i.e., the same limiting distribution as that of the *independent* sum $\alpha\mathbf{Z}_1^\top \mathbf{Z}_1/p + \beta\mathbf{Z}_2/\sqrt{p}$ for \mathbf{Z}_1 with i.i.d. zero mean columns of covariance \mathbf{C}° and \mathbf{Z}_2 a symmetric matrix of i.i.d. zero mean unit variance entries (up to symmetry and with zeros on the diagonal).

Precisely, we have the following result.

theo:lsd-alpha-beta-kernel

Theorem 4.3 (Limiting spectrum of $\alpha\beta$ kernel). *Under the conditions of Theorem 4.2, the empirical spectral measure $\mu_{\check{\mathbf{K}}}$ of $\check{\mathbf{K}} \equiv \sqrt{p}(\mathbf{P}\Phi\mathbf{P} + (f(0) + (\text{tr } \mathbf{C}^\circ/p) \cdot f'(0))\mathbf{P})$ (after centering and rescaling as per Theorem 4.2) satisfies $\mu_{\check{\mathbf{K}}} - \mu \xrightarrow{\text{a.s.}} 0$ weakly, for a probability measure μ defined by its Stieltjes*

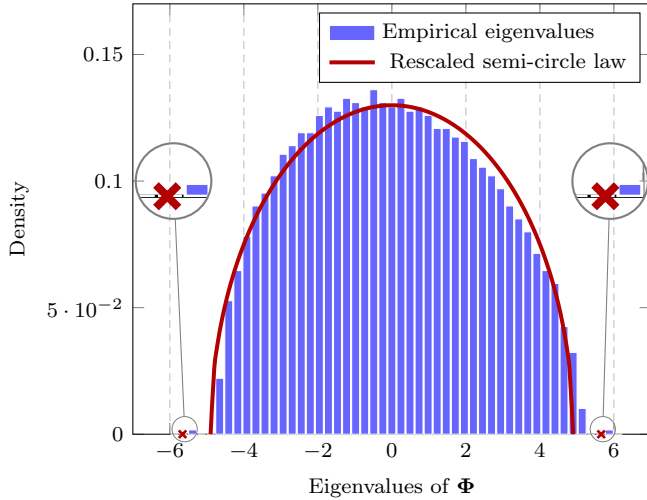


Figure 4.2: Eigenvalues of Φ versus the (rescaled) semi-circle law, for $p = 800$ and $n = 2400$. Two spikes appear here which carry *no information*, with red crosses indicating the location of $\pm(\Omega/c + \omega^2/\Omega)$. [Link to code] [fig:alpha-beta-spike](#)

transform $m(z)$ as the unique solution to

$$\frac{1}{m(z)} = -z + \frac{\alpha}{p} \operatorname{tr} \mathbf{C}^\circ (\mathbf{I}_p + c^{-1}\alpha m(z)\mathbf{C}^\circ)^{-1} - \beta^2 c^{-1} \omega^2 m(z)$$

where we recall $\omega = \frac{\sqrt{2}}{p} \operatorname{tr}(\mathbf{C}^\circ)^2$.

We recognize a semi-circle equation for $\alpha = 0$ and a Bai-Silverstein equation for $\beta = 0$. Figure 4.3 illustrates the transition from the Marčenko–Pastur to the semi-circle law limit for the eigenvalues of \mathbf{K} with different values of α, β .

Back to the statement of Theorem 4.2, note now that α and β also weigh the relative impact of the statistical means (through $\mathbf{M}^\top \mathbf{M}$) and covariances (through \mathbf{S}°) of the data. The spectrum of \mathbf{K} thus has two extreme scenarios: for $\beta = 0$, the main bulk of \mathbf{K} forms a Marčenko–Pastur distribution and isolated eigenvalues can be found only if $\mathbf{M}^\top \mathbf{M}$ is large, with the information in \mathbf{S}° unused; for $\alpha = 0$, the main bulk is a semi-circle law, with isolated eigenvalues only induced by \mathbf{S}° and the information in \mathbf{M} being discarded.

This kernel is deemed “optimal” in the sense that it allows for a separation of different classes at the minimal discriminating rate for $\mathbf{M}^\top \mathbf{M}$ and quasi-optimal rate for \mathbf{S}° (as a significant improvement from the kernel models in the previous sections). This is of particular interest in scenarios where the covariance information is critical to classification, while not discarding the (usually equally important) mean statistics.

While (quasi-)optimal in its discriminating power, the “ α - β ” kernel still has its limitations: (i) it acts solely in the neighborhood of zero so that all functions

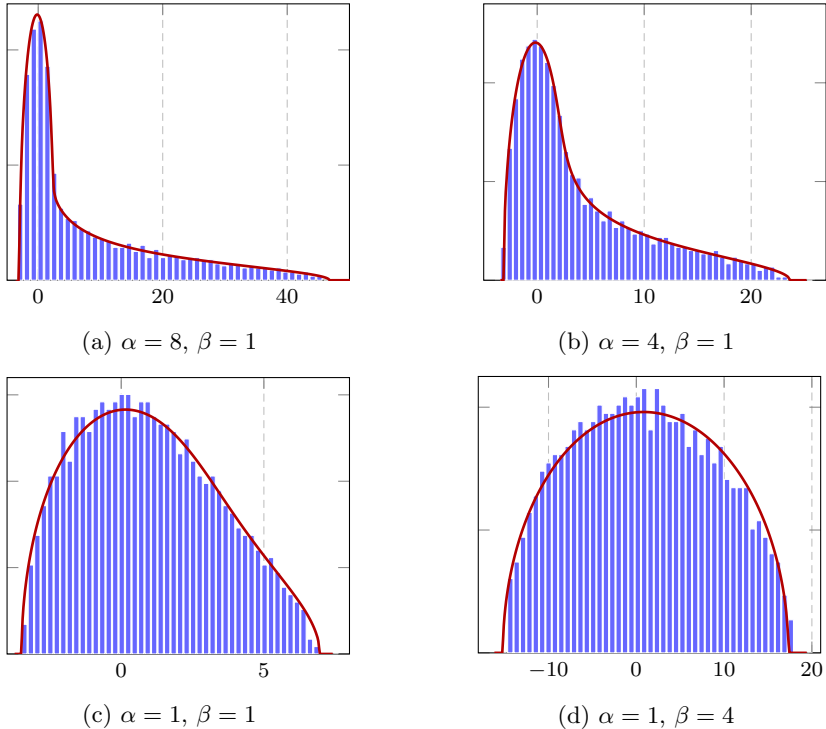


Figure 4.3: Eigenvalues of $\check{\mathbf{K}}$ as defined in Theorem 4.3 versus the limiting laws, for $p = 512$, $n = 1024$, with zero mean and identity covariance, $f(t) = \beta(t + \frac{\alpha}{2\beta}p^{-1/2})^2$. [\[Link to code\]](#)

`fig:alpha_beta_MPvsSC`

f having the same derivatives at zero produce *asymptotic* equivalent kernels, regardless of their behavior on the rest of \mathbb{R} ; (ii) this differentiability request automatically discards a large class of kernel functions of more practical interest, such as the sign function, the rectified linear unit (ReLU) in neural networks, etc.

The next section generalizes the idea of the “ α - β ” kernel, however with a more “proper” scaling of the kernel function. That is, we shall now demand that f operates on $\mathbf{x}_i^\top \mathbf{x}_j / \sqrt{p}$ which does not converge, rather than on $\mathbf{x}_i^\top \mathbf{x}_j / p$ (that “concentrates” around zero for large p). Quite astonishingly, we will see in Section 4.4 that the α - β kernel with f restricted to a second-order polynomial (i) corresponds to a “properly-scaled” polynomial kernel and that (ii) in some respect, is in fact optimal in the class of nonlinear kernels.

4.4 Properly scaling kernels

sec:proper-scaling

4.4.1 Motivation

The concentration of distances $\|\mathbf{x}_i - \mathbf{x}_j\|^2/p - \tau_p \xrightarrow{a.s.} 0$ or of inner products $\mathbf{x}_i^\top \mathbf{x}_j/p \xrightarrow{a.s.} 0$, as $n, p \rightarrow \infty$ discussed in Section 4.2 and 4.3, is advantageous from a computational perspective as it allowed for (entry-wise) Taylor expansions of nonlinear kernel functions. On the downside though, these concentration phenomena strongly restrict the effective impact of the kernel function f : as shown previously, only the first two successive derivatives of f at the point τ_p or zero really affect the kernel (and, as a result, the kernel-based classification or regression performance).

This might be interpreted as an incorrect “scaling” of $\|\mathbf{x}_i - \mathbf{x}_j\|^2$ or $\mathbf{x}_i^\top \mathbf{x}_j$. For the latter, it is in fact rather immediate, from central limit arguments, that, assuming $\mathbb{E}[\mathbf{x}_i] = 0$ for each i , $\mathbf{x}_i^\top \mathbf{x}_j = O(\sqrt{p})$ for $i \neq j$; it is therefore more natural to evaluate f at $(\mathbf{x}_i^\circ)^\top (\mathbf{x}_j^\circ)/\sqrt{p}$ for $\mathbf{x}_i^\circ = \mathbf{x}_i - \frac{1}{n} \sum_{j=1}^n \mathbf{x}_j$. In this case, the whole support of f can be exploited. Similarly, for $\|\mathbf{x}_i - \mathbf{x}_j\|^2$, although not naturally considered in the literature, it turns out to be more appropriate to center and scale it as $(\|\mathbf{x}_i - \mathbf{x}_j\|^2 - p\tau_p)/\sqrt{p}$.

This section precisely studies this “properly scaling” kernels which, as opposed to previous models, cannot be dealt with by means of entry-wise Taylor expansions. A more refined approach, based on orthogonal polynomials for Gaussian measure (here arising as a consequence of the central limit $(\mathbf{x}_i^\circ)^\top (\mathbf{x}_j^\circ)/\sqrt{p} \xrightarrow{d} \mathcal{N}(0, \sigma^2)$), needs to be devised.

Surprisingly enough, despite the initial motivation to avoid concentrating the effect of f at a single point (τ_p or zero, so that the kernel matrix depends on f only via its successive derivative at that point), we will see in the sequel that, under the same non-trivial classification condition, the asymptotics of these “properly scaled” kernels still only depend on two or three key parameters of f and are thus essentially no more powerful than the previously studied kernels. Yet, a few advantages are worth discussing; as we shall see:

- properly-scaled kernels can detect differences in covariances down to the rates of the α - β kernels discussed in Section 4.3; in this respect, they are more powerful than the conventional Gaussian heat kernels;
- we will no longer need to demand f to be smooth and in particular it will not necessarily be differentiable at τ_p or zero. This has the substantial advantage that binary kernels, i.e., kernels such that $f \in \{0, 1\}$, can be shown to meet the same asymptotic performances as the “optimal” α - β kernels when properly defined.

4.4.2 Setting

For simplicity and readability, we will exclusively focus on the inner-product kernel \mathbf{K} , the (i, j) entry of which is given by

$$\mathbf{K}_{ij} = \frac{1}{\sqrt{p}} f \left(\frac{1}{\sqrt{p}} (\mathbf{x}_i^\circ)^\top (\mathbf{x}_j^\circ) \right) \delta_{i \neq j}. \quad \text{eq:proper-scale-K (4.7)}$$

Note here the importance of discarding the diagonal elements, since $\|\mathbf{x}_i\|^2/\sqrt{p} = O(\sqrt{p})$, the diagonal elements essentially evaluate f at ∞ . The leading $1/\sqrt{p}$ term is here to ensure that the main support of \mathbf{K} is of order $O(1)$, for most functions f .

We will show that, under the same (optimal) growth rate assumptions on the data statistics as in the previous sections, and under mild regularity conditions for f , the spectrum of \mathbf{K} defined in (4.7) (asymptotically) still only depends on *three* parameters, that are, however, no longer the derivatives of f at zero.

The loss of ‘‘concentration’’ of $(\mathbf{x}_i^\circ)^\top (\mathbf{x}_j^\circ)/\sqrt{p}$ clearly breaks down the Taylor expansion approach used so far to assess the kernel spectral behavior in the large n, p regime.

The cornerstone idea in this regime is to exploit the fact that $(\mathbf{x}_i^\circ)^\top (\mathbf{x}_j^\circ)\sqrt{p}$ converges *in law* to a Gaussian random variable so that \mathbf{K} may be viewed in the limit as a matrix with *dependent* Gaussian entries to which f is pointwise applied. The main problem posed by this non-trivial dependence is that many elementary tools to determine the limiting eigenvalue distribution or a deterministic equivalent for the resolvent now collapse. Most of all, it is not possible to extract a row/column from \mathbf{K} (or from any simple random matrix asymptotically equivalent to \mathbf{K}) while ensuring its independence with respect to the other columns.

In the seminal works [Cheng and Singer, 2013, Do and Vu, 2013], the authors manage to work the problem around by smartly expanding f in its series of Hermite polynomials; i.e., by approximating f by a sum of *orthogonal polynomials* with respect to the Gaussian measure. In essence, the orthogonal polynomials restore the aforementioned lost independence between the rows/columns of \mathbf{K} . The need to use orthogonal polynomials with respect to the Gaussian measure arises from $(\mathbf{x}_i^\circ)^\top (\mathbf{x}_j^\circ)/\sqrt{p}$ being essentially Gaussian in the $p \rightarrow \infty$ limit.

For ease of presentation, we let here $\mathbf{x}_1, \dots, \mathbf{x}_n \in \mathbb{R}^p$ be drawn independently from one of k classes $\mathcal{C}_1, \dots, \mathcal{C}_k$ (of cardinality n_1, \dots, n_k) with now

$$\mathbf{x}_i \in \mathcal{C}_a \Leftrightarrow \mathbf{x}_i = \boldsymbol{\mu}_a + (\mathbf{I}_p + \mathbf{E}_a)^{\frac{1}{2}} \mathbf{z}_i \sim \mathcal{N}(\boldsymbol{\mu}_a, \mathbf{I}_p + \mathbf{E}_a) \quad \text{eq:inner-prod-GMM (4.8)}$$

so that $\mathbf{C}^\circ = \mathbf{I}_p$. The non-trivial classification assumptions under this setting

are as follows (in essence, the same as for the α - β kernel in Section 4.3).

$$\begin{aligned}\mathbf{M} &= [\boldsymbol{\mu}_1^\circ, \dots, \boldsymbol{\mu}_k^\circ] = O_{\|\cdot\|}(1), \quad \boldsymbol{\mu}_\ell^\circ = \boldsymbol{\mu}_\ell - \sum_{a=1}^k \frac{n_a}{n} \boldsymbol{\mu}_a \\ \mathbf{t} &= [t_1, \dots, t_k]^\top = O_{\|\cdot\|}(1), \quad t_a = \frac{1}{\sqrt{p}} \operatorname{tr} \mathbf{C}_a^\circ = \frac{1}{\sqrt{p}} \operatorname{tr} \mathbf{E}_a \\ \mathbf{S}^\circ &= \{S_{ab}^\circ\}_{a,b=1}^k = O_{\|\cdot\|}(1), \quad S_{ab}^\circ = \frac{1}{\sqrt{p}} \operatorname{tr} \mathbf{C}_a^\circ \mathbf{C}_b^\circ = \frac{1}{\sqrt{p}} \operatorname{tr} \mathbf{E}_a \mathbf{E}_b.\end{aligned}$$

It will appear convenient in the following to first consider the “null model”, that is, for each a , $\boldsymbol{\mu}_a = \mathbf{0}$ and $\mathbf{E}_a = \mathbf{0}$, before discussing the general case.

Under the null model, we write $\mathbf{K} = \mathbf{K}_N$ which is defined as

$$[\mathbf{K}_N]_{ij} = \delta_{i \neq j} f(\mathbf{z}_i^\top \mathbf{z}_j / \sqrt{p}) / \sqrt{p} \quad \text{eq: def-K-n (4.9)}$$

for $\mathbf{z}_i \sim \mathcal{N}(\mathbf{0}, \mathbf{I}_p)$ such that $\mathbf{z}_i^\top \mathbf{z}_j / \sqrt{p} \xrightarrow{d} \mathcal{N}(0, 1)$.

As announced, in order to analyze the spectral behavior of \mathbf{K}_N , we will resort to the theory of orthogonal polynomials and particularly of the class of Hermite polynomials [Olver et al., 2010], as discussed below.

4.4.3 Hermite polynomials

For a probability measure μ , we denote the set of orthogonal polynomials with respect to the scalar product $\langle f, g \rangle = \int f \cdot g d\mu$ as $\{P_l(x), l = 0, 1, \dots\}$, obtained from the Gram-Schmidt procedure on the monomials $\{1, x, x^2, \dots\}$ such that $P_0(x) = 1$, P_l is of degree l and $\langle P_{l_1}, P_{l_2} \rangle = \delta_{l_1-l_2}$. By the Riesz-Fisher theorem [Rudin et al., 1964, Theorem 11.43], for any function $f \in L^2(\mu)$, with $L^2(\mu)$ the set of square-integrable functions with respect to $\langle \cdot, \cdot \rangle$, one can formally expand f as

$$f(x) \sim \sum_{l=0}^{\infty} a_l P_l(x), \quad a_l = \int f(x) P_l(x) d\mu(x) \quad (4.10)$$

where “ $f \sim \sum_{l=0}^{\infty} P_l$ ” indicates that $\|f - \sum_{l=0}^N P_l\| \rightarrow 0$ as $N \rightarrow \infty$ (and $\|f\|^2 = \langle f, f \rangle$).

For our kernel matrix purpose, we demand that f is sufficiently smooth in that it can be well approximated by a sequence of orthogonal polynomials with respect to close-to-Gaussian measures.

ass:Hermite_conditions

Assumption 2. For each p , let $\xi_p = \mathbf{z}_i^\top \mathbf{z}_j / \sqrt{p}$ and let $\{P_{l,p}(x), l \geq 0\}$ be the set of orthogonal polynomials with respect to the probability measure μ_p of ξ_p . For $f \in L^2(\mu_p)$ for each p , we denote

$$f(x) \sim \sum_{l=0}^{\infty} a_{l,p} P_{l,p}(x), \quad a_{l,p} = \int f(x) P_{l,p}(x) d\mu(x)$$

and we demand that

(i) $\sum_{l=0}^{\infty} a_{l,p} P_{l,p}(x) \mu_p(dx)$ converges in $L^2(\mu_p)$ to $f(x)$ uniformly over large p , i.e., for any $\epsilon > 0$ there exists L such that for all p large,

$$\left\| f - \sum_{l=0}^L a_{l,p} P_{l,p} \right\|_{L^2(\mu_p)}^2 = \sum_{l=L+1}^{\infty} |a_{l,p}|^2 \leq \epsilon,$$

(ii) as $p \rightarrow \infty$, $\sum_{l=1}^{\infty} |a_{l,p}|^2 \rightarrow \nu \in [0, \infty)$. Moreover, for $l = 0, 1, 2$, $a_{l,p}$ converges and we denote a_0 , a_1 and a_2 their limits, respectively.

(iii) $a_0 = 0$.

Since $\xi_p \rightarrow \mathcal{N}(0, 1)$, the limiting parameters a_0, a_1, a_2 and ν are indeed (generalized) moments of the standard Gaussian measure involving f . Precisely,

$$a_0 = \mathbb{E}[f(\xi)], \quad a_1 = \mathbb{E}[\xi f(\xi)], \quad \sqrt{2}a_2 = \mathbb{E}[(\xi^2 - 1)f(\xi)], \quad \nu = \underset{\substack{\text{eq: def-hermite-coeff} \\ (4.11)}}{\variance[f(\xi)]} \geq a_1^2 + a_2^2$$

for $\xi \sim \mathcal{N}(0, 1)$. These parameters will be of central significance to determine the eigenspectrum behavior of \mathbf{K} .

Item (iii) above is a simplifying assumption to avoid the existence of a constant component in all (non-diagonal) entries of \mathbf{K} . It suffices to subtract the constant $\mathbb{E}[f(\xi)]$ from f , without affecting the classification or regression performance of kernel methods.

4.4.4 Limiting spectrum of the null model \mathbf{K}_N

As mentioned previously, we start by investigating the null model inner-product kernel matrix $\mathbf{K} = \mathbf{K}_N$ with

$$\mathbf{K}_{ij} = \begin{cases} f(\mathbf{z}_i^\top \mathbf{z}_j / \sqrt{p}) / \sqrt{p} & \text{for } i \neq j \\ 0 & \text{for } i = j \end{cases}$$

for i.i.d. $\mathbf{z}_i \sim \mathcal{N}(\mathbf{0}, \mathbf{I}_p)$. We are, as usual, interested in the associated resolvent

$$\mathbf{Q}(z) \equiv (\mathbf{K} - z\mathbf{I}_n)^{-1}$$

Following the Marčenko-Pastur and Bai-Silverstein approaches (in Theorem 2.3 and 2.5), we first remove the i -th row and the i -th column of the symmetric matrix \mathbf{K} to decompose it as

$$\mathbf{K} = \begin{bmatrix} \mathbf{K}_{-i} & f(\mathbf{Z}_{-i}^\top \mathbf{z}_i / \sqrt{p}) / \sqrt{p} \\ f(\mathbf{z}_i^\top \mathbf{Z}_{-i} / \sqrt{p}) / \sqrt{p} & 0 \end{bmatrix}$$

$$\mathbf{K}_{-i} \equiv f(\mathbf{Z}_{-i}^\top \mathbf{Z}_{-i} / \sqrt{p}) / \sqrt{p} - \text{diag}(\cdot) \in \mathbb{R}^{(n-1) \times (n-1)}$$

(that is, with zeros on the diagonal of \mathbf{K}_{-i}) where $\mathbf{Z}_{-i} \in \mathbb{R}^{p \times (n-1)}$ is the Gaussian matrix \mathbf{Z} without the i -th column \mathbf{z}_i . As such, \mathbf{K}_{-i} is independent of

\mathbf{z}_i , and is asymptotically close to \mathbf{K} for n large. We similarly define the resolvent of \mathbf{K}_{-i} as

$$\mathbf{Q}_{-i} \equiv (\mathbf{K}_{-i} - z\mathbf{I}_{n-1})^{-1}.$$

With Lemma 2.6, the (i, i) -th diagonal entry of \mathbf{Q} is given by

$$\mathbf{Q}_{ii} = \frac{1}{-z - \frac{1}{p}f(\mathbf{z}_i^\top \mathbf{Z}_{-i}/\sqrt{p})\mathbf{Q}_{-i}f(\mathbf{Z}_{-i}^\top \mathbf{z}_i/\sqrt{p})} \stackrel{\text{eq:inner-prod-Qii}}{\equiv} \frac{-z - \delta_i}{-z - \delta_i} \quad (4.12)$$

where we recall that the diagonals of both \mathbf{K} and \mathbf{K}_{-i} are all zero. To evaluate the Stieltjes transform $\frac{1}{n} \sum_{i=1}^n \mathbf{Q}_{ii}(z)$, the key object is the (nonlinear) quadratic form

$$\delta_i \equiv \frac{1}{p}f(\mathbf{z}_i^\top \mathbf{Z}_{-i}/\sqrt{p})\mathbf{Q}_{-i}f(\mathbf{Z}_{-i}^\top \mathbf{z}_i/\sqrt{p}) \stackrel{\text{eq:def-inner-prod-delta}}{\equiv} (4.13)$$

We then wish to relate δ_i to the (normalized) trace of \mathbf{Q}_{-i} (and then to $m(z)$), for instance in the spirit of the trace lemma, Lemma 2.11. However, here Lemma 2.11 does not apply since, the “leave-one-out” kernel matrix \mathbf{K}_{-i} , and thus its resolvent \mathbf{Q}_{-i} , is *not independent* of the random vector $f(\mathbf{z}_i^\top \mathbf{Z}_{-i}/\sqrt{p})/\sqrt{p}$.

To handle the *nonlinear* random vector $f(\mathbf{Z}_{-i}^\top \mathbf{z}_i/\sqrt{p})$, Cheng and Singer [2013] propose to perform the following orthogonal decomposition of \mathbf{z}_j :

$$\mathbf{z}_j = \alpha_j \frac{\mathbf{z}_i}{\|\mathbf{z}_i\|} + \mathbf{z}_j^\perp, \quad \alpha_j \stackrel{\text{eq:in}\mathbf{z}_j^\top\text{prod-single-projection}}{=} \frac{\mathbf{z}_i^\top \mathbf{z}_j}{\|\mathbf{z}_i\|} \quad (4.14)$$

for $j \neq i$, where $\mathbf{z}_i/\|\mathbf{z}_i\|$ is the unit vector in the direction of \mathbf{z}_i and \mathbf{z}_j^\perp lies in the $(p-1)$ -dimensional subspace orthogonal to \mathbf{z}_i . Since $\mathbf{z}_i, \mathbf{z}_j$ are independent standard Gaussian vectors, we have, in the large p limit that, $\alpha_j \sim \mathcal{N}(0, 1)$, $\mathbf{z}_j^\perp \sim \mathcal{N}(0, \mathbf{I}_{p-1})$ and they are *independent*.

The fact that α_j and \mathbf{z}_j^\perp are independent is of crucial significance in the analysis of \mathbf{K} and can be checked by showing that, conditioned on \mathbf{z}_i , they are uncorrelated Gaussian variables.

With this decomposition of \mathbf{z}_i , taking $k \neq j$ and $k \neq i$, the term $\mathbf{z}_j^\top \mathbf{z}_k$ can be expanded as

$$\mathbf{z}_j^\top \mathbf{z}_k = \alpha_j \alpha_k + (\mathbf{z}_j^\perp)^\top \mathbf{z}_k^\perp \stackrel{\text{eq:inner-prod-cross-projection}}{=} \alpha_j \alpha_k + \Phi_{jk}^\perp \quad (4.15)$$

where the cross terms in the product expansion disappear by orthogonality. Note from (4.14) that, both \mathbf{z}_j and \mathbf{z}_j^\perp are of (Euclidean) norm $O(\sqrt{p})$, while $\alpha_j \cdot \|\mathbf{z}_i\|/\|\mathbf{z}_i\| = O(1)$. Similarly, in (4.15), both $\mathbf{z}_j^\top \mathbf{z}_k$ and Φ_{jk}^\perp are of order $O(\sqrt{p})$, while $\alpha_j \alpha_k = O(1)$. In this sense, Φ_{jk}^\perp is asymptotically close to the inner product $\mathbf{z}_j^\top \mathbf{z}_k$, with only the contribution from \mathbf{z}_i excluded and explicitly given by $\alpha_j \alpha_k$.

We further denote $\boldsymbol{\alpha}_{-i} = [\alpha_1, \dots, \alpha_{i-1}, \alpha_{i+1}, \dots, \alpha_n]^\top \in \mathbb{R}^{n-1}$ and $\mathbf{K}_{-i}^\perp \in \mathbb{R}^{(n-1) \times (n-1)}$ with its (j, k) entry given by

$$[\mathbf{K}_{-i}^\perp]_{jk} \equiv \delta_{j \neq k} \cdot f((\mathbf{z}_j^\perp)^\top \mathbf{z}_k^\perp / \sqrt{p}) / \sqrt{p} = \delta_{j \neq k} \cdot f(\Phi_{jk}^\perp / \sqrt{p}) / \sqrt{p} \stackrel{\text{eq: def-inner-prod-K-perp-i}}{=} (4.16)$$

so that the nonlinear random vector $f(\mathbf{Z}_{-i}^\top \mathbf{z}_i/\sqrt{p}) = f(\boldsymbol{\alpha}_{-i} \|\mathbf{z}_i\|/\sqrt{p}) \simeq f(\boldsymbol{\alpha}_{-i})$ for p large. It is also worth remarking here that, the random vector $\boldsymbol{\alpha}_{-i}$ is

merely a standard Gaussian random vector $\boldsymbol{\alpha}_{-i} \sim \mathcal{N}(\mathbf{0}, \mathbf{I}_{n-1})$ in the large n, p limit in the sense that each entry is asymptotically Gaussian and uncorrelated.

The advantage of introducing Φ^\perp and \mathbf{K}_{-i}^\perp is that, $\boldsymbol{\alpha}_{-i}$ is “essentially” asymptotically independent of Φ^\perp in the sense that the expectations $\mathbb{E}[\Phi^\perp \boldsymbol{\alpha}_{-i}]$ and $\mathbb{E}[\mathbf{K}_{-i}^\perp \boldsymbol{\alpha}_{-i}]$ vanish in the large n, p limit. This is, however, not the case for the (original) “leave-one-out” kernel matrix \mathbf{K}_{-i} as previously discussed in (4.13), i.e., $\|\mathbb{E}[\mathbf{K}_{-i} \boldsymbol{\alpha}_{-i}]\| \not\asymp 0$.

The study of \mathbf{K}_{-i} thus boils down to that of \mathbf{K}_{-i}^\perp , we will need in the remainder its resolvent

$$\mathbf{Q}_{-i}^\perp \equiv (\mathbf{K}_{-i}^\perp - z\mathbf{I}_{n-1})^{-1}$$

that is therefore also “asymptotically” independent of $\boldsymbol{\alpha}_{-i}$.

With these preliminary derivations, we now focus on the “leave-one-out” kernel matrix $\mathbf{K}_{-i} \equiv f(\mathbf{Z}_{-i}^\top \mathbf{Z}_{-i}/\sqrt{p})/\sqrt{p} - \text{diag}(\cdot)$. With (4.15), its (k, l) -entry is given by

$$[\mathbf{K}_{-i}]_{jk} = \frac{1}{\sqrt{p}} f\left(\frac{1}{\sqrt{p}} \alpha_j \alpha_k + \frac{1}{\sqrt{p}} \Phi_{jk}^\perp\right)$$

where we recall that $\Phi_{jk}^\perp = O(\sqrt{p})$, $\alpha_j \alpha_k = O(1)$ and they are (asymptotically) independent. As a consequence, with a Taylor expansion of $f(\alpha_j \alpha_k/\sqrt{p} + \Phi_{jk}^\perp/\sqrt{p})$ around the leading term Φ_{jk}^\perp/\sqrt{p} , we obtain⁵

$$f\left(\frac{1}{\sqrt{p}} \alpha_j \alpha_k + \frac{1}{\sqrt{p}} \Phi_{jk}^\perp\right) = f\left(\frac{1}{\sqrt{p}} \Phi_{jk}^\perp\right) + f'\left(\frac{1}{\sqrt{p}} \Phi_{jk}^\perp\right) \frac{1}{\sqrt{p}} \alpha_j \alpha_k + O(p^{-1})$$

so that, for $j \neq k$,

$$\begin{aligned} [\mathbf{K}_{-i}]_{jk} &= \frac{1}{\sqrt{p}} f\left(\frac{1}{\sqrt{p}} \Phi_{jk}^\perp\right) + \frac{a_1}{p} \alpha_j \alpha_k + \frac{1}{p} g\left(\frac{1}{\sqrt{p}} \Phi_{jk}^\perp\right) \alpha_j \alpha_k + O(p^{-3/2}) \\ &= \left[\mathbf{K}_{-i}^\perp + \frac{a_1}{p} \boldsymbol{\alpha}_{-i} \boldsymbol{\alpha}_{-i}^\top + \frac{1}{\sqrt{p}} \text{diag}(\boldsymbol{\alpha}_{-i}) \mathbf{G} \text{diag}(\boldsymbol{\alpha}_{-i}) \right]_{jk} + O(p^{-3/2}) \end{aligned}$$

with the shortcut $g(x) = f'(x) - a_1$, for a_1 the first Hermite coefficient in (4.11), \mathbf{K}_{-i}^\perp defined in (4.16), and another “kernel matrix” \mathbf{G} with its (j, k) -entry given by

$$\mathbf{G}_{jk} \equiv g(\Phi_{jk}^\perp/\sqrt{p})/\sqrt{p}$$

with kernel function $g(x) = f'(x) - a_1$ so that in particular, $\mathbb{E}_{\xi \sim \mathcal{N}(0, 1)}[g(\xi)] = 0$.

Note that we intentionally extract the constant a_1 from the nonlinear function $f'(x)$ since

- for $\boldsymbol{\alpha}_{-i} \sim \mathcal{N}(\mathbf{0}, \mathbf{I}_{n-1})$ in the large n, p limit, we have $\frac{1}{p} \boldsymbol{\alpha}_{-i} \boldsymbol{\alpha}_{-i}^\top = O_{\|\cdot\|}(1)$;

⁵We consider for the moment f to be a Hermite polynomial (and thus differentiable), and extend to square-summable f (with respect to Gaussian measure) under Assumption 2.

- on the other hand, for $\mathbf{G}-\text{diag}(\cdot) = O_{\|\cdot\|}(1)$, we have $\frac{1}{\sqrt{p}} \text{diag}(\boldsymbol{\alpha}_{-i}) \mathbf{G} \text{diag}(\boldsymbol{\alpha}_{-i}) = O_{\|\cdot\|}(p^{-1/2})$ that is of vanishing operator norm as $n, p \rightarrow \infty$.

The fact that $\mathbf{G}-\text{diag}(\cdot) = O_{\|\cdot\|}(1)$ is closely related to Item (iii) of Assumption 2: for $a_0 = \mathbb{E}[f(\xi)] = 0$, it can indeed be shown that the kernel matrix \mathbf{K} has bound operator norm (see, e.g., [Fan and Montanari, 2019, Theorem 1.7]) for n, p large. And similarly for the (slightly different) kernel matrix $\mathbf{G}-\text{diag}(\cdot)$ with $\mathbb{E}[g(\xi)] = 0$. It allows us to conclude that, in matrix form,

$$\mathbf{K}_{-i} = \mathbf{K}_{-i}^\perp + \frac{a_1}{p} \boldsymbol{\alpha}_{-i} \boldsymbol{\alpha}_{-i}^\top + o_{\|\cdot\|}(1) \quad \text{eq:K_i-expansion (4.17)}$$

with $\boldsymbol{\alpha}_{-i}$ “essentially” asymptotically independent of \mathbf{K}_{-i}^\perp .

As a consequence of the above approximation, we have, for $\mathbf{Q}_{-i} \equiv (\mathbf{K}_{-i} - z\mathbf{I}_{n-1})^{-1}$,

$$\begin{aligned} \mathbf{Q}_{-i} &= \left(\mathbf{K}_{-i}^\perp + \frac{a_1}{p} \boldsymbol{\alpha}_{-i} \boldsymbol{\alpha}_{-i}^\top - z\mathbf{I}_{n-1} \right)^{-1} + o_{\|\cdot\|}(1) \\ &= \mathbf{Q}_{-i}^\perp - \frac{a_1 \mathbf{Q}_{-i}^\perp \frac{1}{p} \boldsymbol{\alpha}_{-i} \boldsymbol{\alpha}_{-i}^\top \mathbf{Q}_{-i}^\perp}{1 + \frac{a_1}{p} \boldsymbol{\alpha}_{-i}^\top \mathbf{Q}_{-i}^\perp \boldsymbol{\alpha}_{-i}} + o_{\|\cdot\|}(1) \\ &= \mathbf{Q}_{-i}^\perp - \frac{a_1 \mathbf{Q}_{-i}^\perp \frac{1}{p} \boldsymbol{\alpha}_{-i} \boldsymbol{\alpha}_{-i}^\top \mathbf{Q}_{-i}^\perp}{1 + \frac{a_1}{p} \text{tr } \mathbf{Q}_{-i}^\perp} + o_{\|\cdot\|}(1) \end{aligned}$$

where we recall the definition $\mathbf{Q}_{-i}^\perp \equiv (\mathbf{K}_{-i}^\perp - z\mathbf{I}_{n-1})^{-1}$ that is asymptotically independent of $\boldsymbol{\alpha}_{-i}$. Here we used Lemma 2.8 for the second line and Lemma 2.11 for the approximation in the third line. Also, with (4.17) and Lemma 2.9 we deduce

$$\frac{1}{p} \text{tr } \mathbf{Q}_{-i}^\perp = \frac{1}{p} \text{tr } \mathbf{Q}_{-i} + o(1) = \frac{1}{p} \text{tr } \mathbf{Q} + o(1) \simeq \frac{n}{p} m(z) \equiv \frac{1}{p} \text{tr } \bar{\mathbf{Q}}(z)$$

for $\bar{\mathbf{Q}}(z)$ a deterministic equivalent for $\mathbf{Q}(z)$ (the form of which to be specified) and $m(z) = \frac{1}{n} \text{tr } \bar{\mathbf{Q}}(z)$.

To form an equation for $m(z)$, we would like to use (4.12) and it remains to investigate the nonlinear quadratic form $\delta_i = \frac{1}{p} f(\mathbf{z}_i^\top \mathbf{Z}_{-i} / \sqrt{p}) \mathbf{Q}_{-i} f(\mathbf{Z}_{-i}^\top \mathbf{z}_i / \sqrt{p})$ in (4.13). Note from (4.14) that, for $j \neq i$,

$$\begin{aligned} f(\mathbf{z}_j^\top \mathbf{z}_i / \sqrt{p}) &= f(\alpha_j \|\mathbf{z}_i\| / \sqrt{p}) = f(\alpha_j) + f'(\alpha_j) \cdot \alpha_j (\|\mathbf{z}_i\| / \sqrt{p} - 1) + O(p^{-1}) \\ &= f(\alpha_j) + O(p^{-1/2}) \end{aligned}$$

and therefore

$$\begin{aligned} \delta_i &= \frac{1}{p} f(\boldsymbol{\alpha}_{-i})^\top \mathbf{Q}_{-i} f(\boldsymbol{\alpha}_{-i}) - a_1 \frac{\left(\frac{1}{p} \boldsymbol{\alpha}_{-i}^\top \mathbf{Q}_{-i} f(\boldsymbol{\alpha}_{-i}) \right)^2}{1 + a_1 \cdot \frac{n}{p} m(z)} + o(1) \\ &= \frac{a_1^2}{p} \boldsymbol{\alpha}_{-i}^\top \mathbf{Q}_{-i} \boldsymbol{\alpha}_{-i} + \frac{1}{p} f_{>1}(\boldsymbol{\alpha}_{-i}) \mathbf{Q}_{-i} f_{>1}(\boldsymbol{\alpha}_{-i}) - a_1 \frac{\left(\frac{a_1}{p} \boldsymbol{\alpha}_{-i}^\top \mathbf{Q}_{-i} \boldsymbol{\alpha}_{-i} \right)^2}{1 + a_1 \cdot \frac{n}{p} m(z)} + o(1) \end{aligned}$$

where we decompose again $f(x)$ as the sum of its linear part a_1x and its “purely” nonlinear part $f_{>1}(x) = f(x) - a_1x$ that is *orthogonal* to a_1x in the sense that $\mathbb{E}[\xi f_{>1}(\xi)] = \langle x, f_{>1}(x) \rangle = 0$. As a consequence, we have

$$\begin{aligned}\frac{1}{p}\boldsymbol{\alpha}_{-i}^T \mathbf{A} \boldsymbol{\alpha}_{-i} &= \frac{1}{p} \operatorname{tr} \mathbf{A} + o(1) \\ \frac{1}{p} f_{>1}(\boldsymbol{\alpha}_{-i})^T \mathbf{A} f_{>1}(\boldsymbol{\alpha}_{-i}) &= \operatorname{var}[f_{>1}(\alpha_j)] \cdot \frac{1}{p} \operatorname{tr} \mathbf{A} + o(1) = (\nu - a_1^2) \cdot \frac{1}{p} \operatorname{tr} \mathbf{A} + o(1) \\ \frac{1}{p} \boldsymbol{\alpha}_{-i}^T \mathbf{A} f_{>1}(\boldsymbol{\alpha}_{-i}) &= o(1)\end{aligned}$$

for \mathbf{A} independent of $\boldsymbol{\alpha}_{-i}$ of bounded operator norm, where we recall the definition $\nu = \operatorname{var}[f(\xi)]$ from (4.11). This leads to the following approximation for the quadratic form

$$\delta_i = \frac{1}{p} f(\mathbf{z}_i^T \mathbf{Z}_{-i} / \sqrt{p}) \mathbf{Q}_{-i} f(\mathbf{Z}_{-i}^T \mathbf{z}_i / \sqrt{p}) = \frac{a_1^2 \cdot \frac{n}{p} m(z)}{1 + a_1 \cdot \frac{n}{p} m(z)} + (\nu - a_1^2) \cdot \frac{n}{p} m(z) + o(1).$$

Ultimately, recalling (4.12), we deduce

$$m(z) = \frac{1}{n} \sum_{i=1}^n \frac{1}{-z + \delta_i} + o(1) = \frac{1}{-z - \frac{(a_1^2/c)m(z)}{1+(a_1/c)m(z)} - \frac{\nu-a_1^2}{c}m(z)} + o(1)$$

which entails the following result.

theo:lsd_Cheng

Theorem 4.4 (Limiting spectrum of properly scaling kernel, [Cheng and Singer, 2013, Do and Vu, 2013]). *Let $p/n \rightarrow c \in (0, \infty)$ and Assumption 2 hold. Then, the empirical spectral measure of the null model \mathbf{K}_N defined in (4.9) converges weakly and almost surely to a probability measure μ defined by its Stieltjes transform $m(z)$ as the unique solution to*

$$-\frac{1}{m(z)} = z + \frac{a_1^2 m(z)}{c + a_1 m(z)} + \frac{\nu - a_1^2}{c} m(z). \quad \text{eq:lsd-proper-sacle (4.18)}$$

Despite derived here only in the Gaussian case, Theorem 4.4 holds more generally for the large family of sub-exponential distribution (having finite higher order moments) [Do and Vu, 2013]. While universality is classical in random matrix results, with mostly first and second order statistics involved, the present universality result is much less obvious, due to the nonlinearity and the strong dependence (between entries) in the model under study.

Remark 4.6 (Connection to α - β kernel). *Note that, taking $f(t) = \beta t^2 + \alpha t + \alpha^2/(4\beta)$ in (4.9), one obtains, up to centering, the second-order polynomial α - β kernel discussed in Section 4.3. In a sense, the properly scaling model is a natural extension of the α - β kernel model, allowing for a much larger family of nonlinear functions f (including even non-smooth function).*

Similar to the $\alpha\text{-}\beta$ kernel model in Theorem 4.3, here the limiting spectral measure μ of the null model \mathbf{K}_N is the *free additive convolution* (denoted as ‘ \boxplus ’, see Definition 5) between the Marčenko–Pastur law (denote $\mu_{MP,c}$ of shape parameter $c = \lim p/n$) and the semi-circle law (μ_{SC}) as

$$\mu = a_1(\mu_{MP,c^{-1}} - 1) \boxplus \sqrt{(\nu - a_1^2)c^{-1}}\mu_{SC}$$

where we denote $a_1(\mu_{MP,c^{-1}} - 1)$ the law of $a_1(x - 1)$ for $x \sim \mu_{MP,c^{-1}}$ and $\sqrt{(\nu - a_1^2)c^{-1}}\mu_{SC}$ the law of $\sqrt{(\nu - a_1^2)c^{-1}} \cdot x$ for $x \sim \mu_{SC}$. Intuitively speaking, the Marčenko–Pastur law characterizes the linear part (a_1x) of the kernel function $f(x)$, while the higher-order ‘purely’ nonlinear part $f(x) - a_1x$ contributes to the semi-circle law. These two contributions are asymptotically ‘independent’ so that the resulting limiting spectrum is the free additive convolution of each component. As an illustration, Figure 4.4 compares, for $f(t) = \tanh(t)$, the empirical spectral measure of the null model \mathbf{K}_N to the limiting law μ in Theorem 4.4 that appears to be the ‘sum’ of a Marčenko–Pastur and a semi-circle distribution.

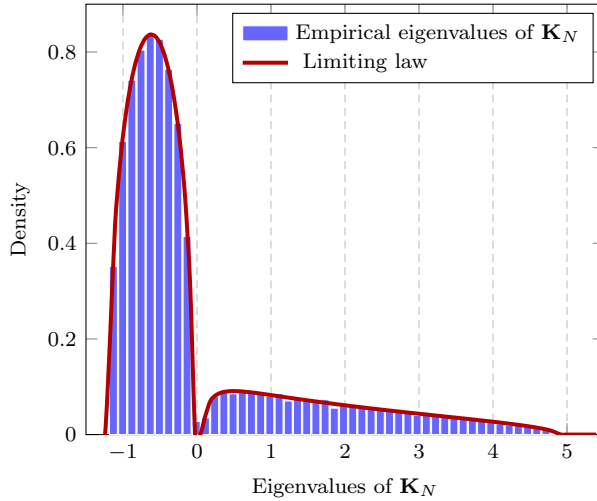


Figure 4.4: Eigenvalues of \mathbf{K}_N versus the limiting law from Theorem 4.4, for $p = 800$, $n = 3200$ and $f(t) = \tanh(t)$. [Link to code]

It is worth mentioning that Theorem 4.4 only characterizes the limiting eigenspectrum and does not provide a description of the possible spikes. Again, akin to the $\alpha\text{-}\beta$ kernel (recall Figure 4.2), the null model \mathbf{K}_N may present *up to two* isolated eigenvalues outside the limiting support in Theorem 4.4. This happens only when the second Hermite coefficient $a_2 \neq 0$ and is precisely described in the following theorem.

theo:DE-proper-scale

Theorem 4.5 (Deterministic equivalent for properly scaling kernel, from [Fan and Montanari, 2019]). *With the notations and assumptions in Theorem 4.4, we have*

$$(\mathbf{K}_N - z\mathbf{I}_n)^{-1} \leftrightarrow m(z)\mathbf{I}_n + \frac{a_2^2(m_4 - 1)m^3(z)}{2c^2 - a_2^2(m_4 - 1)m^2(z)} \cdot \frac{1}{n}\mathbf{1}_n\mathbf{1}_n^\top$$

with $m(z)$ the solution to (4.18) and m_4 the fourth moment of the entries of \mathbf{z} .

As a result of Theorem 4.5, if $a_2 = 0$ or $m_4 = 1$ (for instance for Bernoulli ± 1 entries), there is asymptotically no spike outside the limiting support of the null model \mathbf{K}_N . With $a_2 \neq 0$ and $m_4 > 1$, however, one may have up to two spikes at

$$\lambda = \mp \frac{a_2}{c\delta} \mp \frac{a_2\nu \pm a_1(\nu - a_1^2)\delta}{a_2(a_2 \pm a_1\delta)}\delta, \quad \delta = \sqrt{\frac{2}{m_4 - 1}}.$$

Note that (i) for $a_1 = 0$, the two spikes are at the position $\pm \left(\frac{a_2}{c\delta} + \frac{\nu\delta}{a_2} \right)$ and are symmetric as in the case of the α - β kernel; we recall that in this case the limiting spectrum is a rescaled semi-circle law

$$\mu(dx) = \frac{c}{2\nu\pi} \sqrt{(4\nu/c - x^2)^+} dx$$

and (ii) while the limiting spectrum is universal with respect to the distribution (of the entries), here the spike *does* depend on the fourth moment of the distribution. In Figure 4.5 we observe a farther (left) spike for the Student-t distribution (left) than for the Gaussian distribution (right), with the same limiting law.

In particular, in the case of the Gaussian distribution one has $m_4 = 3$ and by taking $a_2 = \sqrt{2}$ one obtains the same rank-one structure as in (4.6), while the limiting spectrum can be very different.

** Add perhaps the phase transition later**

4.4.5 Main results

Having covered the analysis of the (pure-noise) null mode kernel matrix \mathbf{K}_N , we will establish, in this section, an “information-plus-noise” asymptotic equivalent for the kernel matrix \mathbf{K} , again under the non-trivial classification assumptions for the mixture $\mathbf{x}_i \sim \mathcal{N}(\boldsymbol{\mu}_a, \mathbf{I}_p + \mathbf{E}_a) \in \mathcal{C}_a$, $a \in \{1, \dots, k\}$.

The main idea for this “information-plus-noise” decomposition comes in two steps: (i) first, by an expansion of $\mathbf{x}_i^\top \mathbf{x}_j$ as a function of $\mathbf{z}_i, \mathbf{z}_j$ and the statistical mixture model parameters $\boldsymbol{\mu}, \mathbf{E}$, one can decompose $\mathbf{x}_i^\top \mathbf{x}_j$ into successive orders of magnitudes with respect to p ; this, as we will show, further allows for a Taylor expansion of $f(\mathbf{x}_i^\top \mathbf{x}_j / \sqrt{p})$ for at least twice differentiable functions f around its dominant term $f(\mathbf{z}_i^\top \mathbf{z}_j / \sqrt{p})$. Then, (ii) we rely on the orthogonal polynomial approach of the previous section to “linearize” the resulting matrix terms $\{f(\mathbf{x}_i^\top \mathbf{x}_j / \sqrt{p})\}$, $\{f'(\mathbf{x}_i^\top \mathbf{x}_j / \sqrt{p})\}$ and $\{f''(\mathbf{x}_i^\top \mathbf{x}_j / \sqrt{p})\}$ (all terms corresponding to

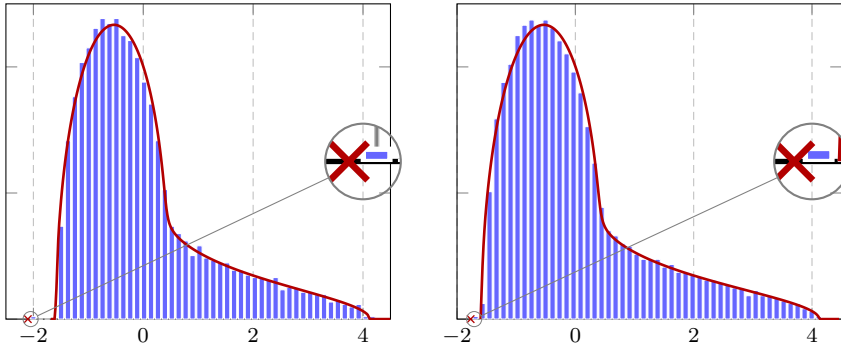


Figure 4.5: Eigenvalues of \mathbf{K}_N versus the limiting laws and spikes in Theorem 4.5, for Student-t (with 7 degrees of freedom, **left**) and Gaussian distribution (**right**) with $p = 512$, $n = 2048$, and $f(t) = \max(t, 0)$. The position of the isolated (non-informative) eigenvalue depends on the kurtosis of the random matrix entries. [Link to code]

`fig:proper_scale_spike`

higher order derivatives asymptotically vanish) and use Assumption 2 to extend the result to all square-summable f .

The main conclusion is that the kernel matrix \mathbf{K} asymptotically behaves like the sum $\tilde{\mathbf{K}} = \mathbf{K}_N + \tilde{\mathbf{K}}_I$ of the full-rank ‘‘noise’’ matrix \mathbf{K}_N (characterized in Theorem 4.4 and 4.5) and a low-rank ‘‘information’’ matrix $\tilde{\mathbf{K}}_I$. This is stated in the following theorem.

`theo:proper-scale-K-approx`

Theorem 4.6 (Properly scaling kernel, [Liao and Couillet, 2019a]). *Let Assumption 2 hold and let $\mathbf{K} \in \mathbb{R}^{n \times n}$ be the properly scaling kernel defined in (4.7) with $\mathbf{x}_i \sim \mathcal{N}(\boldsymbol{\mu}_a, \mathbf{I}_p + \mathbf{E}_a)$, for $\mathbf{x}_i \in \mathcal{C}_a$ satisfying the following growth rate conditions*

$$\mathbf{M} = O_{\|\cdot\|}(1), \quad \mathbf{t} = O_{\|\cdot\|}(1), \quad \mathbf{S}^\circ = O_{\|\cdot\|}(1).$$

Then, as $n, p \rightarrow \infty$ with $p/n \rightarrow c \in (0, \infty)$,

$$\|\mathbf{K} - \tilde{\mathbf{K}}\| \xrightarrow{a.s.} 0, \quad \tilde{\mathbf{K}} = \mathbf{K}_N + \mathbf{V}\mathbf{A}\mathbf{V}^\top$$

with \mathbf{K}_N defined in (4.9) and

$$\begin{aligned} \mathbf{A} &= \begin{bmatrix} a_1 \cdot \mathbf{M}^\top \mathbf{M} + \frac{a_2}{\sqrt{2}} \cdot (\mathbf{t} \mathbf{1}_k^\top + \mathbf{1}_k \mathbf{t}^\top + \mathbf{S}^\circ) & a_1 \mathbf{I}_k \\ a_1 \mathbf{I}_k & \mathbf{0} \end{bmatrix} \\ \mathbf{V} &= \begin{bmatrix} \frac{\mathbf{J}}{\sqrt{p}}, & \frac{\mathbf{Z}^\top \mathbf{M}}{\sqrt{p}} \end{bmatrix} \end{aligned}$$

where we recall the first two Hermite coefficients $a_1 = \mathbb{E}[\xi f(\xi)]$ and $a_2 = \mathbb{E}[(\xi^2 - 1)f(\xi)]/\sqrt{2}$ for $\xi \sim \mathcal{N}(0, 1)$.

Interestingly, different from the noisy spikes in Theorem 4.5 and Figure 4.5, which depends on the fourth moment of the distribution, here the informative

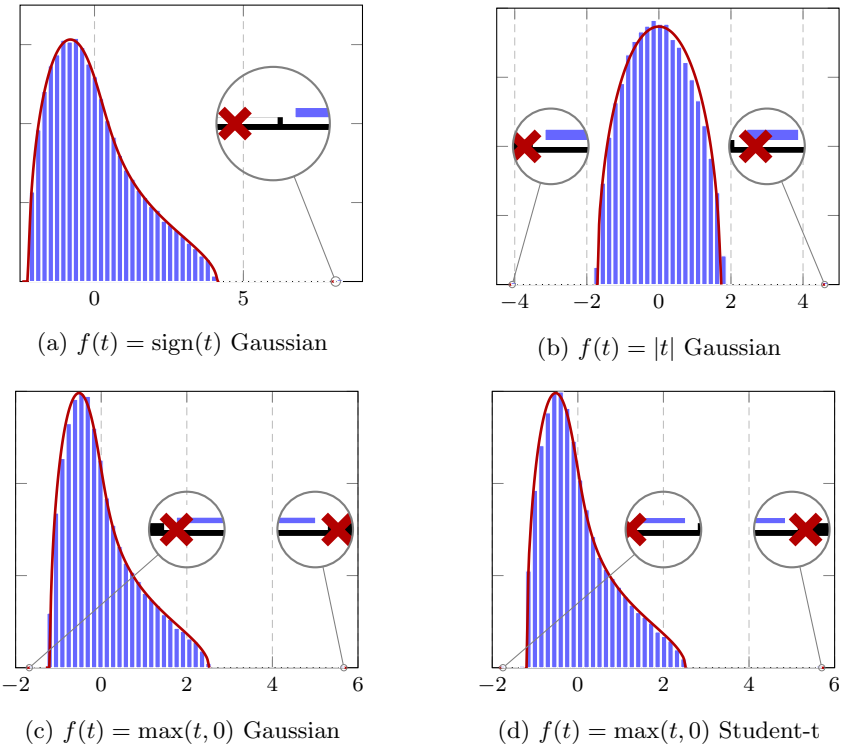


Figure 4.6: Eigenvalues of \mathbf{K} (blue) versus the limiting laws and spikes of $\tilde{\mathbf{K}}$ in Theorem 4.6 (red), for $p = 1024$, $n = 2048$, with two classes $n_1 = n_2 = n/2$ and $\mu_1 = -[2; \mathbf{0}_{p-1}] = -\mu_2$ and $\mathbf{E}_1 = -5 \cdot \mathbf{I}_p / \sqrt{p} = -\mathbf{E}_2$. [\[Link to code\]](#) [\[Fig.validation-approx\]](#)

spikes in Theorem 4.6 are shown to be universal [Liao and Couillet, 2019a], as in the case of limiting spectrum in Theorem 4.4.

Figure 4.6 compares the spectra, and in particular the isolated eigenvalues of \mathbf{K} and $\tilde{\mathbf{K}}$ for $f(t) = \text{sign}(t), |t|$ and $\max(t, 0)$, for random vectors having Gaussian or Student-t entries. These numerical evidences validate Theorem 4.6. Note that we have $a_2 = 0$ for $f(t) = \text{sign}(t)$ and $a_1 = 0$ for $f(t) = |t|$. As a result, different types of spikes (due to means and covariances) are present. More generally, for f odd ($f(-t) = -f(t)$), $a_2 = 0$ and the statistical information on covariances (through \mathbf{E}) asymptotically vanishes in \mathbf{K} ; for f even ($f(-t) = f(t)$), $a_1 = 0$ and information about the means μ vanishes. Thus, only f neither odd nor even can preserve both first and second order discriminating statistics (e.g., the popular ReLU function $f(t) = \max(t, 0)$). Besides, these isolated eigenvalues are informative and, the corresponding eigenvectors are, as expected, noisy versions of linear combinations of \mathbf{J} .

Practical consequences: universality of binary kernels. As a direct consequence of Theorem 4.6, similar to the α - β kernel, the performance of spectral methods with properly scaling kernel only depends on the *three* parameters of the nonlinear function f : $a_1 = \mathbb{E}[\xi f(\xi)]$, $a_2 = \mathbb{E}[\xi^2 f(\xi)]/\sqrt{2}$ and $\nu = \mathbb{E}[f^2(\xi)]$. More precisely, the parameters a_1, ν determine the limiting spectral measure while a_1, a_2 determine the low rank informative structure.

Therefore, arbitrary (square-summable) kernel functions f (with $a_0 = 0$) are asymptotically *equivalent* to the simple cubic function $c_3 x^3 + c_2 x^2 + c_1 x - c_2$ having the *same* Hermite polynomial coefficients a_1, a_2, ν , with the coefficients being related through

$$a_1 = 3c_3 + c_1, \quad a_2 = \sqrt{2}c_2, \quad \nu = (3c_3 + c_1)^2 + 6c_3^2 + 2c_2^2.$$

It is thus possible to design a prototypical family \mathcal{F} of functions f having (i) universal properties with respect to (a_1, a_2, ν) , i.e., for each (a_1, a_2, ν) there exists $f \in \mathcal{F}$ with these Hermite coefficients and (ii) having numerically advantageous properties. Thus, any arbitrary kernel function f can be mapped, through (a_1, a_2, ν) , to a function in \mathcal{F} with good numerical properties. One such prototypical family \mathcal{F} is the set of f , parametrized by (t, s_-, s_+) , and defined as

$$f(x) = \begin{cases} -rt & x \leq \sqrt{2}s_- \\ 0 & \sqrt{2}s_- < x \leq \sqrt{2}s_+ \\ t & x > \sqrt{2}s_+ \end{cases}, \quad \begin{cases} a_1 = \frac{t}{\sqrt{2}\pi}(e^{-s_+^2} + re^{-s_-^2}) \\ a_2 = \frac{t}{\sqrt{2}\pi}(s_+ e^{-s_+^2} + rs_- e^{-s_-^2}) \\ \nu = \frac{t^2}{2}(1 - \text{erf}(s_+))(1 + r) \end{cases} \quad \text{eq: def-piecewise-func (4.19)}$$

where $r \equiv \frac{1 - \text{erf}(s_+)}{1 + \text{erf}(s_-)}$. Figure 4.7 displays such f in (4.19) together with the cubic function $c_3 x^3 + c_2(x^2 - 1) + c_1 x$ sharing the same coefficients (a_1, a_2, ν) , with the gains in storage size shown in Table 4.1.

Table 4.1: Storage size (in Mb) of \mathbf{K} for piecewise constant and cubic f , in the setting of Figure 4.6.

tab:size-time-f	
f	Size
\mathcal{F} -family	4.15
Cubic	16.75

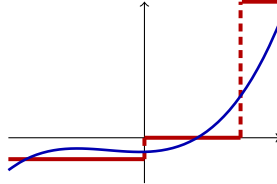


Figure 4.7: Piecewise constant \mathcal{F} -family (green) versus cubic (blue) function with equal (a_1, a_2, ν) .
Fig. illustration nonlinearities

The class of equivalence of kernel functions induced by this mapping (i.e., those having asymptotically equivalent spectral properties) is quite unlike the equivalence class of the previous section for the “improper” scaling $f(\mathbf{x}_i^\top \mathbf{x}_j / p)$ regime. In the latter, functions $f(x)$ of the same class of equivalence are those having common $f'(0)$ and $f''(0)$ values while here these functions may have no similar local behavior (as shown in the example of Figure 4.7).

** performance and complexity trade-off TBD here! **

4.5 Implications to kernel methods

sec:implications_to_kernel_methods

By simply “plugging” the random matrix equivalents of the kernel matrices studied in the previous sections into kernel-based learning algorithms, it is now possible to analyze the asymptotic performance of these algorithms. The present section is dedicated to this analysis, successively for unsupervised (kernel spectral clustering in Section 4.5.1), semi-supervised (with kernel graph Laplacian in Section 4.5.2), and fully supervised (kernel ridge regression in Section 4.5.3) learning.

We shall discover that, as a result of the curse of dimensionality $\|\mathbf{x}_i - \mathbf{x}_j\|^2/p \xrightarrow{a.s.} \tau_p$ and of the resulting inappropriate (low dimensional) intuitions in the large dimensional setting, all these algorithms (i) behave differently from what is expected, (ii) sometimes fail to perform as intended and, (iii) are often far from optimal. Luckily, the random matrix analyses in previous section provide new intuitions and allow for a proper adaptation (such as improved hyperparameter setting) and improvement of the algorithms.

4.5.1 Application to kernel spectral clustering

sec:applications_spectral_clustering

From a machine learning perspective, spectral clustering is often seen as a *discrete-to-continuous relaxation* of a graph min-cut problem [Von Luxburg, 2007]. More precisely, assuming \mathbf{K} to be the adjacency matrix of a graph with nodes $\mathbf{x}_1, \dots, \mathbf{x}_n$ and edges $f(\|\mathbf{x}_i - \mathbf{x}_j\|^2/p)$, the min-cut problem consists in determining a k -class partition $\mathcal{S}_1 \cup \dots \cup \mathcal{S}_k$ of $\{1, \dots, n\}$ that minimizes the affinity across classes, i.e.,

$$(\mathcal{S}_1, \dots, \mathcal{S}_k) \in \arg \min_{\mathcal{S}_1 \cup \dots \cup \mathcal{S}_k = \{1, \dots, n\}} \sum_{a=1}^k \sum_{\substack{i \in \mathcal{S}_a \\ j \notin \mathcal{S}_a}} \frac{f(\frac{1}{p} \|\mathbf{x}_i - \mathbf{x}_j\|^2)}{|\mathcal{S}_a|} \quad \text{eq:graph_cut(4.20)}$$

where the division by the cardinality $|\mathcal{S}_a|$ ensures that classes have approximately balanced weights (this is formally known as the *ratio-cut* adaptation of the original min-cut problem for which the denominator is simply 1). This optimization problem has been shown to be equivalent to finding the orthonormal matrix $\mathbf{S} = [\mathbf{s}_1, \dots, \mathbf{s}_k] \in \mathbb{R}^{n \times k}$ (i.e., $\mathbf{S}^\top \mathbf{S} = \mathbf{I}_k$) with columns defined as $[\mathbf{s}_a]_i = |\mathcal{S}_a|^{-\frac{1}{2}} \cdot \delta_{i \in \mathcal{S}_a}$ which minimize

$$\text{tr } \mathbf{S}^\top (\mathbf{D} - \mathbf{K}) \mathbf{S}$$

where $\mathbf{D} = \text{diag}(\mathbf{K}\mathbf{1}_n)$. Solving this discrete problem is NP-hard [Von Luxburg, 2007], but relaxing \mathbf{S} to be merely an orthonormal matrix with no structure constraint gives the straightforward solution that \mathbf{S} is the collection of the k eigenvectors associated to the smallest eigenvalues of $\mathbf{D} - \mathbf{K}$. This precisely leads to the spectral clustering algorithm.

Yet, performing spectral clustering directly on $\mathbf{D} - \mathbf{K}$ is observed to lead to poor performance in practice. It has instead been proposed to replace $|\mathcal{S}_a|$ in

the min-cut cost function by $\text{vol}(\mathcal{S}_a) = \sum_{i \in \mathcal{S}_a} \mathbf{D}_{ii}$ which is the total weight of the edges connecting the nodes of class \mathcal{S}_a (rather than the number of nodes). With this normalization, the problem now becomes equivalent to minimizing

$$\text{tr } \mathbf{S}^T (\mathbf{I}_n - \mathbf{D}^{-\frac{1}{2}} \mathbf{K} \mathbf{D}^{-\frac{1}{2}}) \mathbf{S}$$

which led to the most popular Ng-Weiss-Jordan spectral clustering algorithm [Ng et al., 2002].

From a random matrix standpoint, the aforementioned heuristic considerations to choose whether 1 , $|\mathcal{S}_a|$ or $\text{vol}(\mathcal{S}_a)$ as normalization is somewhat irrelevant, as we now know that the large dimensional behavior of \mathbf{K} is prone to many erroneous intuitive interpretations. Indeed, the above reasoning is fundamentally based on the fact that f is a decreasing “affinity” function and that $f(\|\mathbf{x}_i - \mathbf{x}_j\|^2/p)$ ought to be large for $\mathbf{x}_i, \mathbf{x}_j$ in the same class, and small otherwise; however, at least as far as non-trivial large dimensional Gaussian mixtures are concerned, this intuition is inappropriate.

Instead, we now need to resort to our novel “large dimensional spectral intuition”, for the moment in the case of standard “improperly scaled” kernels (such as the popular Gaussian kernel).

4.5.1.1 The case of standard distance-kernels

We have seen in Theorem 4.1 that the dominant eigenvectors of \mathbf{K} contain class label information \mathbf{J} and can thus be used for spectral clustering. Yet, \mathbf{K} has the inconvenience that its first two dominant eigenvalues scale like $O(n)$ and $O(\sqrt{n})$. As for the matrix $\mathbf{D} - \mathbf{K}$, it can be readily seen as quite inappropriate for clustering. Indeed, note that, while the informative spectrum of \mathbf{K} is essentially of order $O(1)$ (if we exclude the little informative two dominant eigenvectors), the matrix \mathbf{D} has diagonal elements

$$[\mathbf{D}]_{ii} = n f(\tau_p) + \zeta_i + O(1), \quad \zeta_i = n f'(\tau_p)[\psi]_i = O(\sqrt{n})$$

where the random ζ_i terms are “essentially” of zero mean and asymptotically independent across i . Consequently, the spectrum of $\mathbf{D} - \mathbf{K}$ is largely dominated by the non-informative diagonal elements of \mathbf{D} . As such, $\mathbf{D} - \mathbf{K}$ is not appropriate for spectral clustering, as confirmed by empirical results.

The matrix $\mathbf{D}^{-\frac{1}{2}} \mathbf{K} \mathbf{D}^{-\frac{1}{2}}$ advocated by Ng-Weiss-Jordan is more interesting. First, since $[\mathbf{D}]_{ii} = O(n)$, it is convenient to consider the normalized matrix

$$\mathbf{L} = n \mathbf{D}^{-\frac{1}{2}} \mathbf{K} \mathbf{D}^{-\frac{1}{2}}. \tag{4.21}$$

Note that, $\mathbf{D}^{\frac{1}{2}} \mathbf{1}_n$ is an eigenvector for \mathbf{L} with corresponding eigenvalue n , since

$$n \mathbf{D}^{-\frac{1}{2}} \mathbf{K} \mathbf{D}^{-\frac{1}{2}} (\mathbf{D}^{\frac{1}{2}} \mathbf{1}_n) = \mathbf{D}^{-\frac{1}{2}} \mathbf{K} \mathbf{1}_n = n \mathbf{D}^{-\frac{1}{2}} \mathbf{D} \mathbf{1}_n = n \mathbf{D}^{\frac{1}{2}} \mathbf{1}_n.$$

This is also the largest eigenvalue of \mathbf{L} . Moreover, and quite surprisingly, a thorough Taylor expansion of $\mathbf{D}^{-\frac{1}{2}}$ pre- and post-multiplying the random equivalent

$\tilde{\mathbf{K}}$ of \mathbf{K} , reveals that

$$\mathbf{L}' \equiv n\mathbf{D}^{-\frac{1}{2}}\mathbf{K}\mathbf{D}^{-\frac{1}{2}} - n\frac{\mathbf{D}^{\frac{1}{2}}\mathbf{1}_n\mathbf{1}_n^\top\mathbf{D}^{\frac{1}{2}}}{\mathbf{1}_n^\top\mathbf{D}\mathbf{1}_n} = n\mathbf{D}^{-\frac{1}{2}} \left(\mathbf{K} - \frac{\mathbf{d}\mathbf{d}^\top}{\mathbf{1}_n^\top\mathbf{D}\mathbf{1}_n} \right) \overset{\text{def-L}_2\text{-spectral}}{\mathbf{D}} \quad (4.22)$$

with $\mathbf{d} = \mathbf{D}\mathbf{1}_n$, is asymptotically (with high probability) of bounded operator norm. That is, both matrices \mathbf{A}_n and $\mathbf{A}_{\sqrt{n}}$ (of operator norm of order $O(n)$ and $O(\sqrt{n})$, respectively) from Theorem 4.1 asymptotically disappear after normalization by $\mathbf{D}^{-\frac{1}{2}}$ and projection against the dominant eigen-direction $\mathbf{D}^{\frac{1}{2}}\mathbf{1}_n$. This makes \mathbf{L}' easier to handle mathematically (as no spurious eigenvalue evades from the spectrum at a fast rate) and more “stable” from a statistical viewpoint.

Precisely, we have the following result.

theo:L'

Theorem 4.7 (Random equivalent of normalized Laplacian [Coullet and Benaych-Georges, 2016]). *Under the notations and assumptions of Theorem 4.1, for \mathbf{L}' defined in (4.22), we have*

$$\begin{aligned} \|\mathbf{L}' - \tilde{\mathbf{L}}'\| &\xrightarrow{a.s.} 0 \\ \frac{\mathbf{D}^{\frac{1}{2}}\mathbf{1}_n}{\sqrt{\mathbf{1}_n^\top\mathbf{D}\mathbf{1}_n}} &= \frac{\mathbf{1}_n}{\sqrt{n}} + \frac{1}{n\sqrt{c}} \frac{f'(\tau_p)}{2f(\tau_p)} [\{t_a\mathbf{1}_{n_a}\}_{a=1}^k + \boldsymbol{\psi}] + o(n^{-1}) \end{aligned}$$

where

$$\tilde{\mathbf{L}}' = -2\frac{f'(\tau_p)}{f(\tau_p)} \left(\frac{1}{p} \mathbf{W}^\top \mathbf{W} + \mathbf{U} \mathbf{B} \mathbf{U}^\top \right) + \frac{f(0) - f(\tau_p) + \tau_p f'(\tau_p)}{f(\tau_p)} \mathbf{I}_n$$

and

$$\begin{aligned} \mathbf{U} &= \left[\frac{\mathbf{J}}{\sqrt{p}}, \frac{\mathbf{W}^\top \mathbf{M}}{\sqrt{p}}, \boldsymbol{\psi} \right] \\ \mathbf{B} &= \begin{bmatrix} \mathbf{B}_{11} & \mathbf{I}_k - \mathbf{1}_k \mathbf{c}^\top & \left(\frac{5f'(\tau_p)}{8f(\tau_p)} - \frac{f''(\tau_p)}{2f'(\tau_p)} \right) \mathbf{t} \\ * & \mathbf{0} & \mathbf{0} \\ * & * & \frac{5f'(\tau_p)}{8f(\tau_p)} - \frac{f''(\tau_p)}{2f'(\tau_p)} \end{bmatrix} \\ \mathbf{B}_{11} &= \mathbf{M}^\top \mathbf{M} + \left(\frac{5f'(\tau_p)}{8f(\tau_p)} - \frac{f''(\tau_p)}{2f'(\tau_p)} \right) \mathbf{t} \mathbf{t}^\top - \frac{f''(\tau_p)}{f'(\tau_p)} \frac{\mathbf{S}^\circ}{\sqrt{p}} \\ &\quad + c \cdot \frac{f(0) - f(\tau_p) + \tau_p f'(\tau_p)}{2f'(\tau_p)} \mathbf{1}_k \mathbf{1}_k^\top \\ \frac{\mathbf{S}^\circ}{\sqrt{p}} &= \left\{ \frac{1}{p} \operatorname{tr} \mathbf{C}_a^\circ \mathbf{C}_b^\circ \right\}_{a,b=1}^k, \quad \mathbf{C}_a^\circ = \mathbf{C}_a - \mathbf{C}^\circ \end{aligned}$$

with $\mathbf{c} = [c_1, \dots, c_k]^\top$.

It first provides an explicit characterization of the (exactly known) dominant eigenvector of \mathbf{L}' associated with the eigenvalue n : up to a dominant constant $1/\sqrt{n}$, the eigenvector entries contain small deviations (of order $1/n$) that are

discriminative class information when the t_a 's are of order $O(1)$. These information can be exploited for clustering: indeed, although the deviations t_a/n are small compared to the dominant term $1/\sqrt{n}$, the latter is strictly constant and is thus merely a constant shift and is inconsequential to classification. However, if the t_a 's are equal or only differ by $o(1)$, these information are “buried” in the noisy zero-mean and asymptotically Gaussian vector ψ and cannot be used for clustering.

The projection \mathbf{L}' of the normalized Laplacian matrix \mathbf{L} to the space orthogonal to $\mathbf{D}^{\frac{1}{2}}\mathbf{1}_n$, is then well approximated by an up-to-($2k+1$) rank spiked model (of order $O_{\|\cdot\|}(1)$). The information appears here as a combination of the statistical information $\mathbf{M}^\top \mathbf{M}$, $\mathbf{t}\mathbf{t}^\top$ and \mathbf{S}° , again modulated by the successive derivatives of f at τ_p .

A complete analysis of the asymptotic spectrum of \mathbf{L} is then tractable, leading to the following remarks [Couillet and Benaych-Georges, 2016]:

- due to the presence of the non-informative vector ψ in \mathbf{U} , one *isolated non-informative* eigenvalue may be found in the spectrum of \mathbf{L}' . This has two main consequences: (i) even in the absence of classes, \mathbf{L}' , and thus \mathbf{L} , may contain an isolated eigenvalue which may be confused as information; (ii) in the presence of classes, not all eigenvectors are informative and there is no deciding which one of the isolated eigenvalues is possibly not informative. Figure 4.8 depicts the typical behavior of the spectrum for a Gaussian mixture with equal identity covariance, with emphasis on the non-informative eigenvalue-eigenvector pair;
- unlike \mathbf{MM}^\top and \mathbf{S}° which are matrices of rank at most $k-1$, $\mathbf{t}\mathbf{t}^\top$ is a rank-one matrix; as such, if data are mostly discriminable by the trace of their covariances (i.e., the information in \mathbf{t}), then only one informative eigenvector of \mathbf{L}' (in addition to the eigenvector $\mathbf{D}^{\frac{1}{2}}\mathbf{1}_n$ of \mathbf{L}) can be exploited. This is again counterintuitive since, irrespective of the number of classes, the information is “concentrated” into a single eigenvector. The rule of thumb according to which the number of relevant eigenvectors matches the number of classes thus fails in this case. Figure 4.9 shows the difference between the two informative eigenvectors of \mathbf{L} (the second and third) under a Gaussian mixture with different means and equal covariance, versus the two informative eigenvectors of \mathbf{L} (the first and second) under a common-mean and different-covariance trace scenario. In particular, the bottom display confirms that the discriminative covariance trace information is carried along a one-dimensional axis;
- similar to \mathbf{K} , selecting f such that $f'(\tau_p) \simeq 0$ simultaneously discards the discriminative information of the statistical means across classes as well as the noise terms. The matrix $\mathbf{S}^\circ/\sqrt{p}$ emerges alone and classification becomes asymptotically trivial if $\mathbf{S}^\circ = O_{\|\cdot\|}(\sqrt{p})$.

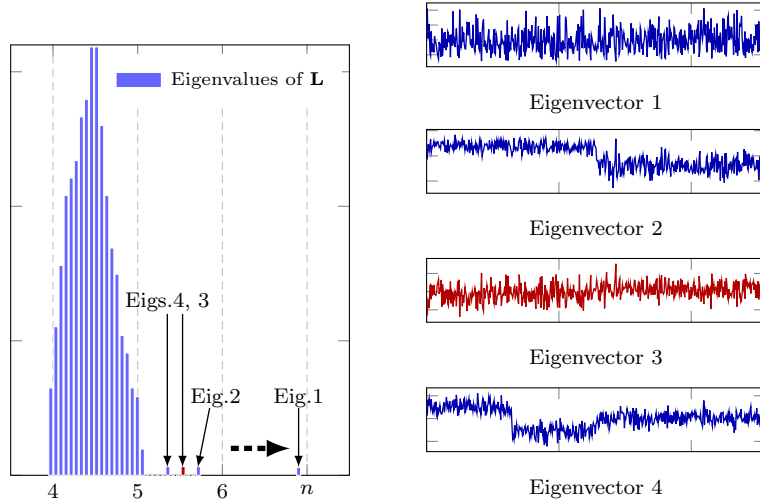


Figure 4.8: Eigenvalues of \mathbf{L} and top four eigenvectors for $\mathbf{C}_a = \mathbf{I}_p$, $f(t) = 4(t - \tau_p)^2 - (t - \tau_p) + 4$ with $\tau_p = 2$, $f(0) = 22$, $f(\tau_p) = 4$, $f'(\tau_p) = -1$, $f''(\tau_p) = 8$, $p = 2048$, $n = 512$, three classes with $n_1 = n_2 = 128$, $n_3 = 256$ and $[\boldsymbol{\mu}_a]_i = 5\delta_{ai}$. Emphasis made on the (third) “non-informative” eigenvalue-eigenvector pair in red. [Link to code]

`fig:eigsL_onlymu`

Implementation on real data. The above results are quite telling of the many misconceptions of, as simple and widely spread an algorithm in machine learning as kernel spectral clustering.

These novel insights can be summarized as follows: under a *large dimensional Gaussian mixture model* setting, (i) the Euclidean distance between data vectors tend to be the same while spectral clustering still performs in a non-trivial fashion, (ii) the number of isolated eigenvalues needs not necessarily match the number of classes, (iii) some dominant eigenvectors may not be informative at all, and possibly most-importantly, (iv) the kernel function f needs not be decreasing and only operates through its first derivatives in the vicinity of τ_p .

Yet, the Gaussian mixture assumption is somewhat fundamental to our analysis as it brings forth the necessary degrees of independence that induce the data concentration. One may wonder whether the results still hold when applied to real-world datasets instead of Gaussian vectors.

Figure 4.11 depicts the four dominant eigenvectors of \mathbf{L} for $\mathbf{K}_{ij} = \exp(-\|\mathbf{x}_i - \mathbf{x}_j\|^2/(2p))$ for $\mathbf{x}_1, \dots, \mathbf{x}_n \in \mathbb{R}^p$ extracted from three classes (zeros, ones, and twos) of the popular MNIST dataset, each class containing 64 vectorized images of size 28×28 pixels (so that $n = 192$ and $p = 784$). Each data vector \mathbf{x}_i is preprocessed by centering and scaling by the empirical mean and variance computed from the whole MNIST database (and then by \sqrt{p} to adhere to the normalization of the theorem statement). An image example from each class are depicted in Figure 4.10.

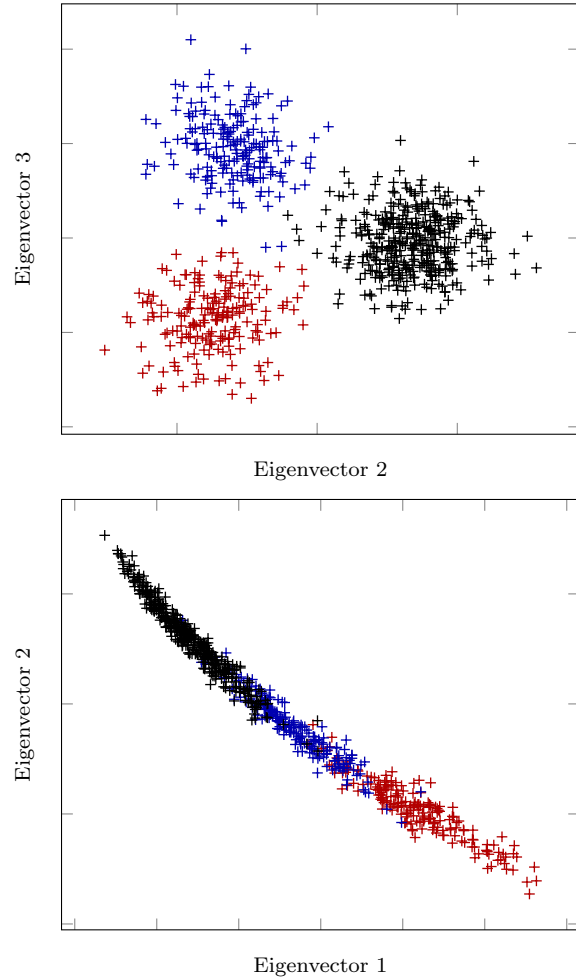


Figure 4.9: Two dimensional representation of (top): eigenvectors two versus three of \mathbf{L} , $[\boldsymbol{\mu}_a]_i = 5\delta_{ai}$, $\mathbf{C}_a = \mathbf{I}_p$, and of (bottom): eigenvectors one versus two of \mathbf{L} , $\boldsymbol{\mu}_a = \mathbf{0}$, $\mathbf{C}_a = (1+4(a-1)/\sqrt{p})\mathbf{I}_p$. In both cases, $p = 3072$, $n_1 = n_2 = 192$, $n_3 = 384$, $f(t) = 1.5(t - \tau_p)^2 - (t - \tau_p) + 5$. [\[Link to code\]](#)

Figure 4.11 precisely shows in red lines the genuine four dominant eigenvectors of \mathbf{L} and in black the eigenvectors of $\tilde{\mathbf{L}}$ from Theorem 4.7. To obtain $\tilde{\mathbf{L}}$, the statistical means and covariances are empirical computed from statistical averaging over the whole set of images of zeros, ones and twos of the MNIST database; as for \mathbf{W} (and thus ψ), it is computed by discarding from \mathbf{X} the evaluated average. Finally, in blue are shown the theoretical class-wise eigenvector means and ± 1 standard deviations obtained from a spiked-model analysis of $\tilde{\mathbf{L}}$ (see for details in [Couillet and Benaych-Georges, 2016]).

It is surprising to see that, despite the obvious non-Gaussianity of the MNIST dataset, the theoretical predictions are in almost perfect accordance with empirical observations.

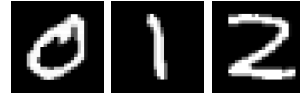


Figure 4.10: Samples from the MNIST database. fig:MNIST

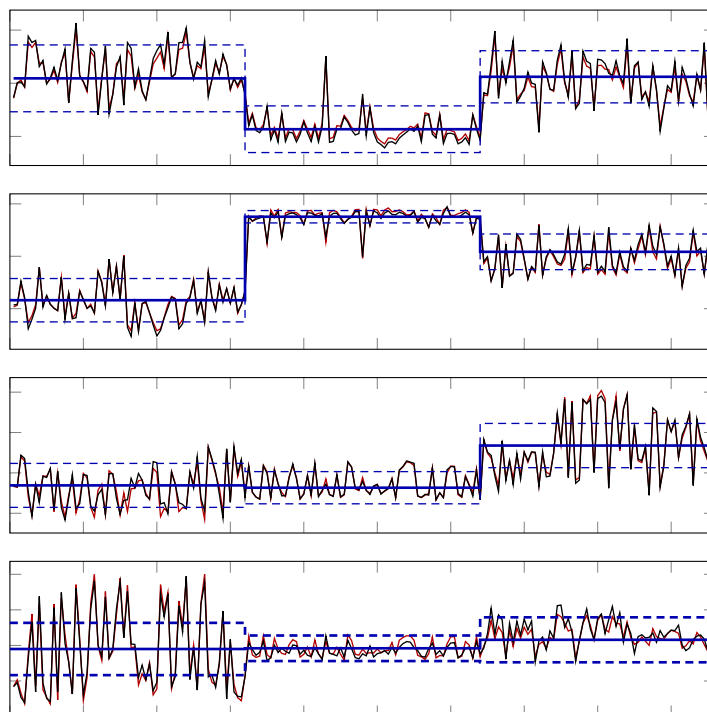


Figure 4.11: Leading four eigenvectors of \mathbf{L} (red) versus $\tilde{\mathbf{L}}$ (black) and theoretical class-wise means and standard deviations (blue) for MNIST data. [\[Link to code\]](#) fig:eigenvectors_L_MNIST

4.5.1.2 The case of “ α - β ” inner-product kernels

The previous section demonstrated that, despite the phenomenon of distance concentration, spectral clustering on the normalized Laplacian \mathbf{L} remains valid under large dimensional data assumption, at the expense of a few unexpected outcomes (presence of non-informative isolated eigenvectors, incoherence between number of classes and number of informative eigenvectors, etc.). These

are immediate consequences of the theoretical study performed in Section 4.2 and were shown to adequately match the actual performance of spectral clustering on, not only Gaussian, but also real-world data.

However, it was also showed in Section 4.2 that kernels of the type $f(\|\mathbf{x}_i - \mathbf{x}_j\|^2/p)$, despite their wide popularity, are suboptimal when it comes to classifying data down to their minimal statistical discrimination. We then proved in Section 4.3 that the α - β kernels, that satisfy $f(\tau_p) = O(1)$, $f'(\tau_p) = \alpha p^{-\frac{1}{2}}$ and $f''(\tau_p) = 2\beta$ for some $\alpha, \beta = O(1)$, are more powerful in discriminating data having close (even equal) means and slightly differing covariances.

We consider this setting here.

Specifically, Figure 4.12 displays the comparative performance of Gaussian versus α - β inner-product kernels in the setting of a two-class Gaussian mixture with equal means but slightly differing covariances (thus here with $\alpha = 0$). We observe that the Gaussian kernel is incapable of resolving the two classes while the α - β kernel is fully adapted. Figure 4.13 then extends the same analysis for an EEG dataset (epileptic versus sane patients)⁶ specifically chosen since, being a more or less stationary zero mean time series, the critical class discriminating features lie more in the second order statistics (i.e., covariance matrices) rather than in the first (means). The dataset vectors were appropriately centered and normalized to be fully compliant with the kernel models. In this case, the Gaussian kernel is observed to have less discriminating power compared to the α - β kernel (chosen here again with $\alpha = 0$, i.e., $f'(\tau_p) = 0$).

We next move to a more general analysis of the α - β kernel for all values of α/β , rather than just for $\alpha = 0$. For a simplified comparison, for varying values of α/β , k-means clustering is performed on the two dominant eigenvectors of the kernels under study. Figure 4.3 and Figure 4.15 provide a comparison of the spectral clustering performance for the “ α - β ” kernel, versus the standard Gaussian kernel on two real datasets: the MNIST image database and the previous EEG database. Figure 4.15 clearly evidences this fact with a strong improvement of the “ α - β ” kernel performance for α/β close to zero (thus when voluntarily disregarding the information about the means and focusing on the covariances instead); the Gaussian kernel in this case has a mediocre performance. But more strikingly, the classification performance on MNIST data in Figure 4.3, where statistical means are (supposedly) more informative than covariances, in general favors a large value for the ratio α/β , but not always: in the case of the pair of digits (3, 8) (which are understandably harder to discriminate than digits (3, 6)), the second order statistics are more valued by the kernel, with a boost of up to 10% of classification rate over the Gaussian kernel.

Setting up the proper value for α, β beforehand is however not immediate as the performance depends on the statistics of each class. Being unknown under a fully unsupervised setting, only iterative procedures (whereby a first iteration provides a crude classification and thus the possibility to estimate the sufficient statistics) can seemingly be exploited to selectively adapt the algorithm

⁶<http://www.meb.unibonn.de/epileptologie/science/physik/eegdata.html>.

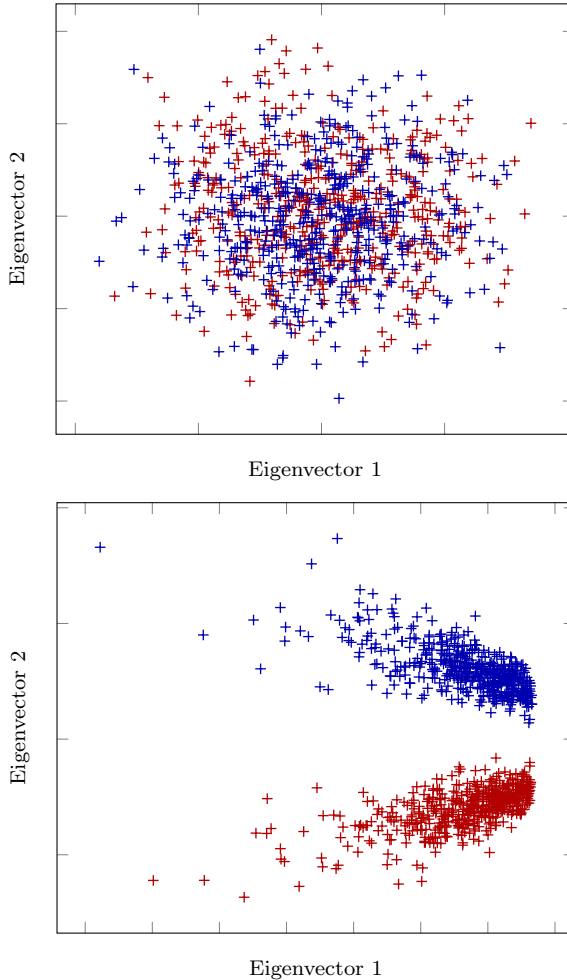


Figure 4.12: Comparison of 2D representation of eigenvectors one and two of (**top**) the Gaussian kernel $\mathbf{K}_{ij} = \exp(-\|\mathbf{x}_i - \mathbf{x}_j\|^2/(2p))$ and (**bottom**) the α - β kernel $\mathbf{K}_{ij} = (\|\mathbf{x}_i - \mathbf{x}_j\|^2/p - 2)^2$ with $\alpha = 0$. Here $k = 2$ classes of even size, $p = 400$, $n = 1000$, $\boldsymbol{\mu}_a = \mathbf{0}$, $\mathbf{C}_a = .1\mathbf{I}_p + 2\mathbf{Z}_a\mathbf{Z}_a^\top/p$ where $\mathbf{Z}_a \in \mathbb{R}^{p \times p/2}$ have independent standard Gaussian entries. [\[Link to code\]](#) `fig:alpha-beta_kernel_onlyCs_2Dplot`

and improve its performance. Alternatively, an informed guess of the relative importance of means versus covariances may be used to adapt the algorithm.

[figures to be done!](#) and y-axis always be misclassification rate.

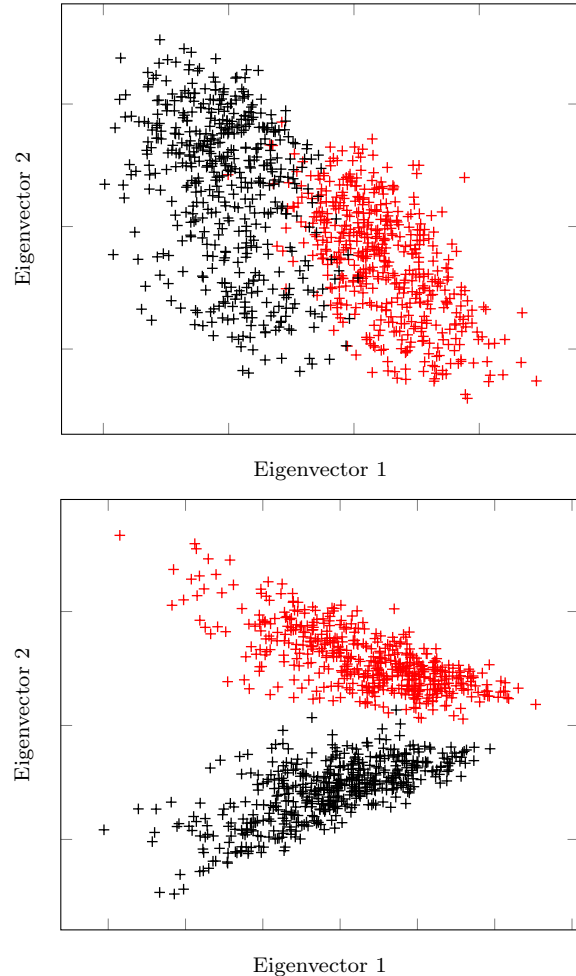


Figure 4.13: Comparison of 2D representation of eigenvectors one and two of (**top**) the Gaussian kernel $\mathbf{K}_{ij} = \exp(-\|\mathbf{x}_i - \mathbf{x}_j\|^2/(2p))$ and (**bottom**) the α - β kernel $\mathbf{K}_{ij} = (\|\mathbf{x}_i - \mathbf{x}_j\|^2/p - 2)^2$ with $\alpha = 0$. Here $k = 2$ classes of even size from the EEG dataset (class ? versus class ?), $p = 100$ and $n = 1000$. [Link to code] [fig:alpha-beta_kernel_EEG_2Dplot](#)

4.5.2 Application to semi-supervised kernel learning

sec:SSL

Semi-supervised learning is possibly the most natural, but paradoxically the least studied, framework in machine learning in that it assumes the existence of a large set of data, say to be classified, with only some of the data already manually labeled. This both encompasses unsupervised learning in the extreme case of no labeled data and supervised learning at the other extreme.

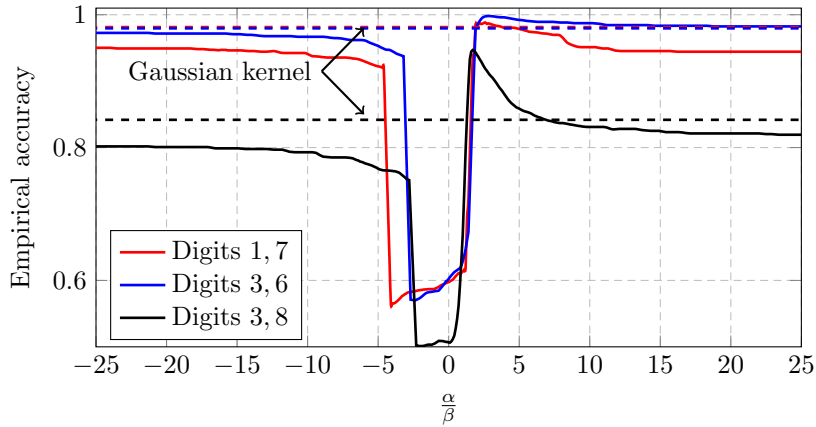


Figure 4.14: Spectral clustering of the MNIST database with the “ α - β ” kernel $\mathbf{K}_{ij} = (\frac{1}{p}\|\mathbf{x}_i - \mathbf{x}_j\|^2 - 2)^2$ for varying $\frac{\alpha}{\beta}$ versus Gaussian kernel ($\mathbf{K}_{ij} = \exp(-\frac{1}{2p}\|\mathbf{x}_i - \mathbf{x}_j\|^2)$). k-means clustering on dominant two eigenvectors. [Link to code]

`fig:real_data_MNIST`

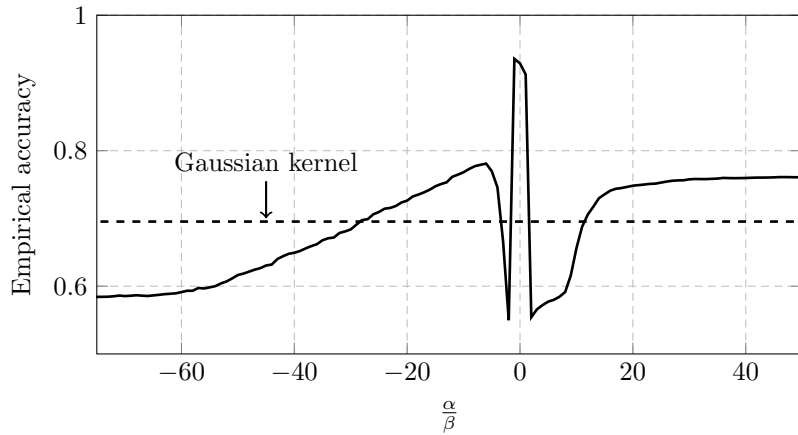


Figure 4.15: Spectral clustering of the EEG database with the “ α - β ” kernel \mathbf{K} for varying $\frac{\alpha}{\beta}$ versus Gaussian kernel ($\mathbf{K}_{ij} = \exp(-\frac{1}{2p}\|\mathbf{x}_i - \mathbf{x}_j\|^2)$). [Link to code]

`fig:alpha_beta_EEG`

We will see in this section that the reason behind its not being profoundly studied may precisely lie in a misunderstanding of the (not so) large dimensional behavior of the devised methods. These lead to often quite erroneous outcomes, which have been worked around in the literature by various intuitions, rarely sustained by theory.

The random matrix approach clarifies the main problems, demonstrates that

some of the popular methods are indeed inconsistent and *must fail*, and most importantly, allows for a novel improved (again in a very counter-intuitive fashion) scheme that is provably consistent.

4.5.2.1 Semi-supervised graph Laplacian and random walk approaches

The likely most common approach to semi-supervised learning are graph-based methods, which have a dual interpretation. In these methods, one considers data $\mathbf{x}_1, \dots, \mathbf{x}_n \in \mathbb{R}^p$ as vertices of a weighted graph with edge weights $\mathbf{K}_{ij} \equiv \kappa(\mathbf{x}_i, \mathbf{x}_j)$ encoding the similarity between \mathbf{x}_i and \mathbf{x}_j . As usual, we consider $\mathbf{K} = \{\mathbf{K}_{ij}\}_{i,j=1}^n$ to be of kernel form, e.g.,

$$\mathbf{K}_{ij} = f\left(\frac{1}{p}\|\mathbf{x}_i - \mathbf{x}_j\|^2\right).$$

From a finite-dimensional intuition, vectors \mathbf{x}_i that are alike should aggregate in clusters, with some nodes in these clusters already labeled. As such, a natural idea to recover the classes of the unknown nodes consists in “spreading” the labels throughout the graph by means of random walks on the graph: either starting from an unlabeled node and having it walk randomly according to edge weights, until it reaches a labeled node, or conversely, walking from labeled nodes to unlabeled nodes; this procedure is iterated randomly on the graph until convergence. In this spirit, assuming k data classes $\mathcal{C}_1, \dots, \mathcal{C}_k$, the random walk method [Jaakkola and Szummer, 2002] or the label propagation approach [Zhu and Ghahramani, 2002] allocates “soft scores” $(\mathbf{S}_{i1}, \dots, \mathbf{S}_{ik}) \in \mathbb{R}^k$ for an unlabeled node \mathbf{x}_i to belong to each class. These k scores are then compared and the argument of the highest score is assigned to \mathbf{x}_i . Of utmost interest for us in the sequel is the particularly popular PageRank approach [Avrachenkov et al., 2012], because of its robustness and high performance.

The alternative viewpoint is more related to the optimization schemes (such as the graph-cut minimization (4.20)) in unsupervised spectral clustering. There again, a matrix scores $\mathbf{S} = \{\mathbf{S}_{ia}\}_{1 \leq i \leq n, 1 \leq a \leq k}$ for the n data vectors in each of the k classes needs to be filled, by solving the optimization problem of the type

$$\begin{aligned} \mathbf{S} = \arg \min_{\mathbf{S} \in \mathbb{R}^{n \times k}} & \sum_{a=1}^k \sum_{i,j=1}^n [\mathbf{K}]_{ij} ([\mathbf{S}]_{ia} d_i^\alpha - [\mathbf{S}]_{ja} d_j^\alpha)^2 && \text{eq:optim_SSL} \\ \text{s.t. } & \mathbf{S}_{ia} = \delta_{\mathbf{x}_i \in \mathcal{C}_a} \text{ for labeled nodes.} \end{aligned} \quad (4.23)$$

Here $d_i = \sum_{j=1}^n \mathbf{K}_{ij}$ is the degree of the node i in the graph representation and $\alpha \in \mathbb{R}$ is some parameter to be specified. Note that the optimization scheme imposes $\mathbf{K}_{ij} \geq 0$ to be meaningful (otherwise, an arbitrarily small negative solution could be found). With this constraint, the optimization scheme naturally induces the scores \mathbf{S}_{ia} and \mathbf{S}_{ja} to be close for \mathbf{K}_{ij} large, and allows them to be distinct if \mathbf{K}_{ij} is close to zero.

Yet, it was empirically observed that, for $\alpha = 0$, the algorithm tends to fail. From a large dimensional perspective, we now understand the fundamental

reason behind this observation is the erroneous assumption that \mathbf{K}_{ij} is either “small” or “large”, while past attempts rather blamed this on the unbalances in the graph. To avoid some (too strongly connected) nodes to create biases, the natural first solution has been to weigh the scores \mathbf{S}_{ij} by a negative power of the degree d^α for some $\alpha < 0$. This is the approach essentially followed, for different choices of α , in [Zhu et al., 2003, Belkin et al., 2004, Joachims et al., 2003, Zhou et al., 2004].

Quite interestingly, the explicit solutions of these (quadratic under linear constraint) optimization problems can essentially be mapped to the stationary points of the aforementioned label propagation or random walk on graphs, as shown in [Avrachenkov et al., 2012] for $\alpha = 0, -1/2$ and -1 . The case $\alpha = -1$, which we shall discuss in depth in the following, precisely corresponds to the PageRank algorithm.

Remark 4.7 (Laplacian versus manifold methods). *Aside from graph-Laplacian approaches, another popular semi-supervised learning scheme is the manifold-based method [Belkin and Niyogi, 2004, Goldberg et al., 2009, Moscovitch et al., 2016]. These algorithms however rely on a first step of “manifold learning” which imposes the unsupervised projection on a dominant subspace that we know, from the previous section, to possibly lead (below a certain phase transition) to a complete loss of information. The Laplacian-based approaches, as shall be seen in this section, do not suffer from this phase transition issue and are thus more robust.*

The solution to (4.23) is explicitly given by

$$\mathbf{S}_{[u]} = \left(\mathbf{I}_{n_u} - \mathbf{D}_{[u]}^{-1-\alpha} \mathbf{K}_{[uu]} \mathbf{D}_{[u]}^\alpha \right)^{-1} \mathbf{D}_{[u]}^{-1-\alpha} \mathbf{K}_{[ul]} \mathbf{D}_{[l]}^\alpha \mathbf{S}_{[l]}^{\text{eq:scores_SSL}} \quad (4.24)$$

where $\mathbf{D} = \text{diag}(d_1, \dots, d_n) \in \mathbb{R}^{n \times n}$ and we divide \mathbf{S} , \mathbf{K} and \mathbf{D} in sub-blocks of labeled (l) versus unlabeled (u) data indices

$$\mathbf{S} = \begin{bmatrix} \mathbf{S}_{[l]} \\ \mathbf{S}_{[u]} \end{bmatrix}, \quad \mathbf{K} = \begin{bmatrix} \mathbf{K}_{[ll]} & \mathbf{K}_{[lu]} \\ \mathbf{K}_{[ul]} & \mathbf{K}_{[uu]} \end{bmatrix}, \quad \text{and } \mathbf{D} = \begin{bmatrix} \mathbf{D}_{[l]} & 0 \\ 0 & \mathbf{D}_{[u]} \end{bmatrix}. \quad \text{eq:S-K-D-block} \quad (4.25)$$

The final decision, i.e., the allocated class index $\hat{\mathcal{C}}_{\mathbf{x}_i}$ for data \mathbf{x}_i , is then given by

$$\hat{\mathcal{C}}_{\mathbf{x}_i} = \mathcal{C}_{\hat{a}} \text{ for } \hat{a} = \arg \max_{1 \leq a \leq k} \mathbf{S}_{ia}.$$

4.5.2.2 Large dimensional performance analysis

As in the previous section for unsupervised classification, we place ourselves under a “non-trivial” Gaussian mixture model, that is

$$\mathbf{x}_i \in \mathcal{C}_a \Leftrightarrow \mathbf{x}_i \sim \mathcal{N}(\boldsymbol{\mu}_a, \mathbf{C}_a).$$

for $\boldsymbol{\mu}_a \in \mathbb{R}^p$ and $\mathbf{C}_a \in \mathbb{R}^{p \times p}$. We assume that there exists k classes $\mathcal{C}_1, \dots, \mathcal{C}_k$ of sizes n_1, \dots, n_k , with in total $n_{[l]}$ labeled and $n_{[u]}$ unlabeled nodes. We denote

$n_{[l]a}, n_{[u]a}$ the number of labeled and unlabeled nodes of class \mathcal{C}_a that are all assumed to be of order $O(n)$.

Since our focus lies in the understanding of the behavior of the semi-supervised learning algorithm, so in particular (but not only) in the statistics of the score matrix \mathbf{S} and the impact of the hyperparameter α , here we merely consider the case $\mathbf{K}_{ij} = f(\frac{1}{p}\|\mathbf{x}_i - \mathbf{x}_j\|^2)$ for $f'(\tau_p)$ away from zero, where we recall

$$\tau_p = \frac{2}{p} \operatorname{tr} \mathbf{C}^{\circ}, \quad \mathbf{C}^{\circ} = \sum_{a=1}^k \frac{n_a}{n} \mathbf{C}_a$$

and demand for every $a, b \in \{1, \dots, k\}$ that

$$\|\boldsymbol{\mu}_a - \boldsymbol{\mu}_b\| = O(1), \quad \operatorname{tr}(\mathbf{C}_a - \mathbf{C}_b) = O(\sqrt{p}), \quad \operatorname{tr}(\mathbf{C}_a - \mathbf{C}_b)^2 = O(p).$$

The fact that these distances are possibly suboptimal for certain classification tasks will not be our primary focus here.

First intuitions. A first key observation is that, under the non-trivial growth rate, since $\max_{ij} |\mathbf{K}_{ij} - \tau_p| \xrightarrow{a.s.} 0$, there are strong reasons to believe that the optimization scheme (4.23), through its solution in (4.24), is bound to fail. However, while the algorithm always behaves differently from our low dimensional intuition, it may not fail in some cases. To see this, let us set $\alpha = -1$ and perform semi-supervised graph learning with a Gaussian kernel on two even-sized classes $\mathcal{N}(\pm \boldsymbol{\mu}, \mathbf{I}_p)$. Figure 4.16 illustrates the scores \mathbf{S} for $p = 1$ (small dimensional case) versus $p = 20$ (moderately large dimensional case).

Recalling that the finite-dimensional intuition behind the optimization framework in (4.23) (or its equivalent walk on graph and label propagation interpretation) is that, the unlabeled data scores should be “drawn” to the scores of neighbors effectively from the same class. This expected behavior of the score vector $\mathbf{S}_{\cdot a} \in \mathbb{R}^n$ of class \mathcal{C}_a is displayed at the top of Figure 4.16 for data of dimension $p = 1$. Yet, as soon as p is slightly larger, this behavior is largely disrupted, as observed in the bottom display for $p = 20$. Note in particular that:

- the unlabeled data scores do not seem affected by the labeled data scores (0 or 1); indeed, a pairwise comparison of \mathbf{S}_{i1} and \mathbf{S}_{i2} reveals that the scores are extremely close to one another but their average is not a fixed value (one would expect 0.5);
- despite this completely different behavior between $p = 1$ and $p = 20$ scenario, the algorithm seems to work properly in that $\mathbf{S}_{i1} > \mathbf{S}_{i2}$ for most $i \leq n/2$ (so for data genuinely in \mathcal{C}_1) and conversely.

As a consequence, although the finite-dimensional intuition is largely disrupted here, the semi-supervised learning scheme does not completely fail, at least in this very elementary Gaussian mixture toy model.

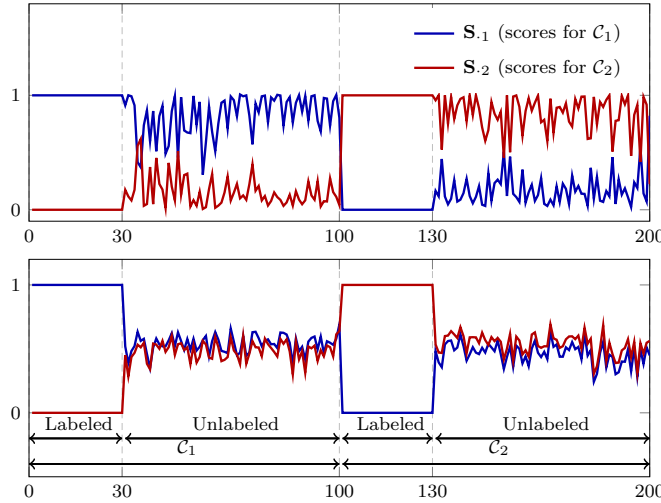


Figure 4.16: Scores \mathbf{S} for Laplacian-based semi-supervised learning with two classes $\mathbf{x}_i \sim \mathcal{N}(\pm\boldsymbol{\mu}, \mathbf{I}_p)$ with $\boldsymbol{\mu} = [2, \mathbf{1}_{p-1}]$, Gaussian kernel, $\alpha = -1$, $n = 200$, $n_{[l]} = 60$, $n_{[u]} = 140$ and (top) $p = 1$, (bottom) $p = 20$. [\[Link to code\]](#) `fig:SSL_p=1_p=20`

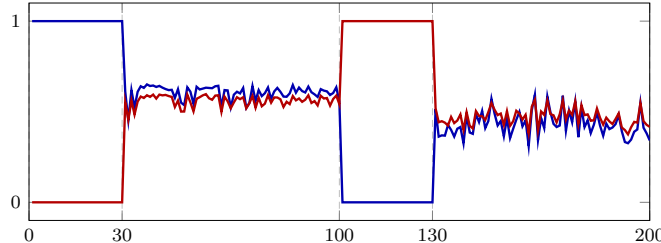


Figure 4.17: Scores \mathbf{S} of MNIST data (ones versus twos) with $p = 784$, in the same setting as Figure 4.16. [\[Link to code\]](#) `fig:SSL_MNIST`

What about real data scenarios? Figure 4.17 proposes the same setting as Figure 4.16 for the MNIST dataset. The situation appears much closer to the bottom than the top display of Figure 4.16, thereby suggesting a closer fit with the large dimensional viewpoint. The situation is even worse since the unlabeled data scores are less close to 1/2. Yet, the algorithm again works decently as the comparison between \mathbf{S}_{i1} and \mathbf{S}_{i2} shows a clear advantage of class \mathcal{C}_1 on the first half of the unlabeled data and class \mathcal{C}_2 on the second half.

But all this is valid here for $\alpha = -1$. The same simulation with for example $\alpha = 0$ or $\alpha = -1/2$ reveals a total failure of the algorithm with all data mapped to the same class.

Derivations and main results. To understand the behavior of Laplacian-based semi-supervised learning observed above, we shall first focus on the large n, p asymptotics of the score vectors $\mathbf{S}_a \in \mathbb{R}^n$ for $1 \leq a \leq k$. Characterizing the ultimate performance of the algorithm will consist instead in studying, for each \mathbf{x}_i unlabeled, the “joint” vector of scores $\mathbf{S}_i \in \mathbb{R}^k$.

Recall from Theorem 4.1 that, the kernel matrix \mathbf{K} under study here admits the random matrix equivalent $\tilde{\mathbf{K}}$ in the sense that $\|\mathbf{K} - \tilde{\mathbf{K}}\| \xrightarrow{a.s.} 0$ in the large n, p limit. In particular, $\|\mathbf{K}_{[ul]} - \tilde{\mathbf{K}}_{[ul]}\| \xrightarrow{a.s.} 0$ and similarly for all sub-blocks of \mathbf{K} under the decomposition in (4.25). From the explicit form (4.24) of the unlabeled data scores $\mathbf{S}_{[u]}$, it is thus tempting to replace all sub-blocks of \mathbf{K} by those of $\tilde{\mathbf{K}}$. This is indeed justified since, almost surely, for all large n , the resolvent $(\mathbf{I}_{n_u} - \mathbf{D}_{[u]}^{-1-\alpha} \mathbf{K}_{[uu]} \mathbf{D}_{[u]}^\alpha)^{-1}$ has bounded spectrum. After calculus, it indeed comes that

$$\mathbf{D}_{[u]}^{-1-\alpha} \mathbf{K}_{[uu]} \mathbf{D}_{[u]}^\alpha = \frac{1}{n} \mathbf{1}_{n_{[u]}} \mathbf{1}_{n_{[u]}}^\top + O_{\|\cdot\|}(n^{-\frac{1}{2}})$$

so that the resolvent can be further expanded as

$$\left(\mathbf{I}_{n_{[u]}} - \mathbf{D}_{[u]}^{-1-\alpha} \mathbf{K}_{[uu]} \mathbf{D}_{[u]}^\alpha \right)^{-1} = \mathbf{I}_{n_{[u]}} + \frac{1}{n_{[l]}} \mathbf{1}_{n_{[u]}} \mathbf{1}_{n_{[u]}}^\top + \underset{\|\cdot\|(n^{-\frac{1}{2}})}{\mathcal{O}} \text{eq:SSL_approx_resolv} \quad (4.26)$$

We will see later, although the $O_{\|\cdot\|}(n^{-\frac{1}{2}})$ term contains statistical information about the classes, this seemingly “trivial” linearization of the resolvent is at the source of various counterintuitive phenomena observed in large dimensional semi-supervised learning.

Once the linearization of the resolvent performed, characterizing the asymptotic behavior of $\mathbf{S}_{[u]}$ becomes a matter of algebraic calculus from the results in Theorem 4.1. This calculus leads to the following first central result (see proof details in [Mai and Couillet, 2018])

$$(\mathbf{S}_{[u]})_{ia} = \frac{n_{[l]a}}{n} \left(\mathbf{1}_{n_{[u]}} + \mathbf{v} + (\alpha + 1) \frac{f'(\tau_p)}{f(\tau_p)\sqrt{c}} \frac{t_a \mathbf{1}_{n_{[u]}}}{\sqrt{n}} \right) + O(n^{-1}) \quad \text{eq:Su_ij} \quad (4.27)$$

where we recall $t_a = \text{tr } \mathbf{C}_a^\circ / \sqrt{p} = O(1)$, $O(n^{-1})$ is understood entry-wise and $\mathbf{v} \in \mathbb{R}^{n_{[u]}}$ is a zero-mean *random vector* with entries of order $O(n^{-1/2})$ which is independent on the class index a .

This first result states that:

1. the score $(\mathbf{S}_{[u]})_{ia}$ of an unlabeled datum \mathbf{x}_i is largely dominated by the constant $n_{[l]a}/n$; as such, if $n_{[l]1}, \dots, n_{[lk]}$ are distinct, all the unlabeled data will be allocated to the class \mathcal{C}_a corresponding to the largest (or smallest) value of $n_{[l]a}$;
2. the next dominant term in $(\mathbf{S}_{[u]})_{ia}$ is the sum of two terms of order $O(n^{-1/2})$: the zero-mean random noise $[\mathbf{v}]_i$ and a term proportional to $(\alpha+1)t_a$ which does not depend on i : as such, provided the $n_{[l]}$ are equal, all unlabeled data \mathbf{x}_i will likely be classified in the class \mathcal{C}_a for which t_a is

maximal (or minimal), unless the t_a 's are all equal (or distinct by at most $O(n^{-1/2})$) or $\alpha = -1$ (or at least equal to $-1 + O(n^{-1/2})$); since the former cannot be guaranteed in practice, one must set the parameter α close to -1 ; this here explains the long observed advantage of the PageRank algorithm over Laplacian methods;

3. once all these constraints are set, what remains in $(\mathbf{S}_{[u]})_{ia}$ is a term of order $O(n^{-1})$, leading to the vector $(\mathbf{S}_{[u]})_{\cdot a}$ being of norm $O(n^{-1/2})$: this “weak” $O(n^{-1})$ term, as we shall see, is the one containing the *relevant classification information* which *must* be protected from the dominant higher $O(n^{-1/2})$ order noise!

From Item 1, we thus conclude that $\mathbf{S}_{[u]}$ is *not* the appropriate metric, and one must instead consider the normalized score matrix

$$\hat{\mathbf{S}}_{[u]} = \mathbf{S}_{[u]} \operatorname{diag} \left(\frac{n}{n_{[l]1}}, \dots, \frac{n}{n_{[l]k}} \right). \quad \text{eq:hatS (4.28)}$$

From Item 3, α must be set to $-1 + \beta/\sqrt{p}$ for some $\beta = O(1)$. This preprocessing step discards all *dominant noise* in $\mathbf{S}_{[u]}$ and therefore now reveals the “hidden” (otherwise buried in noise) class information structure from the residual $O(n^{-1})$ term in the expansion of $(\mathbf{S}_{[u]})_{\cdot a}$ in (4.27). A careful random matrix analysis leads to the following result.

theo:SSL_main

Theorem 4.8 ([Mai and Couillet, 2018, Theorem 2]). *For $\mathbf{x}_i \in \mathcal{C}_b$ an unlabeled data point, let $\hat{\mathbf{S}}$ be defined in (4.28) and $\alpha = -1 + \beta/\sqrt{p}$ for some $\beta \in \mathbb{R}$. Then*

$$p\hat{\mathbf{S}}_{i\cdot} = p(1 + [\mathbf{v}]_i)\mathbf{1}_k + \mathbf{g}_i + o(1), \quad \mathbf{g}_i \sim \mathcal{N}(\mathbf{E}_b, \mathbf{V}_b)$$

where $[\mathbf{v}]_i = O(n^{-1/2})$ only depends on i and

$$\begin{aligned} [\mathbf{E}_b]_a &= -\frac{2f'(\tau_p)}{f(\tau_p)}\tilde{\boldsymbol{\mu}}_a^\top\tilde{\boldsymbol{\mu}}_b + \left(\frac{f''(\tau_p)}{f(\tau_p)} - \frac{f'(\tau_p)^2}{f(\tau_p)^2} \right) \tilde{t}_a \tilde{t}_b \\ &\quad + \frac{2f''(\tau_p)}{f(\tau_p)} \frac{1}{p} \operatorname{tr} \tilde{\mathbf{C}}_a \tilde{\mathbf{C}}_b + \frac{n\beta}{n_{[l]}} \frac{f'(\tau_p)}{f(\tau_p)} t_a \end{aligned} \quad \text{eq:thm:main_mean (4.29)}$$

$$\begin{aligned} [\mathbf{V}_b]_{a_1 a_2} &= 2 \left(\frac{f''(\tau_p)}{f(\tau_p)} - \frac{f'(\tau_p)^2}{f(\tau_p)^2} \right)^2 t_{a_1} t_{a_2} \cdot \frac{1}{p} \operatorname{tr} \mathbf{C}_b \mathbf{C}_b \\ &\quad + 4 \frac{f'(\tau_p)^2}{f(\tau_p)^2} \left[(\boldsymbol{\mu}_{a_1}^\circ)^\top \mathbf{C}_b \boldsymbol{\mu}_{a_2}^\circ + \frac{n\delta_{a_1 a_2}}{n_{[l] a_1} n_{[l]}} \operatorname{tr} \tilde{\mathbf{C}}_{a_1} \tilde{\mathbf{C}}_b \right]. \end{aligned} \quad \text{eq:thm:main_covariance (4.30)}$$

where we introduce the “labeled-data centered” statistics

$$\tilde{\boldsymbol{\mu}}_a \equiv \boldsymbol{\mu}_a - \sum_{b=1}^k \frac{n_{[l]b}}{n_{[l]}} \boldsymbol{\mu}_b, \quad \tilde{t}_a \equiv \frac{1}{\sqrt{p}} \operatorname{tr} \tilde{\mathbf{C}}_a, \quad \tilde{\mathbf{C}}_a \equiv \mathbf{C}_a - \sum_{b=1}^k \frac{n_{[l]b}}{n_{[l]}} \mathbf{C}_b.$$

The main message of Theorem 4.8 is that, up to the irrelevant dominant term $p(1 + z_i \mathbf{v}_i) \mathbf{1}_k$, the normalized score vector $\hat{\mathbf{S}}_{i\cdot} \in \mathbb{R}^k$ of \mathbf{x}_i has a limiting

Gaussian behavior with precisely characterized mean and covariance. Those not surprisingly depend on the statistical means μ_a and covariance matrices \mathbf{C}_a of the data classes and on the first derivatives of f at τ_p . The parameter β also plays a non-trivial “biasing” role that may be helpful in correcting some inherent unbalance between classes.

Yet, generally speaking, most conclusions drawn in the previous section on spectral clustering remain valid (in particular that taking $f'(\tau_p) = 0$ leads to trivial classification of covariance-based classes), at the noticeable exception of the following surprising remark.

Remark 4.8 (Sub-optimality of the Gaussian kernel). *It is interesting to observe that the term $f''(\tau_p)/f(\tau_p) - f'(\tau_p)^2/f(\tau_p)^2$ plays a dominant role in discriminating classes having various “amplitudes” (i.e., distinct values of t_a). For the Gaussian kernel $f(t) = \exp(-t/2\sigma^2)$, this term is exactly zero for all choices of τ_p and thus the Gaussian kernel, in this semi-supervised context, fails for instance to separate two “nested balls” $\mathcal{N}(\mathbf{0}, (1 \pm \epsilon/\sqrt{p})\mathbf{I}_p)$, as in the case of Remark 4.5 for “regular” inner-product kernels, while most polynomial kernels succeed. This is illustrated in Figure 4.18.*

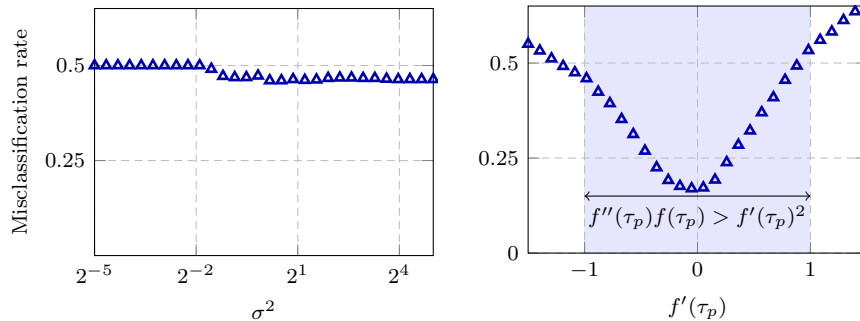


Figure 4.18: Empirical misclassification rate of semi-supervised Laplacian approach on two-class Gaussian mixtures with $\mu_1 = \mu_2$, $\mathbf{C}_1 = \mathbf{I}_p$ and $\mathbf{C}_2 = (1 + 3/\sqrt{p})\mathbf{I}_p$, for (left) Gaussian kernel $f(t) = \exp(-t/(2\sigma^2))$ and (right) polynomial kernel of degree two with $f(\tau_p) = f''(\tau_p) = 1$, $n = 1024$, $p = 512$, $n_{[l]}/n = 1/16$, $n_{[l]1} = n_{[l]2}$ and $\alpha = -1$. [Link to code] fig:SSL_Gaussian_kernel

Looking now more specifically into the “semi-supervised” aspect of the algorithm, a major problem arises immediately: up to renaming β into $\beta n/n_{[l]}$ which is a free parameter, the mean \mathbf{E}_b in Theorem 4.8 depends neither on $n_{[l]}$ nor on $n_{[u]}$. As for the variance \mathbf{V}_b , note that its diagonal elements decrease as $n_{[l]}$ increases (for fixed $p, n_{[u]}$) but *does not decrease* as $n_{[u]}$ increases (for fixed $p, n_{[l]}$). This suggests that the semi-supervised Laplacian approach *does not* learn from unlabeled data. This surprising outcome is in fact well documented in the semi-supervised learning literature: see in particular [Chapelle et al., 2009, Chapter 4] which we quote here

“Our concern is this: it is frequently the case that we would be better off just discarding the unlabeled data and employing a supervised method, rather than taking a semi-supervised route. Thus we worry about the embarrassing situation where the addition of unlabeled data degrades the performance of a classifier.”

The situation is depicted in Figure 4.20 where the performance of the Laplacian approach (blue triangles) is indeed confirmed not to increase with $n_{[u]}$: the popular Laplacian method is thus merely reduced, at least in the large n, p regime, to supervised classification. A particularly problematic consequence is that the fully unsupervised spectral clustering method studied in Section 4.5.1 tends to overtake the Laplacian method.

The next section is dedicated to a more profound analysis of the problem, leading to a random matrix-inspired solution that benefits from more unlabeled data (red circles in Figure 4.20).

4.5.2.3 Improving semi-supervised learning

As pointed out previously, the linearization (4.26) of the resolvent in the expression of $\mathbf{S}_{[u]}$ holds the key to the inefficiency of the use of the unlabeled data in the graph-based semi-supervised learning algorithm.

Main intuition. The situation may be loosely summarized as follows: $\mathbf{S}_{[u]} = \mathbf{A}_{[uu]}\mathbf{A}_{[ul]}$ with $\mathbf{A}_{[uu]}$ the “unsupervised part” of the algorithm and $\mathbf{A}_{[ul]}$ the supervised part. The (operator-norm) dominant-order term of $\mathbf{A}_{[uu]}$ contains the identity matrix $\mathbf{I}_{n_{[u]}}$, while the dominant term of $\mathbf{A}_{[ul]}$ only contains $\frac{1}{n}\mathbf{1}_{n_{[u]}}\mathbf{1}_{n_{[l]}}^\top$; as for the informative terms of least order, call them $\mathbf{B}_{[uu]}$ and $\mathbf{B}_{[ul]}$, they are both such that their (i, a) -entry depends on the class of \mathbf{x}_i and on the class index a . In order for $(\mathbf{S}_{[u]})_{ia}$ to be informative, it must also depend on both the class of \mathbf{x}_i and on a . However, taking the product $\mathbf{A}_{[uu]}\mathbf{A}_{[ul]}$, the only non-vanishing informative terms are the cross-products between the dominant- and least-order terms, so in particular $\mathbf{I}_{n_{[u]}}\mathbf{B}_{[ul]}$ and $\mathbf{B}_{[uu]}\frac{1}{n}\mathbf{1}_{n_{[u]}}\mathbf{1}_{n_{[l]}}^\top$. While the former has entries (i, a) depending on both the class of \mathbf{x}_i and a , this is not true for the latter which does not depend on a . As a consequence, the (unlabeled) informative $\mathbf{B}_{[uu]}$ vanishes from the output and the unsupervised information is not used.

In order to remedy this situation, one must discard the dominant matrices of the type $\mathbf{1}_{n_{[u]}}\mathbf{1}_{n_{[l]}}^\top$ from the derivation. This term is the first order approximation of $\mathbf{K}_{[ul]}\mathbf{D}_{[l]}^{-1}$, and mainly unfolds from the *non-negativity constraint* of (the entries of) \mathbf{K} , which creates this large “bias”. From a purely mathematical standpoint, it stands to reason to remove this bias, for example by changing \mathbf{K} into $\hat{\mathbf{K}}$ with

$$\hat{\mathbf{K}} = \mathbf{P}\mathbf{K}\mathbf{P}, \quad \mathbf{P} = \mathbf{I}_n - \frac{1}{n}\mathbf{1}_n\mathbf{1}_n^\top \quad \text{eq:hatK} \quad (4.31)$$

which is then “orthogonal” to the bias vector $\mathbf{1}_n$. This is not so simple though, as this induces that $\mathbf{D} = \text{diag}(\hat{\mathbf{K}}\mathbf{1}_n) = \mathbf{0}$. Also, replacing \mathbf{K} by $\hat{\mathbf{K}}$ in the original optimization problem (4.23), now that $\hat{\mathbf{K}}$ has negative entries, and leads to an unbounded negative solution.

Adapted optimization framework. The proposed workaround in [Mai and Couillet, 2020] consists in starting from the optimization problem (4.23), replacing \mathbf{K} with $\hat{\mathbf{K}}$ (with thus $\alpha = 0$ since $d_i = 0$ for all i) and imposing an additional constraint on the Frobenius norm $\|\mathbf{S}\|_F$ to avoid the trivial unbounded negative solution.

The optimization framework reads

$$\begin{aligned} \hat{\mathbf{S}} &= \arg \min_{\hat{\mathbf{S}} \in \mathbb{R}^{n \times k}} \sum_{a=1}^k \sum_{i,j=1}^n [\hat{\mathbf{K}}]_{ij} \left([\hat{\mathbf{S}}]_{ia} - [\hat{\mathbf{S}}]_{ja} \right) \stackrel{\text{eq:SSL_optim_improved}}{=} (4.32) \\ \text{s.t. } &\begin{cases} \hat{\mathbf{S}}_{[l]} = \left(\mathbf{I}_{n_{[l]}} - \frac{1}{n_{[l]}} \mathbf{1}_{n_{[l]}} \mathbf{1}_{n_{[l]}}^\top \right) \mathbf{S}_{[l]}, \\ [\mathbf{S}]_{ia} = \delta_{\mathbf{x}_i \in \mathcal{C}_a} \text{ for labeled nodes,} \\ \|\hat{\mathbf{S}}_{[u]}\|_F^2 = n_{[u]} \gamma, \text{ for some } e > 0 \end{cases} \end{aligned}$$

the solution of which is explicitly given by

$$\hat{\mathbf{S}}_{[u]} = \left(\alpha \mathbf{I}_{n_{[u]}} - \hat{\mathbf{K}}_{[uu]} \right)^{-1} \hat{\mathbf{K}}_{[ul]} \stackrel{\text{eq:SSL_centered_solution}}{=} (4.33)$$

where α is the Lagrangian multiplier associated with the constraint $\|\hat{\mathbf{S}}_{[u]}\|_F^2 = n_{[u]} \gamma$ and satisfies $\alpha > \|\hat{\mathbf{K}}_{[uu]}\|$.

Performance analysis. The performance of the random matrix-improved semi-supervised learning approach in (4.33) is studied in [Mai and Couillet, 2020], under the simplified setting of $k = 2$ classes with $\mathbf{C}_1 = \mathbf{C}_2 \equiv \mathbf{C}$ and with the “one-hot” $\hat{\mathbf{S}} \in \mathbb{R}^{n \times k}$ replaced by the “sign” vector $\hat{\mathbf{s}} \in \mathbb{R}^n$ such that

$$\hat{\mathbf{s}}_{[l]} = \left(\mathbf{I}_{n_{[l]}} - \frac{1}{n_{[l]}} \mathbf{1}_{n_{[l]}} \mathbf{1}_{n_{[l]}}^\top \right) \mathbf{s}_{[l]}, \quad [\mathbf{s}]_i = (-1)^a \text{ for labeled node } \mathbf{x}_i \in \mathcal{C}_a. \stackrel{\text{eq: def-hat_s}}{=} (4.34)$$

The derivation of the asymptotic performance is more technically challenging as the resolvent $(\alpha \mathbf{I}_{n_{[u]}} - \hat{\mathbf{K}}_{[uu]})^{-1}$ no longer trivially expands around a leading (non-informative) matrix. For $\hat{\mathbf{K}} = \mathbf{PKP}$, in the notations of Corollary 4.1, it is easily seen that, the random equivalent $\tilde{\mathbf{PKP}}$ is of order $O_{\parallel \cdot \parallel}(1)$ which is the order of the informative terms. Therefore, $\tilde{\mathbf{PKP}}$ may be seen as a low rank perturbation of the (full rank) random matrix $-2f'(\tau_p) \frac{1}{p} \mathbf{PW}^\top \mathbf{WP}$, with known deterministic equivalents for its resolvent (e.g., Theorem 2.7).

This leads to the following performance asymptotics.

theo:SSL_centered

Theorem 4.9 ([Mai and Couillet, 2020]). Let $\hat{\mathbf{s}}_{[u]} = (\alpha \mathbf{I}_{n_{[u]}} - \hat{\mathbf{K}}_{[uu]})^{-1} \hat{\mathbf{K}}_{[ul]} \hat{\mathbf{s}}_{[l]}$ with $\hat{\mathbf{s}}_{[l]}$ defined in (4.34) such that $\|\hat{\mathbf{s}}_{[u]}\|^2 = n_{[u]}\gamma$. Then, for an unlabeled data point $\mathbf{x}_i \in \mathcal{C}_b$ with (a priori) probability $\mathbb{P}(\mathbf{x}_i \in \mathcal{C}_b) = c_b$, $b \in \{1, 2\}$,

$$[\hat{\mathbf{s}}]_i = g_i + o(1), \quad g_i \sim \mathcal{N}((-1)^b(1 - \rho_b)E, V)$$

with $E \equiv E(\xi)$ and $V \equiv V(\xi)$ for ξ the unique solution to $c_1 c_2 E(\xi)^2 + V(\xi) = e^2 = \gamma$ with positive functions $E(t)$ and $V(t)$ defined as

$$E(t) = \frac{2n_{[l]}\theta(t)}{n_{[u]}(1 - \theta(t))}, \quad V(t) = c_1 c_2 \frac{(2n_{[l]} + E(t)n_{[u]})^2 \zeta(t) + (4n_{[l]} + E(t)^2 n_{[u]})p\eta(t)}{n_{[u]}(n_{[u]} - p\eta(t))}$$

where $\Delta\boldsymbol{\mu} \equiv \boldsymbol{\mu}_1 - \boldsymbol{\mu}_2$ and

$$\begin{aligned} \theta(t) &= c_1 c_2 t \Delta\boldsymbol{\mu}^\top (\mathbf{I}_p - t\mathbf{C})^{-1} \Delta\boldsymbol{\mu}, \\ \eta(t) &= t^2 \operatorname{tr}(\mathbf{C}^2 (\mathbf{I}_p - t\mathbf{C})^{-2}) / p, \\ \zeta(t) &= c_1 c_2 t^2 \Delta\boldsymbol{\mu}^\top (\mathbf{I}_p - t\mathbf{C})^{-1} \mathbf{C} (\mathbf{I}_p - t\mathbf{C})^{-1} \Delta\boldsymbol{\mu}. \end{aligned}$$

The formulations of Theorem 4.9, not being explicit, are not immediate to interpret. In the proof of Theorem 4.9, it is shown that θ is of the order of $\|\mathbf{s}_{[u]}\|/\|\mathbf{s}_{[l]}\|$. As such, θ increases with the constraint $e > 0$, itself inversely proportional to the Lagrangian multiplier α . Consequently, raising $\alpha \rightarrow \infty$ brings $\theta \rightarrow 0$ and m/σ no longer depends on $n_{[u]}$: semi-supervised learning is merely a supervised learning. On the opposite, as $\alpha \downarrow \|\hat{\mathbf{K}}_{[uu]}\|$, $\theta \rightarrow \infty$ and now m/σ only depends on $n_{[u]}$: only unlabeled data are used, making the algorithm fully unsupervised. In fact, [Mai and Couillet, 2020] precisely shows that the limit $\alpha \downarrow \|\hat{\mathbf{K}}_{[uu]}\|$ perfectly recovers spectral clustering; this is not difficult to intuit: the resolvent $(\alpha \mathbf{I}_{n_{[u]}} - \hat{\mathbf{K}}_{[uu]})^{-1}$ is strongly dominated by the inverse of the projector $\mathbf{v}\mathbf{v}^\top$ with \mathbf{v} the eigenvector associated with the largest eigenvalue of $\hat{\mathbf{K}}_{[uu]}$, and thus $\hat{\mathbf{s}}_{[u]} \propto \mathbf{v}(\mathbf{v}^\top \hat{\mathbf{K}}_{[ul]} \hat{\mathbf{s}}_{[l]}) \propto \mathbf{v}$, i.e., this is a mere spectral clustering algorithm.

Theorem 4.9, despite taking a rather implicit form, suggests that:

- The classification accuracy is propositional to the ratio E^2/V with

$$\frac{E^2}{V} = \frac{1}{c_1 c_2} \frac{n_{[u]}(n_{[u]} - p\eta(t))E^2}{(2n_{[l]} + E(t)n_{[u]})^2 \zeta(t) + (4n_{[l]} + E(t)^2 n_{[u]})p\eta(t)} \quad (4.35)$$

which, for a well-chosen constraint $\gamma > 0$, is a monotonically increasing function of both $n_{[l]}$ and $n_{[u]}$. As such, the random matrix-improved semi-supervised learning approach is guaranteed to benefit from additional labeled and more importantly, unlabeled data, at least in the simple $\mathcal{N}(\boldsymbol{\mu}_1, \mathbf{C})$ versus $\mathcal{N}(\boldsymbol{\mu}_2, \mathbf{C})$ scenario.

- It can be shown that the quantity $\theta \equiv \theta(\xi) \in (0, 1)$ reflects how much the semi-supervised learning procedure relies on unlabeled data. Precisely, taking $\gamma \rightarrow 0$ leads to $\theta \rightarrow 0$ as well as $\alpha \rightarrow \infty$ and one retrieves (the

performance of) the classical normalized Laplacian approach discussed in Theorem 4.8 that is totally *supervised* in high dimensions; on the other hand, taking $\gamma \rightarrow \infty$ results in $\theta \rightarrow 1$ with $\alpha \downarrow \|\hat{\mathbf{K}}_{[uu]}\|$, and one obtains the same the performance as the *unsupervised* spectral clustering approach.⁷ As a result, tuning the constraint parameter γ allows one to find the best trade-off between the supervised and unsupervised learning schemes. This is confirmed in Figure 4.19 for fixed and varying values of $n_{[u]}$ and $n_{[l]}$.

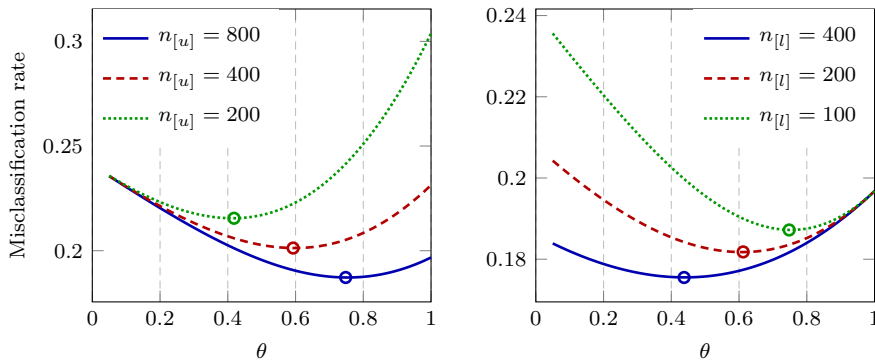


Figure 4.19: Asymptotic misclassification rate as a function of $\theta \equiv \theta(\xi)$ with $c_1 = c_2 = 1/2$, $p = 100$, $\Delta\mu = [2; \mathbf{0}_{p-1}]$, $[\mathbf{C}]_{i,j} = .1^{|i-j|}$. (**Left**): different $n_{[u]}$ with $n_{[l]} = 100$. (**Right**): different $n_{[l]}$ with $n_{[u]} = 800$. Minimal errors are marked in circles. [\[Link to code\]](#)

fig:SSL_theta

Figure 4.20, as already discussed in the previous section, shows that the random matrix-improved semi-supervised learning method significantly improves over the standard Laplacian method, overtaking both the semi-supervised Laplacian and the non-supervised spectral clustering.

Application to real-world datasets. One may wonder why the after-all quite simple solution proposed in [Mai and Couillet, 2020] has not appeared earlier in the literature. A first reason was mentioned previously: the fact that $\hat{\mathbf{K}}$ has negative entries, when placed in the optimization framework of (4.32) is counter-intuitive.

A second reason might follow from the actual output of simulations on real data. The bottom left display of Figure 4.21 compares the performances of the Laplacian versus RMT-improved Laplacian method for a increasing number of unlabeled data $n_{[u]}$: while the RMT-improved method *consistently* outperforms the standard Laplacian, the anticipated incapacity of the latter to use unlabeled data is not observed in practice. This is explained, in the top left display, by the

⁷Since the resolvent $(\alpha \mathbf{I}_{n_{[u]}} - \hat{\mathbf{K}}_{[uu]})^{-1} \simeq (\alpha - \lambda_{\max}(\hat{\mathbf{K}}_{[uu]}))^{-1} \mathbf{v} \mathbf{v}^T$ as $\alpha \downarrow \|\hat{\mathbf{K}}_{[uu]}\|$ with \mathbf{v} the eigenvector associated with the largest eigenvalue of $\hat{\mathbf{K}}_{[uu]}$, we have $\hat{\mathbf{s}}_{[u]} \propto \mathbf{v} (\mathbf{v}^T \hat{\mathbf{K}}_{[ul]} \hat{\mathbf{s}}_{[l]}) \propto \mathbf{v}$ and this is a mere spectral clustering algorithm.

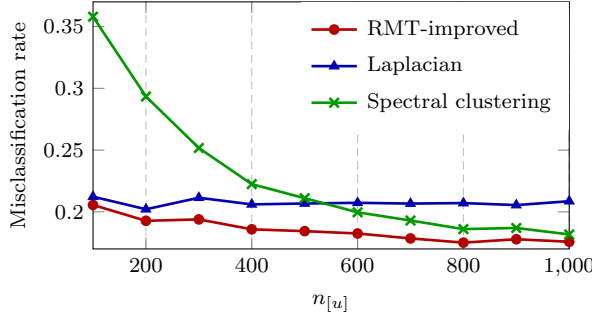


Figure 4.20: Empirical misclassification rate as a function of $n_{[u]}$ with $n_{[l]} = 200$, $p = 100$, $c_1 = c_2 = 1/2$, $\mathbf{x}_i \sim \mathcal{N}(\pm\boldsymbol{\mu}, \mathbf{I}_p)$ for $\boldsymbol{\mu} = [1; \mathbf{0}_{p-1}]$. $\alpha = \|\hat{\mathbf{K}}_{[uu]}\| + 1$ for RMT-improved and $\alpha = -1$ for classical Laplacian method. Gaussian kernel with $f(t) = \exp(-t/2)$. Results averaged over 50 runs. [\[Link to code\]](#) [\[Fig:SSL_comparisons\]](#)

slight but already too large average distance between intra- and inter-class data. Adding Gaussian white noise to the data (middle and right displays), the gap between intra- and inter-class distances vanishes and the performance gain of the RMT-improved method increases significantly, with the standard Laplacian now saturating for larger $n_{[u]}$.

Attempts to reduce the observed limitations of the Laplacian method had in fact been reported in the earlier literature, such as in [Zhou and Belkin, 2011], where an “iterated Laplacian” approach was devised. The basic idea is to replace the kernel matrix \mathbf{K} (or one of its Laplacians, e.g., $\mathbf{D}^{-1}\mathbf{K}$) by powers of the type \mathbf{K}^m : from a label propagation or graph random walk viewpoint, this consists in “iterating” m propagation steps at once, thereby partially avoiding the problem of uninformative direct neighbors. The performances of the iterated Laplacian approach, for a well-chosen m , in general outperform those of the standard Laplacian. Yet, from a purely theoretical standpoint, a random matrix analysis would also reveal that the problem of (asymptotic) uselessness of additional unlabeled data remains (although, for finite p, n , it might be “pushed” and appear only at larger values of $n_{[u]}$). In Table 4.2 and Table 4.3, comprehensive simulations are performed on two-class semi-supervised learning for the popular MNIST (from raw data) and then more advanced German Traffic Signs (from HOG features)⁸ datasets to compare the standard Laplacian, and its RMT-improved version, as well as the iterated Laplacian and its correspondingly RMT-improved equivalent. Performance of manifold-based semi-supervised learning are also reported. For fair comparison, the hyperparameters taken for all these simulations (the α parameter and the power m) are optimized in an oracle manner. For both MNIST and German Traffic Signs, the iterated RMT-improved method (which likely benefits from the ideas of [Zhou and Belkin, 2011]) outperforms all other methods.

⁸<http://benchmark.ini.rub.de/?section=gtsrb&subsection=dataset>.

These numerical evidences on real-world datasets again confirm the strong resilience of the large dimensional statistics approach to real data (or, at least, to some appropriate representation of these data).

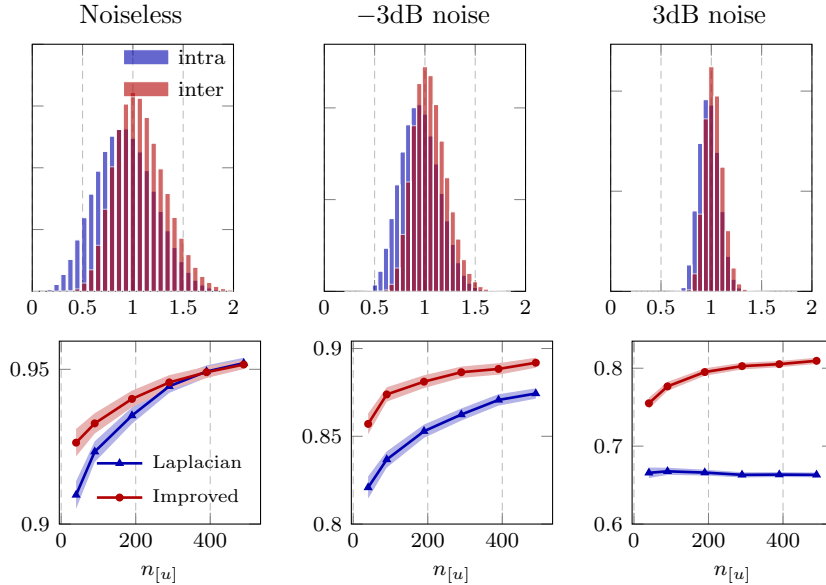


Figure 4.21: (**Top**) Histogram of normalized pairwise distances $\|\mathbf{x}_i - \mathbf{x}_j\|^2$, $i \neq j$ with additive white Gaussian noise of intra- and inter-class MNIST digits (8 versus 9). (**Bottom**) Average accuracy as a function of $n_{[u]}$ with $n_{[l]} = 10$, computed over 1 000 random realizations with 99% confidence intervals represented by shaded regions. [\[Link to code\]](#)

`fig:SSL_noisy_MNIST`

4.5.3 Application to kernel ridge regression

`sec:kernel-ridge`

We have discussed applications of kernel methods to unsupervised learning (kernel spectral clustering in Section 4.5.1) and semi-supervised learning (the graph-based approaches of Section 4.5.2). This section closes the investigation of kernel methods by considering now the most popular supervised learning scenario. The first natural method to supervised learning with kernels is kernel ridge regression, which can be used for both regression and classification purposes. In classification applications, it is also referred to as the least-squares support vector machine, or LS-SVM [Suykens and Vandewalle, 1999], and is considered as a computationally efficient alternative of the classical SVM method (to be discussed later in Chapter 6).

In a binary classification scenario, consider a training set $\{(\mathbf{x}_i, y_i)\}_{i=1}^n$ of size n with data $\mathbf{x}_i \in \mathbb{R}^p$ and labels $y_i = \pm 1$. We denote $\mathbf{x}_i \in \mathcal{C}_1$ if $y_i = -1$ and

Digits	(0, 8)	(2, 7)	(6, 9)
$n_{[u]} = 100$			
RMT-improved	89.5±3.6	89.5±3.4	85.3±5.9
Iterated RMT-improved	89.5±3.6	89.5±3.4	85.3±5.9
Laplacian	75.5±5.6	74.2±5.8	70.0±5.5
Iterated Laplacian	87.2±4.7	86.0±5.2	81.4±6.8
Manifold	88.0±4.7	88.4±3.9	82.8±6.5
$n_{[u]} = 1000$			
RMT-improved	92.2±0.9	92.5±0.8	92.6±1.6
Iterated RMT-improved	92.3±0.9	92.5±0.8	92.9±1.4
Laplacian	65.6±4.1	74.4±4.0	69.5±3.7
Iterated Laplacian	92.2±0.9	92.4±0.9	92.0±1.6
Manifold	91.1±1.7	91.4±1.9	91.4±2.0

Table 4.2: Classification accuracy on MNIST datasets with $n_{[l]} = 10$. Results obtained from 1 000 runs for $n_{[u]} = 100$ and $n_{[u]} = 1 000$. tab:SSL_MNIST

Class ID	(2, 7)	(9, 10)	(11, 18)
$n_{[u]} = 100$			
RMT-improved	79.0±10.4	77.5±9.2	78.5±7.1
Iterated RMT-improved	85.3±5.9	89.2±5.6	90.1±6.7
Laplacian	73.8±9.8	77.3±9.5	78.6±7.2
Iterated Laplacian	83.7±7.2	88.0±6.8	87.1±8.8
Manifold	77.6±8.9	81.4±10.4	82.3±10.8
$n_{[u]} = 1000$			
RMT-improved	83.6±2.4	84.6±2.4	88.7±9.4
Iterated RMT-improved	84.8±3.8	88.0±5.5	96.4±3.0
Laplacian	72.7±4.2	88.9±5.7	95.8±3.2
Iterated Laplacian	83.0±5.5	88.2±6.0	92.7±6.1
Manifold	77.7±5.8	85.0±9.0	90.6±8.1

Table 4.3: Classification accuracy on HOG features of German Traffic Sign datasets with $n_{[l]} = 10$. Results obtained from 1 000 random runs for $n_{[u]} = 100$ and $n_{[u]} = 1 000$. tab:SSL_traffic_signs

$\mathbf{x}_i \in \mathcal{C}_2$ if $y_i = +1$. The objective of LS-SVM is to devise a decision function

$$g(\mathbf{x}) = \mathbf{w}^\top \phi(\mathbf{x}_i) + b \quad (4.36)$$

that ideally maps all the (features $\phi(\mathbf{x}_i)$ of the) training data \mathbf{x}_i to the corresponding y_i , and subsequently an unknown test datum \mathbf{x} to its corresponding y

value, by solving the following optimization problem

$$\begin{aligned} \arg \min_{\mathbf{w}, b} \quad & \|\mathbf{w}\|^2 + \frac{\gamma}{n} \sum_{i=1}^n e_i^2 && \text{eq:LS-SVM-origin (4.37)} \\ \text{s.t.} \quad & y_i = \mathbf{w}^\top \phi(\mathbf{x}_i) + b + e_i, \quad i = 1, \dots, n \end{aligned}$$

for some penalty factor $\gamma > 0$ that weights the structural risk $\|\mathbf{w}\|^2$ against the empirical risk $\frac{1}{n} \sum_{i=1}^n e_i^2$.

By introducing the Lagrange multipliers $\{\alpha_i\}_{i=1}^n$, the solution to (4.37) can be expressed as $\mathbf{w} = \sum_{i=1}^n \alpha_i \phi(\mathbf{x}_i)$, where

$$\begin{cases} \boldsymbol{\alpha} &= \mathbf{Q} \left(\mathbf{I}_n - \frac{\mathbf{1}_n \mathbf{1}_n^\top \mathbf{Q}}{\mathbf{1}_n^\top \mathbf{Q} \mathbf{1}_n} \right) \mathbf{y} \\ b &= \frac{\mathbf{1}_n^\top \mathbf{Q} \mathbf{y}}{\mathbf{1}_n^\top \mathbf{Q} \mathbf{1}_n} \end{cases} \quad \text{eq:LS-SVM-solution (4.38)}$$

for $\mathbf{y} = [y_1, \dots, y_n]^\top$, $\mathbf{Q} \equiv (\mathbf{K} + \frac{n}{\gamma} \mathbf{I}_n)^{-1}$ and $\mathbf{K} \equiv \{\phi(\mathbf{x}_i)^\top \phi(\mathbf{x}_j)\}_{i,j=1}^n$ the kernel matrix from training data, which is assumed to take the following form

$$\mathbf{K} = \{f(\|\mathbf{x}_i - \mathbf{x}_j\|^2/p)\}_{i,j=1}^n$$

for some smooth function f .

Given $\boldsymbol{\alpha}$ and b , a new datum \mathbf{x} is then classified into class \mathcal{C}_1 or \mathcal{C}_2 depending on the value of the following decision function

$$g(\mathbf{x}) = \boldsymbol{\alpha}^\top \mathbf{k}(\mathbf{x}) + b, \quad \mathbf{k}(\mathbf{x}) \equiv \{f(\|\mathbf{x} - \mathbf{x}_i\|^2/p)\}_{i=1}^n. \quad \text{eq:LS-SVM-g(x) (4.39)}$$

One of the most popular choices is to use the sign of $g(\mathbf{x})$, and assign \mathbf{x} to class \mathcal{C}_1 if $g(\mathbf{x}) < 0$ and to class \mathcal{C}_2 otherwise. As we shall see, this decision criterion can be highly biased in some cases, when large dimensional data are considered.

Thanks to the ‘‘kernel trick’’, the decision function $g(\mathbf{x})$ no longer needs the evaluation of $\phi(\cdot)$, and can be fully expressed through the kernel function $(\mathbf{x}_i, \mathbf{x}_j) \mapsto f(\|\mathbf{x}_i - \mathbf{x}_j\|^2/p)$, that is indirectly related to $\phi(\cdot)$ through $\phi(\mathbf{x}_i)^\top \phi(\mathbf{x}_j) = f(\|\mathbf{x}_i - \mathbf{x}_j\|^2/p)$. Yet, to allow for a much larger range of functions $f(\cdot)$ (in particular functions f which do not necessarily arise from a feature mapping $\phi(\cdot)$), in the remainder of this section, we shall allow for arbitrary f with a minimalist set of constraints. We shall in particular observe that some functions f , not positive definite and thus not necessarily deriving from a feature map ϕ , prove extremely powerful in some specific scenarios.

4.5.3.1 Large dimensional performance analysis and its implications

As in the previous sections on unsupervised or semi-supervised classification methods, we place ourselves under the following ‘‘non-trivial’’ Gaussian mixture model

$$\mathbf{x}_i \in \mathcal{C}_a \Leftrightarrow \mathbf{x}_i \sim \mathcal{N}(\boldsymbol{\mu}_a, \mathbf{C}_a), \quad a = 1, 2$$

for $\boldsymbol{\mu}_a \in \mathbb{R}^p$ and $\mathbf{C}_a \in \mathbb{R}^{p \times p}$ such that $\|\mathbf{C}_a\| = O(1)$ and

$$\|\boldsymbol{\mu}_1 - \boldsymbol{\mu}_2\| = O(1), \quad \text{tr}(\mathbf{C}_1 - \mathbf{C}_2) = O(\sqrt{p}), \quad \text{tr}(\mathbf{C}_1 - \mathbf{C}_2)^2 \stackrel{\text{eq:growth-rate-LS-SVM}}{=} O(p). \quad (4.40)$$

We assume a training set of n_1 samples in class \mathcal{C}_1 and n_2 samples in class \mathcal{C}_2 so that $n_1 + n_2 = n$, and that n_1, n_2 and p grow at the same rate (i.e., p/n_a remains away from 0 and ∞ in the large n, p limit). We recall from previous sections on kernel methods that, letting $\tau_p = \frac{2}{p} \text{tr } \mathbf{C}^\circ$ with $\mathbf{C}^\circ = \frac{n_1}{n} \mathbf{C}_1 + \frac{n_2}{n} \mathbf{C}_2$, these non-trivial growth rate conditions ensure that

$$\max_{i,j} \{[\mathbf{K}]_{ij} - \tau_p\} \xrightarrow{a.s.} 0. \quad (4.41)$$

As such, the kernel matrix is dominated by the rank-one matrix $f(\tau_p) \mathbf{1}_n \mathbf{1}_n^\top$, which is of operator norm order $O(n)$, and thus of the same of order as $\frac{n}{\gamma} \mathbf{I}_n$ for $\gamma = O(1)$.

As a result, with the (asymptotic) Taylor expansion of the kernel matrix \mathbf{K} derived in Theorem 4.1, it is possible to similarly “linearize” the resolvent $\mathbf{Q} \equiv \left(\mathbf{K} + \frac{n}{\gamma} \mathbf{I}_n\right)^{-1}$ with a Taylor expansion around the leading $f(\tau_p) \mathbf{1}_n \mathbf{1}_n^\top + \frac{n}{\gamma} \mathbf{I}_n$ term. Since the decision function $g(\mathbf{x})$ depends on $\boldsymbol{\alpha}$ and b , that both depend explicitly on \mathbf{Q} , we can then work out an asymptotic linearization of $g(\mathbf{x})$. An asymptotic expression of the misclassification rate of LS-SVM then unfolds, which is a function of the local behavior of kernel function f around τ_p , as well as the data statistics $\boldsymbol{\mu}_1, \boldsymbol{\mu}_2, \mathbf{C}_1, \mathbf{C}_2$. This result is detailed in the following theorem.

theo:LS-SVM

Theorem 4.10 ([Liao and Couillet, 2019b, Theorem 2]). *Under the non-trivial Gaussian mixture model in (4.40), we have, for $g(\mathbf{x})$ defined in (4.39),*

$$V_a^{-\frac{1}{2}}(g(\mathbf{x}) - E_a) \xrightarrow{d} \mathcal{N}(0, 1), \quad a \in \{1, 2\}$$

for

$$E_a = c_2 - c_1 + \frac{2}{p}(-1)^a(1 - c_a)\gamma c_1 c_2 \mathcal{D}, \quad V_a = \frac{8}{p^2}\gamma^2 c_1^2 c_2^2 \mathcal{V}_a$$

where $c_a = n_a/n$ and

$$\begin{aligned} \mathcal{D} &= -2f'(\tau_p)\|\Delta\boldsymbol{\mu}\|^2 + \frac{f''(\tau_p)}{p} (\text{tr}^2 \Delta\mathbf{C} + 2 \text{tr}(\Delta\mathbf{C}^2)) \\ \mathcal{V}_a &= \frac{(f''(\tau_p))^2}{p^2} \text{tr}^2 \Delta\mathbf{C} \cdot \text{tr}(\mathbf{C}_a^2) + 2(f'(\tau_p))^2 \left(\Delta\boldsymbol{\mu}^\top \mathbf{C}_a \Delta\boldsymbol{\mu} + \frac{1}{n} \text{tr} \mathbf{C}_a \left(\frac{\mathbf{C}_1}{c_1} + \frac{\mathbf{C}_2}{c_2} \right) \right) \end{aligned}$$

in which we denoted $\Delta\boldsymbol{\mu} \equiv \boldsymbol{\mu}_1 - \boldsymbol{\mu}_2$ and $\Delta\mathbf{C} \equiv \mathbf{C}_1 - \mathbf{C}_2$.

An immediate remark from Theorem 4.10 is that, since under the setting of (4.40) both \mathcal{D} and \mathcal{V}_a are of order $O(1)$, the decision function is of order $g(\mathbf{x}) = c_2 - c_1 + O(n^{-1})$. This result contradicts the classical “sign-based”

decision criterion, by which the decision threshold ξ equals zero, i.e., the new datum \mathbf{x} is assigned to \mathcal{C}_1 if $g(\mathbf{x}) < \xi = 0$ and to \mathcal{C}_2 otherwise. When $c_1 - c_2 \neq 0$ (in unbalanced classification scenarios), this would lead to an asymptotic classification of all new data into one of the two classes. Two options to alleviate this issue are;

1. taking the decision threshold ξ , instead of $\xi = 0$ in the sign-based criterion, to be $\xi = \xi_n = c_2 - c_1 + O(n^{-1})$;
2. normalizing the labels $y_i \in \{-1, +1\}$ as $y_i^* \in \{-n/n_1, +n/n_2\}$, while maintaining the decision threshold to $\xi = 0$ (or technically speaking $O(n^{-1})$). This is also referred to as the Fisher's targets in the context of kernel Fisher discriminant analysis [Mika et al., 1999]. It can be shown that, when trained with y_i^* , the associated decision function satisfies $g^*(\mathbf{x}) = 0 + O(n^{-1})$.

As a corollary of Theorem 4.10, the asymptotic misclassification rate is a function of the decision threshold ξ_n , the local behavior of kernel function f , the dimensions p, n_1, n_2 as well as the data statistics $\mu_1, \mu_2, \mathbf{C}_1, \mathbf{C}_2$.
coro: classif-error

Corollary 4.2 (Asymptotic misclassification error rate). *Under the setting of Theorem 4.10, for a decision threshold ξ_n that may depend on n , as $n \rightarrow \infty$,*

$$\begin{aligned} \mathbb{P}(g(\mathbf{x}) > \xi_n \mid \mathbf{x} \in \mathcal{C}_1) - Q\left(\frac{\xi_n - E_1}{\sqrt{V_1}}\right) &\xrightarrow{a.s.} 0 \\ \mathbb{P}(g(\mathbf{x}) < \xi_n \mid \mathbf{x} \in \mathcal{C}_2) - Q\left(\frac{E_2 - \xi_n}{\sqrt{V_2}}\right) &\xrightarrow{a.s.} 0 \end{aligned}$$

for E_a and V_a given in Theorem 4.10 and $Q(x) = \frac{1}{\sqrt{2\pi}} \int_x^\infty \exp(-t^2/2) dt$.

Interestingly, Corollary 4.2 implies that, if one takes $\xi_n = c_2 - c_1 = \frac{n_2}{n} - \frac{n_1}{n}$, the asymptotic classification error is independent of the regularization parameter γ . It is however worth noting that this remark is only valid for $\gamma = O(1)$, i.e., γ is considered to remain a constant as $n, p \rightarrow \infty$, and the threshold is taken to be exactly $c_2 - c_1$.

Remark 4.9 (On non-trivial γ choices). *Since \mathbf{K} is dominated by $f(\tau_p)\mathbf{1}_n\mathbf{1}_n^\top$, taking $\gamma = O(1)$ is a mandatory choice to avoid the asymptotic singularity of the resolvent $\mathbf{Q} = (\mathbf{K} + \frac{n}{\gamma}\mathbf{I}_n)^{-1}$. An alternative approach may consist in working with \mathbf{PKP} for $\mathbf{P} = \mathbf{I}_n - \frac{1}{n}\mathbf{1}_n\mathbf{1}_n^\top$ instead of \mathbf{K} (as in [Elkhalil et al., 2020b]), thereby discarding the dominant (and non-informative) matrix $f(\tau_p)\mathbf{1}_n\mathbf{1}_n^\top$ and allowing for γ to be chosen of order $\gamma = O(n)$. In this case, its specific choice would have a nontrivial impact on the classification performance, as in the case of semi-supervised learning in Section 4.5.2. We do not further elaborate on this setting as this moves us rather far from the conventional LS-SVM formulation.*

Due to the concentration of Euclidean distances in large dimensions, the performance of LS-SVM depends on the kernel function f solely via its successive derivatives at τ_p (which, as recalled from Remark 4.4, can be consistently estimated from the data). More discussions on the choice of f are in order.

1. Note that with $f'(\tau_p) = 0$, the difference in statistical means $\Delta\mu$ vanishes from the expressions of \mathcal{D} and \mathcal{V}_a in Theorem 4.10 and the classification can only be performed based on the covariance structures. In this situation, rather surprisingly, if one further assumes $\text{tr}(\mathbf{C}_1 - \mathbf{C}_2) = \text{tr} \Delta \mathbf{C} = o(\sqrt{p})$ (which is below the minimum “distance” $\text{tr} \Delta \mathbf{C} = O(\sqrt{p})$ in (4.40)), then $\mathcal{D} = 2f''(\tau_p) \text{tr}(\Delta \mathbf{C}^2)/p + o(1)$ and $\mathcal{V}_a = o(1)$ so that with, say $\text{tr}(\Delta \mathbf{C}^2) = O(p)$, perfect classification can be achieved. This remark is of particular interest for example when data in different classes are of zero mean, unit Euclidean norm and thus have indistinguishable $\mathbb{E}[\|\mathbf{x}\|^2] = \text{tr} \mathbf{C}_a$. In this case, the covariance “shape” information can be better exploited with the family of kernels such that $f'(\tau_p) = 0$. Figure 4.22 compares the empirical classification error rate for $p = 512$ and $p = 1024$ to the theoretical asymptotic error predicted in Corollary 4.2, and confirms, when $\text{tr} \Delta \mathbf{C} = 0$, the rapid drop of classification error (which ultimately vanishes) as $f'(\tau_p)$ gets close to zero.
2. Since $|E_1 - E_2|$ is proportional to \mathcal{D} and should, for fixed V_a (which does not depend on the signs of $f'(\tau_p)$ and $f''(\tau_p)$), be made as large as possible to achieve optimal classification performance, the kernel function must satisfy $f'(\tau_p) < 0$ and $f''(\tau_p) > 0$. Incidentally, this condition is naturally satisfied by the popular Gaussian kernel $f(x) = \exp(-x/\sigma^2)$ for any σ , but this is not always the case of polynomial kernels.
3. When the difference in statistical means $\|\Delta\mu\|$ is largely dominant over the difference in covariances $\text{tr}^2 \Delta \mathbf{C}/p$ and $\text{tr}(\Delta \mathbf{C}^2)/p$, from Theorem 4.10, both $E_a - (c_2 - c_1)$ and $\sqrt{V_a}$ are approximately proportionally to $f'(\tau_p)$, making the choice of the kernel function eventually irrelevant in this case, so long that $f'(\tau_p) \neq 0$.

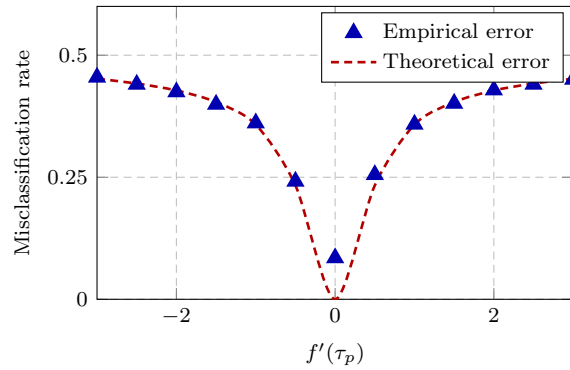


Figure 4.22: Classification error of LS-SVM, $p = 512$, $n = 2048$, $c_1 = c_2 = 1/2$, $\gamma = 1$, second order polynomial kernel with $f(\tau_p) = 4$ and $f''(\tau_p) = 2$. For Gaussian data $\mathbf{x} \sim \mathcal{N}(\mathbf{0}, \mathbf{C}_a)$ with $\mathbf{C}_1 = \mathbf{I}_p$ and $[\mathbf{C}_2]_{ij} = .4^{|i-j|}$. Empirical results averaged over 30 runs. [Link to code] fig:LS-SVM-perf-f' (tau)=0

4.5.3.2 Application to real-world data

Although derived from a simple Gaussian mixture model, the previous theoretical results, when applied to popular large dimensional real-world datasets, again show a (at first unexpected) similar behavior. Figure 4.23 considers the classification of (two from the ten classes of) MNIST and Fashion-MNIST data. Despite the obvious non-Gaussianity as well as the clearly different natures of the data (from the two datasets), the empirical histogram of the decision function $g(\mathbf{x})$ always behaves surprisingly close to its limiting behavior predicted by Theorem 4.10.

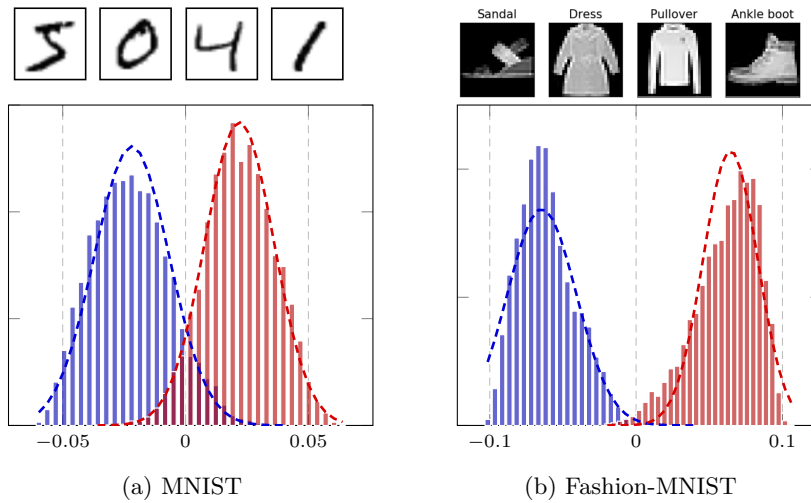


Figure 4.23: Empirical histogram of $g(\mathbf{x})$ versus the Gaussian limiting behavior predicted in Theorem 4.10, $n = 2048$, $p = 784$, $\gamma = 1$ with Gaussian kernel, for MINST (left, 7 versus 9) and Fashion-MNIST (right, 8 versus 9) data. Results averaged over 20 runs. [Link to code] fig:LS-SVM-gaussian-MNIST

In Figure 4.24, the classification error rate is displayed as a function of the decision threshold ξ , again for both MNIST and Fashion-MNIST data. The conclusion that the optimal decision threshold should approximately be $c_2 - c_1$ rather than 0 is conclusively observed to hold true in both cases.

4.5.4 Summary of Section 4.5

Consistent estimation of data statistics, choice of kernel function

4.6 Concluding remarks

Before the present chapter, the first part of the monograph was mostly concerned with the sample covariance matrix model \mathbf{XX}^T/n (as well more marginally as

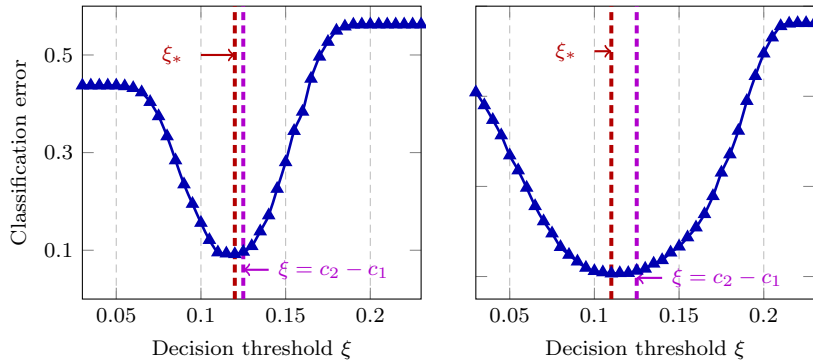


Figure 4.24: Classification error rate as a function of decision threshold ξ , with $n = 512, p = 784, c_2 - c_1 = 1/8$ in **purple**, $\gamma = 1$, Gaussian kernel for MNIST (**left**) and Fashion-MNIST data (**right**). With empirical optimal decision thresholds $\xi_* = 0.12$ (**left**) and 0.11 (**right**) in **red**. [Link to code]

on the Wigner model \mathbf{X}/\sqrt{n} for symmetrical \mathbf{X}), where the columns of \mathbf{X} are independent and the entries of each column are independent or linearly dependent. Historically, this model and its numerous variants (with a variance profile, with right-side correlation, summed up to other independent matrices of the same form, etc.) have covered most of the mathematical and applied interest of the first two decades (since the early nineties) of intense random matrix advances. The main drivers for these early developments were statistics, signal processing, and wireless communications. The present chapter leaped much further in considering now random matrix models with possibly highly correlated entries, with a specific focus on kernel matrices: for the first time, the machine learning applications clearly steered mathematical research towards these models. The main reason lies in the poor understanding and tractability of kernel matrices in finite dimensional settings: where only (as we saw, sometimes wrong) intuitions and heuristics were available, random matrix theory now provides accurate (and asymptotically exact) performance assessment along with the possibility to largely improve the performances of kernel-based machine learning methods. This, in effect, creates a small revolution (not to the extent of the deep learning revolution though) in our understanding of machine learning on realistic large datasets.

A first important finding of the analysis of large dimensional kernel statistics reported here is the ubiquitous character of the Marčenko-Pastur and the semi-circular laws. As a matter of fact, all random matrix models studied in this chapter, and in particular the kernel regimes $f(\mathbf{x}_i^\top \mathbf{x}_j/p)$ (which concentrate around $f(0)$) and $f(\mathbf{x}_i^\top \mathbf{x}_j/\sqrt{p})$ (which tends to $f(\mathcal{N}(0, 1))$), have a limiting eigenvalue distribution akin to a combination of the two laws. This combination may vary from case to case (compare for instance the results of Exercise 3 to Theorem 4.4), but is often parametrized in a such way that the Marčenko-Pastur

and semi-circle laws appear as limiting cases (in the context of Exercise 3, they correspond to the limiting cases of dense versus sparse kernels, and in Theorem 4.4 to the limiting cases of linear versus “purely” nonlinear kernels).

A second point of importance, worth recalling, is the range of valid kernels analyzed: for the “natural” scaling $1/p$ (so kernels of the type $f(\mathbf{x}_i^\top \mathbf{x}_j/p)$ or $f(\|\mathbf{x}_i - \mathbf{x}_j\|^2/p)$), all kernel functions $f(t)$ are equivalent so long that they are differentiable and have the same first three derivatives at the concentration point $t = 0$ (for inner-product) or τ_p (for distance kernels); for the “proper” scaling $1/\sqrt{p}$ (so kernels of the form $f(\mathbf{x}_i^\top \mathbf{x}_j/\sqrt{p})$ or $f(\sqrt{p}[\|\mathbf{x}_i - \mathbf{x}_j\|^2/p - \tau_p])$), kernel functions f are equivalent if they share in common three specific Gaussian moments (i.e., $\int P(t)f(t)\mu(dt)$ for μ the Gaussian measure). As such, while it is not necessarily surprising to see the naturally scaling kernels being equivalent if they have similar behavior near the concentration point, it is quite surprising at first that properly scaling kernel functions f , which “see” values in the whole real axis, do not offer more flexibility or diversity. For both types of kernels, only the first elementary moments of the data are accounted for. The main difference between naturally and properly scaling kernels though, is the possibility of the latter to study very discontinuous kernel functions, such as the sign (or more generally quantization) and thresholding functions: this finds a broad range of applications in low-cost kernel techniques. On this aspect, Chapter 5 recalls the intimate connection between neural networks, random projections, and their limiting kernels: a direct connection can be established between sparsification techniques in neural networks (such as the popular random or deterministic dropout procedure) and sparsification techniques in kernel methods. The present chapter may then provide some keys to understanding and improving computationally constrained methods in the performance-complexity tradeoff of methods beyond kernels.

This being said, the analysis of kernel methods is far from over. Many kernel matrices remain out of analytical reach by the current random matrix machinery. This is in particular the case of “rank correlation” (also referred to as U-statistics) matrices, such as Spearman- ρ [Spearman, 1987] or Kendall- τ [Kendall, 1938]. For data vectors $\mathbf{x}_1, \dots, \mathbf{x}_n \in \mathbb{R}^p$, the entry \mathbf{K}_{ij} of a rank correlation matrix \mathbf{K} evaluates a function on the *ranks* of the entries $[\mathbf{x}_i]_1, \dots, [\mathbf{x}_i]_p$ and $[\mathbf{x}_j]_1, \dots, [\mathbf{x}_j]_p$ of \mathbf{x}_i and \mathbf{x}_j . For Kendall- τ , \mathbf{K}_{ij} evaluates the number of pairs $[\mathbf{x}_i]_a, [\mathbf{x}_i]_b$ such that $\text{sign}([\mathbf{x}_i]_a - [\mathbf{x}_i]_b) = \text{sign}([\mathbf{x}_j]_a - [\mathbf{x}_j]_b)$. As for Spearman- ρ , \mathbf{K}_{ij} evaluates the empirical correlation between the ranks $\text{rg}([\mathbf{x}_i]_a)$ and $\text{rg}([\mathbf{x}_j]_a)$, for $a = 1, \dots, p$. For these kernels, the rank variables create correlations between the entries of the data matrix \mathbf{X} which prevent classical random matrix tools to immediately apply. The problem was worked around in [Bandeira et al., 2017] for \mathbf{X} having fully i.i.d. entries, exploiting there the very fact that the i.i.d. nature of variables induces an i.i.d. distribution of the ranks. The generalization to non-i.i.d. random variables would however fail in general.

Another important family of difficult-to-grasp kernels is that of k-nearest neighbor (kNN) kernels [Fix and Hodges, 1951]. These kernel matrices \mathbf{K} are such that \mathbf{K}_{ij} is only nonzero if \mathbf{x}_j is one of the k-nearest neighbors of \mathbf{x}_i , among

$\mathbf{x}_1, \dots, \mathbf{x}_n$ in the sense of a given metric (typically of the Euclidean distance). The induced dependence between the entries of such matrices is more subtle to grasp, leaving for the moment the study of these kernels, widely used in machine learning applications largely open.

4.7 Practical course material

Zhenyu: TDB

ex:complexity-perf-tradeoff

Practical Lecture Material 3 (Complexity-performance trade-off in spectral clustering with sparse kernel). *In this exercise, we study the spectrum of a “punctured” version $\mathbf{S} = \mathbf{K} \odot \mathbf{B}$ (with $[\mathbf{A} \odot \mathbf{B}]_{ij} = A_{ij}B_{ij}$) of a kernel matrix $\mathbf{K} = \frac{1}{n}\mathbf{X}^T\mathbf{X}$, for $\mathbf{X} \in \mathbb{R}^{p \times n}$ with a symmetric random mask-matrix $\mathbf{B} \in \{0, 1\}^{n \times n}$ with independent $B_{ij} \sim \text{Bern}(\varepsilon)$ entries for $i \neq j$ and $B_{ii} = b$ fixed (i.e., $b = 0$ or $b = 1$) in the limit $p, n \rightarrow \infty$ with $p/n \rightarrow c \in (0, \infty)$, thereby mimicking the behavior of a computation of only a proportion ε of the entries of \mathbf{K} . Letting $\mathbf{X} = [\mathbf{X}_0, \mathbf{X}_1]$ follow a two-class setting with $\mathbf{X}_\ell = (-1)^\ell \boldsymbol{\mu} \mathbf{1}_{n/2}^\top + \mathbf{Z}_\ell \in \mathbb{R}^{p \times \frac{n}{2}}$ for $\boldsymbol{\mu} \in \mathbb{R}^p$ of fixed norm $\|\boldsymbol{\mu}\| = \mu$ (with respect to p, n), the idea is to study the effect of \mathbf{B} on the presence of an isolated spike in the spectrum of \mathbf{S} and thus on the spectral clustering performance of data in class 0 and 1.*

We will study the spectrum of \mathbf{S} using Stein’s lemma and the Gaussian tools. Letting $\mathbf{Z} = [\mathbf{Z}_0, \mathbf{Z}_1]$ and $\mathbf{M} = \boldsymbol{\mu} \mathbf{j}^\top$, where $\mathbf{j} = [\mathbf{1}_{\frac{n}{2}}^\top, -\mathbf{1}_{\frac{n}{2}}^\top]^\top$, first show that, for $\mathbf{Q} \equiv \mathbf{Q}(z) = (\mathbf{S} - z\mathbf{I}_n)^{-1}$,

$$\begin{aligned} \mathbf{Q} &= -\frac{1}{z}\mathbf{I}_n + \frac{1}{z} \left(\frac{\mathbf{Z}^\top \mathbf{Z}}{n} \odot \mathbf{B} \right) \mathbf{Q} + \frac{1}{z} \left(\frac{\mathbf{Z}^\top \mathbf{M}}{n} \odot \mathbf{B} \right) \mathbf{Q} \\ &\quad + \frac{1}{z} \left(\frac{\mathbf{M}^\top \mathbf{Z}}{n} \odot \mathbf{B} \right) \mathbf{Q} + \frac{1}{z} \left(\frac{\mathbf{M}^\top \mathbf{M}}{n} \odot \mathbf{B} \right) \mathbf{Q}. \end{aligned}$$

To proceed, we shall need to go slightly beyond the study of these four terms. Specifically, using Stein’s lemma, show that, for an arbitrary matrix \mathbf{A} of bounded norm,

$$\begin{aligned} \mathbb{E} \left[\left[\left(\frac{\mathbf{Z}^\top \mathbf{Z}}{n} \odot \mathbf{A} \right) \mathbf{Q} \right]_{ij} \right] &= \frac{p}{n} \mathbf{A}_{ii} \mathbb{E}[\mathbf{Q}_{ij}] - \mathbb{E} \left[\frac{1}{n} \text{tr} \left(\mathbf{Q} \mathbf{D}_{\mathbf{b}_i} \frac{\mathbf{Z}^\top \mathbf{Z}}{n} \mathbf{D}_{\bar{\mathbf{a}}_i} \right) \mathbf{Q}_{ij} \right] \\ &\quad - \mathbb{E} \left[\frac{1}{n} \text{tr} \left(\mathbf{Q} \mathbf{D}_{\mathbf{b}_i} \frac{\mathbf{M}^\top \mathbf{Z}}{n} \mathbf{D}_{\bar{\mathbf{a}}_i} \right) \mathbf{Q}_{ij} \right] \\ \mathbb{E} \left[\left[\left(\frac{\mathbf{Z}^\top \mathbf{M}}{n} \odot \mathbf{A} \right) \mathbf{Q} \right]_{ij} \right] &= -\mathbb{E} \left[\frac{1}{n} \text{tr} \left(\mathbf{Q} \mathbf{D}_{\mathbf{b}_i} \frac{\mathbf{Z}^\top \mathbf{M}}{n} \mathbf{D}_{\bar{\mathbf{a}}_i} \right) \mathbf{Q}_{ij} \right] \\ &\quad - \mathbb{E} \left[\frac{1}{n} \text{tr} \left(\mathbf{Q} \mathbf{D}_{\mathbf{b}_i} \frac{\mathbf{M}^\top \mathbf{M}}{n} \mathbf{D}_{\bar{\mathbf{a}}_i} \right) \mathbf{Q}_{ij} \right] \\ \mathbb{E} \left[\left[\left(\frac{\mathbf{M}^\top \mathbf{Z}}{n} \odot \mathbf{A} \right) \mathbf{Q} \right]_{ij} \right] &= -\mathbb{E} \left[\left[\frac{\mathbf{M}^\top \mathbf{Z}}{n} \mathcal{D}_{\mathbf{A}, \mathbf{B}}^{(i)} \mathbf{Q} \right]_{ij} \right] - \mathbb{E} \left[\left[\frac{\mathbf{M}^\top \mathbf{M}}{n} \mathcal{D}_{\mathbf{A}, \mathbf{B}}^{(i)} \mathbf{Q} \right]_{ij} \right] \end{aligned}$$

where

$$\begin{aligned}\mathcal{D}_{\mathbf{A}, \mathbf{B}}^{(i)} &= \begin{bmatrix} \frac{1}{n} \operatorname{tr} \mathbf{Q} \mathbf{D}_{\bar{\mathbf{a}}_i} \mathbf{D}_{\mathbf{b}_1} \\ \ddots \\ \frac{1}{n} \operatorname{tr} \mathbf{Q} \mathbf{D}_{\bar{\mathbf{a}}_i} \mathbf{D}_{\mathbf{b}_n} \end{bmatrix} \\ &= \begin{bmatrix} \frac{1}{n} \operatorname{tr} (\mathbf{Q} \odot \bar{\mathbf{a}}_i \mathbf{b}_1^\top) \\ \ddots \\ \frac{1}{n} \operatorname{tr} (\mathbf{Q} \odot \bar{\mathbf{a}}_i \mathbf{b}_n^\top) \end{bmatrix}\end{aligned}$$

and \mathbf{b}_i is the i -th column of \mathbf{B} , while $\bar{\mathbf{a}}_i$ the i -th (transposed) row of \mathbf{A} , and conclude that

$$\begin{aligned}\mathbb{E}[\mathbf{Q}_{ij}] &\simeq -\frac{1}{z} \delta_{ij} + \frac{1}{z} \left[\frac{p}{n} \mathbf{B}_{ii} - \frac{1}{n} \operatorname{tr} \left(\mathbf{Q} \mathbf{D}_{b_i} \frac{1}{n} (\mathbf{Z} + \mathbf{M})^\top (\mathbf{Z} + \mathbf{M}) \mathbf{D}_{\bar{\mathbf{b}}_i} \right) \right] \mathbb{E}[\mathbf{Q}_{ij}] \\ &\quad + \frac{1}{z} \left[\left(\frac{\mathbf{M}^\top \mathbf{M}}{n} \odot \mathbf{B} \right) \mathbf{Q} \right]_{ij} - \frac{1}{z} \mathbb{E} \left[\left[\frac{\mathbf{M}^\top (\mathbf{Z} + \mathbf{M})}{n} \mathcal{D}_{\mathbf{B}, \mathbf{B}}^{(i)} \mathbf{Q} \right]_{ij} \right].\end{aligned}$$

The main difficulty of the exercise lies in the term $\mathbb{E}[\frac{1}{n} \mathbf{M}^\top (\mathbf{Z} + \mathbf{M}) \mathcal{D}_{\mathbf{B}, \mathbf{B}}^{(i)} \mathbf{Q}]_{ij}$. To study it, we will admit the following result:

$$\begin{aligned}[\mathcal{D}_{\mathbf{B}, \mathbf{B}}^{(i)}]_{ll} &= \frac{1}{n} \operatorname{tr} (\mathbf{D}_{\bar{\mathbf{b}}_i} \mathbf{Q} \mathbf{D}_{\mathbf{b}_l}) = \frac{1}{n} \operatorname{tr} (\mathbf{Q} \odot \bar{\mathbf{b}}_i \mathbf{b}_l^\top) \\ &= \begin{cases} \frac{\varepsilon}{n} \operatorname{tr}(\mathbf{Q}) + o(1) & , \text{ if } i = l \\ \frac{\varepsilon^2}{n} \operatorname{tr}(\mathbf{Q}) + o(1) & , \text{ if } i \neq l. \end{cases}\end{aligned}$$

From this result, along with the remark that $\mathbf{A} = \mathbf{A} \odot \mathbf{1}_n \mathbf{1}_n^\top$ and the fact that $\|\boldsymbol{\mu}\| = O(1)$, show that

$$\mathbb{E} \left[\left[\frac{\mathbf{M}^\top \mathbf{Z} \odot \mathbf{B}}{n} \mathbf{Q} \right]_{ij} \right] = -\mathbb{E} \left[\left[\frac{\mathbf{M}^\top \mathbf{M} \mathbf{Q}}{n} \right]_{ij} \right] \frac{1}{(1 + \frac{\varepsilon}{n} \operatorname{tr}(\mathbf{Q}))} \frac{\varepsilon^2}{n} \operatorname{tr}(\mathbf{Q}) + o(1).$$

To obtain “closing” equations, we finally need to find a recursive relation for the quantities

$$L_{ij} \equiv \frac{1}{n} \operatorname{tr} \left(\mathbf{Q} \left(\frac{1}{n} (\mathbf{Z} + \mathbf{M})^\top (\mathbf{Z} + \mathbf{M}) \odot \mathbf{b}_i \mathbf{b}_j^\top \right) \right)$$

which appeared in the development. By interchangeability, observe that $L_{ij} = L_{\neq} + o(1)$ for all $i \neq j$ and $L_{ii} = L_{=} + o(1)$ for all i , for some L_{\neq} and $L_{=}$. Show that these must then satisfy

$$\begin{aligned}L_{\neq} &= \frac{\frac{\varepsilon^2}{n} \operatorname{tr}(\mathbf{Q})}{1 + \frac{\varepsilon}{n} \operatorname{tr}(\mathbf{Q})} \frac{p}{n} \\ L_{=} &= \frac{\varepsilon}{n} \operatorname{tr}(\mathbf{Q}) \frac{p}{n} - \frac{\varepsilon^3 (\frac{1}{n} \operatorname{tr}(\mathbf{Q}))^2}{1 + \frac{\varepsilon}{n} \operatorname{tr}(\mathbf{Q})} \frac{p}{n}.\end{aligned}$$

Conclude finally from these developments that

$$\mathbf{Q}(z) \leftrightarrow \bar{\mathbf{Q}}(z) = \bar{m}(z) \left(\mathbf{I}_n + \mu^2 \frac{\varepsilon m(z)}{1 + \varepsilon m(z)} \frac{\mathbf{j}\mathbf{j}^\top}{n} \right)^{-1}$$

where $m(z)$ is the Stieltjes transform (the limit of $\frac{1}{n} \operatorname{tr} \mathbf{Q}(z)$) solution to

$$z = -\frac{1}{m(z)} + cb - \varepsilon cm(z) + \frac{\varepsilon^3 cm(z)^2}{1 + \varepsilon m(z)}$$

in which we recall that $c = \lim_n p/n$ and $b = B_{ii}$ for all i . Show in particular that, up to a shift and a well-chosen scaling, we retrieve the Marčenko-Pastur in the limit $\varepsilon = 1$ and the semi-circle law in the limit $\varepsilon \rightarrow 0$.

Using a spiked model approach, show that the largest eigenvalue $\hat{\lambda}$ and associated eigenvector $\hat{\boldsymbol{\mu}}$ of \mathbf{S} satisfy, with high probability,

$$\hat{\lambda} \rightarrow \lambda = \begin{cases} cb + \epsilon(1 + \mu^2) + \frac{c}{1 + \mu^2} + \frac{c\varepsilon}{\mu^2(1 + \mu^2)} & , \mu^2 > \gamma \\ cb + \epsilon(1 + \gamma) + \frac{c}{1 + \gamma} + \frac{c\varepsilon}{\gamma(1 + \gamma)} & , \mu^2 \leq \gamma \end{cases}$$

and

$$\frac{|\hat{\boldsymbol{\mu}}^\top \boldsymbol{\mu}|^2}{\mu^2} \rightarrow \begin{cases} \frac{F(\mu^2)}{\mu^2(1 + \mu^2)^3} & , \mu^2 > \gamma \\ 0 & , \mu^2 \leq \gamma \end{cases}$$

where γ is the largest real solution to $F(\gamma) = 0$ with

$$F(x) = x^4 + 2x^3 + \left(1 - \frac{c}{\varepsilon}\right)x^2 - 2cx - c = 0.$$

Hint: For this last question, it is convenient to evaluate $|\hat{\boldsymbol{\mu}}^\top \boldsymbol{\mu}|^2$ at first to retrieve the separability condition as being the point where $|\hat{\boldsymbol{\mu}}^\top \boldsymbol{\mu}|^2 = 0$.

*** Romain to continue here ***

ex:transfer-learning

Practical Lecture Material 4 (Towards transfer learning with kernel regression). We consider here the extension of the supervised kernel learning to a two-task transfer learning scenario. Specifically, consider two datasets $\mathbf{X}_1 \in \mathbb{R}^{p \times n_1}$ and $\mathbf{X}_2 \in \mathbb{R}^{p \times n_2}$ associated to two learning tasks T_1 and T_2 . The exercise consists in “transferring” the learning of the binary classification of task T_1 with training examples $\mathbf{X}_1 = [\mathbf{x}_1^{(1)}, \mathbf{x}_1^{(2)}]$, $\mathbf{x}_i^{(j)} \in \mathbb{R}^{p \times n_{ij}}$, and labels $\mathbf{y}_1 \in \mathbb{R}^{n_1}$, towards the learning of the binary classification of task T_2 with training examples $\mathbf{X}_2 = [\mathbf{x}_2^{(1)}, \mathbf{x}_2^{(2)}]$ and labels $\mathbf{y}_2 \in \mathbb{R}^{n_2}$. Furthermore, $\mathbf{x}_i^{(j)} = [\mathbf{x}_{i1}, \dots, \mathbf{x}_{in_{ij}}] \in \mathbb{R}^{p \times n_{ij}}$ and we assume, as usual, that $\mathbf{x}_{ij} \sim \mathcal{N}(\boldsymbol{\mu}_{ij}, \mathbf{I}_p)$.

Extending the kernel regression (or LS-SVM) approach of Section 4.5.3, we here seek two hyperplanes $\boldsymbol{\omega}_1 = \boldsymbol{\omega}_0 + \mathbf{v}_1$ and $\boldsymbol{\omega}_2 = \boldsymbol{\omega}_0 + \mathbf{v}_2$ and biases b_1 and b_2 which solves the joint optimization problem:

$$\min_{(\boldsymbol{\omega}_0, \mathbf{V}, \mathbf{b}) \in \mathbb{R}^p \times \mathbb{R}^{p \times 2} \times \mathbb{R}^2} \frac{1}{2\lambda} \|\boldsymbol{\omega}_0\|^2 + \frac{1}{2} \sum_{i=1}^2 \frac{\|\mathbf{v}_i\|^2}{\gamma_i} + \frac{1}{2} \sum_{i=1}^2 \|\boldsymbol{\xi}_i\|^2$$

$$\boldsymbol{\xi}_i = \mathbf{y}_i - (\mathbf{X}_i^\top \boldsymbol{\omega}_i + b_i \mathbf{1}_{n_i}), \quad i \in \{1, 2\}.$$

First show that the problem solves two parallel learning tasks as $\lambda \rightarrow 0$ and a single learning task for $\lambda \rightarrow \infty$, and thus conclude on the role of the hyperparameters γ_i .

Using the Lagrangian multipliers method, show that

$$\begin{aligned} \mathbf{y}_i &= (\lambda + \gamma_i) \mathbf{X}_i^\top \mathbf{X}_i \boldsymbol{\alpha}_i + \lambda \sum_{j \neq i} \mathbf{X}_i^\top \mathbf{X}_j \boldsymbol{\alpha}_j + b_i \mathbf{1}_{n_i} + \boldsymbol{\alpha}_i \\ 0 &= \mathbf{1}_{n_i}^\top \boldsymbol{\alpha}_i \end{aligned}$$

for $\boldsymbol{\alpha} = [\boldsymbol{\alpha}_1^\top, \boldsymbol{\alpha}_2^\top]^\top \in \mathbb{R}^n$ some appropriately chosen Lagrange multipliers. Then, gathering $\mathbf{y} = [\mathbf{y}_1^\top, \mathbf{y}_2^\top]^\top \in \mathbb{R}^n$, $\boldsymbol{\alpha} = [\boldsymbol{\alpha}_1^\top, \boldsymbol{\alpha}_2^\top] \in \mathbb{R}^n$, and using the shortcut notations

$$\mathbf{Z} = \begin{pmatrix} \mathbf{X}_1 & 0 \\ 0 & \mathbf{X}_2 \end{pmatrix} \in \mathbb{R}^{2p \times n}, \quad \text{and} \quad \mathbf{P} = \begin{pmatrix} \mathbf{1}_{n_1} & 0 \\ 0 & \mathbf{1}_{n_2} \end{pmatrix} \in \mathbb{R}^{n \times 2},$$

confirm that we then obtain the compact form for $\boldsymbol{\alpha}$ and \mathbf{b}

$$\mathbf{P}\mathbf{b} + \mathbf{Q}^{-1}\boldsymbol{\alpha} = \mathbf{y} \quad \text{and} \quad \mathbf{P}^\top \boldsymbol{\alpha} = \mathbf{0}_2$$

where

$$\begin{aligned} \mathbf{Q} &\equiv \left(\frac{1}{2p} \mathbf{Z}^\top \mathbf{A} \mathbf{Z} + \mathbf{I}_n \right)^{-1} \\ \mathbf{A} &\equiv (\mathbf{D}_\gamma + \lambda \mathbf{1}_2 \mathbf{1}_2^\top) \otimes \mathbf{I}_p \in \mathbb{R}^{2p \times 2p} \end{aligned}$$

in which ‘ \otimes ’ is the Kronecker product of matrices and \mathbf{D}_x denotes a generic diagonal matrix with diagonal entries x_1, x_2, \dots .

Conclude on the final expressions for $\boldsymbol{\alpha}$ and \mathbf{b} and show finally that

$$\boldsymbol{\omega}_i = \left(\mathbf{e}_i^{[2]\top} \otimes \mathbf{I}_p \right) \mathbf{A} \mathbf{Z} \boldsymbol{\alpha}$$

where $\mathbf{e}_i^{[2]} \in \mathbb{R}^2$ is the canonical vector $(0, 1)$ with entry 1 in position i . Further show that the classification score for task T_i of any test point $\hat{\mathbf{x}}$ is given by

$$g_i(\hat{\mathbf{x}}) = \frac{1}{2p} \left(\mathbf{e}_i^{[2]\top} \otimes \hat{\mathbf{x}}_i \right)^\top \mathbf{A} \mathbf{Z} \boldsymbol{\alpha} + b_i$$

in which $\hat{\mathbf{x}}_i = \hat{\mathbf{x}} - \frac{1}{n_i} \mathbf{X}_i \mathbf{1}_{n_i}$. From these results and the matrix identity $(\mathbf{I} + \mathbf{DB})^{-1} \mathbf{D} = \mathbf{D}(\mathbf{I} + \mathbf{BD})^{-1}$, show that $g_i(\hat{\mathbf{x}})$ can be also expressed as

$$g_i(\hat{\mathbf{x}}) = \frac{1}{2p} \left(\mathbf{e}_i^{[2]\top} \otimes \hat{\mathbf{x}} \right)^\top \mathbf{A}^{\frac{1}{2}} \tilde{\mathbf{Q}} \mathbf{A}^{\frac{1}{2}} \mathbf{Z} (\mathbf{y} - \mathbf{P}\mathbf{b}) + b_i$$

where $\tilde{\mathbf{Q}} = (\frac{1}{2p} \mathbf{A}^{\frac{1}{2}} \mathbf{Z} \mathbf{Z}^\top \mathbf{A}^{\frac{1}{2}} + \mathbf{I}_{2p})^{-1}$.

Using either of the results on deterministic equivalents in the monograph, show then that

$$\mathbf{A}^{\frac{1}{2}} \tilde{\mathbf{Q}} \mathbf{A}^{\frac{1}{2}} \mathbf{Z} \leftrightarrow \mathbf{A}^{\frac{1}{2}} \tilde{\mathbf{Q}} \mathbf{A}^{\frac{1}{2}} \mathbf{M}_\Delta \mathbf{J}^\top$$

where $\tilde{\mathbf{Q}}$ is a deterministic equivalent for $\tilde{\mathbf{Q}}$ given by

$$\tilde{\mathbf{Q}} \leftrightarrow \bar{\tilde{\mathbf{Q}}} \equiv \left(\sum_{i=1}^2 \sum_{j=1}^2 \tilde{\Delta}_{ij} \mathbf{C}_{ij} + \mathbf{I}_{2p} \right)^{-1}$$

$$\mathbf{C}_{ij} = \mathbf{A}^{\frac{1}{2}} \left(\mathbf{e}_i^{[2]} \mathbf{e}_i^{[2]\top} \otimes (\mathbf{I}_p + \boldsymbol{\mu}_{ij} \boldsymbol{\mu}_{ij}^\top) \right) \mathbf{A}^{\frac{1}{2}}$$

and

$$\mathbf{M}_\Delta \equiv \mathbf{M} \sum_{ij} \frac{1}{1 + \Delta_i} \mathbf{e}_{ij}^{[4]} \mathbf{e}_{ij}^{[4]\top}$$

$$\mathbf{M} = \left(e_1^{[2]} \otimes [\boldsymbol{\mu}_{11}, \boldsymbol{\mu}_{12}], e_2^{[2]} \otimes [\boldsymbol{\mu}_{21}, \boldsymbol{\mu}_{22}] \right)$$

$$\Delta_i = \frac{1}{2p} \text{tr} \left(\mathbf{A}^{\frac{1}{2}} \left(\mathbf{e}_i^{[2]} \mathbf{e}_i^{[2]\top} \otimes \mathbf{I}_p \right) \mathbf{A}^{\frac{1}{2}} \bar{\tilde{\mathbf{Q}}} \right)$$

$$\tilde{\Delta}_{ij} = \frac{n_{ij}}{2p(1 + \Delta_i)}$$

$$\mathbf{J} = \begin{bmatrix} \mathbf{1}_{n_{11}} & 0 & 0 & 0 \\ 0 & \mathbf{1}_{n_{12}} & 0 & 0 \\ 0 & 0 & \mathbf{1}_{n_{21}} & 0 \\ 0 & 0 & 0 & \mathbf{1}_{n_{22}} \end{bmatrix}.$$

To go further, using Woodbury's matrix identity, show that

$$\bar{\tilde{\mathbf{Q}}} = \bar{\tilde{\mathbf{Q}}}_0 - \bar{\tilde{\mathbf{Q}}}_0 \bar{\mathbf{M}} \left(\mathbf{I}_{2p} + \bar{\mathbf{M}}^\top \bar{\tilde{\mathbf{Q}}} \bar{\mathbf{M}} \right)^{-1} \bar{\mathbf{M}}^\top \bar{\tilde{\mathbf{Q}}}$$

where $\bar{\tilde{\mathbf{Q}}}_0 = \left[(\mathbf{D}_\gamma + \lambda \mathbf{1}_2 \mathbf{1}_2^\top)^{\frac{1}{2}} \mathbf{D}_{\bar{\Delta}} (\mathbf{D}_\gamma + \lambda \mathbf{1}_2 \mathbf{1}_2^\top)^{\frac{1}{2}} + \mathbf{I}_2 \right]^{-1} \otimes \mathbf{I}_p$ and $\bar{\mathbf{M}} = A^{\frac{1}{2}} \mathbf{M} \mathbf{D}_{\bar{\Delta}}^{\frac{1}{2}}$
with $\bar{\Delta} = [\tilde{\Delta}_{11}, \dots, \tilde{\Delta}_{22}]$ and $\bar{\Delta} = [\tilde{\Delta}_{11} + \tilde{\Delta}_{12}, \tilde{\Delta}_{21} + \tilde{\Delta}_{22}]$.

Finally conclude by deducing the expression of the statistical mean m_{ij} of $g_i(\hat{\mathbf{x}})$ and simulate to verify. To this end, show that

$$m_{ij} = \mathbf{e}_{ij}^\top \mathbf{D}_{\bar{\Delta}}^{-\frac{1}{2}} \left[\mathbf{I}_4 - \left(\mathbf{I}_4 + \bar{\mathbf{M}}^\top \bar{\tilde{\mathbf{Q}}}_0 \bar{\mathbf{M}} \right)^{-1} \right] \mathbf{D}_{\bar{\Delta}}^{\frac{1}{2}} \tilde{\mathbf{y}} + b_i$$

where $\tilde{\mathbf{y}} = [\tilde{y}_{11} - b_1, \dots, \tilde{y}_{22} - b_2]^\top$ in the compacted expression $\mathbf{y} = [\tilde{y}_{11} \mathbf{1}_{n_{11}}^\top, \dots, \tilde{y}_{22} \mathbf{1}_{n_{22}}^\top]^\top$
and $\mathbf{e}_{ij}^{[4]} \in \mathbb{R}^4$ is the canonical vector with entry 1 in position $2(i-1) + j$.

Chapter 5

Large Neural Networks

chap:NN

5.1 Random neural networks

sec:random-NN

Neural networks, and particularly today’s popular deep neural networks, are extremely challenging to study. Even in a large dimensional regime, several technical boundaries are to this day seemingly unbreakable. The most important among these is the highly non-convex nature of their underlying optimization framework. While Chapter 6 later shows that the asymptotic performance analyses accessible to the random matrix framework is not limited to algorithms assuming explicit output functionals (such as linear regressions) and that some implicit (but convex) optimization schemes can be studied in the limit, neural network learning, which involves highly non-convex optimization, is still out of reach.

Although much less popular than modern deep neural networks, neural networks with random fixed weights are simpler to analyze. These have frequently arisen in the past decades as an appropriate solution to handle the possibly restricted number of training data, to reduce the computational and memory complexity and, from another viewpoint, can be seen as efficient *random feature extractors*. These neural networks in fact find their roots in Rosenblatt’s perceptron [Rosenblatt, 1958] and have then been many times revisited, rediscovered, and analyzed in a number of works, both in their feedforward [Schmidt et al., 1992, Albers et al., 1996] and recurrent [Gelenbe, 1993] versions. The simplest modern versions of these random networks are the so-called extreme learning machine [Huang et al., 2012] for the feedforward case, which one may see as a mere linear regression method on random nonlinear features, and the echo-state network [Jaeger, 2001] for the recurrent case, see [Scardapane and Wang, 2017] for a more exhaustive overview of randomness in neural networks.

It is also to be noted that deep neural networks are initialized at random and that random operations (such as random node deletions or voluntarily not-learning a large proportion of randomly-initialized neural network weights) are common and efficient in neural network learning [Srivastava et al., 2014, Fran-

kle and Carbin, 2019]. We may also point the recent endeavor towards neural network “learning without backpropagation” which, inspired by biological neural networks (that do not operate backpropagation learning), proposes learning mechanisms with fixed random *backward* weights and asymmetric *forward* learning procedure [Lillicrap et al., 2016, Nøkland, 2016, Baldi et al., 2018, Frenkel et al., 2019, Han et al., 2019]. As such, the study of random neural network structures may be instrumental to future improved understanding of advanced neural network procedures.

As shall be seen subsequently, the simple models of random neural networks are to a large extent connected to *kernel random matrices*. More specifically, the classification or regression performance at the output of these random neural networks are functionals of random matrices that fall into the wide class of kernel random matrices, yet of a slightly different form from those studied in Section 4. Perhaps more surprisingly, this connection still exists for *deep neural networks* that are (i) randomly initialized and (ii) then trained with gradient descent, via the so-called *neural tangent kernel* [Jacot et al., 2018], by considering the “infinite-neurons” limit, that is, the limit where the network widths of all layers go to infinity simultaneously. This close connection between neural networks and kernels has triggered a renewed interest for the theoretical investigation of deep neural networks from various perspectives including optimization [Du et al., 2019, Chizat et al., 2019], generalization [Allen-Zhu et al., 2019, Arora et al., 2019, Bietti and Mairal, 2019], and learning dynamics [Lee et al., 2019, Advani et al., 2020]. These works shed new light on our theoretical understanding of deep neural network models and specifically demonstrate the significance of studying simple networks with random weights and their associated kernels to assess the intrinsic mechanisms of more elaborate and practical deep networks.

5.1.1 Regression with random neural networks

subsec:ELM

Throughout this section, we consider a feedforward single-hidden-layer neural network, as illustrated in Figure 5.1 (for convenience from right to left). Another important class of neural network models, the (random) recurrent network, will be discussed later in Section 5.3.

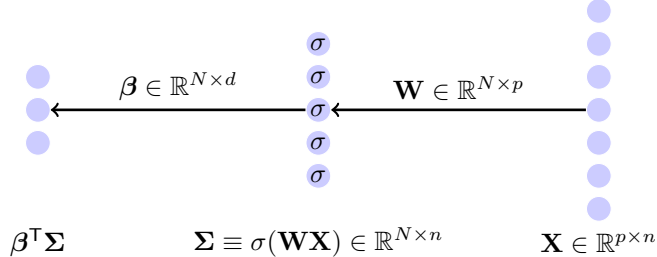


Figure 5.1: Illustration of a single-hidden-layer neural network (from right to left).

fig:ELM

For input data $\mathbf{X} = [\mathbf{x}_1, \dots, \mathbf{x}_n] \in \mathbb{R}^{p \times n}$, we denote $\Sigma \equiv \sigma(\mathbf{W}\mathbf{X}) \in \mathbb{R}^{N \times n}$ the output of the first layer comprising N neurons. This output arises from the pre-multiplication of \mathbf{X} by some random weight matrix $\mathbf{W} \in \mathbb{R}^{N \times p}$ with i.i.d. (say standard Gaussian) entries and the *entry-wise* application of the nonlinear activation function $\sigma : \mathbb{R} \rightarrow \mathbb{R}$. As such, the columns $\sigma(\mathbf{W}\mathbf{x}_i)$ of Σ can be seen as random nonlinear *features* of \mathbf{x}_i . The second layer weight $\beta \in \mathbb{R}^{N \times d}$ is then learned to adapt the feature matrix Σ to the associated target $\mathbf{Y} = [\mathbf{y}_1, \dots, \mathbf{y}_n] \in \mathbb{R}^{d \times n}$, for instance by minimizing the Frobenius norm $\|\mathbf{Y} - \beta^\top \Sigma\|_F^2$.

`rem:RNN-RFF`

Remark 5.1 (Random neural networks, random feature maps and random kernels). *The columns of Σ may be seen as the output of the $\mathbb{R}^p \rightarrow \mathbb{R}^N$ random feature map $\phi : \mathbf{x}_i \mapsto \sigma(\mathbf{W}\mathbf{x}_i)$ for some given matrix \mathbf{W} . In [Rahimi and Recht, 2008], it is shown that, for every nonnegative definite “shift-invariant” kernel of the form $(\mathbf{x}, \mathbf{y}) \mapsto f(\|\mathbf{x} - \mathbf{y}\|^2)$, there exist appropriate choices for σ and the law of the entries of \mathbf{W} so that, as $N \rightarrow \infty$,*

$$\sigma(\mathbf{W}\mathbf{x}_i)^\top \sigma(\mathbf{W}\mathbf{x}_j) \xrightarrow{a.s.} f(\|\mathbf{x}_i - \mathbf{x}_j\|^2).$$

As such, for large enough N (that in general must scale with n, p), the bivariate function $(\mathbf{x}, \mathbf{y}) \mapsto \sigma(\mathbf{W}\mathbf{x})^\top \sigma(\mathbf{W}\mathbf{y})$ approximates a kernel function of the type $f(\|\mathbf{x} - \mathbf{y}\|^2)$ studied in the previous chapter. This result is then generalized, in subsequent works, to a larger family of kernels including inner-product kernels [Kar and Karnick, 2012], additive homogeneous kernels [Vedaldi and Zisserman, 2012], just to name a few. Another, possibly more marginal, connection with the previous sections is that $\sigma(\mathbf{w}^\top \mathbf{x})$ can be interpreted as a “properly scaled” inner-product kernel function applied to the “data” pair $\mathbf{w}, \mathbf{x} \in \mathbb{R}^p$. This technically induces another strong relation between the study of kernels and that of neural networks.

If the network weight β is designed to minimize the regularized mean squared error (MSE) $L(\beta) = \frac{1}{n} \sum_{i=1}^n \|\mathbf{y}_i - \beta^\top \sigma(\mathbf{W}\mathbf{x}_i)\|^2 + \gamma \|\beta\|_F^2$, for some regularization factor $\gamma > 0$, we obtain the explicit *ridge-regressor*¹

$$\beta \equiv \frac{1}{n} \Sigma \left(\frac{1}{n} \Sigma^\top \Sigma + \gamma \mathbf{I}_n \right)^{-1} \mathbf{Y}^\top \quad \text{eq: def-ELM-beta (5.1)}$$

which follows from differentiating $L(\beta)$ with respect to β to obtain $0 = \gamma\beta + \frac{1}{n} \Sigma (\Sigma^\top \beta - \mathbf{Y}^\top)$ so that $(\frac{1}{n} \Sigma \Sigma^\top + \gamma \mathbf{I}_N) \beta = \frac{1}{n} \Sigma \mathbf{Y}^\top$ which, along with $(\frac{1}{n} \Sigma \Sigma^\top + \gamma \mathbf{I}_N)^{-1} \Sigma = \Sigma (\frac{1}{n} \Sigma^\top \Sigma + \gamma \mathbf{I}_n)^{-1}$ for $\gamma > 0$, gives the result.

The single-hidden-layer random neural net model presented above, with fixed random first layer and second layer performing a ridge regression, is sometimes referred to as an “extreme learning machine” in the literature [Huang et al., 2012], but from Remark 5.1 this is merely a random feature-based ridge regression.

¹Here we use a lowercase β to illustrate the fact that $\beta \in \mathbb{R}^{N \times d}$ is a “tall” matrix with $N \gg d$ (often $d = 1$), and acts like a vector from a random matrix point of view.

Note that, for β defined in (5.1), the training MSE (on the given training set (\mathbf{X}, \mathbf{Y})) reads

$$E_{\text{train}} = \frac{1}{n} \|\mathbf{Y}^T - \Sigma^T \beta\|_F^2 = \frac{\gamma^2}{n} \text{tr } \mathbf{Y} \mathbf{Q}^2(\gamma) \mathbf{Y}^T, \quad \mathbf{Q}(\gamma) \equiv \left(\frac{1}{n} \Sigma^T \Sigma + \gamma \mathbf{I}_n \right)^{-1} \quad (\text{eq: def-ELM-E-train})$$

for $\mathbf{Q}(\gamma)$ the resolvent of $\frac{1}{n} \Sigma^T \Sigma$. Similarly, the test MSE on the test set $(\hat{\mathbf{X}}, \hat{\mathbf{Y}}) \in \mathbb{R}^{p \times \hat{n}} \times \mathbb{R}^{d \times \hat{n}}$ of size \hat{n} is given by

$$E_{\text{test}} = \frac{1}{\hat{n}} \|\hat{\mathbf{Y}}^T - \hat{\Sigma}^T \beta\|_F^2, \quad \hat{\Sigma} = \sigma(\mathbf{W} \hat{\mathbf{X}}) \quad (\text{eq: def-ELM-E-test})$$

with $\beta \in \mathbb{R}^{N \times d}$ the same as used in (5.2) which only depends on \mathbf{W} , the training set (\mathbf{X}, \mathbf{Y}) and γ .

The objective of this section is to understand the asymptotic behavior of the training and test MSE, in the large dimensional limit where $n, p, N \rightarrow \infty$ at the same rate, and how they depend on the law of (the entries of) \mathbf{W} , the activation function $\sigma(\cdot)$, the regularization penalty γ , as well as the training and test data (\mathbf{X}, \mathbf{Y}) and $(\hat{\mathbf{X}}, \hat{\mathbf{Y}})$.

5.1.1.1 Intuition and main results

Consider first the training error E_{train} defined in (5.2). Since

$$\text{tr } \mathbf{Y} \mathbf{Q}^2(\gamma) \mathbf{Y}^T = - \frac{\partial}{\partial \gamma} \text{tr } \mathbf{Y} \mathbf{Q}(\gamma) \hat{\mathbf{Y}}, \quad (\text{eq: ELM-relation-E-train})$$

a deterministic equivalent for the resolvent $\mathbf{Q}(\gamma)$ is sufficient to access the asymptotic behavior of E_{train} .

With a linear activation $\sigma(t) = t$, the resolvent of interest

$$\mathbf{Q}(\gamma) = \left(\frac{1}{n} \sigma(\mathbf{W} \mathbf{X})^T \sigma(\mathbf{W} \mathbf{X}) + \gamma \mathbf{I}_n \right)^{-1} \quad (5.5)$$

is the same as in Theorem 2.5. In a sense, the evaluation of E_{train} calls for an extension of Theorem 2.5 to handle the case of nonlinear activations. Recall now that the main ingredients to derive a deterministic equivalent for (the linear case) $\mathbf{Q} = (\mathbf{X}^T \mathbf{W}^T \mathbf{W} \mathbf{X} / n + \gamma \mathbf{I}_n)^{-1}$ are (i) $\mathbf{X}^T \mathbf{W}^T$ has i.i.d. columns, and (ii) its i -th column $[\mathbf{W}^T]_i$ has i.i.d. entries so that the key Lemma 2.11 applies. These hold due to the i.i.d. property of the entries of \mathbf{W} .

However, while for (i) the nonlinear $\Sigma^T = \sigma(\mathbf{W} \mathbf{X})^T$ still has i.i.d. columns, for (ii) its i -th column $\sigma([\mathbf{X}^T \mathbf{W}^T]_i)$ no longer has i.i.d. entries. Therefore, the main technical difficulty here is to obtain a nonlinear version of the trace lemma, Lemma 2.11. That is, we expect that the concentration of quadratic forms around their expectation remains valid despite the application of the entry-wise nonlinear σ . This naturally falls into the concentration of measure theory discussed in Section 2.7 and is given by the following lemma.

lem:ELM-nonlinear-trace-lem

Lemma 5.1 (Concentration of nonlinear quadratic form, [Louart et al., 2018, Lemma 1]). For $\mathbf{w} \sim \mathcal{N}(\mathbf{0}, \mathbf{I}_p)$, 1-Lipschitz $\sigma(\cdot)$, and $\mathbf{A} \in \mathbb{R}^{n \times n}, \mathbf{X} \in \mathbb{R}^{p \times n}$ such that $\|\mathbf{A}\| \leq 1$ and $\|\mathbf{X}\|$ bounded with respect to p, n , then

$$\mathbb{P} \left(\left| \frac{1}{n} \sigma(\mathbf{w}^\top \mathbf{X}) \mathbf{A} \sigma(\mathbf{X}^\top \mathbf{w}) - \frac{1}{n} \operatorname{tr} \mathbf{A} \mathbf{K} \right| > t \right) \leq C e^{-cn \min(t, t^2)}$$

for some $C, c > 0$ with

$$\mathbf{K} \equiv \mathbf{K}_{\mathbf{XX}} \equiv \mathbb{E}_{\mathbf{w}} [\sigma(\mathbf{X}^\top \mathbf{w}) \sigma(\mathbf{w}^\top \mathbf{X})] \in \mathbb{R}^{n \times n}. \quad \text{eq:ELM-def-K (5.6)}$$

In particular, for p, n large together, $\frac{1}{n} \sigma(\mathbf{w}^\top \mathbf{X}) \mathbf{A} \sigma(\mathbf{X}^\top \mathbf{w}) = \frac{1}{n} \operatorname{tr} \mathbf{A} \mathbf{K} + O(n^{-1/2})$ as in the linear case: the convergence rate of the linear case is thus not affected by 1-Lipschitz σ functions.

Equation (5.1) is the core ingredient to generalize Theorem 2.5 to the nonlinear setting, leading to the following result.

theo:ELM-Q

Theorem 5.1 (Nonlinear Gram matrix, Louart et al. [2018]). Let $\mathbf{W} \in \mathbb{R}^{N \times p}$ be a random matrix with i.i.d. standard Gaussian entries, $\sigma(\cdot)$ be 1-Lipschitz continuous, and $\mathbf{X} \in \mathbb{R}^{p \times n}$ be of bounded operator norm (i.e., $\limsup_{n,p} \|\mathbf{X}\| < \infty$). Then, as $n, p, N \rightarrow \infty$ with p/n and N/n bounded away from zero and infinity, for $\mathbf{Q} = (\sigma(\mathbf{X}^\top \mathbf{W}^\top) \sigma(\mathbf{W} \mathbf{X})/n + \gamma \mathbf{I}_n)^{-1}$ with $\gamma > 0$,

$$\mathbf{Q} \leftrightarrow \bar{\mathbf{Q}} = \left(\frac{N}{n} \frac{\mathbf{K}}{1 + \delta} + \gamma \mathbf{I}_n \right)^{-1}$$

for δ the unique positive solution to $\delta = \frac{1}{n} \operatorname{tr} \bar{\mathbf{Q}} \mathbf{K}$ and \mathbf{K} defined in (5.6).

As a direct consequence of Theorem 5.1, we have the following results on the asymptotic training and test mean square errors of a single-hidden-layer random neural network model in Figure 5.1. We refer the interested readers to [Louart et al., 2018] for the detailed proof and more discussions therein.

coro:ELM-MSEs

Corollary 5.1 (Asymptotic training and test MSEs, Louart et al. [2018]). Under the setting and notations of Theorem 5.1, for training and test mean square errors defined in (5.2) and (5.3), respectively, as $n, p, N \rightarrow \infty$,

$$E_{\text{train}} - \bar{E}_{\text{train}} \xrightarrow{a.s.} 0, \quad E_{\text{test}} - \bar{E}_{\text{test}} \xrightarrow{a.s.} 0$$

with

$$\begin{aligned} \bar{E}_{\text{train}} &= \frac{\gamma^2}{n} \operatorname{tr} \mathbf{Y} \bar{\mathbf{Q}} \left(\frac{\frac{1}{N} \operatorname{tr} \bar{\mathbf{Q}} \mathbf{K} \bar{\mathbf{Q}}}{1 - \frac{1}{N} \operatorname{tr} \bar{\mathbf{Q}} \mathbf{K} \bar{\mathbf{Q}}} \bar{\mathbf{K}} + \mathbf{I}_n \right) \bar{\mathbf{Q}} \mathbf{Y}^\top \\ \bar{E}_{\text{test}} &= \frac{1}{\hat{n}} \| \hat{\mathbf{Y}}^\top - \bar{\mathbf{K}}_{\mathbf{X} \hat{\mathbf{X}}}^\top \bar{\mathbf{Q}} \mathbf{Y}^\top \|_F^2 \\ &\quad + \frac{\frac{1}{N} \operatorname{tr} \mathbf{Y} \bar{\mathbf{Q}} \bar{\mathbf{K}} \bar{\mathbf{Q}} \mathbf{Y}^\top}{1 - \frac{1}{N} \operatorname{tr} \bar{\mathbf{Q}} \mathbf{K} \bar{\mathbf{Q}}} \left(\frac{1}{\hat{n}} \operatorname{tr} \bar{\mathbf{K}}_{\mathbf{X} \hat{\mathbf{X}}} - \frac{1}{\hat{n}} \operatorname{tr} (\mathbf{I}_n + \gamma \bar{\mathbf{Q}}) (\bar{\mathbf{K}}_{\mathbf{X} \hat{\mathbf{X}}} \bar{\mathbf{K}}_{\mathbf{X} \hat{\mathbf{X}}}^\top \bar{\mathbf{Q}}) \right) \end{aligned}$$

where, similarly to $\mathbf{K} = \mathbb{E}[\sigma(\mathbf{X}^\top \mathbf{w})\sigma(\mathbf{w}^\top \mathbf{X})]$ in (5.6), we denoted

$$\mathbf{K}_{\mathbf{X}\hat{\mathbf{X}}} \equiv \mathbb{E}[\sigma(\mathbf{X}^\top \mathbf{w})\sigma(\mathbf{w}^\top \hat{\mathbf{X}})], \quad \mathbf{K}_{\hat{\mathbf{X}}\hat{\mathbf{X}}} \equiv \mathbb{E}[\sigma(\hat{\mathbf{X}}^\top \mathbf{w})\sigma(\mathbf{w}^\top \hat{\mathbf{X}})] \quad (5.7)$$

and

$$\bar{\mathbf{K}} \equiv \frac{N}{n} \frac{\mathbf{K}}{1+\delta}, \quad \bar{\mathbf{K}}_{\mathbf{X}\hat{\mathbf{X}}} \equiv \frac{N}{n} \frac{\mathbf{K}_{\mathbf{X}\hat{\mathbf{X}}}}{1+\delta}, \quad \bar{\mathbf{K}}_{\hat{\mathbf{X}}\hat{\mathbf{X}}} \equiv \frac{N}{n} \frac{\mathbf{K}_{\hat{\mathbf{X}}\hat{\mathbf{X}}}}{1+\delta}.$$

The proof of Corollary 5.1 is based on a higher-order deterministic equivalent of the type **QAQ** for some deterministic or structured random matrices \mathbf{A} , as in Exercise 13. More precisely, for the training MSE E_{train} , we have from (5.4) that it suffices to derive a deterministic equivalent for $\mathbf{Q}^2(\gamma)$ (or, alternatively, by considering the derivative with respect to γ). For the test MSE E_{test} , we deduce from (5.3) that

$$E_{\text{test}} = \frac{1}{\hat{n}} \text{tr } \hat{\mathbf{Y}} \hat{\mathbf{Y}}^\top - \frac{2}{n\hat{n}} \text{tr } \mathbf{Y} \mathbf{Q} \Sigma^\top \hat{\Sigma} \hat{\mathbf{Y}}^\top + \frac{1}{n^2 \hat{n}} \text{tr } \mathbf{Y} \mathbf{Q} \Sigma^\top \hat{\Sigma} \hat{\Sigma}^\top \Sigma \mathbf{Q} \mathbf{Y}^\top \quad (5.8)$$

which involves the assessment of, for instance, the more involved expectation $\mathbb{E}_W[\mathbf{Q} \Sigma^\top \hat{\Sigma} \hat{\Sigma}^\top \Sigma \mathbf{Q}]$ with $\hat{\Sigma} = \sigma(\mathbf{W} \hat{\mathbf{X}})$.

Clearly, to evaluate the asymptotic training and test errors in Corollary 5.1, the computation of the expectation of the form \mathbf{K} in (5.6) is needed. To go further, \mathbf{W} being standard Gaussian, the (i, j) entry of matrix \mathbf{K} writes

$$\begin{aligned} \mathbf{K}_{ij} &\equiv \kappa(\mathbf{x}_i, \mathbf{x}_j) \equiv \mathbb{E}[\sigma(\mathbf{w}^\top \mathbf{x}_i)\sigma(\mathbf{w}^\top \mathbf{x}_j)] \\ &= (2\pi)^{-\frac{p}{2}} \int \sigma(\mathbf{w}^\top \mathbf{x}_i)\sigma(\mathbf{w}^\top \mathbf{x}_j)e^{-\frac{1}{2}\|\mathbf{w}\|^2} d\mathbf{w} \end{aligned}$$

and indeed defines the limiting kernel of the random feature map $\mathbf{x}_i \mapsto \sigma(\mathbf{W} \mathbf{x}_i)$ as discussed in Remark 5.1. For a set of commonly used activation functions σ (that are not necessarily Lipschitz), the corresponding kernel matrix \mathbf{K} can be computed explicitly via an integration projection trick (see e.g., [Williams, 1997] for similar calculus). These results are provided in Table 5.1.

Given some data \mathbf{X} , Table 5.1 allows one to compute the “limiting” kernel \mathbf{K} for the listed activation functions $\sigma(\cdot)$. Then, by iterating the fixed-point equation in Theorem 5.1, one obtains the *effective kernel* $\bar{\mathbf{K}} \equiv \frac{N}{n} \frac{\mathbf{K}}{1+\delta}$ in the more practical large n, p, N setting (compared to the $N \rightarrow \infty$ alone limiting kernel \mathbf{K}). In this sense, Theorem 5.1 characterizes the impact of the effective kernel $\bar{\mathbf{K}}$ on the regression performances as detailed in Corollary 5.1.

5.1.1.2 Implications for learning with large neural networks

subsubsec:implication-ELM

To validate the asymptotic analysis in Theorem 5.1 and Corollary 5.1 on real-world finite-dimensional data, Figure 5.2 and 5.3 compare the empirical MSEs with their limiting behaviors predicted in Corollary 5.1, for a random network having $N = 512$ neurons, with various types of Lipschitz and non-Lipschitz activations $\sigma(\cdot)$, respectively. The regressor $\beta \in \mathbb{R}^p$ maps the vectorized images from the Fashion-MNIST dataset (class 1 and 2) to their corresponding

unidimensional ($d = 1$) output labels $\mathbf{Y}_{1i}, \hat{\mathbf{Y}}_{1j} \in \{\pm 1\}$. For n, p, N only of order a few hundreds, a close match between theory and practice is observed for Lipschitz activations in Figure 5.2. The precision is less accurate but still not poor for the case of non-Lipschitz activations (Figure 5.3) which are not supported by the theorem statement – here for $\sigma(t) = 1 - t^2/2$, $\sigma(t) = 1_{t>0}$ and $\sigma(t) = \text{sign}(t)$. For all activations, the deviation from theory is more acute for small values of γ .

$\sigma(t)$	$\kappa(\mathbf{x}, \mathbf{y})$
t	$\mathbf{x}^\top \mathbf{y}$
$ t $	$\frac{2}{\pi} \ \mathbf{x}\ \ \mathbf{y}\ (\angle \cdot \arcsin(\angle) + \sqrt{1 - \angle^2})$
$\text{ReLU}(t) \equiv \max(t, 0)$	$\frac{1}{2\pi} \ \mathbf{x}\ \ \mathbf{y}\ (\angle \arccos(-\angle) + \sqrt{1 - \angle^2})$
$a_+ \max(t, 0) + a_- \max(-t, 0)$	$\frac{1}{2} (a_+^2 + a_-^2) \mathbf{x}^\top \mathbf{y} + \frac{1}{2\pi} \ \mathbf{x}\ \ \mathbf{y}\ (a_+ + a_-)^2 (-\angle \arccos(\angle) + \sqrt{1 - \angle^2})$
$a_2 t^2 + a_1 t + a_0$	$a_2^2 (2(\mathbf{x}^\top \mathbf{y})^2 + \ \mathbf{x}\ ^2 \ \mathbf{y}\ ^2) + a_1^2 \mathbf{x}^\top \mathbf{y} + a_2 a_0 (\ \mathbf{x}\ ^2 + \ \mathbf{y}\ ^2) + a_0^2$
$\text{erf}(t)$	$\frac{2}{\pi} \arcsin \left(\frac{2\mathbf{x}^\top \mathbf{y}}{\sqrt{(1+2\ \mathbf{x}\ ^2)(1+2\ \mathbf{y}\ ^2)}} \right)$
$1_{t>0}$	$\frac{1}{2} - \frac{1}{2\pi} \arccos(\angle)$
$\text{sign}(t)$	$\frac{2}{\pi} \arcsin(\angle)$
$\cos(t)$	$\exp \left(-\frac{1}{2} (\ \mathbf{x}\ ^2 + \ \mathbf{y}\ ^2) \right) \cosh(\mathbf{x}^\top \mathbf{y})$
$\sin(t)$	$\exp \left(-\frac{1}{2} (\ \mathbf{x}\ ^2 + \ \mathbf{y}\ ^2) \right) \sinh(\mathbf{x}^\top \mathbf{y})$
$\exp(-t^2/2)$	$\frac{1}{\sqrt{(1+\ \mathbf{x}\ ^2)(1+\ \mathbf{y}\ ^2)-(x^\top y)^2}}$

tab: ELM-K

Table 5.1: Limiting kernel $\kappa(\mathbf{x}, \mathbf{y})$ for standard Gaussian \mathbf{W} , with $\angle \equiv \frac{\mathbf{x}^\top \mathbf{y}}{\|\mathbf{x}\| \|\mathbf{y}\|}$.

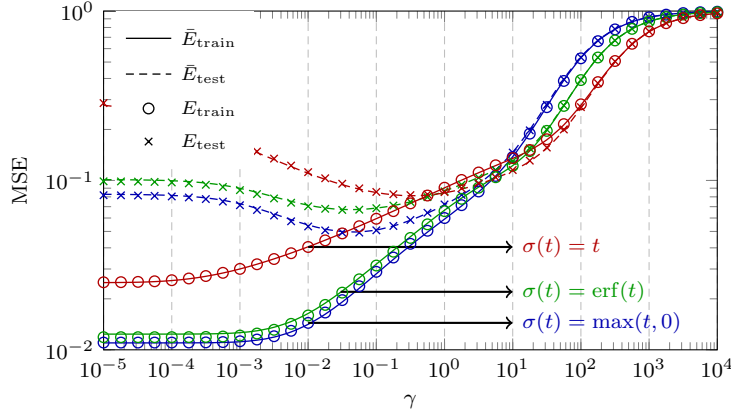


Figure 5.2: Neural network regression errors for Lipschitz $\sigma(\cdot)$ as a function of γ , $\sigma(t) = t$ in red, $\sigma(t) = \text{erf}(t)$ in green, and $\sigma(t) = \text{ReLU}(t)$ in blue, for 2-class Fashion-MNIST data (class 1 versus 2), $N = 512$, $n = 1\,024$, $\hat{n} = 512$, $p = 784$. Results averaged over 30 runs. [Link to code]

fig:ELM-Lips

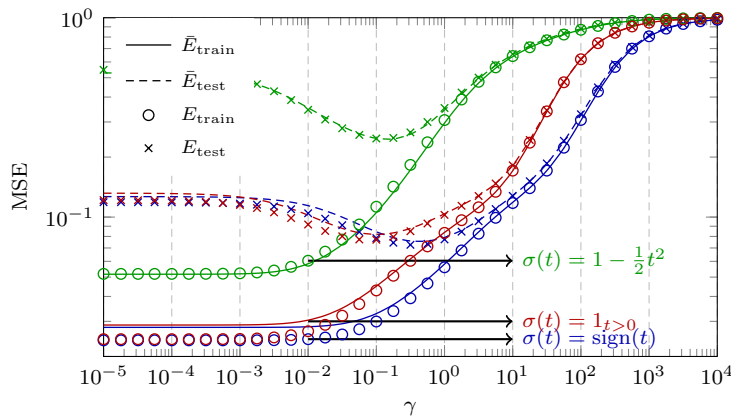


Figure 5.3: Neural network regression errors for non-Lipschitz $\sigma(\cdot)$ as a function of γ , $\sigma(t) = 1_{t>0}$ in red, quadratic $\sigma(t)$ in green, and $\sigma(t) = \text{sign}(t)$ in blue, for 2-class Fashion-MNIST data (class 1 versus 2), $N = 512$, $n = 1\,024$, $\hat{n} = 512$, $p = 784$. Results averaged over 30 runs. [Link to code]

fig:ELM-non-Lips

Figures 5.2 and 5.3 confirm that, while the training error is a monotonically increasing function of the regularization parameter γ , there always exists an optimal value for γ which minimizes the test error. In particular, the theoretical formulas derived in Corollary 5.1 allow for a (data-dependent) fast offline tuning of the hyperparameter γ of the network, in the setting when n, p, N are not too small and comparable. In terms of activation functions (those listed here), we observe that, on the Fashion-MNIST dataset, the ReLU nonlinearity $\sigma(t) =$

$\max(t, 0)$ is optimal and achieves the minimum test error, while the quadratic activation $\sigma(t) = 1 - t^2/2$ is the worst and produces much higher training and test errors compared to others. This observation can be theoretically explained with a deeper analysis of the underlying kernel matrix \mathbf{K} , as performed in Section 5.1.2. Lastly, although not immediate at first sight, the training and test error curves of $\sigma(t) = 1_{t>0}$ and $\sigma(t) = \text{sign}(t)$ are indeed the same, up to a shift in γ , as a consequence of the relation $\text{sign}(t) = 2 \cdot 1_{t>0} - 1$.

Model complexity and the double descent phenomenon. The deterministic equivalent of the limiting performance provided in Corollary 5.1 explicitly depends on the ratio feature-to-sample N/n (as well as, more implicitly through the data, on the size p of the data). The quantity N/n is of crucial significance from a machine learning perspective, as it characterizes the (relative) *model complexity* of the neural network model under investigation. For a training set of size n , the increase of the number of neurons N represents the growth of model complexity and, as a consequence, the increase of its capacity to fit the given training set.

According to the golden “bias-variance tradeoff” rule [Friedman et al., 2001], it is necessary to control the model complexity (N here) to achieve optimal *test* performance. Essentially, as the model size increases, the model tends to better fit the given training set, resulting in a smaller “bias”, while on the other hand, gradually overfits the training set and may perform poorly on an independent test set due to the large “variance”. To prevent overfitting, explicit regularization schemes such as Tikhonov-type regularization or early stopping are proposed to control the model capacity by avoiding too-small training errors.

It has thus been long believed that the optimal choice of model complexity should produce a small but nonzero training error, but the success of deep learning seems to contradict this conventional wisdom. Modern deep neural networks often have a huge number of parameters and are routinely trained to fit the training data almost perfectly, while still yielding remarkably good test performance in many cases [Zhang et al., 2016]. This particularly means that, in some scenarios, it is possible to have good or even optimal models that are much larger than intuitively needed (typically with $N \gg n$).

This counterintuitive phenomenon is empirically observed for various large-scale machine learning models, and more recently, extensively investigated from a theoretical standpoint [Belkin et al., 2019, Hastie et al., 2019, Mei and Montanari, 2019]. More precisely, it is observed that, as the model becomes larger, the test error decreases and then increases, following the traditional “bias versus variance” U-shaped curve, until the interpolation threshold where the model fits perfectly the training set and achieves zero training error, typically at $N = n$. Then, very surprisingly, in the over-parameterization $N > n$ regime, the test error starts to decrease again as N further grows, reaching an error that can (but not always) be even smaller than the optimal error in the under-parametrization $N < n$ regime.

This so-called “double-descent” phenomenon (due to its W-shaped curve)

is depicted in Figure 5.4 for the random neural network model in Figure 5.1, with $\gamma = 10^{-7}$ to mimic the unregularized case. Observe that, when $N = n$, while the training error vanishes, the test error blows up. But then, in the over-parameterization $N > n$ regime, the test error monotonically decreases as N further increases and reaches an even smaller error than the optimal error in the $N < n$ regime, at least in this particular setting.

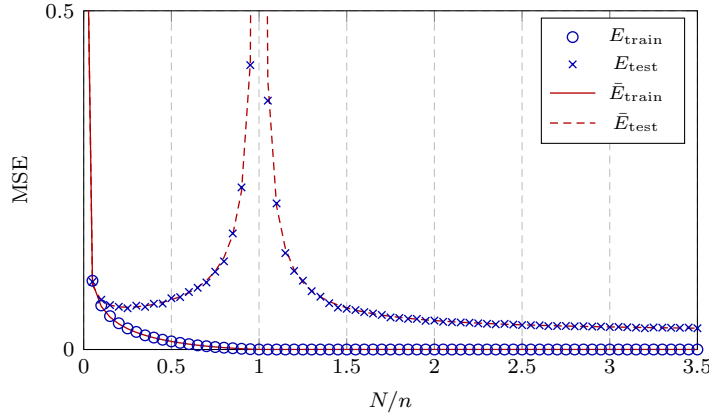


Figure 5.4: Training and test MSEs of random neural network model as a function of the ratio N/n on Fashion-MNIST data (class 1 versus 2), with $p = 784$, $n = 1000$, $\sigma(t) = \text{ReLU}(t)$ and $\lambda = 10^{-7}$. Results averaged over 30 runs.
[\[Link to code\]](#)

`fig:ELM-double-descent`

This unexpected double-descent behavior with a test error singularity at $N = n$ can readily be anticipated from Theorem 5.1 in the unregularized $\gamma = 0$ case. Depending on whether $N > n$ or $N < n$, we indeed have the following *phase transition* behavior:

1. in the over-parameterization $N > n$ regime, by taking $\gamma \rightarrow 0$ in Theorem 5.1, we obtain

$$\delta = \frac{1}{n} \text{tr } \mathbf{K} \left(\frac{N}{n} \frac{\mathbf{K}}{1 + \delta} \right)^{-1} = \frac{\text{eq:ELM-fixed-point-}N>n}{N - n} \quad (5.9)$$

where we assume \mathbf{K} to be invertible, so that $\bar{\mathbf{Q}} \equiv (\frac{N}{n} \frac{\mathbf{K}}{1 + \delta} + \gamma \mathbf{I}_n)^{-1} = \frac{n}{N - n} \mathbf{K}^{-1}$ is well defined at $\gamma = 0$;

2. on the other hand, in the under-parameterization $N < n$ regime, δ diverges when $\gamma \rightarrow 0$, but we remark that

$$\gamma \delta = \frac{1}{n} \text{tr } \mathbf{K} \left(\frac{N}{n} \frac{\mathbf{K}}{\gamma + \gamma \delta} + \mathbf{I}_n \right)^{-1} \quad \text{eq:ELM-fixed-point-}N<n \quad (5.10)$$

converges, as $\gamma \rightarrow 0$, to $\gamma \delta \rightarrow \theta = \frac{1}{n} \text{tr } \mathbf{K} (\frac{N}{n} \frac{\mathbf{K}}{\theta} + \mathbf{I}_n)^{-1}$; that is, $\delta, \bar{\mathbf{Q}}$ both scale like γ^{-1} . We have in particular $\mathbb{E}[\gamma \mathbf{Q}] \sim \gamma \bar{\mathbf{Q}} \sim (\frac{N}{n} \frac{\mathbf{K}}{\theta} + \mathbf{I}_n)^{-1}$. This

is in accordance with the fact that the Gram matrix $\Sigma^\top \Sigma \in \mathbb{R}^{n \times n}$ is of rank at most $\min(N, n)$ and is thus not invertible for $N < n$ (such that $\mathbf{Q} \equiv (\Sigma^\top \Sigma/n + \gamma \mathbf{I}_n)^{-1}$ scales as γ^{-1} as $\gamma \rightarrow 0$).

With this remark, the behavior of the asymptotic test error in Corollary 5.1 as N approaches n , from both sides of $N < n$ and $N > n$ is better understood. In particular, the denominator of \bar{E}_{test} reads

$$\begin{aligned} & 1 - \frac{1}{N} \operatorname{tr} \bar{\mathbf{K}} \bar{\mathbf{Q}} \bar{\mathbf{K}} \bar{\mathbf{Q}} \\ &= \begin{cases} 1 - \frac{n}{N} + \frac{2\gamma}{N} \operatorname{tr} \left(\frac{N}{n} \frac{\mathbf{K}}{1+\delta} + \gamma \mathbf{I}_n \right)^{-1} - \frac{\gamma^2}{N} \operatorname{tr} \left(\frac{N}{n} \frac{\mathbf{K}}{1+\delta} + \gamma \mathbf{I}_n \right)^{-2}, & N > n \\ 1 - \frac{n}{N} + \frac{2}{N} \operatorname{tr} \left(\frac{N}{n} \frac{\mathbf{K}}{\gamma+\theta} + \mathbf{I}_n \right)^{-1} - \frac{1}{N} \operatorname{tr} \left(\frac{N}{n} \frac{\mathbf{K}}{\gamma+\theta} + \mathbf{I}_n \right)^{-2}, & N < n \end{cases} \end{aligned}$$

which, as N approaches n from either side, becomes $1 - \frac{1}{N} \operatorname{tr} \bar{\mathbf{K}} \bar{\mathbf{Q}} \bar{\mathbf{K}} \bar{\mathbf{Q}} \sim \gamma$ (in the small γ regime).

The fact that this denominator scales like γ as $\gamma \rightarrow 0$ explains the major difference between the training and test error behavior in Figure 5.4. Due to the γ^2 prefactor in \bar{E}_{train} , the training error is guaranteed to be finite (in fact to be zero). But for the test error, if the numerator term $\frac{1}{n} \operatorname{tr} \bar{\mathbf{K}}_{\hat{\mathbf{X}}\hat{\mathbf{X}}} - \frac{1}{n} \operatorname{tr} (\mathbf{I}_n + \gamma \bar{\mathbf{Q}})(\bar{\mathbf{K}}_{\mathbf{X}\hat{\mathbf{X}}} \bar{\mathbf{K}}_{\mathbf{X}\hat{\mathbf{X}}}^\top \bar{\mathbf{Q}})$ does not scale like γ as $\gamma \rightarrow 0$, then \bar{E}_{test} diverges to infinity at $N = n$. A first counterexample is of course when $\hat{\mathbf{X}} = \mathbf{X}$, for which the numerator term of \bar{E}_{test} is now

$$\frac{1}{n} - \frac{1}{n} \operatorname{tr} (\mathbf{I}_n + \gamma \bar{\mathbf{Q}})(\bar{\mathbf{K}}_{\mathbf{X}\hat{\mathbf{X}}} \bar{\mathbf{K}}_{\mathbf{X}\hat{\mathbf{X}}}^\top \bar{\mathbf{Q}}) = \frac{\gamma^2}{n} \operatorname{tr} \bar{\mathbf{Q}} \bar{\mathbf{K}} \bar{\mathbf{Q}}$$

where we exploited the fact that $\bar{\mathbf{K}} \bar{\mathbf{Q}} = \mathbf{I}_n - \gamma \bar{\mathbf{Q}}$; of course, the test error \bar{E}_{test} coincides with the training error \bar{E}_{train} in this case. In general though, when $\hat{\mathbf{X}} \neq \mathbf{X}$, the numerator does not vanish with γ and the test error diverges at $N = n$ and $\gamma \rightarrow 0$.

Therefore, this double-descent singularity at $N = n$ only occurs: (i) in the unregularized case as $\gamma \rightarrow 0$ where some sort of invertibility issue arises, and (ii) when the test data $\hat{\mathbf{X}}$ is sufficiently “distinct” from the training data \mathbf{X} , in a kernel matrix sense, and this is fully *independent* of the targets \mathbf{Y} and $\hat{\mathbf{Y}}$.

5.1.2 Delving deeper into limiting kernels

To understand the behavior of different activation functions in Figure 5.2 and 5.3, we would like to build up a *data-dependent* theory that can provide the performance of different nonlinearities in a more explicit manner. According to our previous discussion, the performances depend on the nonlinear activation $\sigma(\cdot)$ only via the kernel matrix of the form

$$\mathbf{K} \equiv \mathbb{E}_{\mathbf{w}}[\sigma(\mathbf{X}^\top \mathbf{w}) \sigma(\mathbf{w}^\top \mathbf{X})] \quad \text{eq: def-K-RNN (5.11)}$$

given explicitly in Table 5.1. The entries of \mathbf{K} are nonlinear functions of $\|\mathbf{x}_i\|$, $\|\mathbf{x}_j\|$ or $\mathbf{x}_i^\top \mathbf{x}_j$, reminiscent of the distance and inner-product random kernel matrices studied in Section 4.2. Following the same idea, under the k -class

Gaussian mixture model for the data \mathbf{x}_i :

$$\mathbf{x}_i \in \mathcal{C}_a \Leftrightarrow \sqrt{p}\mathbf{x}_i \sim \mathcal{N}(\boldsymbol{\mu}_a, \mathbf{C}_a)$$

for $a \in \{1, \dots, k\}$ and the non-trivial classification condition

$$\begin{aligned} \mathbf{M} &= [\boldsymbol{\mu}_1^\circ, \dots, \boldsymbol{\mu}_k^\circ] = O_{\|\cdot\|}(1), \quad \boldsymbol{\mu}_\ell^\circ = \boldsymbol{\mu}_\ell - \sum_{a=1}^k \frac{n_a}{n} \boldsymbol{\mu}_a \\ \mathbf{t} &= [t_1, \dots, t_k]^\top = O_{\|\cdot\|}(1), \quad t_a = \frac{1}{\sqrt{p}} \text{tr}(\mathbf{C}_a - \mathbf{C}^\circ) \\ \mathbf{S} &= \{S_{ab}\}_{a,b=1}^k = O_{\|\cdot\|}(1), \quad S_{ab} = \frac{1}{p} \text{tr} \mathbf{C}_a \mathbf{C}_b. \end{aligned}$$

for $\mathbf{C}^\circ = \sum_{a=1}^k \frac{n_a}{n} \mathbf{C}_a$, we have, for $\mathbf{x}_i \in \mathcal{C}_a$ and $\mathbf{x}_j \in \mathcal{C}_b$, $i \neq j$ that

$$\mathbf{x}_i^\top \mathbf{x}_j = 0 + \frac{1}{p} \mathbf{z}_i^\top \mathbf{C}_a^{\frac{1}{2}} \mathbf{C}_b^{\frac{1}{2}} \mathbf{z}_j + \frac{1}{p} (\boldsymbol{\mu}_a^\top \mathbf{C}_b^{\frac{1}{2}} \mathbf{z}_j + \boldsymbol{\mu}_b^\top \mathbf{C}_a^{\frac{1}{2}} \mathbf{z}_i) + \frac{1}{p} \boldsymbol{\mu}_a^\top \boldsymbol{\mu}_b$$

and

$$\|\mathbf{x}_i\|^2 = \mathbf{x}_i^\top \mathbf{x}_i = \frac{1}{p} \text{tr} \mathbf{C}^\circ + \frac{1}{p} \text{tr}(\mathbf{C}_a - \mathbf{C}^\circ) + [\boldsymbol{\psi}]_i + \frac{1}{p} \|\boldsymbol{\mu}_a\|^2 + \frac{2}{p} \boldsymbol{\mu}_a^\top \mathbf{C}_a^{\frac{1}{2}} \mathbf{z}_i$$

with $\text{tr} \mathbf{C}^\circ / p = O(1)$ and $\boldsymbol{\psi} \in \mathbb{R}^n$ such that $[\boldsymbol{\psi}]_i = \mathbf{z}_i^\top \mathbf{C}_a \mathbf{z}_i / p - \text{tr} \mathbf{C}_a / p = O(p^{-1/2})$ as in Theorem 4.1. As a consequence, a Taylor expansion (around 0 or $-\text{tr} \mathbf{C}^\circ / p$) can be performed, as in Section 4.2, to asymptotically “linearize” these kernel matrices arising from different nonlinear activations in Table 5.1, leading to the following result, which extends Theorem 4.1.

Theorem 5.2 (Liao and Couillet [2018b]). *For all $\sigma(\cdot)$ in Table 5.1 and $\mathbf{P} = \mathbf{I}_n - \frac{1}{n} \mathbf{1}_n \mathbf{1}_n^\top$, we have, as $n, p \rightarrow \infty$ with $p/n \rightarrow c \in (0, \infty)$ and $n_a/n \rightarrow c_a \in (0, 1)$ that*

$$\|\mathbf{PKP} - \mathbf{P}\tilde{\mathbf{K}}\mathbf{P}\| \xrightarrow{a.s.} 0$$

where

$$\tilde{\mathbf{K}} = d_1 \cdot \frac{1}{p} (\mathbf{W} + \mathbf{MJ}^\top)^\top (\mathbf{W} + \mathbf{MJ}^\top) + d_2 \cdot \mathbf{UBU}^\top + d_0 \cdot \mathbf{I}_n$$

for $\mathbf{W} \equiv [\mathbf{W}_1, \dots, \mathbf{W}_k] \in \mathbb{R}^{p \times n}$, $\mathbf{W}_a \equiv \mathbf{C}_a^{\frac{1}{2}} \mathbf{Z}_a \in \mathbb{R}^{p \times n_a}$ and

$$\mathbf{U} = \begin{bmatrix} \mathbf{J} & \boldsymbol{\psi} \end{bmatrix} \in \mathbb{R}^{n \times (k+1)}, \quad \mathbf{B} = \begin{bmatrix} \mathbf{tt}^\top + 2\mathbf{S} & \mathbf{t} \\ \mathbf{t}^\top & 1 \end{bmatrix}, \quad \boldsymbol{\psi} \equiv \frac{1}{p} \{ \|\mathbf{w}_i\|^2 - \mathbb{E}[\|\mathbf{w}_i\|^2] \}_{i=1}^n$$

with the corresponding coefficients d_0 and d_1, d_2 given in Table 5.2.

Following the discussions in Remark 4.2 and 4.5, for simplicity of analysis, the result is presented here under the form of *centered* kernel matrix \mathbf{PKP} , that essentially performs a feature centering in the kernel space.

Theorem 5.2 tells us that, for the (non-trivial) classification of a mixture of k Gaussians, the (centered) kernel matrix \mathbf{K} depends on the nonlinear function $\sigma(\cdot)$ solely via *three* scalars d_0 , d_1 and d_2 , for all nonlinearities listed in Table 5.1. Moreover, note that the coefficient d_0 only introduces a constant shift of *all* eigenvalues of the kernel matrix \mathbf{K} , and has thus no impact on the performance of kernel-based algorithms such as kernel spectral clustering or kernel ridge regression. These two “universal” parameters (d_1, d_2) are reminiscent of the parameters α and β of the α - β kernel in Theorem 4.2 and the properly scaling kernel parameterized by (a_1, a_2) in Theorem 4.6. This is another evidence of large dimensional universality that will be discussed at length in Chapter 8.

Letting the term $d_0\mathbf{I}_n$ aside, the kernel matrix $\tilde{\mathbf{K}}$ has two “information-plus-noise” type components, $\mathbf{W} + \mathbf{M}\mathbf{J}^\top$ and $\mathbf{U} = [\mathbf{J}/\sqrt{p}, \boldsymbol{\psi}]$, weighted by d_1 and d_2 , respectively, where we recall the class structure information matrix $\mathbf{J} = [\mathbf{j}_1, \dots, \mathbf{j}_k] \in \mathbb{R}^{n \times k}$. It is therefore impossible to get rid of the noisy terms (\mathbf{W} and $\boldsymbol{\psi}$) by wisely choosing the function $\sigma(\cdot)$ without affecting \mathbf{J} . This is in sharp contrast to more general kernels (i.e., not arising from random neural networks) as in Corollary 4.1, which allow for a more flexible treatment of information versus noise.

Moreover, since the matrix of statistical means \mathbf{M} is multiplied by d_1 and covariance information \mathbf{t} and \mathbf{S} by d_2 , Theorem 5.2 provides practical instructions in a “data-dependent” choice of the nonlinearity. More precisely, the functions $\sigma(\cdot)$ in Table 5.2 can be divided into the following three groups

1. *mean-oriented*, where $d_1 \neq 0$ while $d_2 = 0$: this is the case of the functions $\sigma(t) = t$, $\text{sign}(t)$ and $\sin(t)$ and $\text{erf}(t)$, which asymptotically capture only the difference in means, with the information in covariance discarded;
2. *covariance-oriented*, where $d_1 = 0$ while $d_2 \neq 0$: this concerns the functions $\sigma(t) = |t|$, $\cos(t)$ and $\exp(-t^2/2)$ which only exploit the information in covariances (\mathbf{t} and \mathbf{S});
3. *balanced*, where both $d_1, d_2 \neq 0$: here for the ReLU $\sigma(t) = \max(t, 0)$, Leaky ReLU (L-ReLU) $a_+ \max(t, 0) + a_- \max(-t, 0)$ [Maas et al., 2013] and the quadratic function $a_2 t^2 + a_1 t + a_0$.

Note that, all mean-oriented functions are odd and all covariance-oriented functions are even. This remark is also reminiscent of a similar conclusion in the α - β kernel discussed in Section 4.3 as well as of the properly scaling inner-product kernel in Section 4.4 on a closely related, yet different, model.

$\sigma(t)$		d_1	d_2	d_0
t		1	0	0
$ t $		0	$\frac{1}{\pi\tau_p}$	$(\frac{1}{2} - \frac{1}{\pi})\tau_p$
$\text{ReLU}(t) \equiv \max(t, 0)$		$\frac{1}{4}$	$\frac{1}{4\pi\tau_p}$	$(\frac{1}{8} - \frac{1}{4\pi})\tau_p$
$\text{LReLU}(t) \equiv a_+ \max(t, 0) + a_- \max(-t, 0)$		$\frac{1}{4}(a_+ - a_-)^2$	$\frac{1}{4\pi\tau_p}(a_+ + a_-)^2$	$\frac{\pi-2}{8\pi}(a_+ + a_-)^2\tau_p$
$a_2 t^2 + a_1 t + a_0$		a_1^2	a_2^2	$\frac{1}{2}\tau_p^2 a_2^2$
$\text{erf}(t)$		$\frac{4}{\pi} \frac{1}{\tau_p+1}$	0	$\frac{2}{\pi} \left(\arccos \frac{\tau_p}{\tau_p+1} - \frac{\tau_p}{\tau_p+1} \right)$
$1_{t>0}$		$\frac{1}{\pi\tau_p}$	0	$\frac{1}{4} - \frac{1}{2\pi}$
$\text{sign}(t)$		$\frac{4}{\pi\tau_p}$	0	$1 - \frac{2}{\pi}$
$\cos(t)$		0	$\frac{1}{4} \cdot e^{-\tau_p/2}$	$\frac{1}{2}(1 + e^{-\tau_p}) - e^{-\tau_p/2}$
$\sin(t)$		$e^{-\tau_p/2}$	0	$\frac{1}{2}(1 - e^{-\tau_p}) - \frac{\tau_p}{2}e^{-\tau_p/2}$
$\exp(-t^2/2)$		0	$\frac{2}{(\tau_p+2)^3}$	$\frac{1}{\sqrt{\tau_p+1}} - \frac{2}{\tau_p+2}$

Table 5.2: Coefficients d_1, d_2 and d_0 for different $\sigma(\cdot)$, with $\tau_p = \frac{2}{p} \text{tr } \mathbf{C}^\circ$. `tab:K-RNN-coef`

Also, similarly to the random kernel matrices discussed in Section 4.5.1, $\tilde{\mathbf{K}}$ in Theorem 5.2 follows a spiked random matrix model and contains the class structural information matrix \mathbf{J} . As a result, the top eigenvectors of the kernel matrix \mathbf{K} are expected to align to (the subspace spanned by the columns of) \mathbf{J} and can be used for spectral clustering.

To corroborate the above classification of different nonlinearities, we perform kernel spectral clustering with **PKP**, in Figure 5.5, on four classes of Gaussian data: $\mathcal{N}(\mu_1, \mathbf{C}_1)$, $\mathcal{N}(\mu_1, \mathbf{C}_2)$, $\mathcal{N}(\mu_2, \mathbf{C}_1)$ and $\mathcal{N}(\mu_2, \mathbf{C}_2)$ with the LReLU function $\text{LReLU}(t) \equiv a_+ \max(t, 0) + a_- \max(-t, 0)$ that takes different values for a_+ and a_- . For $b = 1, 2$, $\mu_b = [\mathbf{0}_{b-1}; 5; \mathbf{0}_{p-b}]$ and $\mathbf{C}_b = (1 + 15(b-1)/\sqrt{p})\mathbf{I}_p$. By choosing $a_+ = -a_- = 1$ (equivalent to $\sigma(t) = |t|$) and $a_+ = a_- = 1$ (equivalent to the linear function $\sigma(t) = t$), with the leading two eigenvectors we always recover two classes instead of four, as each setting of parameters only allows for a part of the statistical information (only mean or only covariance) of the data for clustering. However, by taking $a_+ = 1, a_- = 0$ (i.e., the ReLU function) we distinguish all four classes with the leading two eigenvectors, to which the k-means method can then be applied for a final classification, as shown in Figure 5.6.

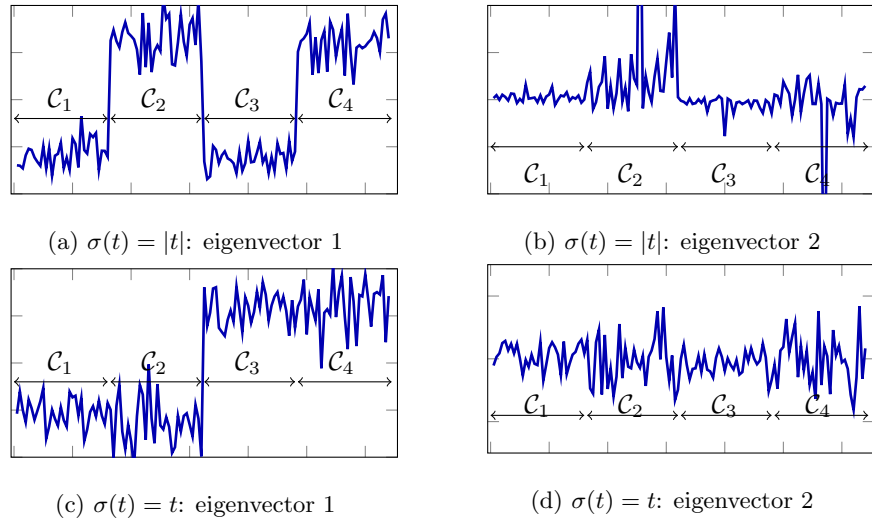


Figure 5.5: Leading two eigenvectors of **PKP** for the LReLU function with $a_+ = -a_- = 1$ (top) and $a_+ = a_- = 1$ (bottom), performed on four classes Gaussian mixture data with $p = 512$, $n = 256$, $c_b = 1/4$ and $\mathbf{j}_b = [\mathbf{0}_{n_{b-1}}; \mathbf{1}_{n_b}; \mathbf{0}_{n-n_b}]$, for $b \in \{1, 2, 3, 4\}$. [Link to code]

`fig:clustering-with-LReLU`

Again, although derived from a simple k -class Gaussian mixture model, Theorem 5.2 establishes an unexpected close match in practice when applied to real-world datasets. To illustrate this claim, we consider two different types of classification tasks: one on the MNIST [LeCun et al., 1998] database (number 6 and 8), and the other on epileptic EEG time series data [Andrzejak et al., 2001]

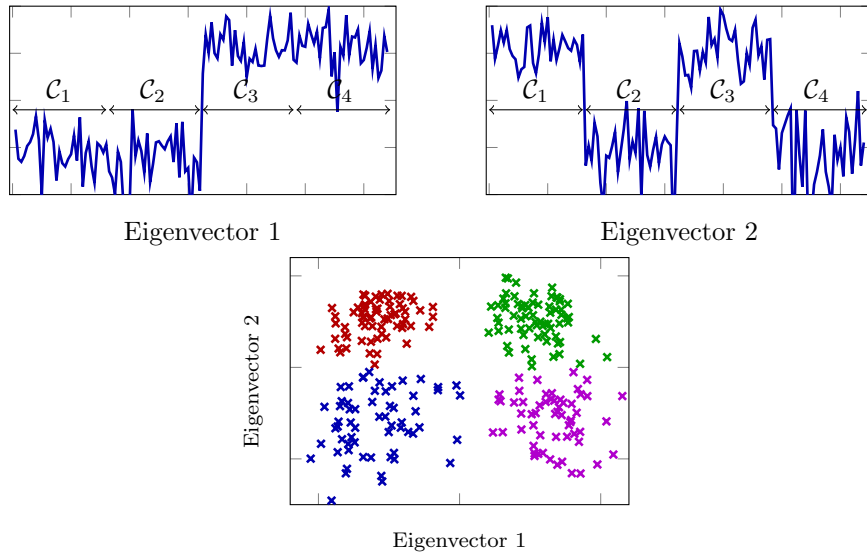


Figure 5.6: Leading two eigenvectors of \mathbf{PKP} (top) for the LReLU function with $a_+ = 1$, $a_- = 0$ (equivalent to $\text{ReLU}(t)$) and two dimensional representation of these eigenvectors (bottom), in the same setting as in Figure 5.5. [Link to code] [fig_clustering_with_ReLU](#)

(set B and E). These two datasets are typical examples of means-dominant (handwritten digits recognition) and covariances-dominant (EEG times series classification) tasks. This is numerically confirmed in Table 5.3.

Table 5.3: Empirical estimation of (normalized) differences in means and covariances of the MNIST and epileptic EEG datasets.

tab:estimation-statistics-data		
	$\ \mathbf{M}^T \mathbf{M}\ $	$\ \mathbf{t} \mathbf{t}^T + 2\mathbf{S}\ $
MNIST data	172.4	86.0
EEG data	1.2	182.7

Recall from (5.11) that the random feature Gram matrix $\frac{1}{N}\sigma(\mathbf{X}^T \mathbf{W}^T)\sigma(\mathbf{W}\mathbf{X}) = \frac{1}{N}\Sigma^T \Sigma$ is an (empirical) estimate of the (expected) kernel matrix \mathbf{K} , and is therefore expected to behave similarly to \mathbf{K} for not-too-small N .

Here we perform random feature-based spectral clustering on data matrices \mathbf{X} that consist of $n = 32, 64$ and 128 randomly selected vectorized images of size $p = 784$ from the MNIST dataset. The k-means method is then applied to the leading two eigenvectors of the Gram matrix $\frac{1}{n}\Sigma^T \Sigma$ that consists of $N = 32$ random features to perform unsupervised classification, with resulting accuracies (averaged over 50 runs) reported in Table 5.4. As seen from Table 5.3, the mean-oriented $\sigma(t)$ functions are expected to outperform the covariance-oriented functions in this task, which is consistent with the results in Table 5.4.

Table 5.4: Classification accuracies for random feature-based spectral clustering with different $\sigma(t)$ on the MNIST dataset.

tab:MNIST-results				
	$\sigma(t)$	$n = 32$	$n = 64$	$n = 128$
mean-oriented	t	85.31%	88.94%	87.30%
	$1_{t>0}$	86.00%	82.94%	85.56%
	$\text{sign}(t)$	81.94%	83.34%	85.22%
	$\sin(t)$	85.31%	87.81%	87.50%
	$\text{erf}(t)$	86.50%	87.28%	86.59%
cov-oriented	$ t $	62.81%	60.41%	57.81%
	$\cos(t)$	62.50%	59.56%	57.72%
	$\exp(-t^2/2)$	64.00%	60.44%	58.67%
balanced	$\text{ReLU}(t)$	82.87%	85.72%	82.27%

For the epileptic EEG dataset [Andrzejak et al., 2001] that is more “covariance-dominant” per Table 5.4, random feature-based spectral clustering on $n = 32, 64$ and 128 randomly picked EEG segments of length $p = 100$ from the dataset. After k-means classification on the leading two eigenvectors of the (centered) Gram matrix composed of $N = 32$ random features, the accuracies (averaged over 50 runs) are reported in Table 5.5 ,where we observe that covariance-oriented functions (i.e., $\sigma(t) = |t|, \cos(t)$ and $\exp(-t^2/2)$) far outperform any other with almost perfect classification accuracies. It is particularly interesting to note that the popular ReLU function is suboptimal in both tasks, but never performs very badly, thereby offering a good risk-performance tradeoff.

Table 5.5: Classification accuracies for random feature-based spectral clustering with different $\sigma(t)$ on the epileptic EEG dataset.

tab:EEG-results				
	$\sigma(t)$	$n = 32$	$n = 64$	$n = 128$
mean-oriented	t	71.81%	70.31%	69.58%
	$1_{t>0}$	65.19%	65.87%	63.47%
	$\text{sign}(t)$	67.13%	64.63%	63.03%
	$\sin(t)$	71.94%	70.34%	68.22%
	$\text{erf}(t)$	69.44%	70.59%	67.70%
cov-oriented	$ t $	99.69%	99.69%	99.50%
	$\cos(t)$	99.00%	99.38%	99.36%
	$\exp(-t^2/2)$	99.81%	99.81%	99.77%
balanced	$\text{ReLU}(t)$	84.50%	87.91%	90.97%

The classification of “mean-oriented”, “covariance-oriented” and “balanced” nonlinearities for nonlinear Gram matrix $\frac{1}{n}\Sigma^\top\Sigma$ also helps explain the performance of different activation functions in neural network models in Figure 5.2 and 5.3. Since the MNIST data have more information in the statistical means, it is not surprising to observe in Figure 5.3 that both training

and test errors of the (covariance-oriented) quadratic activation $\sigma(t) = 1 - t^2/2$ are much higher than the others and the flexible ReLU function achieves the minimal training and test errors in Figure 5.2.

5.2 Gradient descent dynamics in learning linear neural nets

sec:GDD

In Section 5.1 we considered the single-hidden-layer neural network model with random first layer, which, as pointed out in Remark 5.1, is closely connected to random feature maps and kernel methods. More precisely, the analyses in Theorem 5.1 and Corollary 5.1 provide access to the model performance (training and test MSEs) as a function of the nonlinear activation function $\sigma(\cdot)$, through the underlying kernel matrix \mathbf{K} .

Besides these *nonlinear* transformations discussed in Section 5.1, another salient feature of neural network models is that they are routinely trained with the (stochastic) gradient descent method. As a consequence, the network, and thus its performance, are functions of the training time (or the number of descent steps).

In this section, the gradient descent dynamics (GDDs) of learning a ridge regression model (i.e., a single-layer linear network) are considered. For a given training data matrix $\mathbf{X} = [\mathbf{x}_1, \dots, \mathbf{x}_n] \in \mathbb{R}^{p \times n}$ with associated labels $\mathbf{y} = [y_1, \dots, y_n] \in \mathbb{R}^n$, a weight vector $\mathbf{w} \in \mathbb{R}^p$ is learned by minimizing the following (ridge-regularized) square loss

$$L(\mathbf{w}) = \frac{1}{2n} \|\mathbf{y} - \mathbf{X}^\top \mathbf{w}\|^2 + \frac{\gamma}{2} \|\mathbf{w}\|^2 \quad \text{eq:GDD-loss (5.12)}$$

with some regularization penalty $\gamma \geq 0$. The gradient of L with respect to \mathbf{w} is given by $\nabla_{\mathbf{w}} L(\mathbf{w}) = -\frac{1}{n} \mathbf{X}(\mathbf{y} - \mathbf{X}^\top \mathbf{w}) + \gamma \mathbf{w}$ so that with small gradient descent step (or, learning rate) α , we obtain, by performing a continuous-time approximation, the following differential equation

$$\frac{d\mathbf{w}(t)}{dt} = -\alpha \nabla_{\mathbf{w}} L(\mathbf{w}) = \frac{\alpha}{n} \mathbf{X} \mathbf{y} - \alpha \left(\frac{1}{n} \mathbf{X} \mathbf{X}^\top + \gamma \mathbf{I}_p \right) \mathbf{w}$$

the solution of which is explicitly given by

$$\mathbf{w}(t) = e^{-\alpha t \left(\frac{1}{n} \mathbf{X} \mathbf{X}^\top + \gamma \mathbf{I}_p \right)} \mathbf{w}_0 + \left(\mathbf{I}_p - e^{-\alpha t \left(\frac{1}{n} \mathbf{X} \mathbf{X}^\top + \gamma \mathbf{I}_p \right)} \right) \mathbf{w}_\infty \quad \text{eq:w(t) (5.13)}$$

where we denote $\mathbf{w}_0 = \mathbf{w}(t=0)$ the initialization of gradient descent and

$$\mathbf{w}_\infty = \left(\frac{1}{n} \mathbf{X} \mathbf{X}^\top + \gamma \mathbf{I}_p \right)^{-1} \frac{1}{n} \mathbf{X} \mathbf{y} \quad \text{eq:w_inf (5.14)}$$

the ridge regression solution with regularization parameter γ . We recall that the exponential of a symmetric matrix \mathbf{A} is given by $e^{\mathbf{A}} = \sum_{k=0}^{\infty} \frac{1}{k!} \mathbf{A}^k = \mathbf{V} e^{\Lambda} \mathbf{V}^\top$, with $\mathbf{A} = \mathbf{V} \Lambda \mathbf{V}^\top$ the spectral decomposition of \mathbf{A} .

We consider the following symmetric binary Gaussian mixture model for the input data

$$\mathcal{C}_1 : \mathbf{x}_i \sim \mathcal{N}(-\boldsymbol{\mu}, \mathbf{I}_p) \quad \mathcal{C}_2 : \mathbf{x}_i \sim \mathcal{N}(\boldsymbol{\mu}, \mathbf{I}_p)$$

with associated labels $y_i = -1$ and $y_i = 1$, respectively, and we assume as in previous sections the non-trivial setting where $\|\boldsymbol{\mu}\| = O(1)$.

For the linear classifier with $\mathbf{w}(t)$ given by (5.13), the GDDs can be studied by considering the training and test misclassification error rates as

$$\mathbb{P}(\mathbf{x}_i^\top \mathbf{w}(t) > 0 \mid y_i = -1), \quad \mathbb{P}(\hat{\mathbf{x}}^\top \mathbf{w}(t) > 0 \mid \hat{y} = -1)$$

for $\hat{\mathbf{x}} \sim \mathcal{N}(-\boldsymbol{\mu}, \mathbf{I}_p)$ a new test datum (that is independent of the training set (\mathbf{X}, \mathbf{y})), genuinely of label $\hat{y} = -1$.

To evaluate the test performance, since the test datum $\hat{\mathbf{x}}$ is independent of (\mathbf{X}, \mathbf{y}) (and thus of $\mathbf{w}(t)$), conditioned on $\mathbf{w}(t)$, $\mathbf{w}(t)^\top \hat{\mathbf{x}}$ is a Gaussian random variable of mean $\mathbf{w}(t)^\top \boldsymbol{\mu}$ and variance $\|\mathbf{w}(t)\|^2$. The misclassification probability can be retrieved with the Gaussian Q -function and we thus resort to the computation of $\mathbf{w}(t)^\top \boldsymbol{\mu}$ as well as $\mathbf{w}(t)^\top \mathbf{w}(t)$ to assess the classification performance.

For $\boldsymbol{\mu}^\top \mathbf{w}(t)$, with Cauchy's integration formula we have

$$\begin{aligned} \boldsymbol{\mu}^\top \mathbf{w}(t) &= \boldsymbol{\mu}^\top e^{-\alpha t(\frac{1}{n} \mathbf{X} \mathbf{X}^\top + \gamma \mathbf{I}_p)} \mathbf{w}_0 + \boldsymbol{\mu}^\top \left(\mathbf{I}_p - e^{-\alpha t(\frac{1}{n} \mathbf{X} \mathbf{X}^\top + \gamma \mathbf{I}_p)} \right) \mathbf{w}_\infty \\ &= -\frac{1}{2\pi i} \oint_{\Gamma} f_t(z) \boldsymbol{\mu}^\top \left(\frac{1}{n} \mathbf{X} \mathbf{X}^\top + \gamma \mathbf{I}_p - z \mathbf{I}_p \right)^{-1} \mathbf{w}_0 dz \\ &\quad - \frac{1}{2\pi i} \oint_{\Gamma} \frac{1 - f_t(z)}{z} \boldsymbol{\mu}^\top \left(\frac{1}{n} \mathbf{X} \mathbf{X}^\top + \gamma \mathbf{I}_p - z \mathbf{I}_p \right)^{-1} \frac{1}{n} \mathbf{X} \mathbf{y} dz \end{aligned}$$

with $f_t(z) \equiv \exp(-\alpha t z)$ and Γ a positive closed path circling around all the eigenvalues of the (shifted) sample covariance $\frac{1}{n} \mathbf{X} \mathbf{X}^\top + \gamma \mathbf{I}_p$.

Noting that $\mathbf{X} = \boldsymbol{\mu} \mathbf{y}^\top + \mathbf{Z}$ for \mathbf{Z} with i.i.d. standard Gaussian entries, we have, with Lemma 2.7 that

$$\left(\frac{1}{n} \mathbf{X} \mathbf{X}^\top + \gamma \mathbf{I}_p - z \mathbf{I}_p \right)^{-1} = \mathbf{Q}(z) - \mathbf{Q}(z) \mathbf{U} \begin{bmatrix} \|\boldsymbol{\mu}\|^2 m(z) & 1 \\ 1 & -\frac{1}{1 + c m(z)} \end{bmatrix}^{-1} \mathbf{U}^\top \mathbf{Q}(z) + o(1)$$

for $\mathbf{U} = [\boldsymbol{\mu} \quad \frac{1}{n} \mathbf{Z} \mathbf{y}] \in \mathbb{R}^{p \times 2}$ and $\mathbf{Q}(z) \equiv (\frac{1}{n} \mathbf{Z} \mathbf{Z}^\top + \gamma \mathbf{I}_p - z \mathbf{I}_p)^{-1}$ admitting the deterministic equivalent relation (from Theorem 2.3) $\mathbf{Q}(z) \leftrightarrow m(z) \mathbf{I}_p$, with $m(z)$ the unique solution to

$$c(z - \gamma) m^2(z) - (1 - c - z + \gamma) m(z) + 1 = 0. \quad \text{eq:GDD-MP} \quad (5.15)$$

5.2.0.1 Main results

Based on the above deterministic equivalent, the following results on the asymptotic training and test performance can be derived.

theo:GDD-train-test

Theorem 5.3 (Training and test performance of GDD, Liao and Couillet [2018a]). *For random initialization $\mathbf{w}_0 \sim \mathcal{N}(\mathbf{0}, \sigma^2 \mathbf{I}_p/p)$ independent of \mathbf{X} , as $n, p \rightarrow \infty$ with $p/n \rightarrow c \in (0, \infty)$, we have*

$$\begin{aligned}\mathbb{P}(\hat{\mathbf{x}}^\top \mathbf{w}(t) > 0 \mid \hat{y} = -1) - Q\left(\frac{E_{\text{test}}}{\sqrt{V_{\text{test}}}}\right) &\rightarrow 0, \\ \mathbb{P}(\mathbf{x}^\top \mathbf{w}(t) > 0 \mid y = -1) - Q\left(\frac{E_{\text{train}}}{\sqrt{V_{\text{train}}}}\right) &\rightarrow 0,\end{aligned}$$

almost surely, where

$$\begin{aligned}E_{\text{test}} &\equiv -\frac{1}{2\pi i} \oint_{\Gamma} \frac{1-f_t(z)}{z} \frac{\|\boldsymbol{\mu}\|^2 m(z) dz}{(\|\boldsymbol{\mu}\|^2 + c)m(z) + 1} \\ V_{\text{test}} &\equiv \frac{1}{2\pi i} \oint_{\Gamma} \left[\frac{\frac{1}{z^2} (1-f_t(z))^2}{(\|\boldsymbol{\mu}\|^2 + c)m(z) + 1} - \sigma^2 f_t^2(z)m(z) \right] dz \\ E_{\text{train}} &\equiv -\frac{1}{2\pi i} \oint_{\Gamma} \frac{1-f_t(z)}{z} \frac{dz}{(\|\boldsymbol{\mu}\|^2 + c)m(z) + 1} \\ V_{\text{train}} &\equiv \frac{1}{2\pi i} \oint_{\Gamma} \left[\frac{\frac{1}{z} (1-f_t(z))^2}{(\|\boldsymbol{\mu}\|^2 + c)m(z) + 1} - \sigma^2 f_t^2(z)zm(z) \right] dz - E_{\text{train}}^2 - \gamma V_{\text{test}}\end{aligned}$$

with Γ a positive contour surrounding the support of the Marčenko–Pastur law (shifted by $\gamma \geq 0$) and the points $(\gamma, 0)$ and $(\gamma + \lambda_s, 0)$ with $\lambda_s = c + 1 + \|\boldsymbol{\mu}\|^2 + c\|\boldsymbol{\mu}\|^{-2}$, $f_t(z) \equiv \exp(-atz)$ and $m(z)$ given by (5.15).

Note that the point $(\gamma + \lambda_s, 0)$ is the (possible) spike due to the low rank structure $\boldsymbol{\mu}\mathbf{y}^\top$ in \mathbf{X} . We have in particular that

$$\lambda_s = c + 1 + \|\boldsymbol{\mu}\|^2 + \frac{c}{\|\boldsymbol{\mu}\|^2} \geq (\sqrt{c} + 1)^2 \quad \text{eq: def-lambda_s} \quad (5.16)$$

with equality if and only if $\|\boldsymbol{\mu}\|^2 = \sqrt{c}$. As in Theorem 2.12, here we see that the spike isolates from the main bulk of the Marčenko–Pastur support (with right edge $(\sqrt{c} + 1)^2$) only when $\|\boldsymbol{\mu}\|^2 \geq \sqrt{c}$.

However, the expressions in Theorem 5.3 of contour integrations are not easily analyzable nor interpretable. To obtain a more explicit expression, we choose the rectangular contour as in Figure 2.9 that circles around both the main bulk and the isolated eigenvalue (if any). For a shifted version (by γ) of the main bulk of the Marčenko–Pastur law (between $\lambda_- \equiv (1 - \sqrt{c})^2$ and $\lambda_+ \equiv (1 + \sqrt{c})^2$) given by

$$\nu(dx) = \frac{\sqrt{(x - \lambda_-)^+(\lambda_+ - x)^+}}{2\pi cx} dx + (1 - c) \delta(x) \quad \text{eq: def-GDD-MP-measure} \quad (5.17)$$

we know from Theorem 2.9 that the limit $\lim_{\varepsilon_y \rightarrow 0} m(x + i\varepsilon_y)$ exists for x within the support, while the second part which encloses the isolated eigenvalue at

$(\gamma_s + \gamma, 0)$ can be computed by residue calculus. This together leads to the expressions of $(E_{\text{test}}, V_{\text{test}})$ and $(E_{\text{train}}, V_{\text{train}})$ as follows.

$$E_{\text{test}} = \int \frac{1 - f_t(x + \gamma)}{x + \gamma} \omega(dx) \quad \text{eq:GDD-E-test (5.18)}$$

$$V_{\text{test}} = \frac{\|\mu\|^2 + c}{\|\mu\|^2} \int \frac{(1 - f_t(x + \gamma))^2 \omega(dx)}{(x + \gamma)^2} + \sigma^2 \int f_t^2(x + \gamma) \nu(dx) \quad \text{eq:GDD-V-test (5.19)}$$

$$E_{\text{train}} = \frac{\|\mu\|^2 + c}{\|\mu\|^2} \int \frac{1 - f_t(x + \gamma)}{x + \gamma} \omega(dx) \quad \text{eq:GDD-E-train (5.20)}$$

$$V_{\text{train}} = \frac{\|\mu\|^2 + c}{\|\mu\|^2} \int \frac{x(1 - f_t(x + \gamma))^2 \omega(dx)}{(x + \gamma)^2} + \sigma^2 \int x f_t^2(x + \gamma) \nu(dx) - E_{\text{train}}^2 \quad \text{eq:GDD-V-train (5.21)}$$

where we recall $f_t(x) = \exp(-\alpha t x)$, $\nu(x)$ is given by (5.17) and where we introduced the measure

$$\omega(dx) \equiv \frac{\sqrt{(x - \lambda_-)^+ (\lambda_+ - x)^+}}{2\pi(\lambda_s - x)} dx + \frac{(\|\mu\|^4 \text{eq: def-GDD-omega-measure})}{\|\mu\|^2} \delta_{\lambda_s}(x) \quad (5.22)$$

for λ_s defined in (5.16). The expressions in (5.18)-(5.21) are supported by the numerical results in Figure 5.7 with $p = 256$ and $n = 512$.

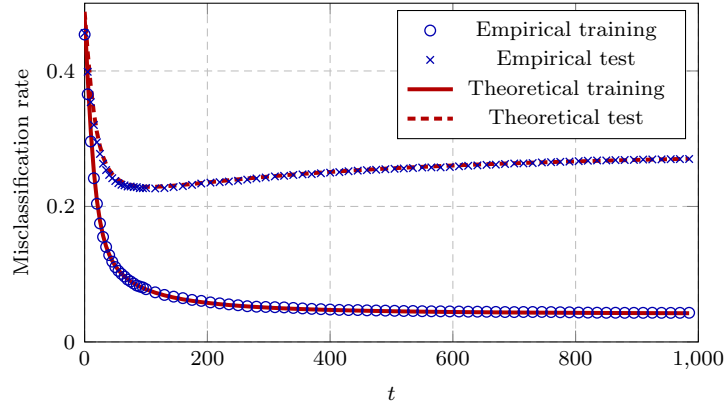


Figure 5.7: Training and test misclassification rate of a linear network as a function of the gradient descent training time t , for $p = 256$, $n = 512$, $\gamma = 0$, $\alpha = 10^{-2}$, $\sigma^2 = 0.1$ and $\mu = [-\mathbf{1}_{p/2}, \mathbf{1}_{p/2}] / \sqrt{p}$. Empirical results averaged over 50 runs. [Link to code]

fig:GDD

5.2.0.2 Practical implications

With the simplified expressions in (5.18)-(5.21), several remarks are in order.

rem:GDD-optimal-perf

Remark 5.2 (Optimal performance). Note that, by the Cauchy–Schwarz inequality and the fact that $\int \omega(dx) = \|\boldsymbol{\mu}\|^2$, we have

$$E_{\text{test}}^2 \leq \int \frac{(1 - f_t(x + \gamma))^2}{(x + \gamma)^2} \omega(dx) \cdot \int \omega(dx) \leq \frac{\|\boldsymbol{\mu}\|^4}{\|\boldsymbol{\mu}\|^2 + c} V_{\text{test}}$$

with equality in the rightmost inequality only when the variance of the random initialization is $\sigma^2 = 0$. We thus have $E_{\text{test}}/\sqrt{V_{\text{test}}} \leq \|\boldsymbol{\mu}\|^2/\sqrt{\|\boldsymbol{\mu}\|^2 + c}$ so that the optimal test performance (lowest misclassification rate) is given by $Q(\|\boldsymbol{\mu}\|^2/\sqrt{\|\boldsymbol{\mu}\|^2 + c})$. This performance bound holds for any classifier obtained by minimizing the ridge-regularization squared loss in (5.12) with gradient descent (for any $t \geq 0$ and any regularization $\gamma \geq 0$). As seen later in Section 6.1, the bound in fact holds for an even larger class of generalized linear classifiers.

Remark 5.3 (Ridge regression and early-stopping). Note that the measures ν and ω defined in (5.17) and (5.22) do not depend on the regularization penalty γ . Since $(1 - f_t(x))/x$ and $f_t(x)$ are both decreasing functions of x , adding a positive ridge regularization $\gamma > 0$ is equivalent to early-stopping the gradient descent algorithm at some $t_\gamma < t$ without regularization (i.e., with $\gamma = 0$). The close connection between ridge regression and early-stopping in gradient descent has been explored in various models and settings [Yao et al., 2007, Suggala et al., 2018, Ali et al., 2019].

Remark 5.4 (Double descent in linear network). As $t \rightarrow \infty$, one obtains the ridge regression solution $\mathbf{w}_\infty = (\mathbf{X}\mathbf{X}^\top + n\gamma\mathbf{I}_p)^{-1}\mathbf{X}\mathbf{y}$, $\lambda \geq 0$ with

$$\frac{\boldsymbol{\mu}^\top \mathbf{w}_\infty}{\|\mathbf{w}_\infty\|} \rightarrow \frac{\|\boldsymbol{\mu}\|^2}{\sqrt{\|\boldsymbol{\mu}\|^2 + c}} \cdot \sqrt{\frac{c\gamma m^2(-\gamma) + 1}{cm(-\gamma) + 1}}$$

for $m(-\gamma)$ the unique positive solution to $-c\gamma m^2(-\gamma) - (1 - c + \gamma)m(-\gamma) + 1 = 0$.

In particular, taking $\lambda \rightarrow 0$ gives the “ridgeless” least-square solution $\mathbf{w}_{LS} = (\mathbf{X}^+)^{\top} \mathbf{y}$ with \mathbf{X}^+ the Moore–Penrose pseudoinverse of \mathbf{X} , that is equivalent to $\mathbf{w}_{LS} = (\mathbf{X}\mathbf{X}^\top)^{-1}\mathbf{X}\mathbf{y}$ for invertible $\mathbf{X}\mathbf{X}^\top$ and $\mathbf{w}_{LS} = \mathbf{X}(\mathbf{X}^\top \mathbf{X})^{-1}\mathbf{y}$ for invertible $\mathbf{X}^\top \mathbf{X}$ so that

$$\frac{\boldsymbol{\mu}^\top \mathbf{w}_{LS}}{\|\mathbf{w}_{LS}\|} \rightarrow \frac{\|\boldsymbol{\mu}\|^2}{\sqrt{\|\boldsymbol{\mu}\|^2 + c}} \cdot \sqrt{1 - \min(c, c^{-1})} \quad \text{eq:perf-w_LS (5.23)}$$

when one of $\mathbf{X}\mathbf{X}^\top$ and $\mathbf{X}^\top \mathbf{X}$ is invertible (which is almost surely the case for $c = \lim p/n \neq 1$). This means that the least-square solution \mathbf{w}_{LS} overfits the training set and the performance drops by a factor $\sqrt{1 - \min(c, c^{-1})}$ compared to the theoretical optimal value in Remark 5.2. This becomes even worse when the ratio p/n gets close to 1 and can be viewed as another manifestation of the “double descent” behavior discussed at the end of Section 5.1.1.2 (here the parameter dimension of $\mathbf{w} \in \mathbb{R}^p$ coincides with the input data dimension p).

Since positive ridge regularization $\gamma > 0$ is known to help alleviate this sharp performance drop at $c = 1$ [Hastie et al., 2019, Mei and Montanari,

[2019], we compare, in Figure 5.8, the misclassification rate as a function of the training time, for $\gamma = 0$ and $\gamma = 0.1$. As t grows large, the regularized classifier with $\gamma = 0.1$ has a test error that saturates at a much lower level than the unregularized classifier with $\gamma = 0$, the test error of which continues to grow (to 0.5 that is equivalent to random guess) as predicted in (5.23).

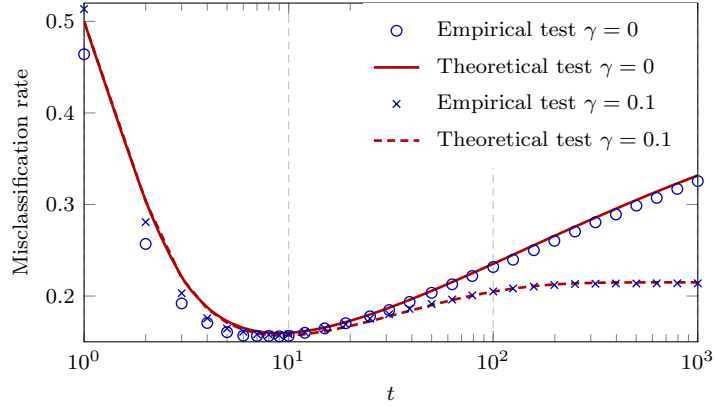


Figure 5.8: Test performance as a function of the training time t , for $n = p = 512$, $\gamma \in \{0, 0.1\}$, $\alpha = 0.1$, $\sigma^2 = 0.1$ and $\mu = [\sqrt{2}, \mathbf{0}_{p-1}]$. Empirical results averaged over 50 runs. [Link to code]

fig:GDD-double-descent

Following a similar direction as presented here, the authors of [Advani et al., 2020] considered the problem of learning, with a gradient descent approach, a similar linear regressor (or a linear single-layer neural network) from n training samples of dimension p , which are however generated by a noisy teacher network; that is, the training labels/targets \mathbf{y} are generated from an independent teacher network taking the same training data \mathbf{X} as input, and then corrupted with additive Gaussian noise. Under the setting of $n, p \rightarrow \infty$ with $p/n \rightarrow c \in (0, \infty)$, they found, by studying the training and test MSEs as a function of the training time (i.e., the number of descent steps), that the overfitting problem becomes most critical when c is close to 1, namely, when the number of parameters of the linear regressor (i.e., the model complexity) p gets close to the number of training data n . Although their theoretical results are limited to the linear regression model, they additionally carried experiments which provide strong evidence that these conclusions extend to deep linear and nonlinear neural networks, as has been discussed in Section 5.1.1.

5.3 Recurrent neural nets: echo-state networks

sec:ESN

5.3.1 Preliminaries and echo state networks

Echo-state neural networks (ESNs), popularized by Jaeger [2001], are elementary and simply parametrized, yet already quite efficient, recurrent neural net-

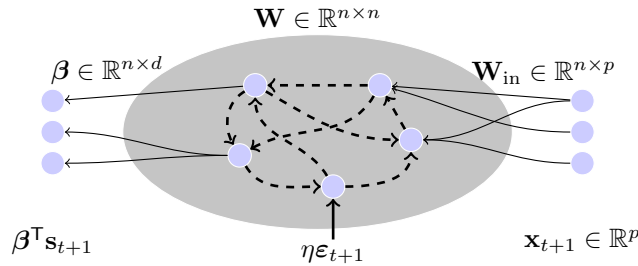


Figure 5.9: Illustration of an echo state network. [fig:ESN](#)

works. Also referred to as *reservoir computing* networks, they consist of a single-hidden layer of size n with state $\mathbf{s}_t \in \mathbb{R}^n$ at time t , which evolves according to:

$$\mathbf{s}_{t+1} = \sigma(\mathbf{W}\mathbf{s}_t + \mathbf{W}_{\text{in}}\mathbf{x}_{t+1} + \eta\varepsilon_{t+1})$$

for $\sigma : \mathbb{R} \rightarrow \mathbb{R}$ an entry-wise activation function, $\mathbf{W} \in \mathbb{R}^{n \times n}$ the neuron connectivity matrix (which induces the recursion), $\mathbf{W}_{\text{in}} \in \mathbb{R}^{n \times p}$ the input layer connection and $\mathbf{x}_t \in \mathbb{R}^p$ the input data at time t . Added to the state is sometimes an independent noise term $\eta\varepsilon_{t+1}$ for $\eta \in \mathbb{R}$, $\varepsilon \sim \mathcal{N}(\mathbf{0}, \mathbf{I}_n)$ mimicking thermal noise inside the network (of relevance in biological modeling of short-term memory neural networks).

In particular, for $\mathbf{W} = \mathbf{0}$ and $\eta = 0$, the network reduces to a nonlinear single-layer projection map, which boils down to a random feature map if \mathbf{W}_{in} is randomly designed.

Assuming the existence of a training dataset $\{(\mathbf{x}_t, \mathbf{y}_t)\}_{t=0}^{T-1}$ over a “time” window T , where $\mathbf{y}_t \in \mathbb{R}^d$ is the expected output at time t , the echo-state network learning consists in a mere linear regression from the state \mathbf{s}_t into the output \mathbf{y}_t by minimizing

$$L(\boldsymbol{\beta}) = \frac{1}{T} \|\mathbf{Y} - \boldsymbol{\beta}^T \mathbf{S}\|_F^2$$

over the regression matrix $\boldsymbol{\beta} \in \mathbb{R}^{n \times d}$, where $\mathbf{X} = [\mathbf{x}_0, \dots, \mathbf{x}_{T-1}] \in \mathbb{R}^{p \times T}$, $\mathbf{Y} = [\mathbf{y}_0, \dots, \mathbf{y}_{T-1}] \in \mathbb{R}^{d \times T}$ and $\mathbf{S} = [\mathbf{s}_0, \dots, \mathbf{s}_{T-1}] \in \mathbb{R}^{n \times T}$. The explicit form of $\boldsymbol{\beta}$ is given by

$$\boldsymbol{\beta} = \begin{cases} \mathbf{S}(\mathbf{S}^T \mathbf{S})^{-1} \mathbf{Y}^T & , n > T; \\ (\mathbf{S} \mathbf{S}^T)^{-1} \mathbf{S} \mathbf{Y}^T & , n < T. \end{cases} \quad (5.24)$$

assuming $\mathbf{S}^T \mathbf{S}$ and $\mathbf{S} \mathbf{S}^T$ is invertible, respectively. Once $\boldsymbol{\beta}$ is set, the corresponding test error on a test set $\hat{\mathbf{X}} \in \mathbb{R}^{p \times \hat{T}}$ with underlying associated output $\hat{\mathbf{Y}} \in \mathbb{R}^{d \times \hat{T}}$ is then given by

$$E_{\text{test}} = \frac{1}{\hat{T}} \|\hat{\mathbf{Y}} - \boldsymbol{\beta}^T \hat{\mathbf{S}}\|_F^2$$

where $\hat{\mathbf{S}} = [\hat{\mathbf{s}}_0, \dots, \hat{\mathbf{s}}_{\hat{T}-1}] \in \mathbb{R}^{n \times \hat{T}}$ and $\hat{\mathbf{s}}_{t+1} = \sigma(\mathbf{W}\hat{\mathbf{s}}_t + \mathbf{W}_{\text{in}}\hat{\mathbf{x}}_{t+1} + \eta\hat{\boldsymbol{\varepsilon}}_{t+1})$, with $\hat{\boldsymbol{\varepsilon}}_t$ independent of $\boldsymbol{\varepsilon}_t$.

Being recursive networks, typical tasks of ESNs are time series regression when \mathbf{y}_t is a function of $\mathbf{x}_t, \mathbf{x}_{t-1}, \dots$, or time series prediction when $\mathbf{y}_t = \mathbf{x}_{t+\tau}$ for a certain $\tau > 0$.

As opposed to more involved recursive networks, such as the popular long short term memory (LSTM) nets [Hochreiter and Schmidhuber, 1997], echo-state networks are extremely easy to train. Yet, they are hyper-parametrized by several key variables: the reservoir connectivity matrix $\mathbf{W} \in \mathbb{R}^{n \times n}$, the input layer $\mathbf{W}_{\text{in}} \in \mathbb{R}^{n \times p}$ and the activation function $\sigma(\cdot)$. Due to the recursive structure though, even in the simplest settings, establishing theoretically the training and test performances remains complex.

Possibly the most important hyperparameter is the spectral radius $\rho(\mathbf{W}) = \max_{1 \leq i \leq n} |\lambda_i(\mathbf{W})|$ (note that the square matrix \mathbf{W} is not imposed to be symmetric so the spectral radius is not necessarily the spectral norm). Indeed, in spirit, the recursive nature of ESNs involves the successive powers \mathbf{W}^t which, for t large, either decays exponentially with t for $\rho(\mathbf{W}) < 1$, thereby only maintaining short term memory in this reservoir, or diverges exponentially for $\rho(\mathbf{W}) > 1$, leading to quickly unstable behavior. The key property of echo-state networks though is that, with a carefully chosen nonlinear activation $\sigma(\cdot)$, values of $\rho(\mathbf{W})$ slightly greater than 1 are still allowed and preserve the stability of the network, placing it in a so-called *near-chaotic* mode.

Yet, the successive iterations involving the nonlinearity $\sigma(\cdot)$ are much less tractable and we shall discuss here the simplified, yet already quite theoretically elaborate, setting where $\sigma(t) = t$ (hence the linear network case), and where \mathbf{W} and \mathbf{W}_{in} are successively fixed deterministic and then set randomly. We also assume the scalar setting where $p = d = 1$ for both input and output variables, letting in particular $\mathbf{W}_{\text{in}} = \mathbf{w}_{\text{in}} \in \mathbb{R}^n$, $\mathbf{X}^\top = \mathbf{x} = [x_0, \dots, x_{T-1}]^\top \in \mathbb{R}^T$, $\mathbf{Y}^\top = \mathbf{y} = [y_0, \dots, y_{T-1}]^\top \in \mathbb{R}^T$, and work under the simultaneously large n, T regime.

5.3.2 Results on ESN asymptotics

Gathering the simplifications above, we consider here the model

$$\mathbf{s}_{t+1} = \mathbf{W}\mathbf{s}_t + \mathbf{w}_{\text{in}}x_{t+1} + \eta\boldsymbol{\varepsilon}_{t+1}$$

with the associated training and test errors given by

$$E_{\text{train}} = \frac{1}{T} \|\mathbf{y} - \mathbf{S}^\top \boldsymbol{\beta}\|^2, \quad E_{\text{test}} = \frac{1}{\hat{T}} \|\hat{\mathbf{y}} - \mathbf{S}^\top \boldsymbol{\beta}\|^2 \stackrel{\text{eq. def. ESN-train-test}}{=} (5.25)$$

and $\boldsymbol{\beta} \in \mathbb{R}^n$ such that

$$\boldsymbol{\beta} = \begin{cases} \mathbf{S}(\mathbf{S}^\top \mathbf{S})^{-1} \mathbf{y} & , n > T; \\ (\mathbf{S} \mathbf{S}^\top)^{-1} \mathbf{S} \mathbf{y} & , n < T. \end{cases} \quad (5.26)$$

For further simplicity of exposition, we particularly focus here on the training performance, which already conveys quite inspiring results. The complete

analyses of both train and test performances are available in [Coullet et al., 2016b].

To investigate the large n, T asymptotics of the training error E_{train} defined in (5.25), first remark that, letting

$$\mathbf{Q}_\gamma \equiv \left(\frac{1}{T} \mathbf{S} \mathbf{S}^\top + \gamma \mathbf{I}_n \right)^{-1} \quad \text{and} \quad \tilde{\mathbf{Q}}_\gamma \equiv \left(\frac{1}{T} \mathbf{S}^\top \mathbf{S} + \gamma \mathbf{I}_T \right)^{-1} \quad (5.27)$$

we have, irrespective of the sign of $n - T$,

$$E_{\text{train}} = \lim_{\gamma \downarrow 0} \frac{\gamma}{T} \mathbf{y}^\top \tilde{\mathbf{Q}}_\gamma \mathbf{y}$$

thereby formulating the estimation problem as the characterization of a quadratic form over the resolvent of $\frac{1}{T} \mathbf{S}^\top \mathbf{S}$.

The specific difficulty induced by \mathbf{S} lies in the intricate dependence between its columns, as successive observations of a multivariate time series. In particular, in order to simplify the analysis and to avoid edge problems at time $t = 0$, we assume (as is conventionally done in practice) that a sufficiently long “washout period” is performed preliminary to observing x_0 , i.e., the considered time series x_0, \dots, x_{T-1} is a finite time extraction of an infinite series $\dots, x_{-1}, x_0, x_1, \dots$; this ensures in particular the stationarity of the random network states $\mathbf{s}_0, \dots, \mathbf{s}_{T-1}$.

With these in mind, we may first describe the state evolution $\mathbf{S} = [\mathbf{s}_0, \dots, \mathbf{s}_{T-1}]$ through the following convenient relation

$$\begin{aligned} \mathbf{S} &= \sqrt{T}(\mathbf{A} + \mathbf{Z}), \quad \mathbf{A} = \mathbf{M}\mathbf{X}, \quad \mathbf{M} = \{\mathbf{W}^j \mathbf{w}_{\text{in}}\}_{j=0}^{T-1} \in \mathbb{R}^{n \times T}, \\ \mathbf{X} &= \frac{\{\mathbf{x}_{j-i}\}_{i,j=0}^{T-1}}{\sqrt{T}} \in \mathbb{R}^{T \times T}, \quad \mathbf{Z} = \frac{\eta}{\sqrt{T}} \left\{ \sum_{k \geq 0} \mathbf{W}^k \boldsymbol{\varepsilon}_{j-k} \right\}_{j=0}^{T-1} \in \mathbb{R}^{n \times T}. \end{aligned}$$

This relation isolates the random part of \mathbf{S} into \mathbf{Z} and the deterministic time series \mathbf{x} into the Toeplitz matrix \mathbf{X} . This expression clearly evidences the important stability condition of the network dynamics, i.e., $\rho(\mathbf{W}) < 1$. We impose this condition from now on.

Using the Gaussian method and Stein’s lemma, Lemma 2.13, we can then evaluate the behavior of the resolvents $\mathbf{Q} \equiv \mathbf{Q}_\gamma$ and $\tilde{\mathbf{Q}} \equiv \tilde{\mathbf{Q}}_\gamma$ by remarking that, for \mathbf{Q} (similar relations being obtained for $\tilde{\mathbf{Q}}$),

$$\mathbb{E}[\mathbf{Q}]_{ij} = \frac{1}{\gamma} \delta_{ij} - \frac{1}{\gamma} \left(\underbrace{\mathbb{E}[\mathbf{Z} \mathbf{Z}^\top \mathbf{Q}]_{ij}}_{(I)} + \underbrace{\mathbb{E}[\mathbf{Z} \mathbf{A}^\top \mathbf{Q}]_{ij}}_{(II)} + \underbrace{\mathbb{E}[\mathbf{A} \mathbf{Z}^\top \mathbf{Q}]_{ij}}_{(III)} + \underbrace{\mathbb{E}[\mathbf{A} \mathbf{A}^\top \mathbf{Q}]_{ij}}_{(IV)} \right)$$

and handle the terms $(I), \dots, (IV)$ subsequently. From the expansion

$$[\mathbf{Z}]_{ab} = \frac{\eta}{\sqrt{T}} \sum_{k \geq 0} \sum_{m=1}^n [\mathbf{W}^k]_{am} \cdot \varepsilon_{m,b-k}$$

we have in particular that

$$\frac{\partial[\mathbf{Z}]_{ab}}{\partial \varepsilon_{il}} = \frac{\eta}{\sqrt{T}} \sum_{k \geq 0} \sum_{q=1}^n \delta_{qi} \delta_{l,b-k} [\mathbf{W}^k]_{aq}$$

and

$$\begin{aligned} \frac{\partial[\mathbf{Q}]_{mj}}{\partial \varepsilon_{il}} &= -\frac{\eta}{\sqrt{T}} \sum_{q=1}^n \delta_{l \leq q} \left([\mathbf{Q}(\mathbf{Z} + \mathbf{A})]_{mq} [(\mathbf{W}^{q-l})^\top \mathbf{Q}]_{ij} \right. \\ &\quad \left. + [(\mathbf{Z} + \mathbf{A})^\top \mathbf{Q}]_{qj} [\mathbf{Q} \mathbf{W}^{q-l}]_{mi} \right). \end{aligned}$$

These two relations are then exploited to develop the terms $(I), \dots, (IV)$, however with a specific difficulty: quite unlike the random matrix models studied so far in the monograph, this formula involves a large sum (over the index q) of successive powers of \mathbf{W} . Fortunately, the exponentially fast decrease of \mathbf{W}^k , due to $\rho(\mathbf{W}) < 1$, makes most of these powers negligible and only roughly $O(\log T)$ of them effectively remain. This, as such, does not impede the technical development and the control of small terms via the Nash-Poincaré inequality, Lemma 2.14; the development is only more cumbersome.

To facilitate the computations and present the results in a simpler form, it is convenient to define the shift matrix $\mathbf{J} \in \mathbb{R}^{T \times T}$ with $[\mathbf{J}^q]_{ij} \equiv \delta_{i+q,j}$, for which $[\mathbf{J}^q \mathbf{B}]_{ij} = [\mathbf{B}]_{q+i,j}$. A careful control of the development ultimately leads to the following deterministic equivalents for \mathbf{Q}_γ and $\tilde{\mathbf{Q}}_\gamma$, established in the limit of simultaneously large n, T ,

$$\begin{aligned} \mathbf{Q}_\gamma \leftrightarrow \bar{\mathbf{Q}}_\gamma &\equiv \frac{1}{\gamma} \left(\mathbf{I}_n + \eta^2 \tilde{\mathbf{R}}_\gamma + \frac{1}{\gamma} \mathbf{A} (\mathbf{I}_T + \eta^2 \mathbf{R}_\gamma)^{-1} \mathbf{A}^\top \right)^{-1} \\ \tilde{\mathbf{Q}}_\gamma \leftrightarrow \bar{\tilde{\mathbf{Q}}}_\gamma &\equiv \frac{1}{\gamma} \left(\mathbf{I}_T + \eta^2 \mathbf{R}_\gamma + \frac{1}{\gamma} \mathbf{A}^\top (\mathbf{I}_n + \eta^2 \tilde{\mathbf{R}}_\gamma)^{-1} \mathbf{A} \right)^{-1} \end{aligned}$$

where $\mathbf{R}_\gamma \in \mathbb{R}^{T \times T}$ and $\tilde{\mathbf{R}}_\gamma \in \mathbb{R}^{n \times n}$ are solutions to

$$\mathbf{R}_\gamma = \left\{ \frac{1}{T} \text{tr} (\mathcal{W}_{i-j} \bar{\mathbf{Q}}_\gamma) \right\}_{i,j=1}^T, \quad \tilde{\mathbf{R}}_\gamma = \sum_{q=-\infty}^{\infty} \frac{1}{T} \text{tr} (\mathbf{J}^q \bar{\tilde{\mathbf{Q}}}_\gamma) \cdot \mathcal{W}_q$$

where $\mathcal{W}_q = \sum_{k \geq 0} \mathbf{W}^{k+(-q)^+} (\mathbf{W}^{k+(q)^+})^\top$ with $(a)^+ = \max(a, 0)$. A detailed development is provided in [Coullet et al., 2016b].

Taking the limit $\lim_{\gamma \downarrow 0} \gamma \tilde{\mathbf{Q}}_\gamma$, we thus find as an immediate corollary that, as $n, T \rightarrow \infty$ with $n/T \rightarrow c \in (0, \infty) \setminus \{1\}$, $E_{\text{train}} - \bar{E}_{\text{train}} \rightarrow 0$ almost surely, with

$$\bar{E}_{\text{train}} = \frac{1}{T} \mathbf{y}^\top \tilde{\mathbf{Q}} \mathbf{y} \cdot 1_{c < 1} + 0 \cdot 1_{c > 1} \quad \text{eq: def-bar-E-train (5.28)}$$

where

$$\begin{aligned}\tilde{\mathcal{Q}} &\equiv \left(\mathbf{I}_T \cdot \delta_{c<1} + \mathcal{R} + \frac{1}{\eta^2} \mathbf{A}^\top \left(\mathbf{I}_n \cdot \delta_{c>1} + \tilde{\mathcal{R}} \right)^{-1} \mathbf{A} \right)^{-1} \\ \mathcal{Q} &\equiv \left(\mathbf{I}_n \cdot \delta_{c>1} + \tilde{\mathcal{R}} + \frac{1}{\eta^2} \mathbf{A} \left(\mathbf{I}_T \cdot \delta_{c<1} + \mathcal{R} \right)^{-1} \mathbf{A}^\top \right)^{-1}\end{aligned}$$

and

$$\begin{aligned}\mathcal{R} &= \left\{ \frac{1}{T} \text{tr} \left(\mathcal{W}_{i-j} \left(\mathbf{I}_n \cdot \delta_{c>1} + \tilde{\mathcal{R}} \right)^{-1} \right) \right\}_{i,j=1}^T \\ \tilde{\mathcal{R}} &= \sum_{q=-\infty}^{\infty} \frac{1}{T} \text{tr} \left(\mathbf{J}^q (\mathbf{I}_T \cdot \delta_{c<1} + \mathcal{R})^{-1} \right) \cdot \mathcal{W}_q.\end{aligned}$$

Due to the ill-defined nature of some of these limits when $\gamma \downarrow 0$, the relations between \mathcal{R} , $\tilde{\mathcal{R}}$, \mathcal{Q} , $\tilde{\mathcal{Q}}$, and their associated \mathbf{R}_γ , $\tilde{\mathbf{R}}_\gamma$, \mathbf{Q}_γ , $\tilde{\mathbf{Q}}_\gamma$ are not mere corresponding limits as $\gamma \downarrow 0$. Specifically, when $c < 1$, we have, as $\gamma \downarrow 0$ that: $\eta^2 \mathbf{R}_\gamma \rightarrow \mathcal{R}$, $\gamma \tilde{\mathbf{R}}_\gamma \rightarrow \tilde{\mathcal{R}}$, $\eta^2 \tilde{\mathbf{Q}}_\gamma \rightarrow \mathcal{Q}$, and $\gamma \tilde{\mathbf{Q}}_\gamma \rightarrow \tilde{\mathcal{Q}}$. When instead $c > 1$, we have correspondingly: $\gamma \mathbf{R}_\gamma \rightarrow \mathcal{R}$, $\eta^2 \tilde{\mathbf{R}}_\gamma \rightarrow \tilde{\mathcal{R}}$, $\gamma \tilde{\mathbf{Q}}_\gamma \rightarrow \mathcal{Q}$, and $\eta^2 \tilde{\mathbf{Q}}_\gamma \rightarrow \tilde{\mathcal{Q}}$.

It is particularly useful to expand the resolvent $\tilde{\mathcal{Q}}$ in the expression of \bar{E}_{train} in (5.28) to retrieve some intuition on this result. Indeed, for $c < 1$, we precisely have

$$\bar{E}_{\text{train}} = \frac{1}{T} \mathbf{y}^\top \left(\mathbf{I}_T + \mathcal{R} + \frac{1}{\eta^2} \mathbf{X}^\top \left\{ \mathbf{w}_{\text{in}}^\top (\mathbf{W}^i)^\top \tilde{\mathcal{R}}^{-1} \mathbf{W}^j \mathbf{w}_{\text{in}} \right\}_{i,j=0}^{T-1} \mathbf{X} \right)^{-1} \mathbf{y}.$$

As such, the memory (training) performance of the network particularly depends on the typical speed of decay of the entries of $\left\{ \mathbf{w}_{\text{in}}^\top (\mathbf{W}^i)^\top \tilde{\mathcal{R}}^{-1} \mathbf{W}^j \mathbf{w}_{\text{in}} \right\}$ as one moves away from its $(1, 1)$ entry. A particularly telling example is the pure-memory task by which $\mathbf{x} = [\sqrt{T}, \mathbf{0}_{T-1}]$ (all the vector energy is concentrated at time 0) and $\mathbf{y} = [\mathbf{0}_{\tau-1}, \sqrt{T}, \mathbf{0}_{T-\tau}]$, that is we wish to recover at time τ the value of x_0 . Then, we find that

$$\bar{E}_{\text{train}} = \left[\left(\mathbf{I}_T + \mathcal{R} + \frac{1}{\eta^2} \mathbf{X}^\top \left\{ \mathbf{w}_{\text{in}}^\top (\mathbf{W}^i)^\top \tilde{\mathcal{R}}^{-1} \mathbf{W}^j \mathbf{w}_{\text{in}} \right\}_{i,j=0}^{T-1} \mathbf{X} \right)^{-1} \right]_{\tau+1, \tau+1}.$$

As shown subsequently, for \mathbf{W} (non-symmetric) having random independent zero mean entries, all off-diagonal entries of \mathcal{R} and $\left\{ \mathbf{w}_{\text{in}}^\top (\mathbf{W}^i)^\top \tilde{\mathcal{R}}^{-1} \mathbf{W}^j \mathbf{w}_{\text{in}} \right\}$ asymptotically vanish, and we have in this case

$$\bar{E}_{\text{train}} = \frac{\eta^2}{\eta^2 (1 + [\mathcal{R}]_{11}) + \mathbf{w}_{\text{in}}^\top (\mathbf{W}^\tau)^\top \tilde{\mathcal{R}}^{-1} \mathbf{W}^\tau \mathbf{w}_{\text{in}}}.$$

For arbitrary \mathbf{W} and \mathbf{w}_{in} , these performance asymptotics may not be quite expressive though. Simpler forms of the performance emerge when considering

randomly drawn connectivity matrices. In particular, for $c < 1$, letting \mathbf{w}_{in} be independent of \mathbf{W} and of unit norm and $\mathbf{W} = \alpha \mathbf{W}^\circ$ where $\mathbf{W}^\circ \in \mathbb{R}^{n \times n}$ is a Haar matrix (see Section 2.6.2.3) and $\alpha < 1$, we find that

$$\bar{E}_{\text{train}} = (1 - c) \frac{1}{T} \mathbf{y}^\top \left(\mathbf{I}_T + \frac{1}{\eta^2} \mathbf{X}^\top \mathbf{D} \mathbf{X} \right)^{-1} \mathbf{y} \quad \text{eq:ESN_perf Haar} \quad (5.29)$$

where $\mathbf{D} = \text{diag}\{(1 - \alpha^2)\alpha^{2(i-1)}\}_{i=1}^T$ and $\alpha < 1$ plays the role of a (short-term) memory depth parameter.

This result may be further expanded into a “multi-modal memory” structure for $\mathbf{W} \in \mathbb{R}^{n \times n}$ by letting $\mathbf{W} = \text{diag}(\mathbf{W}_1, \dots, \mathbf{W}_k)$ where $\mathbf{W}_i = \alpha_i \mathbf{W}_i^\circ$ and $\mathbf{W}_i^\circ \in \mathbb{R}^{n_i \times n_i}$ is a Haar matrix independent of all other \mathbf{W}_j° 's as well as $\sum_{i=1}^k n_i = n$. Writing $c_i = \lim_n n_i/n \in (0, 1)$, \bar{E}_{train} has the same form as in (5.29) above, however with $\mathbf{D} = \text{diag}\{[\mathbf{D}]_{ii}\}_{i=1}^T$ now given by

$$[\mathbf{D}]_{ii} = \frac{\sum_{j=1}^k c_j \alpha_j^{2(i-1)}}{\sum_{j=1}^k c_j (1 - \alpha_j^2)^{-1}}.$$

By letting $\alpha_1 < \dots < \alpha_k < 1$, this form of \mathbf{D} is interesting as it exhibits a “controlled” decay of the memory capacity for a range of memory depths α_j .

In particular, defining formally the memory capacity $\text{MC}(\tau; \mathbf{W})$ as the inverse training error for a pure data recovery shifted by τ in the noiseless limit, i.e.,

$$\text{MC}(\tau; \mathbf{W}) = \lim_{\eta \downarrow 0} \eta^2 E_{\text{train}}^{-1}, \quad \text{for } \mathbf{x} = [\sqrt{T}, \mathbf{0}_{T-1}], \mathbf{y} = [\mathbf{0}_{\tau-1}, \sqrt{T}, \mathbf{0}_{T-\tau}] \quad (5.30)$$

we obtain the typical memory curves depicted in Figure 5.10. This expression of the “memory capacity” of the network is tightly connected with the so-called Fisher memory curve proposed in [Ganguli et al., 2008] as an alternative measure of the network memory.

In these recurrent network structures, symmetry constraints in \mathbf{W} were shown in the literature not to be generally profitable, although few arguments are proposed to support this claim [Canaday, 2019, Section 5.5]. The deterministic equivalents obtained above allow for a better understanding, as exemplified by Figure 5.11 which compares the matrices \mathcal{R} for \mathbf{W} Gaussian symmetric or non-symmetric: the symmetric \mathbf{W} case exhibits an erratic behavior with a quite specific and structured correlation of the time-delayed source data; the associated loss in performances in both mean squared error and memory capacity of symmetric reservoirs is corroborated by the theoretical results displayed in Figure 5.12.

These asymptotic results established in this section, along with the further studies carried out in [Couillet et al., 2016b], allow for a thorough understanding and further improvement of the design of random connectivity matrices aiming for enhanced (possibly selective) memory performance of the networks.

The above study, and the theoretical literature on echo-state network performance as a whole, is nonetheless limited to the case of linear nets, while we

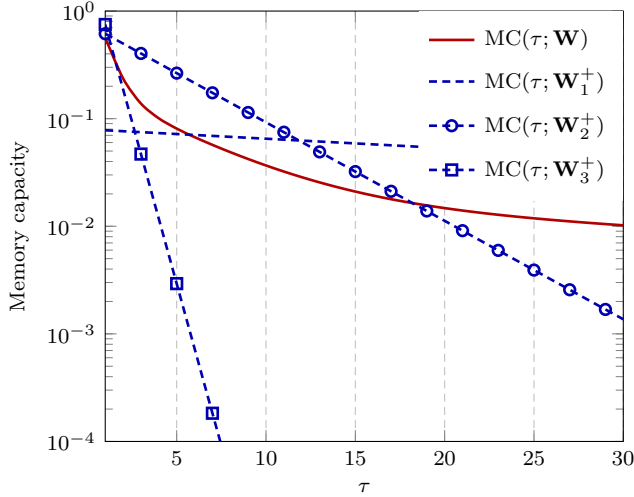


Figure 5.10: Memory curves for $\mathbf{W} = \text{diag}(\mathbf{W}_1, \mathbf{W}_2, \mathbf{W}_3)$, $\mathbf{W}_j = \alpha_j \mathbf{W}_j^o$, $\mathbf{W}_j^o \in \mathbb{R}^{n_j \times n_j}$ Haar distributed, $\alpha_1 = 0.99$, $n_1/n = 0.01$, $\alpha_2 = 0.9$, $n_2/n = 0.1$, and $\alpha_3 = 0.5$, $n_3/n = 0.89$, compared to single-mode memory with \mathbf{W}_i^+ such that $\mathbf{W}_i^+ = \alpha_i \mathbf{W}_i^{+o}$ for Haar $\mathbf{W}_i^{+o} \in \mathbb{R}^{n \times n}$, $n/T = 0.75$. [Link to code] [fig:MC](#)

claimed above the very interest of these networks to lie in the combination of a nonlinear function $\sigma(\cdot)$ and of a carefully chosen spectral radius $\rho(\mathbf{W}) > 1$. In the same way as the performance of deep feedforward neural networks (even trained ones with fully random weight matrices) is difficult to study, notably due to their accumulating nonlinearities under the form $\sigma(\mathbf{W}_L \sigma(\mathbf{W}_{L-1} \cdots \sigma(\mathbf{W}_1 \mathbf{x}_i)))$, the performance of nonlinear echo-state networks remains an open riddle.

5.4 Concluding remarks

In this chapter, by leveraging tools from the concentration of measure theory (see Section 2.7), we went beyond the (mere) Taylor expansion-based approach to the understanding of nonlinear transformations for kernel methods in Chapter 4, and evaluated the large dimensional asymptotics, of a single-hidden-layer *nonlinear* neural network model in Section 5.1 for real-world data. As we shall see later in Chapter 8, this “universal large dimensional concentration” argument has an even more significant impact in practical applications and will be exploited to extend the current analyses and insights (on the choice of kernel function and activation function) to a much broader and more realistic setting.

There has been a growing interest in the eigenspectra, or more generally the large dimensional asymptotics of (random) neural network models. These investigations include the (limiting) eigenspectral measure of the nonlinear Gram matrices [Pennington and Worah, 2017, Benigni and Péché, 2019] (similar to

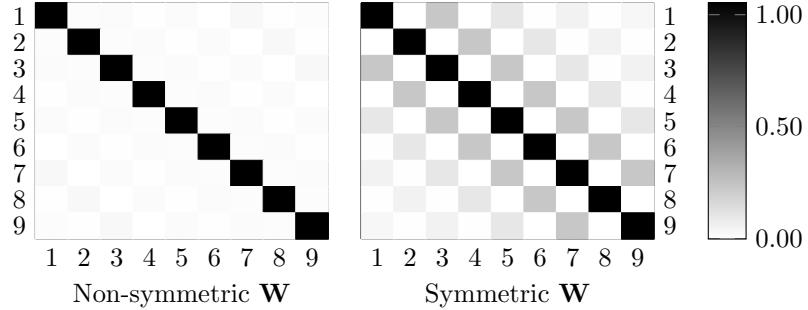


Figure 5.11: Upper 9×9 part of \mathcal{R} for $c = 1/2$ for $\mathbf{W} = \alpha \mathbf{W}^\circ$, $\alpha = 0.9$, and \mathbf{W}° with i.i.d. zero mean and variance $1/n$ non-symmetric Gaussian entries (**left**) and symmetric-Gaussian (**right**). Linear grayscale representation with black being 1 and white being 0. [\[Link to code\]](#)

`fig:checkerboard`

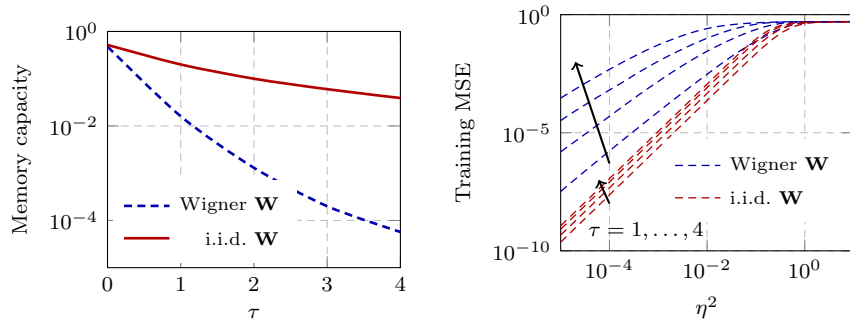


Figure 5.12: Symmetric versus non-symmetric \mathbf{W} performance ($\mathbf{W} = \alpha \mathbf{W}^\circ$, \mathbf{W}° with i.i.d. $\mathcal{N}(0, 1/n)$ entries possibly up to symmetry; $\alpha = 0.9$): (**Left**) Memory curve $MC(\tau; \mathbf{W})$; (**Right**) Training performance of a τ -delay task for $\tau \in \{1, \dots, 4\}$ on the popular Mackey-Glass near-chaotic model [[Glass and Mackey, 1979](#)].

`fig:MC_iid_Wigner`

Section 5.1), as well as that of the input-output Jacobian matrices [Pennington et al., 2017, Pastur, 2020] (closely connected to the behavior of back propagation gradients) of a multilayer neural network with random Gaussian or orthogonal weights. These analyses are not limited to classical feedforward fully connected networks but have been performed on networks with convolutional [Novak et al., 2018, Xiao et al., 2018], recurrent [Chen et al., 2018, Gilboa et al., 2019] and skip-connection structures [Ling and Qiu, 2019] (as in the case of the popular residual network architecture [He et al., 2016]), to name a few. Since random (Gaussian) initializations are widely used in training such deep networks [Glorot and Bengio, 2010], these works shed important light on the initial “landscape” of deep neural networks as well as on the impact of nonlinear activations.

The investigations on randomly weighted neural networks are of even greater interest through the *neural tangent kernel* recently introduced by Jacot et al. [2018]: while the weight matrices *after* training are no longer random, the underlying neural tangent kernel is determined only by the random initialization and remains unchanged during the whole training procedure in the “infinite-neurons” limit. As such, the eigenspectral assessments of the neural tangent kernel of randomly weighted deep networks go beyond the initial stage of training and leads to much richer results on, for example, the learning dynamics of networks [Fan and Wang, 2020, Adlam and Pennington, 2020], at least in this so-called neural tangent limit where the networks widths are *much larger* than both the number of training data n and their dimension p . Nonetheless, most of these works are concerned with random noise-like input data (e.g., i.i.d. Gaussian data or almost orthonormal data [Fan and Wang, 2020, Adlam et al., 2019]) with no information structure, and thus fail to provide sharp qualitative predictions on real-world datasets such as the MNIST dataset. In this respect, considering more involved structural data models, together with the “universal large dimensional concentration” to be discussed later in Chapter 8, is expected to bring greater insights into these elaborate learning systems in a more precise and qualitative manner that better match real-world observations.

Focusing on the optimization methods used in neural network training, we discussed in Section 5.2 the gradient descent dynamics in learning a simple ridge regression model arising from the minimization of the (ridge-regularized) square loss, which enjoys the advantage of having an explicit solution. In the more general context of modern machine learning, however, this is rarely the case: (i) the optimization problem often has no closed-form solution and, perhaps even worse, (ii) it may not be guaranteed to have a *unique* solution, due to the non-convex nature of the problem, for instance in the case of deep neural network models. The non-convexity has long been one of the main technical difficulties for a more solid theoretical understanding of the deep learning method.

In pursuit of the theoretical understanding of the non-convex “loss landscape” of deep networks, Bray and Dean [2007] studied the nature of critical points of *random Gaussian fields* in a high dimensional setting from a statistical physics approach, by evaluating for instance the fraction of negative eigenvalues of the Hessian at critical points. This type of analyses provides precise descrip-

tions on the “chance” of continuing to decrease the loss function as well as on the number of saddle points (with indefinite Hessian) or “bad” local minima (that have significantly higher loss values) [Dauphin et al., 2014, Choromanska et al., 2015, Pennington and Bahri, 2017]. Nonetheless, these works are formally based on statistical physics models quite different from actual neural networks (such as the spin glass model) and require quite restrictive assumptions. A clear and more precise picture of the large dimensional statistical loss landscape of deep networks that accounts for the influence of the network depth, width, choice of nonlinear activation, etc., is still in need.

While optimization problems with non-explicit solutions are ubiquitous in machine learning and pose additional technical difficulty in evaluating their performances, many of the convex problems (that admit a unique solution) still remain accessible in the large dimensional regime. As a telling example, when the more commonly used *cross-entropy* loss (rather than the square loss)

$$L(\boldsymbol{\beta}) = -\frac{1}{n} \sum_{i=1}^n [y_i \log(\sigma(\boldsymbol{\beta}^\top \mathbf{x}_i)) + (1 - y_i) \log(1 - \sigma(\boldsymbol{\beta}^\top \mathbf{x}_i))] \quad (5.31)$$

is adopted to learn a (generalized) linear classifier $\boldsymbol{\beta}$ from a training set $\{(\mathbf{x}_i, y_i)\}_{i=1}^n$, with $\sigma(t) = (1 + e^{-t})^{-1}$ the *logistic sigmoid* function and label $y_i \in \{0, 1\}$, no closed-form solution exists for the loss-minimizing solution $\boldsymbol{\beta}$. In fact, due to the intricate dependence of the learned classifier $\boldsymbol{\beta}$ on $\{\mathbf{x}_i, y_i\}_{i=1}^n$, the statistical behavior of $\boldsymbol{\beta}$ is highly non-trivial to tackle and this gets even worse with the application of the logistic sigmoid nonlinearity $\sigma(\cdot)$. Despite all these technical difficulties, it is nonetheless possible to pursue a large dimensional stochastic description of $\boldsymbol{\beta}$ and consequently to evaluate the performance of, not only the logistic regression classifier, but also any smooth convex loss L that falls into the general *empirical risk minimization* framework discussed in the next chapter.

5.5 Practical course material

Practical Lecture Material 5 (Effective kernel of large dimensional random Fourier features). *As discussed in Remark 5.1, instead of the single-type non-linearity setting in Figure 5.1 thoroughly investigated in Section 5.1.1, from a random feature map and kernel approximation perspective, a mixture of nonlinearities such as ‘cos + sin’ in the case of random Fourier features [Rahimi and Recht, 2008] turns out to be a more natural choice. Specifically, for $\mathbf{W} \in \mathbb{R}^{N \times p}$ with independent standard Gaussian entries, the random Fourier features refer to the cascade of the random features from both ‘cos’ and ‘sin’ activations as*

$$\boldsymbol{\Sigma}^\top = [\cos(\mathbf{W}\mathbf{X})^\top \quad \sin(\mathbf{W}\mathbf{X})^\top] \in \mathbb{R}^{n \times 2N}. \quad (5.32)$$

Using the fact that $\mathbb{E}_{\mathbf{w}}[\cos(\mathbf{w}^\top \mathbf{x}_i) \sin(\mathbf{w}^\top \mathbf{x}_j)] = 0$ for $\mathbf{w} \sim \mathcal{N}(0, \mathbf{I}_p)$ and that both $\cos(\cdot)$ and $\sin(\cdot)$ are 1-Lipschitz, show, with the help of Lemma 5.1 and

similar to Theorem 5.1, that the random Fourier resolvent $(\frac{1}{n}\Sigma^\top \Sigma + \gamma \mathbf{I}_n)^{-1}$ admits the following deterministic equivalent

$$\mathbf{Q} \leftrightarrow \bar{\mathbf{Q}}, \quad \bar{\mathbf{Q}} \equiv \left(\frac{N}{n} \left(\frac{\mathbf{K}_{\cos}}{1 + \delta_{\cos}} + \frac{\mathbf{K}_{\sin}}{1 + \delta_{\sin}} \right) + \gamma \mathbf{I}_n \right)^{-1}$$

for $(\delta_{\cos}, \delta_{\sin})$ the unique positive solution to

$$\delta_{\cos} = \frac{1}{n} \operatorname{tr} \mathbf{K}_{\cos} \bar{\mathbf{Q}}, \quad \delta_{\sin} = \frac{1}{n} \operatorname{tr} \mathbf{K}_{\sin} \bar{\mathbf{Q}}$$

with \mathbf{K}_{\cos} and \mathbf{K}_{\sin} the limiting kernels of ‘cos’ and ‘sin’ nonlinearities enlisted in Table 5.1, respectively.

Then, similar to Corollary 5.1, show that the asymptotic training and test MSEs takes the following forms

$$\begin{aligned} \bar{E}_{\text{train}} &= \frac{\gamma^2}{n} \operatorname{tr} \mathbf{Y} \bar{\mathbf{Q}}^2 \mathbf{Y}^\top \\ &\quad + \frac{N}{n} \frac{\gamma^2}{n} \left[\frac{1}{n} \operatorname{tr} \bar{\mathbf{Q}} \bar{\mathbf{K}}_{\cos} \bar{\mathbf{Q}} - \frac{1}{n} \operatorname{tr} \bar{\mathbf{Q}} \bar{\mathbf{K}}_{\sin} \bar{\mathbf{Q}} \right] \Omega \begin{bmatrix} \operatorname{tr} \mathbf{Y} \bar{\mathbf{Q}} \bar{\mathbf{K}}_{\cos} \bar{\mathbf{Q}} \mathbf{Y}^\top \\ \operatorname{tr} \mathbf{Y} \bar{\mathbf{Q}} \bar{\mathbf{K}}_{\sin} \bar{\mathbf{Q}} \mathbf{Y}^\top \end{bmatrix} \\ \bar{E}_{\text{test}} &= \frac{1}{\hat{n}} \|\hat{\mathbf{Y}}^\top - \Phi_{\mathbf{X}\hat{\mathbf{X}}}^\top \bar{\mathbf{Q}} \mathbf{Y}^\top\|_F^2 \\ &\quad + \left(\frac{N}{n} \right)^2 \frac{1}{\hat{n}} [\Theta_{\cos} \quad \Theta_{\sin}] \Omega \begin{bmatrix} \operatorname{tr} \mathbf{Y} \bar{\mathbf{Q}} \bar{\mathbf{K}}_{\cos} \bar{\mathbf{Q}} \mathbf{Y}^\top \\ \operatorname{tr} \mathbf{Y} \bar{\mathbf{Q}} \bar{\mathbf{K}}_{\sin} \bar{\mathbf{Q}} \mathbf{Y}^\top \end{bmatrix} \end{aligned}$$

with $\bar{\mathbf{K}}_{\cos} \equiv \frac{\mathbf{K}_{\cos}}{1 + \delta_{\cos}}$, $\bar{\mathbf{K}}_{\sin} \equiv \frac{\mathbf{K}_{\sin}}{1 + \delta_{\sin}}$,

$$\Omega^{-1} = \mathbf{I}_2 - \frac{N}{n} \begin{bmatrix} \frac{1}{n} \operatorname{tr} \bar{\mathbf{Q}} \bar{\mathbf{K}}_{\cos} \bar{\mathbf{Q}} \bar{\mathbf{K}}_{\cos} & \frac{1}{n} \operatorname{tr} \bar{\mathbf{Q}} \bar{\mathbf{K}}_{\cos} \bar{\mathbf{Q}} \bar{\mathbf{K}}_{\sin} \\ \frac{(1 + \delta_{\cos})^2}{n} & \frac{(1 + \delta_{\sin})^2}{n} \\ \frac{1}{n} \operatorname{tr} \bar{\mathbf{Q}} \bar{\mathbf{K}}_{\sin} \bar{\mathbf{Q}} \bar{\mathbf{K}}_{\cos} & \frac{1}{n} \operatorname{tr} \bar{\mathbf{Q}} \bar{\mathbf{K}}_{\sin} \bar{\mathbf{Q}} \bar{\mathbf{K}}_{\sin} \\ \frac{(1 + \delta_{\cos})^2}{n} & \frac{(1 + \delta_{\sin})^2}{n} \end{bmatrix}$$

and, for $\sigma \in \{\cos, \sin\}$,

$$\begin{aligned} \Theta_\sigma &\equiv \frac{1}{1 + \delta_\sigma} \left(\frac{1}{N} \operatorname{tr} \bar{\mathbf{K}}_\sigma \hat{\mathbf{x}} \hat{\mathbf{x}}^\top + \frac{N}{n} \frac{1}{n} \operatorname{tr} \bar{\mathbf{Q}} \Phi_{\mathbf{X}\hat{\mathbf{X}}} \Phi_{\mathbf{X}\hat{\mathbf{X}}}^\top \bar{\mathbf{Q}} \bar{\mathbf{K}}_\sigma - \frac{2}{N} \operatorname{tr} \bar{\mathbf{Q}} \Phi_{\mathbf{X}\hat{\mathbf{X}}} (\mathbf{K}_\sigma \hat{\mathbf{x}} \hat{\mathbf{x}}^\top)^\top \right) \\ \Phi &\equiv \frac{N}{n} (\bar{\mathbf{K}}_{\cos} + \bar{\mathbf{K}}_{\sin}), \quad \Phi_{\mathbf{X}\hat{\mathbf{X}}} = \frac{N}{n} (\bar{\mathbf{K}}_{\cos}^{\mathbf{X}\hat{\mathbf{X}}} + \bar{\mathbf{K}}_{\sin}^{\mathbf{X}\hat{\mathbf{X}}}). \end{aligned}$$

Confirm numerically that for not-too-large ratio N/n as in Figure 5.13, a significant gap exists between empirical training MSE of random Fourier ridge regression and the classical Gaussian kernel prediction on MNIST data, while the large N, p, n asymptotics derived above consistently fits empirical observations almost perfectly.

Check also that a double-descent singularity behavior occurs when $\gamma \rightarrow 0$, however at $2N = n$ (rather than $N = n$ as in the case of single nonlinearity discussed at the end of Section 5.1.1.2), due the singular behavior of the two by two matrix Ω^{-1} .

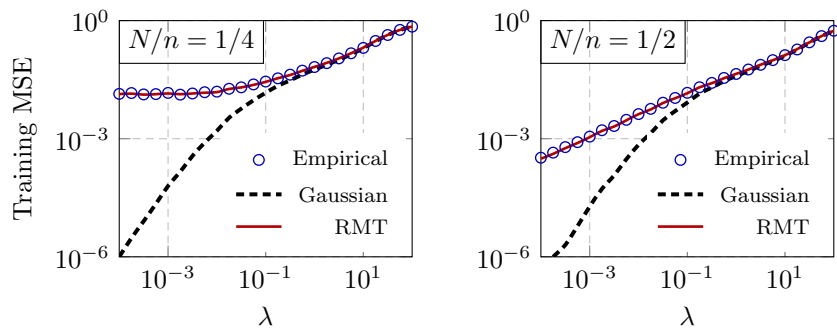


Figure 5.13: Training MSEs of RFF ridge regression on MNIST data (class 3 versus 7), as a function of regression penalty λ , for $p = 784$, $n = 1\,024$, $N = 256$ and 512 . Empirical results displayed in **blue** circles; Gaussian kernel predictions (assuming $N \rightarrow \infty$ alone) in **black** dashed lines; and RMT predictions in **red** solid lines. Results obtained by averaging over 30 runs. [\[Link to code\]](#)
`fig.compare_kernel-RMT`

Chapter 6

Optimization-based Methods with Non-explicit Solutions

chap:optimization

Unlike kernel eigenspectra-based methods in Section 4 or simple neural network models in Section 5, where the objects of study (e.g., kernel matrices and random feature ridge regressors) are given in a rather *explicit* manner, many other machine learning algorithms take the form of (the solutions of) optimization problems, having in general *no closed-form* expressions. A first example is the popular logistic regression algorithm, where one aims to find, in a binary classification setting, an optimal linear classifier $\beta \in \mathbb{R}^p$ by minimizing the logistic loss $\frac{1}{n} \sum_{i=1}^n \log(1 + e^{-y_i \beta^\top \mathbf{x}_i})$ over a training set $\{(\mathbf{x}_i, y_i)\}_{i=1}^n$ with labels $y_i \in \{-1, +1\}$. More generally, by choosing other loss functions rather than the logistic loss, logistic regression can be viewed as a special case of the *empirical risk minimization* [Vapnik, 1992] problem

$$\arg \min_{\beta \in \mathbb{R}^p} \frac{1}{n} \sum_{i=1}^n L(y_i \beta^\top \mathbf{x}_i) + \frac{\gamma}{2} \|\beta\|^2 \quad (6.1)$$

for some convex loss $L : \mathbb{R} \rightarrow \mathbb{R}^+$ and regularization factor $\gamma \geq 0$. With the logistic loss $L(t) = \log(1 + e^{-t})$ one gets the logistic regression, while the least-squares classifier (or ridge regressor) can be obtained with the square loss $L(t) = (t - 1)^2$. Other popular choices of $L(\cdot)$ include the exponential loss $L(t) = e^{-t}$ widely used in boosting algorithms [Freund et al., 1999] and the hinge loss $L(t) = \max(0, 1 - t)$ in the case of support vector machines (SVMs) [Rosasco et al., 2004]. Figure 6.1 illustrates these different losses.

Except for the least-squares solution where $L(t) = (t - 1)^2$, the minimization of a generic loss L generally leads to a classifier β which only takes an *implicit* form. It is thus less clear how the resulting β depends on the data \mathbf{X} , and makes it more challenging to investigate its (large dimensional) statistical behavior.

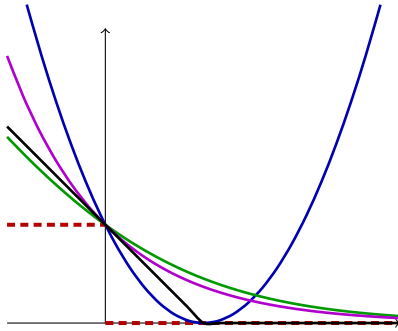


Figure 6.1: Different loss functions for classification: 0–1 loss (red), logistic loss (green), exponential loss (purple), square loss (blue) and hinge loss (black)

The technical challenge from implicit optimization problems appears not only in the analysis of logistic regression, but also in most other machine learning algorithms of daily use, starting with the popular deep learning schemes. It is therefore of crucial importance to adapt the random matrix-based analysis framework discussed in the previous chapters to assess the performance of optimization-based learning methods. In this chapter, we focus on the empirical risk minimization example of (6.1) and evaluate the large dimensional behavior of the classifier β . Technically, a major emphasis will be cast on the “leave-one-out” approach, which aims to “decouple” the intricate statistical dependencies within the learning system.

6.1 Generalized linear classifier

sec:ERM

6.1.1 Basic setting

For simplicity of exposition, we consider the problem of classifying a binary symmetric Gaussian mixture of the form

$$\mathcal{C}_1 : \mathbf{x}_i \sim \mathcal{N}(-\mu, \mathbf{C}), y_i = -1 \quad \mathcal{C}_2 : \mathbf{x}_i \sim \mathcal{N}(+\mu, \mathbf{C}), y_i = +1 \quad \text{eq:ERM-mixture-model (6.2)}$$

each with a class prior probability of 1/2, for some $\mu \in \mathbb{R}^p$ and positive definite $\mathbf{C} \in \mathbb{R}^{p \times p}$. As in the previous chapters, we ensure the classification problem is asymptotically non-trivial by specifying the following growth rate assumptions.

$$\|\mu\| = O(1), \quad \max\{\|\mathbf{C}\|, \|\mathbf{C}^{-1}\|\} = O(1). \quad \text{eq:growth-ERM (6.3)}$$

Note that the mixture model in (6.2) satisfies the logistic model in the sense that the conditional class probability is

$$\begin{aligned} P(y | \mathbf{x}) &= \frac{P(y)P(\mathbf{x} | y)}{P(\mathbf{x})} = \frac{e^{-\frac{1}{2}(\mathbf{x}-y\mu)\mathbf{C}^{-1}(\mathbf{x}-y\mu)}}{e^{-\frac{1}{2}(\mathbf{x}-\mu)\mathbf{C}^{-1}(\mathbf{x}-\mu)} + e^{-\frac{1}{2}(\mathbf{x}+\mu)\mathbf{C}^{-1}(\mathbf{x}+\mu)}} \\ &= \frac{1}{1 + e^{-2y\mu^\top \mathbf{C}^{-1}\mathbf{x}}} \equiv \sigma(\beta_*^\top y\mathbf{x}), \quad \beta_* \equiv 2\mathbf{C}^\top \mu \quad \text{eq:def-ERM-beta-star (6.4)} \end{aligned}$$

with $\sigma(t) = (1 + e^{-t})^{-1}$ the *logistic sigmoid* function and the optimal Bayes solution $\beta_* = 2\mathbf{C}^{-1}\mu$. By the symmetry of (6.2), it is convenient to use the shortcut notation $\tilde{\mathbf{x}}_i \equiv y_i \mathbf{x}_i$ so that

$$\tilde{\mathbf{x}}_i \sim \mathcal{N}(\mu, \mathbf{C})$$

regardless of the class of \mathbf{x}_i .

To investigate the large dimensional asymptotics of the implicit classifier that minimizes the empirical risk in (6.1), the main technical difficulty lies in the fact that β , as the solution of a convex optimization problem, depends on all the random $\tilde{\mathbf{x}}_i$'s in a rather involved manner. Nonetheless, by canceling the loss function derivative with respect to β in (6.1), we can still obtain the following seemingly simple equation satisfied by β ,

$$\gamma\beta = \frac{1}{n} \sum_{i=1}^n -L'(\beta^\top \tilde{\mathbf{x}}_i) \tilde{\mathbf{x}}_i \quad \text{eq:ERM-eq-beta (6.5)}$$

where we assume the loss function L is convex and at least three-times continuously differentiable (making β unique for $\gamma > 0$). We provide, in the following section, the main “leave-one-out” intuition of crucial significance in building up the system of equations which (asymptotically) characterizes the statistical behavior of β .

6.1.2 Intuitions and main results

subsec:intuition-ERM

The proof of the main results on the asymptotic characterization of β is based on the “leave-one-out” intuition similar to the proof of Theorem 2.3, to solve a “leave-one-version” of (6.5) (without the i -th datum $\tilde{\mathbf{x}}_i$), the solution of which should be asymptotically close to the original solution β , so as to form a self-consistent equation for β . Here we focus on providing a few intuitive arguments to convey the main idea, with the proof details given in [Mai and Liao, 2019].

From (6.5), β can be viewed as a linear combination of all $\tilde{\mathbf{x}}_i$'s, weighted by the coefficient $-L'(\beta^\top \tilde{\mathbf{x}}_i)$. The idea is to understand how $\tilde{\mathbf{x}}_i$ affects the corresponding coefficient $-L'(\beta^\top \tilde{\mathbf{x}}_i)$. To handle the complex dependence of β on all $\tilde{\mathbf{x}}_i$'s, we establish a “leave-one-out” version of β , denoted β_{-i} , that is (i) asymptotically close to β by removing the contribution of a single datum and (ii) that is independent of $\tilde{\mathbf{x}}_i$, by solving (6.1) for all data $\tilde{\mathbf{x}}_j$ different from $\tilde{\mathbf{x}}_i$, that is

$$\gamma\beta_{-i} = \frac{1}{n} \sum_{j \neq i} -L'(\beta_{-i}^\top \tilde{\mathbf{x}}_j) \tilde{\mathbf{x}}_j.$$

As a consequence, the difference $\lambda(\beta - \beta_{-i})$ satisfies

$$\gamma(\beta - \beta_{-i}) = \frac{1}{n} \sum_{j \neq i} (L'(\beta_{-i}^\top \tilde{\mathbf{x}}_j) - L'(\beta^\top \tilde{\mathbf{x}}_j)) \tilde{\mathbf{x}}_j - \frac{1}{n} L'(\beta^\top \tilde{\mathbf{x}}_i) \tilde{\mathbf{x}}_i. \quad \text{eq:diff-beta (6.6)}$$

Intuitively, the difference $\|\beta - \beta_{-i}\|$ must vanish as $n, p \rightarrow \infty$ so that, by Taylor expanding L' around $\beta_{-i}^\top \tilde{\mathbf{x}}_j$, $j \neq i$, one obtains

$$L'(\beta^\top \tilde{\mathbf{x}}_j) = L'(\beta_{-i}^\top \tilde{\mathbf{x}}_j) + L''(\beta_{-i}^\top \tilde{\mathbf{x}}_j)(\beta - \beta_{-i})^\top \tilde{\mathbf{x}}_j + O(\|\beta - \beta_{-i}\|^2).$$

Ignoring higher order terms, together with (6.6), this leads to the following equation for $\beta - \beta_{-i}$

$$\gamma(\beta - \beta_{-i}) \simeq -\frac{1}{n} \sum_{j \neq i} L''(\beta_{-i}^\top \tilde{\mathbf{x}}_j) \tilde{\mathbf{x}}_j \tilde{\mathbf{x}}_j^\top (\beta - \beta_{-i}) - \frac{1}{n} L'(\beta^\top \tilde{\mathbf{x}}_i) \tilde{\mathbf{x}}_i$$

or equivalently

$$\left(\frac{1}{n} \tilde{\mathbf{X}}_{-i} \mathbf{D}_{-i} \tilde{\mathbf{X}}_{-i}^\top + \gamma \mathbf{I}_p \right) (\beta - \beta_{-i}) \simeq -\frac{1}{n} L'(\beta^\top \tilde{\mathbf{x}}_i) \tilde{\mathbf{x}}_i$$

with $\tilde{\mathbf{X}}_{-i} = [\tilde{\mathbf{x}}_1, \dots, \tilde{\mathbf{x}}_{i-1}, \tilde{\mathbf{x}}_{i+1}, \dots, \tilde{\mathbf{x}}_n] \in \mathbb{R}^{p \times (n-1)}$ and diagonal $\mathbf{D}_{-i} \in \mathbb{R}^{(n-1) \times (n-1)}$ with $[\mathbf{D}_{-i}]_{jj} = L''(\beta_{-i}^\top \tilde{\mathbf{x}}_j)$ that are both independent of \mathbf{x}_i .

Note further by the convexity of L that $L''(t) \geq 0$ for all t , so that for any $\gamma > 0$, the matrix $\frac{1}{n} \tilde{\mathbf{X}}_{-i} \mathbf{D}_{-i} \tilde{\mathbf{X}}_{-i}^\top + \gamma \mathbf{I}_p$ is positive definite (and invertible). Thus we may write

$$\beta - \beta_{-i} \simeq -\frac{1}{n} L'(\beta^\top \tilde{\mathbf{x}}_i) \left(\frac{1}{n} \tilde{\mathbf{X}}_{-i} \mathbf{D}_{-i} \tilde{\mathbf{X}}_{-i}^\top + \gamma \mathbf{I}_p \right)^{-1} \tilde{\mathbf{x}}_i$$

which, while not solving a linear regression problem, once again involves the *resolvent* of (a “weights” version of) the sample covariance matrix of the training data.

In particular, projecting against $\tilde{\mathbf{x}}_i$ gives

$$(\beta - \beta_{-i})^\top \tilde{\mathbf{x}}_i \simeq -\frac{1}{n} L'(\beta^\top \tilde{\mathbf{x}}_i) \tilde{\mathbf{x}}_i^\top \left(\frac{1}{n} \tilde{\mathbf{X}}_{-i} \mathbf{D}_{-i} \tilde{\mathbf{X}}_{-i}^\top + \gamma \mathbf{I}_p \right)^{-1} \tilde{\mathbf{x}}_i. \quad (6.7)$$

At this point, note that $(\frac{1}{n} \tilde{\mathbf{X}}_{-i} \mathbf{D}_{-i} \tilde{\mathbf{X}}_{-i}^\top + \gamma \mathbf{I}_p)^{-1}$ is of bounded spectral norm (by $1/\gamma$) and independent of $\tilde{\mathbf{x}}_i = \mu + \mathbf{C}^{\frac{1}{2}} \mathbf{z}_i$ for $\mathbf{z}_i \sim \mathcal{N}(\mathbf{0}, \mathbf{I}_p)$. By the trace lemma (Lemma 2.11), one must therefore have under the growth rate (6.3) that, as $n \rightarrow \infty$

$$\frac{1}{n} \tilde{\mathbf{x}}_i^\top \left(\frac{1}{n} \tilde{\mathbf{X}}_{-i} \mathbf{D}_{-i} \tilde{\mathbf{X}}_{-i}^\top + \gamma \mathbf{I}_p \right)^{-1} \tilde{\mathbf{x}}_i - \delta \xrightarrow{\text{eq.:ERM-approx-quadratic}} 0 \quad (6.8)$$

with δ the unique positive solution to¹

$$\delta = \frac{1}{n} \operatorname{tr} \mathbf{C} \left(\mathbb{E} \left[\frac{L''(\beta^\top \tilde{\mathbf{x}})}{1 + \delta L''(\beta^\top \tilde{\mathbf{x}})} \right] \mathbf{C} + \gamma \mathbf{I}_p \right)^{-1}. \quad (6.9)$$

¹Formally, \mathbf{D}_{-i} is *not independent* of \mathbf{X}_{-i} , so that Lemma 2.11 does not lead straightforwardly to the form in (6.9); yet, with additional arguments detailed in [Mai and Liao, 2019], this dependence can be shown to asymptotically vanish.

The positiveness of δ follows from the quadratic form in (6.8). As for uniqueness, it is guaranteed by rewriting the trace relation under the form

$$1 = \frac{1}{n} \sum_{i=1}^p \frac{\lambda_i}{\left(1 - \mathbb{E}\left[\frac{1}{1+\delta L''(\cdot)}\right]\right) \lambda_i + \gamma \delta} \equiv g(\delta)$$

with $\{\lambda_i\}_{i=1}^p$ the eigenvalues of \mathbf{C} and noticing that, for $L''(\cdot) \geq 0$, $g(\delta)$ is a decreasing function of δ with $\lim_{\delta \rightarrow 0} g(\delta) \rightarrow \infty$ and $\lim_{\delta \rightarrow \infty} g(\delta) \rightarrow 0$. This ensures the uniqueness of δ as g is thus one-to-one from $(0, \infty)$ to $(0, \infty)$.

Back to the expression of (6.8), it now unfolds from (6.7) that

$$\boldsymbol{\beta}^\top \tilde{\mathbf{x}}_i \simeq \boldsymbol{\beta}_{-i}^\top \tilde{\mathbf{x}}_i - \delta L'(\boldsymbol{\beta}^\top \tilde{\mathbf{x}}_i).$$

Solving for $\boldsymbol{\beta}^\top \tilde{\mathbf{x}}_i$, we may remark that $\boldsymbol{\beta}^\top \tilde{\mathbf{x}}_i$ is (approximately) explicitly given by the proximal operator of $\boldsymbol{\beta}_{-i}^\top \tilde{\mathbf{x}}_i$ for the function δL , i.e.,

$$\boldsymbol{\beta}^\top \tilde{\mathbf{x}}_i \simeq \text{prox}_{\delta L}(\boldsymbol{\beta}_{-i}^\top \tilde{\mathbf{x}}_i)$$

with $\text{prox}_{\delta L}(t)$ the *proximal mapping* [Bauschke and Combettes, 2011], defined as the *unique* solution of the minimization problem

$$\text{prox}_{\delta L}(t) \equiv \arg \min_{x \in \mathbb{R}} \left\{ \delta L(x) + \frac{1}{2}(x - t)^2 \right\}. \quad \text{eq: def-prox (6.10)}$$

As a consequence, replacing in (6.5) gives the approximation

$$\gamma \boldsymbol{\beta} \simeq \frac{1}{n} \sum_{i=1}^n -L'(\text{prox}_{\delta L}(\boldsymbol{\beta}_{-i}^\top \tilde{\mathbf{x}}_i)) \tilde{\mathbf{x}}_i \equiv \frac{1}{n} \sum_{i=1}^n f(\boldsymbol{\beta}_{-i}^\top \tilde{\mathbf{x}}_i) \tilde{\mathbf{x}}_i, \quad \text{eq: ERM-f (6.11)}$$

where we denoted $f(x) \equiv -L'(\text{prox}_{\delta L}(x)) = (\text{prox}_{\delta L}(x) - x)/\delta$, which follows from differentiating the (convex) right-hand side of (6.10).

Equation (6.11) establishes an asymptotic connection between $\boldsymbol{\beta}$ and (the average of) the “leave-one-out” $\boldsymbol{\beta}_{-i}$. One may want for instance to take the expectation (6.11) to retrieve $\mathbb{E}[\boldsymbol{\beta}]$ as a function of the expectation of $\tilde{\mathbf{x}}_i$. However, the expectation of the type $\mathbb{E}_{\tilde{\mathbf{x}}_i}[f(\boldsymbol{\beta}_{-i}^\top \tilde{\mathbf{x}}_i) \tilde{\mathbf{x}}_i]$ is delicate to handle due to the $\tilde{\mathbf{x}}_i$ inside the nonlinear function $f(\cdot)$. This can be resolved by using the Gaussianity of $\tilde{\mathbf{x}}_i$ with the following decomposition: recall now that $\tilde{\mathbf{x}}_i = \boldsymbol{\mu} + \mathbf{C}^{\frac{1}{2}} \mathbf{z}_i$ for $\mathbf{z}_i \sim \mathcal{N}(\mathbf{0}, \mathbf{I}_p)$, so that by conditioning on $\boldsymbol{\beta}_{-i}$ (which is independent of \mathbf{z}_i), one can decompose \mathbf{z}_i under the form

$$\mathbf{z}_i = \eta_i \frac{\mathbf{C}^{\frac{1}{2}} \boldsymbol{\beta}_{-i}}{\sqrt{\boldsymbol{\beta}_{-i}^\top \mathbf{C} \boldsymbol{\beta}_{-i}}} + \mathbf{z}_i^\perp, \quad \eta_i = \frac{\boldsymbol{\beta}_{-i}^\top \mathbf{C}^{\frac{1}{2}} \mathbf{z}_i}{\sqrt{\boldsymbol{\beta}_{-i}^\top \mathbf{C} \boldsymbol{\beta}_{-i}}} \quad \text{eq: ERM-decom (6.12)}$$

with $\mathbf{C}^{\frac{1}{2}} \boldsymbol{\beta}_{-i} / \sqrt{\boldsymbol{\beta}_{-i}^\top \mathbf{C} \boldsymbol{\beta}_{-i}}$ the unit vector oriented in the direction of $\mathbf{C}^{\frac{1}{2}} \boldsymbol{\beta}_{-i}$ and \mathbf{z}_i^\perp lying on the $(p-1)$ -dimensional subspace orthogonal to $\mathbf{C}^{1/2} \boldsymbol{\beta}_{-i}$. By the

orthogonal invariance of the standard multivariate Gaussian distribution, both η_i and \mathbf{z}_i^\perp are Gaussian and orthogonal, thus independent. This is a natural decomposition of \mathbf{z}_i to reduce the fluctuation $\beta_{-i}^\top \mathbf{C}^{1/2} \mathbf{z}_i$ in the expansion of $\beta_{-i}^\top \tilde{\mathbf{x}}_i$ to the scalar fluctuation of $\eta_i \sim \mathcal{N}(0, 1)$ (since $\beta_{-i}^\top \mathbf{C}^{1/2} \mathbf{z}_i^\perp = 0$).

Exploiting this decomposition, (6.11) becomes

$$\begin{aligned}\gamma\beta &\simeq \frac{1}{n} \sum_{i=1}^n f(\beta_{-i}^\top \tilde{\mathbf{x}}_i)(\mu + \mathbf{C}^{1/2} \mathbf{z}_i) = \frac{1}{n} \sum_{i=1}^n f(\beta_{-i}^\top \mu + \beta_{-i}^\top \mathbf{C}^{1/2} \mathbf{z}_i)(\mu + \mathbf{C}^{1/2} \mathbf{z}_i) \\ &= \frac{1}{n} \sum_{i=1}^n f\left(\beta_{-i}^\top \mu + \sqrt{\beta_{-i}^\top \mathbf{C} \beta_{-i}} \eta_i\right) \left(\mu + \frac{\eta_i \mathbf{C} \beta_{-i}}{\sqrt{\beta_{-i}^\top \mathbf{C} \beta_{-i}}} + \mathbf{C}^{1/2} \mathbf{z}_i^\perp\right)\end{aligned}$$

for $\eta_i \sim \mathcal{N}(0, 1)$ (conditioned on β_{-i}) and *independent* of \mathbf{z}_i^\perp , which is more convenient to work with.

By construction, β_{-i} is independent of $\tilde{\mathbf{x}}_i$, so that, conditioning on β_{-i} the norm of which should converge to a limit (the same as that of $\|\beta\|$), one expects to have $\beta_{-i}^\top \tilde{\mathbf{x}}_i \sim \mathcal{N}(M, \sigma^2)$ in the large p, n limit. The deterministic pair (M, σ^2) is however so far unknown, but it must satisfy

$$M \simeq \mathbb{E}[\beta_{-i}^\top \mu] \simeq \beta_{-i}^\top \mu, \quad \sigma^2 \simeq \mathbb{E}[\beta_{-i}^\top \mathbf{C} \beta_{-i}] \simeq \beta_{-i}^\top \mathbf{C} \beta_{-i} \tag{6.13} \quad \text{eq: ERM-M-sigma2}$$

with a concentration argument. Intuitively, the variable variable $\beta^\top \mu$ characterizes the (expected) projection of β on a new datum (of mean μ) and determines the classification performance of β that should be asymptotically deterministic. A similar argument holds for $\beta_{-i}^\top \mathbf{C} \beta_{-i}$.

Assuming this indeed holds, we have, as $n, p \rightarrow \infty$,

$$\begin{aligned}\frac{1}{n} \sum_{i=1}^n f(\beta_{-i}^\top \tilde{\mathbf{x}}_i) \mu &\simeq \mathbb{E}[r] \mu, \\ \frac{1}{n} \sum_{i=1}^n f(\beta_{-i}^\top \tilde{\mathbf{x}}_i) \frac{\eta_i \mathbf{C} \beta_{-i}}{\sqrt{\beta_{-i}^\top \mathbf{C} \beta_{-i}}} &= \frac{1}{n} \sum_{i=1}^n f\left(\beta_{-i}^\top \mu + \sqrt{\beta_{-i}^\top \mathbf{C} \beta_{-i}} \cdot \eta_i\right) \frac{\eta_i \mathbf{C} \beta_{-i}}{\sqrt{\beta_{-i}^\top \mathbf{C} \beta_{-i}}} \\ &\simeq \left(\frac{1}{n} \sum_{i=1}^n f(M + \sigma \eta_i) \eta_i\right) \cdot \frac{\mathbf{C} \beta}{\sigma} \\ &\simeq \frac{\mathbb{E}[f(r)(r - M)]}{\sigma^2} \mathbf{C} \beta,\end{aligned}$$

for $r \sim \mathcal{N}(M, \sigma^2)$ with the law of large numbers, where for the second term we use that $\beta_{-i} \simeq \beta$. As such, (6.11) further reads

$$\gamma\beta \simeq \mathbb{E}[f(r)] \mu + \frac{\mathbb{E}[f(r)(r - M)]}{\sigma^2} \mathbf{C} \beta + \frac{1}{n} \sum_{i=1}^n f(M + \sigma \cdot \eta_i) \mathbf{C}^\perp \mathbf{z}_i^\perp \tag{6.14} \quad \text{eq: ERM-beta-eq}$$

for η_i behaves asymptotically like a standard Gaussian variable, where we retain the last term under the form of (the sum of) random vectors \mathbf{z}_i^\perp since, unlike

the second term where all β_{-i} are asymptotically “in the same direction”, the \mathbf{z}_i^\perp ’s asymptotically behave like \mathbf{z}_i and are totally random (in fact, uniformly distributed on the unit sphere of radius \sqrt{p}), so we do not see “the effect of averaging” for the third term as for the second term. Further remark that with the decomposition in (6.12), \mathbf{z}_i^\perp is independent of η_i , so that by denoting $\mathbf{u} = \frac{1}{n} \sum_{i=1}^n f(M + \sigma \cdot \eta_i) \mathbf{C}^{\frac{1}{2}} \mathbf{z}_i^\perp$, we should have

$$\mathbb{E}[\mathbf{u}] = \mathbf{0}, \quad \mathbb{E}[\mathbf{u}\mathbf{u}^\top] \simeq \frac{\mathbb{E}[f^2(r)]}{n} \mathbf{C} \quad (6.15)$$

which, together with an asymptotically Gaussian fluctuation argument, leads to

$$\mathbf{u} \sim \mathcal{N} \left(\mathbf{0}, \frac{\mathbb{E}[f^2(r)]}{n} \mathbf{C} \right)$$

which is of the same amplitude as $\boldsymbol{\mu}$, and thus not negligible.

Solving (6.14) for $\boldsymbol{\beta}$ gives

$$(\mathbb{E}[f'(r)]\mathbf{C} + \gamma \mathbf{I}_p)\boldsymbol{\beta} \simeq \mathbb{E}[f(r)]\boldsymbol{\mu} + \mathbf{u} \quad \text{eq: ERM-f-improve} \quad (6.16)$$

which unfolds from an integration by parts to write $\mathbb{E}[f(r)(r - M)]/\sigma^2 = -\mathbb{E}[f'(r)]$. This provides a *stochastic* characterization of $\boldsymbol{\beta}$ as the sum of a deterministic ($\mathbb{E}[f(r)]\boldsymbol{\mu}$) and a random (\mathbf{u}) part.

To close the loop and connect (M, σ^2) to the data statistics $\boldsymbol{\mu}, \mathbf{C}$ and particularly to those of $\boldsymbol{\beta}$, recall from (6.13) and $\boldsymbol{\beta}_{-i} \simeq \boldsymbol{\beta}$ that

$$M \simeq \mathbb{E}[\boldsymbol{\beta}]^\top \boldsymbol{\mu}, \quad \sigma^2 \simeq \text{tr}(\mathbf{C}\mathbb{E}[\boldsymbol{\beta}\boldsymbol{\beta}^\top]).$$

Therefore, taking the expectation of both sides of (6.16) and solving for $\mathbb{E}[\boldsymbol{\beta}]$, one reaches

$$\mathbb{E}[\boldsymbol{\beta}] \simeq \mathbb{E}[f(r)](\mathbb{E}[f'(r)]\mathbf{C} + \gamma \mathbf{I}_p)^{-1}\boldsymbol{\mu}.$$

Recalling the definition $f : x \mapsto -(x - \text{prox}_{\delta L}(x))/\delta$ where $\delta > 0$, by the firmly non-expansive nature of the proximal mapping (see detail in [Bauschke and Combettes, 2011, Chapter 12]), it unfolds that $f'(\cdot) \geq 0$ and that the inverse in (6.16) is well defined for any $\gamma > 0$.

Lastly, using again (6.16),

$$\begin{aligned} \mathbb{E}[\boldsymbol{\beta}\boldsymbol{\beta}^\top] &\simeq (\mathbb{E}[f(r)])^2 (\mathbb{E}[f'(r)]\mathbf{C} + \gamma \mathbf{I}_p)^{-1} \boldsymbol{\mu} \boldsymbol{\mu}^\top (\mathbb{E}[f'(r)]\mathbf{C} + \gamma \mathbf{I}_p)^{-1} \\ &\quad + (\mathbb{E}[f'(r)]\mathbf{C} + \gamma \mathbf{I}_p)^{-1} \mathbb{E}[\mathbf{u}\mathbf{u}^\top] (\mathbb{E}[f'(r)]\mathbf{C} + \gamma \mathbf{I}_p)^{-1} \end{aligned}$$

so that

$$\begin{aligned} \sigma^2 &\simeq (\mathbb{E}[f(r)])^2 \cdot \boldsymbol{\mu}^\top (\mathbb{E}[f'(r)]\mathbf{C} + \gamma \mathbf{I}_p)^{-1} \mathbf{C} (\mathbb{E}[f'(r)]\mathbf{C} + \gamma \mathbf{I}_p)^{-1} \boldsymbol{\mu} \\ &\quad + \mathbb{E}[f^2(r)] \cdot \frac{1}{n} \text{tr} [(\mathbb{E}[f'(r)]\mathbf{C} + \gamma \mathbf{I}_p)^{-2} \mathbf{C}^2]. \end{aligned}$$

The above heuristic derivation is summarized in the following theorem.

Theorem 6.1 (Asymptotic behavior of β , [Mai and Liao, 2019, Theorem 1])
 $\text{theo:ERM-regularize}$
). For $\max\{\|\mu\|, \|\mathbf{C}\|, \|\mathbf{C}^{-1}\|\} = O(1)$, convex and three-times continuously differentiable L and β the unique solution to (6.1), we have, as $n, p \rightarrow \infty$,

$$\|\beta - \tilde{\beta}\| \rightarrow 0, \quad (\mathbb{E}[f'(r)]\mathbf{C} + \gamma\mathbf{I}_p)\tilde{\beta} \sim \mathcal{N}(\mathbb{E}[f(r)]\mu, \mathbb{E}[f^2(r)]\mathbf{C}/n)$$

where $f(r) = -L'(\text{prox}_{\delta L}(r))$, $r \sim \mathcal{N}(M, \sigma^2)$, and (M, σ^2) solution to

$$\begin{aligned} M &= \mathbb{E}[f(r)] \cdot \mu^\top (\mathbb{E}[f'(r)]\mathbf{C} + \gamma\mathbf{I}_p)^{-1}\mu, \\ \sigma^2 &= (\mathbb{E}[f(r)])^2 \cdot \mu^\top (\mathbb{E}[f'(r)]\mathbf{C} + \gamma\mathbf{I}_p)^{-1}\mathbf{C}(\mathbb{E}[f'(r)]\mathbf{C} + \gamma\mathbf{I}_p)^{-1}\mu \\ &\quad + \mathbb{E}[f^2(r)] \cdot \frac{1}{n} \text{tr}[(\mathbb{E}[f'(r)]\mathbf{C} + \gamma\mathbf{I}_p)^{-2}\mathbf{C}^2] \end{aligned}$$

with δ the unique positive solution to

$$\delta = \frac{1}{n} \text{tr} \mathbf{C} \left(\mathbb{E} \left[\frac{L''(\text{prox}_{\delta L}(r))}{1 + \delta L''(\text{prox}_{\delta L}(r))} \right] \mathbf{C} + \gamma\mathbf{I}_p \right)^{-1}.$$

Note that here $\tilde{\beta}$ (and thus β) is of norm order $O(1)$ (like μ), so if μ (and thus the mean $\mathbb{E}[f(t)](\mathbb{E}[f'(r)]\mathbf{C} + \gamma\mathbf{I}_p)^{-1}\mu$ of $\tilde{\beta}$) is *delocalized* in the sense that its entries are of order $O(1/\sqrt{p})$, the entries of $\tilde{\beta}$ then fluctuate as $O(1/\sqrt{p})$, thus at the same order as their means: the vector is therefore not asymptotically deterministic. We will come back to this point in more detail later.

From the above “leave-one-out” derivation, since β_{-i} is by construction independent of $\tilde{\mathbf{x}}_i$, the random variable $r_i = \beta_{-i}^\top \tilde{\mathbf{x}}_i$ is asymptotically close to $\beta^\top \tilde{\mathbf{x}}$, that is, the projection of the classifier β on a new datum $\tilde{\mathbf{x}} \sim \mathcal{N}(\mu, \mathbf{C})$. This gives access to the asymptotic test classification error rate

$$\mathbb{P}(\beta^\top \tilde{\mathbf{x}} < 0) - Q(M/\sigma) \rightarrow 0 \quad \text{eq:ERM-test-error} \quad (6.17)$$

with $Q(\cdot)$ the Gaussian Q -function. Similarly, since $\beta^\top \tilde{\mathbf{x}}_i \simeq \text{prox}_{\delta L}(\beta_{-i}^\top \tilde{\mathbf{x}}_i)$, the training classification error is given by

$$\mathbb{P}(\beta^\top \tilde{\mathbf{x}}_i < 0) - \mathbb{P}(\text{prox}_{\delta L}(r) < 0) \rightarrow 0 \quad \text{eq:ERM-train-error} \quad (6.18)$$

for $r \sim \mathcal{N}(M, \sigma^2)$ given in Theorem 6.1.

6.1.3 Practical consequences and further discussions

subsec:ERM-discussion

To validate the asymptotic results given in Theorem 6.1 for n, p of reasonable sizes, Figure 6.2 compares the empirical distribution of $\{\beta_{-i}^\top \tilde{\mathbf{x}}_i\}_{i=1}^n$ to the limiting Gaussian distribution $\mathcal{N}(M, \sigma^2)$ from the system of fixed-point equations in Theorem 6.1. The theoretical results are seen to fit the simulations almost perfectly, already for $p = 256$ and $n = 1024$.

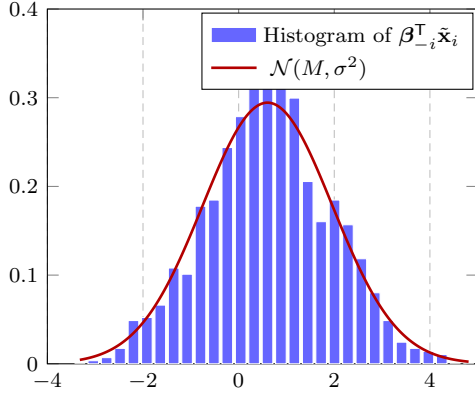


Figure 6.2: Histogram of $\beta_{-i}^\top \tilde{\mathbf{x}}_i$ and the Gaussian distribution $\mathcal{N}(M, \sigma^2)$ defined in Theorem 6.1 with $\mu = \mathbf{1}_p / \sqrt{p}$, $\mathbf{C} = \text{diag}[\mathbf{1}_{p/4}; 3 \cdot \mathbf{1}_{p/4}; 5 \cdot \mathbf{1}_{p/2}]$, for logistic loss $L(t) = \log(1 + e^{-t})$, $\lambda = 0.1$, $p = 256$ and $n = 1024$. fig:ERM-CLT

6.1.3.1 The existence and uniqueness of empirical risk minimizer

We now interpret the results in Theorem 6.1. First, let us for simplicity restrict ourselves to the unregularized case where $\gamma = 0$ and assume the existence and uniqueness of the solution to the (unregularized) optimization problem

$$\arg \min_{\beta \in \mathbb{R}^p} \frac{1}{n} \sum_{i=1}^n L(y_i \beta^\top \mathbf{x}_i) \quad \text{eq: def-empirical-risk-min-unregulariz} \quad (6.19)$$

and the asymptotic boundedness of the solution (i.e., $\limsup_p \|\beta\| < \infty$). This assumption is necessary since, in the unregularized $\gamma = 0$ case, such a minimizer may not exist, and if it does, may not be unique or may have a diverging behavior. A well-known counter-example in the logistic regression $L(t) = \log(1 + e^{-t})$ setting is as follows: if the training data $\{(\mathbf{x}_i, y_i)\}_{i=1}^n$ are *linearly separable* in the sense that there exists a linear decision boundary $\mathbf{b} \in \mathbb{R}^p$ so that

$$y_i \mathbf{x}_i^\top \mathbf{b} \geq 0, \quad i \in \{1, \dots, n\}$$

then, since $L(t)$ is strictly decreasing, one can always decrease the objective function and have $\frac{1}{n} \sum_{i=1}^n L(y_i \alpha_1 \mathbf{b}^\top \mathbf{x}_i) < \frac{1}{n} \sum_{i=1}^n L(y_i \alpha_2 \mathbf{b}^\top \mathbf{x}_i)$ as long as $\alpha_1 > \alpha_2 > 0$, and the (global) minimizer of (6.19) does not exist.

rem:existence-ERM

Remark 6.1 (Existence and uniqueness of a well-defined empirical risk minimizer). *In the large dimensional setting under consideration, the existence of a unique and well-behaved minimizer can be characterized, as a function of the problem setting (μ, \mathbf{C} and the loss L) and of the ratio p/n . For instance, it was shown in [Candès and Sur, 2020] for the logistic regression that a sharp phase transition exists for the existence of the minimizer of (6.19) in the sense*

that, for $g(\cdot)$ some decreasing function, if $p/n > g(\boldsymbol{\mu}^\top \mathbf{C}^{-1} \boldsymbol{\mu})$, the minimizer exists with probability approaching zero; but if $p/n < g(\boldsymbol{\mu}^\top \mathbf{C}^{-1} \boldsymbol{\mu})$, the probability approaches one. The function g additionally has the property that $g(\cdot) \leq 1/2$, meaning that the minimizer (asymptotically) does not exist if $n < 2p$.² This result was then extended in [Taheri et al., 2019] to more general convex losses.

According to the above discussion, assume the existence of a bounded solution to the unregularized optimization problem (6.19), from which one may simplify the expression in Theorem 6.1 as

$$\tilde{\boldsymbol{\beta}} \sim \mathcal{N}\left(\frac{\mathbb{E}[f(r)]}{\mathbb{E}[f'(r)]} \mathbf{C}^{-1} \boldsymbol{\mu}, \frac{\mathbb{E}[f^2(r)]}{(\mathbb{E}[f'(r)])^2} \frac{\mathbf{C}^{-1} \boldsymbol{\mu}}{n}\right) \quad \text{eq:beta-unregularize (6.20)}$$

for $r \sim \mathcal{N}(M, \sigma^2)$, $f(r) = -L'(\text{prox}_{\delta L}(r))$ with

$$M = \frac{\mathbb{E}[f(r)]}{\mathbb{E}[f'(r)]} \boldsymbol{\mu}^\top \mathbf{C}^{-1} \boldsymbol{\mu}, \quad \sigma^2 = \left(\frac{\mathbb{E}[f(r)]}{\mathbb{E}[f'(r)]}\right)^2 \boldsymbol{\mu}^\top \mathbf{C}^{-1} \boldsymbol{\mu} + \frac{\mathbb{E}[f^2(r)]}{(\mathbb{E}[f'(r)])^2} \frac{p}{n}$$

and δ the unique positive solution of

$$\mathbb{E}\left[\frac{1}{1 + \delta L''(\text{prox}_{\delta L}(r))}\right] = 1 - \frac{p}{n}. \quad \text{eq:ERM-delta (6.21)}$$

Note already from the convexity of L that one must have (at least) $n > p$ so as to have $\delta > 0$, in accordance with the existence and uniqueness condition in [Candès and Sur, 2020, Taheri et al., 2019]. Also, taking $L''(t) = 0$, which excludes the existence of $\delta > 0$ for $p/n > 0$, is not allowed.

6.1.3.2 Implications to large dimensional empirical risk minimization

Debiasing the estimator in large dimensions. Recall from (6.4) that the underlying model follows a logistic model, with the optimal Bayes solution given by $\boldsymbol{\beta}_* = 2\mathbf{C}^{-1} \boldsymbol{\mu}$. However, from the asymptotic characterization in (6.20) the expectation of the minimizer $\boldsymbol{\beta}$ of the logistic loss $L(t) = \log(1 + e^{-t})$, despite being the maximum likelihood estimator, instead of being equal to $\boldsymbol{\beta}_*$ as the large- n asymptotic suggests [Rosasco et al., 2004], is only a scaled version of $\boldsymbol{\beta}_*$, due to the non-vanishing ratio p/n .

Although in a classification context one has $\text{sign}(\boldsymbol{\beta}^\top \mathbf{x}) = \text{sign}(\alpha \boldsymbol{\beta}^\top \mathbf{x})$ for $\alpha > 0$, so that a positive constant rescaling of the classifier $\boldsymbol{\beta}$ does not affect the classification performance, it is often still desirable to have a large- (n, p) consistent estimator of $\boldsymbol{\beta}_*$, for inference or risk management purposes. For instance, such an estimator is necessary to predict the variability of the obtained solution by means of standard errors, confidence intervals or p-values [Sur and Candès, 2019].

²This remark is reminiscent of the similar, yet formally different, phenomenon where the minimizer to (6.19) for square loss $L(t) = (t - 1)^2/2$ and $\gamma = 0$ exists but is *not unique* in the under-determined regime $n < p$.

To this end, we see from (6.20) that it suffices to estimate $\mathbb{E}[f(r)]$ and $\mathbb{E}[f'(r)]$ in a consistent manner, which, according to the derivation in the previous section, can be evaluated as follows.

lem:rescale-ERM

Lemma 6.1. *Under the notations of the conditions of Theorem 6.1, we have*

$$\begin{aligned} -\frac{1}{n} \sum_{i=1}^n L'(\boldsymbol{\beta}^\top \tilde{\mathbf{x}}_i) - \mathbb{E}[f(t)] &\xrightarrow{a.s.} 0 \\ \frac{1}{n} \sum_{i=1}^n [L'(\boldsymbol{\beta}^\top \tilde{\mathbf{x}}_i)]^2 - \mathbb{E}[f^2(t)] &\xrightarrow{a.s.} 0 \\ \frac{1}{n} \sum_{i=1}^n \frac{L'(\boldsymbol{\beta}^\top \tilde{\mathbf{x}}_i)(r_i - \frac{1}{n} \sum_{i=1}^n r_i)}{\frac{1}{n} \sum_{i=1}^n (r_i - \frac{1}{n} \sum_{i=1}^n r_i)^2} - \mathbb{E}[f'(t)] &\xrightarrow{a.s.} 0 \end{aligned}$$

for $r_i = \boldsymbol{\beta}^\top \tilde{\mathbf{x}}_i + \hat{\delta} L'(\boldsymbol{\beta}^\top \tilde{\mathbf{x}}_i)$ with $\hat{\delta}$ the (unique) positive solution to

$$\hat{\delta} = \frac{p}{n} \left(\frac{1}{n} \sum_{i=1}^n \frac{L''(\boldsymbol{\beta}^\top \tilde{\mathbf{x}}_i)}{1 + \hat{\delta} L''(\boldsymbol{\beta}^\top \tilde{\mathbf{x}}_i)} \right)^{-1}.$$

We have in particular $|\hat{\delta} - \delta| \xrightarrow{a.s.} 0$.

Figure 6.3 examines the empirical mean (as an estimate of the expectation) of $\boldsymbol{\beta}$, the proposed rescaling version and the optimal Bayes solution $\boldsymbol{\beta}_*$ and confirms that, by rescaling $\boldsymbol{\beta}$ with the plug-in estimators in Lemma 6.1, one retrieves on average the optimal $\boldsymbol{\beta}_*$.

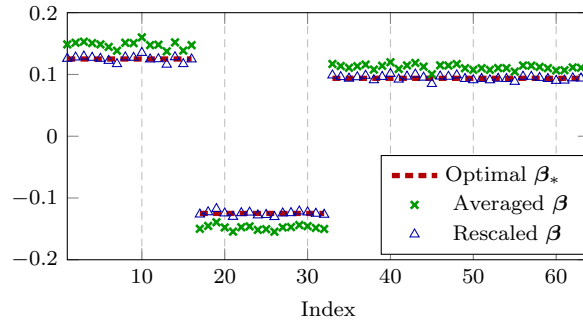


Figure 6.3: Comparison of the averaged $\boldsymbol{\beta}$ (over 500 realizations, to estimate the expectation), the optimal Bayes solution $\boldsymbol{\beta}_*$ and the (averaged) rescaled solution $\boldsymbol{\beta}$ proposed in Lemma 6.1, for logistic loss with $\boldsymbol{\mu} = [\mathbf{1}_{p/4}, -\mathbf{1}_{p/4}, \frac{3}{4}\mathbf{1}_{p/2}] / \sqrt{p}$, $\mathbf{C} = 2\mathbf{I}_p$, for $p = 64$ and $n = 512$. fig:ERM-compare-beta-expectation

Let us now focus on the random fluctuations of $\boldsymbol{\beta}$, which are (asymptotically) Gaussian with covariance \mathbf{C}^{-1}/n (so that the entry-wise noise is typically of the order $O(n^{-1/2})$) under (6.3). Therefore, since $\|\boldsymbol{\beta}_*\| = O(1)$, depending on the nature of $\boldsymbol{\beta}_*$, either of the following two situations may arise:

1. $\beta_* \in \mathbb{R}^p$ is *sparse* in the sense that the number of its nonzero entries (i.e., its ℓ_0 norm) is of order $O(1)$ and each nonzero element is of order $O(1)$. In this case, one may wish to perform some sort of soft-thresholding and to set noise-like small valued entries to zero, with a wisely chosen threshold;
2. $\beta_* \in \mathbb{R}^p$ is more “*delocalized*” with $\|\beta_*\|_0 = O(n)$ and $\|\beta_*\|_\infty = O(n^{-1/2})$, which is of the same order as the random noise. Intuitively, the energy of β_* is spread over all $O(n)$ entries and it is unlikely to recover the desired β_* from a single realization in this case. An alternative, yet computational more burdensome, approach is to solve n times the “leave-one-out” version of (6.19) by removing different datum each time, and then average the obtained solutions.

Optimal loss for classification. From a classification standpoint, it follows from (6.17) that the optimal design of the loss L is the function that maximizes the ratio M^2/σ^2 or, equivalently, as per (6.20), the function solution to

$$\max_f \frac{M^2}{\sigma^2} = \max_f \frac{(\mathbb{E}[f(r)])^2 (\boldsymbol{\mu}^\top \mathbf{C}^{-1} \boldsymbol{\mu})^2}{(\mathbb{E}[f(r)])^2 (\boldsymbol{\mu}^\top \mathbf{C}^{-1} \boldsymbol{\mu})^2 + \mathbb{E}[f^2(r)] \frac{p}{n}}.$$

An immediate remark is that, by the Cauchy–Schwarz inequality,

$$(\mathbb{E}[f(r)])^2 \leq \mathbb{E}[f^2(r)]$$

with equality if and only if $f(r) = -L'(\text{prox}_{\delta L}(r))$ is constant (which is however unattainable with the current framework as discussed previously below (6.21)). Yet, a theoretical misclassification error rate “lower bound” is given by

$$Q\left(\frac{M}{\sigma}\right) = Q\left(\frac{\boldsymbol{\mu}^\top \mathbf{C}^{-1} \boldsymbol{\mu}}{\sqrt{\boldsymbol{\mu}^\top \mathbf{C}^{-1} \boldsymbol{\mu} + p/n}}\right).$$

This extends the optimal performance bound for linear classifier from gradient descent minimizing squared loss in Remark 5.2 to more general loss functions.

For a given problem with fixed $\boldsymbol{\mu}^\top \mathbf{C}^{-1} \boldsymbol{\mu}$ and p/n , it thus suffices to maximize the ratio $(\mathbb{E}[f(r)])^2/\mathbb{E}[f^2(r)]$ or, alternatively, according to Lemma 6.1, to maximize the following empirical version for n, p large

$$\max_L \frac{|L'(\boldsymbol{\beta}^\top \tilde{\mathbf{X}}) \mathbf{1}_n|}{\sqrt{L'(\boldsymbol{\beta}^\top \tilde{\mathbf{X}}) L'(\tilde{\mathbf{X}}^\top \boldsymbol{\beta})}} \quad \text{eq:ERM-loss-empirical} \quad (6.22)$$

where the function $L'(\cdot)$ is applied entry-wise to the vector $\boldsymbol{\beta}^\top \tilde{\mathbf{X}} \in \mathbb{R}^n$. At this point, note from (6.5) that in the unregularized case ($\gamma = 0$) one must have

$$\tilde{\mathbf{X}} L'(\tilde{\mathbf{X}}^\top \boldsymbol{\beta}) = \mathbf{0}$$

so that, by considering the singular value decomposition of $\tilde{\mathbf{X}}$

$$\tilde{\mathbf{X}} = \mathbf{U} \boldsymbol{\Sigma} \mathbf{V}^\top = \mathbf{U} [\mathbf{S} \quad \mathbf{0}] \begin{bmatrix} \mathbf{V}_1^\top \\ \mathbf{V}_2^\top \end{bmatrix}$$

for $\tilde{\mathbf{X}} \in \mathbb{R}^{p \times n}$ with $\Sigma \in \mathbb{R}^{p \times n}$, orthogonal $\mathbf{U} \in \mathbb{R}^{p \times p}$, $\mathbf{V} \in \mathbb{R}^{n \times n}$, diagonal $\mathbf{S} \in \mathbb{R}^{p \times p}$ and $\mathbf{V}_1 \in \mathbb{R}^{n \times p}$, $\mathbf{V}_2 \in \mathbb{R}^{n \times (n-p)}$ (recall the necessary $n > p$ condition when $\gamma = 0$ case), one must have

$$\mathbf{V}_1^T L'(\tilde{\mathbf{X}}^T \boldsymbol{\beta}) = \mathbf{0}.$$

That is, $L'(\tilde{\mathbf{X}}^T \boldsymbol{\beta})$ lies on the subspace spanned by the column vectors of \mathbf{V}_2 , i.e., there exists $\mathbf{a} \in \mathbb{R}^{n-p}$ for which

$$L'(\tilde{\mathbf{X}}^T \boldsymbol{\beta}) = \mathbf{V}_2 \mathbf{a}$$

and thus (6.22) further simplifies to

$$\max_L \frac{\mathbf{a}^T \mathbf{V}_2^T \mathbf{1}_n}{\|\mathbf{a}\|}$$

which attains the maximum if and only if \mathbf{a} is aligned to $\mathbf{V}_2^T \mathbf{1}_n$, i.e., $\mathbf{a} = a \mathbf{V}_2^T \mathbf{1}_n$ for some $a > 0$. This optimality condition is met with the square loss $L(t) = (t - 1)^2/2$.

Consequently, the surprising conclusion of this section is that, in the unregularized case, among all convex and smooth functions, the simplest square loss turns out to be optimal. In particular, it *uniformly* outperforms the maximum likelihood solution induced by the logistic loss, as it systematically reaches lower classification error. Perhaps even more surprisingly, a similar conclusion can be reached in the *regularized case*, where is more subtle to establish as one needs to consider the possible different levels of regularization for different losses; we refer the interested readers to [Mai and Liao, 2019] for more details.³

The analysis framework presented in this section is based on a “local” Taylor expansion of the loss L . This analysis however excludes the non differentiable hinge loss of the popular and important method of support vector machines (SVMs). The following section develops the intuitive ideas to handle this non-smooth implicit optimization case.

6.2 Large dimensional support vector machines

As one of most popular classification methods in the machine learning literature, the support vector machine (SVM), and in particular the hard-margin SVM, is based on the intuition of finding two separating hyperplanes with a maximum “margin” between them, so as to make robust future predictions.

Assuming the *linear separability* of the training set $\{(\mathbf{x}_i, y_i)\}_{i=1}^n$ with $y_i \in \{-1, +1\}$, the max margin classifier given by the solution to the hard-margin

³The (approximate) optimality of the square loss among all *convex* losses was recently established by Taheri et al. [2020c,a,b] on similar, yet formally different, models, showing the (somewhat unexpected) advantageous performance of the simple square loss in large dimensional problems.

SVM, is formulated as the following optimization problem

$$\begin{aligned} \arg \min_{\beta \in \mathbb{R}^p} \quad & \|\beta\|^2, \\ \text{s.t.} \quad & y_i \beta^\top \mathbf{x}_i \geq 1, \quad i \in \{1, \dots, n\}. \end{aligned} \quad \text{eq:hard-SVM} \quad (6.23)$$

It is interesting to note that, unlike for logistic regression where the training set *must not be* linearly separable as mentioned in Remark 6.1, the hard-margin SVM, on the contrary, assumes explicitly the *linear separability* of data.

Remark 6.2 (Connection between linear, logistic regression and SVM). *It has been shown in [Soudry et al., 2018] that, on a linearly separable dataset, the gradient descent method, when applied to minimize the unregularized logistic loss, converges in direction to the max margin classifier, that is, the solution to the hard-margin SVM.*

This can be understood by drawing an analogy to the linear (ridgeless) regression on the pair (\mathbf{X}, \mathbf{y}) for $\mathbf{X} \in \mathbb{R}^{p \times n}$, $\mathbf{y} \in \mathbb{R}^n$: in the under-parameterized $p < n$ regime there exists a unique solution $\beta = (\mathbf{X}\mathbf{X}^\top)^{-1}\mathbf{X}\mathbf{y}$ that minimizes the unregularized square loss $L(\beta) = \|\mathbf{y}^\top - \beta^\top \mathbf{X}\|^2$, when $\mathbf{X}\mathbf{X}^\top \in \mathbb{R}^{p \times p}$ is invertible; while for $p > n$ there are infinitely many solutions, and by running gradient descent (for almost all initializations) we obtain the minimal norm solution given by the Moore–Penrose pseudo-inverse $(\mathbf{X}\mathbf{X}^\top)^+ \mathbf{X}\mathbf{y} = \mathbf{X}(\mathbf{X}^\top \mathbf{X})^{-1}\mathbf{y}$ when $\mathbf{X}^\top \mathbf{X} \in \mathbb{R}^{n \times n}$ is invertible. In the linear regression case, having $p > n$ implies that there always exists $\beta_0 \in \mathbb{R}^p$ that can interpolate all the n training samples so that $\mathbf{X}^\top \beta_0 = \mathbf{y}$. Analogously, when the training set is linearly separable, there also exists β_0 such that $\text{sign}(\beta_0^\top \mathbf{x}_i) = y_i$ for $i \in \{1, \dots, n\}$ that perfectly classifies all training samples. In this respect, the hard-margin SVM solution is nothing more than the minimum norm solution (as per (6.23)) among all “interpolation” classifiers.

When the training set is *not linearly separable*, the “hard” constraints in (6.23) are not attainable. Nonetheless, by allowing residual small errors in the linear “separation”, the “soft-margin” alternative can be introduced

$$\begin{aligned} \arg \min_{\beta \in \mathbb{R}^p} \quad & \frac{1}{2} \|\beta\|^2 + \frac{\gamma}{n} \sum_{i=1}^n \varepsilon_i \\ \text{s.t.} \quad & y_i \beta^\top \mathbf{x}_i \geq 1 - \varepsilon_i, \quad \varepsilon_i \geq 0, \quad i \in \{1, \dots, n\} \end{aligned} \quad \text{eq:soft-SVM} \quad (6.24)$$

with some regularization parameter $\gamma > 0$, which is, as one may note, equivalent to solving the general empirical risk minimization problem in (6.1) with the hinge loss $L(t) = \max(0, 1 - t)$, by introducing the variable $\varepsilon_i = \max(0, 1 - y_i \beta^\top \mathbf{x}_i)$ which is the smallest nonnegative number satisfying $y_i \beta^\top \mathbf{x}_i \geq 1 - \varepsilon_i$.

Solving the associated Lagrangian dual, (6.24) can be further reduced to the

following simplified optimization problem

$$\begin{aligned} \max_{c_i, i \in \{1, \dots, n\}} \quad & \sum_{i=1}^n c_i - \frac{1}{2n} \sum_{i,j=1}^n c_i c_j \tilde{\mathbf{x}}_i^\top \tilde{\mathbf{x}}_j \\ \text{s. t.} \quad & \sum_{i=1}^n c_i y_i = 0, \quad 0 \leq c_i \leq \gamma, \quad i \in \{1, \dots, n\} \end{aligned} \quad (6.25) \quad \text{eq:soft-SVM-dual}$$

where we use again the shortcut $\tilde{\mathbf{x}}_i \equiv y_i \mathbf{x}_i$ and assume for simplicity the symmetric Gaussian mixture

$$\mathcal{C}_1 : \mathbf{x}_i \sim \mathcal{N}(-\boldsymbol{\mu}, \mathbf{C}), \quad y_i = -1 \quad \mathcal{C}_2 : \mathbf{x}_i \sim \mathcal{N}(+\boldsymbol{\mu}, \mathbf{C}), \quad y_i = +1 \quad (6.26)$$

with class prior probability of 1/2 as in the previous section. The hard-margin solution, if it exists, can be retrieved by taking $\gamma \rightarrow \infty$. With the dual variables c_i , the SVM classifier $\boldsymbol{\beta}$ is given by

$$\boldsymbol{\beta} = \frac{1}{n} \sum_{i=1}^n c_i \tilde{\mathbf{x}}_i \quad \text{eq:solution-SVM} \quad (6.27)$$

which is very reminiscent of (6.5) in the previous section, with the dependence of c_i on the $\boldsymbol{\beta}$ and all $\tilde{\mathbf{x}}_i$'s seemingly more involved. Yet, the core idea remains the same: we need to “unwrap” this complex statistical dependence by introducing a series of self-consistent *nonlinear* equations as in (6.11) of the previous section, which allows for the evaluation of the statistics of $\boldsymbol{\beta}$.

Precisely, with the Karush–Kuhn–Tucker (KKT) conditions, the variable c_i satisfies the following constraints

$$\begin{cases} c_i = 0, & \text{for } \boldsymbol{\beta}^\top \tilde{\mathbf{x}}_i > 1 \\ 0 < c_i < \gamma, & \text{for } \boldsymbol{\beta}^\top \tilde{\mathbf{x}}_i = 1 \\ c_i = \gamma, & \text{for } \boldsymbol{\beta}^\top \tilde{\mathbf{x}}_i < 1 \end{cases} \quad (6.28)$$

which, by (6.27), can be further compactly rewritten as

$$c_i = f\left(\frac{1 - \frac{1}{n} \sum_{j \neq i} c_j \tilde{\mathbf{x}}_j^\top \tilde{\mathbf{x}}_i}{\|\tilde{\mathbf{x}}_i\|^2/n}\right) \equiv f\left(\frac{1 - \boldsymbol{\alpha}^\top \tilde{\mathbf{x}}_i}{\|\tilde{\mathbf{x}}_i\|^2/n}\right), \quad \boldsymbol{\alpha} = \frac{1}{n} \sum_{j \neq i} c_j \tilde{\mathbf{x}}_j \quad (6.29) \quad \text{eq: def-alpha=SVM}$$

for $f(t) = \max(0, \min(t, \gamma))$. Note importantly here that $\boldsymbol{\alpha}$ is already a (first) “leave-one-out” version of the solution $\boldsymbol{\beta}$ in the sense that

$$\boldsymbol{\beta} = \boldsymbol{\alpha} + \frac{c_i}{n} \tilde{\mathbf{x}}_i \quad (6.30)$$

with the contribution from a *single* datum $c_i \tilde{\mathbf{x}}_i$ of negligible impact to $\boldsymbol{\beta}$.

Similar to the derivation in Section 6.1, we introduce a second (standard) “leave-one-out” solution $\boldsymbol{\beta}_{-i}$ by solving the optimization problem (6.24) for all training data except \mathbf{x}_i . As a consequence, we shall have

$$\boldsymbol{\beta}_{-i} = \frac{1}{n} \sum_{j \neq i}^n c_j^{-i} \tilde{\mathbf{x}}_j, \quad c_j^{-i} = f\left(\frac{1 - \frac{1}{n} \sum_{l \neq i, j} c_l^{-i} \tilde{\mathbf{x}}_l^\top \tilde{\mathbf{x}}_j}{\|\tilde{\mathbf{x}}_j\|^2/n}\right) \quad (6.31) \quad \text{eq:SVM-beta-i}$$

with c_j^{-i} the associated dual coefficients. Despite taking similar forms, α and β_{-i} crucially differ from each other in the fact that α depends on the \mathbf{x}_i (through the coefficients c_j), while β_{-i} not. Our objective is, again similar to Section 6.1, to derive the (asymptotic) relation between the dual coefficient c_j^{-i} and c_j , as well as α and β_{-i} (that should both be asymptotically “close to” β).

We start by writing, for all $j \neq i$,

$$c_j - c_j^{-i} = f\left(\frac{1 - \frac{1}{n} \sum_{l \neq i,j} c_l \tilde{\mathbf{x}}_l^\top \tilde{\mathbf{x}}_j - \frac{1}{n} c_i \tilde{\mathbf{x}}_i^\top \tilde{\mathbf{x}}_j}{\|\tilde{\mathbf{x}}_j\|^2/n}\right) - f\left(\frac{1 - \frac{1}{n} \sum_{l \neq i,j} c_l^{-i} \tilde{\mathbf{x}}_l^\top \tilde{\mathbf{x}}_j}{\|\tilde{\mathbf{x}}_j\|^2/n}\right).$$

Since $f(t) = \max(0, \min(t, \gamma))$, there exists $d \in [0, 1]$ such that for $t_1, t_2 \in \mathbb{R}$ we have $f(t_1) - f(t_2) = d(t_1 - t_2)$. Denote $d_j \in [0, 1]$ the constant that satisfies⁴

$$c_j - c_j^{-i} = d_j \left(\frac{-\frac{1}{n} \sum_{l \neq i,j} (c_l - c_l^{-i}) \tilde{\mathbf{x}}_l^\top \tilde{\mathbf{x}}_j - \frac{1}{n} c_i \tilde{\mathbf{x}}_i^\top \tilde{\mathbf{x}}_j}{\|\tilde{\mathbf{x}}_j\|^2/n} \right) \stackrel{\text{eq:SVM-def-d}}{\equiv} [\Delta c]_j \quad (6.32)$$

so that, for $\Delta c \in \mathbb{R}^{n-1}$ the column vector composed of the differences $c_j - c_j^{-i}$ and $\mathbf{D}_{-i} \in \mathbb{R}^{(n-1) \times (n-1)}$ the diagonal matrix of all nonzero d_j 's, we have the following (matrix form) relation

$$\left(\frac{1}{n} \mathbf{D}_{-i} \tilde{\mathbf{X}}_{-i}^\top \tilde{\mathbf{X}}_{-i} + \text{diag} \left(\frac{1}{n} \tilde{\mathbf{X}}_{-i}^\top \tilde{\mathbf{X}}_{-i} - \frac{1}{n} \mathbf{D}_{-i} \tilde{\mathbf{X}}_{-i}^\top \tilde{\mathbf{X}}_{-i} \right) \right) \Delta c = -c_i \frac{1}{n} \mathbf{D}_{-i} \tilde{\mathbf{X}}_{-i}^\top \tilde{\mathbf{x}}_i$$

so that

$$\Delta c = -\frac{c_i}{n} \mathbf{M}_{-i}^{-1} \tilde{\mathbf{X}}_{-i}^\top \tilde{\mathbf{x}}_i, \quad \mathbf{M}_{-i} \equiv \frac{1}{n} \tilde{\mathbf{X}}_{-i}^\top \tilde{\mathbf{X}}_{-i} + \text{diag} \left((\mathbf{D}_{-i}^{-1} - \mathbf{I}_{n-1}) \frac{1}{n} \tilde{\mathbf{X}}_{-i}^\top \tilde{\mathbf{X}}_{-i} \right). \quad \stackrel{\text{eq: def-SVM-Delta-c}}{\equiv} \quad (6.33)$$

As a consequence, we deduce

$$\alpha - \beta_{-i} = \frac{1}{n} \sum_{j \neq i} (c_j - c_j^{-i}) \tilde{\mathbf{x}}_j = \frac{1}{n} \tilde{\mathbf{X}}_{-i} \Delta c = -\frac{c_i}{n^2} \tilde{\mathbf{X}}_{-i} \mathbf{M}_{-i}^{-1} \tilde{\mathbf{X}}_{-i}^\top \tilde{\mathbf{x}}_i \quad (6.34)$$

which again takes a similar form as (6.7) in the previous section. As such

$$\beta^\top \tilde{\mathbf{x}}_i = \alpha^\top \tilde{\mathbf{x}}_i + \frac{c_i}{n} \|\mathbf{x}_i\|^2 = \beta_{-i}^\top \tilde{\mathbf{x}}_i + c_i \tilde{\delta}_i, \quad c_i = f \left(\frac{1 - \beta_{-i}^\top \tilde{\mathbf{x}}_i}{\tilde{\delta}_i} \right) \stackrel{\text{relation-c}}{\equiv} \quad (6.35)$$

where we recall $f(t) = \max(0, \min(t, \gamma))$ and denote the random variable

$$\tilde{\delta} \equiv \frac{1}{n} \tilde{\mathbf{x}}_i^\top \left(\mathbf{I}_p - \frac{1}{n} \tilde{\mathbf{X}}_{-i} \mathbf{M}_{-i}^{-1} \tilde{\mathbf{X}}_{-i}^\top \right) \tilde{\mathbf{x}}_i \stackrel{\text{eq:SVM-def-tilde-delta}}{\equiv} \quad (6.36)$$

⁴Here we observe a similar form as (6.6) in the previous section, the main difference being that, due to the non-differentiability of the hinge loss, the auxiliary variables d_j 's are introduced, the statistics of which remain to be determined.

which, as in (6.8) in the previous section, is expected to “converge” to a deterministic limit δ as $n, p \rightarrow \infty$, by the trace lemma, Lemma 2.11. As such, by (6.35) the random variable c_i is expected to behave as a nonlinear transformation of a Gaussian random variable (depending on the data statistics μ, \mathbf{C} and δ) in the large $n, p \rightarrow \infty$ limit (since $\beta_{-i}^\top \tilde{\mathbf{x}}_i$ is Gaussian conditioned on β_{-i} , the norm of which should converge to a limit). Nonetheless, the self-consistent equation of δ must involve the statistics of the d_j 's that remain unknown for the moment.

To investigate the statistics of the d_j 's as well as that of $\tilde{\delta}$, note that with a Taylor expansion-type argument, we have for $t \in \mathbb{R} \setminus \{0, \gamma\}$ that

$$f(t + \varepsilon) - f(t) = f'(t) \cdot \varepsilon + O(\varepsilon^2)$$

for $f'(t) = 1$ for $t \in (0, \gamma)$ and 0 otherwise. Therefore, by (6.32) we have that d_j is nonzero only when the associated c_j^{-i} lies in $(0, \gamma)$.

With (6.36) we thus conclude that

$$\tilde{\delta}_i = \frac{1}{n} \tilde{\mathbf{x}}_i^\top \left(\mathbf{I}_p - \tilde{\mathbf{X}}_{-i} (\tilde{\mathbf{X}}_{-i,S}^\top \tilde{\mathbf{X}}_{-i,S})^{-1} \tilde{\mathbf{X}}_{-i}^\top \right) \tilde{\mathbf{x}}_i \quad (6.37)$$

where the j -th column of $\tilde{\mathbf{X}}_{-i,S}$ is $\tilde{\mathbf{x}}_j$ such that the associated coefficient c_j^{-i} lies in $(0, \gamma)$ and $\tilde{\delta} \xrightarrow{a.s.} \delta$ for δ the unique solution to

$$\delta = \frac{1}{n} \text{tr } \mathbf{C} \left(\mathbf{I}_p + \frac{\mathbb{E}[c \cdot 1_{(0,\gamma)}]}{\delta} \mathbf{C} \right)^{-1}, \quad c \sim f \left(\frac{1-r}{\delta} \right) \quad (6.38)$$

for $r \sim \mathcal{N}(M, \sigma^2)$ with

$$M = \mathbb{E}[\beta]^\top \mu, \quad \sigma^2 = \text{tr}(\mathbf{C} \mathbb{E}[\beta \beta^\top]) \quad (6.39)$$

which presents a close analogy to (6.9) and (6.13) in the previous section, respectively.

To close the loop, it remains, as in the previous section, to express the statistics of β via (6.27) as a function of those of c_i and μ, \mathbf{C} . This leads to the following result on the (asymptotically) statistical behavior of SVM, as an extension of Theorem 6.1 in the previous section.

[ref below to be updated](#)

[theo:SVM-main](#)

Theorem 6.2 (Asymptotic behavior of β for SVM, [Mai, 2019, Theorem 5.3.1]). *For $\max\{\|\mu\|, \|\mathbf{C}\|, \|\mathbf{C}^{-1}\|\} = O(1)$ and β the unique solution to (6.24), we have, as $n, p \rightarrow \infty$,*

$$\|\beta - \tilde{\beta}\| \rightarrow 0, \quad \left(\mathbf{I}_p + \frac{\mathbb{E}[c \cdot 1_{(0,\gamma)}]}{\delta} \mathbf{C} \right) \tilde{\beta} \sim \mathcal{N}(\mathbb{E}[c] \mu, \mathbb{E}[c^2] \mathbf{C} / n)$$

where $c \sim f((1-r)/\delta)$ for $f(t) = \max(0, \min(t, \gamma))$ and $r \sim \mathcal{N}(M, \sigma^2)$ for (M, σ^2) solution to

$$M = \mathbb{E}[\tilde{\beta}]^\top \mu, \quad \sigma^2 = \text{tr}(\mathbf{C} \mathbb{E}[\tilde{\beta} \tilde{\beta}^\top]) \quad (6.40)$$

with δ the unique positive solution to

$$\delta = \frac{1}{n} \operatorname{tr} \mathbf{C} \left(\mathbf{I}_p + \frac{\mathbb{E}[c \cdot 1_{(0,\gamma)}]}{\delta} \mathbf{C} \right)^{-1}.$$

One may wish to take the limit of $\gamma \rightarrow \infty$ in the above theorem to retrieve the solution of hard-margin SVM. However, attention must be paid here since, as in Remark 6.1 for logistic regression, a *sharp* phase transition on the ratio p/n also exists in the case of hard-margin SVM, see for instance [Kammoun and Alouini, 2020] for a more detailed discussion on this point.

Analogy to (6.17) and (6.18), the asymptotic test classification error rates of SVM can also be given, for a new datum $\tilde{\mathbf{x}}$, by

$$\mathbb{P}(\boldsymbol{\beta}^T \tilde{\mathbf{x}} < 0) - Q(M/\sigma) \rightarrow 0 \quad \text{eq:SVM-test-error} \quad (6.41)$$

with $Q(\cdot)$ the Gaussian Q -function and similarly the asymptotic training classification error

$$\mathbb{P}(\boldsymbol{\beta}^T \tilde{\mathbf{x}}_i < 0) - \mathbb{P}(r + c\delta < 0) \rightarrow 0 \quad \text{eq:SVMtrain-error} \quad (6.42)$$

for $r \sim \mathcal{N}(M, \sigma^2)$ and $c \sim f((1-r)/\delta)$ defined in Theorem 6.2.

** it would be good if we could find a simple argument to show that least-squares outperforms SVM**

In this section, we provided the heuristic derivation of the asymptotic performance of the soft-margin SVM classifier defined in (6.24) arising from the minimization of the non smooth hinge loss $L(t) = \max(0, 1 - t)$, with a focus on the similarities and differences from the large dimensional analysis of, say, the logistic regression, in Section 6.1 where the loss is at least three-times differentiable.

Recall from the discussions at the end of Section 6.1.3 that the simple square loss is proved to be optimal in the classification of the Gaussian mixture $\mathcal{N}(\pm \boldsymbol{\mu}, \mathbf{C})$ and beyond [Taheri et al., 2020c,a,b]. The theoretical analyses in these two sections unveil the surprising and counterintuitive facts that, for large dimensions problems, classical empirical risk minimization solutions may fail to exist (e.g., the maximum likelihood solution discussed in Remark 6.1 or the hard-margin SVM), and if they exist, may fail to meet the performance of the simple square loss. These results challenge the conventional wisdom from classical statistical learning theory where the data dimension p is considered negligibly small with respect to the sample size n , in which case the maximum likelihood solution is believed to produce the minimum regression error and the hinge loss is proved to be optimal in a classification context [Rosasco et al., 2004]. The theoretical analysis proposed in this section, although performed on relatively simple statistical models, opens the door to a renewed understanding of machine learning basics, starting with the long-proclaimed SVM method, when considering large (and even moderately large) dimensional data.

6.3 Conclusion

After covering the analysis of machine learning algorithms involving optimization methods with *explicit* solutions (such as least-square regression or spectral methods), this chapter pushed into the large dimensional analysis of algorithms with solution expressed as the (*unique*) *minimum of a convex optimization problem*. Unlike in the explicit case where the structure of dependence within the solution (such as between the entries of a least-square regression vector) more-or-less easily relates to a functional of the underlying random matrix model, the main difficulty involved in the implicit case lies in a possibly very intricate structure of dependence. The chapter proposed to “break” this dependence by exploiting a “leave-one-out” approach, by which an arbitrary (large dimensional) data vector is isolated from the dataset to perturb the solution in a controlled manner.

Other options in the large dimensional statistics literature exist which may tackle the same problem in a different manner. Among these, we find

- the “double leave-one-out” approach adopted early on in [El Karoui et al., 2013], in order to study the statistical behavior of a family of (robust) M-estimators. This approach hinges on the intuition that, as both dimensions n, p grow, the “leave-one-sample-out” approach, popular in asymptotic (large- n alone) statistics and upon which we based our derivations in the present chapter, could be extended into a double “leave-one-sample-out” and “leave-one-feature-out” approach. Specifically, having reached step (6.11) in Section 6.1, in order to evaluate the statistics of β , the double leave-one-out method would not decompose $\tilde{\mathbf{x}}_i$ as in (6.12) but rather extract an arbitrary entry j from each vector $\tilde{\mathbf{x}}_i$ (and accordingly from β) to understand the statistics of the entry $[\beta]_j$. However, this approach is only valid (or easily adaptable) when the $[\beta]_j$ ’s are statistically exchangeable or linearly related, so essentially for “*unstructured*” feature vectors with *no informative* pattern. This is in particular not directly applicable to data mixture models as simple as $\mathcal{N}(\pm\mu, \mathbf{C})$ discussed at length in this chapter;
- the convex Gaussian min-max theorem (CGMT), first introduced by Gordon [1985] and then largely popularized by Thrampoulidis et al. [2018]. The idea of the CGMT lies in an opportunistic result relating two “Gaussian” min-max optimization problems:

$$\Phi(\mathbf{G}) = \min_{\mathbf{v}} \max_{\mathbf{u}} \{ \mathbf{u}^T \mathbf{G} \mathbf{v} + \psi(\mathbf{v}, \mathbf{u}) \} \quad \text{eq: CGMT-PQ} \quad (6.43)$$

$$\phi(\mathbf{g}, \mathbf{h}) = \min_{\mathbf{v}} \max_{\mathbf{u}} \{ \|\mathbf{v}\| \cdot \mathbf{g}^T \mathbf{u} + \|\mathbf{u}\| \cdot \mathbf{h}^T \mathbf{v} + \psi(\mathbf{v}, \mathbf{u}) \} \quad \text{eq: CGMT-AQ} \quad (6.44)$$

where $\mathbf{G} \in \mathbb{R}^{n \times p}$, $\mathbf{g} \in \mathbb{R}^n$ and $\mathbf{h} \in \mathbb{R}^p$ are matrix and vectors composed of i.i.d. $\mathcal{N}(0, 1)$ entries, and $\psi : \mathbb{R}^p \times \mathbb{R}^n \rightarrow \mathbb{R}$ is continuous and convex-concave, and for which it can be shown that, for any $x, t \in \mathbb{R}$,

$$\mathbb{P}(|\Phi(\mathbf{G}) - x| > t) \leq 2\mathbb{P}(|\phi(\mathbf{g}, \mathbf{h}) - x| > t).$$

Evidently, the second optimization being simpler than the first, if $\phi(\mathbf{g}, \mathbf{h})$ concentrates around x as $n, p \rightarrow \infty$, then so does $\Phi(\mathbf{G})$. The idea to apply the above CGMT inequality is then to express the studied optimization problem under the form $\Phi(\mathbf{G})$. This is usually performed by introducing an additional slack variable \mathbf{u} to enforce the constraints. For instance, in the hard-margin SVM setting, one may rewrite (6.23) under the form

$$\begin{aligned} & \min_{\boldsymbol{\beta}} \max_{\mathbf{u} \leq \mathbf{0}} \left\{ \|\boldsymbol{\beta}\|^2 + \frac{1}{n} \sum_{i=1}^n u_i (y_i \boldsymbol{\beta}^\top \mathbf{x}_i - 1) \right\} \\ &= \min_{\boldsymbol{\beta}} \max_{\mathbf{u} \leq \mathbf{0}} \left\{ \frac{1}{n} \mathbf{u}^\top \tilde{\mathbf{X}}^\top \boldsymbol{\beta} + \|\boldsymbol{\beta}\|^2 - \frac{1}{n} \mathbf{u}^\top \mathbf{1}_n \right\} \end{aligned}$$

for $\tilde{\mathbf{X}} = [y_1 \mathbf{x}_1, \dots, y_n \mathbf{x}_n] \in \mathbb{R}^{p \times n}$ and $\mathbf{u} \leq \mathbf{0}$ understood in an entry-wise sense, in which we recognize the form $\mathbf{u}^\top \mathbf{G} \mathbf{v}$ of $\Phi(\mathbf{G})$ in the term $\frac{1}{n} \mathbf{u}^\top \tilde{\mathbf{X}}^\top \boldsymbol{\beta}$. A thorough analysis of SVM and logistic regression under the CGMT framework is performed in [Deng et al., 2019].

As such, the CGMT approach does not solve the “zero-gradient” equation implied by the optimization problem, but rather rewrites the optimization problem itself to make it simpler to solve. Specifically, the major interest here is to “break” the bilinear form $\mathbf{u}^\top \mathbf{G} \mathbf{v}$ in the primal optimization (6.43) into the sum of two linear optimizations $\|\mathbf{v}\| \mathbf{g}^\top \mathbf{u} + \|\mathbf{u}\| \mathbf{h}^\top \mathbf{v}$ (conditionally on the norms of \mathbf{v} and then \mathbf{u}) in (6.44). This also interestingly breaks the very random matrix structure of the original problem, turning the random Gaussian matrix \mathbf{G} into the random Gaussian vectors \mathbf{g} and \mathbf{h} . The method however strongly relies on the CGMT inequality and thus requires \mathbf{G} to have strictly i.i.d. $\mathcal{N}(0, 1)$ entries. Any deviation from this setting (for instance by adding correlation structures within \mathbf{G}) may pose new challenges to the CGMT framework;

- the approximate message passing (AMP) and the state evolution techniques [Donoho and Montanari, 2016]. Unlike the previous methods, AMP proposes to directly solve the optimization problem by following the dynamics of an iterative fixed-point algorithm ultimately converging to the sought-for solution. The method is reminiscent and indeed strongly related with the message passing (also known as belief propagation [Pearl, 1986]) approach from statistical physics, yet enjoys a mathematical sound framework (unlike belief propagation). The AMP approach however requires the introduction of many additional tools which would drive us too far from our present topic.

Having in hand numerous tools to handle convex optimization problems in machine learning, a natural next step would be to deal with *non-convex optimization problems*. These problems are deemed hard to solve (and consequently to study) due to the possible existence of multiple, even perhaps infinity many, critical points which can all be candidate solutions of the problem. In practice,

initialization may play a crucial role in gradient-based learning and one may wish to start the algorithm at a “good guess” starting point, sufficient close to the sought-for (global) optimal solution. In this respect, RMT analyses provide efficient *spectral-based initialization* schemes widely used in many non-convex problems, such as phase retrieval [Fienup, 1982], matrix completion [Keshavan et al., 2010], low-rank matrix recovery [Jain et al., 2013], blind deconvolution [Lee et al., 2016], sparse coding [Arora et al., 2015], to name a few; a detailed example on the problem of phase retrieval is developed as a practical course exercise in the next section. Yet, many non-convex optimization problems need to be confronted with directly, without resorting to first approximations. This is the case notably of neural network training, and particularly in the large dimensional setting of deep learning, as well as of other popular, yet still ill-understood, machine learning methods such as stochastic neighborhood embedding (SNE [Hinton and Roweis, 2003] or its popular t-SNE variant [Maaten and Hinton, 2008]). For these challenging problems, the strong hope is that, while as $n, p \rightarrow \infty$, the number of critical points in these problems typically grows at a fast (possibly exponential) rate, these critical points share numerous symmetries and their associated performances (the “depth” of a given local minimum for instance) often reduce to a few states. This is indeed to be expected as one of the strong arguments in favor of the observed very stable behavior of deep neural networks [Choromanska et al., 2015]: irrespective of the learning initialization point, gradient descent learning in these highly non-convex optimization problems is expected to converge to a local minimum with essentially the same performance level as the vast majority of the local minima. The article [Choromanska et al., 2015] provides tentative theoretical insights in this direction, yet for an overly simplified version of a deep learning network (modeled as a mere Gaussian random field), using the Kac-Rice formula (which assesses the number of critical points of a problem) in conjunction to random matrix arguments.

6.4 Practical course material

read over and simu to be done!

Practical Lecture Material 6 (Phase retrieval). *The object of phase retrieval is to recover an unknown (deterministic) signal $\mathbf{a} \in \mathbb{R}^p$ (say with $\|\mathbf{a}\| = 1$) from magnitude measurements of the type $y_i = (\mathbf{a}^\top \mathbf{x}_i)^2$, for i.i.d. Gaussian sensing vectors $\mathbf{x}_i \sim \mathcal{N}(\mathbf{0}, \mathbf{I}_p)$, $i \in \{1, \dots, n\}$. One popular algorithm to solve this problem is the so-called “Wirtinger Flow algorithm” proposed by Candes et al. [2015] which comes in two steps: (i) a careful initialization obtained by means of a spectral method, and (ii) a series of updates fine-tuning this initial estimate using for instance a gradient descent procedure on a target cost function. Due to the non-convex nature of the underlying problem, the initialization step (i) is of crucial significance to ensure decent performance. Candes et al. [2015] proposed to use the dominant eigenvector of the sample covariance-like matrix $\frac{1}{n} \sum_{i=1}^n y_i \mathbf{x}_i \mathbf{x}_i^\top$ as initialization. The target of this exercise is to understand*

the relevance of this idea through the analysis of the spectral properties of this matrix.

To this end, first decompose (the columns of) $\mathbf{X} = [\mathbf{x}_1, \dots, \mathbf{x}_n]$ into the sum of a component aligned to \mathbf{a} and a component orthogonal to \mathbf{a} , and show that we may then express \mathbf{X} under the form $\mathbf{X} = \mathbf{aa}^\top \mathbf{X} + \mathbf{X}^\perp$ with $\mathbf{X}^\perp = (\mathbf{I}_p - \mathbf{aa}^\top)\mathbf{X} \in \mathbb{R}^{p \times n}$; confirm in particular that $\mathbf{a}^\top \mathbf{X}^\perp = 0$ and, more importantly, that $\mathbf{X}^\top \mathbf{a} = \mathbf{v} \in \mathbb{R}^n$ and \mathbf{X}^\perp are both Gaussian and independent of each other.

Based on the above decomposition, show that the limiting spectral measure of $\frac{1}{n}\mathbf{X}^\perp \mathbf{D}(\mathbf{X}^\perp)^\top$ for diagonal $\mathbf{D}_{ii} = y_i^2$, if it exists, coincides with that of the original model $\frac{1}{n}\mathbf{X}\mathbf{D}\mathbf{X}^\top = \frac{1}{n}\sum_{i=1}^n y_i \mathbf{x}_i \mathbf{x}_i^\top$.

With this decomposition in mind, and using similar steps as in the proof of Theorem 2.5, determine the limiting spectrum of $\frac{1}{n}\mathbf{X}\mathbf{D}\mathbf{X}^\top$ via its Stieltjes transform. Show that it is asymptotically close to that of $\frac{1}{n}\sum_{i=1}^n \tau_i \mathbf{x}_i \mathbf{x}_i^\top$ for i.i.d. τ_i following a χ^2 distribution with one degree of freedom which is independent of \mathbf{x}_i . In other words, the dependence between $y_i = \mathbf{x}_i^\top \mathbf{a}$ and \mathbf{x}_i does not “contribute” to the limiting spectral measure of $\frac{1}{n}\mathbf{X}\mathbf{D}\mathbf{X}^\top$.

Recalling that the χ^2 distribution with one degree of freedom admits the density

$$\nu(dt) = \frac{1}{\sqrt{2\Gamma(1/2)}} \frac{e^{-\frac{t}{2}}}{\sqrt{t}}, \quad t > 0 \quad (6.45)$$

and has unbounded support. Conclude, using the argument in Section 2.3.1, that the support of limiting spectrum of $\frac{1}{n}\mathbf{X}\mathbf{D}\mathbf{X}^\top$ is also unbounded and that it may not be possible to have (an almost sure) isolated eigenvalue “jumping out” in the large n, p limit.

Further consider the truncated model $\frac{1}{n}\mathbf{X}f(\mathbf{D})\mathbf{X}^\top = \frac{1}{n}\sum_{i=1}^n f(y_i) \mathbf{x}_i \mathbf{x}_i^\top$ for some truncation function $f : \mathbb{R}_+ \rightarrow \mathbb{R}_+$ that is of bounded support, for instance $f(t) = 1_{t \leq \tau}$ for some (predefined) threshold $\tau > 0$. This is indeed the trimming strategy proposed in [Chen and Candès, 2017] and was shown there to play a crucial role in the success of the algorithm in the large n, p regime. Again with the decomposition used above and Theorem 2.5, show that the resolvent $\mathbf{Q} = (\frac{1}{n}\mathbf{X}^\perp f(\mathbf{D})(\mathbf{X}^\perp)^\top - z\mathbf{I}_p)^{-1}$ and the co-resolvent $\tilde{\mathbf{Q}}$ admit the following deterministic equivalents

$$\mathbf{Q} \leftrightarrow m(z)(\mathbf{I}_p - \mathbf{aa}^\top) - \frac{1}{z}\mathbf{aa}^\top, \quad \tilde{\mathbf{Q}} \leftrightarrow -\frac{1}{z}(\mathbf{I}_n + cm(z)f(\mathbf{D}))^{-1}$$

for $(z, m(z))$ the unique solution in $\mathcal{Z}(\mathbb{C} \setminus \mathbb{R}^+)$ to

$$m(z) = \left(-z + \frac{1}{n} \text{tr } f(\mathbf{D})(\mathbf{I}_n + cm(z)f(\mathbf{D}))^{-1} \right)^{-1}$$

or equivalently

$$m(z) = \left(-z + \int \frac{f(t)\nu(dt)}{1 + cm(z)f(t)} \right)^{-1}$$

attention here! The definition of c seems not good!

for ν the χ^2 distribution with one degree of freedom (recall that $\|\mathbf{a}\| = 1$ and $\mathbb{E}[\mathbf{x}^\perp(\mathbf{x}^\perp)^\top] = \mathbf{I}_p - \mathbf{a}\mathbf{a}^\top$). With the deterministic equivalents derived above, following the proof of Theorem 2.12, solve $\det(\frac{1}{n}\mathbf{X}f(\mathbf{D})\mathbf{X}^\top - \lambda\mathbf{I}_p) = 0$ to find an (hypothetically) isolated spike λ and check that the associated $m(\lambda)$ then satisfies

$$-\frac{1}{m(\lambda)} + \int \frac{f(t)\nu(dt)}{1 + cf(t)m(\lambda)} = \int \frac{tf(t)\nu(dt)}{1 + cf(t)m(\lambda)} \quad (6.46)$$

with $\nu(dt)$ defined in (6.45). Determine then μ , the limiting spectral support of $\frac{1}{n}\mathbf{X}^\perp f(\mathbf{D})(\mathbf{X}^\perp)^\top$ (and thus of $\frac{1}{n}\mathbf{X}f(\mathbf{D})\mathbf{X}^\top$), with the help of the functional inverse

$$x(m) = -\frac{1}{m} + \int \frac{f(t)\nu(dt)}{1 + cmf(t)}$$

introduced in Section 2.3.1. Conclude on the (phase transition) condition for the spike λ to exist, using the sign of the derivative $x'(m_*)$, with m_* the solution to (6.46).

Denote the shortcut $\alpha \equiv -\frac{1}{cm}$, $\alpha_* \equiv -\frac{1}{cm_*}$ and

$$x(m) = \psi_c\left(\alpha \equiv -\frac{1}{cm}\right) = \alpha \left(c + \int \frac{f(t)\nu(dt)}{\alpha - f(t)} \right)$$

as well as

$$\phi(\alpha) = \alpha \int \frac{tf(t)\nu(dt)}{\alpha - f(t)}$$

so that (6.46) can be compactly rewritten as $\phi(\alpha_*) = \psi_c(\alpha_*)$.

Check that, on the interval $\alpha \in (\tau, \infty)$ (recall τ the upper bound of the truncation function f , i.e., $f(\cdot) \leq \tau$), $\phi(\alpha)$ is a non-increasing function and $\psi_c(\alpha)$ is a convex function, attaining its unique minimum at $\bar{\alpha}$ that satisfies

$$\psi'_c(\bar{\alpha}) = 0 \Leftrightarrow \int \frac{f^2(t)\nu(dt)}{(\bar{\alpha} - f(t))^2} = c.$$

Check that the phase transition condition on the sign of $x'(m_*)$ derived above is equivalent to

$$\begin{cases} \phi(\bar{\alpha}) > \psi_c(\bar{\alpha}) \Leftrightarrow \bar{\alpha} < \alpha_* \text{ and } \psi'_c(\alpha_*) > 0; \\ \phi(\bar{\alpha}) \leq \psi_c(\bar{\alpha}) \Leftrightarrow \bar{\alpha} \geq \alpha_* \text{ and } \psi'_c(\alpha_*) \leq 0. \end{cases}$$

As a consequence, in pursuit of an optimal design for the truncation function $f(\cdot)$ with maximum phase transition threshold c_{th} , it suffices to find $f(\cdot)$ such that

$$\int \frac{f^2(t)\nu(dt)}{(\bar{\alpha} - f(t))^2} = c, \quad \int \frac{f(t)(t-1)\nu(dt)}{\bar{\alpha} - f(t)} > c \quad (6.47)$$

holds for a maximal value of c . Using Cauchy-Schwarz inequality, show that we must then have

$$c^2 \leq 2c$$

with equality if and only if $\int \frac{f^2(t)\nu(dt)}{(\bar{\alpha}-f(t))^2} = \int (t-1)^2\nu(dt)$. Deduce that the optimal phase transition threshold is $c_{th} = 2$, in the sense that there is (almost surely) no spike in the spectrum of $\frac{1}{n}\mathbf{X}f(\mathbf{D})\mathbf{X}^\top$ so long that $c < c_{th} = 2$. Conclude then that the associated optimal truncation function is therefore given by

$$f(t) = \frac{\max(t, 0) - 1}{\max(t, 0) + \sqrt{2/c} - 1}$$

such that $\frac{f(t)}{1-f(t)} - (t-1) \rightarrow 0$ as $c \rightarrow c_{th} = 2$.

We refer the interested readers to [Lu and Li, 2019] for the asymptotic behavior of the associated isolated eigenvector and [Mondelli and Montanari, 2019] for the complex sensing matrix case.

** ajoute-on une question à un moment qui demande de retrouver le résultat avec ta méthode à la Zheng-Singer? **

Chapter 7

Community Detection on Graphs

`chap:community-detection`

In the previous chapters, our attention has been long cast on numerous applications involving sample covariance matrix models $\frac{1}{n}\mathbf{XX}^\top \in \mathbb{R}^{p \times p}$ for some random matrix $\mathbf{X} \in \mathbb{R}^{p \times n}$ following a certain statistical model, as well as on the quite related Gram matrix $\frac{1}{n}\mathbf{X}^\top\mathbf{X} \in \mathbb{R}^{n \times n}$ and kernel matrices $f(\frac{1}{n}\mathbf{X}^\top\mathbf{X})$ (with f applied here entry-wise). The starting point of the asymptotic analysis of machine learning algorithms for most of these models is the Marčenko-Pastur law (Theorem 2.3) and its various generalizations.

When it comes to studying the statistical behavior of randomly generated graphs and networks, starting with the so-called Erdős-Rényi graphs, which randomly and independently draws connections between each pair of nodes in the graph according to a Bernoulli law, the raw random matrix model will be instead a Wigner matrix (for undirected graphs) and theoretical analyses will rely instead on Wigner's semi-circle law (Theorem 2.4) and its variations.

In this chapter, we will be particularly interested in the question of *community detection* on large dimensional and *dense* undirected and unweighted n -node graphs. By unweighted, we mean that an edge between node i and node j carries a unit weight 1, and zero otherwise. By undirected, we mean that, if node i connects to node j , then node j connects to node i , which in particular implies that the *adjacency matrix* $\mathbf{A} \in \{0, 1\}^{n \times n}$ of the graph is symmetric ($\mathbf{A}_{ij} = \mathbf{A}_{ji}$). By dense graphs, we mean graphs for which the typical number of neighbors of each node scales proportionally to the graph size n as $n \rightarrow \infty$. This will cover the main Section 7.1 of this chapter. A few notes and remarks on the more involved case of *sparse* graphs, those graphs for which each node instead has $O(1)$ neighbors, will be given in Section 7.2.

7.1 Community detection in dense graphs

sec:commu-detec-dense

7.1.1 The stochastic block model

sec:SBM

7.1.1.1 Erdős-Rényi random graphs and the modularity matrix

The adjacency matrix The most natural random undirected graph is the Erdős-Rényi graph, defined by the fact that its adjacency matrix $\mathbf{A} \in \{0, 1\}^{n \times n}$ is composed, up to symmetry ($\mathbf{A}_{ij} = \mathbf{A}_{ji}$) and to a null diagonal ($\mathbf{A}_{ii} = 0$), of *independent and identically distributed Bernoulli* entries: for all $i \neq j$,

$$\mathbf{A}_{ij} = \mathbf{A}_{ji} \sim \text{Bern}(p)$$

where $p \in (0, 1)$. To ensure that the graph is dense, we demand that, for each i , $\sum_j \mathbf{A}_{ij} = O(n)$, which implies that $p = O(1)$ with respect to n .

This setting implies that, for all $i < j$, the \mathbf{A}_{ij} are independent with $\mathbb{E}[\mathbf{A}_{ij}] = p$ and $\text{var}[\mathbf{A}_{ij}] = p(1-p)$. In particular, by the central limit theorem, the degree d_i of node i , satisfies

$$d_i \equiv \sum_{j=1}^n \mathbf{A}_{ij} = np + \sqrt{p(1-p)n}(\mathcal{N}(0, 1) + o(1)).$$

and the average degree d_i/n converges almost surely to p .

Writing

$$\mathbf{A} = \mathbb{E}[\mathbf{A}] + \sqrt{p(1-p)}\mathbf{X} = p(\mathbf{1}_n \mathbf{1}_n^\top - \mathbf{I}_n) + \sqrt{p(1-p)}(\mathbf{X} - \text{diag}(\mathbf{X}))$$

where $\mathbf{X} \in \mathbb{R}^{n \times n}$ has entries or zero mean and unit variance and $\text{diag}(\mathbf{X})$ is the diagonal matrix containing only the diagonal entries of \mathbf{X} , we find that

$$\frac{1}{\sqrt{n}}\mathbf{A} = \frac{p}{\sqrt{n}}\mathbf{1}_n\mathbf{1}_n^\top + \frac{\sqrt{p(1-p)}}{\sqrt{n}}\mathbf{X} + O_{\|\cdot\|}(n^{-\frac{1}{2}})$$

is a rank-one perturbation of a ($\sqrt{p(1-p)}$ -scaled) Wigner matrix (where $O_{\|\cdot\|}(\cdot)$ is in probability). Theorem 2.4 therefore applies and we have

- in the first order, $\frac{1}{n}\mathbf{A} = \frac{p}{n}\mathbf{1}_n\mathbf{1}_n^\top + O_{\|\cdot\|}(n^{-\frac{1}{2}})$ is essentially a unit-rank matrix with eigendirection $\mathbf{1}_n$ and eigenvalue p .
- the limiting spectral measure of $\frac{1}{\sqrt{n}}\mathbf{A}$ is a semi-circle law scaled by $\sqrt{p(1-p)}$, so in particular supported on $[-2\sqrt{p(1-p)}, 2\sqrt{p(1-p)}]$.

The modularity matrix To avoid the technically problematic, and practically irrelevant, largely dominant $\frac{p}{\sqrt{n}}\mathbf{1}_n\mathbf{1}_n^\top$ matrix in \mathbf{A} , it is customary to rather work with the so-called *modularity* matrix

$$\mathbf{B} = \frac{1}{\sqrt{n}} \left(\mathbf{A} - \frac{\mathbf{d}\mathbf{d}^\top}{\mathbf{d}^\top \mathbf{1}_n} \right)$$

introduced in [Newman, 2006], where $\mathbf{d} = [d_1, \dots, d_n]^\top = \mathbf{A}\mathbf{1}_n$. The advantage of \mathbf{B} versus \mathbf{A} is that $\mathbf{B}\mathbf{1}_n = \mathbf{0}$. This eliminates the dominant contribution of the vector $\mathbf{1}_n$. However, as a negative side effect, the matrix $\mathbf{A} - \frac{\mathbf{d}\mathbf{d}^\top}{\mathbf{d}^\top\mathbf{1}_n}$ is the summation of two strongly dependent random matrices. Let us try to decipher this dependence and study the spectrum of \mathbf{B} for n large.

First, using the fact that $\mathbf{d} = \mathbf{A}\mathbf{1}_n$ gives

$$\mathbf{d} = pn\mathbf{1}_n + \sqrt{p(1-p)}\mathbf{X}\mathbf{1}_n + O_{\|\cdot\|}(n^{\frac{1}{2}})$$

from which it follows that

$$\begin{aligned} \mathbf{d}^\top\mathbf{1}_n &= pn^2 + O(n) \\ \mathbf{d}\mathbf{d}^\top &= p^2n^2\mathbf{1}_n\mathbf{1}_n^\top + pn\sqrt{p(1-p)}(\mathbf{X}\mathbf{1}_n\mathbf{1}_n^\top + \mathbf{1}_n\mathbf{1}_n^\top\mathbf{X}) + O_{\|\cdot\|}(n^2) \end{aligned}$$

and thus

$$\frac{1}{\sqrt{n}} \frac{\mathbf{d}\mathbf{d}^\top}{\mathbf{d}^\top\mathbf{1}_n} = p \frac{\mathbf{1}_n\mathbf{1}_n^\top}{\sqrt{n}} + \sqrt{p(1-p)} \left(\frac{\mathbf{1}_n\mathbf{1}_n^\top\mathbf{X}}{n\sqrt{n}} + \frac{\mathbf{X}\mathbf{1}_n\mathbf{1}_n^\top}{n\sqrt{n}} \right) + O_{\|\cdot\|}(n^{-\frac{1}{2}}).$$

Thus, we obtain

$$\frac{1}{\sqrt{p(1-p)}}\mathbf{B} = \frac{\mathbf{X}}{\sqrt{n}} - \left(\frac{\mathbf{1}_n\mathbf{1}_n^\top\mathbf{X}}{n\sqrt{n}} + \frac{\mathbf{X}\mathbf{1}_n\mathbf{1}_n^\top}{n\sqrt{n}} \right) + O_{\|\cdot\|}(n^{-\frac{1}{2}}). \quad \text{eq:(7.1)}$$

As a consequence, the modularity matrix \mathbf{B} may be asymptotically seen as a rank 2 perturbation of a random Wigner matrix \mathbf{X} . Solving $\det(\mathbf{B} - \lambda\mathbf{I}_n) = 0$ for $\lambda \notin [-2\sqrt{p(1-p)}, 2\sqrt{p(1-p)}]$ (the support of the limiting spectral measure of \mathbf{B}) reveals that there asymptotically exists no solution. A detailed derivation will be performed in the next section for the more interesting stochastic block model. As such, as one would have expected, all the eigenvalues of \mathbf{B} are compactly supported within the limiting semi-circle support.

7.1.1.2 From Erdős-Rényi to the SBM

In order to account for the presence of communities of nodes in the graphs, we introduce now the stochastic block model (SBM) by assuming the possibility for the Bernoulli parameter of \mathbf{A}_{ij} to depend on the pair of nodes (i, j) . Specifically, letting $\mathcal{C}_1, \dots, \mathcal{C}_k$ be k communities of cardinalities $n_a \equiv |\mathcal{C}_a|$, we define $\mathbf{C} \in \mathbb{R}^{k \times k}$ the matrix of Bernoulli parameters such that, if node i belongs to class \mathcal{C}_a and node $j \neq i$ belongs to class \mathcal{C}_b with $a, b \in \{1, \dots, k\}$,

$$\mathbf{A}_{ij} = \mathbf{A}_{ji} \sim \text{Bern}(\mathbf{C}_{ab}).$$

We further consider that all classes are of “large size” in the sense that $n_a/n \rightarrow c_a \in (0, 1)$ as $n \rightarrow \infty$.

As in the case of spectral clustering discussed in Section 4, in order to avoid trivial scenarios in the large n asymptotics, a careful control of the differences

between elements of the matrix \mathbf{C} is needed. As we shall see next, the proper normalization is such that

$$\mathbf{C}_{ab} = p \left(1 + \frac{\mathbf{M}_{ab}}{\sqrt{n}} \right)$$

for $\mathbf{M} \in \mathbb{R}^{k \times k}$ a deterministic matrix, independent of n , and $p \in (0, 1)$ as above, also independent of n . That is, as n increases, communities with Bernoulli parameter differences scaling as $1/\sqrt{n}$ can still be distinguished in SBM.

here!

Following the same analysis as above, it comes immediately that

$$\mathbb{E}[\mathbf{A}] = p \left(\mathbf{1}_n \mathbf{1}_n^\top + \frac{1}{\sqrt{n}} \mathbf{J} \mathbf{M} \mathbf{J}^\top \right)$$

where, as in the previous chapters, we defined $\mathbf{J} = [\mathbf{j}_1, \dots, \mathbf{j}_k] \in \mathbb{R}^{n \times k}$ for $[\mathbf{j}_a]_i = \delta_{i \in C_a}$ the canonical vector of community C_a . Also,

$$\begin{aligned} \text{var}[\mathbf{A}_{ij}] &= p \left[1 + \frac{\mathbf{M}_{ab}}{\sqrt{n}} \right] \left(1 - p \left[1 + \frac{\mathbf{M}_{ab}}{\sqrt{n}} \right] \right) \\ &= p(1-p) + O(n^{-\frac{1}{2}}). \end{aligned}$$

As such, since $\mathbf{1}_n = \mathbf{J} \mathbf{1}_k$, we can anticipate from the previous section that $\frac{1}{\sqrt{np(1-p)}} \mathbf{A}$ is well approximated by a rank (at most) k perturbation of a random matrix $\frac{1}{\sqrt{n}} \mathbf{X}$ having i.i.d. entries of zero mean and unit variance. The perturbation matrix has a largely dominant eigenvalue of order \sqrt{n} and up-to $k-1$ isolated eigenvalues outside the bulk of the limiting spectrum of $\frac{1}{\sqrt{n}} \mathbf{X}$; here “up-to” translates the fact that, $\frac{1}{n} \mathbf{J} \mathbf{M} \mathbf{J}^\top$ being of operator norm $O(1)$ (same as $\frac{1}{\sqrt{n}} \mathbf{X}$), phase transition phenomena are bound to occur.

As for $\mathbf{B} = \frac{1}{\sqrt{n}} (\mathbf{A} - \frac{\mathbf{d}\mathbf{d}^\top}{\|\mathbf{d}\|^2})$, it will likely have the same effect of discarding the dominant eigenvalue-eigenvector pair, thereby ensuring that $\|\mathbf{B}\| = O(1)$ and that the dominant (possibly isolated) and bulk eigenvalues of \mathbf{B} are comparable.

Performing the same analysis as in the Erdős-Rényi setting brings additional terms which, after carefully discarding the terms of vanishing norms (as usual, special care is needed when taking the product of matrices or vectors with varying different norms and different levels of dependence), gives the SBM version of (7.1):

$$\begin{aligned} \frac{1}{\sqrt{p(1-p)}} \mathbf{B} &= \frac{\mathbf{X}}{\sqrt{n}} + \frac{p}{\sqrt{p(1-p)}} \frac{\mathbf{J} \mathbf{M}^\circ \mathbf{J}^\top}{n} \\ &\quad - \left(\frac{\mathbf{1}_n \mathbf{1}_n^\top}{n} \frac{\mathbf{X}}{\sqrt{n}} + \frac{\mathbf{X}}{\sqrt{n}} \frac{\mathbf{1}_n \mathbf{1}_n^\top}{n} \right) + O_{\|\cdot\|}(n^{-\frac{1}{2}}) \quad \text{eq:B_SBM (7.2)} \end{aligned}$$

where we defined $\mathbf{M}^\circ = (\mathbf{I}_k - \mathbf{1}_k \mathbf{c}^\top) \mathbf{M} (\mathbf{I}_k - \mathbf{c} \mathbf{1}_k^\top)$ with $\mathbf{c} = (\frac{n_1}{n}, \dots, \frac{n_k}{n})^\top$ the community size ratios. Matrix \mathbf{M}° is a “centered” version of \mathbf{M} accounting for the community sizes in the sense that $\mathbf{M}^\circ \mathbf{c} = 0$ (i.e., for all a , $\sum_{b=1}^k n_b M_{ab}^\circ = 0$).

Consequently, \mathbf{B} is again (up to scaling) the sum of a symmetric random matrix \mathbf{X} with zero mean unit variance entries and of a perturbation matrix of rank up to k (since $\mathbf{1}_n$ is in the span of the columns of \mathbf{J}). Clearly, in expectation,

$$\mathbb{E}[\mathbf{B}] = p \frac{\mathbf{JM}^\circ \mathbf{J}^\top}{n} + O_{\|\cdot\|}(n^{-\frac{1}{2}})$$

so that the dominant eigenvectors of \mathbf{B} are, as one would expect, linear combinations of the class vectors $\mathbf{j}_1, \dots, \mathbf{j}_k$, weighted here by the coefficients of \mathbf{M}° . The additional fluctuations being due to the matrices \mathbf{X} and $(\mathbf{1}_n \mathbf{1}_n^\top \mathbf{X} + \mathbf{X} \mathbf{1}_n \mathbf{1}_n^\top)$, which are “isotropic” with respect to the class structures, they should not affect the quality of a k-means of expectation-maximization clustering of the eigenvectors of \mathbf{B} . We will see in the next section that this important remark no longer holds for stochastic block models with *heterogeneous* degrees.

Pursuing our derivation, to stress the presence of a rank- k perturbation, note that \mathbf{B} may be rewritten conveniently as

$$\frac{\mathbf{B}}{\sqrt{p(1-p)}} = \frac{\mathbf{X}}{\sqrt{n}} + \begin{bmatrix} \frac{\mathbf{J}}{\sqrt{n}} & \frac{\mathbf{X}\mathbf{1}_n}{n} \end{bmatrix} \begin{bmatrix} \frac{p}{\sqrt{p(1-p)}} \mathbf{M}^\circ & -\mathbf{1}_k \\ -\mathbf{1}_k^\top & 0 \end{bmatrix} \begin{bmatrix} \frac{\mathbf{J}^\top}{\sqrt{n}} \\ \frac{\mathbf{1}_n^\top \mathbf{X}^\top}{n} \end{bmatrix} + O_{\|\cdot\|}(n^{-\frac{1}{2}}).$$

It is interesting to note that \mathbf{B} is here a rank- k perturbation of \mathbf{X} which is *not* independent of \mathbf{X} , from the presence of the vector $\mathbf{X}\mathbf{1}_n$ (although, as we will see subsequently, the term $\mathbf{X}\mathbf{1}_n$ will have asymptotically no effect on the limiting spectral properties of \mathbf{B}).

Studying the (limiting) location of the possibly isolated eigenvalues of \mathbf{B} thus consists in solving, for $\lambda > 2$ (i.e., the right-edge of the semi-circle law, which is the limiting support of the eigenvalues of the full-rank matrix \mathbf{X}/\sqrt{n}),

$$\begin{aligned} & \det \left(\frac{\mathbf{X}}{\sqrt{n}} - \lambda \mathbf{I}_n + \begin{bmatrix} \frac{\mathbf{J}}{\sqrt{n}} & \frac{\mathbf{X}\mathbf{1}_n}{n} \end{bmatrix} \begin{bmatrix} \frac{p}{\sqrt{p(1-p)}} \mathbf{M}^\circ & -\mathbf{1}_k \\ -\mathbf{1}_k^\top & 0 \end{bmatrix} \begin{bmatrix} \frac{\mathbf{J}^\top}{\sqrt{n}} \\ \frac{\mathbf{1}_n^\top \mathbf{X}^\top}{n} \end{bmatrix} \right) = 0 \\ & \Leftrightarrow \det \left(\mathbf{I}_n + \mathbf{Q} \begin{bmatrix} \frac{\mathbf{J}}{\sqrt{n}} & \frac{\mathbf{X}\mathbf{1}_n}{n} \end{bmatrix} \begin{bmatrix} \frac{p}{\sqrt{p(1-p)}} \mathbf{M}^\circ & -\mathbf{1}_k \\ -\mathbf{1}_k^\top & 0 \end{bmatrix} \begin{bmatrix} \frac{\mathbf{J}^\top}{\sqrt{n}} \\ \frac{\mathbf{1}_n^\top \mathbf{X}^\top}{n} \end{bmatrix} \right) = 0 \\ & \Leftrightarrow \det \left(\mathbf{I}_{k+1} + \begin{bmatrix} \frac{\mathbf{J}^\top}{\sqrt{n}} \\ \frac{\mathbf{1}_n^\top \mathbf{X}^\top}{n} \end{bmatrix} \mathbf{Q} \begin{bmatrix} \frac{\mathbf{J}}{\sqrt{n}} & \frac{\mathbf{X}\mathbf{1}_n}{n} \end{bmatrix} \begin{bmatrix} \frac{p}{\sqrt{p(1-p)}} \mathbf{M}^\circ & -\mathbf{1}_k \\ -\mathbf{1}_k^\top & 0 \end{bmatrix} \right) = 0 \end{aligned}$$

where we introduced the resolvent $\mathbf{Q} = \mathbf{Q}(\lambda) = (\frac{\mathbf{X}}{\sqrt{n}} - \lambda \mathbf{I}_n)^{-1}$.

From the deterministic equivalent $\mathbf{Q} \leftrightarrow m(\lambda) \mathbf{I}_n$ of Theorem 2.4, where $m(\lambda)$ is here the unique negative solution to $m^2(\lambda) + \lambda m(\lambda) + 1 = 0$, we find that

$$\begin{bmatrix} \frac{\mathbf{J}^\top}{\sqrt{n}} \\ \frac{\mathbf{1}_n^\top \mathbf{X}^\top}{n} \end{bmatrix} \mathbf{Q} \begin{bmatrix} \frac{\mathbf{J}}{\sqrt{n}} & \frac{\mathbf{X}\mathbf{1}_n}{n} \end{bmatrix} = \begin{bmatrix} m(\lambda) \mathbf{D}_c & (1 + \lambda m(\lambda)) \mathbf{c} \\ (1 + \lambda m(\lambda)) \mathbf{c}^\top & \lambda(1 + \lambda m(\lambda)) \end{bmatrix} + o(1)$$

(almost surely) where $\mathbf{D}_c = \text{diag}(\mathbf{c})$ and the bottom right entry follows from a repeated use of the relation $\mathbf{QX}/\sqrt{n} = \mathbf{I}_n + \lambda\mathbf{Q}$ and of the above deterministic equivalent. This gives the (asymptotically) equivalent determinantal equation

$$\det \begin{pmatrix} \mathbf{I}_k + \frac{pm(\lambda)}{\sqrt{p(1-p)}} \mathbf{D}_c \mathbf{M}^\circ & (1 + \lambda m(\lambda)) \mathbf{c} \mathbf{1}_k^\top & -m(\lambda) \mathbf{c} \\ & -\lambda(1 + \lambda m(\lambda)) \mathbf{1}_k^\top & -\lambda m(\lambda) \end{pmatrix} \quad (7.3)$$

which, using the block-determinant relation $\det(\begin{smallmatrix} \mathbf{A}^\top & \mathbf{u} \\ \mathbf{v}^\top & w \end{smallmatrix}) = \det(\mathbf{A} - \frac{1}{w}\mathbf{u}\mathbf{v}^\top)$, is simply

$$\det \left(\mathbf{I}_k + \frac{pm(\lambda)}{\sqrt{p(1-p)}} \mathbf{D}_c \mathbf{M}^\circ \right) = \det \left(\mathbf{I}_k + \frac{pm(\lambda)}{\sqrt{p(1-p)}} \mathbf{D}_{\sqrt{c}} \mathbf{M}^\circ \mathbf{D}_{\sqrt{c}} \right)$$

where in the last equality, $\sqrt{\mathbf{c}} = (\sqrt{c_1}, \dots, \sqrt{c_k})^\top$. The cancellation of the term proportional to $\mathbf{c} \mathbf{1}_k^\top$ in the last calculus stresses the asymptotic “inaction” of the vector $\mathbf{X} \mathbf{1}_n$ on the *informative* (for community detection) eigenvalues of \mathbf{B} .

This leads to the following result on isolated eigenvalues.

Theorem 7.1 (Isolated eigenvalues in the SBM). *Under the setting of this section, to each eigenvalue ℓ of $\mathbf{D}_c \mathbf{M}^\circ$ for which*

$$|\ell| > \sqrt{\frac{1-p}{p}}$$

there exists an associated eigenvalue λ_ℓ of $\frac{1}{\sqrt{p(1-p)}} \mathbf{B}$ such that, for all large n almost surely, $|\lambda_\ell| > 2$ and

$$\begin{aligned} \lambda_\ell &= m^{-1} \left(-\sqrt{\frac{1-p}{p}} \frac{1}{\ell} \right) + o(1) \\ &= \frac{p\ell + \frac{1-p}{\ell}}{\sqrt{p(1-p)}} + o(1) \end{aligned}$$

for $m^{-1}(\cdot) : (-1, 0) \rightarrow (2, \infty)$, $t \mapsto (-1 - t^2)/t$ is the local inverse of $m(\cdot)$.

Obviously, as with spectral clustering (recall Chapter 4.5.1), isolated eigenvalues in the spectrum of \mathbf{B} are associated with eigenvectors aligned to $\mathbb{E}[\mathbf{B}]$ and thus here to some informative linear combination of the class-vectors $\mathbf{j}_1, \dots, \mathbf{j}_k$.

To assess the limiting projection of these eigenvectors of \mathbf{B} on each (normalized) direction $\mathbf{j}_1, \dots, \mathbf{j}_k$, we may next evaluate

$$\begin{aligned} &\frac{1}{n} \mathbf{D}_c^{-\frac{1}{2}} \mathbf{J}^\top \hat{\mathbf{u}}_\ell \hat{\mathbf{u}}_\ell^\top \mathbf{J} \mathbf{D}_c^{-\frac{1}{2}} \\ &= -\frac{1}{2\pi i} \oint_{\Gamma_\ell} \frac{1}{n} \mathbf{D}_c^{-\frac{1}{2}} \mathbf{J}^\top \left(\frac{\mathbf{B}}{\sqrt{p(1-p)}} - z \mathbf{I}_n \right)^{-1} \mathbf{J} \mathbf{D}_c^{-\frac{1}{2}} dz \end{aligned}$$

where $\frac{1}{n} \mathbf{J} \mathbf{D}_c^{-1} \mathbf{J}^\top$ is a projector on $\text{span}(\mathbf{j}_1, \dots, \mathbf{j}_k)$ and Γ_ℓ a fixed small complex contour circling around λ_ℓ only (for all large n). Using the same approach consisting in isolating $\frac{\mathbf{X}}{\sqrt{n}} - z\mathbf{I}_n$ from $\frac{\mathbf{B}}{\sqrt{p(1-p)}} - z\mathbf{I}_n$, and using matrix inversion lemmas and several algebraic simplifications, we obtain

*** I should clearly give some details here... ***

$$\begin{aligned} & \frac{1}{n} \mathbf{D}_c^{-\frac{1}{2}} \mathbf{J}^\top \hat{\mathbf{u}}_\ell \hat{\mathbf{u}}_\ell^\top \mathbf{J} \mathbf{D}_c^{-\frac{1}{2}} \\ &= \frac{-1}{2\pi i} \oint_{\Gamma_\ell} m(z) \left(\mathbf{I}_k + \frac{pm(z)\mathbf{D}_c^{-\frac{1}{2}} \mathbf{M}^\circ \mathbf{D}_c^{-\frac{1}{2}}}{\sqrt{p(1-p)}} \right)^{-1} dz + o(1) \end{aligned}$$

where we neglected all terms leading to a vanishing residue in the large n limit. Residue calculus leads to the existence of a unique pole of order 1 with associated residue given by

$$\begin{aligned} & \frac{1}{n} \mathbf{D}_c^{-\frac{1}{2}} \mathbf{J}^\top \hat{\mathbf{u}}_\ell \hat{\mathbf{u}}_\ell^\top \mathbf{J} \mathbf{D}_c^{-\frac{1}{2}} \\ &= \lim_{z \rightarrow \lambda_\ell} -(z - \lambda_\ell)m(z) \left(\mathbf{I}_k + \frac{pm(z)\mathbf{D}_c^{-\frac{1}{2}} \mathbf{M}^\circ \mathbf{D}_c^{-\frac{1}{2}}}{\sqrt{p(1-p)}} \right)^{-1} + o(1) \\ &= \frac{-m(\lambda_\ell)}{\frac{p}{\sqrt{1-p}} \ell m'(\lambda_\ell)} \mathbf{u}_\ell \mathbf{u}_\ell^\top + o(1) \end{aligned}$$

where \mathbf{u}_ℓ is the eigenvector of $\mathbf{D}_{\sqrt{c}} \mathbf{M}^\circ \mathbf{D}_{\sqrt{c}}$ associated with eigenvalue ℓ . Recalling that λ_ℓ is solution to $1 + \sqrt{p/(1-p)}\ell m(\lambda_\ell) = 0$ and that $m(z)^2 + zm(z) = -1$ (which we can differentiate along z), this is more simply written as

$$\begin{aligned} & \frac{1}{n} \mathbf{D}_c^{-\frac{1}{2}} \mathbf{J}^\top \hat{\mathbf{u}}_\ell \hat{\mathbf{u}}_\ell^\top \mathbf{J} \mathbf{D}_c^{-\frac{1}{2}} = (1 - m(\lambda_\ell)^2) \mathbf{u}_\ell \mathbf{u}_\ell^\top + o(1) \\ &= \left(1 - \frac{1-p}{p\ell^2} \right) \mathbf{u}_\ell \mathbf{u}_\ell^\top + o(1). \end{aligned}$$

These two alternative formulas are nicely interpreted: outside the support of the semi-circle law, $\lambda \mapsto 1 - m(\lambda)^2$ is positive, increasing and maps $(2, \infty)$ onto $(0, 1)$. In particular, the alignment of $\hat{\mathbf{u}}_\ell$ on the subspace spanned by $\mathbf{j}_1, \dots, \mathbf{j}_k$ is given by $\|\frac{1}{n} \mathbf{D}_c^{-\frac{1}{2}} \mathbf{J}^\top \hat{\mathbf{u}}_\ell\|^2 = 1 - m(\lambda_\ell)^2 + o(1)$. Equivalently, recalling that one needs $|\ell| > \sqrt{(1-p)/p}$ to achieve separability, as $|\ell|$ increases in $(\sqrt{(1-p)/p}, \infty)$, the alignment increases to 1 at rate $1/\ell^2$.

This is summarized in the following result.

theo:eigv_SBM

Theorem 7.2 (Eigenvector alignment in the SBM). *Under the setting and notations of Theorem 7.1, if $|\ell| > \sqrt{\frac{1-p}{p}}$ for (ℓ, \mathbf{u}_ℓ) an eigenvalue-eigenvector pair of $\mathbf{D}_{\sqrt{c}} \mathbf{M}^\circ \mathbf{D}_{\sqrt{c}}$, then the eigenvalue-eigenvector pair $(\lambda_\ell, \hat{\mathbf{u}}_\ell)$ of \mathbf{B} satisfies*

$$\frac{1}{n} \mathbf{D}_c^{-\frac{1}{2}} \mathbf{J}^\top \hat{\mathbf{u}}_\ell \hat{\mathbf{u}}_\ell^\top \mathbf{J} \mathbf{D}_c^{-\frac{1}{2}} = (1 - m(\lambda_\ell)^2) \mathbf{u}_\ell \mathbf{u}_\ell^\top + o(1)$$

as $n \rightarrow \infty$, almost surely.

7.1.1.3 Case study: 2-class symmetric SBM

Let us observe the consequences of the previous results on the popular two-class symmetric stochastic block model. In this setting, we generally define the connection probability matrix as

$$\mathbf{C} = \begin{bmatrix} p_{\text{in}} & p_{\text{out}} \\ p_{\text{out}} & p_{\text{in}} \end{bmatrix}$$

for some $p_{\text{in}}, p_{\text{out}} > 0$ the inner-class and outer-class connection probabilities. We also set the class cardinalities as $\mathbf{c} = [\frac{1}{2}, \frac{1}{2}]^T$. By exchangeability arguments, the statistics of the eigenvectors of \mathbf{B} are in this case completely symmetric and thus more expressive.

In the context of the previous section, this choice implies for instance that

$$\begin{aligned} p &= p_{\text{out}} \\ \mathbf{M} &= \sqrt{n} \frac{p_{\text{in}} - p_{\text{out}}}{p_{\text{out}}} \mathbf{I}_2 \end{aligned}$$

which indicates, of course, that p_{in} depends on n and must scale as $p_{\text{out}} + O(n^{-\frac{1}{2}})$ for \mathbf{M} to remain of bounded norm. As a consequence,

$$\mathbf{D}_{\sqrt{c}} \mathbf{M}^\circ \mathbf{D}_{\sqrt{c}} = \frac{\sqrt{n}(p_{\text{in}} - p_{\text{out}})}{p_{\text{out}}} \frac{1}{2} \left(\mathbf{I}_2 - \frac{1}{2} \mathbf{1}_2 \mathbf{1}_2^T \right) \xrightarrow{\text{eq:M_2classSBM}} (7.4)$$

which has a unique nonzero eigenvalue, equal to

$$\ell = \frac{\sqrt{n}(p_{\text{in}} - p_{\text{out}})}{2p_{\text{out}}}$$

and with associated eigenvector

$$\mathbf{u}_\ell = \frac{1}{\sqrt{2}} \begin{pmatrix} 1 \\ -1 \end{pmatrix}.$$

The detectability phase transition thus occurs under the condition

$$p_{\text{in}} > p_{\text{out}} + \frac{2\sqrt{p_{\text{out}}(1-p_{\text{out}})}}{\sqrt{n}}.$$

The isolated eigenvalue of $\frac{1}{\sqrt{p_{\text{out}}(1-p_{\text{out}})}} \mathbf{B}$ is defined by

$$m(\lambda_\ell) = -\frac{2\sqrt{p_{\text{out}}(1-p_{\text{out}})}}{\sqrt{n}(p_{\text{in}} - p_{\text{out}})} + o(1)$$

or equivalently, using $m(\cdot)^{-1}(t) = (-1 - t^2)/t$,

$$\lambda_\ell = \frac{\sqrt{n}(p_{\text{in}} - p_{\text{out}})}{2\sqrt{p_{\text{out}}(1-p_{\text{out}})}} + \frac{2\sqrt{p_{\text{out}}(1-p_{\text{out}})}}{\sqrt{n}(p_{\text{in}} - p_{\text{out}})} + o(1).$$

Consequently, the asymptotic projection of $\hat{\mathbf{u}}_\ell$ on each vector $\mathbf{j}_1, \mathbf{j}_2$ is given by

$$\frac{2}{n} [\mathbf{j}_1 \quad \mathbf{j}_2]^\top \hat{\mathbf{u}}_\ell \hat{\mathbf{u}}_\ell^\top [\mathbf{j}_1 \quad \mathbf{j}_2] = \frac{1}{2} \left(1 - \frac{4p_{\text{out}}(1-p_{\text{out}})}{n(p_{\text{in}}-p_{\text{out}})^2} \right) \begin{bmatrix} 1 & -1 \\ -1 & 1 \end{bmatrix} + o(1).$$

By exchangeability and symmetry, these results also give access to the mean and variance of every entry $[\hat{\mathbf{u}}_\ell]_i$ of the vector $\hat{\mathbf{u}}_\ell$. Specifically,

$$\frac{2}{n} (\mathbf{j}_1^\top \hat{\mathbf{u}}_\ell)^2 = \frac{n}{2} \left(\frac{1}{n/2} \sum_{i=1}^{n/2} [\hat{\mathbf{u}}_\ell]_i \right)^2$$

gives access to the empirical average value of the entries $[\hat{\mathbf{u}}_\ell]_i$ which are of course identically distributed on $1 \leq i \leq \frac{n}{2}$ and on $\frac{n}{2} + 1 \leq i \leq n$. Also

$$\frac{2}{n} (\mathbf{j}_1^\top \hat{\mathbf{u}}_\ell)(\mathbf{j}_2^\top \hat{\mathbf{u}}_\ell) = \frac{n}{2} \left(\frac{1}{n/2} \sum_{i=1}^{n/2} [\hat{\mathbf{u}}_\ell]_i \right) \left(\frac{1}{n/2} \sum_{i=n/2+1}^n [\hat{\mathbf{u}}_\ell]_i \right)$$

gives access to the correlation between the first $n/2$ and last $n/2$ elements of $\hat{\mathbf{u}}_\ell$. We thus find that

$$\begin{aligned} \mathbb{E}[[\hat{\mathbf{u}}_\ell]_i] &= \begin{cases} \sqrt{\frac{1}{n} \left(1 - \frac{4p_{\text{out}}(1-p_{\text{out}})}{n(p_{\text{in}}-p_{\text{out}})^2} \right)} + o(1) & , i \leq \frac{n}{2} \\ -\sqrt{\frac{1}{n} \left(1 - \frac{4p_{\text{out}}(1-p_{\text{out}})}{n(p_{\text{in}}-p_{\text{out}})^2} \right)} + o(1) & , i > \frac{n}{2} \end{cases} \\ \text{var}[[\hat{\mathbf{u}}_\ell]_i] &= \frac{4p_{\text{out}}(1-p_{\text{out}})}{n^2(p_{\text{in}}-p_{\text{out}})^2} + o(1) \end{aligned}$$

where the result on the average is of course valid up to sign (since eigenvectors are defined up to a sign) and the result on the variance exploits the constraint $\sum_{i=1}^n |[\hat{\mathbf{u}}_\ell]_i|^2 = 1$.

As it can be further shown that the fluctuations of $[\hat{\mathbf{u}}_\ell]_i$ are asymptotically Gaussian and asymptotically independent across i , see Remark 7.1, (only asymptotically of course, since the constraint $\|\hat{\mathbf{u}}_\ell\| = 1$ creates a finite-dimensional dependence), the result immediately leads to the evaluation of the empirical classification error, i.e.,

$$\begin{aligned} \frac{1}{n} \left(\# \left\{ [\hat{\mathbf{u}}_\ell]_i < 0 \mid i \leq \frac{n}{2} \right\} + \# \left\{ [\hat{\mathbf{u}}_\ell]_i > 0 \mid i > \frac{n}{2} \right\} \right) \\ - Q \left(\sqrt{\frac{n(p_{\text{in}}-p_{\text{out}})^2}{4p_{\text{out}}(1-p_{\text{out}})}} - 1 \right) \xrightarrow{\text{a.s.}} 0 \end{aligned} \quad \text{eq:SBM_proba_err} \quad (7.5)$$

with the sign convention $[\hat{\mathbf{u}}_\ell]_1 > 0$ and with $Q(t) = \frac{1}{\sqrt{2\pi}} \int_t^\infty e^{-\frac{u^2}{2}} du$. Be careful that this does not depend on n as $n(p_{\text{in}}-p_{\text{out}})^2 = O(1)$.

rem:SBM_CLT

Remark 7.1 (On the asymptotic Gaussianity of the error rate). *It is interesting to realize that the asymptotic Gaussianity of the misclassification probability, despite depending on all the entries of the vector $\hat{\mathbf{u}}_\ell$, only requires to prove the asymptotic two-dimensional Gaussianity of any pair $([\hat{\mathbf{u}}_\ell]_i, [\hat{\mathbf{u}}_\ell]_j)$ of entries of the eigenvector $\hat{\mathbf{u}}_\ell$. It suffices indeed to proceed as follows:*

1. **Pairwise Gaussianity using the resolvent.** As usual, we first seek to express the quantities of interest (here $[\hat{\mathbf{u}}_\ell]_i$) as a function of the resolvent $\mathbf{Q}_z = (\mathbf{X}/\sqrt{n} - z\mathbf{I}_n)^{-1}$. This is obtained first the defining equation

$$\frac{1}{\sqrt{p_{\text{out}}(1-p_{\text{out}})}} \mathbf{B}\hat{\mathbf{u}}_\ell = \lambda_\ell \hat{\mathbf{u}}_\ell$$

from which, after basic algebraic manipulations, we obtain

$$\sqrt{n}[\hat{\mathbf{u}}_\ell]_i = \frac{p_{\text{out}}}{\sqrt{p_{\text{out}}(1-p_{\text{out}})}} \left(\sqrt{n}\mathbf{e}_i^\top \mathbf{Q}_\lambda \frac{\mathbf{J}}{\sqrt{n}} \right) \left(\mathbf{M}^\circ \frac{\mathbf{J}^\top}{\sqrt{n}} \hat{\mathbf{u}}_\ell \right) + o_p(1)$$

with $[\mathbf{e}_i]_j = \delta_{ij}$. The right parenthesis term converges to known limits (from standard eigenvector alignment results such as e.g., Theorem 2.13), while the first parenthesis term “fluctuates”. Using central limit arguments for random matrices (either based on a martingale difference approach as in [Bai and Silverstein, 2010] or a Gaussian integration-by-part technique as in [Pastur and Shcherbina, 2011]; see Section 2.6.3), it is not difficult to show, as a result, that the vector $[\sqrt{n}[\hat{\mathbf{u}}_\ell]_i, \sqrt{n}[\hat{\mathbf{u}}_\ell]_j]^\top$ has a two-dimensional Gaussian limit.

2. From there, the misclassification rate in the left-hand side of (7.5) corresponds to

$$S \equiv \frac{1}{(n/2)} \sum_{i \leq n/2} 1_{\sqrt{n}[\hat{\mathbf{u}}_\ell]_i < 0} + \frac{1}{(n/2)} \sum_{i > n/2} 1_{\sqrt{n}[\hat{\mathbf{u}}_\ell]_i > 0}.$$

Writing $S = S - \mathbb{E}[S] + \mathbb{E}[S]$, by exchangeability we have from the previous item that $\mathbb{E}[S] = P(\sqrt{n}[\hat{\mathbf{u}}_\ell]_1 < 0)$ has a Gaussian limit while $P(|S - \mathbb{E}[S]| > \varepsilon) \leq \frac{1}{\varepsilon} \text{var}[S]$, which exclusively depends on $\mathbb{E}[n[\hat{\mathbf{u}}_\ell]_i [\hat{\mathbf{u}}_\ell]_j]$ for any pair (i, j) , is vanishes. This completes the result without having to resort to any further joint statistics of the entries of $\hat{\mathbf{u}}_\ell$.

Figure 7.1 depicts the probability of correct classification for a 2-class SBM under the present symmetric setting. The asymptotic predictions closely match the simulated values, with a slight mismatch for small n around the phase transition (around 1 in the x-axis). This is no surprise as the second order discontinuity observed in the limit cannot be observed in finite (especially small) dimensions. This is a typical example where random matrix asymptotics tend to be slow to converge.

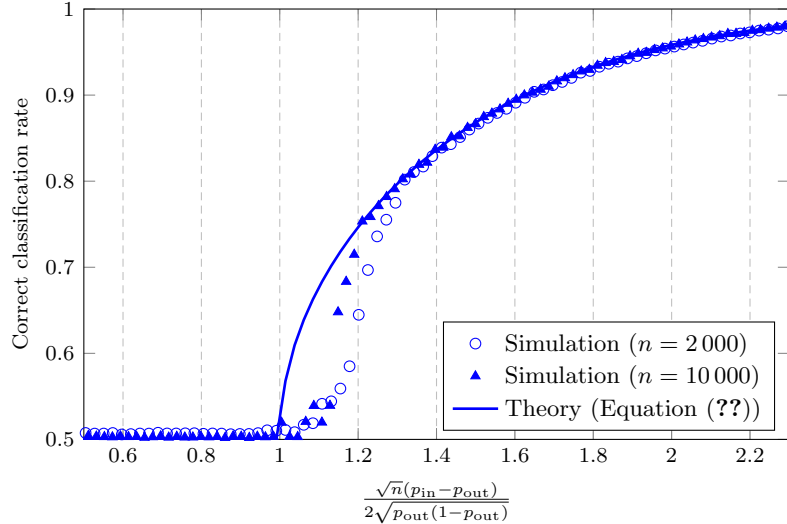


Figure 7.1: Classification performance for a 2-class SBM with $n_1 = n_2$, as a function of $p_{in} - p_{out}$ with $p_{in} = .4$. Simulations averaged over 10 realizations. fig:SBM_perfs

The limiting results are quite simple and have the advantage of being in closed form. The SBM setting is however quite unrealistic in that the average degree of each node is constant (converging to p), which does not translate the heterogeneity of node connectivity in real graphs and, as a result, cannot provide a typical “power-law” scaling of the degrees.

The next section brings the present analysis into more realistic graph models by considering the so-called degree-corrected SBM (DC-SBM) which does account for degree heterogeneity. This has major non-trivial consequences on: (i) the shape of the limiting eigenvalue distribution of \mathbf{B} (no longer a semi-circle in general), (ii) the resulting position of the phase transition, and (iii) the content of the dominant eigenvectors themselves which do not lead as straightforward an access to the classes as in the SBM case. The expressions of the resulting limits are less simple but provide a sufficiently clear account of the (mis)behavior of spectral clustering to envision several directions of improvements.

7.1.2 The degree-corrected stochastic block model

sec:DC-SBM

In this section, we generalize the stochastic block model by allowing, in addition to the existence of communities, different “intrinsic” degrees for the nodes in the graph. This better translates the nature of real-world graphs in which nodes have possibly very heterogeneous degrees.

Precisely, we here demand that

$$A_{ij} = A_{ji} \sim \text{Bern}(q_i q_j C_{g_i g_j})$$

for $q_i > 0$ some weight factor accounting for the connectivity of node i and $g_i \in \{1, \dots, k\}$ the class of node i . Similar to before, we ask the cardinality $n_a = |\mathcal{C}_a|$ of class \mathcal{C}_a to be of the same order as n , i.e., $n_a/n \rightarrow c_a \in (0, 1)$. For the moment, we maintain the q_i 's as deterministic, but we will soon take them random i.i.d., yet independent of the Bernoulli realization.

As in the SBM case, we also request the non-trivial clustering setting corresponding to

$$C_{ab} = 1 + \frac{M_{ab}}{\sqrt{n}}$$

where, as opposed to the SBM setting, the parameters p is no longer necessary.

A first important remark is that, in this configuration,

$$\mathbb{E}[\mathbf{A}] = \mathbf{D}_{\mathbf{q}} \left(\mathbf{1}_n \mathbf{1}_n^T + \frac{1}{\sqrt{n}} \mathbf{J} \mathbf{M} \mathbf{J}^T \right) \mathbf{D}_{\mathbf{q}}$$

where $\mathbf{q} = (q_1, \dots, q_n)^T$ and $\mathbf{D}_{\mathbf{q}} = \text{diag}(\mathbf{q})$. In particular, observe that the eigenvectors of $\mathbb{E}[\mathbf{A}]$ are no longer linear combinations of the vectors $\mathbf{j}_1, \dots, \mathbf{j}_k$ but are “deformed” by the (usually unknown) weights q_1, \dots, q_n . Compensating for this eigenvector deformation is not completely obvious and will be the major technical point of interest in this section.

As for the variance of the elements of \mathbf{A} , similar to the SBM setting, we find that

$$\text{var}[A_{ij}] = q_i q_j (1 - q_i q_j) + O(n^{-\frac{1}{2}})$$

which does not depend on the communities of nodes i and j .

As such, up to low-rank centering, \mathbf{A} is a matrix with independent entries of zero mean and variance $q_i q_j (1 - q_i q_j)$. Consequently, the limiting spectral measure of $\frac{1}{\sqrt{n}} \mathbf{A}$ (and of its rank-one perturbation $\mathbf{B} = \frac{1}{\sqrt{n}} (\mathbf{A} - \frac{\mathbf{d}\mathbf{d}^T}{\mathbf{d}^T \mathbf{1}_n})$), is that of a *deformed* Wigner matrix with variance profile.

It is instructive to first analyze this spectrum. From Theorem 2.8 in which we set $\sigma_{ij}^2 = q_i q_j (1 - q_i q_j)$, we find that the Stieltjes transform of the eigenvalue distribution of \mathbf{B} satisfies

$$\frac{1}{n} \text{tr}(\mathbf{B} - z \mathbf{I}_n)^{-1} - \frac{1}{n} \text{tr}(\mathbf{D}_{\mathbf{g}} - z \mathbf{I}_n)^{-1} \xrightarrow{a.s.} 0$$

where $\mathbf{g} = (g_1, \dots, g_n)^{-1}$ and

$$\begin{aligned} g_i &= \frac{1}{n} \sum_{j=1}^n \frac{q_i q_j - q_i^2 q_j^2}{-z - g_j} = q_i \frac{1}{n} \sum_{j=1}^n \frac{q_j}{-z - g_j} - q_i^2 \frac{1}{n} \sum_{j=1}^n \frac{q_j^2}{-z - g_j} \\ &\equiv q_i g_{10} - q_i^2 g_{20} \end{aligned}$$

in which we introduced g_{10} and g_{20} the solutions to

$$g_{10} = \frac{1}{n} \sum_{j=1}^n \frac{q_j}{-z - q_j g_{10} + q_i^2 g_{20}}$$

$$g_{20} = \frac{1}{n} \sum_{j=1}^n \frac{q_j^2}{-z - q_j g_{10} + q_i^2 g_{20}}.$$

Thus, finally,

$$\frac{1}{n} \text{tr}(\mathbf{B} - z\mathbf{I}_n)^{-1} - \frac{1}{n} \text{tr}(g_{10}\mathbf{D}_{\mathbf{q}} - g_{20}\mathbf{D}_{\mathbf{q}^2} - z\mathbf{I}_n)^{-1} \xrightarrow{\text{a.s.}} 0$$

where $\mathbf{q}^2 = (q_1^2, \dots, q_n^2)^\top$ and g_{10}, g_{20} are defined as the solution of the previous two equations.

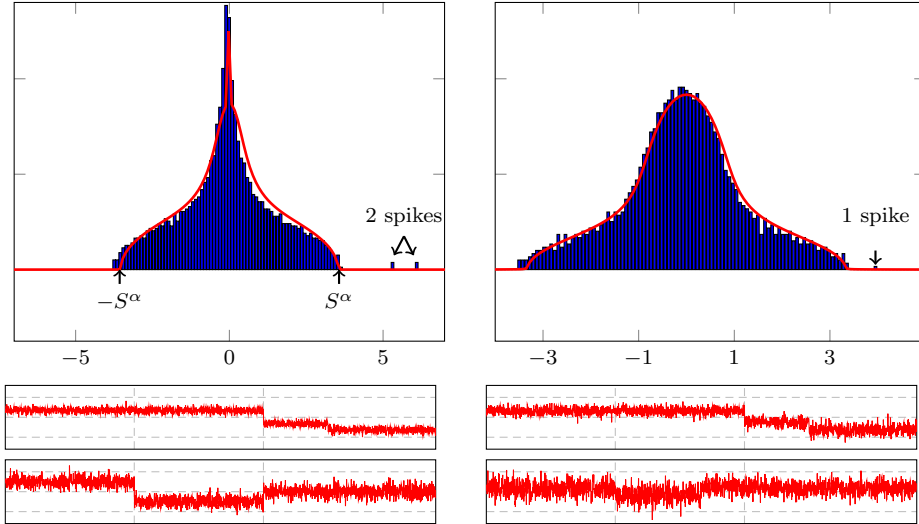


Figure 7.2: Two graphs generated upon the DCSBM with $k = 3$ communities, $n = 2000$, $c_1 = 0.3$, $c_2 = 0.3$, $c_3 = 0.4$, q_i 's drawn i.i.d. from the measure $\frac{1}{2}\delta_{q_{(1)}} + \frac{1}{2}\delta_{q_{(2)}}$ where $q_{(1)} = 0.4$, $q_{(2)} = 0.9$, for two different affinity matrices \mathbf{M} . (Left) $M_{ii} = 12$, $M_{ij} = -4$, $i \neq j$, (Right): $M_{ii} = -3$, $M_{ij} = -10$, $i \neq j$, (Top): Eigenvalue distribution of \mathbf{L}_α , with $\alpha = 0$. (Bottom): First and second leading eigenvectors of \mathbf{L}_α , with $\alpha = 0$. *** Il y a un probleme avec cette figure. Il faut la refaire... ***

`fig:hist_L_synthetic`

As shown in Figure 7.2, different distributions for the q_i 's lead to different spreads of the spectra of \mathbf{A} and \mathbf{B} . As a consequence, it is expected that phase transitions for the appearance of isolated eigenvalues due to the presence of communities will occur more or less easily depending on this eigenvalue spreading. Specifically, Figure 7.2 shows that for a bi-modal law for the q_i 's the limit

spectrum is far more spread out than a semi-circle. Besides, depending on \mathbf{M} , either two isolated eigenvalues or only one are found in the spectrum (with corresponding eigenvectors displaying more or less informative structure).

An intuitive way to reduce this spread is to pre-process the matrix \mathbf{B} in such a way that its spectrum is “as close as possible” to a semi-circle. For not too large q_i , $q_i q_j (1 - q_i q_j) \simeq q_i q_j$, and at the same time $d_i / \sqrt{\mathbf{d}^\top \mathbf{1}_n} \simeq q_i$ (see Lemma (7.1) below), so an idea is to pre- and post- multiply \mathbf{B} by \mathbf{D}^{-1} .

However, while affecting positively the spread of the spectrum of \mathbf{B} , its effect on isolated eigenvalues is not trivial and may be deleterious (as we will see next). An improved strategy consists in pre- and post-multiplying \mathbf{B} by $\mathbf{D}^{-\alpha}$ for some well chosen α . We will hereafter denote

$$\mathbf{L}_\alpha \equiv \frac{(\mathbf{d}^\top \mathbf{1}_n)^\alpha}{\sqrt{n}} \mathbf{D}^{-\alpha} \left(\mathbf{A} - \frac{\mathbf{d}\mathbf{d}^\top}{\mathbf{d}^\top \mathbf{1}_n} \right) \mathbf{D}^{-\alpha}$$

for which the normalization by $(\mathbf{d}^\top \mathbf{1}_n)^\alpha$ will appear later to be the natural one. This strategy in particular allows one to retrieve, for $\alpha = 0$ the modularity matrix \mathbf{B} (up to scaling), for $\alpha = \frac{1}{2}$ the normalized Laplacian matrix

$$\mathbf{L}_{\frac{1}{2}} = \sqrt{\frac{\mathbf{d}^\top \mathbf{1}_n}{n}} \mathbf{D}^{-\frac{1}{2}} \left(\mathbf{A} - \frac{\mathbf{d}\mathbf{d}^\top}{\mathbf{d}^\top \mathbf{1}_n} \right) \mathbf{D}^{-\frac{1}{2}}$$

and for $\alpha = -1$ the bi-lateral random walk Laplacian matrix

$$\mathbf{L}_1 = \frac{\mathbf{d}^\top \mathbf{1}_n}{\sqrt{n}} \left(\mathbf{D}^{-1} \mathbf{A} \mathbf{D}^{-1} - \frac{\mathbf{1}_n \mathbf{1}_n^\top}{\mathbf{d}^\top \mathbf{1}_n} \right)$$

which admits $\mathbf{1}_n$ as dominant eigenvector.

In a similar manner as in the previous decomposition of \mathbf{A} and \mathbf{B} for the Erdős-Rényi and SBM cases, it can be shown (see details in [Tiomoko Ali and Couillet \[2017\]](#)) that, in the large n regime,

$$\begin{aligned} \mathbf{L}_\alpha &= \frac{1}{\sqrt{n}} \mathbf{D}_\mathbf{q}^{-\alpha} \mathbf{X} \mathbf{D}_\mathbf{q}^{-\alpha} \\ &+ \begin{bmatrix} \mathbf{D}_\mathbf{q}^{1-\alpha} \frac{\mathbf{J}}{\sqrt{n}} & \frac{\mathbf{D}_\mathbf{q}^{-\alpha} \mathbf{X} \mathbf{1}_n}{\mathbf{q}^\top \mathbf{1}_n} \end{bmatrix} \begin{bmatrix} \mathbf{M}^\circ & -\mathbf{1}_k \\ -\mathbf{1}_k^\top & 0 \end{bmatrix} \begin{bmatrix} \frac{\mathbf{J}}{\sqrt{n}} \mathbf{D}_\mathbf{q}^{1-\alpha} \\ \frac{\mathbf{1}_n^\top \mathbf{X} \mathbf{D}_\mathbf{q}^{-\alpha}}{\mathbf{q}^\top \mathbf{1}_n} \end{bmatrix} + O_{\|\cdot\|}(n^{-\frac{1}{2}}). \end{aligned}$$

We immediately see from this expression that, for high information to noise ratios (i.e., when the nonzero eigenvalues of \mathbf{M}° dominate those of \mathbf{X}), the dominant eigenvectors of \mathbf{L}_α are contained in linear combinations of the vectors $\mathbf{D}_\mathbf{q}^{1-\alpha} \mathbf{j}_a$ for $a = 1, \dots, k$. To retrieve the sought-for \mathbf{j}_a , it is thus necessary to post-process the eigenvectors by $\mathbf{D}_\mathbf{q}^{\alpha-1}$ which, in the absence of a perfect knowledge of the vector \mathbf{q} , can be performed empirically by post-processing the eigenvectors by $\mathbf{D}^{\alpha-1}$ instead.

The resulting algorithm for spectral clustering under realistic heterogeneous degree graphs thus consists in the following steps:

1. select a scalar $\alpha \in \mathbb{R}$
2. identify isolated eigenvalues in the spectrum of \mathbf{L}_α and extract the corresponding eigenvectors, say $\mathbf{V} = [\mathbf{v}_1, \dots, \mathbf{v}_m] \in \mathbb{R}^{n \times m}$, where $m < k$
3. perform a k -class k-means (or expectation-maximization) clustering on the m -dimensional row vectors of the matrix $\mathbf{D}^{\alpha-1}\mathbf{V} \in \mathbb{R}^{n \times m}$.

By an asymptotic analysis similar to the SBM case (see [Tiomoko Ali and Couillet \[2017\]](#) for details), this method is granted to outperform standard spectral clustering approaches. Yet, it remains to properly identify an appropriate value for α . An idea would be to select the value α which maximizes the asymptotic classification performance as $n \rightarrow \infty$: however, this choice strongly depends on \mathbf{M} which is naturally unknown (and cannot be estimated without performing some sort of clustering in the first place).

Instead, we may choose α to be the value for which the “worse case detectability” is achieved. That is, for each α , there exists a smallest value for $\|\mathbf{M}^\circ\|$ for which community detection performs asymptotically better than random guess. We thus decide to choose this value of α for which, under the constraint that community detection remains doable, $\|\mathbf{M}^\circ\|$ is the smallest possible. This does not require any information on the actual value of \mathbf{M} .

To identify this value of α , it suffices again to evaluate the limiting spectrum of \mathbf{L}_α and the condition under which spectrum separability is achieved (by solving $\det(\mathbf{L}_\alpha - \lambda \mathbf{I}_n) = 0$ as in the SBM case). The result is summarized as follows:

Theorem 7.3 (Limiting spectrum and separability for \mathbf{L}_α). *For $\alpha \in \mathbb{R}$, let $\mu_n^\alpha = \frac{1}{n} \sum_{i=1}^n \delta_{\lambda_i(\mathbf{L}_\alpha)}$ be the empirical spectrum measure of \mathbf{L}_α . Then, as $n \rightarrow \infty$, $\mu_n^\alpha \xrightarrow{a.s.} \mu^\alpha$, where μ^α is determined by its Stieltjes transform $m_{\mu^\alpha}(z) = \int (t-z)^{-1} \mu^\alpha(dt)$ defined by*

$$m_{\mu^\alpha}(z) = g_{2\alpha,\alpha}(z)$$

where

$$g_{ab}(z) = \frac{1}{n} \sum_{j=1}^n \frac{q_j^{a-2b}}{-z - q_j g_{1,\alpha}(z) + q_j^2 g_{2,\alpha}(z)}.$$

In particular, g_{ab} for all a, b is obtained by solving the fixed-point equation in $(g_{1,\alpha}, g_{2,\alpha})$. The limiting spectrum of μ^α is continuous, symmetric, of the form $\mathcal{S}_a = [-S_a, S_a]$. Besides, if there exists an eigenvalue ℓ of $\mathbf{D}_c \mathbf{M}^\circ$ such that

$$|\ell| > \tau^\alpha \equiv - \lim_{x \downarrow S^\alpha} \frac{1}{m_{\mu^\alpha}(x)}$$

then there exists a corresponding isolated eigenvalue λ_ℓ in the spectrum of \mathbf{L}_α given by

$$\lambda_\ell = (m_{\mu^\alpha})^{-1} \left(-\frac{1}{\ell} \right).$$

When compared to the SBM case, the separability result above is not surprising. The main difference though is that the Stieltjes transform m_{μ^α} and its inverse do not assume closed-form formulas.

As for the optimal value for α , discussed above, it is then defined as

$$\alpha^* \in \arg \min_{\alpha \in \mathbb{R}} \{\tau^\alpha\}$$

where we used an inclusion (rather than equality) sign in case the minimum is not unique (which is for instance the case in the SBM setting where all q_i 's are equal). By this definition, α^* is indeed defined as the smallest possible phase transition value which ensures in the worst case the existence of isolated eigenvalues, as desired.

From a practical standpoint, of course, since the q_i 's are unknown, it is not possible to identify α^* precisely. Yet, as mentioned several times above, it can be shown that $d_i/\sqrt{\mathbf{d}^\top \mathbf{1}_n} \xrightarrow{a.s.} q_i$ uniformly over i . More precisely, we have

lem:di_qi

Lemma 7.1. *Assume that*

$$0 < \liminf_n \min_{1 \leq i \leq n} \{q_i\} \leq \limsup_n \max_{1 \leq i \leq n} \{q_i\} < 1.$$

Then,

$$\max_{1 \leq i \leq n} \left| \frac{d_i}{\sqrt{\mathbf{d}^\top \mathbf{1}_n}} - q_i \right| \xrightarrow{a.s.} 0.$$

It is fundamental to understand here that the condition $C_{ab} = 1 + \frac{M_{ab}}{\sqrt{n}}$, that is $C_{ab} - C_{a'b'} = O(n^{-\frac{1}{2}})$, plays a key role in the above estimate: d_i is a consistent estimate of q_i (up to scaling) irrespective of the class affinities of node i precisely because the difference between the affinities is asymptotically negligible. Note also that the condition for q_i to be bounded away from zero, which ensures that the graph is nowhere sparse, is somewhat limiting when applied to realistic graph models (typically having power laws for their degrees), but is theoretically necessary here.

From Lemma 7.1, it is possible to estimate every τ^α from the fact that, for all a, b and all $x \in \mathbb{R}$ large enough,

$$\hat{g}_{a,b}(x) - g_{a,b}(x) \xrightarrow{a.s.} 0$$

where

$$\hat{g}_{a,b}(x) \equiv \frac{1}{n} \sum_{j=1}^n \frac{\hat{q}_j^{a-2b}}{-x - \hat{q}_j \hat{g}_{1,\alpha}(x) + \hat{q}_j^2 \hat{g}_{2,\alpha}(x)}$$

with $(\hat{g}_{1,\alpha}, \hat{g}_{2,\alpha})$ being solution of their defining fixed-point equation, and $\hat{q}_j \equiv d_j/\sqrt{\mathbf{d}^\top \mathbf{1}_n}$. Thus one can estimate $1/m_{\mu^\alpha}(x) = 1/g_{2\alpha,\alpha}(x)$ for all x large. The last difficulty consists in estimating S^α since one needs $\lim_{x \downarrow S^\alpha} 1/m_{\mu^\alpha}(x)$.

This is unfortunately not easily performed, and to our knowledge there exists no standard estimate of S^α (or of any limiting spectrum edge based on the defining fixed-point equations in general). Numerically, the idea implemented in [Tiomoko Ali and Couillet, 2017] consists in solving the fixed-point equation in $(\hat{g}_{1,\alpha}(x), \hat{g}_{2,\alpha}(x))$ for decreasing values of x until convergence fails (indeed, the fixed-point equation cannot have a solution inside the support of μ^α). More practically, a dichotomy approach can be pursued to identify the pivotal value of x for which solving for $(\hat{g}_{1,\alpha}(x), \hat{g}_{2,\alpha}(x))$ becomes possible. This value (the first one for which the fixed-point algorithm does converge) is called \hat{S}^α .

With this (algorithmic) definition of \hat{S}^α , the estimate $\hat{\alpha}^*$ of α^* is given by

$$\begin{aligned}\hat{\alpha}^* &\in \arg \min_{\alpha \in \mathbb{R}} \{\hat{\tau}^\alpha\} \\ \hat{\tau}^\alpha &= \lim_{x \downarrow \hat{S}^\alpha} \frac{1}{\hat{g}_{\alpha,2\alpha}(x)}.\end{aligned}$$

To evaluate the performance gains incurred by the improved choice of α , Figure 7.3 and Figure 7.4 depict the so-called “overlap” metric (adapted to $k > 2$ classes) defined as

$$\text{Overlap} = \frac{\frac{1}{n} \sum_{i=1}^n \delta_{g_i, \hat{g}_i} - \frac{1}{k}}{1 - \frac{1}{k}}$$

where \hat{g}_i is the class allocated by the algorithm to node i , compared for various algorithms (notably against the recent Bethe Hessian method discussed in the next section). Figure 7.3 considers a DCSBM with fixed \mathbf{M} , while 3/4 of the nodes connect with a fixed weight $q_{(1)} = 0.1$ and 1/4 with a higher varying weight $q_{(2)}$. In Figure 7.4, a more realistic synthetic graph setting is considered with the q_i 's following a power law truncated to a support $[0.05, 0.3]$ (to avoid nodes with no neighbors) and with \mathbf{M} proportional to the identity matrix for simplicity. In both cases, choosing α optimally (at least in such a way that phase transitions are observed at the lowest values of $\|\mathbf{M}\|$) largely overtakes the performance of more standard methods, even beyond the phase transition point.

The DC-SBM setting is another telling example of a scenario where the conventional algorithms (here spectral clustering on the adjacency or modularity matrix) may severely fail. Spectral clustering on the matrix $\mathbf{D}^{-\alpha} \mathbf{A} \mathbf{D}^{-\alpha}$ provides a work around, but does not come along with a proof of optimality (more elaborate algorithms may perform better, and even improve the phase transition point).

More generally, another strong limiting aspect of our analysis of spectral clustering for graphs and data (Section 4.5.1) is that they fundamentally rely on “dense” graphs and affinity matrices, which are possibly unrealistic in practice (real graphs tend to be rather sparse with each node having a number of neighbors irrespective of the size of the graph). It is indeed central to the

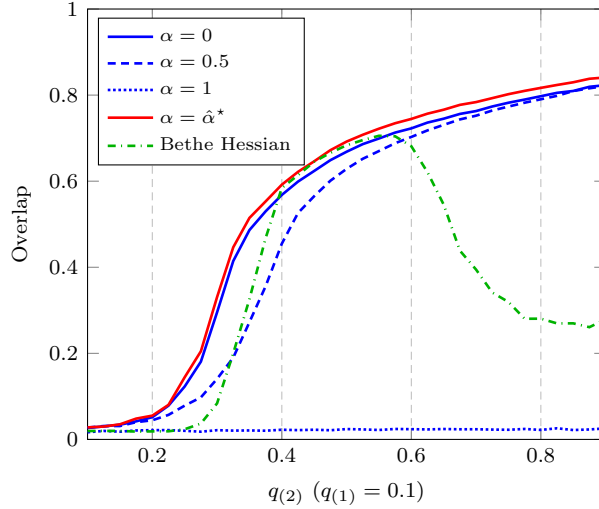


Figure 7.3: Overlap for $n = 3000$, $K = 3$, q_i 's i.i.d. with law $\frac{3}{4}\delta_{q_{(1)}} + \frac{1}{4}\delta_{q_{(2)}}$ for $q_{(1)} = 0.1$ and $q_{(2)} \in [0.1, 0.9]$, \mathbf{M} defined by $M_{ii} = 10$, $M_{ij} = -10$, $i \neq j$, $n_i/n = \frac{1}{3}$.

`fig:overlap_2masses_q`

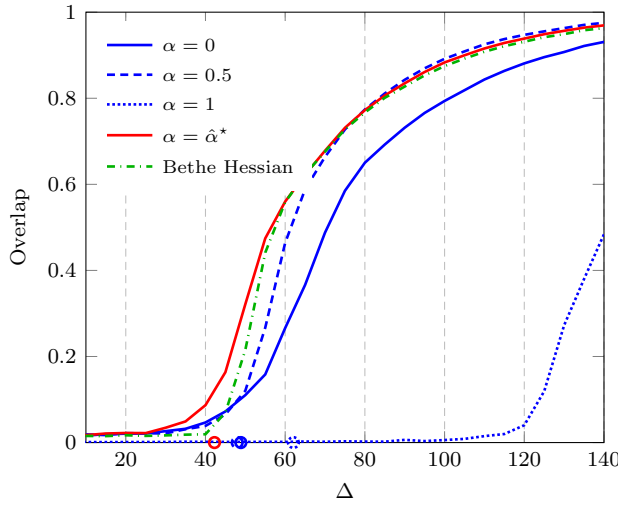


Figure 7.4: Overlap for $n = 3000$, $K = 3$, $n_i/n = \frac{1}{3}$, q_i 's following a power law with exponent 3 and support $[0.05, 0.3]$, $\mathbf{M} = \Delta \mathbf{I}_3$. Here $\alpha^* = 0.28$. In circles are indicated the theoretical positions of the phase transitions.

`fig:overlap_powerlaw`

random matrix framework that the rows and columns of the adjacency matrices have $O(n)$ degrees of freedom (i.e., are constituted from $O(n)$ independent random variables), so and the matrix itself be made of $O(n^2)$ degrees of free-

dom. If instead the number of degrees of freedom per row or column scales as $O(1)$, most random matrix results collapse. Remark for instance that the trace lemma according to which $\frac{1}{n}\mathbf{x}^T\mathbf{A}\mathbf{x} \simeq \frac{1}{n}\text{tr } \mathbf{A}$, which is at the core of most of the derivations in this monograph, would no longer be valid if $\mathbf{x} \in \mathbb{R}^n$ had independent (say zero-mean) Bernoulli entries with parameter $O(1/n)$: in this case, $\mathbb{E}[\frac{1}{n}\mathbf{x}^T\mathbf{A}\mathbf{x}] = \frac{1}{n}\text{tr } \mathbf{A}$ remains valid but $\frac{1}{n}\mathbf{x}^T\mathbf{A}\mathbf{x}$ no longer converges.

Handling sparse models of random matrix theory requires fundamentally different approaches and the mathematical tools under this setting are almost nonexistent. These will not be presented in this monograph, as they would demand an altogether very different set of prerequisite. Instead, the subsequent section discusses the few findings arising either from these alternative mathematical tools or, more often, from strikingly different intuitions from statistical physicists (however in general non rigorous).

7.2 From dense to sparse graphs: a different approach

sec:sparse-graphs

In sparse graph settings, spectral clustering on the adjacency matrix is largely suboptimal, even under a stochastic block model for the graph. This follows from the fact that, for a Erdős-Rényi graph with $O(1)$ node degrees (that is, $\mathbf{A}_{ij} \sim \text{Bern}(p/n)$ where $p = O(1)$), the limiting spectrum of \mathbf{A} is no longer a semi-circle law. Surprisingly enough, while a limiting spectrum does exist, very little is known about it. But, as opposed to the semi-circle law, we know it has an *unbounded support* and has localized point masses [].

The unboundedness of the support in the sparse regime is problematic for spectral clustering in presence of communities and explains why spectral clustering on \mathbf{A} (or the modularity matrix \mathbf{B}) is bound to fail. One must then devise other methods and possibly find alternative matrices to the adjacency.

7.2.1 The non-backtracking matrix

The first convincing idea arose from a statistical physics interpretation [Krzakala et al., 2013]: the nodes of a graph may be seen as interacting particles with interaction strength given by the entries of the adjacency matrix (in the binary case, particles i and j interact if $\mathbf{A}_{ij} = 1$). If let free of external “force fields”, the system tends to minimize its energy, that is to fall into a state of high probability. By establishing expressions for the probability of each state and performing linear approximations around some trivial solution, it appears that the dominant eigenvectors of the so-called *non-backtracking matrix* must be correlated to the communities of the graph. The non-backtracking matrix \mathbf{N} is defined on the set \mathcal{E} of edges of the graph as

$$\mathbf{N}_{(ij)(kl)} = \delta_{jk}(1 - \delta_{il}), \quad \forall (ij), (kl) \in \mathcal{E}.$$

It is thus a non-symmetric matrix. Its limiting spectrum is mostly unknown but, in the SBM case, it is importantly known that all eigenvalues are asymptotically

found inside a disc of controlled radius, with a possible exception for finitely many real eigenvalues of larger amplitude: the associated eigenvectors are those correlated to the classes. Precisely, letting \mathbf{v} be such an eigenvector (of size the number of edges in the graph), the vector $\tilde{\mathbf{v}} \in \mathbb{R}^n$ defined by

$$\tilde{\mathbf{v}}_i = \sum_{j \in \partial i} \mathbf{v}_{(ij)}$$

provides a clustering vector of the graph communities. As in the dense setting, the presence of isolated eigenvalues is ruled by a phase transition phenomenon. In the symmetric stochastic block model where $\mathbf{A}_{ij} \sim \text{Bern}(p_{\text{in}}/n)$ if i, j are in the same community and $\mathbf{A}_{ij} \sim \text{Bern}(p_{\text{out}}/n)$ otherwise, this phase transition has been proved (rigorously) in [Mossel et al., 2012, Massoulié, 2014] to occur whenever

$$\frac{p_{\text{in}} - p_{\text{out}}}{\sqrt{\frac{1}{2}(p_{\text{in}} + p_{\text{out}})}} > 2.$$

Note in particular that, as opposed to the dense regime where $(p_{\text{in}} - p_{\text{out}})/(p_{\text{in}} + p_{\text{out}})$ would be requested to scale as $O(n^{-\frac{1}{2}})$, here it is necessary to have $(p_{\text{in}} - p_{\text{out}})/(p_{\text{in}} + p_{\text{out}}) = O(1)$ for communities to arise in spectral clustering: in the absence of strong redundancy, the classification task is thus (not surprisingly) much harder.

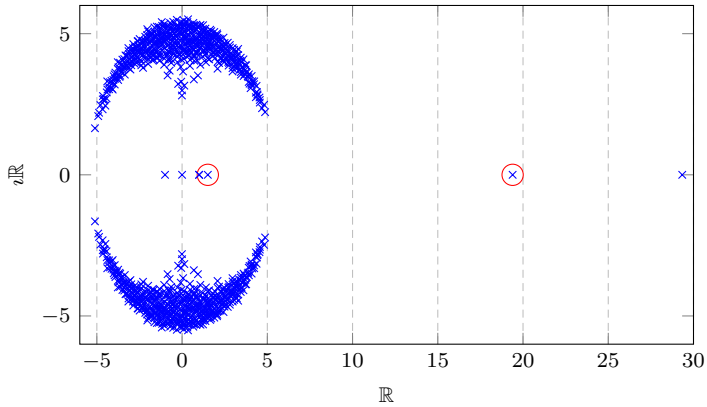


Figure 7.5: Complex spectrum of the non-backtracking matrix \mathbf{N} ; $n = 1\,000$, $p_{\text{in}} = 25$, $p_{\text{out}} = 5$. Emphasized in red circles are the two informative eigenvalues.

`fig:NonBacktracking`

The non-backtracking approach is however quite expensive to implement as the matrix is non-symmetric and possibly of large dimensions (scaling as the number of edges rather than the number of nodes in the graph). Also, the vector $\tilde{\mathbf{v}}$, while indeed correlated to the node classes, is seen in simulations to

be largely affected by heterogeneity in the node degrees: that is, it becomes largely inconsistent beyond the SBM setting.

It in fact turns out though that the spectrum of the non-backtracking operator is intimately related to that of another matrix, called the Bethe Hessian operator, also familiar of statistical physicists and which, as shown later in Section 7.2.4, can be exploited to naturally fight against degree heterogeneity.

7.2.2 The Bethe Hessian matrix

It can indeed be shown that, if $\mathbf{N}\mathbf{v} = \gamma\mathbf{v}$, then, letting $\tilde{\mathbf{v}}_i = \sum_{j \in \partial i} \mathbf{v}_{(ij)}$ as above,

$$((\gamma^2 - 1)\mathbf{I}_n + \mathbf{D} - \gamma\mathbf{A})\tilde{\mathbf{v}} = 0.$$

Thus, $\tilde{\mathbf{v}}$ is also an eigenvector (associated to a zero eigenvalue) of the so-called *Bethe Hessian* matrix

$$\mathbf{H}_\gamma \equiv (\gamma^2 - 1)\mathbf{I}_n + \mathbf{D} - \gamma\mathbf{A}.$$

The parameter γ defining \mathbf{H}_γ is however unknown, since it requires to solve an eigenvector equation for \mathbf{N} , which we precisely want to avoid.

But the Bethe Hessian \mathbf{H}_γ also finds a parallel origin, again from a statistical physics interpretation: the isolated eigenvectors of \mathbf{H}_γ (associated to the smallest eigenvalues) correspond to particle states of minimal *Bethe free energy*, where $1/\gamma$ is the *temperature* of the system of interacting particles. Under this interpretation, [Saade et al., 2014] heuristically proposes to chose $\gamma = \sqrt{\rho(\mathbf{N})}$ with $\rho(\mathbf{N})$ the spectral radius (largest eigenvalue in amplitude) of \mathbf{N} and to perform clustering on the eigenvector associated with the second smallest eigenvalue of \mathbf{H}_γ . Figure 7.6 reports the histogram of the eigenvalues and the informative eigenvector of \mathbf{H}_γ for two choices of γ .

In the specific case of the stochastic block model, the choice $\gamma = \sqrt{\rho(\mathbf{N})}$ corresponds in the limit to $\gamma = \sqrt{\frac{1}{2}(p_{\text{in}} + p_{\text{out}})}$. This choice of γ , inspired by a stochastic block model analysis, seems indeed rather optimal in this setting. Yet, the same remark on degree heterogeneity reported for the non-backtracking matrix still holds here: for $\gamma = \sqrt{\frac{1}{2}(p_{\text{in}} + p_{\text{out}})}$, spectral clustering on \mathbf{H}_γ is tainted by the heterogeneity of node degrees.

7.2.3 Degree regularization

An alternative approach to improve the adjacency matrix \mathbf{A} or the various normalized Laplacian matrices $\mathbf{D}^{-1}\mathbf{A}$ or $\mathbf{D}^{-\frac{1}{2}}\mathbf{A}\mathbf{D}^{-\frac{1}{2}}$ consists in observing that their main defect in dealing with sparse graphs is linked to: (i) the instability in \mathbf{D}^{-1} caused by nodes with low connectivity and (ii) the existence of spurious “hubs”, that is nodes i with exceptionally high degrees, which “pull” their own eigenvectors ($\mathbf{v}_j \simeq \delta_{ij}$).

The non-backtracking matrix \mathbf{N} precisely handles item (ii) by reducing the number of rows with large “degrees” (through the non-backtracking walks that escape hubs without returning to them).

Alternatively, several authors proposed (heuristically) to correct the adjacency or normalized Laplacian matrices by adding a regularization term, such as: $\mathbf{A} + \tau \mathbf{1}_n \mathbf{1}_n^\top$ in [Amini et al., 2013] or $\mathbf{L}_\tau = (\mathbf{D} + \tau \mathbf{I}_n)^{-\frac{1}{2}} \mathbf{A} (\mathbf{D} + \tau \mathbf{I}_n)^{-\frac{1}{2}}$ in [Qin and Rohe, 2013]. In the latter, the authors, still heuristically, propose to let $\tau = \frac{1}{2}(p_{\text{in}} + p_{\text{out}})$ (despite their few theoretical results suggesting to take much larger values for τ).

Interestingly, as opposed to the Bethe Hessian and non-backtracking methods described above which sometimes fail on realistic (especially heterogeneous) graphs, spectral clustering on L_τ for this choice of τ is seen in simulations to be extremely efficient and resilient to real graph clustering.

7.2.4 A unifying approach adapted to DC-SBM

sec:unified_approach

In [Dall'Amico et al., 2019], a unified approach is proposed which explains how Bethe Hessian and regularized Laplacian relate, and most importantly, provides values for γ and τ that make spectral clustering insensitive to degree heterogeneity.

The authors simply observe that, in a two-class symmetric DC-SBM setting, letting $\mathbf{j} = [\mathbf{1}_{n/2}^\top, -\mathbf{1}_{n/2}^\top]^\top$, one has

$$[(\mathbf{D} - \zeta \mathbf{A})\mathbf{j}]_i = d_i \mathbf{j}_i \left[1 - \zeta \left(\frac{|\partial_i^{(\text{in})}|}{d_i} - \frac{|\partial_i^{(\text{out})}|}{d_i} \right) \right]$$

with $\partial_i^{(\text{in})}$ the nodes connected to i within the same community and $\partial_i^{(\text{out})}$ the nodes connected to i within the other community. Assuming the average degree not too small, this gives

$$[(\mathbf{D} - \zeta \mathbf{A})\mathbf{j}]_i \simeq d_i \mathbf{j}_i \left[1 - \gamma \frac{p_{\text{in}} - p_{\text{out}}}{p_{\text{in}} + p_{\text{out}}} \right].$$

Thus, \mathbf{j} is an approximate eigenvector of $\mathbf{D} - \gamma \mathbf{A}$ if one chooses

$$\zeta = \frac{p_{\text{in}} + p_{\text{out}}}{p_{\text{in}} - p_{\text{out}}}.$$

As opposed to the regularization values γ and τ in the previous sections, it is interesting to note here that ζ depends on the clustering task difficulty (since it depends explicitly on $p_{\text{in}} - p_{\text{out}}$).

Since $\mathbf{D} - \zeta \mathbf{A}$ has the same eigenvectors as \mathbf{H}_ζ , this choice of ζ offers a new value for the Bethe Hessian parameter (γ) which now is insensitive to degree heterogeneity. Yet, as opposed to $\gamma = \sqrt{\frac{1}{2}(p_{\text{in}} + p_{\text{out}})}$ which can be estimated consistently by evaluating the average node degree in the graph, ζ cannot be directly estimated from the graph. But the authors in [Dall'Amico

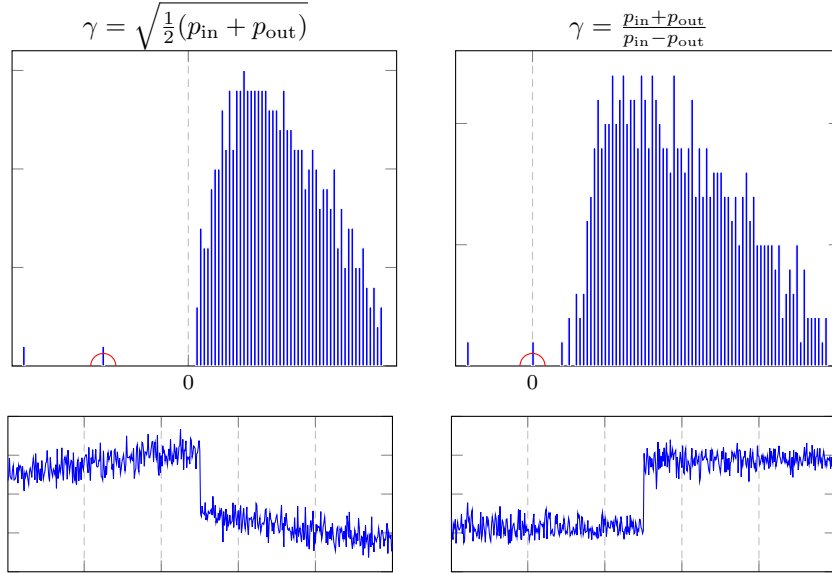


Figure 7.6: Histogram of the empirical spectral distribution of \mathbf{H}_γ and informative eigenvector under a DC-SBM model for (left) $\gamma = \sqrt{\frac{1}{2}(p_{in} + p_{out})}$ and (right) $\gamma = \frac{p_{in}+p_{out}}{p_{in}-p_{out}}$. Here $n = 1000$ nodes. Informative eigenvalue emphasized in red circle.

[fig:BetheHessian](#)

[et al., 2019] showed that ζ corresponds (asymptotically) to the smallest value for which $\lambda_2(\mathbf{H}_\zeta) = 0$ (with λ_2 the second smallest eigenvalue). The eigenvector \mathbf{v} carrying the class information is then the one associated with the zero eigenvalue of \mathbf{H}_ζ (i.e., such that $\mathbf{H}_\zeta \mathbf{v} = 0$). The right-hand side displays of Figure 7.6 demonstrates the better resilience of this choice to graph heterogeneity.

In a k -class setting, it is similarly shown that spectral clustering can be performed, no longer on a single matrix \mathbf{H}_ζ , but on the matrices $\mathbf{H}_{\zeta_2}, \dots, \mathbf{H}_{\zeta_k}$ where ζ_p is the value of ζ such that $\lambda_p(\mathbf{H}_\zeta) = 0$ (with λ_p the p -th smallest eigenvalue) and the corresponding informative eigenvector \mathbf{v}_p is the one for which $\mathbf{H}_\zeta \mathbf{v}_p = 0$.

Besides, it is observed by the authors that the following two equations are equivalent:

$$\begin{aligned} &[(\zeta_p^2 - 1)\mathbf{I}_n + \mathbf{D} - \zeta_p \mathbf{A}] \mathbf{v}_p = 0 \\ &(\mathbf{D} + (\zeta_p^2 - 1)\mathbf{I}_n)^{-1} \mathbf{A} \mathbf{v}_p = \frac{1}{\zeta_p} \mathbf{v}_p. \end{aligned}$$

This means that \mathbf{v}_p is also an eigenvector for the random-walk Laplacian $(\mathbf{D} + (\zeta_p^2 - 1)\mathbf{I}_n)^{-1} \mathbf{A}$. Since the eigenvalues of the latter are the same as the eigenvalues of $(\mathbf{D} + (\zeta_p^2 - 1)\mathbf{I}_n)^{-\frac{1}{2}} \mathbf{A} (\mathbf{D} + (\zeta_p^2 - 1)\mathbf{I}_n)^{-\frac{1}{2}}$ and that the associated eigenvectors

Dataset	n	p	k	$\{\mathbf{H}_{\zeta_p}\}$	\mathbf{A}	\mathbf{H}_γ	\mathbf{N}	$\mathbf{D}^{-1}\mathbf{A}$	\mathbf{L}_τ
Dolphins	62	5	<u>2</u>	0.38	0.21	0.34	0.22	0.38	0.38
Polbook	105	8.4	<u>3</u>	0.5	0.44	0.5	0.45	0.5	0.5
Mail	1133	9.6	21	0.5	0.32	0.4	0.37	0.5	0.5
Polblogs	1222	27.4	<u>2</u>	0.43	0.23	0.27	0.24	0	0.43
Tv	3892	8.9	41	0.8	0.51	0.58	0.55	0.55	0.8
Facebook	4039	43.7	55	0.78	0.43	0.49	0.49	0.78	0.57
Power grid	4941	2.7	25	0.93	0.18	0.37	0.31	0.93	0.85
GrQc	5242	5.5	29	0.53	0.45	0.49	0.49	0.42	0.79
Politicians	5908	14.1	<u>62</u>	0.85	0.48	0.54	0.5	0.83	0.74
GNutella P2P	6301	6.6	4	0.26	0.16	0.14	0.19	0	0.35
Wikipedia	7115	28.3	22	0.23	0.15	0.17	0.17	0.23	0.27
Vip	11565	11.6	53	0.62	0.27	0.33	0.3	0.55	0.54
HepPh	12008	19.7	60	0.37	0.42	0.42	0.42	0.11	0.52
Croatia	57573	18.3	<u>84</u>	0.65	0.33	0.39	0.34	0.69	0.62

Table 7.1: Modularity comparison on real networks [Leskovec and Krevl, 2014]. k (unless underlined) and ground truth labels are unknown. Special emphasis is made on the technique $\{\mathbf{H}_{\zeta_p}\}_{p=1}^{\hat{k}}$ devised in [Dall’Amico et al., 2019], which outperforms most competing approaches.

`tab:unlabeled`

tors are just scaled by the normalized degrees, we also find a natural connection to the regularized Laplacian matrix discussed in the previous sections.

Using an efficient procedure to evaluate the number of class \hat{k} and the values $\zeta_2, \dots, \zeta_{\hat{k}}$ (without resorting to expensive line searches), the authors in [Dall’Amico et al., 2019] provide a comparative performance table of all aforementioned spectral clustering procedures on real benchmark graphs. This is reported in Table 7.1, in which p denotes the average node degree.

These studies remain largely at a heuristic level. To the noticeable exception of [Massoulié, 2014] which theoretically proves that the phase transition empirically obtained by the physicists for the non-backtracking operator is indeed optimal, very few random matrix analyses exist that are able to tackle the spectrum of sparse graphs. Here, Stieltjes transform approaches collapse, and are mostly replaced by combinatorics and random graph techniques.

Yet, the analysis of sparse graphs is fundamental for at least two reasons: (i) as said, the reality of real networks tends more towards the sparse than the dense side, and (ii) sparsification techniques may also be used in practice to reduce computational costs; in clustering data using kernel methods, one may use k-NN (k-nearest neighbors) with a small value of k , or alternatively only compute few entries of the kernel matrix. The spectral and, more generally, algorithmic implications of sparse data and sparsification procedures will surely be a subject of active future interest in large dimensional statistics and random matrices for machine learning.

7.3 Concluding remarks

Spectral methods for community detection are the “Wigner semi-circle” counterpart of spectral clustering for large dimensional data (which, in its simplest setting, is the “Wishart Marčenko-Pastur” equivalent). The random matrix tools and proof methods being equally applicable to each setting, their ultimate study is quite similar.

A second difference relates to the matrix entries: the entries of the adjacency matrices are typically Bernoulli distributed (in unweighted graphs) where instead kernel matrices tend to be filled with continuous variables (aside from k-NN kernels). But in dense (or moderately dense) graphs, from the universality of first order random matrix results, this difference also vanishes. In particular, the case of weighted dense graphs, although not quite studied in the literature, would be easily handled.

Major differences start instead to appear when considering sparse graph settings. It is likely that the limiting spectral measure of the adjacency matrix A of a graph, and its associated Laplacian, depends on the law of the entries beyond first and second moment. This may be understood from the fact that the columns of A no longer “concentrate” in the sparse regime (e.g., their norm does not converge) but remain a random variable fully dependent on the law of the entries. This behavior, although possibly averaged over the columns to some extent, breaks the convenient universality phenomena arising in dense random matrices.

An alternative approach to partially account for the sparse regime while remaining tractable to classical tools in random matrix theory is to assume that the average degree of the nodes of the graph grows slowly (as $O(\log n)$) with the size n of the graph. In doing so, slow convergence behavior appear, with Wigner’s semi-circle law being valid again. The major problem though is that, under the classical SBM model, for which $p_{\text{in}} - p_{\text{out}} = O(1)$, classification becomes asymptotically trivial: that is, the dominant eigenvalue of A grows unbounded, yet at a very slow rate. Studying this setting remains interesting though, as one is able to precisely “control” the evolution, *for all finite but large n* , of the spectrum of A and of the Laplacian, Bethe Hessian, non-backtracking matrices, etc. Under the not completely unsatisfying $O(\log n) \approx O(1)$ approximation, for these large but finite n values, these studies may provide a sufficiently accurate picture of the behavior of real (deemed sparse) graphs. This path is currently at the center of focus of research in random matrix theory for graphs, see e.g., [Coste and Zhu, 2019] in which results on the position of the real eigenvalues of the non-backtracking matrix are “tracked”.

7.4 Practical course material

Practical Lecture Material 7 (Gaussian fluctuations of the SBM eigenvectors). *This exercise aims to complete Remark 7.1 on the asymptotic joint Gaussian fluctuations of the entries of the dominant eigenvector of the modularity*

exo:2-classSBM

matrix \mathbf{B} in a stochastic-block model setting, thereby leading to the asymptotic Gaussianity of the classification error rate.

We consider for simplicity the two even class $\mathcal{C}_1, \mathcal{C}_2$ (with $|\mathcal{C}_1| = |\mathcal{C}_2|$) setting where the graph affinity matrix $\mathbf{A} \in \mathbb{R}^{n \times n}$ has i.i.d. Bernoulli entries $A_{ij} \sim \text{Bern}(\mathbf{C}_{ab})$ entries where $i \in \mathcal{C}_a$, $j \in \mathcal{C}_b$ and $\mathbf{C} = [\begin{smallmatrix} p_{\text{in}} & p_{\text{out}} \\ p_{\text{out}} & p_{\text{in}} \end{smallmatrix}]$, where $p_{\text{in}} - p_{\text{out}} = O(n^{-\frac{1}{2}})$. We denote $\mathbf{d} = [d_1, \dots, d_n]^\top$ where $d_i = \sum_j A_{ij}$.

Letting $\mathbf{B} = \frac{1}{\sqrt{n}}(\mathbf{A} - \frac{\mathbf{d}\mathbf{d}^\top}{\mathbf{d}^\top \mathbf{1}_n})$, first establish, from the results of this chapter (in particular (7.2) and (7.4)) that

$$\begin{aligned} \frac{1}{\sqrt{p_{\text{out}}(1-p_{\text{out}})}} \mathbf{B} &= \frac{\mathbf{X}}{\sqrt{n}} + \frac{p_{\text{in}} - p_{\text{out}}}{2\sqrt{n}\sqrt{p_{\text{out}}(1-p_{\text{out}})}} \mathbf{j}\mathbf{j}^\top \\ &\quad - \left(\frac{\mathbf{1}_n \mathbf{1}_n^\top}{n} \frac{\mathbf{X}}{\sqrt{n}} + \frac{\mathbf{X}}{\sqrt{n}} \frac{\mathbf{1}_n \mathbf{1}_n^\top}{n} \right) + O_{\|\cdot\|}(n^{-\frac{1}{2}}) \end{aligned}$$

where $\mathbf{j} = [\mathbf{1}_{n/2}^\top, -\mathbf{1}_{n/2}^\top]^\top \in \mathbb{R}^n$ and \mathbf{X} is a matrix with i.i.d. zero mean and unit variance entries. Since $p_{\text{in}} - p_{\text{out}} = O(n^{-\frac{1}{2}})$, our interest is on matrices of the form

$$\mathbf{Y} \equiv \frac{\mathbf{X}}{\sqrt{n}} + \frac{\gamma}{n} \mathbf{j}\mathbf{j}^\top - \left(\frac{\mathbf{1}_n \mathbf{1}_n^\top}{n} \frac{\mathbf{X}}{\sqrt{n}} + \frac{\mathbf{X}}{\sqrt{n}} \frac{\mathbf{1}_n \mathbf{1}_n^\top}{n} \right)$$

for some $\gamma > 0$ and \mathbf{X} an arbitrary random matrix with i.i.d. zero mean and unit variance entries. We further assume γ large enough (in fact $\gamma > 1$) for the existence of an isolated eigenvalue $\hat{\lambda}$ in the spectrum of \mathbf{Y} to be enforced and we let $\hat{\mathbf{j}}$ be its associated eigenvector.

Show that $\mathbf{1}_n$ is an eigenvector of \mathbf{Y} associated with an eigenvalue tending to zero and conclude that $\hat{\mathbf{j}}^\top \mathbf{1}_n = 0$.

Based ob this result, and since $\mathbf{Y}\hat{\mathbf{j}} = \hat{\lambda}\hat{\mathbf{j}}$, show that

$$\hat{\mathbf{j}} = \frac{\mathbf{1}_n^\top \mathbf{X} \hat{\mathbf{j}}}{n\sqrt{n}} \mathbf{Q}(\hat{\lambda}) \mathbf{1}_n - \frac{\gamma \mathbf{j}^\top \hat{\mathbf{j}}}{n} \mathbf{Q}(\hat{\lambda}) \mathbf{j}$$

where $\mathbf{Q}(z) \equiv (\frac{\mathbf{X}}{\sqrt{n}} - z\mathbf{I}_n)^{-1}$ and that, in particular, for $\mathbf{e}_i \in \mathbb{R}^n$ the canonical vector with $[\mathbf{e}_i]_j = \delta_{ij}$,

$$\sqrt{n}\hat{j}_i = \frac{\mathbf{1}_n^\top \mathbf{X} \hat{\mathbf{j}}}{n} \mathbf{e}_i^\top \mathbf{Q}(\hat{\lambda}) \mathbf{1}_n - \frac{\gamma \mathbf{j}^\top \hat{\mathbf{j}}}{\sqrt{n}} \mathbf{e}_i^\top \mathbf{Q}(\hat{\lambda}) \mathbf{j}.$$

Using a spiked model approach, first establish that

$$\begin{aligned} \lambda &= \gamma + \frac{1}{\gamma} \\ \left| \frac{1}{\sqrt{n}} \mathbf{j}^\top \hat{\mathbf{j}} \right| &\xrightarrow{\text{a.s.}} \sqrt{1 - \frac{1}{\gamma^2}} \\ \left| \frac{1}{n} \mathbf{1}_n^\top \mathbf{X} \hat{\mathbf{j}} \right| &\xrightarrow{\text{a.s.}} 0. \end{aligned}$$

Note in particular that $\hat{\lambda}$ and $|\frac{1}{\sqrt{n}}\hat{\mathbf{j}}^\top \hat{\mathbf{j}}|$ thus have the same limit as in the deformed semi-circle model $\mathbf{Y}^\circ = \frac{\mathbf{X}}{\sqrt{n}} + \frac{\gamma}{n}\mathbf{j}\mathbf{j}^\top$.

Next, using the resolvent identity, establish in parallel that, for any deterministic vectors $\mathbf{u}_1, \mathbf{u}_2$, and scalars ℓ_1, ℓ_2 ,

$$\sqrt{n}\mathbf{u}_1^\top \mathbf{Q}(\ell_1)\mathbf{u}_2 = \sqrt{n}\mathbf{u}_1^\top \mathbf{Q}(\ell_2)\mathbf{u}_2 - \sqrt{n}(\ell_1 - \ell_2)\mathbf{u}_1^\top \mathbf{Q}(\ell_1)\mathbf{Q}(\ell_2)\mathbf{u}_2$$

Apply this result to the bilinear forms $\mathbf{e}_i^\top \mathbf{Q}(\hat{\lambda})\mathbf{1}_n$ and $\mathbf{e}_i^\top \mathbf{Q}(\hat{\lambda})\mathbf{j}$ so to discard the dependence between \mathbf{X} (in the definition of $\mathbf{Q}(\hat{\lambda})$) and $\hat{\lambda}$.

Assume for the moment that \mathbf{X} has independent $\mathcal{N}(0, 1)$ entries and show, by a diagonalization of \mathbf{X} (recalling that eigenvalues and eigenvectors are independent in the Gaussian case) and a standard central limit theorem argument, that

$$\mathbf{e}_i^\top \mathbf{Q}(\lambda)\mathbf{1}_n = \mathcal{N}(m(\lambda), m'(\lambda) - m(\lambda)^2) + O_p(n^{-1})$$

for $m(z)$ the Stieltjes transform of the semi-circle distribution and $m'(z)$ its derivative. Confirm by a universality argument that this result holds true beyond the Gaussian distribution for \mathbf{X} , so long that \mathbf{X} has entries of zero mean and unit variance.

Recalling that $m^2(z) + zm(z) + 1 = 0$ is the defining equation of the semi-circle Stieltjes transform and that $m(\lambda) = -1/\gamma$, conclude that

$$\sqrt{n}\hat{j}_i = \pm\sqrt{1 - \gamma^{-2}} + \gamma^{-1}w_i + o_p(1)$$

where $w_i \sim \mathcal{N}(0, 1)$.

Generalize now this result to a k -dimensional setting by showing that, for any k entries $\hat{j}_{i_1}, \dots, \hat{j}_{i_k}$ of $\hat{\mathbf{j}}$, with the same line of arguments

$$\sqrt{n} \begin{bmatrix} \hat{j}_{i_1} \\ \vdots \\ \hat{j}_{i_k} \end{bmatrix} = \pm\sqrt{1 - \gamma^{-2}}\mathbf{1}_k + \gamma^{-1}\mathbf{w} + o_{\|\cdot\|}(1)$$

where $\mathbf{w} \sim \mathcal{N}(0, \mathbf{I}_k)$. In particular, the fluctuations of the entries of $\hat{\mathbf{j}}$ are asymptotically decorrelated under the SBM setting.

Conclude, from this result and the help of Remark 7.1-2., that the probability of misclassification is asymptotically given by $Q(\sqrt{\gamma^2 - 1})$ for Q the Gaussian tail function, and translate this result in terms of the parameters p_{out} and $\sqrt{n}(p_{\text{in}} - p_{\text{out}})$ to recover, as expected, the asymptotic error rate

$$Q\left(\sqrt{\frac{n(p_{\text{in}} - p_{\text{out}})^2}{4p_{\text{out}}(1 - p_{\text{out}})}} - 1\right)$$

established in Equation (7.5).

Chapter 8

Discussions on Universality and Practical Applications

chap:universality-and-concentration

8.1 From Gaussian mixtures to concentrated random vectors and GAN images

8.1.1 On data models in large dimensions

In the previous chapters, we have repeatedly worked under the assumption that data arise from a Gaussian mixture model to elaborate asymptotic performance analyses of a wide range of machine learning algorithms. This assumption primarily arises for mathematical convenience: the Gaussian model has many mathematical virtues (it is parameterized only through its first two moments, specific mathematical tools are available, Gaussian vectors are up to centering and scaling vectors with independent entries, etc.).

From a small dimensional viewpoint (p small and fixed), it is clear that Gaussian vectors $\mathbf{x} \in \mathbb{R}^p$ are extremely limited models for most realistic datasets: Gaussian vectors of small dimensions are restricted to ellipsoid-shaped distributions and cannot account for the possibly complex dependence relations between the entries of \mathbf{x} . By extrapolation, the many possible interactions between the entries of a large dimensional vector \mathbf{x} are even less prone to modelling by means of a Gaussian vector.

Yet, we have seen in the previous chapters a systematic, sometimes seemingly perfect, match between the performances machine learning algorithms achieve on real datasets and those predicted on Gaussian (mixture) models sharing the same statistical means and covariances as the real data (these means and covariances being evaluated empirically from the whole dataset).

The objective of this chapter is to demonstrate that this is far from a coincidence. It is indeed possible to prove that many of the results of this monograph *do extend* to a wide range of “almost” real data. More specifically, we will

successively show in this chapter that

- as already hinted at in Theorem 2.17 which proves that Theorem 2.5 not only holds for vectors with independent entries (up to centering and scaling) but also for the much larger class of *concentrated random* vectors, many core results from the previous chapters *hold* almost identically under a data model of (mixture of) concentrated random vectors. In particular, it appears that the salient information, that dictates the behavior of most machine learning algorithms, lies in the first two statistical moments: those are sufficient to capture the essence of most learning mechanisms;
- the class of concentrated random vectors in particular contains all random vectors arising from a Lipschitz transformation of large standard Gaussian vectors, which in particular comprises all random vectors produced by generative adversarial networks (the now popular GANs): as a consequence of the previous item, *the performance of many machine learning algorithms on data produced by GANs is theoretically predictable*;
- extensive simulations have been run on state-of-the-art classification frameworks for real versus GAN-simulated data: while the performances are not identical between GAN and real data (GAN data are easier to discriminate), the *theoretical performances predicted by random matrix theory on real data* are indeed a systematic accurate match to the actual performances.

From these observations, a careless conclusion may be to claim that Gaussian (mixture) vectors are accurate models for real data. In a way, this hasty conclusion is not necessarily inappropriate: it all depends on what is meant by “an accurate model”. If a model is appropriate because a human observer (or a machine) cannot distinguish real data from the model (as GANs have been designed to do), then Gaussian models are not accurate: Figure 8.1 evidences this fact by comparing digits from the MNIST database to their Gaussian model counterpart.

But, if an “accurate model” is defined as correctly *testifying of the performance of a given data processing method* on real data, then, as we already saw and will see next in more detail, the Gaussian model is quite accurate when studying a host of classification and regression problems in machine learning.

The conclusion here is quite fundamental to the vision of machine learning methods for (not so) large dimensional data: the conservative approach according to which real data need be appropriately modelled from a human eye standpoint to be worth theoretical analysis, reducing Gaussian vectors to “toy examples”, is strikingly disrupted in large dimensions. For large data, Gaussian models are often more than enough to account for the behavior of statistical learning mechanisms.

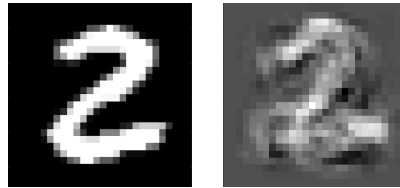


Figure 8.1: Image of digit “2” from the MNIST database (**left**) and random Gaussian generation from a model with the same mean and covariance (**right**), empirically estimated from all digits “2” from the entire database.
fig:MNIST_vs_Gaussian

8.1.2 A study of GAN data

8.1.2.1 Reminders on deep neural networks and GANs

The field of computer vision has recently experienced two successive tidal waves that brushed aside (i) years of conventional mathematical research in image classification with the arrival of deep convolutional networks [Krizhevsky et al., 2012], the performance of which is now near superhuman in some tasks (while previous wavelet-based approaches were far below human performances), and (ii) the conventional thinking that modern computers could not generate arbitrary samples of deceptively realistic images, here with the construction of generative adversarial networks (GANs) [Goodfellow et al., 2014], which are merely two competing instances of deep (convolutional) networks.

For reminder, a neural network is a succession of L linear and point-wise nonlinear maps, associating input data $\mathbf{x} \in \mathbb{R}^p$ to an output $\mathbf{y} \in \mathbb{R}^q$ as

$$\mathbf{y} = \phi_L(\mathbf{W}_L \phi_{L-1}(\mathbf{W}_{L-1} \dots \phi_1(\mathbf{W}_1 \mathbf{x}) \dots))$$

with $\mathbf{W}_i \in \mathbb{R}^{l_i \times l_{i-1}}$ the linear maps and $\phi_i : \mathbb{R} \rightarrow \mathbb{R}$ the nonlinear maps applied entry-wise (with the slight abuse of notation $\phi_i(\mathbf{z}) = \{\phi(z_j)\}_{j=1}^{l_i}$). Based on a (usually quite numerous) sequence of known input-output pairs $(\mathbf{x}_i, \mathbf{y}_i)$ and from a random initialization of the weights $\mathbf{W}_1, \dots, \mathbf{W}_L$, neural networks adapt these weights (for fixed ϕ_i) in a gradient descent manner, so to minimize some loss function of the type

$$\frac{1}{n} \sum_{i=1}^n \ell(\phi_L(\mathbf{W}_L \phi_{L-1}(\mathbf{W}_{L-1} \dots \phi_1(\mathbf{W}_1 \mathbf{x}_i) \dots)), \mathbf{y}_i).$$

When the gradient vanishes, the algorithm is stopped, the weights $\mathbf{W}_1, \dots, \mathbf{W}_L$ ideally corresponding to a (not too bad) local minimum of the optimization framework.

Convolutional neural networks are simply more structured versions of this generic neural network for which the weight matrices \mathbf{W}_i have a block Toeplitz structure (so to enforce local filtering of the data). State-of-the-art methods also use more elaborate versions of gradient descent, add extra tricks to the general

architecture, but are mostly based on this elementary model. They are called “deep” whenever both the number of “layers” L and the number of “neurons” per layer l_i ’s are large numbers.

Generative adversarial networks are the combination of two such neural networks: (i) a so-called *generator* which creates, from Gaussian input vectors $\mathbf{x} \sim \mathcal{N}(0, \mathbf{I}_p)$, output “data” vectors $\mathbf{y} \in \mathbb{R}^q$, which are then compared by (ii) the *discriminator* to real data. The objective function of the generator is to minimize the objective function of the generator (hence the “adversarial” name), the latter objective function being to maximally discriminate genuine data from the generated ones. Upon convergence of this adversarial game, the expected output is that the discriminator, while having become skillful at discriminating true from fake data, can no longer distinguish them: the GAN (precisely the generator) has learned to generate fake but extremely realistic data.

The top display of Figure 8.2 schematically depicts the diagram of a generative adversarial network.

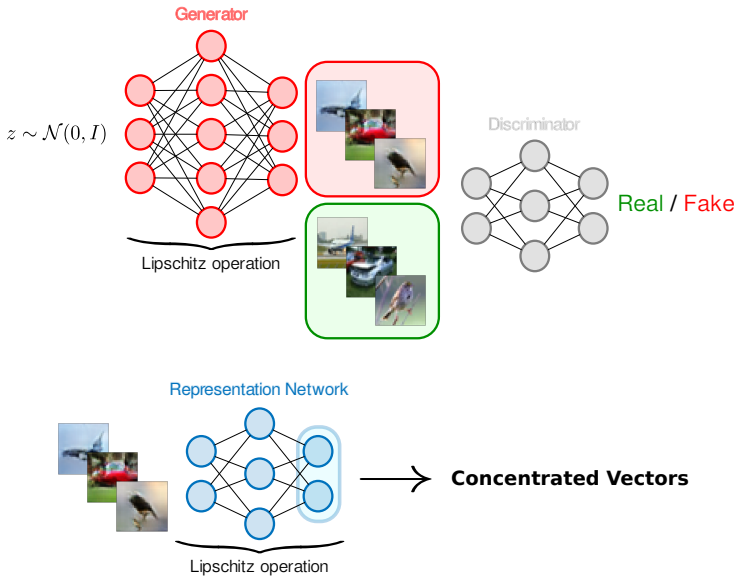


Figure 8.2: Schematics of modern data generation and representation frameworks: GANs (**top**) and CNNs (**bottom**). fig:GAN-CNN

8.1.2.2 GAN-induced data are concentrated random vectors

It is generally assumed that the weight matrices \mathbf{W}_i in neural networks have bounded operator norms (with respect to the data dimensions and numbers). Similarly, the functions ϕ_i are restricted to be 1-Lipschitz (typical functions are the ReLU operator $\phi(x) = \max(x, 0)$, the sign function, or sigmoid functions).

As such, since the input of GANs are random Gaussian vectors $\mathbf{x} \sim \mathcal{N}(0, \mathbf{I}_p)$ and that the successive operations $\mathbf{y} \mapsto \mathbf{W}_i \mathbf{y}$ and $\mathbf{y} \mapsto \phi_i(\mathbf{y})$ are all bounded Lipschitz operations, the output of a GAN is, by definition, a bounded Lipschitz function of a Gaussian $\mathcal{N}(0, \mathbf{I}_p)$ vector.

From the Lipschitz stability of concentrated random vectors (recall (2.40)) and the fact that $\mathbf{x} \sim \mathcal{N}(0, \mathbf{I}_p)$ is concentrated, it then comes that the output of the GAN generator is a concentrated random vector with head and tail parameters of order $O(1)$ (i.e., the same as for \mathbf{x}). In practice, other operations are performed on neural networks, such as pooling operations, random or deterministic dropouts, various connectivity matrix normalization procedures, etc. All these, sometimes precisely designed to avoid the “explosion” of the norm of the layers, can be shown to also consist in Lipschitz operations with $O(1)$ Lipschitz constants. This thus extends our previous statement on the concentration of GAN vectors to state-of-the-art deep neural networks, and in particular to the very popular convolutional neural networks (CNN).

While being concentrated vectors, GAN data (say fake images of dog and cat images) do not necessarily “cluster” in their ambient space as a well separated mixture model of concentrated random vectors. This is even obviously far from being the case: well performing GANs must have a large variance (or entropy) in ambient space so to avoid generating systematically similar data. Images of dogs (1) versus images of cats (2) differ in their being generated by two different neural network maps $\mathbf{x} \mapsto \Phi_1(\mathbf{x})$ and $\mathbf{x} \mapsto \Phi_2(\mathbf{x})$ having differing statistical means $\boldsymbol{\mu}_j = \mathbb{E}[\Phi_j(\mathbf{x})]$ and covariances $\mathbf{C}_j = \mathbb{E}[\Phi_j(\mathbf{x})\Phi_j(\mathbf{x})^\top] - \boldsymbol{\mu}_j\boldsymbol{\mu}_j^\top$ (or alternatively by a conditional GAN having the same effect). Yet, they are clearly not linearly separable (as are real images), therefore implying that $\|\boldsymbol{\mu}_1 - \boldsymbol{\mu}_2\|$, $\|\mathbf{C}_1 - \mathbf{C}_2\|_F$ are likely quite small (when compared to the typical values of $\|\boldsymbol{\mu}_j\|$ and $\|\mathbf{C}_j\|_F$) and thus not prone to immediate classification by standard clustering methods. Feature extraction methods (from simple histograms of oriented gradients (HOG) to modern CNNs (VGG, ResNet, etc.)) precisely aim at increasing these distances by further transforming $\Phi_j(\mathbf{x})$ into some $\Psi(\Phi_j(\mathbf{x}))$ for which distances in means and covariances are larger.

is that right ??? We need to add some confirming table here... (Mohamed is on it)

8.1.2.3 From GAN-data to CNN-features to GMM

State-of-the-art feature extractors in current machine learning research are based on deep neural networks, and specifically for multimedia data on convolutional neural networks. These networks, such as the popular VGG or ResNet, have been pretrained on huge collections of independent databases and are thus fixed, independently functions of the dataset of interest to the experimenter. The associated feature extractor, say $\psi : \mathbb{R}^p \rightarrow \mathbb{R}^q$, is then usually taken to be the function that maps the data to the one-before-last layer of the trained deep network: that is, the very last layer (in general a “fully connected” layer from $\mathbb{R}^q \rightarrow \mathbb{R}^d$, with d the number of classes that the deep learning was trained to learn) is discarded from the network and only the mapping from input to

q -dimensional output is maintained to form ψ .

Being based on a neural network map, ψ is naturally a Lipschitz function with usually well controlled and bounded Lipschitz parameter. The resulting features $\Psi(\mathbf{z}_i) \in \mathbb{R}^q$ handled by the machine learning algorithm are therefore some bounded Lipschitz images of the raw data $\mathbf{z}_i \in \mathbb{R}^p$. When these raw data \mathbf{z}_i are themselves the (realistic multimedia data) output from a GAN, i.e., $\mathbf{z}_i = \Phi_j(\mathbf{x}_i)$ with our previous notations, we obtain that the data $\tilde{\mathbf{x}}_i$ at the input of the classification or regression algorithm under study are of the form $\tilde{\mathbf{x}}_i = \Psi(\Phi_j(\mathbf{x}_i))$ with $\mathbf{x}_i \sim \mathcal{N}(0, 1)$, which by definition are concentrated random vectors (since $\Psi \circ \Phi_j$ is Lipschitz with bounded parameter).

As a consequence, the dataset $\{\tilde{\mathbf{x}}_i\}$ in which each $\tilde{\mathbf{x}}_i$ is of the form $\tilde{\mathbf{x}}_i = \Psi(\Phi_j(\mathbf{x}_i))$, for some j identifying the class of $\tilde{\mathbf{x}}_i$, is a *mixture of concentrated random vectors*.

As such, to treat more realistic data models than the “toy” Gaussian mixture models, the many results presented in the previous chapters should be updated to data $\{\tilde{\mathbf{x}}_i = \Psi(\Phi_j(\mathbf{x}_i))\}$ (where j implicitly depends on the class of \mathbf{x}_i) arising from a mixture of concentrated random vectors. But, from a concentration of measure perspective, it is not formally necessary to specify the concentration origin of $\tilde{\mathbf{x}}_i$ and we may, in all generality, simply ask for the data to be *generic concentrated random vectors from a mixture model*.

Therefore, in the following, we will assume that the data (be they the raw random data or any feature representation), which we redefine as $\mathbf{x}_1, \dots, \mathbf{x}_n \in \mathbb{R}^p$, are simply issued from any mixture of concentrated random vectors as follows:

$$\mathbf{x}_1, \dots, \mathbf{x}_{n_1} \sim \mathcal{L}_1, \quad \dots, \quad \mathbf{x}_{n-n_k}, \dots, \mathbf{x}_n \sim \mathcal{L}_k$$

where \mathcal{L}_j is the law of a concentrated random vector of size p . We further denote, as usual, the statistics means and covariances of the law \mathcal{L}_j as $\boldsymbol{\mu}_j$ and \mathbf{C}_j . For technical reason, it is also necessary to demand that the joint matrix $\mathbf{X} = [\mathbf{x}_1, \dots, \mathbf{x}_n] \in \mathbb{R}^{p \times n}$ be concentrated.

The fundamental result and message of this section are the following: if we recall Theorem 2.17, it appears, in a single-class setting ($k = 1$), that the resolvent $\mathbf{Q}(z) = (\frac{1}{n}\mathbf{X}^\top \mathbf{X} - z\mathbf{I}_n)^{-1}$ of $\frac{1}{n}\mathbf{X}^\top \mathbf{X}$, which is at the core of most of the machine learning algorithms studied thus far, appears to have a deterministic equivalent $\bar{\mathbf{Q}}(z)$ which *only depends on* $\boldsymbol{\Phi} = \boldsymbol{\mu}_1 \boldsymbol{\mu}_1^\top + \mathbf{C}_1$, and thus on the first two order statistics of the law \mathcal{L}_1 .

It is not difficult to infer from this result that, for a multi-class setting ($k > 1$ finite), the same will hold. Besides, from Theorem 4.1 and the discussion preceding it, it is likely that kernel matrices with the classical normalization, e.g., $\mathbf{K} = \{f(\frac{1}{p}\|\mathbf{x}_i - \mathbf{x}_j\|^2)\}_{i,j=1}^n$, and their spectral properties, which asymptotically essentially depend on the behavior of a low-rank perturbation of $\mathbf{X}^\top \mathbf{X}$, will also mostly depend on the first two order statistics.

8.1.2.4 Kernel asymptotics and GAN-generated data

This intuition turns out to be correct, at least to some extent. It is indeed shown in [Seddik et al., 2019, Theorem 1] that, under the setting of concentrated random vectors, Theorem 4.1, Theorem 4.1 holds identically under the present concentration of measure assumptions. Precisely, it is shown for technical simplicity that $\|\mathbf{P}(\mathbf{K} - \tilde{\mathbf{K}})\mathbf{P}\| \xrightarrow{a.s.} 0$ where $\mathbf{P} = \mathbf{I}_n - \frac{1}{n}\mathbf{1}_n\mathbf{1}_n^\top$: this discards several terms in the expansion of $\tilde{\mathbf{K}}$ which however do not affect the practical relevance of the result (for instance, all terms in the expansion of matrices $\mathbf{A}_n, \mathbf{A}_{\sqrt{n}}, \mathbf{A}_1$ of the form $\mathbf{1}_k$ or $\mathbf{1}_k\mathbf{1}_k^\top$ disappear). This aspect notwithstanding, the random $\tilde{\mathbf{K}}$ has the same expression under a Gaussian or concentrated random vector mixture model. However, $\tilde{\mathbf{K}}$ does not solely depend on the first and second order moments of the data, due to the presence of the vector ψ , the entries of which have zero mean but variance function of the fourth-order moment of \mathbf{x}_i (precisely of $\mathbf{w}_i = \mathbf{C}_a^{-\frac{1}{2}}(\mathbf{x}_i - \boldsymbol{\mu}_a)$ for $\mathbf{x}_i \sim \mathcal{L}_a$). Yet, this vector ψ (i) only intervenes in the low-rank part of the expansion of $\tilde{\mathbf{K}}$ and thus does not asymptotically affects the limiting spectrum of \mathbf{K} , and (ii) does not affect the component $\mathbf{A}_{1,11}$ which essentially rules the isolated spectrum behavior of \mathbf{K} (position of isolated eigenvalues and content of the eigenvectors). As a consequence, standard operations on \mathbf{K} , such as devised in the algorithms described in the previous chapters (extraction of “informative” eigenvectors, use within a semi-supervised or supervised learning filter), are essentially *universal* with respect to the laws $\mathcal{L}_j = \mathcal{L}_j(\boldsymbol{\mu}_j, \mathbf{C}_j)$ in that they only depend on $\boldsymbol{\mu}_j, \mathbf{C}_j$.

The immediate outcome of this discussion is that most results above, defined for machine learning algorithms based on \mathbf{K} , *provably identically hold for realistic (GAN-generated) data and for their Gaussian mixture model equivalent* (i.e., for the Gaussian mixture model with same first order statistics).

This is visually confirmed in Figure 8.4 which provides a concrete comparison of the finite-dimensional spectrum (eigenvalues and two dominant eigenvectors) of $\mathbf{K} = \{\exp(-\frac{1}{p}\|\mathbf{x}_i - \mathbf{x}_j\|^2)\}_{i,j=1}^n$ for \mathbf{x}_i CNN-features of real images, GAN images (arising from the training of a GAN on the same real images), versus a Gaussian mixture with same empirical (mean and covariance) statistics as those CNN-features. The visual fit, which we now know to be theoretically asymptotically perfect in the GAN-data case, is extremely accurate in this finite-dimensional case (p of order a few thousands), even for the real data for which no guarantee can of course be claimed (so long that the theoretical relation between real data and their GAN-generated counterpart is not elucidated).

8.1.2.5 Beyond “classical” kernels

The previous section emphasized the universality of the kernel $\mathbf{K} = \{f(\frac{1}{p}\|\mathbf{x}_i - \mathbf{x}_j\|^2)\}_{i,j=1}^n$ with respect to the concentrated random vector statistics of \mathbf{x}_i . The main reason follows from the fact that the higher-than-two order moments of \mathbf{K} play a marginal role, if not no role, in the asymptotics of \mathbf{K} (as we saw, only through the vector ϕ which has no asymptotic impact on the relevant



Figure 8.3: Images produced by a high-resolution GAN for three data classes (hamburger, mushroom, pizza) (**top**) versus the dataset of real images used to learn the GAN (**bottom**). fig:GAN_pictures

eigenvectors and low-rank informative terms in \mathbf{K}).

This may no longer be the case for more elaborate kernel models, such as the $\alpha\text{-}\beta$ kernel and the properly scaled kernels discussed in Chapter 4.

For the $\alpha\text{-}\beta$ kernel, the “second-order noise” matrix Φ with entries related to $(\mathbf{w}_i^\top \mathbf{w}_j)^2$: from the independence of \mathbf{w}_i and \mathbf{w}_j , the variance of this term depends on the fourth order moments of the (independent) entries of \mathbf{w}_i and \mathbf{w}_j , which impacts the overall spectrum of Φ . Yet, since the diagonal terms $(\mathbf{w}_i^\top \mathbf{w}_i)^2$ are discarded, the up-to-eighth order moments are not accounted for. The universality thus holds in this case only up to the fourth order moments: the Gaussian mixture model likely becomes insufficient to properly model its behavior on concentrated random vectors and thus on realistic datasets.

As for the more involved properly scaled kernels, such as the kernel $\mathbf{K} = \{f(\frac{1}{\sqrt{p}} \mathbf{x}_i^\circ \mathbf{x}_j^{\circ\top})\}_{i,j=1}^n$ (with $\mathbf{x}_i^\circ = \mathbf{x}_i - \frac{1}{n} \sum_j \mathbf{x}_j$), recall that its asymptotics are inherently related to the Gaussian asymptotics (central limit) of $\frac{1}{\sqrt{p}} \mathbf{x}_i^\circ \mathbf{x}_j^{\circ\top}$. This central limit must be preserved in concentrated random vectors for universality to hold. Yet, this is far from obvious and demands additional constraints on the laws \mathcal{L}_j . In this setting, it is quite possible that important deviations to universality be observed. In the specific setting of GAN-data, which arise from deep neural network learning, one is tempted to assume some sort of an inherent “isotropic” nature of the successive layers of the large trained network, which may smooth-out the concentrated random vectors in a way to make them “more

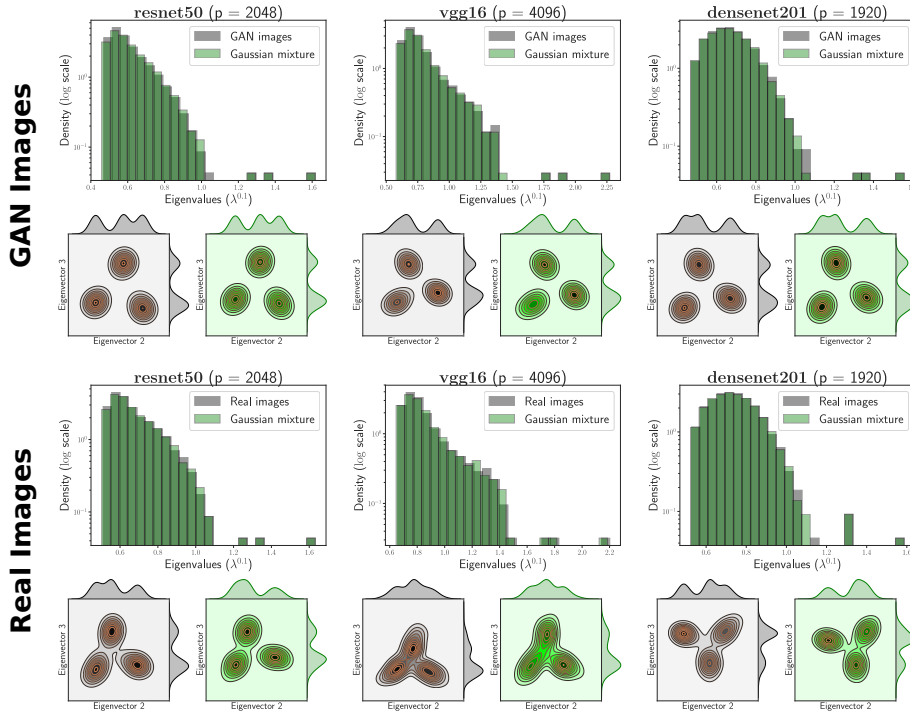


Figure 8.4: Eigenvalue distribution and two dominant eigenvectors of $\mathbf{K} = \{\exp(-\frac{1}{p}\|\mathbf{x}_i - \mathbf{x}_j\|^2)\}_{i,j=1}^n$ for datasets $\mathbf{X} = [\mathbf{x}_1, \dots, \mathbf{x}_n] \in \mathbb{R}^{p \times n}$ of features obtained from different convolutional neural networks (from left to right: ResNet50 with $p = 2048$ features, the VGG16 with $p = 4096$ features and DenseNet201 with $p = 1920$) of the dataset of original images in Figure 8.3. Comparison of the results obtained for the GAN-generated data (**top**) versus the real data (**bottom**), empirically on the dataset (gray) and on independent Gaussian vectors following the same statistical (means and covariances) mixture `fig:GAN_results`

Gaussian”, and one may still be confident that the Gaussian mixture model assumption may still be somewhat relevant.

***** detail more here! *****

8.2 Wide-sense universality in large dimensional machine learning

The example of GANs in the previous section underlies a seemingly more fundamental aspect of real (large dimensional) data processing: so long that real data can be assumed to be inherently constituted of a large number of degrees of freedom (or of randomness), a dual phenomenon arises:

- these degrees of freedom tend to regularize and induce robustness into machine learning algorithms; this is in particular at the very source of well-behaved deep neural networks (based on numerous data and numerous randomly-initialized neurons) versus ill-behaved small perceptrons.
- the machine learning algorithms essentially extract basic small dimensional statistics from the data (scalar comparisons of first order moments and deterministic patterns) from the data, thereby completely “eliminating” the noise, irrespective of its nature (distribution, higher order moments).

This suggests that, beyond images and sounds, data representations sufficiently rich in degrees of freedom should be similarly handled in a robust and theoretically tractable manner by standard machine learning methods. The recent success of word embeddings (derivatives of the word2vec method for instance [Mikolov et al., 2013]) which aim to represent word, sentences and other structures in the complex field of natural language processing via vectors in a rather large dimensional space, confirms this intuition: these representations are likely quite rich and diverse, and thus probably amenable to theoretical analysis by means of Gaussian mixture approximations. A typical counter-example in this very field of natural language processing is the so-far exploited “bag of words” representation which consists in large dimensional *extremely sparse* dictionary vectors (each sentence or paragraph being represented by one such vector counting the number of instances of each dictionary word in the sentence); being very sparse, these vectors *do not concentrate*, thereby poorly contributing to adding degrees of freedom to stabilize the machine learning algorithms. We may even go as far as claiming that it is no wonder that so little theory is available in the field of natural language processing, until recently essentially based on these unstable data representations.

Figure 8.5 compares the typical kernel matrix structures observed when evaluating the distances between CNN features for real images (of dimension $p = 1024$) in two classes, versus word2vec embeddings for words (of dimensions $p = 300$) in two categories. The colormap strongly suggests the aforementioned concentration effect arising in real data, even here in a natural language processing context.

This being said, we must stress that the validity of the random matrix predictions and improvements of algorithms fundamentally relies on the *preexistence* of convenient data representations. Aside from subspace or manifold-based algorithms, the field of random matrix theory does not in itself propose such elaborate representations. If anything, it would naturally suggest to operate random (nonlinear) projections on real data so to “generate” more randomness, and thus more predictability and robustness. However, random projections are a rather poor elementary representation technique which does not account for the data context and structure (as opposed to convolutional neural nets which intrinsically exploit the locality and multiclass nature of the data).

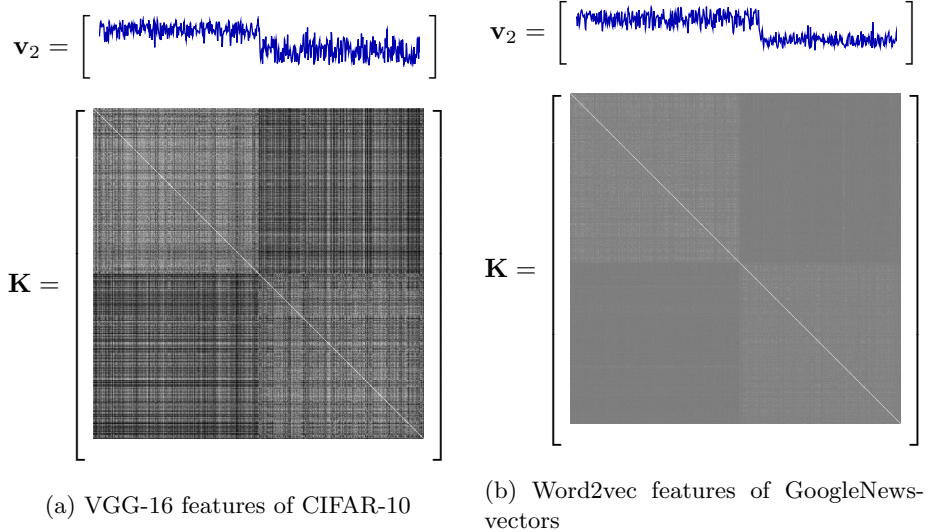


Figure 8.5: Kernel matrices \mathbf{K} (Gaussian kernel) and the second top eigenvectors \mathbf{v}_2 for (left) VGG-16 [Simonyan and Zisserman, 2014] features of CIFAR-10 data (airplane versus bird) and (right) word2vec [Mikolov et al., 2013] features of GoogleNews-vectors data (“sports” versus “sales”), with $\mathbf{x}_1, \dots, \mathbf{x}_{n/2} \in \mathcal{C}_1$ and $\mathbf{x}_{n/2+1}, \dots, \mathbf{x}_n \in \mathcal{C}_2$.

`fig:kernel-plot-word2vec`

Recalling that machine learning can be seen as the elegant merger of “representation + classification”, random matrix theory is so far merely able to operate on the “classification” aspect, assuming that the data representation is given and rather convenient. Better understanding and contributing to the “representation” part of machine learning would require to add supplementary data-related contextual ingredients to random matrix theory, so most likely more complex random and deterministic structures. Alternatively, knowing the powerful capability of deep neural networks to design appropriate representations of data, random matrix theory could contribute by improving its understanding of the deep learning mechanisms. This would mean understanding the dynamics of learning in the multi-layer, nonlinear, and non-convex setting of deep learning, which raises multiple (so far unsurpassable) difficulties:

- “tracking” the gradient descent evolution of the deep network weights involves intricate correlation between descent steps; also, the number of required steps to convergence scales with the size N of the network: a sudden sheer gain in performance is usually observed (similarly observed in other network dynamics) after at least $O(\log N)$ descent steps, so that it is insufficient to study the network behavior after finitely many steps of descent. This may seem at first contradictory to the recent findings on the so-called neural tangent kernels (NTK) [Jacot et al., 2018], which predicts

that deep neural networks converge close to their initialization point *in the limit of infinitely many neurons per layer*. This last statement is however key to the NTK convergence: for a number of neurons per layer N scaling like the size p and number n of data, the proof of the NTK asymptotics no longer holds;

- several works predict that, despite the highly non-convex nature of the underlying optimization, deep network learning owes its stability to the simultaneously large dimensions in data size, number as well as network depth and width. This has not been formally proved but related optimization problems in random Gaussian fields (formally not a neural network but that could resemble one [Choromanska et al., 2015]) show that in the large dimensional regime, while the number of local minima increases exponentially with the network size, these minima tend to reach the same level, thereby ensuring that, with high probability, all initialization points reach the approximate same performance after convergence [Dauphin et al., 2014]. These results however do not say much more: what are the performances reached? How do they relate to the data statistics? How could they be improved? Besides, the setting of Gaussian random fields remains far from actual deep networks and notably ignores some of its key features, such as the nonlinear activations, their structure in multiple layers, their convolutive nature for convolutional nets, etc.

If deep neural networks do not converge to a limiting kernel, as predicted by the NTK analysis [Jacot et al., 2018], it nonetheless remains true that neural networks and kernels are intimately related, so that further studies and explorations of the former may help improve the understanding of the latter.

8.3 Discussions and conclusions

Concentration of measure theory provides a powerful tool, quite complementary to random matrix theory, to analyze the performance of statistical learning algorithms applied to a host of real data models. According to our previous discussions, one is tempted to state that the existence of “good concentrated vector models” of real data, such as the images produced by GANs, fully justifies (through the proofs of universality) the further development of random matrix theory for the performance analysis and improvement of Gaussian mixture-based algorithms. However, claiming that a model is “good” is a fairly subjective statement (do GANs produce all images of a class one could possibly think of or do they over-produce a limited set of images?), and if ever a measure of goodness was appropriately designed, confirming that the analyses made on Gaussian mixtures are robust to deviations in the data models which would include real data is likely difficult. On this point, only extensive simulations can be used as a measure of faith.

This is the case of images, which differ from text, language, and some complex signals, in their not requiring “long-term memory”: correlations in images

are indeed mostly localized and may thus be produced by feedforward networks. Textual contents are rather produced by recurrent networks, and most particularly by long short-term memory (LSTM) networks. A possible parallel path to proving that learning in natural language processing can be theoretically analyzed by random matrix and concentration of measure methods would then consist in showing that LSTM networks are also Lipschitz mappings (for instance from and into some word embedding space). Similar to deep feedforward networks, understanding the behavior of LSTMs is difficult (as they use the same gradient descent learning) but the study of simpler networks, such as echo-state networks, already capable of faithful predictions, may help improve our present lack of understanding.

In spirit though, without having to formally prove that “real data learning” is amenable to random matrix analysis, the validity of the random matrix approximation mostly holds on two complementary pillars: (i) a “concentration-like behavior” of the real data representation, and (ii) a good “Lipschitz mixing behavior” of the studied algorithm. That is: (i) the data representation under study should resemble a vector with *rather independent and delocalized entries*, i.e., the data representation must exploit most of the degrees of freedom offered by its ambient space, in the manner of Gaussian random vectors: this ensures that their scalar Lipschitz observations have a more or less predictable behavior, and (ii) the learning algorithm maintains the delocalized behavior or data, or even reinforces it: this avoids the creation of outlying (thus difficult to predict) behavior; most well-performing algorithms tend to satisfy this rule (activation functions in neural networks are Lipschitz, their weight matrices are normalized, kernels are rarely more than quadratic to remain stable, etc.). In a sense, even data that would not be concentrated per se may be appropriately mixed (Gaussianized one may say) by the learning algorithm so to stabilize the performances. Conversely, well-concentrated data may suffer the effects of non-strictly Lipschitz transformations (so to extract exotic or marginal features for instance) while remaining stable under random matrix analysis. This in essence justifies the wide applicability and robustness of the various random matrix analyses presented in the course of the monograph on various real data.

Some data, however, are frankly not concentrated: this is notably the case of sparse vectors and sparse graphs. A typical example in natural language processing is that of the bag-of-words or tf*idf (for term frequency-inverse document frequency) method, which use large dictionary vectors (typically of size in the hundreds or thousands of words) filled with the number of occurrence or frequency of each word in a paragraph or text. These vectors are naturally quite empty and clearly do not adhere to the concentration of distance phenomenon observed in Gaussian-like vectors. The adjacency matrix of sparse graphs (that is graphs of n nodes with $O(1)$ neighbors per node) also loses key concentration properties to random matrix analysis: the norm or inner product between arbitrary columns of the adjacency matrix do not converge: this makes most classical random matrix tools (starting with the trace lemma, Lemma 2.11) collapse at once. When additional statistical symmetries are assumed, for in-

stance if the entries of the adjacency matrix are independent and identically distributed, stable asymptotic behavior (of the eigenspectrum in particular) is observed, but is often to date not tractable to random matrix theory. If ever possible, the observed behavior would at any rate not be universal and thus quite dependent on the detailed model statistics: this raises a major issue in practice since, Gaussian approximations no longer being valid, the data models must be extremely accurate for the theoretical analysis to be of any value. With difficult-to-understand real data, this severely reduces the interest of large dimensional statistical results.

Nonetheless, where random matrix theory fails to work, ingredients of statistical physics (despite their often lacking mathematical rigor) can sometimes be exploited. Informal techniques such as the replica method, the various linearizations and approximations of the belief-propagation algorithm using statistical physics concepts (of free energy, Hamiltonian, Bethe-Hessian approximation, etc.) have provided tremendous advances in large dimensional statistical learning, precisely under scenarios where random matrices still lag behind. This is particularly the case of sparse graph mining, where heuristic but powerful new algorithms were designed out of statistical physics ideas [Krzakala et al., 2013, Saade et al., 2014]. Mathematicians are only recently managing to formally prove some of the fundamental predictions proposed in these articles. So long that no formal theory of sparse random matrices exist, the future of large dimensional statistical learning may in part lie in this two-stage process where physicists come first with intuitive ideas and new algorithm proposals, before random matrix experts formalize and mathematically push further these ideas.

Solutions to exercises in Section 2.9

chap:solutions_exo

Exercise 1 (Stieltjes transform and moments). *Show that the Stieltjes transform $m_\mu(z)$, of a probability measure μ with bounded support (and thus finite moments), is a moment generating function in the sense that, for all $z \in \mathbb{C}$ such that $|z| > \max\{|\inf(\text{supp}(\mu))|, |\sup(\text{supp}(\mu))|\}$,*

$$m_\mu(z) = -\frac{1}{z} \sum_{n=0}^{\infty} M_n z^{-n}$$

where $M_n = \int t^n \mu(dt)$.

From this formulation, propose a method to evaluate the successive moments of μ .

Correction 1 (Stieltjes transform and moments). *For the first part, it suffices to note that*

$$\begin{aligned} m_\mu(z) &= \int \frac{1}{t-z} \mu(dt) \\ &= -\frac{1}{z} \int \frac{1}{1-\frac{t}{z}} \mu(dt) \\ &= -\frac{1}{z} \sum_{k=0}^{\infty} \int \frac{t^k}{z^k} \mu(dt) \\ &= -\frac{1}{z} \sum_{k=0}^{\infty} M_k z^{-k}. \end{aligned}$$

Thus, differentiating successively $\delta(z) \equiv -\frac{1}{z} m_\mu(z^{-1}) = \int \frac{1}{1-zt} \mu(dt)$, we find

$$\frac{d^\ell}{dz^\ell} \delta(z) = \sum_{k \geq \ell} \frac{k!}{(k-\ell)!} M_k z^{k-\ell}$$

and so, in particular, setting $z = 0$ in this expression, we find

$$\frac{d^\ell}{dz^\ell} \delta(0) = \ell! M_\ell.$$

Exercise 2 (Non-immediate Stieltjes transforms). Let $\mathbf{X} \in \mathbb{R}^{n \times n}$ be a Hermitian matrix and $\mathbf{Q}(z) = (\mathbf{X} - z\mathbf{I}_n)^{-1}$ its resolvent. Show that, for any $\mathbf{u} \in \mathbb{R}^n$ unitary ($\|\mathbf{u}\| = 1$) and any \mathbf{A} with $\text{tr } \mathbf{A} = 1$, the quantities $\mathbf{u}^\top \mathbf{Q}(z)\mathbf{u}$ and $\text{tr } \mathbf{A}\mathbf{Q}(z)$ are the Stieltjes transform of probability measures.

What are these measures and what are their supports?

Correction 2 (Non-immediate Stieltjes transforms). It suffices to observe that, letting $\mathbf{X} = \mathbf{V}\Lambda\mathbf{V}^\top$ with $\mathbf{V} = [\mathbf{v}_1, \dots, \mathbf{v}_n]$ and $\Lambda = \text{diag}(\lambda_1, \dots, \lambda_n)$, and denoting $\mathbf{w} = \mathbf{V}^\top \mathbf{u}$,

$$\mathbf{u}^\top \mathbf{Q}(z)\mathbf{u} = \mathbf{u}^\top \mathbf{V} \text{diag} \left(\frac{1}{\lambda_i - z} \right)_{i=1}^n \mathbf{V}^\top \mathbf{u} = \sum_{i=1}^n \frac{|w_i|^2}{\lambda_i - z} = \int \frac{1}{t - z} \mu(dt)$$

where $\mu = \sum_{i=1}^n |w_i|^2 \delta_{\lambda_i}$. This measure is such that

$$\int \mu(dt) = \sum_{i=1}^n |w_i|^2 = \mathbf{w}^\top \mathbf{w} = \mathbf{u}^\top \mathbf{V} \mathbf{V}^\top \mathbf{u} = 1$$

and is thus a probability measure.

All the same, letting $\mathbf{B} = \mathbf{V}\Lambda\mathbf{V}^\top$,

$$\text{tr } \mathbf{A}\mathbf{Q} = \text{tr } \mathbf{B} \text{diag} \left(\frac{1}{\lambda_i - z} \right)_{i=1}^n = \sum_{i=1}^n \frac{B_{ii}}{\lambda_i - z} = \int \frac{1}{t - z} \mu(dt)$$

where $\mu = \sum_{i=1}^n B_{ii} \delta_{\lambda_i}$ and $\int \mu(dt) = \text{tr } \mathbf{B} = \text{tr } \mathbf{A} = 1$.

Exercise 3 (Stieltjes transform and singular values). Let μ be a probability measure on \mathbb{R}^+ and ν, ν' be the measures defined by

$$\begin{aligned} \int f(t)\nu(dt) &= \int f(\sqrt{t})\mu(dt) \\ \int f(t)\nu'(dt) &= \frac{1}{2} \left(\int f(t)\nu(dt) + \int f(-t)\nu(dt) \right) \end{aligned}$$

for all bounded continuous f .

What are ν, ν' when $\mu = \frac{1}{n} \sum_{i=1}^n \delta_{x_i}$ for $x_1, \dots, x_n \geq 0$?

Show that the Stieltjes transform $m_{\nu'}$ of ν' satisfies

$$m_{\nu'}(z) = zm_\mu(z^2).$$

Letting $\mathbf{X} \in \mathbb{R}^{n \times n}$ and μ the empirical spectral distribution of $\mathbf{X}\mathbf{X}^\top$, relate the Stieltjes transform of the matrix

$$\Gamma = \begin{bmatrix} 0 & \mathbf{X} \\ \mathbf{X}^\top & 0 \end{bmatrix}$$

to that of the measure μ , and conclude on the nature of this Stieltjes transform.

Correction 3 (Stieltjes transform and singular values). For $\mu = \frac{1}{n} \sum_{i=1}^n \delta_{x_i}$, $\nu = \frac{1}{n} \sum_{i=1}^n \delta_{\sqrt{x_i}}$ and $\nu' = \frac{1}{2n} \sum_{i=1}^n (\delta_{x_i} + \delta_{-x_i})$.

The Stieltjes transform relation is then given by

$$\begin{aligned} m_{\nu'}(z) &= \frac{1}{2} \int \frac{1}{t-z} \nu(dt) + \frac{1}{2} \int \frac{1}{-t-z} \nu(dt) \\ &= \frac{1}{2} \int \frac{1}{\sqrt{t}-z} \mu(dt) + \frac{1}{2} \int \frac{1}{-\sqrt{t}-z} \mu(dt) \\ &= -z \int \frac{1}{z^2-t} \mu(dt) \\ &= zm_\mu(z^2). \end{aligned}$$

The Stieltjes transform of the empirical spectral measure of Γ is given by

$$\begin{aligned} \frac{1}{2n} \text{tr} \begin{pmatrix} -z\mathbf{I}_n & \mathbf{X} \\ \mathbf{X}^\top & -z\mathbf{I}_n \end{pmatrix}^{-1} &= \frac{-z}{2n} \text{tr}(z^2\mathbf{I}_n - \mathbf{X}\mathbf{X}^\top)^{-1} + \frac{-z}{2n} \text{tr}(z^2\mathbf{I}_n - \mathbf{X}^\top\mathbf{X})^{-1} \\ &= \frac{-z}{n} \text{tr}(z^2\mathbf{I}_n - \mathbf{X}\mathbf{X}^\top)^{-1} \end{aligned}$$

where we used the block-matrix inverse lemma. This Stieltjes transform has its singularities for z one of the singular values of \mathbf{X} (i.e., the square-root of the eigenvalues of $\mathbf{X}\mathbf{X}^\top$). It thus relates to the singular spectrum of \mathbf{X} .

Exercise 4 (Partial proof of Lemma 2.9). For \mathbf{A}, \mathbf{M} symmetric nonnegative definite matrices, $\tau > 0$ and $z < 0$, using inversion lemmas and norm inequalities, prove that

$$\left| \text{tr } \mathbf{A} (\mathbf{M} + \tau \mathbf{u} \mathbf{u}^\top - z \mathbf{I}_p)^{-1} - \text{tr } \mathbf{A} (\mathbf{M} - z \mathbf{I}_p)^{-1} \right| \leq \frac{\|\mathbf{A}\|}{|z|}.$$

Correction 4 (Partial proof of Lemma 2.9). There is a slight subtlety not to ignore when upper bounding the difference: we start with the resolvent identity $\mathbf{A}^{-1} - \mathbf{B}^{-1} = \mathbf{A}^{-1}(\mathbf{B} - \mathbf{A})\mathbf{B}^{-1}$ followed by the rank-one perturbation inverse lemma $(\mathbf{A} + t\mathbf{v}\mathbf{v}^\top)^{-1}\mathbf{v} = \mathbf{A}^{-1}\mathbf{v}/(1 + t\mathbf{V}^\top\mathbf{A}^{-1}\mathbf{v})$,

$$\begin{aligned} &\left| \text{tr } \mathbf{A} (\mathbf{M} + \tau \mathbf{u} \mathbf{u}^\top - z \mathbf{I}_p)^{-1} - \text{tr } \mathbf{A} (\mathbf{M} - z \mathbf{I}_p)^{-1} \right| \\ &= \left| \text{tr } \mathbf{A} (\mathbf{M} + \tau \mathbf{u} \mathbf{u}^\top - z \mathbf{I}_p)^{-1} \tau \mathbf{u} \mathbf{u}^\top (\mathbf{M} - z \mathbf{I}_p)^{-1} \right| \\ &= \frac{\left| \text{tr } \mathbf{A} (\mathbf{M} + \tau \mathbf{u} \mathbf{u}^\top - z \mathbf{I}_p)^{-1} \tau \mathbf{u} \mathbf{u}^\top (\mathbf{M} - z \mathbf{I}_p)^{-1} \right|}{1 + \tau \mathbf{u}^\top (\mathbf{M} - z \mathbf{I}_p)^{-1} \mathbf{u}} \\ &= \frac{\left| \tau \mathbf{u}^\top (\mathbf{M} - z \mathbf{I}_p)^{-1} \mathbf{A} (\mathbf{M} + \tau \mathbf{u} \mathbf{u}^\top - z \mathbf{I}_p)^{-1} \mathbf{u} \right|}{1 + \tau \mathbf{u}^\top (\mathbf{M} - z \mathbf{I}_p)^{-1} \mathbf{u}}. \end{aligned}$$

At this point, we use the fact that $|\mathbf{x}^\top \mathbf{B} \mathbf{x}| \leq \|\mathbf{B}\| \|\mathbf{x}\|^2$ where we smartly take

$\mathbf{B} = (\mathbf{M} - z\mathbf{I}_p)^{-\frac{1}{2}} \mathbf{A} (\mathbf{M} - z\mathbf{I}_p)^{-\frac{1}{2}}$ and $\mathbf{x} = (\mathbf{M} - z\mathbf{I}_p)^{-\frac{1}{2}} \mathbf{u}$, so to obtain

$$\begin{aligned} & \left| \operatorname{tr} \mathbf{A} (\mathbf{M} + \tau \mathbf{u} \mathbf{u}^\top - z\mathbf{I}_p)^{-1} - \operatorname{tr} \mathbf{A} (\mathbf{M} - z\mathbf{I}_p)^{-1} \right| \\ & \leq \|(\mathbf{M} - z\mathbf{I}_p)^{-\frac{1}{2}} \mathbf{A} (\mathbf{M} - z\mathbf{I}_p)^{-\frac{1}{2}}\| \frac{\tau \mathbf{u}^\top (\mathbf{M} - z\mathbf{I}_n)^{-1} \mathbf{u}}{1 + \tau \mathbf{u}^\top (\mathbf{M} - z\mathbf{I}_n)^{-1} \mathbf{u}}. \end{aligned}$$

Using finally $\|(\mathbf{M} - z\mathbf{I}_p)^{-\frac{1}{2}} \mathbf{A} (\mathbf{M} - z\mathbf{I}_p)^{-\frac{1}{2}}\| \leq \|\mathbf{A}\| \|(\mathbf{M} - z\mathbf{I}_n)^{-1}\|$, $\|(\mathbf{M} - z\mathbf{I}_n)^{-1}\| \leq \frac{1}{|z|}$ and $\frac{x}{1+x} \leq 1$ for $x > 0$, we retrieve the sought-for result.

Exercise 5 (The $\sqrt{|x-b|}$ behavior of the edges). Show that both the semi-circle and the Marčenko-Pastur laws (for $c \neq 1$) have a local $\sqrt{|x-b|}$ behavior at each of the edges b of their support.

Conclude on the typical number of eigenvalues of the Wishart matrix $\frac{1}{n} \mathbf{X} \mathbf{X}^\top \in \mathbb{R}^{p \times p}$ with $\mathbf{X}_{ij} \sim \mathcal{N}(0, 1)$ independent, and the Wigner $\mathbf{X} \in \mathbb{R}^{n \times n}$ with $\mathbf{X}_{ij} = \mathbf{X}_{ji} \sim \mathcal{N}(0, 1)$ independent up to symmetry, found near the edges of their respective supports.

Relate this finding to the fluctuations of the Tracy-Widom distribution of the largest and smallest eigenvalues.

What happens for the left-edge of the support of the Marčenko-Pastur law and to the associated smallest eigenvalues of Wishart matrices when $\lim p/n = c = 1$? How many eigenvalues are then found close to the left edge in this so-called “hard-edge” setting? Conclude on the typical fluctuations of these eigenvalues and confirm numerically.

Correction 5 (The $\sqrt{|x-b|}$ behavior of the edges). The Marčenko-Pastur density can be approximated around, say, the right-edge E^+ ($x = (1 + \sqrt{c})^2 - \varepsilon$, $\varepsilon > 0$ small) of its support as

$$\mu(dx) \simeq_{x \sim E^+} \frac{\sqrt{(1 + \sqrt{c})^2 - (1 - \sqrt{c})^2}}{2\pi c(1 + \sqrt{c})^2} \sqrt{|x - (1 + \sqrt{c})^2|} dx.$$

Similarly, around $E^+ = 2$, the semi-circle distribution has approximate density

$$\mu(dx) = \frac{1}{2\pi} \sqrt{(x^2 - 4)^+} dx \simeq_{x \sim E^+} \frac{1}{\pi} \sqrt{|x - 2|} dx.$$

As a consequence, for both models, within the interval $[E^+ - \varepsilon, E^+]$ of size ε small, the typical integral of the density is of order

$$\int_{E^+ - \varepsilon}^{E^+} \mu(dx) \simeq C \int_{E^+ - \varepsilon}^{E^+} \sqrt{E^+ - x} dx =_{y=E^+-x} -C \int_{\varepsilon}^0 \sqrt{y} dy = \frac{2C}{3} \varepsilon^{\frac{3}{2}}$$

where $C > 0$ is one of the constants provided above for each measure.

As a consequence, the number of eigenvalues of the corresponding finite-dimensional matrix models falling within an interval of small (but $O(1)$) size near E^+ is of order $n^{\frac{2}{3}}$. This is particularly interesting as, elsewhere in the support, the typical number of eigenvalues within a space of size $O(1)$ is naturally

of order $O(n)$ (i.e., a non-trivial proportion of the total number of eigenvalues). As a consequence, the typical “spacing” between adjacent eigenvalues near the edge E^+ is of order $1/n^{2/3} = n^{-2/3}$, which is (not surprisingly) also the typical fluctuation of the largest eigenvalues according to the Tracy-Widom theorem.

When $c = 1$ in the Marčenko-Pastur limit though, due to the presence of the term x in the denominator of the density $\mu(dx)$, we obtain instead that, for x near the left edge $E^- = 0$,

$$\mu(dx) \simeq_{x \sim 0} \frac{1}{\pi\sqrt{x}}$$

so that the density diverges in zero and the integral of the density on $[0, \varepsilon]$ is instead of order $\frac{2}{\pi}\sqrt{\varepsilon}$: the typical number of eigenvalues is here instead extremely large, of order $n^{2/3}$ (extremely locally of course).

*** check the final reasoning here ***

Exercise 6 (The $\sqrt{|x - b|}$ behavior in elaborate models). We here seek to extend the results of Exercise 5 to the sample covariance matrix model $\frac{1}{n}\mathbf{X}\mathbf{X}^\top$ where $\mathbf{X} = \mathbf{C}^{1/2}\mathbf{Z}$ with \mathbf{Z} having independent standard Gaussian entries and \mathbf{C} having a bounded limiting spectral measure ν with fast decaying tails. We denote $\tilde{m}(z)$ the Stieltjes transform of the limiting spectral measure $\tilde{\mu}$ of $\frac{1}{n}\mathbf{X}^\top\mathbf{X}$.

Using Figure 2.5 as a reference and recalling the formulation for the inverse Stieltjes transform

$$x(\tilde{m}) = -\frac{1}{\tilde{m}} + c \int \frac{t\nu(dt)}{1+t\tilde{m}}$$

visually justify that $x''(\tilde{m})$ can be (complex) analytically extended in the neighborhood of each point \tilde{m} where $x'(\tilde{m}) = 0$ into a function $z(\tilde{m})$ which must locally coincide with the inverse Stieltjes transform of $\tilde{m}(z)$.

Deduce that $\tilde{m}(z)$ must be of the form $\sqrt{z - b}$ near an edge and conclude.

Correction 6 (The $\sqrt{|x - b|}$ behavior in elaborate models). We observe visually that $x''(\tilde{m}) \neq 0$ near the edges of the support ($x(\tilde{m})$ has a quadratic behavior). As such, the function $z(\tilde{m})$, defined similar to $x(\tilde{m})$ but for $\tilde{m} \in \mathbb{C} \setminus \{-1/\text{supp}(\nu)\}$, is analytic and locally invertible into a function $\tilde{M}(z)$. This function $\tilde{M}(z)$ coincides with the Stieltjes transform $\tilde{m}(z)$ of $\tilde{\mu}$ for all z real outside the support. By analyticity (in particular of all its derivatives), for z at the edges of – but inside – the support, $\tilde{m}(z)$ and its inverse $z(\tilde{m})$ must enjoy the same functional behavior: the latter is in particular locally quadratic, and thus, as its inverse, the former has a local square-root behavior. Since the density equals the imaginary part of $\tilde{m}(z)$ for z near the real axis, this square-root behavior propagates to the density which must then be of the form $\sqrt{z - E}$.

Exercise 7 (Further results on $x(\tilde{m})$). We aim in this exercise to justify some of the visual observations made on Figure 2.5.

Show that, for $\tilde{m}_1 \neq \tilde{m}_2$ such that $x'(\tilde{m}_1), x'(\tilde{m}_2) > 0$, we cannot have $x(\tilde{m}_1) = x(\tilde{m}_2)$: that is, the increasing segments of $x(\tilde{m})$ never “overlap”.

Besides, show that, if $\tilde{m}_1 < \tilde{m}_2$ are both of the same sign, and $x'(\tilde{m}_1), x'(\tilde{m}_2) > 0$, then $x(\tilde{m}_1) < x(\tilde{m}_2)$: that is, the increasing segments of $x(\tilde{m})$ never “swap”. To this end, we may prove the intermediary result

$$(\tilde{m}_1 - \tilde{m}_2) \left(1 - \int \frac{c\tilde{m}_1\tilde{m}_2 t^2 \nu(dt)}{(1+t\tilde{m}_1)(1+t\tilde{m}_2)} \right) = \tilde{m}_1\tilde{m}_2(x(\tilde{m}_1) - x(\tilde{m}_2))$$

and use Cauchy–Schwarz inequality to control the left-hand side parenthesis.

Finally show that, if ν has bounded support, then $x(\tilde{m}) \rightarrow 0$ as $\tilde{m} \rightarrow \pm\infty$.

As a final remark, note that the only important observation about Figure 2.5 which we have not shown here is the fact that the points \tilde{m} where $x'(\tilde{m}) = 0$ must exist. In fact, this is not always the case and heavily depends on the nature of the tails of the underlying measure ν . Justify in particular that, for some ν , there may be no asymptote on the edges of the domain of definition of $x(\cdot)$ (as opposed to what is seen in Figure 2.5).

Correction 7 (Further results on $x(\tilde{m})$). If $x(\tilde{m}_1) = x(\tilde{m}_2)$ for \tilde{m}_1, \tilde{m}_2 such that $x'(\tilde{m}_1), x'(\tilde{m}_2) > 0$, then $x(\tilde{m})$ is locally invertible around both \tilde{m}_1 and \tilde{m}_2 with inverse the Stieltjes transform $\tilde{m}(\cdot)$ of $\tilde{\mu}$. In particular, $\tilde{m}(x(\tilde{m}_1))$ and $\tilde{m}(x(\tilde{m}_2))$ are both uniquely defined (since the Stieltjes transform of a valid z outside the support is unique) and equal to $\tilde{m}_1 \neq \tilde{m}_2$, respectively. It is thus impossible that $x(\tilde{m}_1) = x(\tilde{m}_2)$ if $\tilde{m}_1 \neq \tilde{m}_2$.

If $\tilde{m}_1 < \tilde{m}_2$ and $x'(\tilde{m}_1), x'(\tilde{m}_2) > 0$, then

$$x(\tilde{m}_1) - x(\tilde{m}_2) = (\tilde{m}_1 - \tilde{m}_2) \left[\frac{1}{\tilde{m}_1\tilde{m}_2} - c \int \frac{t^2 \nu(dt)}{(1+t\tilde{m}_1)(1+t\tilde{m}_2)} \right]$$

or equivalently

$$(x(\tilde{m}_1) - x(\tilde{m}_2))\tilde{m}_1\tilde{m}_2 = (\tilde{m}_1 - \tilde{m}_2) \left[1 - c \int \frac{t^2 \tilde{m}_1 \tilde{m}_2 \nu(dt)}{(1+t\tilde{m}_1)(1+t\tilde{m}_2)} \right].$$

At the same time, observe that, taking the limit where $\tilde{m}_1 - \tilde{m}_2 \rightarrow 0$, we have the derivative formulation

$$x'(\tilde{m})\tilde{m}^2 = 1 - c \int \frac{t^2 \tilde{m}^2}{(1+t\tilde{m})^2} \nu(dt)$$

which is positive for both $\tilde{m} = \tilde{m}_1$ and $\tilde{m} = \tilde{m}_2$. Using Cauchy–Schwarz inequality, we thus find that

$$\left| c \int \frac{t^2 \tilde{m}_1 \tilde{m}_2}{(1+t\tilde{m}_1)(1+t\tilde{m}_2)} \right| \leq \sqrt{c \int \frac{t^2 \tilde{m}_1^2 \nu(dt)}{(1+t\tilde{m}_1)^2} c \int \frac{t^2 \tilde{m}_2^2 \nu(dt)}{(1+t\tilde{m}_2)^2}} < 1.$$

As a consequence,

$$(x(\tilde{m}_1) - x(\tilde{m}_2)) \frac{\tilde{m}_1 \tilde{m}_2}{\tilde{m}_1 - \tilde{m}_2} > 0.$$

Since $\tilde{m}_1 \tilde{m}_2 > 0$ (both are of the same sign), we conclude that $x(\tilde{m}_1) - x(\tilde{m}_2)$ is of the same sign as $\tilde{m}_1 - \tilde{m}_2$, as requested.

If ν has bounded support, by dominated convergence, it easily follows that $x(\tilde{m}) \rightarrow 0$ when $\tilde{m} \rightarrow \pm\infty$.

Exercise 8 (Alternative estimates of $\frac{1}{p} \text{tr}(\frac{1}{n} \mathbf{XX}^\top)^2$). Let $\mathbf{X} = \mathbf{C}^{\frac{1}{2}} \mathbf{Z}$ for $\mathbf{Z} \in \mathbb{R}^{p \times n}$ with independent standard Gaussian entries, and \mathbf{C} deterministic symmetric nonnegative definite, of bounded spectral norm, and limiting eigenvalue distribution ν .

By a direct calculus, determine the limit, as $n, p \rightarrow \infty$ and $p/n \rightarrow c > 0$ of the second order moment

$$M_2 = \frac{1}{p} \text{tr} \left(\frac{1}{n} \mathbf{XX}^\top \right)^2$$

as a function of the moments of ν .

Retrieve the same result using the results of Exercise 1 along with the expression of the Stieltjes transform $m(z)$ of the limiting spectrum μ of $\frac{1}{n} \mathbf{XX}^\top$. Hint: It may be useful here to first show that $m(z)$ is solution to

$$m(z) = \int \frac{\nu(dt)}{-z(1 + ctm(z)) + (1 - c)t}$$

with ν the limiting spectral measure of \mathbf{C} .

Correction 8 (Alternative estimates of $\frac{1}{p} \text{tr}(\frac{1}{n} \mathbf{XX}^\top)^2$). A direct estimate is easily obtained by merely evaluating $\mathbb{E}[\frac{1}{p} \text{tr} \left(\frac{1}{n} \mathbf{C}^{\frac{1}{2}} \mathbf{ZZ}^\top \mathbf{C}^{\frac{1}{2}} \right)^2]$. By the unitary invariance of the Gaussian matrix \mathbf{Z} (i.e., $U\mathbf{Z} \sim \mathbf{Z}$ in law for all orthogonal matrix U), we may assume $\mathbf{C} = \text{diag}(C_{11}, \dots, C_{pp})$ diagonal. Therefore,

$$\mathbb{E} \left[\frac{1}{p} \text{tr} \left(\frac{1}{n} \mathbf{C}^{\frac{1}{2}} \mathbf{ZZ}^\top \mathbf{C}^{\frac{1}{2}} \right)^2 \right] = \frac{1}{n^2 p} \sum_{i,i'=1}^p \sum_{j,j'=1}^n C_{ii} C_{i'i'} \mathbb{E}[Z_{ij} Z_{i'j} Z_{i'j'} Z_{ij'}].$$

Of these sums, the case $i = i'$ and $j = j'$ simultaneously brings $\mathbb{E}[Z_{ij} Z_{i'j} Z_{i'j'} Z_{ij'}] = \mathbb{E}[|Z_{ij}|^4] = 3$; the other non-trivial case is when $i = i'$ and $j \neq j'$, or $j = j'$ and $i \neq i'$ which both yield $\mathbb{E}[Z_{ij} Z_{i'j} Z_{i'j'} Z_{ij'}] = \mathbb{E}[|Z_{ij}|^2] \mathbb{E}[|Z_{ij'}|^2] = 1$. Summing all contributions, we find

$$\begin{aligned} \mathbb{E} \left[\frac{1}{p} \text{tr} \left(\frac{1}{n} \mathbf{C}^{\frac{1}{2}} \mathbf{ZZ}^\top \mathbf{C}^{\frac{1}{2}} \right)^2 \right] &= \frac{3n \text{tr } \mathbf{C} + n(n-1) \text{tr } \mathbf{C}^2 + n[(\text{tr } \mathbf{C})^2 - \text{tr } \mathbf{C}^2]}{n^2 p} \\ &= \frac{1}{p} \text{tr } \mathbf{C}^2 + c \left(\frac{1}{p} \text{tr } \mathbf{C} \right)^2 + O(n^{-1}) \end{aligned}$$

where we recall that $c = \lim p/n$. In the large n, p limit, all empirical moments almost surely converge, and we thus find that

$$M_2 = \frac{1}{p} \text{tr } \mathbf{C}^2 + c \left(\frac{1}{p} \text{tr } \mathbf{C} \right)^2 + O(n^{-1})$$

almost surely. It is in particular interesting to note that, as $c \rightarrow 0$, we correctly recover the standard $\frac{1}{p} \operatorname{tr} \mathbf{C}^2$ estimate. In the large dimensional random matrix regime though, the additional non-negligible bias $c \left(\frac{1}{p} \operatorname{tr} \mathbf{C} \right)^2$ contributes.

Solving Exercise 1, we have that

$$M_2 = \frac{1}{2} \frac{d^2 \delta}{dz^2}(0) + o(1)$$

almost surely, where $\delta(z) = -\frac{1}{z}m(z^{-1})$. Using the defining equation $m(z) = \frac{1}{c}\tilde{m}(z) + \frac{1-c}{cz}$ with $\tilde{m}(z) = (-z + c \int \frac{t\nu(dt)}{1+t\tilde{m}(z)})^{-1}$, we may verify that

$$m(z) = \int \frac{\nu(dt)}{-z(1+ctm(z)) + (1-c)t}$$

(it suffices to replace $m(z)$ by $\frac{1}{c}\tilde{m}(z) + \frac{1-c}{cz}$ in this equation to fall back on the defining equation for $\tilde{m}(z)$). From this expression, we find that

$$\delta(z) = -\frac{1}{z}m(z^{-1}) = \int \frac{\nu(dt)}{1-ctz\delta(z) - (1-c)tz}.$$

Differentiating a first time, we find

$$\delta'(z) = \int \frac{(1-c)t + ct\delta(z) + ctz\delta'(z)}{(1-ctz\delta(z) - (1-c)tz)^2}.$$

Remarking that $\delta(z) = \int \frac{\mu(dt)}{1-tz}$ leads directly to $\delta(0) = 1$ and thus $\delta'(0) = \int t\nu(dt)$ (as expected from Exercise 1). Differentiating a second time, we have

$$\begin{aligned} \delta''(z) &= \int \frac{2ct\delta'(z) + ctz\delta''(z)}{(1-ctz\delta(z) - (1-c)tz)^2} \\ &\quad - 2 \int \frac{((1-c)t + ct\delta(z) + ctz\delta'(z))(-(1-c)t - ct\delta(z) - ctz\delta'(z))}{(1-ctz\delta(z) - (1-c)tz)^3} \end{aligned}$$

which, after setting $z = 0$, gives

$$\delta''(z) = 2c(\int t\nu(dt))^2 + 2 \int t^2 \nu(dt).$$

Consequently, we have the almost sure relation

$$M_2 = c \left(\int t\nu(dt) \right)^2 + \int t^2 \nu(dt) + o(1) = c \left(\frac{1}{p} \operatorname{tr} \mathbf{C} \right)^2 + \frac{1}{p} \operatorname{tr} \mathbf{C}^2 + o(1)$$

as requested.

Exercise 9 (Location of the zeros of $\tilde{m}(z)$). Figure 2.7 and Remark 2.13 both show that the zeros η_1, \dots, η_n of $m_{\mathbf{X}}(z)$, the Stieltjes transform of a symmetric matrix $\mathbf{X} \in \mathbb{R}^{n \times n}$, are interlaced with the eigenvalues $\lambda_1, \dots, \lambda_n$ of \mathbf{X} .

In the sample covariance matrix case $\frac{1}{n}\mathbf{Z}^\top \mathbf{C} \mathbf{Z}$ with $\mathbf{Z} \in \mathbb{R}^{p \times n}$ having independent standard Gaussian entries and \mathbf{C} with limited spectral measure ν of bounded and connected support, this means that (up to zero eigenvalues) the roots η_i of $m_{\frac{1}{n}\mathbf{Z}^\top \mathbf{C} \mathbf{Z}}(z)$ are all found in the limiting support $\tilde{\mu}$ of the empirical spectral distribution, at the possible exception of the leftmost η_1 .

Using a variable change involving $\tilde{m}(z)$ on the formula

$$0 = \frac{1}{2\pi i} \oint_{\Gamma} \frac{1}{w} dw$$

for all Γ not enclosing zero, then the approximation $\tilde{m}(z) = m_{\frac{1}{n}\mathbf{Z}^\top \mathbf{C} \mathbf{Z}}(z) + o(1)$ and finally a residue calculus, show that no root of $m_{\frac{1}{n}\mathbf{Z}^\top \mathbf{C} \mathbf{Z}}(z)$ can be found at macroscopic distance from the limiting support of μ . Conclude.

Correction 9 (Location of the zeros of $\tilde{m}(z)$). Letting $w = -1/\tilde{m}(z)$, we find that, upon the validity of the variable change for the contour Γ ,

$$\frac{1}{2\pi i} \oint_{\Gamma} \frac{1}{w} dw = \frac{1}{2\pi i} \oint_{\Gamma'} \frac{\tilde{m}'(z)}{\tilde{m}(z)} dz.$$

The idea is to take Γ' to be any complex contour with leftmost real crossing slightly larger than zero and rightmost real crossing slightly smaller than the left edge of the support of μ (excluding the possible mass at 0 of course). From Figure 2.5 (and the discussions in this chapter), it appears that, for such a Γ' , the associated Γ does not circle around zero, and thus the integral is null.

As such, in the large n, p limit, we have

$$0 = \frac{1}{2\pi i} \oint_{\Gamma'} \frac{\tilde{m}'_{\frac{1}{n}\mathbf{Z}^\top \mathbf{C} \mathbf{Z}}(z)}{\tilde{m}_{\frac{1}{n}\mathbf{Z}^\top \mathbf{C} \mathbf{Z}}(z)} dz + o(1)$$

almost surely. By residue calculus, the right-hand side integral equals the cardinality of the η_i 's found inside Γ' . As this is an integer and that, for all n, p large $o(1) < 1$, this cardinal must be zero: we conclude that η_1 (the smallest of η_i 's) must be found at an asymptotically vanishing distance from λ_1 (the smallest nonzero eigenvalue of $\frac{1}{n}\mathbf{Z}^\top \mathbf{C} \mathbf{Z}$) almost surely.

Exercise 10 (Additive spiked model). Similar to Theorem 2.12, show the phase transition threshold for the additive model $\mathbf{Y} \equiv \frac{1}{n}\mathbf{X}\mathbf{X}^\top + \mathbf{P}$ for \mathbf{X} having i.i.d. entries of zero mean, unit variance and low rank $\mathbf{P} = \sum_{i=1}^k \ell_i \mathbf{u}_i \mathbf{u}_i^\top$, with $\ell_1 > \dots > \ell_k > 0$, is determined by the condition

$$\ell_i > \sqrt{c}(1 + \sqrt{c})$$

with $c = \lim p/n$ as $p, n \rightarrow \infty$. Under this condition, show that the (almost sure) limiting value of the corresponding isolated eigenvalue $\hat{\gamma}_i$ of \mathbf{Y} is given by

$$\hat{\gamma}_i \xrightarrow{a.s.} \gamma_i = 1 + \ell_i + \frac{c}{\ell_i - c}.$$

Further show that, letting $\hat{\mathbf{u}}_i$ be the eigenvector of \mathbf{Y} associated with γ_i , we have the convergence

$$|\hat{\mathbf{u}}_i^\top \mathbf{u}_i|^2 \xrightarrow{a.s.} 1 - \frac{c}{(\ell_i - c)^2}.$$

Correction 10 (Additive spiked model). *This case is simpler to handle than the model of Theorem 2.12. We may answer the three questions (determination of the phase transition threshold, spike position and asymptotic alignment) at once by writing*

$$|\hat{\mathbf{u}}_i^\top \mathbf{u}_i|^2 = -\frac{1}{2\pi i} \oint_{\Gamma_{\gamma_i}} \mathbf{u}_i^\top \mathbf{Q}(z) \mathbf{u}_i dz$$

for all large n almost surely, where Γ_{γ_i} surrounds γ_i and is positively oriented, while $\mathbf{Q}(z) = (\mathbf{Y} - z\mathbf{I}_p)^{-1}$ is the resolvent of \mathbf{Y} . By Woodbury's identity, and exploiting the fact that $\mathbf{Q}(z)$ itself asymptotically has no residue inside Γ_{γ_i} , we obtain

$$|\hat{\mathbf{u}}_i^\top \mathbf{u}_i|^2 = \frac{1}{2\pi i} \oint_{\Gamma_{\gamma_i}} \mathbf{u}_i^\top \mathbf{Q}^\circ(z) \mathbf{U} \mathbf{L}(\mathbf{I}_k + \mathbf{U}^\top \mathbf{Q}^\circ(z) \mathbf{U} \mathbf{L})^{-1} \mathbf{U}^\top \mathbf{Q}^\circ(z) \mathbf{u}_i dz$$

with $\mathbf{Q}^\circ(z) = (\frac{1}{n} \mathbf{X} \mathbf{X}^\top - z\mathbf{I}_p)^{-1}$. Since $\mathbf{U}^\top \mathbf{Q}^\circ(z) \mathbf{U} \xrightarrow{a.s.} m(z)\mathbf{I}_k$, we immediately find that, in the limit,

$$|\hat{\mathbf{u}}_i^\top \mathbf{u}_i|^2 \xrightarrow{a.s.} \frac{1}{2\pi i} \oint_{\Gamma_{\gamma_i}} \frac{\ell_i m^2(z)}{1 + \ell_i m(z)} dz.$$

By residue calculus, this term is null, unless $1 + \ell_i m(\gamma_i) = 0$: this is the defining equation for γ_i . Since $m(x)$ increases on $((1 + \sqrt{c})^2, \infty)$ with image $(-1/(c + \sqrt{c}), 0)$ (the left edge being obtained from the defining equation of $m(z)$), this equation has a solution if and only if $\ell_i > c + \sqrt{c}$. Using again the definition of $m(z)$ (either the explicit form or rather its defining fixed-point relation), we find in this case that $\gamma_i = 1 + \ell_i + c/(\ell_i - c)$ as requested.

Exploiting the expression $m'(z) = m(z)^2/(1 - cm(z)^2/(1 + cm(z))^2)$, the residue calculus over the complex integral finally gives, by l'Hospital's rule

$$|\hat{\mathbf{u}}_i^\top \mathbf{u}_i|^2 \xrightarrow{a.s.} \frac{m^2(\gamma_i)}{m'(\gamma_i)} = 1 - \frac{c}{(\ell_i - c)^2}$$

which completes the proof.

Exercise 11 (Additive spiked model: the Wigner case). Let \mathbf{X} be symmetric with X_{ij} , $i \geq j$, i.i.d. zero mean and unit variance. As in Exercise 10, show that the “spiked” phase transition threshold for the model $\mathbf{Y} \equiv \frac{1}{\sqrt{n}} \mathbf{X} + \mathbf{P}$, where $\mathbf{P} = \sum_{i=1}^k \ell_i \mathbf{u}_i \mathbf{u}_i^\top$, with $\ell_1 > \dots > \ell_k > 0$, is determined by the condition

$$\ell_i > 1$$

and that, under this condition, the isolated eigenvalue $\hat{\gamma}_i$ of \mathbf{Y} associated with ℓ_i is given by

$$\hat{\gamma}_i \xrightarrow{a.s.} \gamma_i = \ell_i + \frac{1}{\ell_i}.$$

Show finally that, for $\hat{\mathbf{u}}_i$ the eigenvector of \mathbf{Y} associated with $\hat{\gamma}_i$, we have

$$|\hat{\mathbf{u}}_i^\top \mathbf{u}_i|^2 \xrightarrow{a.s.} 1 - \frac{1}{\ell_i^2}.$$

Correction 11 (Additive spiked model: the Wigner case). *The results of the proof of Exercise 10 can be extensively reused, merely by replacing the definition of $m(z)$ with that of the Stieltjes transform of the semi-circle law. In particular, here, $m(z) = 1/(-z - m(z))$ so that $m'(z) = m(z)^2/(1 - m(z)^2)$.*

Now, the asymptotic alignment $|\hat{\mathbf{u}}_i^\top \mathbf{u}_i|^2$ is still provided by

$$|\hat{\mathbf{u}}_i^\top \mathbf{u}_i|^2 \xrightarrow{a.s.} \frac{1}{2\pi i} \oint_{\Gamma_{\gamma_i}} \frac{\ell_i m^2(z)}{1 + \ell_i m(z)} dz$$

almost surely, where the result is non-trivial only if $1 + \ell_i m(\gamma_i) = 0$, i.e., if $m(\gamma_i) = -1/\ell_i$. On the set $(2, \infty)$ (outside the support of the semi-circle law), $m(z)$ is increasing with $m(2^+) = -1$. The condition of existence of a solution to $m(\gamma_i) = -1/\ell_i$ is thus $\ell_i > 1$. In this case, we find $\gamma_i = \ell_i + 1/\ell_i$ as requested.

The residue of the above integral is $m^2(\gamma_i)/m'(\gamma_i)$ (again, as in Exercise 10) and we thus find that

$$|\hat{\mathbf{u}}_i^\top \mathbf{u}_i|^2 \xrightarrow{a.s.} 1 - \frac{1}{\ell_i^2}$$

as requested.

8.3.1 Deterministic equivalent

Exercise 12 (Proof of Theorem 2.16). *Inspired by the proofs of Theorem 2.5, prove Theorem 2.16 using*

1. the trace method adapted to Haar random matrices, Lemma 2.16; and
2. Stein's lemma adapted to Haar random matrices, Lemma 2.17.

Correction 12 (Proof of Theorem 2.16). *We first provide the derivation of Theorem 2.16 with the Haar trace lemma, Lemma 2.16. Recall from Theorem 2.16 that, for $\mathbf{Q}(z) = (\frac{p}{n} \mathbf{C}^{\frac{1}{2}} \mathbf{U} \mathbf{U}^\top \mathbf{C}^{\frac{1}{2}} - z \mathbf{I}_p)^{-1}$ for $\mathbf{U} \in \mathbb{R}^{p \times n}$ having $n < p$ columns from a $p \times p$ Haar random matrix, we have, for $z < 0$,*

$$\mathbf{Q}(z) \leftrightarrow \bar{\mathbf{Q}}(z) = \left(\frac{p/n}{1 + \delta(z)} \mathbf{C} - z \mathbf{I}_p \right)^{-1}$$

where $\delta(z)$ is the unique positive solution to

$$\delta(z) = \frac{p}{n} - 1 + \frac{p}{n} \frac{\delta(z)}{1 + \delta(z)} \frac{1}{n} \operatorname{tr} \mathbf{C} \bar{\mathbf{Q}}(z).$$

This is equivalent to the expression in Theorem 2.5 by taking $\delta(z) = -\frac{p}{n} \frac{1}{z \tilde{m}_p(z)} - 1 > 0$ for $0 < -z \tilde{m}_p(z) < p/n \in (1, \infty)$. We will thus proceed similarly to the proof of Theorem 2.5.

Since

$$\begin{aligned} \mathbf{I}_p + z\mathbb{E}[\mathbf{Q}] &= \mathbb{E} \left[\mathbf{Q} \cdot \frac{p}{n} \mathbf{C}^{\frac{1}{2}} \mathbf{U} \mathbf{U}^\top \mathbf{C}^{\frac{1}{2}} \right] \\ &= \frac{p}{n} \sum_{i=1}^n \mathbb{E}[\mathbf{Q} \mathbf{C}^{\frac{1}{2}} \mathbf{u}_i \mathbf{u}_i^\top \mathbf{C}^{\frac{1}{2}}] \\ &= \frac{p}{n} \sum_{i=1}^n \mathbb{E} \left[\frac{\mathbf{Q}_{-i} \mathbf{C}^{\frac{1}{2}} \mathbf{u}_i \mathbf{u}_i^\top \mathbf{C}^{\frac{1}{2}}}{1 + \frac{p}{n} \mathbf{u}_i^\top \mathbf{C}^{\frac{1}{2}} \mathbf{Q}_{-i} \mathbf{C}^{\frac{1}{2}} \mathbf{u}_i} \right] \end{aligned}$$

where we denoted $\mathbf{Q}_{-i} = (\frac{p}{n} \mathbf{C}^{\frac{1}{2}} \mathbf{U}_{-i} \mathbf{U}_{-i}^\top \mathbf{C}^{\frac{1}{2}} - z \mathbf{I}_p)^{-1}$ and $\mathbf{U}_{-i} \mathbf{U}_{-i}^\top = \mathbf{U} \mathbf{U}^\top - \mathbf{u}_i \mathbf{u}_i^\top$. At this point, note that, unlike in the proof of Theorem 2.5, here \mathbf{Q}_{-i} is no longer independent of \mathbf{u}_i and the usual “trace lemma” (Lemma 2.11) can no longer be used. Instead, with Lemma 2.16, we have

$$\begin{aligned} \frac{p}{n} \mathbb{E}[\mathbf{Q}_{-i} \mathbf{C}^{\frac{1}{2}} \mathbf{u}_i \mathbf{u}_i^\top \mathbf{C}^{\frac{1}{2}}] &\simeq \frac{p}{n} \frac{1}{p-n} \mathbb{E}[\mathbf{Q}_{-i} \mathbf{C}^{\frac{1}{2}} (\mathbf{I}_p - \mathbf{U}_{-i} \mathbf{U}_{-i}^\top) \mathbf{C}^{\frac{1}{2}}] \\ &= \frac{1}{p-n} \mathbb{E} \left[\frac{p}{n} \mathbf{Q}_{-i} \mathbf{C} - (\mathbf{I}_p + z \mathbf{Q}_{-i}) \right] \end{aligned}$$

as well as

$$\begin{aligned} \frac{p}{n} \mathbf{u}_i^\top \mathbf{C}^{\frac{1}{2}} \mathbf{Q}_{-i} \mathbf{C}^{\frac{1}{2}} \mathbf{u}_i &\simeq \frac{1}{p-n} \left(\frac{p}{n} \operatorname{tr} \mathbf{C} \mathbf{Q}_{-i} - (p + z \operatorname{tr} \mathbf{Q}_{-i}) \right) \\ &\simeq \frac{1}{p-n} \left(\frac{p}{n} \operatorname{tr} \mathbf{C} \bar{\mathbf{Q}} - (p + z \operatorname{tr} \bar{\mathbf{Q}}) \right) \end{aligned}$$

with $\mathbb{E}[\mathbf{Q}] \leftrightarrow \bar{\mathbf{Q}}$, for some $\bar{\mathbf{Q}}$ to be defined. Denoting the previous right-hand side, scaled by $(p-n)/n$, as

$$\delta(z) \equiv \frac{p-n}{n} + \frac{p}{n} \frac{1}{n} \operatorname{tr} \mathbf{C} \bar{\mathbf{Q}} - \left(\frac{p}{n} + \frac{z}{n} \operatorname{tr} \bar{\mathbf{Q}} \right) \stackrel{\text{eq:proof-Haar-1}}{=} (8.1)$$

we have

$$\mathbf{I}_p + z\mathbb{E}[\mathbf{Q}] \simeq \frac{1}{n} \frac{\sum_{i=1}^n \mathbb{E}[\mathbf{Q}_{-i}] \left(\frac{p}{n} \mathbf{C} - z \mathbf{I}_p \right) - \mathbf{I}_p}{\delta(z)} \simeq \frac{\mathbb{E}[\mathbf{Q}] \left(\frac{p}{n} \mathbf{C} - z \mathbf{I}_p \right) - \mathbf{I}_p}{\delta(z)}$$

and thus

$$\mathbb{E}[\mathbf{Q}(z)] \simeq \left(\frac{p/n}{1 + \delta(z)} \mathbf{C} - z \mathbf{I}_p \right)^{-1} \equiv \bar{\mathbf{Q}}(z).$$

Plugging back into (8.1) we obtain $\delta(z) = \frac{p}{n} - 1 + \frac{p}{n} \frac{\delta(z)}{1+\delta(z)} \frac{1}{n} \operatorname{tr} \mathbf{C} \bar{\mathbf{Q}}(z)$ and thus the conclusion.

We now present the derivation of Theorem 2.16 with Haar Stein's lemma, Lemma 2.17, in the complex case. Since Lemma 2.17 only applies to square Haar random matrices, we may rewrite the resolvent as

$$\mathbf{Q}(z) = \left(\mathbf{C}^{\frac{1}{2}} \mathbf{U} \mathbf{D} \mathbf{U}^* \mathbf{C}^{\frac{1}{2}} - z \mathbf{I}_p \right)^{-1} \leftrightarrow \bar{\mathbf{Q}}(z)$$

for $\mathbf{U} \in \mathbb{C}^{p \times p}$ a random Haar matrix and diagonal $\mathbf{D} \in \mathbb{R}^{p \times p}$ with $\mathbf{D}_{ii} = \delta_{i \leq n} = d_i$ and some $\bar{\mathbf{Q}}(z)$ to be specified. We start again from the relation $\mathbb{E}[\mathbf{C}^{\frac{1}{2}} \mathbf{U} \mathbf{D} \mathbf{U}^* \mathbf{C}^{\frac{1}{2}} \mathbf{Q}] = \mathbf{I}_p + z \mathbb{E}[\mathbf{Q}]$. Since \mathbf{U} is unitary, it suffices to consider the case of diagonal \mathbf{C} with $\mathbf{C}_{ii} = \alpha_i$. As such, define

$$f(\mathbf{U}) = \sqrt{\alpha_q} \mathbf{U}_{qk} d_l [\mathbf{U}^*]_{lm} \sqrt{\alpha_m} \mathbf{Q}_{mq}$$

we have

$$\begin{aligned} \frac{\partial \mathbf{U}^*}{\partial \mathbf{U}_{ij}} &= -\mathbf{U}^* \mathbf{E}_{ij} \mathbf{U}^* \\ \frac{\partial \mathbf{Q}}{\partial \mathbf{U}_{ij}} &= -\mathbf{Q} \mathbf{C}^{\frac{1}{2}} \mathbf{E}_{ij} \mathbf{D} \mathbf{U}^* \mathbf{C}^{\frac{1}{2}} \mathbf{Q} + \mathbf{Q} \mathbf{C}^{\frac{1}{2}} \mathbf{U} \mathbf{D} \mathbf{U}^* \mathbf{E}_{ij} \mathbf{U}^* \mathbf{C}^{\frac{1}{2}} \mathbf{Q} \end{aligned}$$

and

$$\begin{aligned} f'_{ij} \mathbf{U}_{ij'} &= \sqrt{\alpha_q} \delta_{qi} \delta_{kj} d_l [\mathbf{U}^*]_{lm} \sqrt{\alpha_m} \mathbf{Q}_{mq} \mathbf{U}_{ij'} - \sqrt{\alpha_q} \mathbf{U}_{qk} d_l [\mathbf{U}^*]_{li} [\mathbf{U}^*]_{jm} \sqrt{\alpha_m} \mathbf{Q}_{mq} \mathbf{U}_{ij'} \\ &\quad - \sqrt{\alpha_q} \mathbf{U}_{qk} d_l [\mathbf{U}^*]_{lm} \sqrt{\alpha_m} [\mathbf{Q} \mathbf{C}^{\frac{1}{2}}]_{mi} [\mathbf{D} \mathbf{U}^* \mathbf{C}^{\frac{1}{2}} \mathbf{Q}]_{jq} \mathbf{U}_{ij'} \\ &\quad + \sqrt{\alpha_q} \mathbf{U}_{qk} d_l [\mathbf{U}^*]_{lm} \sqrt{\alpha_m} [\mathbf{Q} \mathbf{C}^{\frac{1}{2}} \mathbf{U} \mathbf{D} \mathbf{U}^*]_{mi} [\mathbf{U}^* \mathbf{C}^{\frac{1}{2}} \mathbf{Q}]_{jq} \mathbf{U}_{ij'} \end{aligned}$$

so that with Lemma 2.17 for $j = k$ and $j' = l$,

$$\begin{aligned} 0 &= \mathbb{E} \left[\sum_{i=1}^p f'_{ij} \mathbf{U}_{ij'} \right] = \mathbb{E}[\sqrt{\alpha_q} \mathbf{U}_{ql} d_l [\mathbf{U}^*]_{lm} \sqrt{\alpha_m} \mathbf{Q}_{mq}] \\ &\quad - \mathbb{E}[\sqrt{\alpha_q} \mathbf{U}_{qk} [\mathbf{U}^*]_{km} \sqrt{\alpha_m} \mathbf{Q}_{mq} d_l] \\ &\quad - \mathbb{E}[\sqrt{\alpha_q} \mathbf{U}_{qk} [\mathbf{D} \mathbf{U}^* \mathbf{C}^{\frac{1}{2}} \mathbf{Q}]_{kj} d_l [\mathbf{U}^*]_{lm} \sqrt{\alpha_m} [\mathbf{Q} \mathbf{C}^{\frac{1}{2}} \mathbf{U}]_{ml}] \\ &\quad + \mathbb{E}[\sqrt{\alpha_q} \mathbf{U}_{qk} [\mathbf{U}^* \mathbf{C}^{\frac{1}{2}} \mathbf{Q}]_{kj} d_l [\mathbf{U}^*]_{lm} \sqrt{\alpha_m} [\mathbf{Q} \mathbf{C}^{\frac{1}{2}} \mathbf{U} \mathbf{D}]_{ml}] \end{aligned}$$

where we use $\mathbf{U}^* \mathbf{U} = \mathbf{I}_p$. By definition, for $d_l = 1$, summing over k, l and m we get

$$\begin{aligned} 0 &= p \mathbb{E}[\alpha_q \mathbf{Q}_{qq}] - p \mathbb{E}[\alpha_q \mathbf{Q}_{qq}] - \mathbb{E}[[\mathbf{C}^{\frac{1}{2}} \mathbf{U} \mathbf{D} \mathbf{U}^* \mathbf{C}^{\frac{1}{2}} \mathbf{Q}]_{qq} \operatorname{tr}(\mathbf{Q} \mathbf{C})] \\ &\quad + \mathbb{E}[\alpha_q [\mathbf{Q}]_{qq} \operatorname{tr}(\mathbf{U}^* \mathbf{C}^{\frac{1}{2}} \mathbf{Q} \mathbf{C}^{\frac{1}{2}} \mathbf{U} \mathbf{D})] \end{aligned}$$

and with a concentration argument for the traces we have

$$\begin{aligned}\mathbb{E}[\mathbf{Q}]_{qq} &\simeq \frac{\text{tr } \mathbb{E}[\mathbf{Q}]\mathbf{C}}{\alpha_q \mathbb{E}[\text{tr}(\mathbf{C}^{\frac{1}{2}} \mathbf{U} \mathbf{D} \mathbf{U}^* \mathbf{C}^{\frac{1}{2}} \mathbf{Q})] - z \text{tr}(\mathbb{E}[\mathbf{Q}]\mathbf{C})} \\ &\simeq \frac{\frac{1}{p} \text{tr } \bar{\mathbf{Q}}\mathbf{C}}{\alpha_q + \alpha_q \frac{z}{p} \text{tr } \bar{\mathbf{Q}} - \frac{z}{p} \text{tr } \bar{\mathbf{Q}}\mathbf{C}}\end{aligned}$$

so that $\bar{\mathbf{Q}}$ should take the form

$$\bar{\mathbf{Q}} = \left(\frac{p + z \text{tr } \bar{\mathbf{Q}}}{\text{tr } \mathbf{C} \bar{\mathbf{Q}}} \mathbf{C} - z \mathbf{I}_p \right)^{-1}$$

and thus

$$\frac{1}{p} \text{tr } \mathbf{C} \bar{\mathbf{Q}} \simeq \frac{1}{p} \text{tr } \mathbf{C} \left(\frac{1 + \frac{z}{p} \text{tr } \bar{\mathbf{Q}}}{\frac{1}{p} \text{tr } \mathbf{C} \bar{\mathbf{Q}}} \mathbf{C} - z \mathbf{I}_p \right)^{-1}. \quad \text{eq:proof-Haar-2 (8.2)}$$

Similarly, for $\tilde{\mathbf{Q}}(z) = (\mathbf{C}^{\frac{1}{2}} \mathbf{U} \mathbf{D} \mathbf{U}^* \mathbf{C}^{\frac{1}{2}} - z \mathbf{I}_p)^{-1}$ we have

$$\frac{1}{p} \text{tr } \mathbf{D} \tilde{\mathbf{Q}} \simeq \frac{1}{p} \text{tr } \mathbf{D} \left(\frac{1 + \frac{z}{p} \text{tr } \bar{\mathbf{Q}}}{\frac{1}{p} \text{tr } \mathbf{D} \tilde{\mathbf{Q}}} \mathbf{D} - z \mathbf{I}_p \right)^{-1}. \quad \text{eq:proof-Haar-3 (8.3)}$$

To connect (8.2) to (8.3) and close the loop, it suffices to note that

$$\frac{1}{p} \text{tr } \mathbf{C} \bar{\mathbf{Q}} \cdot \frac{1}{p} \text{tr } \mathbf{D} \tilde{\mathbf{Q}} \simeq \left(1 + \frac{z}{p} \text{tr } \bar{\mathbf{Q}} \right) \cdot \frac{1}{p} \text{tr } \bar{\mathbf{Q}}.$$

where we use the fact that $\mathbf{D}^{\frac{1}{2}} \mathbf{U}^* \mathbf{C}^{\frac{1}{2}} \mathbf{Q} = \tilde{\mathbf{Q}} \mathbf{D}^{\frac{1}{2}} \mathbf{U}^* \mathbf{C}^{\frac{1}{2}}$. As a consequence, denoting $\delta(z) = \frac{p+z \text{tr } \bar{\mathbf{Q}}}{\text{tr } \mathbf{C} \bar{\mathbf{Q}}}$ so that $\bar{\mathbf{Q}} = (\delta(z)\mathbf{C} - z\mathbf{I}_p)^{-1}$, we deduce

$$\delta(z) = \left(1 + (c - \delta(z)) \frac{1}{p} \text{tr } \mathbf{C} \bar{\mathbf{Q}} \right)^{-1}.$$

This is equivalent to the expression in Theorem 2.16, and thus concludes the proof.

Exercise 13 (Higher-order deterministic equivalent). *Theorem 2.3 provides an deterministic equivalent for the resolvent $\mathbf{Q} = (\frac{1}{n} \mathbf{X} \mathbf{X}^T - z \mathbf{I}_p)^{-1}$ for $\mathbf{X} \in \mathbb{R}^{p \times n}$ having i.i.d. zero mean and unit variance entries, which, according to Notation 1, provides access to the asymptotic behavior of $\mathbf{a}^T \mathbf{Q} \mathbf{b}$. In many machine learning applications, however, the object of natural interest (e.g., mean squared error in regression analysis and variance analysis in a classification context) often involves the asymptotic behavior of $\mathbf{a}^T \mathbf{Q} \mathbf{A} \mathbf{Q} \mathbf{b}$ which requires a deterministic equivalent for random matrices of the type $\mathbf{Q} \mathbf{A} \mathbf{Q}$, for arbitrary \mathbf{A} independent of \mathbf{Q} . In particular, for $\mathbf{Q} \leftrightarrow \bar{\mathbf{Q}}$ (such that $\|\mathbb{E}[\mathbf{Q}] - \bar{\mathbf{Q}}\| \rightarrow 0$), $\bar{\mathbf{Q}} \mathbf{A} \bar{\mathbf{Q}}$ is in general not a deterministic equivalent for $\mathbf{Q} \mathbf{A} \mathbf{Q}$, due to the fact that*

$$\mathbb{E}[\mathbf{Q} \mathbf{A} \mathbf{Q}] \neq \mathbb{E}[\mathbf{Q}] \mathbf{A} \mathbb{E}[\mathbf{Q}].$$

Instead, prove that, in the setting of Theorem 2.3, one has

$$\mathbf{Q}(z)\mathbf{A}\mathbf{Q}(z) \leftrightarrow m(z)^2\mathbf{A} + \frac{1}{n} \operatorname{tr} \mathbf{A} \cdot \frac{m'(z)m(z)^2}{(1+cm(z))^2} \mathbf{I}_p. \quad (8.4)$$

For sanity check, using the fact that $\partial\mathbf{Q}(z)/\partial z = \mathbf{Q}^2(z)$ and taking $\mathbf{A} = \mathbf{I}_p$ in the equation above, confirm that

$$\mathbf{Q}^2(z) \leftrightarrow m'(z)\mathbf{I}_p$$

for $m'(z) = \frac{m(z)^2}{1 - \frac{cm(z)^2}{(1+cm(z))^2}}$ obtained by differentiating the Marčenko–Pastur equation (2.9).

Correction 13 (Higher-order deterministic equivalent). We provide the following intuitive derivation of a deterministic equivalent for $\bar{\mathbf{Q}}\mathbf{A}\bar{\mathbf{Q}}$. First recall from Theorem 2.3 that

$$\mathbf{Q} \leftrightarrow \bar{\mathbf{Q}} = m(z)\mathbf{I}_p = \left(\frac{1}{1+cm(z)} - z \right)^{-1} \mathbf{I}_p, \quad m(z) = \frac{1}{-z + \frac{1}{1+cm(z)}}.$$

We then have the following sequence of approximations

$$\begin{aligned} \mathbb{E}[\mathbf{Q}\mathbf{A}\mathbf{Q}] &= \mathbb{E}[\mathbf{Q}\mathbf{A}\bar{\mathbf{Q}}] + \mathbb{E}[\mathbf{Q}\mathbf{A}(\mathbf{Q} - \bar{\mathbf{Q}})] \\ &\simeq \mathbf{Q}\mathbf{A}\bar{\mathbf{Q}} + \mathbb{E}\mathbf{Q}\mathbf{A}\mathbf{Q} \left(\frac{\mathbf{I}_p}{1 + \frac{1}{n} \operatorname{tr} \bar{\mathbf{Q}}} - \frac{1}{n} \mathbf{X}\mathbf{X}^\top \right) \bar{\mathbf{Q}} \\ &= \mathbf{Q}\mathbf{A}\bar{\mathbf{Q}} + \frac{\mathbb{E}[\mathbf{Q}\mathbf{A}\mathbf{Q}]\bar{\mathbf{Q}}}{1 + \frac{1}{n} \operatorname{tr} \bar{\mathbf{Q}}} - \frac{1}{n} \sum_{i=1}^n \mathbb{E} \left[\frac{\mathbf{Q}\mathbf{A}\mathbf{Q}_{-i}\mathbf{x}_i\mathbf{x}_i^\top}{1 + \frac{1}{n} \mathbf{x}_i^\top \mathbf{Q}_{-i} \mathbf{x}_i} \right] \bar{\mathbf{Q}} \\ &= \bar{\mathbf{Q}}\mathbf{A}\bar{\mathbf{Q}} + \frac{\mathbb{E}[\mathbf{Q}\mathbf{A}\mathbf{Q}]\bar{\mathbf{Q}}}{1 + \frac{1}{n} \operatorname{tr} \bar{\mathbf{Q}}} - \frac{1}{n} \sum_{i=1}^n \frac{\mathbb{E}[\mathbf{Q}_{-i}\mathbf{A}\mathbf{Q}_{-i}\mathbf{x}_i\mathbf{x}_i^\top]}{1 + \frac{1}{n} \operatorname{tr} \bar{\mathbf{Q}}} \bar{\mathbf{Q}} \\ &\quad + \frac{1}{n} \sum_{i=1}^n \mathbb{E} \left[\frac{\mathbf{Q}_{-i}\mathbf{x}_i \frac{1}{n} \mathbf{x}_i^\top \mathbf{Q}_{-i} \mathbf{A} \mathbf{Q}_{-i} \mathbf{x}_i \mathbf{x}_i^\top}{(1 + \frac{1}{n} \operatorname{tr} \bar{\mathbf{Q}})^2} \right] \bar{\mathbf{Q}} \\ &\simeq \bar{\mathbf{Q}}\mathbf{A}\bar{\mathbf{Q}} + \frac{1}{n} \sum_{i=1}^n \mathbb{E} \left[\mathbf{Q}_{-i} \frac{\frac{1}{n} \operatorname{tr}(\mathbf{Q}_{-i}\mathbf{A}\mathbf{Q}_{-i})}{(1 + \frac{1}{n} \operatorname{tr} \bar{\mathbf{Q}})^2} \right] \bar{\mathbf{Q}} \simeq \bar{\mathbf{Q}}\mathbf{A}\bar{\mathbf{Q}} + \frac{\frac{1}{n} \operatorname{tr}(\mathbb{E}[\mathbf{Q}\mathbf{A}\mathbf{Q}])}{(1 + \frac{1}{n} \operatorname{tr} \bar{\mathbf{Q}})^2} \bar{\mathbf{Q}}^2 \end{aligned}$$

where we applied Lemma 2.8 twice and used the fact that $\mathbb{E}[\mathbf{Q}\mathbf{A}\mathbf{Q}] \simeq \mathbb{E}[\mathbf{Q}_{-i}\mathbf{A}\mathbf{Q}_{-i}]$ for \mathbf{A} of bounded norm. Taking the (normalized) trace and gathering the terms proportional to $\operatorname{tr}(\mathbb{E}[\mathbf{Q}\mathbf{A}\mathbf{Q}])$, we obtain

$$\begin{aligned} \frac{1}{n} \operatorname{tr}(\mathbb{E}[\mathbf{Q}\mathbf{A}\mathbf{Q}]) &\simeq \left(1 - \frac{\frac{1}{n} \operatorname{tr} \bar{\mathbf{Q}}^2}{(1 + \frac{1}{n} \operatorname{tr} \bar{\mathbf{Q}})^2} \right)^{-1} \frac{1}{n} \operatorname{tr} \bar{\mathbf{Q}}\mathbf{A}\bar{\mathbf{Q}} = \frac{m(z)^2 \frac{1}{n} \operatorname{tr} \mathbf{A}}{1 - \frac{cm(z)^2}{(1+cm(z))^2}} \\ &= m'(z) \frac{1}{n} \operatorname{tr} \mathbf{A} \end{aligned}$$

where we recall that $m'(z) = \frac{m(z)^2}{1 - \frac{cm(z)^2}{(1+cm(z))^2}}$ by differentiating (2.9) and

$$\mathbf{Q}\mathbf{A}\mathbf{Q} \leftrightarrow \bar{\mathbf{Q}}\mathbf{A}\bar{\mathbf{Q}} + \frac{1}{n} \operatorname{tr} \mathbf{A} \cdot \frac{m'(z)}{(1+cm(z))^2} \bar{\mathbf{Q}}^2 = m(z)^2 \mathbf{A} + \frac{1}{n} \operatorname{tr} \mathbf{A} \cdot \frac{m'(z)m(z)^2}{(1+cm(z))^2} \mathbf{I}_p.$$

In particular, with $\mathbf{A} = \mathbf{I}_p$, we have $\mathbf{Q}\mathbf{A}\mathbf{Q} \leftrightarrow m'(z)\mathbf{I}_p$.

** Peut-être ajouter un exo ici avec des probas libres, en guidant un peu le lecteur **

** Exercise from Cosme, to clean **

Exercise 14 (Concentration of matrix quadratic forms). *Recalling the definitions and notations of Section 2.7, let $\mathbf{X} \in \mathbb{R}^{p \times n}$ be a random matrix satisfying*

$$\mathbf{X} \propto C e^{c \cdot^2}, \text{ and } \|\mathbb{E}[\mathbf{X}]\| \leq K$$

for some $K, C, c > 0$. Given $\mathbf{A} \in \mathbb{R}^{p \times p}$ deterministic, we wish to prove the linear concentration of $\mathbf{X}^\top \mathbf{A} \mathbf{X}$ in $(\mathbb{R}^{n \times n}, \|\cdot\|_F)$. To this end, we thus consider a deterministic matrix $\mathbf{B} \in \mathbb{R}^{n \times n}$ such that $\|\mathbf{B}\|_F \leq 1$ and study the behavior of $\operatorname{tr}(\mathbf{B}\mathbf{X}^\top \mathbf{A}\mathbf{X})$. First decompose

$$\mathbf{A} = \mathbf{P}_A \boldsymbol{\Lambda} \mathbf{Q}_A \text{ and } \mathbf{B} = \mathbf{P}_B \boldsymbol{\Gamma} \mathbf{Q}_B,$$

with $\mathbf{P}_A, \mathbf{Q}_A \in \mathbb{R}^{p \times p}$ and $P_B, Q_B \in \mathbb{R}^{n \times n}$ orthogonal matrices and $\boldsymbol{\Lambda} \in \mathbb{R}^{p \times p}$, $\boldsymbol{\Gamma} \in \mathbb{R}_+^{n \times n}$ diagonal matrices, and define $\check{\mathbf{X}} = \mathbf{P}_A \mathbf{X} \mathbf{Q}_B \in \mathbb{R}^{p \times n}$. In the next items, the constants $K', C', c' > 0$ are understood only depending on K, C, c and might change from one line to the other.

First show that there exist $K', C', c' > 0$ such that, for any $t > K' \log(np)$,

$$\mathbb{P}(\|\check{\mathbf{X}} - \mathbb{E}[\check{\mathbf{X}}]\|_\infty \geq t) \leq C' e^{-c't^2/\log(np)},$$

and deduce from Fubini's theorem and the bound on $\|\mathbb{E}[\check{\mathbf{X}}]\|$ that there exists a constant $K' > 0$ depending only on K, C, c such that:

$$\mathbb{E}[\|\check{\mathbf{X}}\|_\infty] \leq K' \sqrt{\log(pn)}.$$

This established, introduce the subset $\mathcal{A}_\theta = \{\mathbf{M} \in \mathbb{R}^{p \times n}, \|\mathbf{P}_A \mathbf{M} \mathbf{Q}_B\|_\infty \leq \theta\} \subset \mathbb{R}^{p \times n}$ and show that for all $\theta \geq K' \sqrt{\log(pn)}$, $\mathbb{P}(\mathbf{X} \in \mathcal{A}_\theta^c) \leq C e^{-c\theta^2/4}$ and that the mapping $\mathbf{M} \mapsto \operatorname{tr}(\mathbf{B}\mathbf{M}^\top \mathbf{A}\mathbf{M})$ is $\theta \|\mathbf{A}\|_F$ -Lipschitz on \mathcal{A}_θ .

Introducing m , a median of $\operatorname{tr}(\mathbf{B}\mathbf{X}^\top \mathbf{A}\mathbf{X})$, denote now

$$\mathcal{C} = \{\mathbf{M} \in \mathbb{R}^{p \times n} \mid \operatorname{tr}(\mathbf{B}\mathbf{M}^\top \mathbf{A}\mathbf{M}) \leq m\},$$

and for $\mathcal{B} \subset \mathbb{R}^{p \times n}$, $\mathcal{B} \neq \emptyset$, define the map $d(\cdot, \mathcal{B}) : z \mapsto \inf\{\|z - b\|, b \in \mathcal{B}\}$ and show that

$$\begin{aligned} & \mathbb{P}(|\operatorname{tr}(\mathbf{B}\mathbf{X}^\top \mathbf{A}\mathbf{X}) - m| \geq t, \mathbf{X} \in \mathcal{A}_\theta) \\ & \leq \mathbb{P}\left(d(\mathbf{X}, \mathcal{C}) \geq \frac{t}{\theta \|\mathbf{A}\|_F}\right) + \mathbb{P}\left(d(\mathbf{X}, \mathcal{C}^c) \geq \frac{t}{\theta \|\mathbf{A}\|_F}\right). \end{aligned}$$

Cleverly choosing the parameter $\theta \geq K' \sqrt{\log(np)}$, conclude by showing that

$$\mathbf{X}^\top \mathbf{A} \mathbf{X} \in \mathbb{E}[\mathbf{X}^\top \mathbf{A} \mathbf{X}] \pm C'e^{-c'^2/(\log(np)\|\mathbf{A}\|_F)} + C'e^{-c'/\|\mathbf{A}\|_F}.$$

Correction 14 (Concentration of matrix quadratic forms). *Letting $\mathbf{e}_i^k \in \mathbb{R}^k$ be the canonical vector of \mathbb{R}^k for the i -th entry, we first have*

$$\mathbb{P}(\|\check{\mathbf{X}} - \mathbb{E}[\check{\mathbf{X}}]\|_\infty \geq t) \leq \mathbb{P}\left(\sup_{\substack{1 \leq i \leq p \\ 1 \leq j \leq n}} (\mathbf{e}_i^n)^\top (\check{\mathbf{X}} - \mathbb{E}[\check{\mathbf{X}}]) \mathbf{e}_j^n \geq t\right) \leq npCe^{-ct^2}.$$

Now it can be shown that $\min(1, Ce^{\log(np)}e^{-ct^2}) \leq C'e^{-c't^2/\log(np)}$ for some constants C', c' depending only on C, c . Therefore

$$\begin{aligned} \mathbb{E}[\|\check{\mathbf{X}}\|_\infty] &\leq \|\mathbb{E}[\check{\mathbf{X}}]\|_\infty + \mathbb{E}[\|\check{\mathbf{X}} - \mathbb{E}[\check{\mathbf{X}}]\|_\infty] \\ &\leq \|\mathbb{E}[\check{\mathbf{X}}]\| + \int_0^\infty \mathbb{P}(\|\check{\mathbf{X}} - \mathbb{E}[\check{\mathbf{X}}]\|_\infty \geq t) dt \\ &\leq K + C'\sqrt{\log(np)} \int_0^\infty e^{-c't^2} dt \leq K'\sqrt{\log(np)}. \end{aligned}$$

Next, note that for $\theta \geq 2K'\sqrt{\log(np)}$, $\theta \geq \frac{\theta}{2} + \mathbb{E}[\|\check{\mathbf{X}}\|_\infty]$. Since $\|\check{\mathbf{X}}\|_\infty \propto Ce^{-c^2}$, we may bound

$$\mathbb{P}(\mathbf{X} \in \mathcal{A}_\theta^c) = \mathbb{P}(\|\check{\mathbf{X}}\|_\infty \geq \theta) = \mathbb{P}\left(\|\check{\mathbf{X}}\|_\infty - \mathbb{E}[\|\check{\mathbf{X}}\|_\infty] \geq \frac{\theta}{2}\right) \leq Ce^{-c\theta^2/4}.$$

Besides, with the notation $\boldsymbol{\Lambda} = \text{diag}(\boldsymbol{\lambda})$ and $\boldsymbol{\Gamma} = \text{diag}(\boldsymbol{\gamma})$, we find that for any $\mathbf{M} \in \mathcal{A}_\theta$,

$$\text{tr}(\mathbf{B}\mathbf{M}^\top \mathbf{A}\mathbf{M}) = \text{tr}(\boldsymbol{\Gamma}\check{\mathbf{M}}^\top \boldsymbol{\Lambda}\check{\mathbf{M}}) = \sum_{\substack{1 \leq i \leq p \\ 1 \leq j \leq n}} \lambda_i \gamma_j \check{M}_{i,j} \check{M}_{i,j} = \boldsymbol{\gamma}^\top (\check{\mathbf{M}} \odot \check{\mathbf{M}}) \boldsymbol{\lambda},$$

where \odot is the hadamard (entry-wise) product. Therefore

$$|\text{tr}(\mathbf{B}\mathbf{M}^\top \mathbf{A}\mathbf{M})| \leq \|\boldsymbol{\lambda}\| \|\boldsymbol{\gamma}\| \|\mathbf{M} \odot \mathbf{M}\|_F \leq \|\mathbf{A}\|_F \|\mathbf{B}\|_F \|\mathbf{M}\|_F \|\mathbf{M}\|_\infty \leq \theta \|\mathbf{A}\|_F \|\mathbf{M}\|_F,$$

which means that the 2-linear form $\mathbf{M} \mapsto \text{tr}(\mathbf{B}\mathbf{M}^\top \mathbf{A}\mathbf{M})$ is $\theta \|\mathbf{A}\|_F$ -Lipschitz on \mathcal{A}_θ . This implies, as a consequence of the fact that for all $M \in \mathbb{R}^{p \times n}$,

$$|f(\phi(\mathbf{M})) - m_f| \geq t \implies d(\mathbf{M}, \mathcal{C}) \geq \frac{t}{K^{(p-1)}} \quad \text{or} \quad d(\mathbf{M}, \mathcal{C}^c) \geq \frac{t}{K^{(p-1)}}.$$

We may next bound

$$\begin{aligned} &\mathbb{P}(|\text{tr}(\mathbf{B}\mathbf{M}^\top \mathbf{A}\mathbf{M}) - \mathbb{E}[\text{tr}(\mathbf{B}\mathbf{M}^\top \mathbf{A}\mathbf{M})]| \geq t) \\ &\leq \mathbb{P}(|\text{tr}(\mathbf{B}\mathbf{X}^\top \mathbf{A}\mathbf{X}) - m| \geq t, \mathbf{X} \in \mathcal{A}_\theta) + \mathbb{P}(\mathbf{X} \in \mathcal{A}_\theta^c) \\ &\leq 2Ce^{-c(t/\theta)^2} + Ce^{-c\theta^2/4}. \end{aligned}$$

Since $\mathbf{M} \rightarrow d(\mathbf{M}, \mathcal{C})$ and $\mathbf{M} \rightarrow d(\mathbf{M}, \mathcal{C}^c)$ are both 1-Lipschitz. Now, if we choose $\theta = \max(K' \sqrt{\log(np)}, \sqrt{t})$, we can bound

$$\mathbb{P}(|\text{tr}(\mathbf{B}\mathbf{M}^\top \mathbf{A}\mathbf{M}) - \mathbb{E}[\text{tr}(\mathbf{B}\mathbf{M}^\top \mathbf{A}\mathbf{M})]| \geq t) \leq 2Ce^{-c(t/K' \sqrt{\log(pn)})^2} + 3Ce^{-ct/4},$$

from which we conclude on the linear concentration of $\mathbf{X}^\top \mathbf{A}\mathbf{X}$.

Exercise 15 (Towards Spiked Models in Random Tensors). Let $\mathcal{Y} \in \mathbb{R}^{n \times n \times n}$ be a three-way symmetric tensor, i.e., such that \mathcal{Y}_{ijk} is constant to exchanges of its indexes, defined by

$$\mathcal{Y} = \lambda \mathbf{x} \otimes \mathbf{x} \otimes \mathbf{x} + \frac{1}{\sqrt{n}} \mathcal{W}$$

where $\mathcal{W} \in \mathbb{R}^{n \times n \times n}$ has independent $\mathcal{N}(0, 1)$ entries up to symmetry, $\mathbf{x} \in \mathbb{R}^n$ is of unit norm, and $[\mathbf{a} \otimes \mathbf{b} \otimes \mathbf{c}]_{ijk} = a_i b_j c_k$.

A possible definition of the “eigenvalue-eigenvector” pair (ℓ, \mathbf{u}) with $\|\mathbf{u}\| = 1$ of the symmetric tensor \mathcal{Y} is given by the solutions to

$$\mathcal{Y} \cdot \mathbf{u} \cdot \mathbf{u} = \ell \mathbf{u}$$

where $\mathcal{A} \cdot \mathbf{a} \cdot \mathbf{b} = \sum_{ijk} \mathcal{A}_{ijk} a_i b_j \in \mathbb{R}^n$ is the contraction of tensor \mathcal{A} on the vectors \mathbf{a}, \mathbf{b} . The objective is to characterize the largest eigenvalue ℓ_{\max} as well as the associated alignment $|\mathbf{u}_{\max}^\top \mathbf{x}|$ between the dominant eigenvector and the spike \mathbf{x} .

Show first that the matrix $\mathbf{Y}_x = \mathcal{Y} \cdot \mathbf{x} = \sum_{i=1}^n \mathcal{Y}_{i,\cdot,\cdot} x_i$ is given by

$$\mathbf{Y}_x = \lambda \mathbf{x} \mathbf{x}^\top + \frac{1}{\sqrt{n}} \sum_{i=1}^n x_i \mathbf{W}_{i,\cdot,\cdot}$$

where $\mathbf{W}_{i,\cdot,\cdot} \in \mathbb{R}^{n \times n}$ is the i -th “layer” matrix of the tensor \mathcal{W} with $[\mathbf{W}_{i,\cdot,\cdot}]_{ab} = \mathcal{W}_{iab}$.

Using Pastur’s Stein approach, show that the limiting empirical spectral measure of \mathbf{Y}_x is the semi-circle distribution supported on $[-2, 2]$ (we may discard the rank-one matrix $\lambda \mathbf{x} \mathbf{x}^\top$ to retrieve this result). Then, using a spiked analysis, show that

- for all $\lambda > 0$, there must exist an isolated eigenvalue $\hat{\gamma}$ of \mathbf{Y}_x (thus no phase transition) asymptotically equal to (with high probability)

$$\hat{\gamma} \rightarrow \gamma = \sqrt{\lambda^2 + 4};$$

- the eigenvector $\hat{\mathbf{u}}$ associated with $\hat{\gamma}$ satisfies (with high probability)

$$|\hat{\mathbf{u}}^\top \mathbf{x}|^2 \rightarrow \frac{\lambda}{\sqrt{\lambda^2 + 4}}.$$

Conclude on a (asymptotic) bound for the quantity $\ell_{\max} |\mathbf{u}_{\max}^\top \mathbf{x}|$.

Correction 15 (Towards Spiked Models in Random Tensors). *** to update ***

To obtain the semi-circle limit, the main difficulty is to handle the multi-way symmetry of the tensor \mathcal{W} . Denoting $\mathbf{Q} = (\mathbf{Y}_x^\circ - z\mathbf{I}_n)^{-1}$ where $\mathbf{Y}_x^\circ = \frac{1}{\sqrt{n}} \sum_{i=1}^n x_i \mathbf{W}_{i,\cdot,\cdot}$, we use the relation $\mathbf{Q} = -\frac{1}{z}\mathbf{I}_n + \frac{1}{z}\mathbf{Y}_x^\circ\mathbf{Q}$ and evaluate, with the help of Stein's lemma,

$$\begin{aligned}\mathbb{E}[(\mathbf{Y}_x^\circ\mathbf{Q})_{ij}] &= \frac{1}{\sqrt{n}} \sum_{m,\ell} x_l \mathbb{E}[W_{im\ell} Q_{mj}] \\ &= \frac{1}{\sqrt{n}} \sum_{m,\ell} x_l \mathbb{E}\left[\frac{\partial Q_{mj}}{\partial W_{im\ell}}\right].\end{aligned}$$

Here, note that $W_{abc} = W_{bac} = W_{cab} = W_{cba} = W_{bca} = W_{acb}$ and thus

$$\begin{aligned}\frac{\partial \mathbf{Q}}{\partial W_{abc}} &= -\frac{1}{\sqrt{n}} \sum_{\ell=1}^n x_\ell \mathbf{Q} \frac{\partial W_{\ell,\cdot,\cdot}}{\partial W_{abc}} \mathbf{Q} \\ &= -\frac{1}{\sqrt{n}} \sum_{\ell=1}^n x_\ell \mathbf{Q} [(E_{ab} + E_{ba})\delta_{\ell c} + (E_{ca} + E_{ac})\delta_{\ell b} + (E_{bc} + E_{cb})\delta_{\ell a}] \mathbf{Q}\end{aligned}$$

with $E_{ab} \in \mathbb{R}^{n \times n}$ the indicator matrix with $[E_{ab}]_{a'b'} = \delta_{aa'}\delta_{bb'}$. Plugging this expression into the previous equation gives

$$\begin{aligned}\mathbb{E}[(\mathbf{Y}_x^\circ\mathbf{Q})_{ij}] &= -\frac{1}{n} \mathbb{E}[(\mathbf{Q}^2)_{ij}] - \frac{1}{n} \mathbb{E}[\text{tr } \mathbf{Q} Q_{ij}] - \frac{1}{n} \mathbb{E}[\mathbf{x}^\top \mathbf{Q} \mathbf{x} Q_{ij}] \\ &\quad - \frac{1}{n} \mathbb{E}[(\mathbf{Q} \mathbf{x})_i (\mathbf{Q} \mathbf{x})_j] - \frac{1}{n} \mathbb{E}[\text{tr } \mathbf{Q} (\mathbf{Q} \mathbf{x})_j x_i] - \frac{1}{n} \mathbb{E}[(\mathbf{Q}^2 \mathbf{x})_j x_i].\end{aligned}$$

Using $\mathbf{Q} = -\frac{1}{z}\mathbf{I}_n + \frac{1}{z}\mathbf{Y}_x^\circ\mathbf{Q}$, we then find

$$\begin{aligned}\mathbb{E}[Q_{ij}] &= -\frac{1}{z}\delta_{ij} - \frac{1}{z} \frac{1}{n} \mathbb{E}[\text{tr } \mathbf{Q} Q_{ij}] - \frac{1}{z} \frac{1}{n} \mathbb{E}[(\mathbf{Q}^2)_{ij}] - \frac{1}{z} \frac{1}{n} \mathbb{E}[\mathbf{x}^\top \mathbf{Q} \mathbf{x} Q_{ij}] \\ &\quad - \frac{1}{z} \frac{1}{n} \mathbb{E}[(\mathbf{Q} \mathbf{x})_i (\mathbf{Q} \mathbf{x})_j] - \frac{1}{z} \frac{1}{n} \mathbb{E}[\text{tr } \mathbf{Q} (\mathbf{Q} \mathbf{x})_j x_i] - \frac{1}{z} \frac{1}{n} \mathbb{E}[(\mathbf{Q}^2 \mathbf{x})_j x_i]\end{aligned}$$

in which we notably used $\|\mathbf{x}\| = 1$. This leads, with a proper control of orders and variances (using for instance the Nash-Poincaré inequality to show that the variances of $\frac{1}{n} \text{tr } \mathbf{Q}$ and $\mathbf{x}^\top \mathbf{Q} \mathbf{x}$ vanish as $n \rightarrow \infty$), to

$$\begin{aligned}\frac{1}{n} \text{tr } \mathbf{Q} &= -\frac{1}{z} - \frac{1}{z} \left(\frac{1}{n} \text{tr } \mathbf{Q} \right)^2 + O_p(1/n) \\ \mathbf{x}^\top \mathbf{Q} \mathbf{x} &= -\frac{1}{z} - \frac{2}{z} \mathbf{x}^\top \mathbf{Q} \mathbf{x} \frac{1}{n} \text{tr } \mathbf{Q} + O_p(1/n).\end{aligned}$$

Since $\frac{1}{n} \text{tr } \mathbf{Q}$ satisfies in the limit the fixed-point equation characteristic of the Wigner semi-circle law (i.e., $m(z)^2 + zm(z) + 1 = 0$), the first part of the result unfolds. An interesting consequence of the previous equalities though is that, because of the dependence of \mathbf{x} in the expression of matrix \mathbf{Y}_x , $\mathbf{x}^\top \mathbf{Q} \mathbf{x}$ does not

satisfy the same equation as $\frac{1}{n} \operatorname{tr} \mathbf{Q}$ (due to the extra factor 2). Precisely, we find that

$$\begin{aligned}\frac{1}{n} \operatorname{tr} \mathbf{Q} &= -\frac{z}{2} + \frac{1}{2} \sqrt{z^2 - 4} + O_p(1/n) \\ \mathbf{x}^\top \mathbf{Q} \mathbf{x} &= \frac{1}{\sqrt{z^2 - 4}} + O_p(1/n)\end{aligned}$$

where the branch of the square root is chosen so that the right-hand side terms are Stieltjes transforms of (probability) measures. For further use, note that

$$\frac{d}{dz} \mathbf{x}^\top \mathbf{Q}(z) \mathbf{x} = \mathbf{x}^\top \mathbf{Q}'(z) \mathbf{x} = -\frac{z}{(z^2 - 4)^{\frac{3}{2}}} + O_p(1/n) \quad (8.5)$$

with the same convention on the square root.

As for the spike eigenvalue and eigenvector alignment analysis, it may be performed at once by writing

$$\begin{aligned}|\hat{\mathbf{u}}^\top \mathbf{x}|^2 &= -\frac{1}{2\pi i} \oint_{C_\gamma} \mathbf{x}^\top (\mathbf{Y}_x - z \mathbf{I}_n)^{-1} \mathbf{x} dz \\ &= -\frac{1}{2\pi i} \oint_{C_\gamma} \frac{\mathbf{x}^\top \mathbf{Q} \mathbf{x}}{1 + \lambda \mathbf{x}^\top \mathbf{Q} \mathbf{x}} dz\end{aligned}$$

which holds for all large n with high probability over a sufficiently small contour C_γ surrounding the limiting isolated eigenvalue γ (upon existence). By residue calculus, we find that this integral can only be non-vanishing if γ is a limiting root of $1 + \lambda \mathbf{x}^\top \mathbf{Q}(z) \mathbf{x} = 0$, that is, if

$$\gamma = \sqrt{\lambda^2 + 4}$$

and the corresponding limiting residue is given by (applying for instance l'Hospital's rule)

$$\begin{aligned}|\hat{\mathbf{u}}^\top \mathbf{x}|^2 &= -\frac{\mathbf{x}^\top \mathbf{Q}(\lambda) \mathbf{x}}{\lambda \mathbf{x}^\top \mathbf{Q}'(\gamma) \mathbf{x}} + o_p(1) \\ &= \frac{\lambda}{\sqrt{\lambda^2 + 4}} + o_p(1)\end{aligned}$$

as requested.

The proof is then concluded by remarking that

$$\begin{aligned}\ell_{\max} |\mathbf{u}_{\max}^\top \mathbf{x}| &= |\mathbf{Y} \cdot \mathbf{u}_{\max} \cdot \mathbf{u}_{\max} \cdot \mathbf{x}| \\ &\leq \max_{\|\mathbf{v}\|=1} |\mathbf{Y} \cdot \mathbf{v} \cdot \mathbf{v} \cdot \mathbf{x}| \\ &= \max_{\|\mathbf{v}\|=1} \mathbf{v}^\top \mathbf{Y}_x \mathbf{v} \\ &= \hat{\gamma}\end{aligned}$$

which, in the limit, provides the upper bound

$$\ell_{\max} |\mathbf{u}_{\max}^\top \mathbf{x}| \leq \sqrt{\lambda^2 + 4} + o(1).$$

Bibliography

- Radoslaw Adamczak et al. On the marchenko-pastur and circular laws for some classes of random matrices with dependent entries. *Electronic Journal of Probability*, 16:1065–1095, 2011.
- Ben Adlam and Jeffrey Pennington. The neural tangent kernel in high dimensions: Triple descent and a multi-scale theory of generalization. *arXiv preprint arXiv:2008.06786*, 2020.
- Ben Adlam, Jake Levinson, and Jeffrey Pennington. A random matrix perspective on mixtures of nonlinearities for deep learning. *arXiv preprint arXiv:1912.00827*, 2019.
- Madhu S Advani, Andrew M Saxe, and Haim Sompolinsky. High-dimensional dynamics of generalization error in neural networks. *Neural Networks*, 2020.
- Oskari Ajanki, László Erdős, and Torben Krüger. *Quadratic vector equations on complex upper half-plane*, volume 261. American Mathematical Society, 2019.
- Naum Ilich Akhiezer and Izrail Markovich Glazman. *Theory of linear operators in Hilbert space*. Courier Corporation, 2013.
- DJ Albers, JC Sprott, and WD Dechert. Dynamical behavior of artificial neural networks with random weights. *Intelligent Engineering Systems Through Artificial Neural Networks*, 6:17–22, 1996.
- Alnur Ali, J Zico Kolter, and Ryan J Tibshirani. A continuous-time view of early stopping for least squares regression. In *The 22nd International Conference on Artificial Intelligence and Statistics*, pages 1370–1378, 2019.
- Zeyuan Allen-Zhu, Yuanzhi Li, and Yingyu Liang. Learning and generalization in overparameterized neural networks, going beyond two layers. In *Advances in neural information processing systems*, pages 6158–6169, 2019.
- Arash A Amini, Aiyou Chen, Peter J Bickel, Elizaveta Levina, et al. Pseudo-likelihood methods for community detection in large sparse networks. *The Annals of Statistics*, 41(4):2097–2122, 2013.

- Greg W Anderson, Alice Guionnet, and Ofer Zeitouni. *An introduction to random matrices*, volume 118. Cambridge university press, 2010.
- Ralph G Andrzejak, Klaus Lehnertz, Florian Mormann, Christoph Rieke, Peter David, and Christian E Elger. Indications of nonlinear deterministic and finite-dimensional structures in time series of brain electrical activity: Dependence on recording region and brain state. *Physical Review E*, 64(6):061907, 2001.
- Ludwig Arnold, Volker Matthias Gundlach, Lloyd Demetrius, et al. Evolutionary formalism for products of positive random matrices. *The Annals of Applied Probability*, 4(3):859–901, 1994.
- Sanjeev Arora, Rong Ge, Tengyu Ma, and Ankur Moitra. Simple, efficient, and neural algorithms for sparse coding. *Journal of Machine Learning Research*, 40(2015), 2015.
- Sanjeev Arora, Simon Du, Wei Hu, Zhiyuan Li, and Ruosong Wang. Fine-grained analysis of optimization and generalization for overparameterized two-layer neural networks. In *International Conference on Machine Learning*, pages 322–332, 2019.
- Benson Au, Guillaume Cébron, Antoine Dahlqvist, Franck Gabriel, and Camille Male. Large permutation invariant random matrices are asymptotically free over the diagonal. *arXiv preprint arXiv:1805.07045*, 2018.
- Nicolas Auguin, David Morales-Jimenez, Matthew R McKay, and Romain Couillet. Large-dimensional behavior of regularized maronna’s m-estimators of covariance matrices. *IEEE Transactions on Signal Processing*, 66(13):3529–3542, 2018.
- Konstantin Avrachenkov, Alexey Mishenin, Paulo Gonçalves, and Marina Sokol. Generalized optimization framework for graph-based semi-supervised learning. In *Proceedings of the 2012 SIAM International Conference on Data Mining*, pages 966–974. SIAM, 2012.
- ZD Bai and Jack W Silverstein. Exact separation of eigenvalues of large dimensional sample covariance matrices. *Annals of probability*, pages 1536–1555, 1999.
- Zhi-Dong Bai and Jack W Silverstein. No eigenvalues outside the support of the limiting spectral distribution of large-dimensional sample covariance matrices. *The Annals of Probability*, 26(1):316–345, 1998.
- Zhidong Bai and Jack W Silverstein. *Spectral analysis of large dimensional random matrices*, volume 20. Springer, 2010.
- Zhidong Bai and Jian-feng Yao. Central limit theorems for eigenvalues in a spiked population model. In *Annales de l’IHP Probabilités et statistiques*, volume 44, pages 447–474, 2008.

- Zhidong D Bai and Jack W Silverstein. Clt for linear spectral statistics of large-dimensional sample covariance matrices. In *Advances In Statistics*, pages 281–333. World Scientific, 2008.
- Zhidong D Bai, Jack W Silverstein, and Yong Q Yin. A note on the largest eigenvalue of a large dimensional sample covariance matrix. *Journal of Multivariate Analysis*, 26(2):166–168, 1988.
- Jinho Baik and Jack W Silverstein. Eigenvalues of large sample covariance matrices of spiked population models. *Journal of multivariate analysis*, 97(6):1382–1408, 2006.
- Jinho Baik, Gérard Ben Arous, Sandrine Péché, et al. Phase transition of the largest eigenvalue for nonnull complex sample covariance matrices. *The Annals of Probability*, 33(5):1643–1697, 2005.
- Pierre Baldi, Peter Sadowski, and Zhiqin Lu. Learning in the machine: random backpropagation and the deep learning channel. *Artificial intelligence*, 260:1–35, 2018.
- Afonso S Bandeira, Asad Lodhia, Philippe Rigollet, et al. Marčenko-pastur law for kendall’s tau. *Electronic Communications in Probability*, 22, 2017.
- Richard G Baraniuk. Compressive sensing. *IEEE signal processing magazine*, 24(4), 2007.
- Heinz H Bauschke and Patrick L Combettes. *Convex analysis and monotone operator theory in Hilbert spaces*, volume 408. Springer, 2011.
- Amine Bejaoui, Khalil Elkhailil, Abla Kammoun, Mohamed Slim Alouini, and Tarek Alnaffouri. Improved design of quadratic discriminant analysis classifier in unbalanced settings. *arXiv preprint arXiv:2006.06355*, 2020.
- Mikhail Belkin and Partha Niyogi. Semi-supervised learning on riemannian manifolds. *Machine learning*, 56(1-3):209–239, 2004.
- Mikhail Belkin, Irina Matveeva, and Partha Niyogi. Regularization and semi-supervised learning on large graphs. In *International Conference on Computational Learning Theory (COLT)*, pages 624–638. Springer, 2004.
- Mikhail Belkin, Daniel Hsu, Siyuan Ma, and Soumik Mandal. Reconciling modern machine-learning practice and the classical bias–variance trade-off. *Proceedings of the National Academy of Sciences*, 116(32):15849–15854, 2019.
- Gérard Ben Arous and Sandrine Péché. Universality of local eigenvalue statistics for some sample covariance matrices. *Communications on Pure and Applied Mathematics: A Journal Issued by the Courant Institute of Mathematical Sciences*, 58(10):1316–1357, 2005.

- Florent Benaych-Georges and Romain Couillet. Spectral analysis of the Gram matrix of mixture models. *ESAIM: Probability and Statistics*, 20:217–237, 2016.
- Florent Benaych-Georges and Raj Rao Nadakuditi. The eigenvalues and eigenvectors of finite, low rank perturbations of large random matrices. *Advances in Mathematics*, 227(1):494–521, 2011.
- Florent Benaych-Georges and Raj Rao Nadakuditi. The singular values and vectors of low rank perturbations of large rectangular random matrices. *Journal of Multivariate Analysis*, 111:120–135, 2012.
- Lucas Benigni and Sandrine Péché. Eigenvalue distribution of nonlinear models of random matrices. *arXiv preprint arXiv:1904.03090*, 2019.
- Pascal Bianchi, Merouane Debbah, Mylène Maida, and Jamal Najim. Performance of statistical tests for single-source detection using random matrix theory. *IEEE Transactions on Information theory*, 57(4):2400–2419, 2011.
- Philippe Biane. Free probability for probabilists. *arXiv preprint math/9809193*, 1998.
- Alberto Bietti and Julien Mairal. On the inductive bias of neural tangent kernels. In *Advances in Neural Information Processing Systems*, pages 12893–12904, 2019.
- Patrick Billingsley. *Probability and measure*. John Wiley & Sons, third edition, 2012. ISBN 9781118122372.
- Charles Bordenave. Eigenvalues of euclidean random matrices. *Random Structures & Algorithms*, 33(4):515–532, 2008.
- Charles Bordenave and Djalil Chafaï. Lecture notes on the circular law. *Modern aspects of random matrix theory*, 72(1):57, 2014.
- Charles Bordenave and Marc Lelarge. The rank of diluted random graphs. In *Proceedings of the twenty-first annual ACM-SIAM symposium on Discrete algorithms*, pages 1389–1402. Society for Industrial and Applied Mathematics, 2010a.
- Charles Bordenave and Marc Lelarge. Resolvent of large random graphs. *Random Structures & Algorithms*, 37(3):332–352, 2010b.
- Alan J Bray and David S Dean. Statistics of critical points of gaussian fields on large-dimensional spaces. *Physical review letters*, 98(15):150201, 2007.
- Andrew Brock, Jeff Donahue, and Karen Simonyan. Large scale GAN training for high fidelity natural image synthesis. In *International Conference on Learning Representations*, 2018.

- Joël Bun, Jean-Philippe Bouchaud, and Marc Potters. Cleaning large correlation matrices: tools from random matrix theory. *Physics Reports*, 666:1–109, 2017.
- Daniel M Canaday. *Modeling and Control of Dynamical Systems with Reservoir Computing*. PhD thesis, The Ohio State University, 2019.
- Emmanuel J Candès. The restricted isometry property and its implications for compressed sensing. *Comptes rendus mathematique*, 346(9-10):589–592, 2008.
- Emmanuel J Candès and Pragya Sur. The phase transition for the existence of the maximum likelihood estimate in high-dimensional logistic regression. *The Annals of Statistics*, 48(1):27–42, 02 2020. doi: 10.1214/18-AOS1789. URL <https://doi.org/10.1214/18-AOS1789>.
- Emmanuel J Candès, Xiaodong Li, and Mahdi Soltanolkotabi. Phase retrieval via wirtinger flow: Theory and algorithms. *IEEE Transactions on Information Theory*, 61(4):1985–2007, 2015.
- Mireille Capitaine. Exact separation phenomenon for the eigenvalues of large information-plus-noise type matrices, and an application to spiked models. *Indiana University Mathematics Journal*, pages 1875–1910, 2014.
- Olivier Chapelle, Bernhard Scholkopf, and Alexander Zien. Semi-supervised learning (chapelle, o. et al., eds.; 2006)[book reviews]. *IEEE Transactions on Neural Networks*, 20(3):542–542, 2009.
- Minmin Chen, Jeffrey Pennington, and Samuel Schoenholz. Dynamical isometry and a mean field theory of rnns: Gating enables signal propagation in recurrent neural networks. In *International Conference on Machine Learning*, pages 873–882, 2018.
- Yuxin Chen and Emmanuel J Candès. Solving random quadratic systems of equations is nearly as easy as solving linear systems. *Communications on Pure and Applied Mathematics*, 70(5):822–883, 2017.
- Xiuyuan Cheng and Amit Singer. The spectrum of random inner-product kernel matrices. *Random Matrices: Theory and Applications*, 2(04):1350010, 2013.
- Marco Chiani. Distribution of the largest eigenvalue for real wishart and gaussian random matrices and a simple approximation for the tracy–widom distribution. *Journal of Multivariate Analysis*, 129:69–81, 2014.
- Lenaic Chizat, Edouard Oyallon, and Francis Bach. On lazy training in differentiable programming. In *Advances in Neural Information Processing Systems*, pages 2937–2947, 2019.
- Anna Choromanska, Mikael Henaff, Michael Mathieu, Gérard Ben Arous, and Yann LeCun. The loss surfaces of multilayer networks. In *Artificial intelligence and statistics*, pages 192–204, 2015.

- Simon Coste and Yizhe Zhu. Eigenvalues of the non-backtracking operator detached from the bulk. *arXiv preprint arXiv:1907.05603*, 2019.
- R. Couillet, M. Debbah, and J. W. Silverstein. A deterministic equivalent for the analysis of correlated MIMO multiple access channels. *IEEE Transactions on Information Theory*, 57(6):3493–3514, June 2011.
- Romain Couillet. Robust spiked random matrices and a robust g-music estimator. *Journal of Multivariate Analysis*, 140:139–161, 2015.
- Romain Couillet and Florent Benaych-Georges. Kernel spectral clustering of large dimensional data. *Electronic Journal of Statistics*, 10(1):1393–1454, 2016.
- Romain Couillet and Merouane Debbah. *Random matrix methods for wireless communications*. Cambridge University Press, 2011.
- Romain Couillet and Walid Hachem. Fluctuations of spiked random matrix models and failure diagnosis in sensor networks. *IEEE Transactions on Information Theory*, 59(1):509–525, 2013.
- Romain Couillet and Walid Hachem. Analysis of the limiting spectral measure of large random matrices of the separable covariance type. *Random Matrices: Theory and Applications*, 3(04):1450016, 2014.
- Romain Couillet and Abla Kammoun. Random matrix improved subspace clustering. In *2016 50th Asilomar Conference on Signals, Systems and Computers*, pages 90–94. IEEE, 2016.
- Romain Couillet and Matthew McKay. Large dimensional analysis and optimization of robust shrinkage covariance matrix estimators. *Journal of Multivariate Analysis*, 131:99–120, 2014.
- Romain Couillet, Jakob Hoydis, and Mérourane Debbah. Random beamforming over quasi-static and fading channels: A deterministic equivalent approach. *IEEE Transactions on Information Theory*, 58(10):6392–6425, 2012.
- Romain Couillet, Frédéric Pascal, and Jack W Silverstein. The random matrix regime of maronna’s m-estimator with elliptically distributed samples. *Journal of Multivariate Analysis*, 139:56–78, 2015.
- Romain Couillet, Abla Kammoun, and Frédéric Pascal. Second order statistics of robust estimators of scatter. application to glrt detection for elliptical signals. *Journal of Multivariate Analysis*, 143:249–274, 2016a.
- Romain Couillet, Gilles Wainrib, Harry Sevi, and Hafiz Tiomoko Ali. The asymptotic performance of linear echo state neural networks. *The Journal of Machine Learning Research*, 17(1):6171–6205, 2016b.

- Romain Couillet, Malik Tiomoko, Steeve Zozor, and Eric Moisan. Random matrix-improved estimation of covariance matrix distances. *Journal of Multivariate Analysis*, 174:104531, 2019.
- Lorenzo Dall’Amico, Romain Couillet, and Nicolas Tremblay. Revisiting the bethe-hessian: improved community detection in sparse heterogeneous graphs. In *Advances in Neural Information Processing Systems*, pages 4039–4049, 2019.
- Yann N Dauphin, Razvan Pascanu, Caglar Gulcehre, Kyunghyun Cho, Surya Ganguli, and Yoshua Bengio. Identifying and attacking the saddle point problem in high-dimensional non-convex optimization. In *Advances in neural information processing systems*, pages 2933–2941, 2014.
- Chandler Davis. All convex invariant functions of hermitian matrices. *Archiv der Mathematik*, 8(4):276–278, 1957.
- Mérouane Debbah, Walid Hachem, Philippe Loubaton, and Marc De Courville. Mmse analysis of certain large isometric random precoded systems. *IEEE Transactions on Information theory*, 49(5):1293–1311, 2003.
- Zeyu Deng, Abla Kammoun, and Christos Thrampoulidis. A model of double descent for high-dimensional binary linear classification. *arXiv preprint arXiv:1911.05822*, 2019.
- Yen Do and Van Vu. The spectrum of random kernel matrices: universality results for rough and varying kernels. *Random Matrices: Theory and Applications*, 2(03):1350005, 2013.
- David Donoho and Andrea Montanari. High dimensional robust M-estimation: Asymptotic variance via approximate message passing. *Probability Theory and Related Fields*, 166(3-4):935–969, 2016.
- David L Donoho, Matan Gavish, and Iain M Johnstone. Optimal shrinkage of eigenvalues in the spiked covariance model. *arXiv preprint arXiv:1311.0851*, 2013.
- R Brent Dozier and Jack W Silverstein. On the empirical distribution of eigenvalues of large dimensional information-plus-noise-type matrices. *Journal of Multivariate Analysis*, 98(4):678–694, 2007.
- Simon Du, Jason Lee, Haochuan Li, Liwei Wang, and Xiyu Zhai. Gradient descent finds global minima of deep neural networks. In *International Conference on Machine Learning*, pages 1675–1685, 2019.
- Julien Dumont, Walid Hachem, Samson Lasaulce, Philippe Loubaton, and Jamal Najim. On the capacity achieving covariance matrix for rician mimo channels: an asymptotic approach. *arXiv preprint arXiv:0710.4051*, 2007.

- Noureddine El Karoui. Concentration of measure and spectra of random matrices: Applications to correlation matrices, elliptical distributions and beyond. *The Annals of Applied Probability*, 19(6):2362–2405, 2009.
- Noureddine El Karoui, Derek Bean, Peter J Bickel, Chinghway Lim, and Bin Yu. On robust regression with high-dimensional predictors. *Proceedings of the National Academy of Sciences*, page 201307842, 2013.
- Noureddine El Karoui et al. Spectrum estimation for large dimensional covariance matrices using random matrix theory. *The Annals of Statistics*, 36(6):2757–2790, 2008.
- Khalil Elkhailil, Abla Kammoun, Romain Couillet, Tareq Y Al-Naffouri, and Mohamed-Slim Alouini. A large dimensional study of regularized discriminant analysis. *IEEE Transactions on Signal Processing*, 68:2464–2479, 2020a.
- Khalil Elkhailil, Abla Kammoun, Xiangliang Zhang, Mohamed-Slim Alouini, and Tareq Al-Naffouri. Risk convergence of centered kernel ridge regression with large dimensional data. *IEEE Transactions on Signal Processing*, 68:1574–1588, 2020b.
- László Erdős. Universality of wigner random matrices: a survey of recent results. *Russian Mathematical Surveys*, 66(3):507, 2011.
- László Erdős, Sandrine Péché, José A Ramírez, Benjamin Schlein, and Horng-Tzer Yau. Bulk universality for wigner matrices. *Communications on Pure and Applied Mathematics: A Journal Issued by the Courant Institute of Mathematical Sciences*, 63(7):895–925, 2010.
- Zhou Fan and Andrea Montanari. The spectral norm of random inner-product kernel matrices. *Probability Theory and Related Fields*, 173(1-2):27–85, 2019.
- Zhou Fan and Zhichao Wang. Spectra of the conjugate kernel and neural tangent kernel for linear-width neural networks. *arXiv preprint arXiv:2005.11879*, 2020.
- James R Fienup. Phase retrieval algorithms: a comparison. *Applied optics*, 21(15):2758–2769, 1982.
- Evelyn Fix and J.L. Hodges. *Discriminatory analysis: nonparametric discrimination, consistency properties*. USAF School of Aviation Medicine, 1951.
- Jonathan Frankle and Michael Carbin. The lottery ticket hypothesis: Finding sparse, trainable neural networks. In *International Conference on Learning Representations*, 2019. URL <https://openreview.net/forum?id=rJl-b3RcF7>.
- Charlotte Frenkel, Martin Lefebvre, and David Bol. Learning without feedback: Direct random target projection as a feedback-alignment algorithm with layerwise feedforward training. *arXiv preprint arXiv:1909.01311*, 2019.

- Yoav Freund, Robert Schapire, and Naoki Abe. A short introduction to boosting. *Journal-Japanese Society For Artificial Intelligence*, 14(771-780):1612, 1999.
- Jerome Friedman, Trevor Hastie, and Robert Tibshirani. *The elements of statistical learning*, volume 1. Springer series in statistics New York, 2001.
- Surya Ganguli, Dongsung Huh, and Haim Sompolinsky. Memory traces in dynamical systems. *Proceedings of the National Academy of Sciences*, 105(48):18970–18975, 2008.
- Erol Gelenbe. Learning in the recurrent random neural network. *Neural computation*, 5(1):154–164, 1993.
- Dar Gilboa, Bo Chang, Minmin Chen, Greg Yang, Samuel S Schoenholz, Ed H Chi, and Jeffrey Pennington. Dynamical isometry and a mean field theory of LSTMs and GRUs. *arXiv preprint arXiv:1901.08987*, 2019.
- Viacheslav Leonidovich Girko. *Theory of stochastic canonical equations*, volume 2. Springer Science & Business Media, 2001.
- Leon Glass and Michael C Mackey. A simple model for phase locking of biological oscillators. *Journal of Mathematical Biology*, 7(4):339–352, 1979.
- Xavier Glorot and Yoshua Bengio. Understanding the difficulty of training deep feedforward neural networks. In *Proceedings of the thirteenth international conference on artificial intelligence and statistics*, pages 249–256, 2010.
- Andrew Goldberg, Xiaojin Zhu, Aarti Singh, Zhiting Xu, and Robert Nowak. Multi-manifold semi-supervised learning. In *Artificial Intelligence and Statistics*, pages 169–176, 2009.
- Ian Goodfellow, Jean Pouget-Abadie, Mehdi Mirza, Bing Xu, David Warde-Farley, Sherjil Ozair, Aaron Courville, and Yoshua Bengio. Generative adversarial nets. In *Advances in neural information processing systems*, pages 2672–2680, 2014.
- Yehoram Gordon. Some inequalities for gaussian processes and applications. *Israel Journal of Mathematics*, 50(4):265–289, 1985.
- Robert M Gray. *Toeplitz and circulant matrices: A review*. now publishers inc, 2006.
- Bernard Haasdonk. Feature space interpretation of svms with indefinite kernels. *IEEE Transactions on pattern analysis and machine intelligence*, 27(4):482–492, 2005.
- Walid Hachem, Philippe Loubaton, Jamal Najim, et al. Deterministic equivalents for certain functionals of large random matrices. *The Annals of Applied Probability*, 17(3):875–930, 2007.

- Walid Hachem, Philippe Loubaton, and Jamal Najim. A CLT for information-theoretic statistics of gram random matrices with a given variance profile. *The Annals of Applied Probability*, 18(6):2071–2130, 2008.
- James D Hamilton. *Time series analysis*, volume 2. Princeton New Jersey, 1994.
- Donghyeon Han, Jinsu Lee, Jinmook Lee, and Hoi-Jun Yoo. A 1.32 tops/w energy efficient deep neural network learning processor with direct feedback alignment based heterogeneous core architecture. In *2019 Symposium on VLSI Circuits*, pages C304–C305. IEEE, 2019.
- Trevor Hastie, Andrea Montanari, Saharon Rosset, and Ryan J Tibshirani. Surprises in high-dimensional ridgeless least squares interpolation. *arXiv preprint arXiv:1903.08560*, 2019.
- Kaiming He, Xiangyu Zhang, Shaoqing Ren, and Jian Sun. Deep residual learning for image recognition. In *Proceedings of the IEEE conference on computer vision and pattern recognition*, pages 770–778, 2016.
- Fumio Hiai and Dénes Petz. *The semicircle law, free random variables and entropy*. Number 77. American Mathematical Soc., 2000.
- Geoffrey E Hinton and Sam T Roweis. Stochastic neighbor embedding. In *Advances in neural information processing systems*, pages 857–864, 2003.
- Sepp Hochreiter and Jürgen Schmidhuber. Long short-term memory. *Neural computation*, 9(8):1735–1780, 1997.
- Roger A. Horn and Charles R. Johnson. *Matrix Analysis*. Cambridge University Press, second edition, 2012. ISBN 9780521548236.
- Sebastian Houben, Johannes Stallkamp, Jan Salmen, Marc Schlipsing, and Christian Igel. Detection of traffic signs in real-world images: The German Traffic Sign Detection Benchmark. In *International Joint Conference on Neural Networks*, number 1288, 2013.
- Guang-Bin Huang, Hongming Zhou, Xiaojian Ding, and Rui Zhang. Extreme learning machine for regression and multiclass classification. *IEEE Transactions on Systems, Man, and Cybernetics, Part B (Cybernetics)*, 42(2):513–529, 2012.
- Peter J Huber. *Robust statistics*. Springer, 2011.
- Martin Szummer Tommi Jaakkola and Martin Szummer. Partially labeled classification with markov random walks. *International Conference in Neural Information Processing Systems*, 14:945–952, 2002.
- Arthur Jacot, Franck Gabriel, and Clément Hongler. Neural tangent kernel: Convergence and generalization in neural networks. In *Advances in neural information processing systems*, pages 8571–8580, 2018.

- Herbert Jaeger. The “echo state” approach to analysing and training recurrent neural networks-with an erratum note. *Bonn, Germany: German National Research Center for Information Technology GMD Technical Report*, 148(34):13, 2001.
- Prateek Jain, Praneeth Netrapalli, and Sujay Sanghavi. Low-rank matrix completion using alternating minimization. In *Proceedings of the forty-fifth annual ACM symposium on Theory of computing*, pages 665–674, 2013.
- Thorsten Joachims et al. Transductive learning via spectral graph partitioning. In *International Conference on Machine Learning*, volume 3, pages 290–297, 2003.
- Iain M Johnstone. On the distribution of the largest eigenvalue in principal components analysis. *Annals of statistics*, pages 295–327, 2001.
- Iain M Johnstone. Multivariate analysis and jacobi ensembles: Largest eigenvalue, tracy–widom limits and rates of convergence. *Annals of statistics*, 36(6):2638, 2008.
- Abla Kammoun and Mohamed-Slim Alouini. On the precise error analysis of support vector machines. *arXiv preprint arXiv:2003.12972*, 2020.
- Abla Kammoun and Romain Couillet. Subspace kernel spectral clustering of large dimensional data. *Technical Report*, 2017.
- Abla Kammoun, Malika Kharouf, Walid Hachem, and Jamal Najim. A central limit theorem for the sinr at the lmmse estimator output for large-dimensional signals. *IEEE Transactions on Information Theory*, 55(11):5048–5063, 2009.
- Abla Kammoun, Romain Couillet, Frédéric Pascal, and Mohamed-Slim Alouini. Optimal design of the adaptive normalized matched filter detector using regularized Tyler estimators. *IEEE Transactions on Aerospace and Electronic Systems*, 54(2):755–769, 2018.
- Purushottam Kar and Harish Karnick. Random feature maps for dot product kernels. In *Artificial Intelligence and Statistics*, pages 583–591, 2012.
- Maurice G Kendall. A new measure of rank correlation. *Biometrika*, 30(1/2):81–93, 1938.
- Raghunandan H Keshavan, Andrea Montanari, and Sewoong Oh. Matrix completion from a few entries. *IEEE transactions on information theory*, 56(6):2980–2998, 2010.
- Alexei M Khorunzhy and Leonid A Pastur. On the eigenvalue distribution of the deformed wigner ensemble of random matrices. *Spectral operator theory and related topics*, 19:97–127, 1994.

- Alex Krizhevsky, Ilya Sutskever, and Geoffrey E Hinton. Imagenet classification with deep convolutional neural networks. In *Advances in neural information processing systems*, pages 1097–1105, 2012.
- Florent Krzakala, Cristopher Moore, Elchanan Mossel, Joe Neeman, Allan Sly, Lenka Zdeborová, and Pan Zhang. Spectral redemption in clustering sparse networks. *Proceedings of the National Academy of Sciences*, 110(52):20935–20940, 2013.
- Laurent Laloux, Pierre Cizeau, Marc Potters, and Jean-Philippe Bouchaud. Random matrix theory and financial correlations. *International Journal of Theoretical and Applied Finance*, 3(03):391–397, 2000.
- Yann LeCun, Léon Bottou, Yoshua Bengio, Patrick Haffner, et al. Gradient-based learning applied to document recognition. *Proceedings of the IEEE*, 86(11):2278–2324, 1998.
- Olivier Ledoit and Sandrine Péché. Eigenvectors of some large sample covariance matrix ensembles. *Probability Theory and Related Fields*, 151(1-2):233–264, 2011.
- Olivier Ledoit, Michael Wolf, et al. Nonlinear shrinkage estimation of large-dimensional covariance matrices. *The Annals of Statistics*, 40(2):1024–1060, 2012.
- Michel Ledoux. *The concentration of measure phenomenon*. Number 89. American Mathematical Soc., 2001. ISBN 9780821837924.
- Jaehoon Lee, Lechao Xiao, Samuel Schoenholz, Yasaman Bahri, Roman Novak, Jascha Sohl-Dickstein, and Jeffrey Pennington. Wide neural networks of any depth evolve as linear models under gradient descent. In *Advances in neural information processing systems*, pages 8572–8583, 2019.
- Kiryung Lee, Yanjun Li, Marius Junge, and Yoram Bresler. Blind recovery of sparse signals from subsampled convolution. *IEEE Transactions on Information Theory*, 63(2):802–821, 2016.
- Jure Leskovec and Andrej Krevl. SNAP Datasets: Stanford large network dataset collection. <http://snap.stanford.edu/data>, June 2014.
- Jian Li and Petre Stoica. Mimo radar with colocated antennas. *IEEE Signal Processing Magazine*, 24(5):106–114, 2007.
- Zhenyu Liao and Romain Couillet. The dynamics of learning: A random matrix approach. In *Proceedings of the 35th International Conference on Machine Learning*, volume 80, pages 3072–3081. PMLR, 2018a. URL <http://proceedings.mlr.press/v80/liao18b.html>.

- Zhenyu Liao and Romain Couillet. On the spectrum of random features maps of high dimensional data. In *Proceedings of the 35th International Conference on Machine Learning*, volume 80, pages 3063–3071. PMLR, 2018b. URL <http://proceedings.mlr.press/v80/liao18a.html>.
- Zhenyu Liao and Romain Couillet. Inner-product kernels are asymptotically equivalent to binary discrete kernels. *arXiv preprint arXiv:1909.06788*, 2019a.
- Zhenyu Liao and Romain Couillet. A large dimensional analysis of least squares support vector machines. *IEEE Transactions on Signal Processing*, 67(4):1065–1074, 2019b.
- Timothy P Lillicrap, Daniel Cownden, Douglas B Tweed, and Colin J Akerman. Random synaptic feedback weights support error backpropagation for deep learning. *Nature communications*, 7(1):1–10, 2016.
- Zenan Ling and Robert C Qiu. Spectrum concentration in deep residual learning: a free probability approach. *IEEE Access*, 7:105212–105223, 2019.
- Cosme Louart and Romain Couillet. Concentration of measure and large random matrices with an application to sample covariance matrices. 2019.
- Cosme Louart, Zhenyu Liao, and Romain Couillet. A random matrix approach to neural networks. *The Annals of Applied Probability*, 28(2):1190–1248, 2018. doi: 10.1214/17-AAP1328. URL <https://doi.org/10.1214/17-AAP1328>.
- Philippe Loubaton, Pascal Vallet, et al. Almost sure localization of the eigenvalues in a gaussian information plus noise model. application to the spiked models. *Electronic Journal of Probability*, 16:1934–1959, 2011.
- Lu Lu, Geoffrey Ye Li, A Lee Swindlehurst, Alexei Ashikhmin, and Rui Zhang. An overview of massive mimo: Benefits and challenges. *IEEE journal of selected topics in signal processing*, 8(5):742–758, 2014.
- Yue M Lu and Gen Li. Phase transitions of spectral initialization for high-dimensional non-convex estimation. *Information and Inference: A Journal of the IMA*, 2019.
- Ronny Luss and Alexandre d’Aspremont. Support vector machine classification with indefinite kernels. In *Advances in Neural Information Processing Systems*, pages 953–960, 2008.
- Anna Lytova, Leonid Pastur, et al. Central limit theorem for linear eigenvalue statistics of random matrices with independent entries. *The Annals of Probability*, 37(5):1778–1840, 2009.
- Zongming Ma et al. Accuracy of the tracy–widom limits for the extreme eigenvalues in white wishart matrices. *Bernoulli*, 18(1):322–359, 2012.

- Andrew L Maas, Awni Y Hannun, and Andrew Y Ng. Rectifier nonlinearities improve neural network acoustic models. In *Proc. icml*, volume 30, page 3, 2013.
- Laurens van der Maaten and Geoffrey Hinton. Visualizing data using t-SNE. *Journal of machine learning research*, 9(Nov):2579–2605, 2008.
- Xiaoyi Mai. *Methods of random matrices for large dimensional statistical learning*. PhD thesis, Université Paris-Saclay, 2019.
- Xiaoyi Mai and Romain Couillet. A random matrix analysis and improvement of semi-supervised learning for large dimensional data. *The Journal of Machine Learning Research*, 19(1):3074–3100, 2018.
- Xiaoyi Mai and Romain Couillet. Consistent semi-supervised graph regularization for high dimensional data. *arXiv preprint arXiv:2006.07575*, 2020.
- Xiaoyi Mai and Zhenyu Liao. High dimensional classification via empirical risk minimization: Improvements and optimality. *arXiv preprint arXiv:1905.13742*, 2019.
- Vladimir A Marcenko and Leonid Andreevich Pastur. Distribution of eigenvalues for some sets of random matrices. *Mathematics of the USSR-Sbornik*, 1(4):457, 1967.
- Ricardo A Maronna, R Douglas Martin, Victor J Yohai, and Matías Salibián-Barrera. *Robust statistics: theory and methods (with R)*. Wiley, 2018.
- Ricardo Antonio Maronna. Robust m-estimators of multivariate location and scatter. *The annals of statistics*, pages 51–67, 1976.
- Laurent Massoulié. Community detection thresholds and the weak ramanujan property. In *Proceedings of the forty-sixth annual ACM symposium on Theory of computing*, pages 694–703. ACM, 2014.
- Madan Lal Mehta and Michel Gaudin. On the density of eigenvalues of a random matrix. Technical report, Commissariat à l'Énergie Atomique, 1960.
- Song Mei and Andrea Montanari. The generalization error of random features regression: Precise asymptotics and double descent curve. *arXiv preprint arXiv:1908.05355*, 2019.
- Xavier Mestre. Improved estimation of eigenvalues and eigenvectors of covariance matrices using their sample estimates. *IEEE Transactions on Information Theory*, 54(11):5113–5129, 2008.
- Xavier Mestre and Miguel Ángel Lagunas. Modified subspace algorithms for doa estimation with large arrays. *IEEE Transactions on Signal Processing*, 56(2):598–614, 2008.

- Sebastian Mika, Gunnar Ratsch, Jason Weston, Bernhard Scholkopf, and Klaus-Robert Mullers. Fisher discriminant analysis with kernels. In *Neural networks for signal processing IX: Proceedings of the 1999 IEEE signal processing society workshop*, pages 41–48. IEEE, 1999.
- Tomas Mikolov, Kai Chen, Greg Corrado, and Jeffrey Dean. Efficient estimation of word representations in vector space. *arXiv preprint arXiv:1301.3781*, 2013.
- James A Mingo and Roland Speicher. *Free probability and random matrices*, volume 35. Springer, 2017.
- Marco Mondelli and Andrea Montanari. Fundamental limits of weak recovery with applications to phase retrieval. *Foundations of Computational Mathematics*, 19(3):703–773, 2019.
- David Morales-Jimenez, Romain Couillet, and Matthew R McKay. Large dimensional analysis of robust m-estimators of covariance with outliers. *IEEE Transactions on Signal Processing*, 63(21):5784–5797, 2015.
- Amit Moscovich, Ariel Jaffe, and Boaz Nadler. Minimax-optimal semi-supervised regression on unknown manifolds. *arXiv preprint arXiv:1611.02221*, 2016.
- Elchanan Mossel, Joe Neeman, and Allan Sly. Stochastic block models and reconstruction. *arXiv preprint arXiv:1202.1499*, 2012.
- Jamal Najim, Jianfeng Yao, et al. Gaussian fluctuations for linear spectral statistics of large random covariance matrices. *The Annals of Applied Probability*, 26(3):1837–1887, 2016.
- John Ashworth Nelder and Robert WM Wedderburn. Generalized linear models. *Journal of the Royal Statistical Society: Series A (General)*, 135(3):370–384, 1972.
- Mark EJ Newman. Modularity and community structure in networks. *Proceedings of the national academy of sciences*, 103(23):8577–8582, 2006.
- Andrew Y Ng, Michael I Jordan, and Yair Weiss. On spectral clustering: Analysis and an algorithm. In *Advances in neural information processing systems*, pages 849–856, 2002.
- Alexandru Nica and Roland Speicher. *Lectures on the combinatorics of free probability*, volume 13. Cambridge University Press, 2006.
- Arild Nøkland. Direct feedback alignment provides learning in deep neural networks. In *Advances in neural information processing systems*, pages 1037–1045, 2016.

- Roman Novak, Lechao Xiao, Yasaman Bahri, Jaehoon Lee, Greg Yang, Jiri Hron, Daniel A Abolafia, Jeffrey Pennington, and Jascha Sohl-dickstein. Bayesian deep convolutional networks with many channels are gaussian processes. In *International Conference on Learning Representations*, 2018.
- Frank WJ Olver, Daniel W Lozier, Ronald F Boisvert, and Charles W Clark. *NIST handbook of mathematical functions hardback and CD-ROM*. Cambridge university press, 2010.
- Sean O'Rourke et al. A note on the marchenko-pastur law for a class of random matrices with dependent entries. *Electronic Communications in Probability*, 17, 2012.
- Alain Pajor and Leonid Pastur. On the limiting empirical measure of eigenvalues of the sum of rank one matrices with log-concave distribution. *Studia Mathematica*, 195:11–29, 2009.
- Anastasios K Papazafeiropoulos and Tharmalingam Ratnarajah. Deterministic equivalent performance analysis of time-varying massive mimo systems. *IEEE Transactions on Wireless Communications*, 14(10):5795–5809, 2015.
- Leonid Pastur. On random matrices arising in deep neural networks. gaussian case. *arXiv preprint arXiv:2001.06188*, 2020.
- Leonid A Pastur. A simple approach to the global regime of gaussian ensembles of random matrices. *Ukrainian Mathematical Journal*, 57(6):936–966, 2005.
- Leonid Andreevich Pastur and Mariya Shcherbina. *Eigenvalue distribution of large random matrices*. Number 171. American Mathematical Soc., 2011.
- Debashis Paul. Asymptotics of sample eigenstructure for a large dimensional spiked covariance model. *Statistica Sinica*, pages 1617–1642, 2007.
- Debashis Paul and Jack W Silverstein. No eigenvalues outside the support of the limiting empirical spectral distribution of a separable covariance matrix. *Journal of Multivariate Analysis*, 100(1):37–57, 2009.
- Judea Pearl. Fusion, propagation, and structuring in belief networks. *Artificial intelligence*, 29(3):241–288, 1986.
- Jeffrey Pennington and Yasaman Bahri. Geometry of neural network loss surfaces via random matrix theory. In *International Conference on Machine Learning*, pages 2798–2806, 2017.
- Jeffrey Pennington and Pratik Worah. Nonlinear random matrix theory for deep learning. In *Advances in Neural Information Processing Systems*, pages 2637–2646, 2017.
- Jeffrey Pennington, Samuel Schoenholz, and Surya Ganguli. Resurrecting the sigmoid in deep learning through dynamical isometry: theory and practice. In *Advances in neural information processing systems*, pages 4785–4795, 2017.

- Tai Qin and Karl Rohe. Regularized spectral clustering under the degree-corrected stochastic blockmodel. In *Advances in Neural Information Processing Systems*, pages 3120–3128, 2013.
- Ali Rahimi and Benjamin Recht. Random features for large-scale kernel machines. In *Advances in neural information processing systems*, pages 1177–1184, 2008.
- Lorenzo Rosasco, Ernesto De Vito, Andrea Caponnetto, Michele Piana, and Alessandro Verri. Are loss functions all the same? *Neural Computation*, 16(5):1063–1076, 2004.
- Frank Rosenblatt. The perceptron: a probabilistic model for information storage and organization in the brain. *Psychological review*, 65(6):386, 1958.
- Yu. A. Rozanov. *Stationary random processes*. Holden-Day, San Francisco, CA, 1967.
- Walter Rudin et al. *Principles of mathematical analysis*, volume 3. McGraw-hill New York, 1964.
- Alaa Saade, Florent Krzakala, and Lenka Zdeborová. Spectral clustering of graphs with the bethe hessian. In *Advances in Neural Information Processing Systems*, pages 406–414, 2014.
- Justin Salez. *Some implications of local weak convergence for sparse random graphs*. PhD thesis, Université Pierre et Marie Curie-Paris VI; Ecole Normale Supérieure de Paris . . . , 2011.
- Simone Scardapane and Dianhui Wang. Randomness in neural networks: an overview. *Wiley Interdisciplinary Reviews: Data Mining and Knowledge Discovery*, 7(2), 2017.
- Ralph Schmidt. Multiple emitter location and signal parameter estimation. *IEEE transactions on antennas and propagation*, 34(3):276–280, 1986.
- Wouter F Schmidt, Martin A Kraaijveld, and Robert PW Duin. Feed forward neural networks with random weights. In *International Conference on Pattern Recognition*, pages 1–1. IEEE Computer Society Press, 1992.
- Mohamed El Amine Seddik, Mohamed Tamaazousti, and Romain Couillet. Kernel random matrices of large concentrated data: the example of gan-generated images. In *ICASSP 2019-2019 IEEE International Conference on Acoustics, Speech and Signal Processing (ICASSP)*, pages 7480–7484. IEEE, 2019.
- Jack W Silverstein. The limiting eigenvalue distribution of a multivariate F matrix. *SIAM Journal on Mathematical Analysis*, 16(3):641–646, 1985.
- Jack W Silverstein and ZD Bai. On the empirical distribution of eigenvalues of a class of large dimensional random matrices. *Journal of Multivariate analysis*, 54(2):175–192, 1995.

- Jack W Silverstein and Sang-Il Choi. Analysis of the limiting spectral distribution of large dimensional random matrices. *Journal of Multivariate Analysis*, 54(2):295–309, 1995.
- Karen Simonyan and Andrew Zisserman. Very deep convolutional networks for large-scale image recognition. *arXiv preprint arXiv:1409.1556*, 2014.
- Alexander Soshnikov. Universality at the edge of the spectrum in wigner random matrices. *Communications in mathematical physics*, 207(3):697–733, 1999.
- Alexander B Soshnikov. Gaussian fluctuation for the number of particles in airy, bessel, sine, and other determinantal random point fields. *Journal of Statistical Physics*, 100(3-4):491–522, 2000.
- Daniel Soudry, Elad Hoffer, Mor Shpigel Nacson, Suriya Gunasekar, and Nathan Srebro. The implicit bias of gradient descent on separable data. *The Journal of Machine Learning Research*, 19(1):2822–2878, 2018.
- Charles Spearman. The proof and measurement of association between two things. *The American journal of psychology*, 100(3/4):441–471, 1987.
- Roland Speicher and Carlos Vargas. Free deterministic equivalents, rectangular random matrix models, and operator-valued free probability theory. *Random Matrices: Theory and Applications*, 1(02):1150008, 2012.
- Nitish Srivastava, Geoffrey Hinton, Alex Krizhevsky, Ilya Sutskever, and Ruslan Salakhutdinov. Dropout: a simple way to prevent neural networks from overfitting. *The journal of machine learning research*, 15(1):1929–1958, 2014.
- Charles M Stein. Estimation of the mean of a multivariate normal distribution. *The annals of Statistics*, pages 1135–1151, 1981.
- Arun Suggala, Adarsh Prasad, and Pradeep K Ravikumar. Connecting optimization and regularization paths. In *Advances in Neural Information Processing Systems*, pages 10608–10619, 2018.
- Pragya Sur and Emmanuel J Candès. A modern maximum-likelihood theory for high-dimensional logistic regression. *Proceedings of the National Academy of Sciences*, 116(29):14516–14525, 2019.
- Johan AK Suykens and Joos Vandewalle. Least squares support vector machine classifiers. *Neural processing letters*, 9(3):293–300, 1999.
- Hossein Taheri, Ramtin Pedarsani, and Christos Thrampoulidis. Sharp guarantees for solving random equations with one-bit information. In *2019 57th Annual Allerton Conference on Communication, Control, and Computing (Allerton)*, pages 765–772. IEEE, 2019.
- Hossein Taheri, Ramtin Pedarsani, and Christos Thrampoulidis. Fundamental limits of ridge-regularized empirical risk minimization in high dimensions. *arXiv preprint arXiv:2006.08917*, 2020a.

- Hossein Taheri, Ramtin Pedarsani, and Christos Thrampoulidis. Optimality of least-squares for classification in gaussian-mixture models. In *2020 IEEE International Symposium on Information Theory (ISIT)*, pages 2515–2520. IEEE, 2020b.
- Hossein Taheri, Ramtin Pedarsani, and Christos Thrampoulidis. Sharp asymptotics and optimal performance for inference in binary models. *arXiv preprint arXiv:2002.07284*, 2020c.
- Michel Talagrand. Concentration of measure and isoperimetric inequalities in product spaces. *Publications Mathématiques de l’Institut des Hautes Etudes Scientifiques*, 81(1):73–205, 1995.
- Terence Tao. *Topics in random matrix theory*, volume 132. American Mathematical Soc., 2012.
- Terence Tao and Van Vu. Random matrices: the circular law. *Communications in Contemporary Mathematics*, 10(02):261–307, 2008.
- Christos Thrampoulidis, Ehsan Abbasi, and Babak Hassibi. Precise error analysis of regularized m -estimators in high dimensions. *IEEE Transactions on Information Theory*, 64(8):5592–5628, 2018.
- Malik Tiomoko and Romain Couillet. Random matrix-improved estimation of the wasserstein distance between two centered gaussian distributions. In *2019 27th European Signal Processing Conference (EUSIPCO)*, pages 1–5, 2019.
- Hafiz Tiomoko Ali and Romain Couillet. Improved spectral community detection in large heterogeneous networks. *The Journal of Machine Learning Research*, 18(1):8344–8392, 2017.
- Hafiz Tiomoko Ali, Abla Kammoun, and Romain Couillet. Random matrix-improved kernels for large dimensional spectral clustering. In *2018 IEEE Statistical Signal Processing Workshop (SSP)*, pages 453–457. IEEE, 2018.
- Craig A Tracy and Harold Widom. On orthogonal and symplectic matrix ensembles. *Communications in Mathematical Physics*, 177(3):727–754, 1996.
- Antonia M Tulino, Sergio Verdú, et al. Random matrix theory and wireless communications. *Foundations and Trends® in Communications and Information Theory*, 1(1):1–182, 2004.
- David E Tyler. Robustness and efficiency properties of scatter matrices. *Biometrika*, 70(2):411–420, 1983.
- Aad W Van der Vaart. *Asymptotic statistics*, volume 3. Cambridge university press, 2000.
- Vladimir Vapnik. Principles of risk minimization for learning theory. In *Advances in neural information processing systems*, pages 831–838, 1992.

- Andrea Vedaldi and Andrew Zisserman. Efficient additive kernels via explicit feature maps. *IEEE transactions on pattern analysis and machine intelligence*, 34(3):480–492, 2012.
- Roman Vershynin. Introduction to the non-asymptotic analysis of random matrices. *arXiv preprint arXiv:1011.3027*, 2010.
- Dan V Voiculescu, Ken J Dykema, and Alexandru Nica. *Free random variables*. Number 1. American Mathematical Soc., 1992.
- Ulrike Von Luxburg. A tutorial on spectral clustering. *Statistics and computing*, 17(4):395–416, 2007.
- Sebastian Wagner, Romain Couillet, Mérouane Debbah, and Dirk TM Slock. Large system analysis of linear precoding in correlated miso broadcast channels under limited feedback. *IEEE transactions on information theory*, 58(7):4509–4537, 2012.
- Chao-Kai Wen, Guangming Pan, Kai-Kit Wong, Meihui Guo, and Jung-Chieh Chen. A deterministic equivalent for the analysis of non-gaussian correlated mimo multiple access channels. *IEEE transactions on information theory*, 59(1):329–352, 2012.
- Eugene P. Wigner. Characteristic vectors of bordered matrices with infinite dimensions. *Annals of Mathematics*, 62(3):548–564, 1955.
- Christopher KI Williams. Computing with infinite networks. In *Advances in neural information processing systems*, pages 295–301, 1997.
- John Wishart. The generalised product moment distribution in samples from a normal multivariate population. *Biometrika*, 20(1/2):32–52, 1928.
- Svante Wold, Kim Esbensen, and Paul Geladi. Principal component analysis. *Chemometrics and intelligent laboratory systems*, 2(1-3):37–52, 1987.
- Han Xiao, Kashif Rasul, and Roland Vollgraf. Fashion-mnist: a novel image dataset for benchmarking machine learning algorithms, 2017.
- Lechao Xiao, Yasaman Bahri, Jascha Sohl-Dickstein, Samuel Schoenholz, and Jeffrey Pennington. Dynamical isometry and a mean field theory of cnns: How to train 10,000-layer vanilla convolutional neural networks. In *International Conference on Machine Learning*, pages 5393–5402, 2018.
- Liusha Yang, Romain Couillet, and Matthew R McKay. A robust statistics approach to minimum variance portfolio optimization. *IEEE Transactions on Signal Processing*, 63(24):6684–6697, 2015.
- Jianfeng Yao, Romain Couillet, Jamal Najim, and Merouane Debbah. Fluctuations of an improved population eigenvalue estimator in sample covariance matrix models. *IEEE Transactions on Information Theory*, 59(2):1149–1163, 2013.

- Yuan Yao, Lorenzo Rosasco, and Andrea Caponnetto. On early stopping in gradient descent learning. *Constructive Approximation*, 26(2):289–315, 2007.
- Chiyuan Zhang, Samy Bengio, Moritz Hardt, Benjamin Recht, and Oriol Vinyals. Understanding deep learning requires rethinking generalization. *arXiv preprint arXiv:1611.03530*, 2016.
- Teng Zhang, Xiuyuan Cheng, and Amit Singer. Marchenko-pastur law for tyler’s and maronna’s m-estimators. *arXiv preprint arXiv:1401.3424*, 2014.
- Shurong Zheng, Zhidong Bai, Jianfeng Yao, et al. Clt for eigenvalue statistics of large-dimensional general fisher matrices with applications. *Bernoulli*, 23(2):1130–1178, 2017.
- Dengyong Zhou, Olivier Bousquet, Thomas Navin Lal, Jason Weston, and Bernhard Schölkopf. Learning with local and global consistency. volume 16, pages 321–328, 2004.
- Xueyuan Zhou and Mikhail Belkin. Semi-supervised learning by higher order regularization. In *Proceedings of the Fourteenth International Conference on Artificial Intelligence and Statistics*, pages 892–900, 2011.
- Xiaojin Zhu and Zoubin Ghahramani. Learning from labeled and unlabeled data with label propagation. Technical report, Citeseer, 2002.
- Xiaojin Zhu, Zoubin Ghahramani, John Lafferty, et al. Semi-supervised learning using gaussian fields and harmonic functions. In *International Conference on Machine Learning*, volume 3, pages 912–919, 2003.
- Xiaojin Jerry Zhu. Semi-supervised learning literature survey. Technical report, University of Wisconsin-Madison Department of Computer Sciences, 2005.